



Proceedings of the

6th | NATIONAL CONFERENCE

on Research and Development
in Science, Engineering
and Technology

Organized by

ST. ANNE'S

COLLEGE OF ENGINEERING AND TECHNOLOGY

Association with



INSTITUTION'S
INNOVATION
COUNCIL

(Ministry of HRD Initiative)

N
C
R
D
S
E
T

'22

**Proceedings of
National Conference on Research and Development in
Science, Engineering and Technology**

NCRDSET '22

27th May 2022

Organised by



St. Anne's College of Engineering and Technology
Panruti, Cuddalore District – 607106.
Tamilnadu, India.

PREFACE

The 6th National Conference on Research and Development in Science, Engineering and Technology (NCRDSET'22) in association with Indian Society for Technical Education (ISTE) was held on the campus of St. Anne's College of Engineering and Technology in Anguchettypalayam, Panruti of Cuddalore District on 27th May 2022.

Conferences pave way to bring together people with common interests and discuss issues and ideas related to various topics. Sixth National Conference on Research, Development, Science and Technology 2022 (NCRDSET'22) will target state-of-the-art as well as emerging topics pertaining in the field of Science, Engineering and Technology and effective strategies for its implementation. It also provides a premier interdisciplinary platform for researchers, academicians, industry persons, practitioners, educators and students to present and discuss the most recent innovations, trends, and concerns as well as practical challenges encountered, and solutions adopted in the fields of innovation. The objective of this National conference is to provide opportunity for the participants to interact and exchange ideas, experience and expertise in the current trend and strategies. Besides this, participants will also be enlightened about vast avenues, current and recent technological developments in various domain and its applications will be thoroughly explored and discussed.

The proceedings is a compilation of the 76 accepted papers and represent an interesting outcome of the conference. This year, NCRDSET'22 has attracted Academicians and students across the country who have submitted their contributions with their latest advances. The accepted papers reflect the current trends in the following 5 broad research areas. 1) Computer Science, 2) Electrical 3) Electronics and Communications 4) Mechanical and 5) Engineering Science.

Before concluding this preface of these proceedings, I would like to express my thanks to all authors, members of the program committee, members of the organizing committee and the rest of the people involved in planning and developing of NCRDSET'22 for their unconditional support, their great effort, and their valuable time. I would like to devote special thanks to the members of the program committee for providing excellent reviews of the submitted papers. I also wish to give special thanks to all the non-teaching members for their hard work and devotion, which made the conference a great success. All of them have made possible the successful accomplishment of NCRDSET'22.

Special thanks to the authors, the committee members and the sponsors. I hope all the participants can obtain useful information from the proceedings.

Convener

Mrs.D.Pauline Freeda,

Associate Professor and Head,

Department of Computer Science Engineering,

St. Anne's College of Engineering and Technology.

ORGANISING COMMITTEE

CHIEF PATRON

Rev. Sr. Dr. Y. Yesu Thangam, SAT,

Secretary

St. Anne's College of Engineering and Technology

PATRON

Dr. R. Arokiadass,

Principal

St. Anne's College of Engineering and Technology

Co-PATRON

Sr. Punitha Jilt, SAT,

Vice Principal

St. Anne's College of Engineering and Technology

CONVENOR

Mrs. D. Pauline Freeda,

Associate Professor and Head

Department of Computer Science and Engineering

St. Anne's College of Engineering and Technology

STEERING COMMITTEE

Dr. D. Ommurugadasan,

Professor and Head

Department of Mechanical Engineering

Dr. Sr. S. Anita,

Professor and Head

Department of Electronics and communication Engineering

Mr. V.C. Eugin Martin Raj,

Associate Professor and Head

Department of Electrical and Electronics Engineering

Mr. N. Syed Mubarak,

Assistant Professor and Head

Department of Science and Humanities

MESSAGE FROM CHIEF GUEST

Science and Engineering research conducted in academic institutions plays a critical role in raising our standard of living, creating jobs, improving health, and providing for national security. Conference is timely and an excellent opportunity for academicians to establish meaningful collaborations around the world.

It is a great privilege and profound honour bestowed on me for being the Chief Guest for the National Conference on Research and Development in Science, Engineering & Technology (NCRDSET22) and to share my thoughts and ideas through this message column with the maverick and creative minds of this reputed Institute committed to scholastic excellence.

This National Conference, NCRDSET '22, provides many opportunities to the Faculty, Industrialists and Students to exhibit their research articles, share, exchange their views and aspirations, learn novel methods, and approach in their respective field.

This premier institute, St. Anne's College of Engineering and Technology has put forth concerted efforts to align in focus with the national goal of achieving technological self-reliance through conducting this 6th National Conference on Research and Development in Science, Engineering and Technology in the thrust areas of Engineering like Computer science, Electrical, Electronics and Communication, Mechanical along with Engineering Sciences.

I look forward to an excellent meeting with great engineering minds, sharing exciting and innovative presentations and ideas. I take great pride in inviting all participants of the Conference and I am sure that each one of you will identify subjects of his/her interest and will benefit from many fruitful and enriching interactive discussions. Let me thank the local organizing committee, participants, session chairs, keynote and plenary

speakers for what promises to be an exciting conference program. I wish for inspiring and successful ideas.

My best wishes to all.

Dr.S.Selvam,

Director,
National Power Training Institute,
(Ministry of Power,Govt.of India)
Neyveli

MESSAGE FROM KEYNOTE SPEAKER

I am extremely delighted about the 6th National Conference on Research and Development in Science, Engineering and Technology organized by St. Annes College of Engineering and Technology, Panruti on 27th May 2022. Over the years, intense improvements have been made in the field of Science, Engineering and Technology. This forum will address various research challenges and latest innovation. The development in these areas have made the world get closer, communication easier and faster. The need of the hour is to bridge the gap between the academia and industry. This conference is sure to provide a venue for researchers and practitioners to address the research problems and identify better solutions. I believe it will also aim at increasing the synergy between the academic and industry professionals.

I congratulate the organizing committee members, supporting staff, research scholars and delegates for their initiatives. My sincere and best wishes for the success of the conference.

Dr.S.P.Mangaiyarkarasi

Assistant professor Sr. Grade,
Department of Electrical and Electronics Engineering
University College of Engineering
Panruti

MESSAGE FROM SECRETARY'S DESK

St. Anne's College of Engineering and Technology (SACET), since its inception, aims at character formation, excellence in teaching, learning, research, training and placement, empowerment of rural youth, and has been steadily growing in all directions with its Motto: To Build a Holistic Society. A serene and green campus, and pure fresh air warmly welcome everyone who enters the portals of SACET. Our faculty members are highly dedicated to the noble cause of teaching, learning and research, by imbibing human values as well as subject knowledge in the students so as to develop themselves as integrated persons. The students are motivated to make use of every opportunity in expanding the horizon of their knowledge and they actively participate in curricular, co-curricular and extra-curricular activities.

Through organizing the National Conference on "Research and Development in Science, Engineering and Technology" (NCRDSET), every year, SACET provides a platform to initiate, foster and trigger thought exchange between Engineers by focusing on the recent trends as well as future prospects for research and projects, experiences and applications in the field of Engineering, to promote research, improve the existing processes and finding new solutions to upcoming problems. With immense joy I congratulate the Principal, Convener and committee members and all the Faculty and Non-teaching staff for their involvement and cooperation to conduct this NCRDSET.

I congratulate the staff, researchers and budding Engineers for their participation and contribution of research papers in this conference. The topics of the NCRDSET reflect the current trends, recent advances and new approaches in all the disciplines of Engineering and Technology and many other inter-disciplinary fields which are of concerns for the society. I pray that the Almighty God may shower His abundant blessings on this conference which in turn may enrich everyone to enhance their knowledge for their life and the welfare of the society. Best wishes for the fruitful deliberations in this NCRDSET.

Rev. Sr. Dr. Y. Yesu Thangam, S.A.T.

Secretary

St. Anne's College of Engineering and Technology

MESSAGE FROM PRINCIPAL

It gives me immense pleasure that St. Anne's College of Engineering and Technology is organizing 6th National Conference on Research and development in Science, Engineering and Technology on 27th May, 2022.

This conference aims to bring novel ideas from inquisitive minds to a common platform for deliberation, consideration and appreciation. Besides that, candidates get an opportunity to showcase their talents in their respective fields. We are pleased with the enthusiastic response we have received from participants across the country.

Quite a lot of commitment and hard work has gone into organising this conference and I sincerely congratulate the convener and the organizing team, and all coordinators for their united efforts.

I sincerely convey my heartily congratulation to all authors and participants from our and other institutions for their efforts and interest in participating in this conference.

I am sure that this conference will help the next generation researchers to gain insight knowledge in their area of interest.

I wish the conference all the success.

Best wishes to all.

Dr. R. Arokiadass, M.E., Ph.D.,

Principal

St. Anne's College of Engineering and Technology

MESSAGE FROM VICE-PRINCIPAL

I am delighted in acknowledging the National Conference on Research and Development in Science, Engineering and Technology (ICRDSET'22) organized by our institution.

The Conference aims to bring different ideologies under one roof and provide opportunities to exchange ideas face to face, to establish research relations and to find global partners for future collaboration. The themes and sub-themes for this conference are indicative of relevant research areas to give the prospective authors innovative prepositions about the ambit of discussion.

I am sure that the conference will provide an opportunity to interact and share your knowledge and ideas with peers, to create new collaborations and partnerships to create a better tomorrow.

I welcome you all to St. Annes College of Engineering and Technology and hope that this conference will act as a medium for all of us present here to ponder upon the topic of discussion, challenge us to strive towards it and inspire us at the same time

I wish the best of fortune, peace and prosperity to all those who contribute to the noble task of spreading knowledge and its manifest qualities, aims and objectives. I would also like to thank the staff, the organisers and the students for their contribution in successfully organising and managing this event. This event wouldn't have been possible without their guidance and constant support.

I wish the Conference a grand success!!!

Sr. Punitha Jilt, SAT

Vice Principal
St. Anne's College of Engineering and Technology

INDEX

Computer Science and Engineering

NCRDSET-1027	Smart Ration card using Face recognition <i>R.Ranjithkumar, M.Labilan ,G.Ravindiran, P.Saravanabhava</i>	1
NCRDSET-1034	Implementation Of Dna Cryptography In Cloud Computing And Using Socket Programming <i>S. Nithya, R. Sharmila, N. Thanigaivel</i>	5
NCRDSET-1035	Online product price and comparison using web mining and machine learning <i>Sandhiya.R, Senthamizhselvi.P, AnnaiTherasammal.A, Brittadevi.v</i>	9
NCRDSET-1036	Heart attack prediction for stroke patients using machine learning <i>S.Manavalan, A.Bckiya priy, A.Ezakia selvam , R.Kamatchi</i>	14
NCRDSET-1039	KBot: Approach for Understanding NL Over Linked Data <i>D.Sakthi Sankar, T.Sivasubramanian, R.Sridharan, T.Periyasamy</i>	19
NCRDSET-1041	Massive MIMO Transmission for LEO Satellite Communication <i>Gayathiri.T, Reshma Taaaj .M, Sangeetha .S, T. Periyasamy</i>	20
NCRDSET-1045	Cyberbullying Detection on Social Networks Using Neural Networks <i>P.Nivetha, A. Archana, R.Vimala Roshini</i>	21
NCRDSET-1046	Classification of video metadata <i>K. Bakkiyalakshmi, R. Kowsalya, R. Krishnaveni</i>	27
NCRDSET-1050	Towards Achieving Keyword Search over Dynamic Encrypted Cloud Data with Symmetric-Key Based Verification <i>S.Ramalingam, Abinash S, Prem S, Karthikeyan S</i>	31
NCRDSET-1051	DL- CNN based hardware state enable using hand gesture <i>E.Indhuma, N.Subasri, M.Jayaveena</i>	36
NCRDSET-1052	Optimizing Spectrum Sensing for Energy Efficient Cognitive Radio Sensor Network <i>Abirami.S, Priyadharshini.P, Ragulya.S, Gayathiri.N, ST.Preethi,</i>	41
NCRDSET-1054	Smart Ration System Using Face Recognition. <i>A.Ammeerunnish, R. Elavarasi, V. Lakshmi, T.Hemalatha</i>	42
NCRDSET-1055	Modified Secure Multi Clouds Mobile Computing for the Data Computing in Cloud <i>A. Akilan, R.Aadhithyan, S.Dinesh, S.Karthikeyan</i>	46

NCRDSET-1056	Secure Message Communication Protocol For Warship Establishment <i>Arivumathi.V, Jothika.S, Keerthana.S, Ramalingam.S</i>	51
NCRDSET-1059	User Choice-Based Alpha Numerical Random Password Generator For Securing the Data Assets <i>M.Saleth Reena, Z.Asmathunnisa</i>	52
NCRDSET-1061	Blind Assistance System with Voice Enabled and Real time Object Detection <i>S. Sri Ram, S. Syed Thameem, P.A.Yokesh, E.Indhuma</i>	57
NCRDSET-1063	Video Compression <i>Z. Asmathunnisa, B.Dhivagar, K.Rajesh, P.A.Vasanth</i>	63
NCRDSET-1079	Automation using IoT in Greenhouse Environment <i>Jasmine Medona .A</i>	69
NCRDSET-1086	Drowsiness Detection of Driver by Using Transfer Learning of Deep Learning <i>N.Kanishya, B. Ranjani, A.Reshma, V.Sindhu, P.M.Kamatchi</i>	77
NCRDSET-1053	Hybrid key splitting scheme for data sharing and prevention of cyber security <i>A.Nandhini., D. sowmiya., S. Subalakshmi , S. T. Preethi</i>	81
NCRDSET-1057	AI Based transport system in real time traffic monitoring with machine learning <i>B.Harine, E.Premalatha, S.Sivaranjani, S.Sneha, R.Vijayabharathi</i>	82

Electronics and Communication Engineering

NCRDSET-1006	Green energy harvesting from Radio frequency to direct current <i>Elakiya, Heera, Pavithra, Sathyamoorthy.S</i>	86
NCRDSET-1008	IOT Approach to vehicle accident detection and live location tracking <i>K.Mohanapriya, G.Indumathi</i>	92
NCRDSET-1015	Smart and secure voting machine using biometric authentication <i>S.Abinandhini, R.Iyshwarya, R.Sivapratha</i>	97
NCRDSET-1018	Implementation Of Speed Assistance In Vehicle By Using IoT <i>Mohanraj. R,Sanjay. T,Yogeshraja. R Prithiviraj.K</i>	104
NCRDSET-1019	Abandoned Bore Well Rescue System For Toddlers Using Apl Device <i>R.Aasha, M.Shylaja, S.Nivetha , T.Karthiga</i>	111

NCRDSET-1022	IOT Based Implementation Of River Water Flow And Water Quality Monitoring For Pico Hydro Power Plant <i>V.Heera, P.Paruthi Ilam Vazhuthi</i>	118
NCRDSET-1024	Form Monitoring By Augmented Reality Using Under Ground Sensor Network <i>Abinaya.S, Bavadharini.R, Kalki.V, Ramapriya.S</i>	124
NCRDSET-1032	Military Robot For Surveillance And Protection System <i>Ajay.K, Gokul Raj.R, Santhosh Kumar.S , Venkatesan.G</i>	130
NCRDSET-1033	Bus Tracking System For Visually Impaired Person <i>K.Santhini. G.Gayathri V.Thiyagarajan/ASP, G.Sadiq Basha</i>	133
NCRDSET-1037	Audio Data Transmission On Light Using Li-Fi Technology <i>Bhuvanitha K, Anupriya K, Deivanai E, Raju S</i>	139
NCRDSET-1049	Design And Fabrication Of Optimized Rail gate Control And Obstacle Detection Using Wireless Protocol <i>Jeevanandam.V, Manikandan.R,Mohamed Akshith.M, Thivagar.T</i>	142
NCRDSET-1065	Cascade attentive refinenet for blood vessels Segmentation of diabetic retinopathy <i>Abinesh.M, Ravichandran.P , D. Uma maheswari</i>	145
NCRDSET-1066	IoT- Based Intelligent Aquaculture Monitoring System For Fish Farming <i>R.Radhakrishnan/AP, S.Balabasker</i>	153
NCRDSET-1072	Design And Implementation Of Microcontroller Based Vehicular Smart Helmet For Safe Journey Using Sensors <i>B. Arunkumar/AP, S. Durai Ra/ AP, V.Venkatesan</i>	161
NCRDSET-1073	Microfluidic Syringe Pump <i>R. Sineka, Dr. S. Anita</i>	167
NCRDSET-1078	Design And Analysis Of Multi-Patient Monitoring System Using Cloud Computing <i>V. Ramya, G. Seetha Lakshmi, R.Radhakrishnan</i>	173
NCRDSET-1080	Design of GaAs Based Low Noise Amplifier For 5G Frond-End System <i>K.Kaveri, P.Sivasakthi , M.Sahinippiriya</i>	179
NCRDSET-1081	Remote Health Monitoring System For Visually Impaired <i>Kavitha.K, Delisya.D, B. Arunkumar</i>	184
NCRDSET-1082	Saline Level Monitoring System Using Lora Technology <i>G.Parameswari, R.Preethi, S.Krishna Dharshini, S.Balabaker</i>	189

NCRDSET-1083	Design Of Fast Full By Exploring New Xor/X Nor Gates <i>R.Manju, K.Vijayalakshmi , V.venkatesan</i>	193
NCRDSET-1093	High Speed Gate Level Synchronous Full Adder Designs <i>V.Venkatesan B.Arunkumar M.sahinipriya</i>	199
NCRDSET-1098	Design of Rectangular Patch 4×4 Array For Satellite Communication <i>S.Selvapraveena, R.Sandhiya S.Durai Raj</i>	205

Electrical and Electronics Engineering

NCRDSET-1062	Optimal Placement and Sizing of Distributed Generator Based on Multi objective Particle Swarm Optimization <i>A. Richard Pravin, J. Aarthiroja, M. Eswari, S. Sivapriya</i>	210
NCRDSET-1067	Cost Saving on Micro Grid Operation using Grey Wolf Optimization Algorithm <i>K. Sriram, B. Anbumani, S. KalaiPriyan, C. Naveenkumar</i>	215
NCRDSET-1069	A 129-level Asymmetrical Cascaded H-Bridge Multilevel Inverter with Reduced Switches and Low THD <i>A. Annai Theresa, P. Vivethitha, K. Srilekha, M. Nivetha</i>	221
NCRDSET-1071	Monitoring the Microgrid using IoT <i>J. Ramesh, C. Boobathi, K. Mohanraj, R. Rasu</i>	227
NCRDSET-1074	Power Loss Reduction and Voltage Profile Improvement using Optimal Placement of FACTS Devices <i>M. Prema Latha, S. Kannan, G. Sampathkumar, K. Surendhar</i>	233
NCRDSET -1075	A Novel Circuit for Battery Charging and Motor Control of Electric Vehicle <i>V. Balaji, K. Bhuvaneshwaran, M. Muralikrishnan, V. Vijay</i>	240
NCRDSET-1076	Wireless Power Transmission System <i>J. Arul Martinal, A. Pieorex, A. Arockiaraj, I. Kavnilavan, D. Vijaykumar</i>	245
NCRDSET-1077	Solution to Combine Economic and Emission Dispatch Problem using Adaptive Particle Swarm Optimization Algorithm <i>M. Gnanaprakash, S. P. Mangaiyarkarasi, R. Vijayakumar, S. Sathishkumar</i>	250
NCRDSET-1099	Design of Efficient Electric Motorcycle Using Brushless DC Motor <i>A. Sundarapandiyan</i>	256
NCRDSET-1100	Electrical Motor Topologies for Aircraft Propulsion <i>V. C. Eugin Martin Raj</i>	261

Mechanical Engineering

NCRDSET-1038	Performance Enhancement Study for Single Slope Solar Desalination Plant <i>M.Kavitha, K. Anandavelu, K. Thiruvvasagamoorthy</i>	267
NCRDSET -1088	1 A Brief Review On The Influence Of Nanofillers On Composite Efficiency <i>A.Abinesh, Jayakrishnan, Robin Paul, A.Shanmugarajan</i>	273
NCRDSET-1089	Experimental Analysis Of Diesel Engine Using Bio Fuel Blended With Aluminium Oxide <i>R.Sasikumar , Krishanakumar.S, D.Manivel, B.Karunakaran</i>	282
NCRDSET-1090	Electrical Discharge Coating Of Aluminium Alloy Using Ws2/Cu Green Compact Electrode <i>K.Shanmuga Elango(S), J.Arockiatony Play , A. Vigneshkumar, R. Arun Prakash</i>	285
NCRDSET-1091	Analysis Of Mechanical Properties Of Tic Reinforced Aluminium Alloy Composites <i>D.Ommurugadhasan, M. Arulselvam, K. Dhinakaran, A. Krishnaraj, V. Senthamilselvan, Dr.</i>	294
NCRDSET -1094	Taguchi optimization of end milling parameters on 316L stainless steel <i>R.Arokiadass, S.Daniel, R.Devendiran, T.Anbhazhagan, S.Fralick</i>	301
NCRDSET-1095	Optimization Of Machining Parameter On Ss316l Material Using Orthogonal Array Method <i>K.Saravanan , M.Sivamanikandan, R.Jayakumar</i>	306
NCRDSET -1096	An Over View Of Biomass Dryer For Cashew Product <i>P.Murugan, Dhanushkodi</i>	309
NCRDSET-1097	A Review on Recent Development In Design and Energy Enhancement of Flat Plate Hybrid Photovoltaic Thermal (PV/T) Air Collector. <i>K.Sakthivel , P.Murugan , S.Dhanushkodi</i>	318

Science and Humanities

NCRDSET-1013	Analysis of MAP/PH/1 Queueing model subject to Two-stage vacations policy with imperfect service, Setup time, Breakdown, Delayed Phase type repair and Reneging customer <i>G. Ayyappan, N. Arulmozhi</i>	322
NCRDSET-1020	Analysis of MAP/PH/1 Queueing Model with Degrading Service Rate, Phase-type Vacation, Repairs, Starting failure and Closedown <i>G. Ayyappan, S. Meena</i>	323

NCRDSET-1058	Analysis of MAP/PH/1 Queueing Model with Differentiated Vacation, Vacation Interruption under N-Policy, Optional Service, Breakdown and Repair, Setup and Discouragement of customers <i>G. Ayyappan, G. Archana @ Gurulakshmi</i>	324
NCRDSET-1060	Analysis of $M^{[X1]}$, $M^{[X2]}$/G_1, $G_2^{(a,b)}$ /1 Queue with Priority Services, Server Breakdown, Repair, Modified Bernoulli Vacation, Immediate Feedback <i>G. Ayyappan, S. Nithya, B. Somasundaram</i>	325
NCRDSET-1064	MAP/PH(1), PH(2)/2 queue with backup server, multiple vacations, optional Service, breakdowns and repairs <i>G. Ayyappan, S. Sankeetha</i>	326
NCRDSET-1084	Enhanced Internal Quantum Efficiency of Organic Light-Emitting Diodes: A Synergistic Effect <i>G. Abirama sundari, S. Ramya</i>	327

SMART RATION SYSTEM USING FACE RECOGNITION

R.Ranjithkumar, CSE, St.Anne's CET
M.Labilan ,CSE, St.Anne's CET
G.Ravindiran, CSE, St.Anne's CET
Mr.P.Saravanabhava,,CSE, St.Anne's CET

Abstract

Ration card plays a vital role for the household details such as to get gas connection, family member details. Technique and IOT to thwart the derelictions and corruption in the current ration distribution system. In this system conventional quota card will be replaced by a Face Recognition system. This Faces will be verified with family members for authentication of the user. If user is found to be authentic then monthly quota of the ration available for the user is displayed. After successful transaction the database will be updated stating the ration content delivered to the user. This system will require very less human efforts for operation and is also very secure. By implementing this system government can keep track of all the delivered ration content very easily.

Keywords: *Face Detection, Face Recognition, Capture Face.*

1 INTRODUCTION

Distribution of ration in a country like India is not an easy task. India is second largest populated country in the world. Public distribution system is a major public sector which manages and distributes the essential commodities to all the citizens of the India below the poverty line and some reserved categories such as police and military persons. In ration shop, materials such as rice, wheat, sugar, dales, kerosene, and oil are provided.

2 EXISTING SYSTEM

In our current ration distribution system of India there are many limitations and malpractice at various levels, which needs to be improved. Furthermost of the helping shopkeepers keep fake allotment greetings card with them. Due en route for fake ration cards, the dealer receives the extra helping from higher govt.

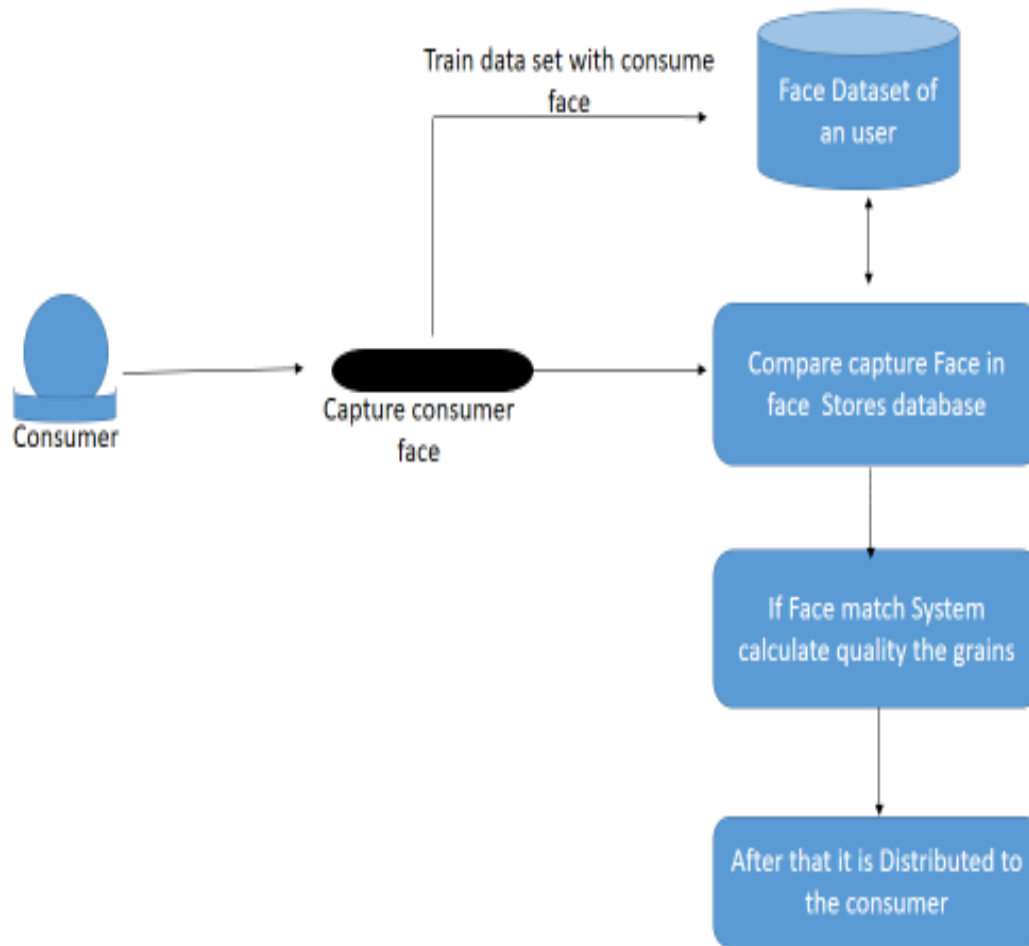
3 DISADVANTAGES OF EXISTING SYSTEM

Due to fake ration cards, the dealer receives the extra ration from higher govt. authority and he sales it into the open market at higher price to earn some extra profit. The quantity of ration that is being allocated might differ significantly from the actual allocated ration quota.

4 PROPOSED SYSTEM

The Smart ration card system uses Face Recognition. This system successfully eliminates the errors due to manual monitoring of ration data as all the data is automatically updated in the cloud based database. To access the database and authentication of user requires internet connectivity which can be a problem in remote locations.

5 SYSTEM ARCHITECTURE:



6 Algorithm

Local Binary Pattern (LBP) is a simple yet very efficient texture operator which labels the pixels of an image by thresholding the neighborhood of each pixel and considers the result as a binary number. Human beings perform face recognition automatically every day and practically with no effort. Although it sounds like a very simple task for us, it has proven to be a complex task for a computer, as it has many variables that can impair the accuracy of the methods, for example: illumination variation, low resolution, occlusion, amongst other.

Step-by-Step

Now that we know a little more about face recognition and the LBPH, let's go further and see the steps of the algorithm:

1. Parameters: the LBPH uses 4 parameters:

Radius: the radius is used to build the circular local binary pattern and represents the radius around the central pixel. It is usually set to 1.

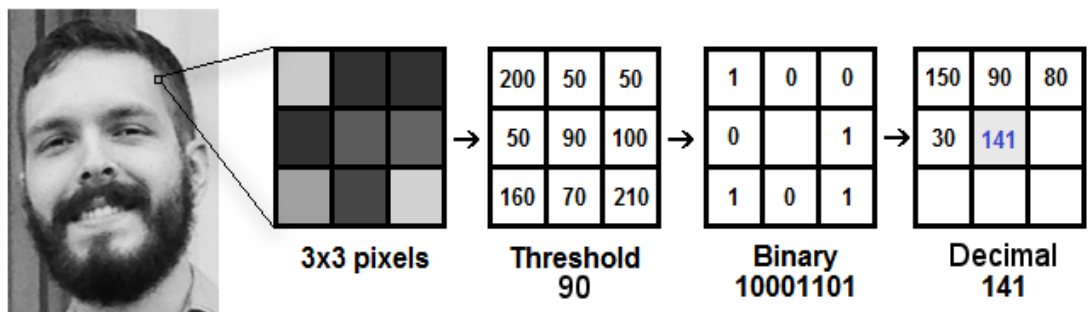
Neighbours: the number of sample points to build the circular local binary pattern. Keep in mind: the more sample points you include, the higher the computational cost. It is usually set to 8.

Grid X: the number of cells in the horizontal direction. The more cells, the finer the grid, the higher the dimensionality of the resulting feature vector. It is usually set to 8.

Grid Y: the number of cells in the vertical direction. The more cells, the finer the grid, the higher the dimensionality of the resulting feature vector. It is usually set to 8.

Don't worry about the parameters right now, you will understand them after reading the next steps.

2. Training the Algorithm: First, we need to train the algorithm. To do so, we need to use a dataset with the facial images of the people we want to recognize. We need to also set an ID (it may be a number or the name of the person) for each image, so the algorithm will use this information to recognize an input image and give you an output. Images of the same person must have the same ID. With the training set already constructed, let's see the LBPH computational steps.



3. Applying the LBP operation: The first computational step of the LBPH is to create an intermediate image that describes the original image in a better way, by highlighting the facial characteristics. To do so, the algorithm uses a concept of a sliding window, based on the parameters radius and neighbours.

7 LITERATURE SURVEY

In paper [1], E-ration PDS using SMART CARD and GSM technology is an innovative approach in public distribution system (PDS) which is very useful for efficient, accurate, and automated distribution of ration distribution system. Presently ration distribution system has drawbacks like inaccurate quantity of goods, large waiting time, low processing speed and material theft in ration shop. Main objective of the designed system is to replace manual work with the atomization of ration shop to have a transparency in PDS. Proposed E- ration shop for public distribution system

8 CONCLUSION

The Smart ration card system uses Face Recognition. This system successfully eliminates the errors due to manual monitoring of ration data as all the data is automatically updated in the cloud based database. Also this system will enable the government to keep track of the consumers and their transactions. Although the system will reduce the security issues and malpractices present in the current PDS the starting cost of the system is high. To access the database and authentication of user requires internet connectivity which can be a problem in remote locations.

9 REFERENCES

- [1] Gaikwad PriyaB Prof. Sangita Nikumbh , “E – Public distribution system using SMART card and GSM technology” International Conference on Intelligent Sustainable Systems(ICISS 2017) IEEEISBN:978-1-5386-1959-9
- [2] Mrs. Subhasini Shukla, Mr. Akash Patil, Mr. BrightsonSelvin , “A Step Towards Smart Ration Card System Using RFID & IOT” , IEEE International Conference on Inventive Communication and Computational Technologies(ICICCT), 2017
- [3] Prof. Shital A. Aher, Akshay D. Saindane, Suved P. Patil, Shivsagar K. Chakor , “Smart Ration Card Using RFID and Biometrics ”, Vol-3 Issue-2 2017, IJARIE-ISSN(O)-2395-4396,2017
- [4] Vinayak T. Shelar, Mahadev S. Patil , “RFID and GSM based Automatic Rationing System using LPC2148”, International Journal of Advanced Research in Computer Engineering & Technology (IJARCET) Volume 4 Issue 6, June 2015
- [5] Anshu Prasad, Aparna Ghenge, SonaliZende, Sashikala Mishra, Prashant Godakhi, “Smart Ration Card Using RFID, Biometrics and SMS Gateway”, IEEE International Conference on Inventive Communication and Computational Technologies(ICICCT), 2017
- [6] Dr. M. PallikondaRajeseakaran, D.Balaji, P.Daniel”,Automatic Smart Ration Distribution System for Prevention of Civil Supplies Hoarding In India”, 2017 International Conference on Advanced Computing and Communication Systems (ICACCS -2017), Jan. 06 – 07, 2017, Coimbatore, INDIA.
- [7] Anshu Prasad, Aparna Ghenge, Prof. Sashikala Mishra, Prof. Prashant Gadakh,”Smart Ration Card Using RFID, Biometrics and SMS Gateway” IEEE Conference on Inventive Communication and Computational Technologies(ICICCT 2017).
- [8] K. BalaKarthik , “Cloud Based Ration Card System Using RFID And GSM Technology”, International Journal of Engineering Research & Technology (IJERT), ISSN:2278-0181, Vol. 2 Issue 4, April 2013
- [9] Mr. A .chimgave ,prof.shaileshjadhavi: E-Rationing , International Engineering Research Journal (IERJ) Volume 2 Issue 2 Page 467-469, 2016, ISSN 2395-1621@IEEE 2016.
- [10] Swapnil r kurkute,chetanmedhe : “automatic ration distribution system-A review”, 2016 International Conference on Computing for Sustainable Global Development (INDIA Com).).

IMPLEMENTATION OF DNA CRYPTOGRAPHY IN CLOUD COMPUTING AND USING SOCKET PROGRAMMING

S. Nithya, Cse, Krishnasamy College of Engineering and Technology
R. Sharmila, Cse Krishnasamy College of Engineering and Technology
N. Thanigaivel, Cse, Krishnasamy College of Engineering and Technology

Abstract

Cloud computing is the latest technology in the field of distributed computing. It provides various online and on-demand services for data storage, network services, platform services and etc. Many organizations are unenthusiastic to use cloud services due to data security issues as the data resides on the cloud services provider's servers. To address this issue, there have been several approaches applied by various researchers worldwide to strengthen security of the stored data on cloud computing. The Bi-directional DNA Encryption Algorithm (BDEA) is one such data security techniques. However, the existing technique focuses only on the ASCII character set, ignoring the non-English user of the cloud computing. Thus, this proposed work focuses on enhancing the BDEA to use with the Unicode characters.

Key Words: *Cloud computing, Data security issues, Bi-directional DNA Encryption Algorithm, DNA digital code, Socket Programming.*

1 Introduction

Cloud computing has recently reached popularity and developed into a major trend in IT. We perform such a systematic review of cloud computing and explain the technical challenges facing in this paper. In Public cloud the "Pay per use" model is used. In private cloud, the computing service is distributed for a single society. In Hybrid cloud, the computing services is consumed both the private cloud service and public cloud service. Cloud computing has three types of services. Software as a Service (SaaS), in which customer prepared one service and run on a single cloud, then multiple consumer can access this service as per on demand. Platform as a Service (PaaS), in which, it provides the platform to create application and maintains the application. Infrastructure as a Service (IaaS), as per term suggest to provides the data storage, Network capacity, rent storage, Data centers etc. It is also known as Hardware as a Service (HaaS).

2 Literature Survey

In cloud computing the major issue is to provide the security of data. In Cloud computing data security is prepared by the Authentication, Encryption & Decryption, Message authentication code, Hash function, and Digital signature and so on. So here we discuss about some security problems and their solutions

Use of Digital Signature with Diffie Hellman Key Exchange and AES Encryption Algorithm to Enhance Data Security in Cloud Computing. Mr. Prashant Rewagad and Ms. Yogita Pawar Here in this paper, the researcher using three way architecture protection schemes. Firstly Diffie-Hellman algorithm is used to generate keys for key exchange step. Then digital signature is used for authentication, thereafter AES encryption algorithm is used to encrypt or decrypt user's data file. Diffie- Hellman key exchange algorithm is vulnerable to main in the middle attack. The most serious limitation is the lack of the authentication.

Union of RSA algorithm, Digital Signature and Kerberos in Cloud Security. Mehdi Hojabri and Mona Heidari

Here in this paper, the researcher first performs the concept of Kerberos authentication services. At the next step the Authenticate Server (AS) of Kerberos do verifies users and created the ticket granting ticket and session key and it sent to the users. The next step users send the ticket granting ticket and session key to Ticket Granting Server (TGS) for getting the service. Then TGS send ticket and session key for user. In final step the users send the request service to cloud service provider for using the cloud service and also cloud service, provide service to users. After doing this step user can used the cloud service provider. But for more security they performed RSA algorithm for encryption & decryption and then they use Digital Signature for Authentication.

Implementation Digital signature with RSA Encryption algorithm to enhance the Data security of cloud in Cloud Computing. Uma Somani, Kanika Lakhani, and Manish Mundra

In this paper, there are two enterprises A and B. An enterprise A has some data that are public data and enterprise has public cloud. Now B wants some secure data from A's cloud. So RSA algorithm and Digital signature are used for secure

communication. In this method, enterprise A takes data from cloud, which B wants. Now the data or document is crushed into little line using Hash code function that is called Message digest. Then A encrypts the message digest within private key the result is in the Digital signature form. Using RSA algorithm, A will encrypt the digital signed signature with B's public key and B will decrypt the cipher text to plain text with his private key and A's public key for verification of signature.

3 PROPOSED SYSTEM

Previous section describes the study about the cloud computing, basics of cloud computing and security problems occurs in cloud. Then study some papers to solve these security problems. Here in this paper, the Bi-serial DNA encryption algorithm is performing, that providing the two level of security.

3.1 DNA DIGITAL CODING

In information science, the binary digital coding encoded by two state 0 or 1 and a combination of 0 and 1. But DNA digital coding can be encoded by four kind of base as shown in table 1. That is ADENINE (A) and THYMINE (T) or CYTOSINE (C) and GUANINE (G). There are possibly $4! = 24$ pattern by encoding format like (0123/ATGC) [4].

Binary value	DNA Digital Coding
00	A
01	T
10	G
11	C

Table 1. DNA Digital Coding

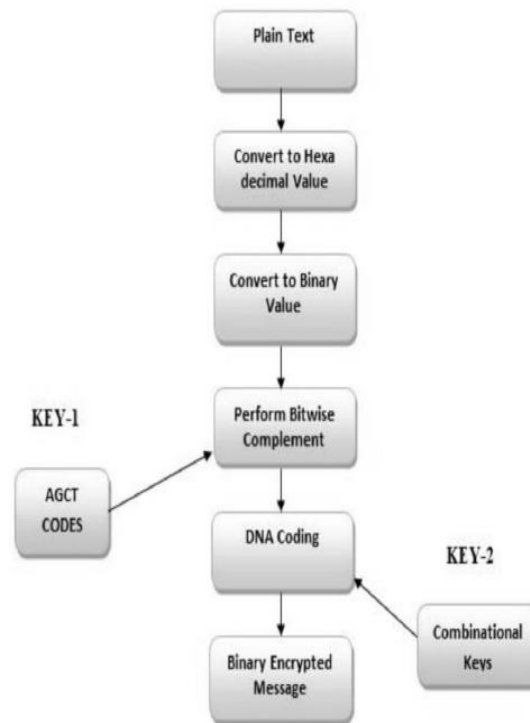
3.2 KEY COMBINATION

Here in this work, we are using ATGC as a key. Every bit have 2 bits like A=00, T=01, G=10, and C=11 and by using ATGC, key combinations is generated and give numbering respectively that is given into table. From the table 2, we can generate 64 bit key values and adding ATGC, we can generate 72-bit key (64 bits of key combination and 8 bits of ATGC). ATGC key is sending to the receiver side by using Diffie Hellman key sharing algorithm. In this work, every time the key value will be randomly changed.

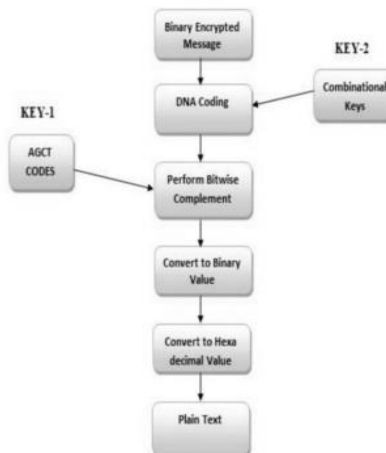
KEY COMBINATION	PATTERNS	VALUES
AA	0101	5
AT	0011	3
AG	0001	1
AC	0010	2
TA	0110	6
TT	1111	15
TG	0111	7
TC	1001	9
GA	1010	10
GT	0100	4
GG	1000	8
GC	1100	12
CA	1110	14
CT	1011	11
CG	0000	0
CC	1101	13

Table 2: Key combination

ENCRYPTION PROCESS



DECRYPTION PROCESS



4 Conclusion

Data security is the main challenge for cloud usability. Various algorithms like RSA, Diffie -Hellman, DNA encryption etc. are available to provide data security for the data stored on cloud. Digital signatures, Extensible Authentication Protocols are used for authentications. Using BDEA algorithm, we achieve 2-layer security for ASCII character sets. The proposed system focuses on extending the BDEA algorithm to be used with Unicode character set. This can help reach to the wider community of the cloud users. The future work will focus on the possible attacks and cryptanalysis of the cipher text and measure its strength.

5 References

- [1] Prashantrewagad, Yogitapawar, “*Use Of Digital Signature With Diffie-Hellman Key Exchange And AES Encryption Algorithm To Enhance Data Security In Cloud Computing*” 2013 International Conference On Communication System And Network Technologies (IEEE Computer Society).
- [2] Uma Somani, Kanika Lakhani, Manishamundra, “*Implementing Digital Signature With RSA Encryption Algorithm To Enhance The Data Security Of Cloud In Cloud Computing*”-2010 IEEE 1st International Conference On Parallel, Distributed And Grid Computing (PDGC-2010).
- [3] Mehdi Hojabri & Mona Heidari “*Union Of RSA Algorithm, Digital Signature And KERBEROS In Cloud Computing*” International Conference On Software Technology And Computer Engineering (STACE-2012).
- [4] Ashish Prajapati, Amit Rathod “*Enhancing Security In Cloud Computing Using Bi-Directional DNA Encryption Algorithm*”, International Conference On Intelligent Computing, Communication & Devices. (ICCD-2014), Springer.

Online Product Price and Comparison Using Web Mining and Machine Learning

Sandhiya.R, CSE, St.Anne's college of Engineering and Technology,Anguchettypalayam.
Senthamizhselvi.P,CSE, St.Anne's college of Engineering and Technology,Anguchettypalayam.
AnnaiTherasammal.A, CSE, St.Anne's college of Engineering and Technology,Anguchettypalayam.
Brittadevi.v , AP/CSE, St.Anne's college of Engineering and Technology,Anguchettypalayam.

Abstract

Web mining is an application data-mining technique used to extract information from web services. E-commerce websites nowadays have become one of the most important sources for buying all kinds of products. Many strategies have been developed by analyzing customer's behavior so as to attract more business and participation of people. As there are many e-commerce websites available it becomes difficult for users to choose best deal for desired product amongst these websites. Comparison of E-commerce products using web mining enables users to analyze prices and get desired product at minimum price. Users can also select multiple products that belong to same category for comparing its features. In order to make our system dynamic and to keep pace with real-time changes occurring on the sites, our database is automatically updated in every 12 hours. Our system displays the result with 93.06% accuracy according to the user's query. To obtain best deals from e-commerce websites web crawlers and web scrapping techniques are used to fetch detailed information. This way, project aims to provide solution for online customers to buy products at good deal and save their valuable time, effort and money.

Keywords:Price Comparison, Web Crawling, Web Scapping, MangoDB, Django.

1 Introduction

Nowadays, e-commerce websites have been prevalent and growing up in an unprecedented manner. In the current era of online business, ecommerce have become a huge market for the people to buy goods online. E-commerce website holders are deliberately putting prices on their websites derailed from actual rates leveraging on people's demand. Increasing use of smart devices and other mediums has paved the way for users to buy products almost from anywhere. Thus people are being deceived, paying more money than necessary to buy a product. Synthesizing the fact above, the importance of the price comparison tool is beyond gainsaying. This has increased involvement of online buyers evolving e-commerce business.

Our Solution aims for a collaborative platform for allowing a consumer to evaluate the price and make the purchase decision more manageable according to their budget. These large numbers of ecommerce websites put users in turmoil to search and choose to buy a single product from multiple ecommerce websites . They designed a tool for price comparison which uses scrapping scripts written with a python library and improvise the storage for scrapped data. formulated a pattern analysis recommender system by analyzing buying patterns using data mining technique. established a website with Django framework and Mongo DB for comparing price using web crawling and also used request and BeautifulSoup4 library for web scrapped.

We have designed User Interface for a user-friendly interaction while searching for query and for showing results appertaining to correspondent query. This paper is organized as follows: In section , we describe the proposed system and step by step explanations of our work and algorithm. The paper illustrates the experimental result and performance analysis in section , while section encompasses the paper with limitation of our system and plan for future work. .The proposed solution helps online users to grab best deal for their product from multiple ecommerce websites on single web interface

2 Proposed System

To obtain best deals from e-commerce websites web crawlers and web scrapping techniques are used to fetch detailed information. This way, paper aims to provide solution for online customers to buy products at good deal and save their valuable time, effort and money. The proposed system is as follows: The backend system consists of two important techniques web crawling and web scrapping. Web scrapping is a technique that is used to extract information in the human readable format and display it on destination terminal. In this section, we have demonstrated different aspects and the procedure of implementation of our price comparison tool. Algorithm 1 demonstrates the pseudo code for the creation of the database where Algorithm 2 represents the pseudo code for the language processing and comparison methods.

2.1 System Architecture

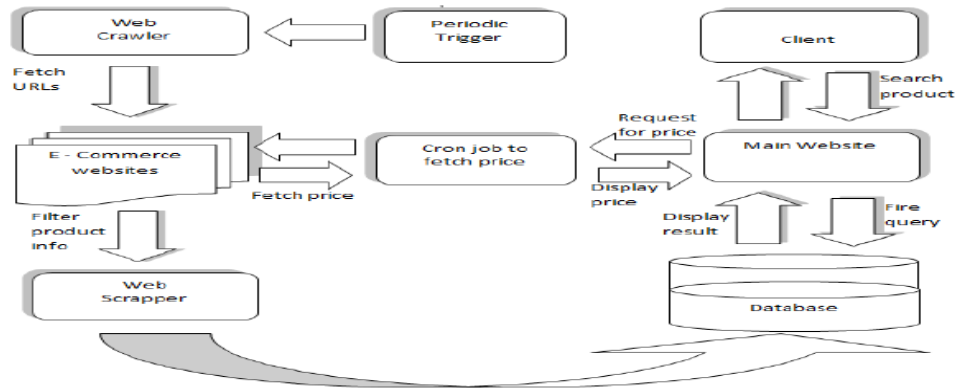


Fig 2.1 system architecture

2.2 Dataset creation

In this paper used web crawling approach to collect necessary data from different websites in a fast and efficient way . We have built different spiders for different websites using Python’s powerful Scrapy framework to collect information about products..After that, we store the extracted data in an individual CSV file under the column named “Image”, “Product name”, “Product price”, “Offer”, and “Website link” for every website . Once the crawler has completed it traversing through the whole website, it starts to scrape off the correspondents to a particular product discarding superfluous information. Since websites tend to perform changes in products after a specific time, our system has been equipped with dynamicity to keep pace with the changes. We have introduced an automated script that runs in every seconds and renews the data in our database.

2.3 Processing of Bag of Words & Vectorization

In this paper implemented a text modeling algorithm, “Bag of Words”. Bag of words approach preprocess the raw data by turning all the words that exist in the database into a bag of words, including the words presented in queries and paired with their word count per database. We have generated a vector representation of the database using TF-IDF. It has been used to depict the significance of word to its corresponding single document in digital libraries, around 83 percent of text-based recommendation .

2.4 Algorithm for similarity checking

The product with a lower price ranks first in that order. To find the congruence between user input and the data present in the database, we have constructed the cosine similarity algorithm by using the Sci-kit learn library. Cosine similarity distinguishes between two or more documents on account of the orientation (angle), not the magnitude . The similarity between two documents is calculated by the cosine of the angle of two vectors. Cosine similarity overcomes the flaw of zero matches between two documents irrespective of their sizes. For instance, if a and b are two vectors then cosine similarity uses the following rule:

$$\cos \theta = \frac{\vec{a} \cdot \vec{b}}{\|\vec{a}\| \|\vec{b}\|} = \frac{\sum_{i=1}^n a_i b_i}{\sqrt{\sum_{i=1}^n a_i^2} \sqrt{\sum_{i=1}^n b_i^2}} \text{----- (1)}$$

Where, $\vec{a} \cdot \vec{b} = \sum_{i=1}^n a_i b_i = a_1 b_1 + a_2 b_2 + \dots + a_n b_n$ is the dot product of the two vectors.

If the cosine value is 0, then the angle between a and b vector, two vectors are at 90 degrees to each other and share no similarity. Thus it can be depicted that two vectors are similar when the cosine of the angle of two vectors is smaller.

3 System Methodology

3.1 Web Crawler and Scapper

The system deals with price comparison engine. The first thing required are to gather large amount of data from different e-commerce websites. It is not possible to manually collect the data from websites. Hence the best way is to create a web crawler that will navigate to these e-commerce websites. The fetched URL's are send to scrapper for scrapping process. Web Scrapping is used to extract HTML data from URL's and use it for personal purpose. As this is price comparison website, data is scrapped from multiple e-commerce websites. In this system, Scrapping is done using python libraries like requests and beautifulsoup4. Beautifulsoup4 is a python library which is used for parsing html pages. Using these, product information from different e-commerce sites is scrapped and stored in database.

3.2 MongoDB and Django Web Framework

MongoDB is classified as NoSQL database which is a document oriented database. As system deals with large amount of unstructured data, it is flexible to use mongodb as database. Data extracted from scrapper is stored in MongoDB database. Django is a python web framework. Comparison of E-commerce products using web mining is product and price comparison website which is created using Django framework. Products that are been requested by user are queried in mongodb database using an object relational mapper mongo engine. Admissions in reputed varsity.

4 Techniques

To obtain best deals from e-commerce websites web crawlers and web scrapping techniques are used to fetch detailed information. This way, paper aims to provide solution for online customers to buy products at good deal and save their valuable time, effort and money

4.1 Algorithm

```
for each E-commerce site do
  for each category in the site do
    for each product in the category do
      Product Details → Name, Price, link, Image
      Use CSS selector to find Product Details
      remove garbage data
      CSV dataset ← Product Details
    end for
  end for
end for
```

4.2 Algorithm

```
InSent ← Product to be searched
T ← Minimal similarity threshold
DetectLanguage(InSent)
if detected language of the input is Bengali then
  Transliterate InSent to English as TSent
else
  Transliterate InSent to Bengali as TSent
end if
for each website in our data set do
  generate bag of words with TF-IDF
  for all products do
    PN ← product name
    if PN matches with InSent then
      put product details in ExactList
    end if
    if PN matches with TSent then
      put product details in ExactList
    end if
    if cosine similarity(P N, InSent) >=T then
      put product details in SimilarList
```

```
end if
if cosine similarity(P N, T Sent) >=T the
    put product details in SimilarList
end if
end for
end for
Sort ExactList according to price in ascending order
Sort SimilarList according to similarity in descending order and price in ascending order.
```

5 System Implementation

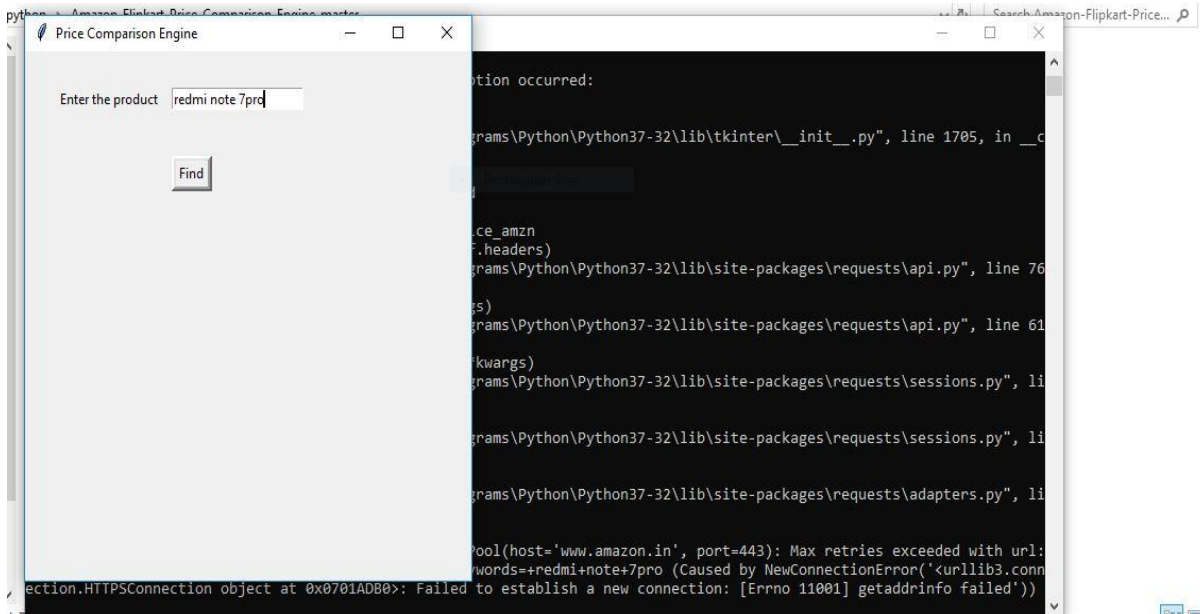


Fig 5.1:

select the product

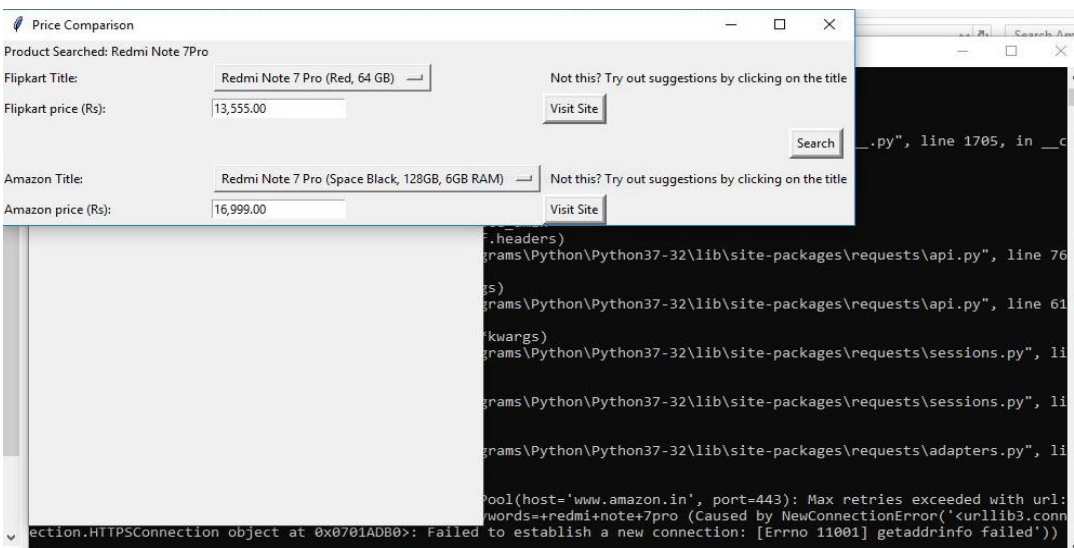


Fig 5.2: comparing the product

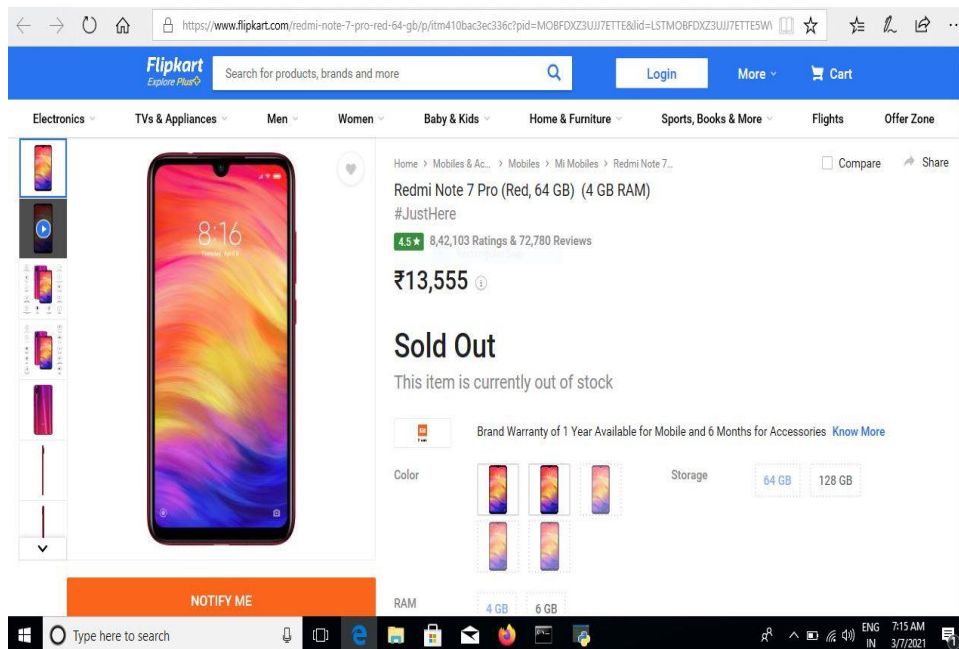


Fig 5.3: Identify the product which one is low price

6 Conclutions

Comparison of E-commerce products using web mining is web based system which will help users in decision making while buying products online. We have suggested the lowest price for the same product based on the similarity between the user's query and products stored in the database. This website will facilitate users to analyze prices that are present on different e-commerce shopping websites so that they get to know the cheapest price of product with best deal. The website will also have the facility of comparing products with all its specifications that belong to same category. This will surely save buyers efforts and valuable time. Ultimately, this will bring together strategies, best offers and deals from all leading online stores and will help buyers to shop online. In the future, we are planning to arrange a manifestation of consumer reviews and ratings to help consumers to identify the right product to cover their needs according to their budget. Moreover, we will use Neural Networks to generate different predictions and suggestions based on the user's query.

7 References

- [1] Amna Shifia Nisafani, Rully Agus Hendrawan, and Arif Wibisono. Eliciting data from website using scrapy: An example. SEMNASTEKNOMEDIA ONLINE.
- [2] Shakra Mehak, Rabia Zafar, Sharaz Aslam, and Sohail Masood Bhatti. Exploiting filtering approach with web scrapping for smart online shopping penny wise a wise tool for online shopping. In 2019 2nd International Conference on Computing, Mathematics and Engineering Technologies (iCoMET), pages 1–5. IEEE, 2019.
- [3] Kali Pradeep, I Bhagyasri, and P Praneetha. E-commerce with backbone of data mining. International Journal of Engineering and Technical Research, 2:460, 10 2018.
- [4] Tiago Pessoa, Raul Medeiros, Thiago Nepomuceno, Gui-Bin Bian, V.H.C. Albuquerque, and Pedro Pedrosa Filho. Performance analysis of google colab as a tool for accelerating deep learning applications. IEEE Access, PP:1–1, 10 2018.
- [5] Christopher D. Manning, Prabhakar Raghavan, and Hinrich Schütze, Introduction to Information Retrieval.: Cambridge University Press, 2008.

Heart Attack Prediction For Stroke Patients Using Machine Learning

S.Manavalan,Cse, St.Anne's college of engineering and technology.
A.Bckiya priya ,Cse , St.Anne's college of engineering and technology.
A.Ezakia selvam ,Cse , St.Anne's college of engineering and technology.
R.Kamatchi ,Cse, st.Anne's college of engineering and technology.

Abstract

Early predicting heart attack out of stroke patients in a view of data analysis is an approach to reduce a high mortality rate. Stroke-patient data in Intensive Care Unit are imbalanced due to that stroke patients with heart attack are in the minority of stroke patients. How to predict heart attack in the stroke-patient data becomes a challenge. For processing the imbalanced data, this paper designs an algorithm by leveraging Linear regression. Linear Regression is a machine learning algorithm based on supervised learning. It performs a regression task. Regression models a target prediction value based on independent variables . Our results show that classifier achieves the best Predicting performance with accuracy of 80.30%, precision of 80.05%. It could be well-predicted using Linear regression that whether a stroke patient will have heart attack or not.

Keywords: stroke, heart attack, Linear regression, imbalanced data, variable.

1 Introduction

Stroke, also known as “ischemic stroke”, refers to ischemic necrosis or softening of localized brain tissue caused by cerebral blood supply, ischemia and hypoxia. The main clinical manifestations are sudden collapse, mental coma, unclear speech, and hemiplegia . Heart attack is a myocardial necrosis caused by acute and persistent ischemia and hypoxia of coronary artery which manifestations are arrhythmia, shock or heart failure, which can be fatal . Stroke complicated with heart attack is cerebral infarction accompanied by heart attack. As we know, the stroke complicated by heart attack was 30%, and the mortality rate was as high as 54%. The main causes of death are ventricular arrhythmia, acute left heart failure and cardiogenic shock. . On the other side, the onset of heart attack is rapid, and sudden deaths easily happen on the heart attack patients. This paper attempts to predict heart attack for the stroke patients based on analyzing medical indication. Such a prediction is to gain more treatment time for the stroke patients with heart attack.

1.1 Factors Of Stroke

- High blood pressure
- Cigarette smoking or second hand smoke exposure
- High cholesterol
- Diabetes
- Obstructive sleep apnea
- Cardiovascular disease, including heart failure, heart defects, heart infection or irregular heart rhythm, such as atrial fibrillation.
- Personal or family history of stroke, heart attack or transient ischemic attack
- COVID-19 infection

1.2 Symptoms

- Trouble speaking and understanding what others are saying.
- Paralysis or numbness of the face, arm or leg. Problems seeing in one or both eyes.
- Headache.
- Trouble walking .
- sudden behavioral changes, especially increased agitation.

2 Attributes

2 a.Demographic:

- Sex: male or female(Nominal)

•Age: Age of the patient;(Continuous — Although the recorded ages have been truncated to whole numbers, the concept of age is continuous)

2.b. Behavioral:

•Current Smoker: whether or not the patient is a current smoker (Nominal)

•Cigs Per Day: the number of cigarettes that the person smoked on average in one day.(can be considered continuous as one can have any number of cigarettes, even half a cigarette.)

2.c. Information on medical history:

•BP Meds: whether or not the patient was on blood pressure medication (Nominal)

•Prevalent Stroke: whether or not the patient had previously had a stroke (Nominal)

•Prevalent Hyp: whether or not the patient was hypertensive (Nominal)

•Diabetes: whether or not the patient had diabetes (Nominal)

2.d.Information on current medical condition:

•Tot Chol: total cholesterol level (Continuous)

•Sys BP: systolic blood pressure (Continuous)

•Dia BP: diastolic blood pressure (Continuous)

•BMI: Body Mass Index (Continuous)

•Heart Rate: heart rate (Continuous — In medical research, variables such as heart rate though in fact discrete, yet are considered continuous because of large number of possible values.)

•Glucose: blood glucose level (Continuous)

3 Module Description

The study of predicting heart attack in stroke patients is to reduce the mortality of stroke patients with heart attack. For the prediction problems, machine learning methods are extensively utilized in recent years. How to process well imbalanced data is a challenge in the prediction of heart attack in stroke patients. In this section, research work about heart attack prediction in stroke patients and imbalanced data processing are presented separately.

3.1 Data cleaning and pre-processing:

Here we have to check and dealt with missing and duplicate variables from the data set as these can grossly affect the performance of different machine learning algorithms (many algorithms do not tolerate missing data).

3.2 Data Analysis:

We have to gain important statistical insights from the data and the things that I checked for were the distributions of the different attributes, correlations of the attributes with each other and the target variable and calculated important odds and proportions for the categorical attributes.

3.3 Feature Selection:

Since having irrelevant features in a data set can decrease the accuracy of the models applied, I used the Boruta Feature Selection technique to select the most important features which were later used to build different models.

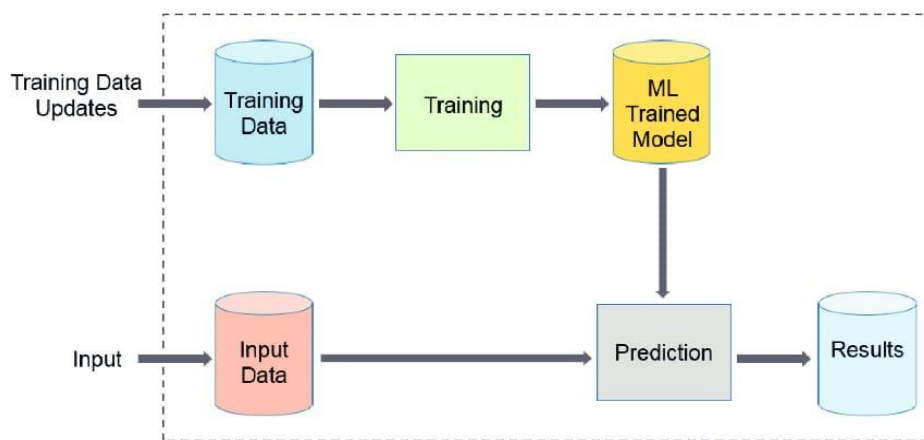
3.4 Model development and comparison:

We are going to use the classification models such as Logistic Regression, K-Nearest Neighbors, Decision Trees and Support Vector Machine, After which the performance of the models can be compared using their accuracy and F1 scores.

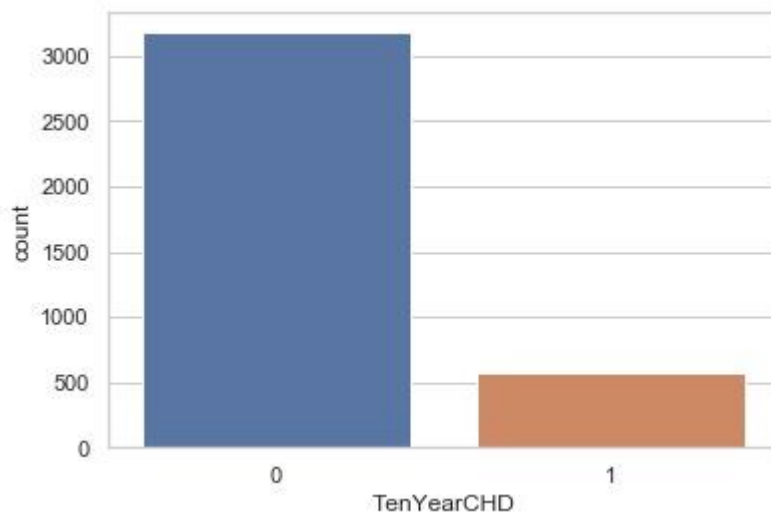
4 Algorithm

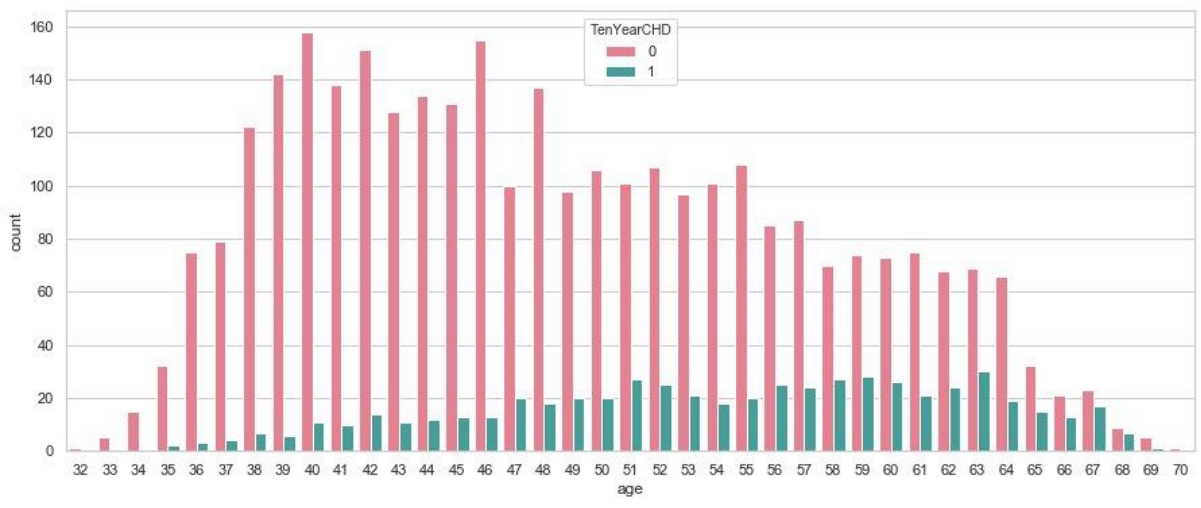
Linear Regression is a machine learning algorithm based on supervised learning. It performs a regression task. Regression models a target prediction value based on independent variables. It is mostly used for finding out the relationship between variables and forecasting. Different regression models differ based on – the kind of relationship between dependent and independent variables they are considering, and the number of independent variables getting used. Linear regression performs the task to predict a dependent variable value (y) based on a given independent variable (x). So, this regression technique finds out a linear relationship between x (input) and y (output). Hence, the name is Linear Regression. In the figure above, X (input) is the work experience and Y (output) is the salary of a person. The regression line is the best fit line for our model.

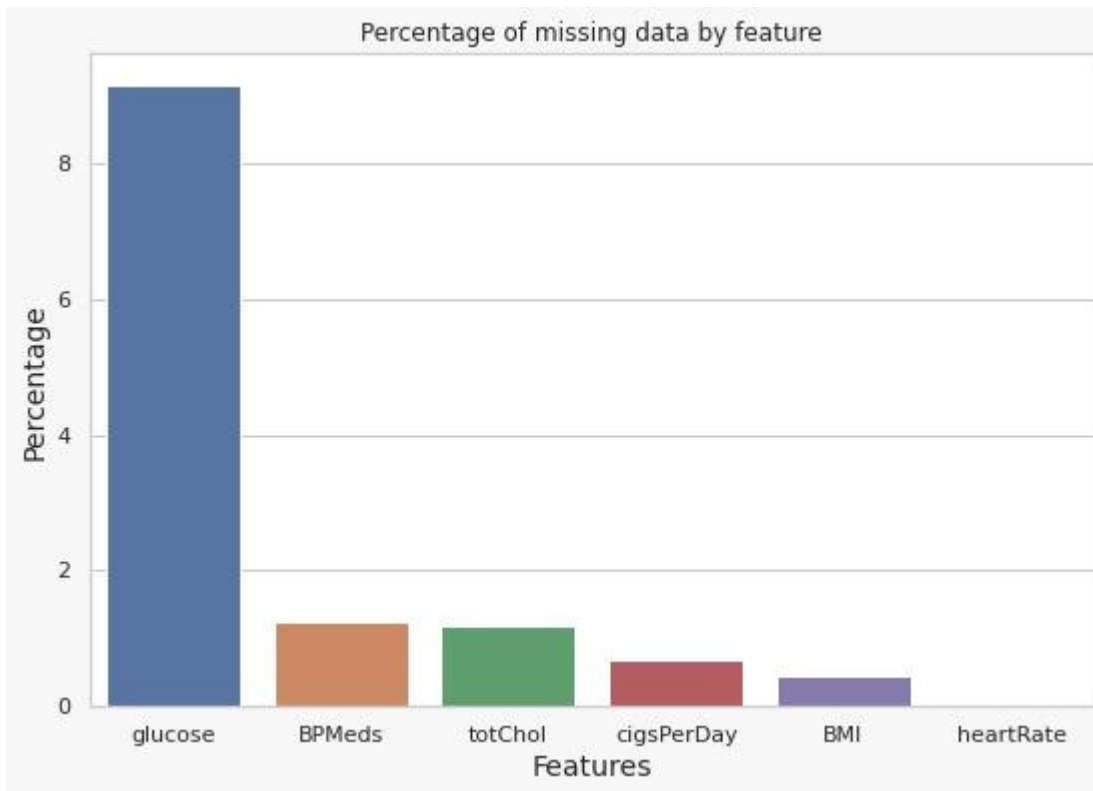
5 Block Diagram



5 Experimental Results







6 REFERENCES

- [1] L. Junfan, Observation of Clinical Effect of 'Stroke Integration' in the Treatment of Ischemic Stroke. Beijing, China: Beijing Univ. Chinese Medicine, 2019.
- [2] S. Diekmann, L. Hörster, S. Evers, M. Hiligsmann, G. Gelbrich, K. Gröschel, R. Wachter, G. F. Hamann, P. Kermer, J. Liman, M. WeberKrüger, J. Wasem, and A. Neumann, "Economic evaluation of prolonged and enhanced ECG holter monitoring in acute ischemic stroke patients," *Current Med. Res. Opinion*, vol. 35, no. 11, pp. 1859–1866, Nov. 2019.
- [3] Y. Rongfeng and X. Minhui, "A report of 9 cases of acute stroke complicated with acute myocardial infarction," *Hunan Med.*, to be published.
- [4] G. V. Dous, A. C. Grigos, and R. Grodman, "Elevated troponin in patients with acute stroke—Is it a true heart attack," *Egyptian Heart J.*, vol. 69, no. 3, pp. 165–170, 2017.
- [5] D. Bhatnagar, I. Kaur, and A. Kumar, "Ultrasensitive cardiac troponin i antibody based nanohybrid sensor for rapid detection of human heart attack," *Int. J. Biol. Macromolecules*, vol. 95, pp. 505–510, Feb. 2017.
- [6] B. Week, "Heart disorders and diseases; Data on heart attack described by researchers at capital medical University (over expression of protein kinase C epsilon improves retention and survival of transplanted mesenchymal stem cells in rat acute myocardial infarction)," *Tech. Rep.*, 2016.
- [7] Q. Wang, Y. Zhou, W. Zhang, Z. Tang, and X. Chen, "Adaptive sampling using self-paced learning for imbalanced cancer data pre-diagnosis," *Expert Syst. Appl.*, vol. 152, Aug. 2020, Art. no. 113334.
- [8] R. A. Bauder, T. M. Khoshgoftaar, and T. Hasanin, "Data sampling approaches with severely imbalanced big data for medicare fraud detection," in *Proc. IEEE 30th Int. Conf. Tools Artif. Intell. (ICTAI)*, Nov. 2018, pp. 137–142.
- [9] Z. Fenglan, *Electrocardiogram QTcd Changes and Prognosis in Different Periods of Acute Myocardial Infarction*. Shanxi, China: Shanxi Clinical Medicine, 2001.
- [10] Y. Yuejin et al., "Spontaneous improvement of exercise abnormality in acute myocardial infarction and the predictive value of low-dose dobutamine echocardiographic test," *Chin. J. Circulat.*, to be published.

KBot: Approach for Understanding NL Over Linked Data

D.Sakthi Sankar, Cse, MRK Institute Of Technology

T.Sivasubramanian, Cse, MRK Institute Of Technology

R.Sridharan, Cse, MRK Institute Of Technology

Mr.T.Periyasamy, Cse, MRK Institute Of Technology

Abstract

Building a chatbot over linked data raises different challenges, including user queries understanding, multiple knowledge base support, and multilingual aspect. To address these challenges, we first design and develop an architecture to provide an interactive user interface. Secondly, we propose a machine learning approach based on intent classification and natural language understanding to understand user intents and generate SPARQL queries. Furthermore, evaluation and application cases in the chatbot are provided to show how it facilitates interactive semantic data towards different real application scenarios and showcase the proposed approach for a knowledge graph and data-driven chatbot. Making these data accessible and useful for end-users is one of the main objectives of chatbots over linked data.

Key Words: *Linked data, Chatbot, SPARQL, intent classification, natural language myPersonality dataset.*

Massive MIMO Transmission For LEO Satellite Communications

Gayathiri .T, CSE, MRK Institute Of Technology
Reshma Taaj .M, CSE, MRK Institute Of Technology
Sangeetha .S, CSE, MRK Institute Of Technology
T. Periyasamy AP/CSE, MRK Institute Of Technology

Abstract

Satellite orbiting the earth would appear to be the ideal way to obtain worldwide coverage to mobile users. We propose Bipolar Pulse Amplitude (BPAM) based Amplification algorithm to enhance the mobile signal transmission distance into different Leo Satellite groups. By using the proposed BPAM methodology is usual mobile tower based communication can be eliminated with LEO Satellites. Results shows that the proposed BPAM based LEO Satellite communication scheme enhances the data rate of Mobile communication systems.

Index Terms—*Random access, timing advance, LEO satellite, time difference of arrival (TDOA)*

CYBERBULLYING DETECTION ON SOCIAL NETWORKS USING NEURAL NETWORKS.

Ms.P.Nivetha, Computer Science and Engineering ,St.Anne's college of engineering and technology.

A. Archana , Computer Science and Engineering, St.Anne's college of engineering and technology.

R.Vimala Roshini , Computer Science and Engineering ,St.Anne's college of engineering and technology.

Abstract

Online users now share their information with each other easily using by communication, collaboration, knowledge and ideas. However, this has led to the growth of cyber criminal acts, for example, cyberbullying which has become a worldwide epidemic. Cyberbullying is the use of electronic communication to bully a person by sending harmful messages using social media, instant messaging, or digital messages. It has emerged as a platform for insulting and humiliating a person which can affect the person either physically or emotionally and sometimes lead to suicidal attempts in the worst case. The main issue in preventing cyberbullying is detecting its occurrence so that appropriate action can be taken at the initial stages. These social technologies have created a revolution in user-generated information, online human networks, and rich human behaviour-related data. However, the misuse of social technologies such as social media platforms has introduced a new form of aggression and violence that occurs in online. To overcome this problem, many methods and techniques had been worked upon till now to control this problem. Cyberbullying is the use of electronic communication to bully a person by sending harmful messages using social media, instant messaging, or digital messages. It has emerged as a platform for insulting and humiliating a person which can affect the person either physically or emotionally and sometimes lead to suicidal attempts in the worst case. The main issue in preventing cyberbullying is detecting its occurrence so that appropriate action can be taken at the initial stages. To overcome this problem, many methods and techniques had been worked upon till now to control this problem.

INDEX TERMS: Cyberbullying, Cybercriminals Online users and communicators.

1 Introduction

Online communication is how people communicate, connect, transact to send, retrieve, or receive information of any kind via the internet using digital media. All the communication that is carried out via the internet is known as Online communication. Because of our increasing presence online, this type of communication is becoming equally important as offline communication. More and more information is being churned out online ever than before. There is a lot of information for the reader to read online. People have started doing everything online, including but not limited to banking, reserving tickets, booking travel, planning travel, purchasing any and every kind of thing, teaching, conducting meetings and seminars, one on one or group discussions, dating, sending information. Every other activity which is possible is being done online. While basic tech literacy is essential for online activities, many can perform activities even with very little knowledge. The growth of online communication is fast and rapidly replacing traditional communication methods. Paper-based communication has reduced a lot since the evolution of online communication. It is convenient, easy, and does not cause any harm to nature. It is also fast and can be communicated anywhere in the world.

1.1 Cybers talking:

Cybers talking is a form of online harassment in which the perpetrator uses electronic communications to stalk a victim. This is considered more dangerous than other forms of cyberbullying because it generally involves a credible threat to the victim's safety. Cybers talkers may send repeated messages intended to threaten or harass, and they may encourage others to do the same, either explicitly or by impersonating their victim and asking others to contact them..

1.1.1 Trolling:

Internet trolls intentionally try to provoke or offend others in order to elicit a reaction. Trolls and cyberbullies do not always have the same goals: while some trolls engage in cyberbullying, others may be engaged in comparatively harmless mischief. A troll may be disruptive either for their own amusement or because they are genuinely a combative person.

1.2 . Cyber bullying:

Social Media, such as Facebook, Instagram, Snapchat, and Tik Tok, Text Messaging and Messaging apps on mobile or tablet devices, Instant Messaging, Direct messaging, and online chatting over the internet, Online forums, chat rooms, and message boards, such as Reddit Email. Online gaming communities

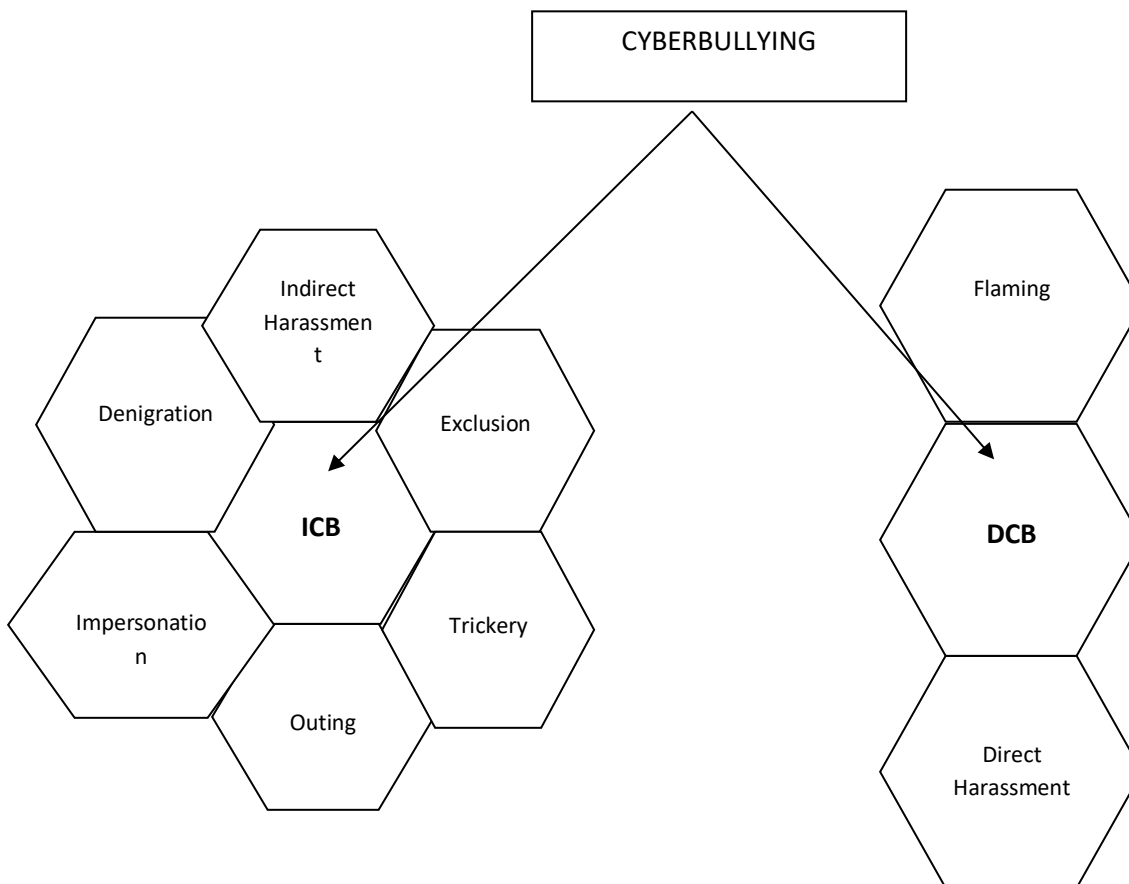
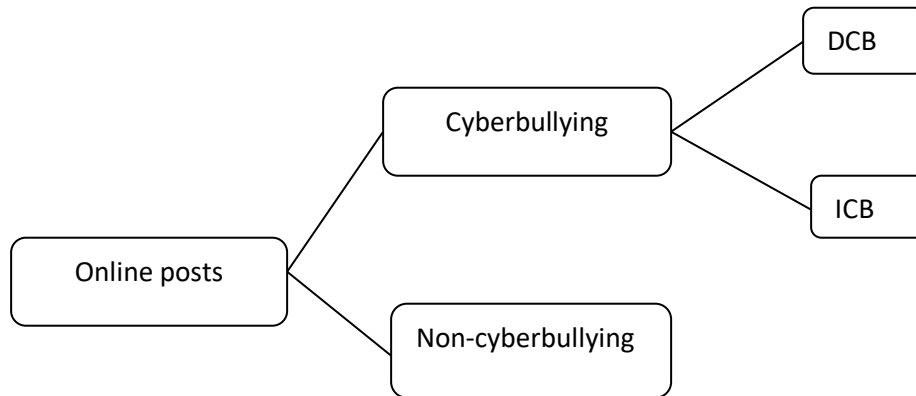
Some of the most common forms of cyberbullying are as follows. Flaming: Heated online arguments and fights using vulgar and abusive language. Harassment: Repeatedly sending cruel, offensive, or threatening messages. Denigration: Exposing secrets of a person or gossip in order to damage the reputation of a person Impersonation: Breaking into the victim's account and sending emails. Trickery: Tricking the victim into revealing sensitive information and passing it on to others. Interactive Gaming: Most gaming consoles allow people to connect and play online providing a chance to abuse using chats and comments.

2 In search engines:

Information cascades happen when users start passing along information they assume to be true, but cannot know to be true, based on information on what other users are doing. This can be accelerated by search engines' ranking technologies and their tendency to return results relevant to a user's previous interests. This type of information spreading is hard to stop. Information cascades over social media and the Internet may also be harmless, and may contain truthful information. Bullies use Google bombs (a term applicable to any search engine) to increase the prominence of favored posts sorted by the most popular searches, done by linking to those posts from as many other web pages as possible. Examples include the campaign for the neologism "santorum" organized by the LGBT lobby. Google bombs can manipulate the Internet's search engines regardless of how authentic the pages are, but there is a way to counteract this type of manipulation as well. Of those who reported having experienced online harassment in a Pew Research poll, 16% said the most recent incident had occurred in an online game. A study from National Sun Yat-sen University observed that children who enjoyed violent video games were significantly more likely to both experience and perpetrate cyberbullying. Another study that discusses the direct correlation between exposure to violent video games and cyber bullying also took into account personal factors such as "duration of playing online games, alcohol consumption in the last 3 months, parents drunk in the last 3 months, anger, hostility, ADHD, and a sense of belonging" as potential contributing factors of cyberbullying. Gaming was a more common venue for men in which to experience harassment, whereas women's harassment tended to occur more via social media. Most respondents considered gaming culture to be equally welcoming to both genders, though 44% thought it favored men. Sexual harassment in gaming generally involves slurs directed towards women, sex role stereotyping, and overaggressive language. Keza MacDonald writes in The Guardian that sexism exists in gaming culture, but is not mainstream within it. U.S. President Barack Obama made reference to the harassment of women gamers during his remarks in honor of Women's History Month. Competitive gaming scenes have been less welcoming of women than has broader gaming culture. In an internet-streamed fighting game competition, one female gamer forfeited a match after the coach of her team, Aris Bakhtanians, stated, "The sexual harassment is part of the culture. If you remove that from the fighting game community, it's not the fighting game community." The comments were widely condemned by gamers, with comments in support of sexual harassment "drowned out by a vocal majority of people expressing outrage, disappointment, and sympathy." The incident built momentum for action to counter sexual harassment in gaming. Some game developers have been subjected to harassment and death threats by players upset by changes to a game or by a developer's online policies. Harassment also occurs in reaction to critics such as Jack Thompson or Anita Sarkeesian, whom some fans see as threats to the medium. Various people have been harassed in connection with the Gamergate controversy. Harassment related to gaming is not of notably different severity or tenor compared to online harassment motivated by other subcultures or advocacy issues. Other developers have been harassed simply due to misogyny or anti-LGBTQ+ stances. A notable case was the death of "Near", the developer of Higan, a console emulator, who took their own life after becoming the subject of ridicule from members of the online Kiwi Farms board following their announcement of being nonbinary.

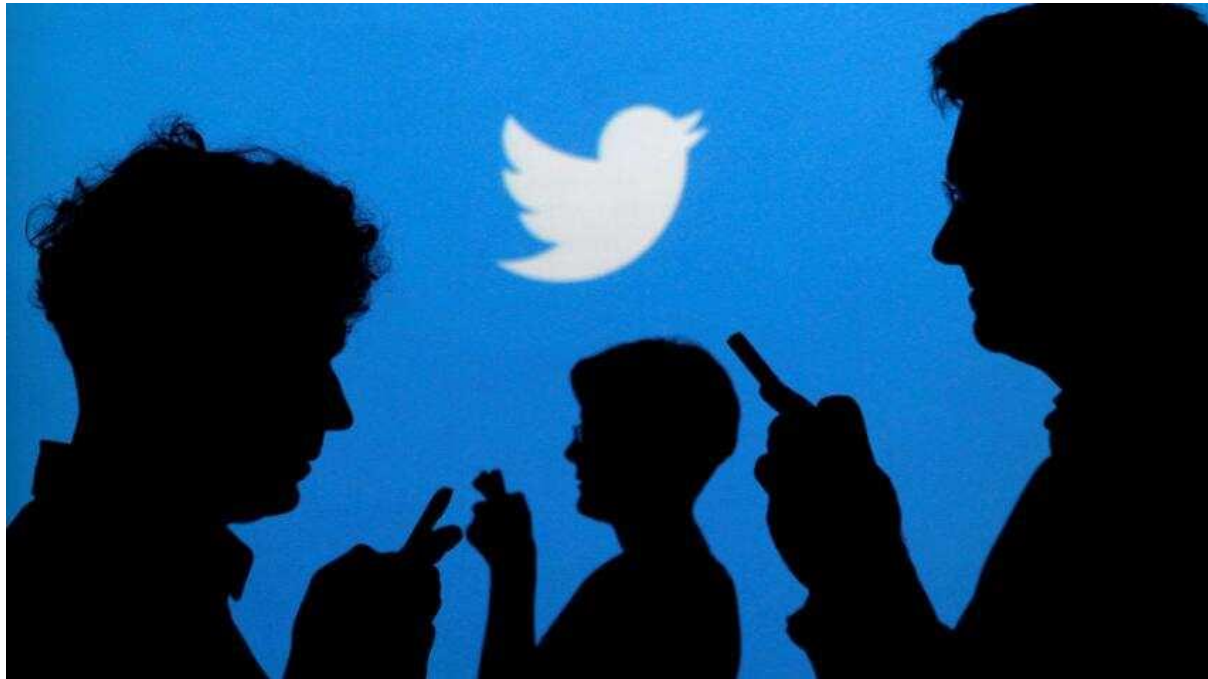
Sections and sub-sections should be referred to as shown in the next sentence. Section 3 explained how figures and tables should be formatted. In this section, the formatting of footnotes and references is discussed.

Cyberbullying detection on social multimedia using soft computing techniques:

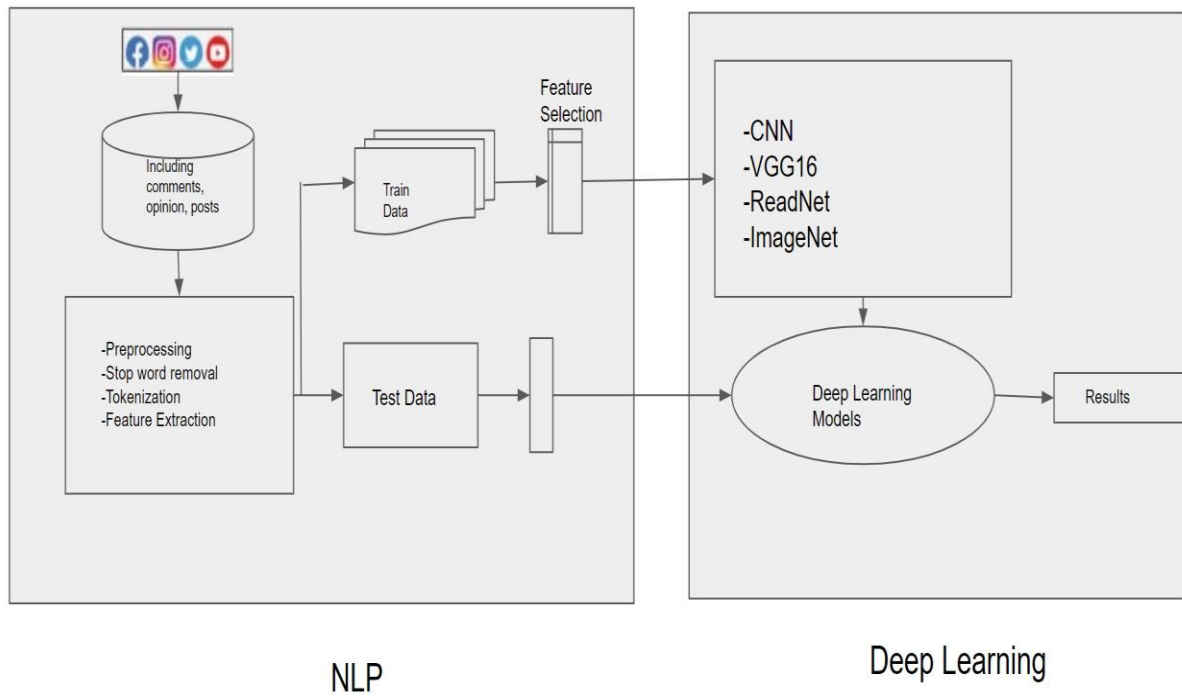


3 Problem Statement :

As I am a Network Admin/Application Owner/Social Media Admin, I need to Find out which one is the bullying message and who is the author .



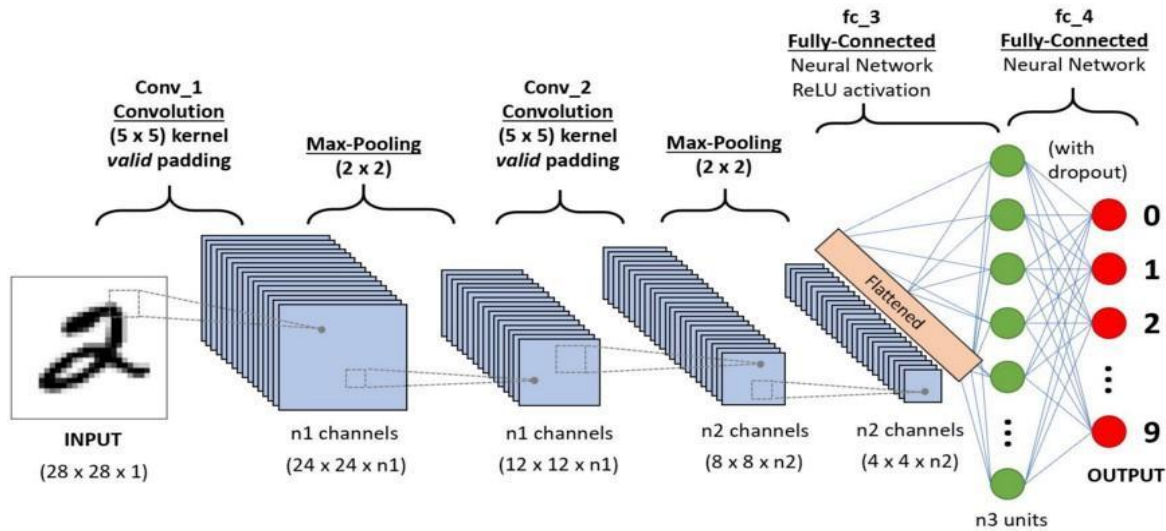
4 Architecture :



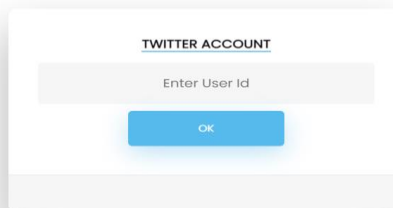
5 Proposed system:

A Convolutional Neural Network (CNN) is a Deep Learning algorithm that can take in an input image, assign importance (learnable weights and biases) to various aspects/objects in the image, and be able to differentiate one from the other. The pre-processing required in a CNN is much lower as compared to other classification algorithms. While in primitive methods filters are hand-engineered, with enough training, CNN has the ability to learn these filters/characteristics. Find out the bullying messages/tweets on social networks using neural networks. By the use of Neural networks, predicting the unwanted and vulgar, abusive messages.

CNN - Convolutional Neural Networks is one of the Deep Learning approaches. CNN is one of the Neural Network algorithms. Neural Network structure is inspired by the human brain, mimicking the way that biological neurons signal to one another.



6 Screenshot:



7 Conclusions:

In this paper, we proposed an approach to detect the cyber bullying on social network using neutral networks. Cyberbullying has become an alarming social threat for today's world and has gained huge attention from the research community. To the extent the misuse comes with any new technology. These techniques lead to cyberbullying. Efficiency of cyberbullying detection will decrease due to a constrained word set of negative words. These techniques make automatic detection of bullying messages in social media and this could help to construct a healthy and safe social media environment.

8 References:

- [1] <https://www.stopbullying.gov/cyberbullying/>
- [2] J. Patchin, & S. Hinduja, "Bullies move beyond the schoolyard; a preliminary look at cyberbullying." Youth violence and juvenile justice. 4:2 (2006). 148-169.
- [3] Sourabh Parime, Vaibhav Suri "Cyberbullying Detection and Prevention: Data Mining and Psychological Perspective", 2014 International Conference on Circuit, Power and Computing Technologies [ICCPCT]
- [4] <http://www.TIMESOFINDIA.com>
- [5] <http://www.nepc.org/cyberbullying>
- [6] K. Reynolds, A. Kontostathis, and L. Edwards, "Using Machine Learning to Detect Cyberbullying," In Proceedings of the 2011 10th International Conference on Machine Learning and Applications Workshops (ICMLA 2011), vol. 2, December 2011. pp. 241-244.
- [7] <http://www.statisticbrain.com/cyber-bullying-statistics/>
- [8] <http://en.wikipedia.org/wiki/Cyber-bullying/>
- [9] A. M. Chandrashekar, Muktha G S & Anjana D "Cyberstalking and Cyberbullying: Effects and prevention measures" Imperial Journal of Interdisciplinary Research (IJIR) Vol-2, Issue-3, 2016 ISSN: 2454-1362.

Classification of Video Metadata

K. Bakkiyalakshmi, CSE, St. Anne's CET
R. Kowsalya, CSE, St. Anne's CET
R. Krishnaveni, CSE, St. Anne's CET

Abstract

This paper proposes a model of the video metadata generation approach for detecting human action in video. The idea is to develop a framework, which uses a semantic approach on the action recognition and classification level. This paper will stress on the metadata generation process for extracting all the features needed. The processes are video acquisition, feature extraction, action detection, inference and presentation level. The samples are trained on one entire clip and tested on all other clips. This process is repeated for each video as the training set. To evaluate the performance of the proposed approach, two measurement of accuracy were computed: precision and recall. Detection accuracy was measured as the number of actions correctly detected over total number of samples.

Keywords: *Deep learning, Convolutional neural networks, Recurrent neural networks, Video classification, metadata generation*

1 Introduction

Metadata is a set of data that describes and gives information about other data. Some examples of basic metadata are author, date created, date modified, and file size. Metadata is also used for unstructured data such as images, video, web pages, spreadsheets, etc.

The purpose of Metadata is:

- Metadata makes finding and working with data easier – allowing the user to sort or locate specific documents.
- *Metadata helps us understand the structure, nature, and context of the data.*

There are various kinds of metadata files. They are Document Metadata, Image Metadata and Video Metadata. Document metadata is information attached to a text-based file that may not be visible on the face of the document; documents may also contain supporting elements such as graphic images, photographs, tables and charts, each of which can have its own metadata.

Metadata summarizes basic information about data, which can make finding and working with particular instances of data easier. Having the ability to filter through that metadata makes it much easier for someone to locate a specific document or other data asset in a variety of different ways. Document metadata in Microsoft Word, for example, includes the file size, date of document creation, the names of the author and most recent modifier, the dates of any changes and the total edit time. Further metadata can be added, including title, tags and comments.

Photo metadata is the information and specific details concerning a particular image file (Figure 1). This information often includes date created, author, file name, content, themes and more. Photo metadata offers users a better way to organize, sort and maintain image files within a system. This picture in Figure 2 is a photograph of a small dog wearing a Champion brand yellow shirt in front of a blue background. Metadata adds to that, with elements such as: Date created, geographical location, author (photographer), image title, pixels, camera type, file type and more. It may seem minor, but if the title of the picture is “The King’s Dog”, the metadata is crucial in understanding it.



Figure 1



Figure 2

Video metadata is used to provide information about specific video and audio streams or files, also known as essence for television broadcasting and video streaming. Metadata can either be embedded directly into the video or included as a separate file within a container such as MP4 or MKV. Metadata can include information about the entire video stream or file or specific video frames. Created by cameras, encoders, and other video processing elements, metadata can include timestamps, video resolution, file size, closed captioning, audio languages, ad-insertion points, color spaces, error messages, and much more.

For the metadata to be useful, it must be recognized by whichever element or device it is intended for. For example, a set-top box needs to be able to recognize metadata about a video's picture resolution in order to display it in the right format. Once a live video has been captured and recorded, further metadata can be included for describing the content allowing users to search for content without having to sift through potentially long video Files.

2 Literature Review

Over the last decade, active researchers have produced methods for improving Video Classification.. In [1], this paper gives a method to reduce the computation time for video classification using the idea of distillation. Specifically, we first train a teacher network that computes a representation of the video using all the frames in the video. The proposed approach in [2] used an improved CNN-based classification algorithm with a softmax loss function to classify mine video scenes. Compared to the older algorithms this CNN algorithm showed higher accuracy, precision, and recall in classifying mine videos. It did solve the drawbacks that were there in the traditional model but as it requires massive data to give a more accurate result which was not available at that moment so it was predicted that future massive data and complex training would make that model more efficient. The presented method in paper [3] considers the problem constructing a minimum representative set of video physical features that can be used in different regression and classification tasks when working with video. To test the resulting set of features, the problem of classifying video into 4 classes was considered: cartoon, drone shooting, computer game and sports broadcast. [4] uses a support vector machine. This system is capable of extracting keyframes from videos and classifying them as natural scenery, personality, animal and plant. For feature extraction, new methods like edge histogram, dominant color, color layout and face feature were used for image retrieval.

3 Methodology

Dataset

The dataset consists of 1827 videos related to 10 different tasks, which were all collected from various websites. The average length of a video is 2 minutes. Each video is labelled with 3 step segments, where each segment lasts 12 seconds on average. In total, the dataset contains videos of 10 hours. We have considered 5 classes out of the given 6 classes and have taken 200 images for training and testing purpose.

Keyframe

Extraction Key-frames are defined as the representative frames of a video stream, the frames that provide the most accurate and compact summary of the video content. Frame extraction and selection criteria for key-frame extraction.

- Frame that are sufficiently different from previous ones using absolute differences in LUV color space
- Brightness score filtering of extracted frames
- Entropy/contrast score filtering of extracted frames
- K-Means Clustering of frames using image histogram
- Selection of best frame from clusters based on and variance of laplacian (image blur detection)

Video Classification Model

- Suppose we have n number of classes , let's name them $\{c_1, c_2, c_3 \dots c_n\} \in C$ and 'S' video containing 'M' number of frames present in it as $\{F_0, F_1, F_2, \dots, F_{M-1}\}$. The purpose of this model is to classify the frames by identifying the classes they belong to.
- For each of the unique 'n' number of classes we have we will be predicting the probability $P(c_n | S) P(c_n | S) = \{F_0, F_1, F_2, \dots, F_{M-1}\}$.
- The mentioned κ can be a Neural Network that does the job of predicting the frames 'F'.

3.1 CNN Architecture

Neural networks are considered a very powerful and intelligent technique to classify different types of data for important applications. New types of neural networks called convolutional neural networks. They were developed for classification and recognition tasks in many applications. It makes a breakthrough in image processing, video, speech, and text recognition research, and the concentration it earned is due to the capability and the high performance.

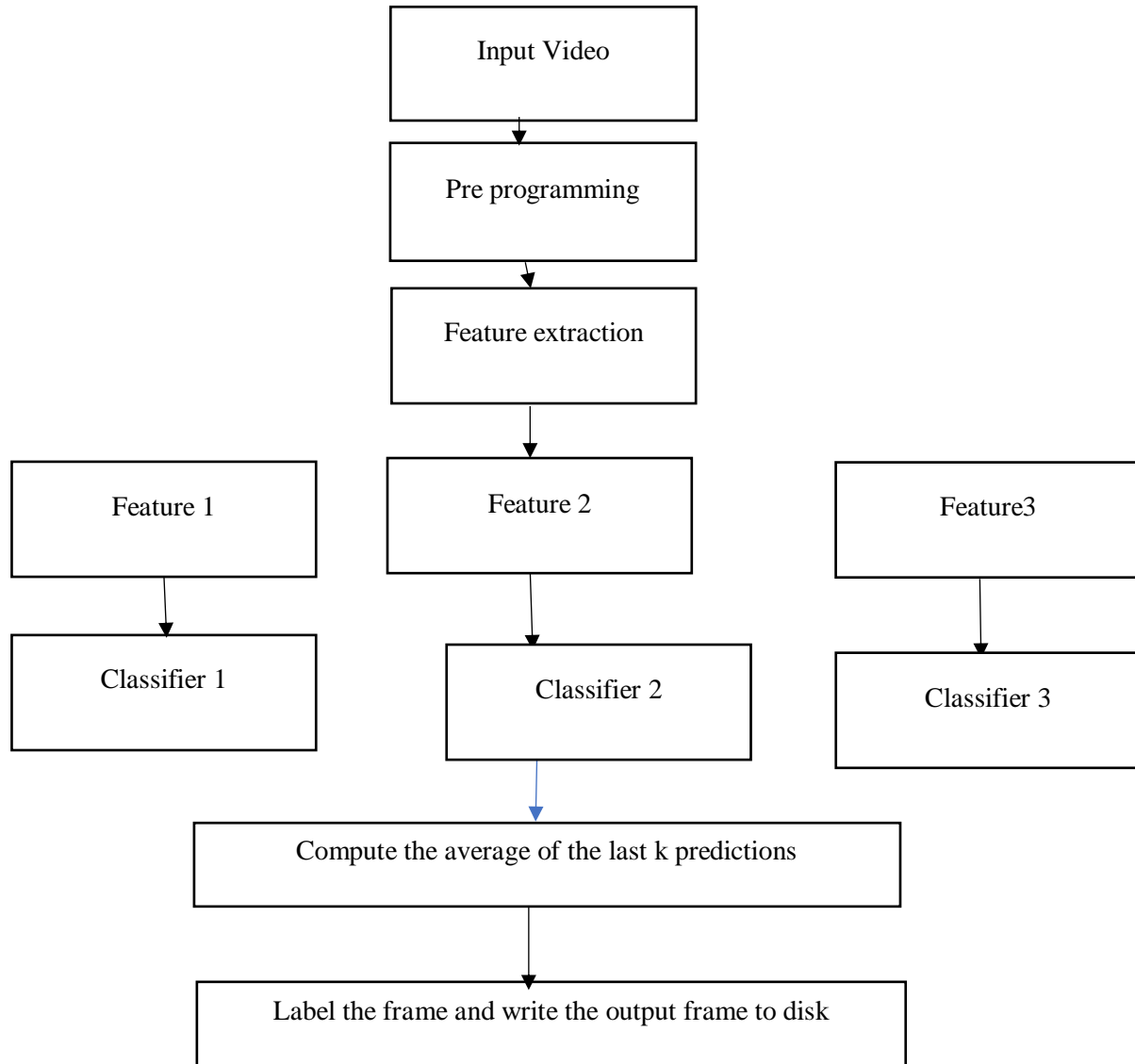


Figure 3 – Video Classification Model

Convolutional Neural Networks can take in an input image, assign importance to various aspects/objects in the image and be able to differentiate one from the other which means it can work on the spatial features of the video while RNN i.e Recurrent Neural networks which uses sequential data or time-series data so it can work on the temporal features. It extracts and finds the features in following layers.

a. Convolution Layer

It contains a set of digital filters to perform the function of convolution in the input data. It is the number of filters the convolutional layers will learn from. It is the absolute value and determines the number of filters that come out of convolution. It uses the 'Relu' activation function here.

b. Average Pooling Layer

It involves calculating the average for each part of the feature map. This means that each 2×2 square of the feature map is down sampled to the average value in the square

c. Max Pooling Layer

It is an operation that calculates the maximum value for patches of a feature map, and uses it to create a down sampled (pooled) feature map. It is used to reduce the dimensions of the feature maps

d. Drop Out Layer

It is a technique used to prevent a model from overfitting. It works by randomly setting the outgoing edges of hidden units to 0 at each update of the training phase.

e. Dense Layer

We can call it a deeply connected network. Each neuron in the dense layer receives input from all neurons of its previous layer. Acts like output layer and gives results according to classified classes.

3.2 Workflow

- a. Firstly the dataset is loaded.
- b. The images frames are resized to a common scale of 224 x224.
- c. As we do not have any separate testing dataset we will be dividing the current dataset into training and validation dataset. in the ratio of 80:2
- d. The datasets are loaded with a batch size of 128 and then the dataset is shuffled to avoid biased conditions.
- e. And the class mode will be categorical.
- f. Then the images are preprocessed for training using feature extraction and edge detection methods.
- g. The above process gives a compiled model so from here the model has to be fit to train. So the model is trained over the training dataset under 15 epochs.
- h. For the Testing Part, Video input is taken and the keyframes are then fed in the pre-trained model, where the input frame image of size 224 x 224 is given to the model.
- i. The result of prediction is given in form of percentage where it tells that by what percentage does the video resembles each class.

4 RESULTS AND DISCUSSIONS

The model after compilation is trained and then tested after this process the model has given an accuracy of 80.27%. This accuracy was possible because of introducing some complex layers like the Dense layer and Dropout layer where the random neurons are dropped for training. Also as we used the softmax function which helped in quicker training coverage.

5 CONCLUSION

The proposed model is able to emulate the accuracy of approximately 80 % as expected using the dataset. This accuracy was possible because of introducing some complex layers like the Dense layer and Dropout layer where the random neurons are dropped for training. Also as we used the softmax function which helped in quicker training coverage

References

- [1] Bhardwaj, S., Srinivasan, M., & Khapra, M. M "Efficient Video Classification Using Fewer Frames" 2019 IEEE/CVF Conference on Computer Vision and Pattern Recognition (CVPR).
- [2] O. Ye, Y. Li, G. Li, Z. Li, T. Gao and T. Ma, "Video scene classification with complex background algorithm based on improved CNNs," 2018 IEEE International Conference on Signal Processing, Communications and Computing (ICSPCC), 2018, pp. 1-5.
- [3] R. A. Kazantsev, S. V. Zvezdakov, D. S. Vatolin, "Application of physical video features in a classification problem," International Journal of Open Information Technologies ISSN: 2307-8162 vol. 7, no.5, 2019
- [4] Z. Min, "Scenery video type classification based on SVM," 2009 Asia Pacific Conference on Postgraduate Research in Microelectronics & Electronics (PrimeAsia), 2009, pp. 287-289.

Towards Achieving Keyword Search over Dynamic Encrypted Cloud Data with Symmetric-Key Based Verification

Mr S.Ramalingam..ME.,AP/CSE Assistant professor, MRK Institute of Technology,
Abinash S, UG Scholar, MRK Institute of Technology, Cuddalore,India,
Prem S, UG Scholar, MRK Institute of Technology, Cuddalore,India,
Karthikeyan S, UG Scholar, MRK Institute of Technology, Cuddalore,India,

Abstract

Identity-based encryption is used to build data sharing system. in order, access control is not static. In this project, we address this practical problem. Proposed system suggests the novel concept of key aggregate searchable encryption (KASE) and instantiating the concept through a concrete KASE scheme. In which a data owner only needs to distribute a single key to a user for sharing a large number of documents, and the user only needs to submit a two key to the cloud for querying the shared documents. The security analysis and performance evaluation both confirm that our proposed schemes are provably secure and practically efficient.

1 Introduction

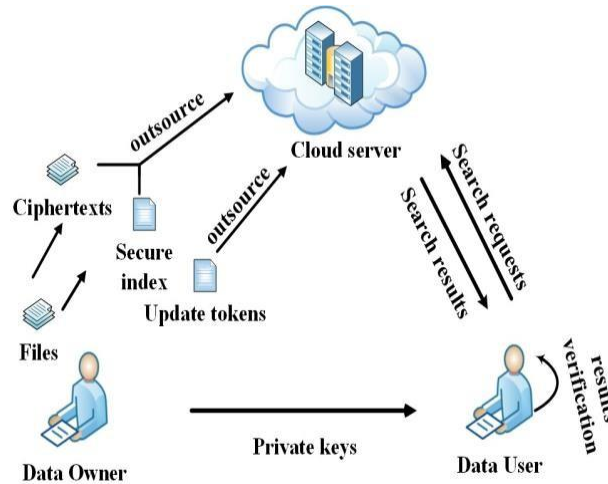
Cloud computing provides the flexible architecture to share the application(software) as well as the other network resources(hardware) Cloud storage enables networked online storage where data is stored on multiple virtual servers, generally hosted by third parties , rather than being hosted on dedicated servers key management and key sharing plays the main role in the data sharing concept of cloud computing. Traditional key cryptosystems lack the enhanced security techniques as the keys are generated by the existing random key generation Proposed system said to have aggregate key cryptosystem in which key generated by means of various derivations of cipher text class properties of data and its associated key.

Searchable Semantic Encryption(SSE) is a practical way for users to securely retrieve the interested cipher texts from the encrypted cloud data through keywords. Cloud computing provides the flexible architecture to share the application(software) as well as the other network resources(hardware) Cloud storage enables networked online storage where data is stored on multiple virtual servers, generally hosted by third parties , rather than being hosted on dedicated servers key management and key sharing plays the main role in the data sharing concept of cloud computing. Traditional key cryptosystems lack the enhanced security techniques as the keys are generated by the existing random key generation Proposed system said to have aggregate key cryptosystem in which key generated by means of various derivations of cipher text class properties of data and its associated keys It has become a hot research topic in cloud computing security and numerous SSE schemes have been proposed. Nonetheless, most of them only consider realizing keyword search over static encrypted cloud data. In practice, the data stored on the cloud server might often need to be updated(added, deleted or modified) by data owners

2 Related Works

In recent years, cloud computing has been applied to securely perform various tasks, such as healthcare monitoring [11], deep packet inspection [12] and key updates [13]. Cloud storage is universally viewed as one of the most important services of cloud computing. Although cloud storage provides great benefit to users, it brings some new security challenges. Firstly, users may worry about whether their data is intently stored in the cloud because the cloud data is out of their physical control. In order to solve this problem, some cloud storage auditing schemes [14–16] are proposed to check the integrity of cloud data. In addition, users usually need to encrypt the data for keeping the privacy before outsource them to the cloud. It makes performing keyword search over encrypted cloud data become a new challenge. In order to address this issue, searchable encryption is proposed, which allows users to selectively retrieve cipher documents stored in the cloud by keyword-based search. Compared with searchable public key encryption [17, 18], searchable symmetric encryption draws more attention owing to its high efficiency. Static SSE. Song et al. [19] firstly proposed the searchable symmetric encryption scheme, in which a special two-layered encryption structure is constructed to encrypt each keyword. Goh et al. [20] proposed a keyword search scheme over encrypted cloud data based on the Bloom filter. Curtmola et al. [21] proposed two efficient keyword search schemes(SSE1 and SSE-2) over encrypted cloud data. These schemes can realize sublinear search, that is, the search cost is proportional to the number of the files matching the queried keyword. Cao et al. [22] proposed a privacy-preserving multi-keyword ranked search scheme over encrypted cloud data by utilizing the similarity measure of “Coordinate matching” and “inner product similarity”. In addition, some other static SSE schemes, such as semantic search scheme [23, 24], similarity search scheme [25–28], ranked keyword search schemes [29–32], central keyword- based semantic extension search scheme [33], and keyword search scheme supporting deduplication [34], have also been proposed. Dynamic SSE. In order to support data dynamic update, some dynamic SSE schemes [1–4, 35–38] have been proposed. Kamara et al. [1] proposed a dynamic SSE scheme by extending the inverted index approach. This scheme can achieve sub linear search and CKA2-security. Subsequently, they proposed another dynamic SSE scheme [4] based on keyword red-black tree index structure. This scheme supports parallel keyword search as well as parallel addition and deletion of files. Naveed et al. [38] presented a dynamic SSE scheme via blind storage. Blind storage allows a data owner to store files on a cloud server in such a way that the cloud server does not learn the number of files. Xia et al. [3] proposed a dynamic keyword search scheme over encrypted cloud data based on the tree-based index structure, which can support multi-keyword rank. Guo et al. [2] proposed a dynamic SSE scheme based on the inverted index. It enables the data user to search several phrases in a query request. Also, their proposed scheme supports the sorting of the search results. Verifiable SSE. In order to prevent the cloud server from returning the invalid search results,

scheme. In order to support dynamic data update for verifiable SSE schemes, Sun et al. [10] proposed a verifiable dynamic conjunctive keywords search scheme based on the bilinear-map accumulator and the accumulation tree. Zhu et al. [9] introduced a verifiable and dynamic fuzzy keyword search scheme based on the inverted index. Liu et al. [7] presented a verifiable dynamic keyword search scheme supporting the search results rank. This scheme and scheme [9] both leverage RSA accumulator to realize the results verification and the data dynamics. The verification techniques used in above verifiable and dynamic schemes are all based on asymmetric-key cryptography, which involves time-consuming operations. As a result, the verification efficiency is very low in these scheme



3 Problem Formulation

A. System Model

As shown in Fig.1, the system model consists of three entities: data owner, data user and cloud server

- Data owner: He encrypts his plain files and constructs a secure index with private keys. He uploads the cipher texts and the secure index to the cloud server. When the data owner wants to update files, he generates the update tokens locally and sends them to the cloud server.
- Data user: He is authorized by the data owner who shares the private keys with him. When he wants to search the files containing the interested keywords, he sends the search requests to the cloud server. After the data user receives the search results from the cloud server, he can verify the validity of the results.
- Cloud server: It stores the ciphertexts and the secure index from the data owner. Upon receiving the search requests from the data user, it performs search operation over the secure index, and returns the search results.

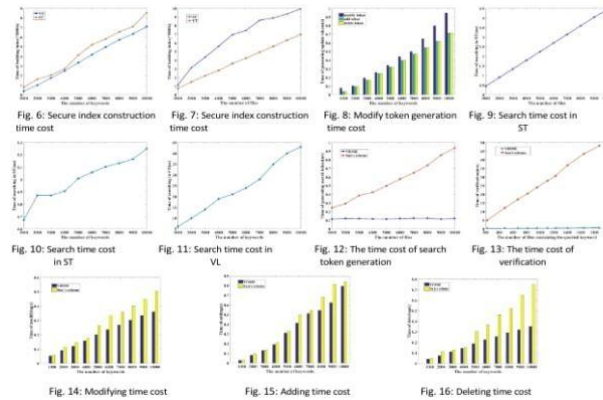
In addition, upon receiving the update information from the data owner, it updates the secure index and the related ciphertexts. In this model, the data owner and the data user are assumed to be always trusted. That is, the data owner honestly encrypts files and builds a secure index. The data user honestly generates the search request for the queried keyword. The cloud server is regarded as an untrusted entity. It is allowed to learn which encrypted files contain the queried keyword by performing the search operation. However, it might try to learn more valuable information from the encrypted files, the secure index, and the search trapdoors. For example, it might try to find which files contain two queried keywords and which keywords have changed in the modified file. Besides, the cloud server may return invalid or non-updated search results to the data user for saving computation cost or other reasons.

B. Design Goals

To address the above challenges, we aim at making the proposed scheme meet the following goals. Supporting efficient keyword search over encrypted cloud data. The scheme should retrieve all matching files for the search token and also should achieve sub linear search efficiency. Supporting efficient data dynamic update. The scheme should support efficient data dynamic update, such as modification, addition or deletion.

4 Performance And Experiments

In this section, we analyse the performance of the proposed VDSSE scheme. Experiments are implemented using C++ language on a Linux OS equipped with 2.4GHz Inter(R) Core(TM) i5 CPU and 4GB RAM, and constructed on a real-world data set [45]. Index construction efficiency. To evaluate the efficiency of our proposed schemes, we conduct the experiments for building ST and building VL. Fig.6 shows the time cost of building the secure index when the number of files is set to 10000 and the number of keywords varies from 1000 to 10000. We can observe that the time cost grows linearly with the number of keywords. In our scheme, as the row list number in ST equals to the number of keywords,



the increase of the row list number leads to the increase of ST construction time cost. As the node number in VL equals to the number of keywords, the increase of the node number leads to the increase of VL construction time. Fig.7 shows the time cost of building the secure index when the number of keywords is set to 10000 and the number of files varies from 1000 to 10000. We can observe that the time cost of building index grows linearly with the number of files. In our scheme, as the column list number in ST equals to the number of files, the increase of the column list number leads to the increase of ST construction time cost. The time cost of computing tags in VL is related to the number of files.

5 CONCLUSION

To share data flexibly is vital thing in cloud computing. Users prefer to upload there data on cloud and among different users. Outsourcing of data to server may lead to leak the private data of user to everyone. Encryption is a one solution which provides to share selected data with desired candidate Sharing of decryption keys in secure way plays important role Public-key cryptosystems provides delegation of secret keys for different cipher text classes in cloud storage. The delegate gets securely an aggregate key of constant size It is required to keep enough number of cipher texts classes as they increase fastand the ciphertext classes are bounded that is the limitation utilizes the bilinear-map accumulator to verify the searchresults.

6 References

- [1] S. Kamara, C. Papamanthou and T. Roeder, "Dynamic searchable symmetric encryption," presented at ACM Conference on Computer and Communications Security, pp.965-976, 2012.
- [2] C. Guo, X. Chen, Y. M. Jie, Z. J. Fu, M. C. Li and B. Feng, "Dynamic Multi-phrase Ranked Search over Encrypted Data with Symmetric Searchable Encryption," in IEEE Transactions on Services Computing, vol. 99, No. 1939, pp. 1-1, 2017.
- [3] Z. H. Xia, X. H. Wang, X. M. Sun and Q. Wang, "A Secure and Dynamic Multi-Keyword Ranked Search Scheme over Encrypted Cloud Data," in IEEE Transactions on Parallel and Distributed Systems, vol. 27, No. 2, pp. 340-352, 2016.
- [4] S. Kamara and C. Papamanthou, "Parallel and Dynamic Searchable Symmetric Encryption," presented at the International Conference on Financial Cryptography and Data Security, pp. 258-274, 2013.
- [5] J. B. Yan, Y. Q. Zhang and X. F. Liu, "Secure multi-keyword search supporting dynamic update and ranked retrieval," in China Communication, vol. 13, No. 10, pp.209-221, 2016.
- [6] K. Kurosawa and Y. Ohtaki, "How to Update Documents Verifiably in Searchable Symmetric Encryption," presented at International Conference on Cryptology and Network Security, pp. 309-328, 2013.
- [7] Q. Liu, X. H. Nie, X. H. Liu, T. Peng and J. Wu, "Verifiable Ranked Search over dynamic echnol., vol. 29, no. 7, pdsp. 1985–1997, Jul. 2019 encrypted data in cloud computing," presented at the IEEE/ACM International Symposium on Quality of Service, pp. 1-6, 2017.
- [8] X. H. Nie, Q. Liu, X. H. Liu, T. Peng and Y. P. Lin, "Dynamic Verifiable Search Over Encrypted Data in Un-trusted Clouds," presented at the International Conference Algorithm and Architectures for Parallel Processing, pp.557-571, 2016.

DL-CNN BASED HARDWARE STATE ENABLED USING HAND GESTURE

Mrs.E.Indhuma,cse,St.Anne's college of engineering and technology.

N.Subasri,cse,St.Anne's college of engineering and technology

M.Jayaveena, cse,St.Anne's college of engineering and technology

Abstract

Gesture recognition is a technology that is becoming increasingly relevant, given the recent growth and popularity of Virtual and Augmented Reality technologies. It is one key aspect to HCI, allowing for two-way interaction in virtual spaces. However, many instances of such interaction are currently limited to specialized uses or more expensive devices such as the Kinect and the Oculus Rift. In this paper we explore the methods for hand gesture recognition using a more common device the mobile Hand camera. Specifically, we explore and test 3 different methods of segmenting the hand, and document the pros and cons of each method. We will also cover one method for hand gesture recognition.

Keywords: convolutional neural network, IoT devices, anomaly detection; UAV videos; deep Learning.

1 Introduction

Hand gesture recognition is the first step for a computer to understand human body language. It plays a pivotal role in a wide range of human-computer interaction (HCI) applications such as smart mobile and TV control, video games, telesurgery, and virtual reality applications of hand gesture recognition. The hand gestures involved in sign language are structured in a very complex way as they convey important human communication information and feelings the time dependence of these frames makes it difficult to directly compare the primitives in Euclidean space. Most of the existing recognition systems only consider the local configuration of the hand. These systems either receive a segmented hand region as input or perform a hand segmentation preprocessing step using skin color models or colored gloves. However, such systems perform well only for gestures involving simple alphabets and numbers, which slightly rely on the global configuration, but not for real sign language gestures. Traditionally, dynamic hand gesture recognition systems use different techniques to extract handcrafted features followed by a sequence modeling technique such as a hidden Markov model (HMM). However, the recent success of deep learning techniques in image classification, object recognition, speech recognition, and human activity recognition has encouraged many researchers to exploit them for hand gesture recognition. For example, convolutional neural networks (CNN) have been widely used for learning visual features in computer vision. The most important characteristic of 3DCNN is its ability to directly create hierarchical representations of spatiotemporal data. However, it requires more parameters than 2DCNN, which is one of its disadvantages. Moreover, 3DCNN has an additional kernel dimension, which makes it harder to train. Hence, instead of training a 3DCNN from scratch, using domain adaptation on pretrained instances is preferred.

2 Related Works

S. Kausar and M. Y. [1] Javed presented a paper on the survey of the current research trends in the field of SL recognition to highlight the current status of different research aspects of the area. Paper also critically analyzed the current research to identify the problem areas and challenges faced by the researchers. This identification is aimed at providing guideline for the future advances in the field. M. B. Waldron and S. Kim [2] presented a paper on design and evaluation of a two-stage neural network which can recognize isolated ASL signs is given. The input to this network is the hand shape and position data obtained from a DataGlove mounted with a Polhemus sensor. The first level consists of four backpropagation neural networks which can recognize the sign language phonology, namely, the 36 hand shapes, 10 locations, 11 orientations, and 11 hand movements.

The recognized phonemes from the beginning, middle, and end of the sign are fed to the second stage which recognizes the actual signs. C. Chansri and J. Srinonchat [3] presented a paper on the article which investigates and develops the technique to recognize hand posture of Thai sign language in a complex background using fusion of depth and color video. The new technology of sensors, such as the Microsoft Kinect, recently provides the depth video which helps researchers to find the hand position in the scene. This advantage is used to segment the hand sign in the color video without the environment interference such as skin color background. M.-H. Yang, N. Ahuja, and M. Tabb [4] presented a paper on algorithm for extracting and classifying two-dimensional motion in an image sequence based on motion trajectories. First, a multiscale segmentation is performed to generate homogeneous regions in each frame. Regions between consecutive frames are then matched to obtain two-view correspondences. Affine transformations are computed from each pair of corresponding regions to define pixel matches. T. Starner, J. Weaver, and A. Pentland [5] presented a paper on two real-time hidden Markov model-based systems for recognizing sentence-level continuous American sign language (ASL) using a single camera to track the user's unadorned hands. The first system observes the user from a desk mounted camera and achieves 92 percent word accuracy. The second system mounts the camera in a cap worn by the user and achieves 98 percent accuracy (97 percent with an unrestricted grammar).

3 Proposed System

We have used different datasets to evaluate the proposed deep learning algorithm.detection method. The proposed system is vision based, that uses image processing techniques and inputs from a camera. The input frame would be captured from the digital camera and system is broken down into four stages, skin detection, hand contour extraction, hand the skin region would be detected victimization skin detection. The hand contour would then be found and used for hand trailing and gesture recognition. Hand trailing would be used to change the state of the mobile APP like whatsapp on and gallery on and off control..

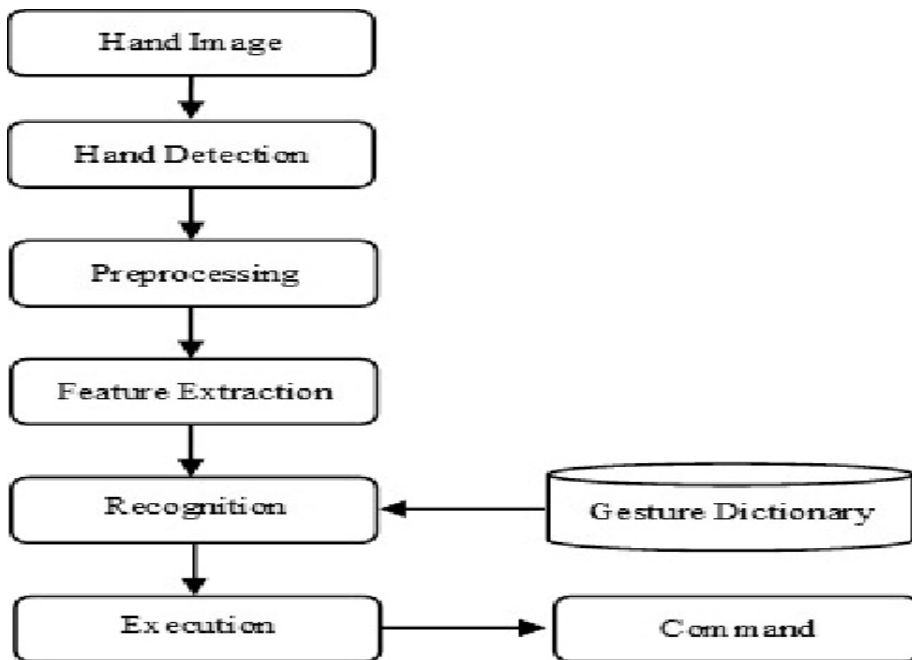


Figure 1: System Architecture of proposed system

4 Implementation

The project constitute of below modules,

4.1 Data Collection and Preprocessing

Data collection is the process of gathering and measuring information on targeted variables in an established system, which then enables one to answer relevant questions and evaluate outcomes. Data collection is a component of research in all fields of study including physical and social sciences, humanities and business. While methods vary by discipline, the emphasis on ensuring accurate and honest collection remains the same. The goal for all data collection is to capture quality evidence that allows analysis to lead to the formulation of convincing and credible answers to the questions that have been posed. Preprocessing can refer to the following topics in computer science Preprocessor, a program that processes its input data to produce output that is used Preprocessing as input to another program like a compilers Data preprocessing used in deep learning and data mining to make input data easier to work with disambiguation page lists articles associated with the title the preprocessing.

4.2 Segmentation

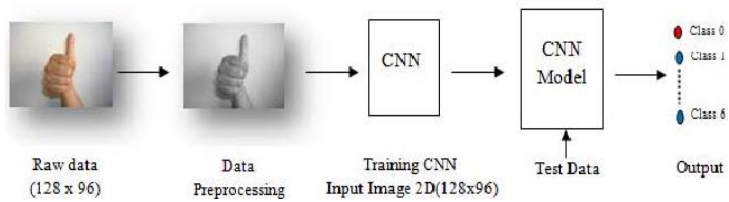
In computer vision, image segmentation is the process of partitioning a digital image into multiple segments sets of pixels, also known as image objects. The goal of segmentation is to simplify and/or change the representation of an image into something that is more meaningful and easier to analyze. Image segmentation is typically used to locate objects and boundaries in images. More precisely, image segmentation is the process of assigning a label to every pixel in an image such that pixels with the same label share certain characteristics.

5 Classification Based On Feature Expectation

Interesting part of an image from where the required informations are extracted is called as feature extraction. Once the frames of video are represented using feature expectation subgraphs, we can use them to classify and recognize anomaly. In this section, we will combine with convolutional neural network classifiers and feature expectation subgraphs to calibrate the classification of a single linear convolutional neural network classifier.

5.1 Convolutional Neural Networks (CNN)

Convolutional Neural Networks (CNN) (inspired by the mammalian visual cortex) is one of the most successful and widely used architectures in the deep learning community (especially for computer vision tasks). CNN's mainly consist of three types of layers: convolutional layers, where a sliding kernel is applied to the image (as in image convolution operation) features are extracted by a feature extraction layer; nonlinear layers are applied element-wise, enabling the network to model nonlinear functions; and pooling layers take a small neighborhood of the feature map and replace it with some statistical information (mean, max, etc.). Nodes in the CNN layers are locally connected; that is, each unit in a layer receives input from a small neighborhood of the previous layer (known as the receptive field). The main advantage of CNN is the weight sharing mechanism through the use of the sliding kernel, which goes through the images, and aggregates the local information to get the features. In contrast to a similar-connected neural network, CNNs have a significantly smaller number of parameters since the kernel weights are shared across the entire image. Moreover, the higher levels learn features from wider receptive fields through the stacking of multiple convolution layers



6 Results and Discussion

In this section, analyse the results of the proposed system which is implemented on the Android platform. The screenshots the experimental results our system. The gesture is detected Figure 3,4,5,6

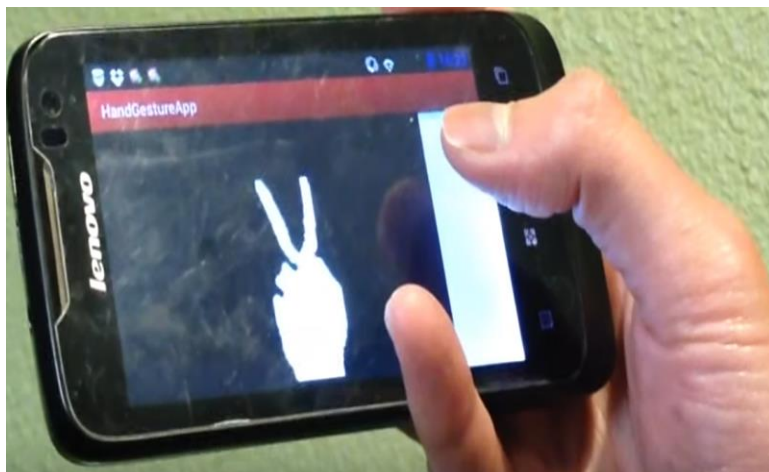


Figure 4: ImageClassification
39



Figure 5 Feature Extraction



Figure 6: App open

7 Conclusion

In this paper A novel system for dynamic hand gesture recognition via a combination of multiple deep learning techniques. The proposed system represented the hand gesture using local hand shape features as well as global body configuration features, which is very efficient for complicated structured hand gestures of the sign language. The openpose framework was used in this study for hand region detection and estimation. The proposed system was evaluated on a real and challenging sign language dataset. The experimental results showed that the proposed system outperformed state-of-the-art methods in terms of recognition rate, demonstrating its effectiveness.

8 Reference

1. S. Kausar and M. Y. Javed, "A survey on sign language recognition," in Proc. Frontiers Inf. Technol., Islamabad, Pakistan, Dec. 2011, pp. 95–98.
2. M. B. Waldron and S. Kim, "Isolated ASL sign recognition system for deaf persons," IEEE Trans. Rehabil. Eng., vol. 3, no. 3, pp. 261–271, Sep. 1995.
3. C. Chansri and J. Srinonchat, "Hand gesture recognition for thai sign language in complex background using fusion of depth and color video," ProcediaComput. Sci., vol. 86, pp. 257–260, Jan. 2016.
4. M.-H. Yang, N. Ahuja, and M. Tabb, "Extraction of 2D motion trajectories and its application to hand gesture recognition," IEEE Trans. Pattern Anal. Mach. Intell., vol. 24, no. 8, pp. 1061–1074, Aug. 2002.

Optimizing Spectrum Sensing For Energy Efficient Cognitive Radio Sensor Network

Abirami.S, Priyadharshini.P, Ragulya.S, Gayathiri.N,
Ms.ST.Preethi,
UG_student, Assistant Professor
Department of Computer science and Engineering,
MRK institute of Technology

Abstract

Designing energy-efficient cognitive radio sensor networks is important to intelligently use battery energy and to maximize the sensor network life. In this project a new spectrum sensing method is used to improve spectrum sensing performance and energy efficiency. It provide fast transmission to secondary users Fuzzy Cleans algorithm is used to estimate shortest path to the destination is calculated and data is transmitted with less energy consumption.. By continuously interacting and learning with the environment, the method guides the secondary user(SU) to select the channel with better channel quality. Moreover, we also propose a resource management and allocation mechanism with guaranteed QoS requirements for node traffic based on the framework of Lyapunov optimization theory. We design a low- complex online algorithm based on the optimization framework, which is then validated through extensive simulations. The results demonstrate that our design achieves higher accuracy with the QoS guarantee.

Smart Ration System Using Face Recognition

A.Ammeerunnish, Cse, ,Krishnasamy College of Engineering and Technology

R. Elavarasi, Cse, ,Krishnasamy College of Engineering and Technology

V. Lakshmi, Cse, ,Krishnasamy College of Engineering and Technology

T.Hemalatha, Cse, ,Krishnasamy College of Engineering and Technology

Abstract

Ration card plays a vital role for the household details such as to get gas connection, family member details; it acts as address proof etc. In this rag, we have wished-for a smart measure card system using Face Recognition Technique and IOT to thwart the derelictions and corruption in the current ration distribution system. In this system conventional quota card will be replaced by a Face Recognition system. This Faces will be verified with family members for authentication of the user. If user is found to be authentic then monthly quota of the ration available for the user is displayed. After successful transaction the database will be updated stating the ration content delivered to the user. This system will require very less human efforts for operation and is also very secure. By implementing this system government can keep track of all the delivered ration content very easily.

Key Words: Face Detection, Face Recognition, Capture Face, SMS, Purchase.

1 INTRODUCTION

The public distribution stores or ration stores use ration cards which are in the form of a book are used for general identification of the customer and holds the user's personal information and purchase history. On successful purchase, the details of purchase are entered in the card and in the purchase register at the employee's side. This is the system which exists at the ration stores now. This system has a lot of drawbacks. The ration card should be renewed every year by pasting additional leaves in the same card. There is a possibility of the ration card being torn. In some ration stores, dealers involve in malpractices like diverting food grains to open market to make profits. As a result there is a possibility of consumers sent back with a no stock sign even though there are food grains in stock. Having said the limitations imposed by the conventional ration system, we propose a solution in the form of a ration card system based on Face Recognition technology. The user will be authenticated and the user details are retrieved from the user database from the web server and are updated in the window application which is open in a computer system at the employee side. When the user asks for a particular quantity and type of food grain, the details are entered in the application by the employee and are updated in the web server. Additionally the users can check their purchase history and their details in the dedicated website by entering their registered username and password.

2 LITERATURE SURVEY

2.1 E-ration PDS using SMART CARD and GSM technology

Is an innovative approach in public distribution system (PDS) which is very useful, efficient, accurate, and automated distribution of ration distribution system. Presently ration distribution system has drawbacks like inaccurate quantity of goods, large waiting time, low processing speed and material theft in ration shop. Main objective of the designed system is to replace manual work with the atomization of ration shop to have a transparency in PDS. Proposed E-ration shop for public distribution system replaces conventional ration card by smart cards which consist of all the details about the card holder like family details, type of card and its validity etc.

2.2 Ration card plays a vital role for the household details

To get gas connection, family member details; it acts as address proof etc. In this paper, we have proposed a smart ration card system using Radio Frequency Identification (RFID) Technique and IOT to prevent the malpractices and corruption in the current ration distribution system.

In this system conventional ration card will be replaced by a unique RFID tag. This RFID tag will be verified at the fair price shop for the authentication of the user. The user's identity will be verified by microcontroller which is connected to an Amazon Web Services (AWS) database. For added security One Time Password (OTP) is also sent to user's registered mobile number which needs to be entered in the system

2.3 System is to reduce forgery from ration shops

The users will get their grocery in easy way. Also to reduce manual work. In this system we will develop the smart ration card system based on the RFID and the BIOMETRICS, in which the user can fill their data online. And also the manual working is not there. When user wants a ration, he/she comes with the Smart ration card, then the card is swiped and checked whether the user is valid or not. The fingerprints of that user also checked and the allocated ration is distributed to that particular user, changes of adding and issuing of ration is done automatically in the government database.

3 PROPOSED SYSTEM

The Smart ration card system uses Face Recognition. This system successfully eliminates the errors due to manual monitoring of ration data as all the data is automatically updated in the cloud-based database. Also this system will enable the government to keep track of the consumers and their transactions. Although the system will reduce the security issues and malpractices present in the current PDS the starting cost of the system is high. To access the database and authentication of user requires internet connectivity which can be a problem in remote locations.

3.1 ALGORITHM LBPH ALGORITHM

LBPH (Local Binary Pattern Histogram) is a Face-Recognition algorithm it is used to recognize the face of a person. It is known for its performance and how it is able to recognize the face of a person from both front face and side face.

3.2 CNN LAYER

3.2.1 Convolutional

The convolution procedure brings a solution to this problem as it reduces the number of free parameters, allowing the network in the direction of being deeper with fewer parameters

3.2.2 Pooling

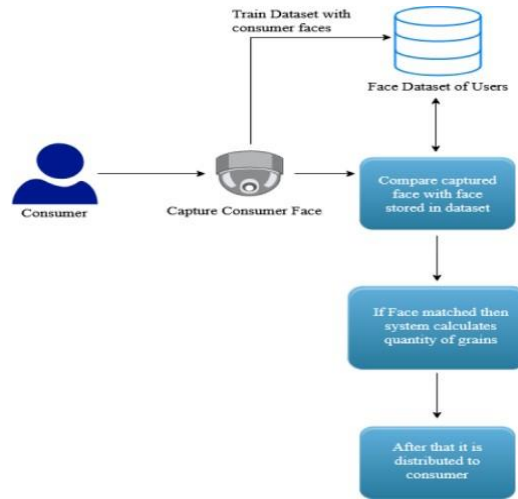
Convolutional networks may include global pooling covers to streamline the underlying multiplication. Sharing layers reduce the dimensions of the data by mingling the harvests of neuron clusters at one and only deposit into a single neuron in the next layer. Local pooling combines small clusters, normally 2×2 . Comprehensive pooling acts proceeding all the neurons of the convolutional layer. Trendy addition, pooling may reproduce a max or an averaging. Max pooling through integrating uses the thorough going value beginning each of a cluster of neurons at the prior sheet. Average pooling amalgamates uses the middling value from each of a gathering of neurons at the prior layer.

3.2.3 Fully connected

Abundantly connected withdrawals connect every single neuron in one layer en route for every neuron in a new layer. It is fashionable assessment the same as the traditional multi-layer perceptron neural complex (MLP). The compacted matrix goes through a effusively connected withdrawal to classify the images.

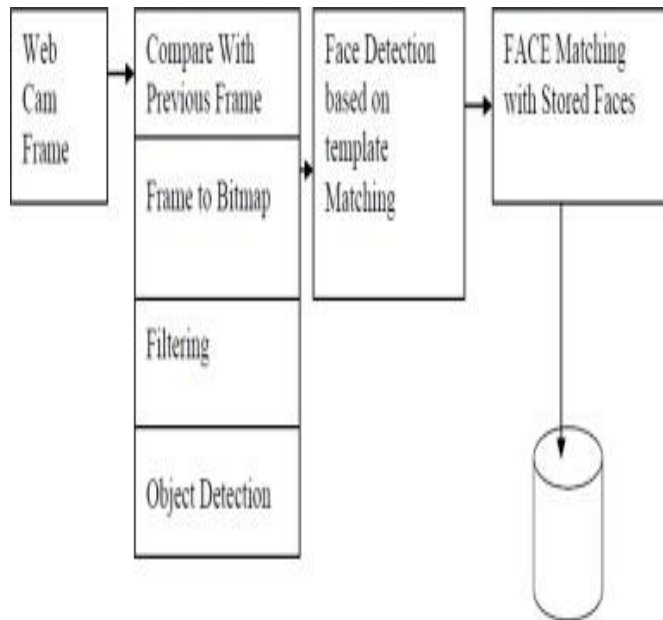
3.2.4 Receptive field

Up-to-the-minute neural complexes, every single neuron bring together input from some encryption of localities in the previous deposit. In an abundantly discrete layer, each one neuron convey together input foundation every single detachment of the previous layer. Contemporary a convolutional layer, neurons collect input on or after individual a controlled subarea of the aforementioned layer. Typically the subarea is of a square shape (e.g., size 5×5). The participation area of a neuron represent called its concerned field. Weights Each one neuron in a neural linkage divides an output assessment by spread over a unambiguous function to the input values coming beginning the approachable field in the previous layer. The function that is applied to the input values is firm by a vector of weights and a preference (typically real numbers).



ARCHITECTUR DIAGRAM

Flow Chart



4 CONCLUSION

The Smart ration card system uses Face Recognition algorithm. This system successfully eliminates the errors due to manual monitoring of ration data as all the data is automatically updated in the cloud based database. Also this system will enable the government to keep track of the consumers and their transactions. Although the system will reduce the security issues and misuse of ration in the current PDS the starting cost of the system is high. To access the database and authentication of user requires internet connectivity which can be a problem in remote locations.

5 REFERENCES

- [1] Gaikwad PriyaB.. Prof. Sangita Nikumbh , “E – Public distribution system using SMART card and GSM technology” International Conference on Intelligent Sustainable Systems(ICISS 2017) IEEE ISBN:978-1-5386-1959-9
- [2] Mrs. Subhasini Shukla, Mr. Akash Patil, Mr. Brightson Selvin , “A Step Towards Smart Ration Card System Using RFID & IOT” , IEEE International Conference on Inventive Communication and Computational Technologies(ICICCT), 2017
- [3] Prof. Shital A. Aher, Akshay D. Saindane, Suved P. Patil, Shivsagar K. Chakor , “Smart Ration Card Using RFID and Biometrics ”, Vol-3 Issue-2 2017, IJARIE-ISSN(O)-2395-4396,2017
- [4] Vinayak T. Shelar, Mahadev S. Patil , “RFID and GSM based Automatic Rationing System using LPC2148”, International Journal of Advanced Research in Computer Engineering & Technology(IJARCET) Volume 4 Issue 6, June 2015
- [5] Anshu Prasad, Aparna Ghenge, Sonali Zende, Sashikala Mishra, Prashant Godakh, “Smart Ration Card Using RFID, Biometrics and SMS Gateway”, IEEE International Conference on Inventive Communication and Computational Technologies(ICICCT), 2017
- [6] Dr. M. Pallikonda Rajesekaran, D. Balaji, P. Daniel”, Automatic Smart Ration Distribution System for Prevention of Civil Supplies Hoarding In India”, 2017 International Conference on Advanced Computing and Communication Systems (ICACCS -2017), Jan. 06 – 07, 2017, Coimbatore, INDIA.

Modified Secure Multi Clouds Mobile Computing for the Data Computing in Cloud

.A. Akilan, R.Aadhithyan, S.Dinesh, S.Karthikeyan, , Computer Science Engineering, MRK Institute Of Technology, Cuddalore,India

Abstract— The rapid growth of mobile device (e.g., smart phone and bracelet) has spawned a lot of new applications. During which the requirements of applications are increasing, while the capacities of some mobile devices are still limited. In this project work, we focus on addressing the cloud migration oriented resource allocation problem among mobile cloud devices. Additionally, the proposed scheme can satisfy the public verifiability without requiring any trusted third party. Finally, we also develop a simulation implementation that demonstrates the practicality and efficiency of our proposal. Finally, we also develop a simulation implementation that demonstrates the practicality and efficiency of our proposal.

Keywords—Cloud storage, Data deletion, Data transfer, Counting Bloom filter, Public verifiability.

1 Introduction

Cloud computing, an emerging and very promising computing paradigm, connects large-scale distributed storage resources, computing resources and network bandwidths together[1,2]. By using these resources, it can provide tenants with plenty of high-quality cloud services. Due to the attractive advantages, the services (especially cloud storage service) have been widely applied[3,4], by which the resource-constraint data owners can outsource their data to the cloud server, which can greatly reduce the data owners' local storage overhead[5,6]. According to the report of Cisco[7], the number of Internet consumers will reach about 3.6 billion in 2019, and about 55 percent of them will employ cloud storage service. Because of the promising market prospect, an increasing number of companies (e.g., Microsoft, Amazon, Alibaba) offer data owners cloud storage service with different prices, security, access speed, etc. To enjoy more suitable cloud storage service, the data data transfer, integrity verification, verifiable deletion. These challenges, if not solved suitably, might prevent the public from accepting and employing cloud storage service.

2 Related works

Verifiable data deletion has been well studied for a long time, resulting in many solutions[12–18]. Xue et al. [19] studied the goal of secure data deletion, and put forward a key-policy attribute based encryption scheme, which can achieve data finegrained access control and assured deletion. They reach data deletion by removing the attribute and use Merkle hash tree (MHT) to achieve verifiability, but their scheme requires a trusted authority. Du et al. [20] designed a scheme called Associated deletion scheme for multi-copy (ADM), which uses pre-deleting sequence and MHT to achieve data integrity verification and provable deletion. However, their scheme also requires a TTP to manage the data keys. In 2018, Yang et al. [21] presented a Blockchain-based cloud data deletion scheme, in which the cloud executes deletion operation and publishes the corresponding deletion evidence on Blockchain. Then any verifier can check the deletion result by verifying the deletion proof. Besides, they solve the bottleneck of requiring a TTP. Although these schemes all can achieve verifiable data deletion, they cannot realize secure data transfer.

To migrate the data from one cloud to another and delete the transferred data from the original cloud, many methods have been proposed[22–26]. In 2015, Yu et al. [22] presented a Provable data possession (PDP) scheme that can also support secure data migration. To the best of our knowledge, their scheme is the first one to solve the data transfer between two clouds efficiently, but it's inefficient in data deletion process since they reach deletion by re-encrypting the transferred data, which requires the data owner to provide many information. Xue et al. [24] designed a provable data migration scheme,

which characterized by PDP and verifiable deletion. The data owner can check the data integrity through PDP protocol and verify the deletion result by Rank-based Merkle hash tree (RMHT). However, Liu et al. [25] pointed out that there exists a security flaw in the scheme of Ref.[24] and they designed an improved scheme that can solve the security flaw. In 2018, Yang et al. [26] adopted vector commitment to design a new data transfer and deletion scheme, which offers the data owner the ability to verify the transfer and deletion results without any TTP. Moreover, their scheme can realize data integrity verification on the target cloud.

3 The Proposed Scheme

In this part, we introduce our new scheme in detail. Notethat the cloud storage service provider must authenticate the data owner. For simplicity, we assume that the data owner has passed the identification and become a legal tenant of cloud A and cloud B. In our scenario, we aim to achieve verifiable data transferand deletion, which is similar to Ref.[26]. The main processes are shown in Fig.4. Firstly, the data owner encrypts the data and outsources the ciphertext to the cloud A. Then he checks the storage result and deletesthe local backup. Later, the data owner may change the cloud storage service provider and migrate some data from cloud A to cloud B. After that the data owner wantsto check the transfer result. Finally, when the data transfer is successful, the data owner requires the cloud A to remove the transferred data and check the deletion result.

3.1 Data encryption

To protect the data confidentiality, the data owner uses secure encryption algorithm to encrypt the outsourced file before uploading. For every data block C_i , the data owner randomly chooses a distinct integer a_i as the index of C_i and computes the hash values $H_i = H(\text{tagf} \parallel a_i \parallel C_i)$. Thus, the outsourced data set can be denoted as $D = ((a_1, C_1), \dots$

$(a_n, C_n))$. Firstly, the data owner sends D to the cloudA, along with the file tag tagf . Firstly, the data owner computes encryption key $k = H(\text{tagf} \parallel \text{SKO})$, and then uses k to encrypt the file $C = \text{Enc}_k(F)$, where Enc is an IND-CPA secure encryption algorithm. After that the data owner divides the ciphertext C into n' blocks, meanwhile, inserts $n - n'$ random blocks into the n' blocks at random positions, which can guarantee that the CBF will not be null after data transfer and deletion. Then the data owner records these random positions in a table P . For every data block C_i , the data owner randomly chooses a distinct integer a_i as the index of C_i , and computes the hash values $H_i = H(\text{tagf} \parallel a_i \parallel C_i)$. Thus, the outsourced data set can be denoted as $D = ((a_1, C_1), \dots, (a_n, C_n))$. Finally, the data owner sends D to the cloud A, along with the file tag tagf .

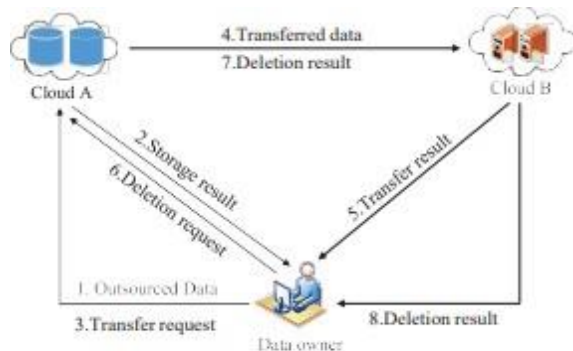


Fig. 4. The main processes of our scheme

3.2 Data outsourcing

The cloud A stores D and generates storage proof. Then the data owner checks the storage result and deletes the local backup. Upon receiving data set D and file tag tagf , the cloud A stores D , and uses the indexes (a_1, a_2, \dots, a_n) to construct accounting Bloom filter CBFs, where $i = 1, 2, \dots, n$. Meanwhile, the cloud A stores tagf as the index of D . Finally, the cloud A computes a signature $\text{sigs} = \text{SignSKA}(\text{storage} \parallel \text{tagf} \parallel \text{CBFs} \parallel \text{Ts})$, and sends the proof $\lambda = (\text{CBFs}, \text{Ts}, \text{sigs})$ to the data owner, where Sign is a ECDSA signature algorithm, Ts is a timestamp. On receipt of storage proof λ , the data owner checks its validity. Specifically, the data owner first checks the validity of the signature sigs . If sigs is invalid, the data owner quits and outputs failure; otherwise, the data owner randomly chooses half of the indexes from (a_1, a_2, \dots, a_n) to check the correctness of the CBFs. If the CBFs is not correct, the data owner quits and outputs failure; otherwise, the data owner deletes the local backup. Upon receiving data set D and file tag tagf , the cloud A stores D , and uses the indexes (a_1, a_2, \dots, a_n) to construct a counting Bloom filter CBFs, where $i = 1, 2, \dots, n$. Meanwhile, the cloud A stores tagf as the index of D . Finally, the cloud A computes a signature $\text{sigs} = \text{SignSKA}(\text{storage} \parallel \text{tagf} \parallel \text{CBFs} \parallel \text{Ts})$, and sends the proof $\lambda = (\text{CBFs}, \text{Ts}, \text{sigs})$ to the data owner, where Sign is a ECDSA signature algorithm, Ts is a timestamp.

3.3 Data transfer

When the data owner wants to change the service provider, he migrates some data blocks, even the whole file from the cloud B. Firstly, the data owner generates the index set of block indices ϕ , which will identify the data blocks that need to be migrated. Then the data owner computes a signature $\text{sig}_t = \text{SignSKO}(\text{transfer} \parallel \text{tagf} \parallel \phi \parallel T_t)$, where T_t is a timestamp. After that the data owner generates a transfer request $R_t = (\text{transfer}, \text{tagf}, \phi, T_t, \text{sig}_t)$, and then sends it to the cloud A. Meanwhile, the data owner sends the hash values $\{H_i\}_{i \in \phi}$ to the cloud B. On receipt of the transfer request R_t , the cloud A checks the validity of R_t . If R_t is not valid, the cloud A quits and outputs failure; otherwise, the cloud A computes a signature $\text{sig}_a = \text{SignSKA}(R_t \parallel T_t)$, and sends the data blocks.

3.4 Transfer check

The cloud B wants to check the correctness of the transfer and returns the transfer result to the data owner. Firstly, the cloud B checks the validity of the transfer request R_t and signature sig_a . If not both of them are valid, the cloud B quits and outputs failure; otherwise, the cloud B checks that whether the equation $H_i = H(\text{tagf} \parallel a_i \parallel m_i)$ holds, where $i \in \phi$. If $H_i \neq H(\text{tagf} \parallel a_i \parallel C_i)$, the cloud B requires the cloud A to send (a_i, C_i) again; otherwise, the cloud B goes to Step ii) The cloud B stores the blocks $\{(a_i, C_i)\}_{i \in \phi}$, and uses the indexes $\{a_i\}_{i \in \phi}$ to construct a new counting Bloom filter CBF_b . Then the cloud B computes a signature $\text{sig}_b = \text{SignSKB}(\text{success} \parallel \text{tagf} \parallel \phi \parallel T_t \parallel \text{CBF}_b)$. Finally, the cloud B returns the transfer proof $\pi = (\text{sig}_a, \text{sig}_b, \text{CBF}_b)$ to the data owner. Upon receipt of π , the data owner checks the transfer result. To be specific, the data owner checks the validity of the signature sig_b . Meanwhile, the data owner randomly chooses half of the indexes from set ϕ to verify the correctness of the counting Bloom filter CBF_b . If and only if all the verifications pass, the data owner trusts the transfer proof is valid, and the cloud B stores the transferred data honestly.

3.5 Data deletion

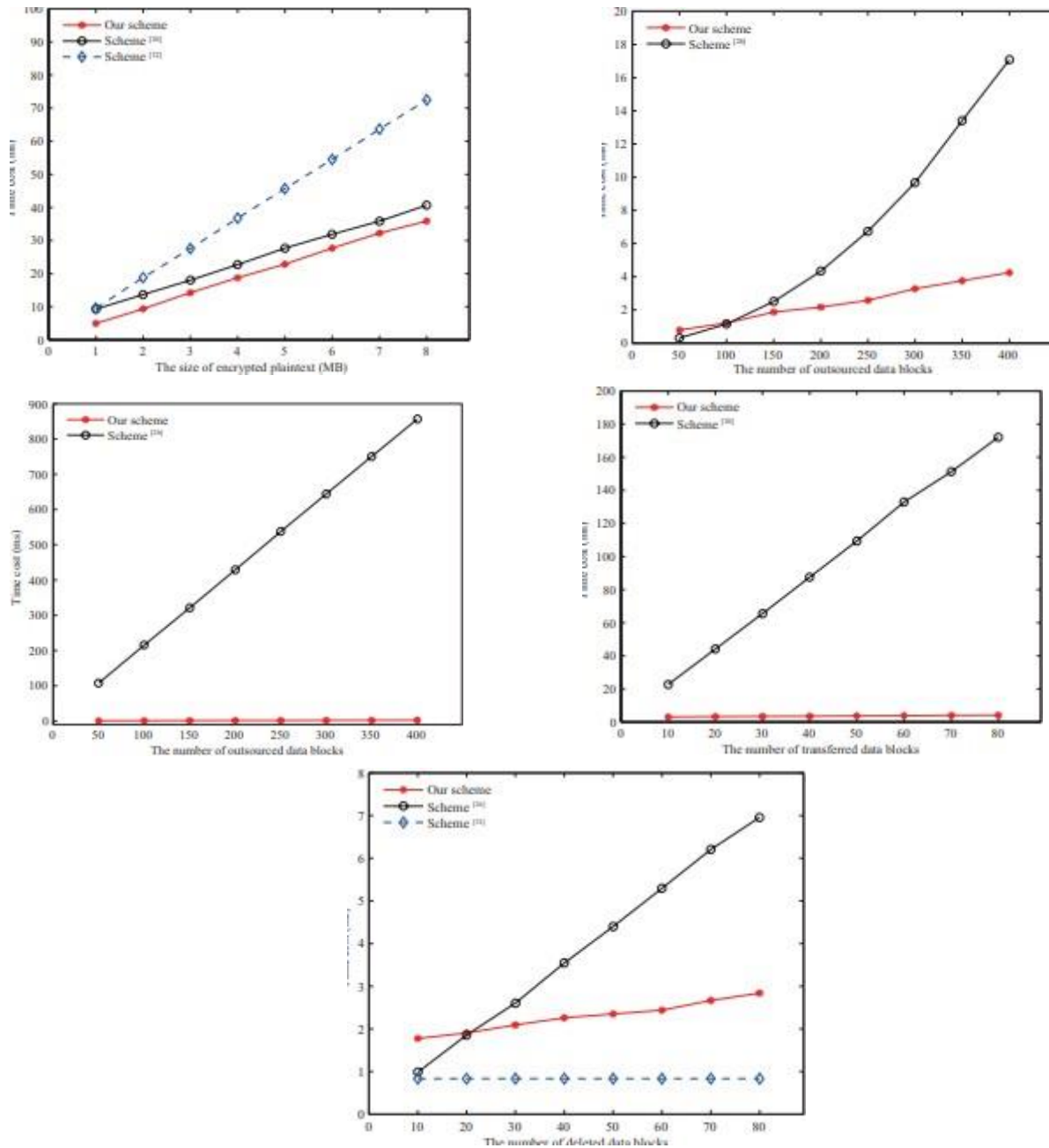
The data owner might require the cloud A to delete some data blocks when they have been transferred to the cloud B successfully. Firstly, the data owner computes a signature $\text{sig}_d = \text{SignSKA}(\text{delete} \parallel \text{tagf} \parallel \phi \parallel T_d)$, where T_d is a timestamp. Then the data owner generates a data deletion request $R_d = (\text{delete}, \text{tagf}, \phi, T_d, \text{sig}_d)$ and sends it to cloud A. Upon receiving R_d , the cloud A checks R_d . If R_d is invalid, the cloud A quits and outputs failure; otherwise, the cloud A deletes the data blocks $\{(a_i, C_i)\}_{i \in \phi}$ by overwriting. Meantime, the cloud A removes indexes $\{a_q\}_{q \in \phi}$ from the CBFs and obtains a new counting Bloom filter CBF_d . Finally, the cloud A computes a signature $\text{sig}_d = \text{Sign}(\text{delete} \parallel R_d \parallel \text{CBF}_d)$, and returns the data deletion evidence $\tau = (\text{sig}_d, \text{CBF}_d)$ to the data owner. After receiving τ , the data owner checks the signature sig_d . If sig_d is invalid, the data owner quits and outputs failure; otherwise, the data owner randomly chooses half of the indexes from ϕ to check the equations $\text{CBF}(a_q) = 0$ and determines if a_q belongs to the CBF_d . If the equations hold, the data owner trusts τ is valid.

4 Efficiency Evaluation

In this part, we provide the theoretical comparison among our scheme and two previous schemes [26,32]. From Table 1 we can have the following findings. Firstly, all of these three schemes can achieve verifiable data deletion. Secondly, our scheme and the scheme of Ref.[26] can realize provable data transfer, meanwhile, they can check the transferred data integrity on the new cloud, which is different from the scheme of Ref.[32]. Last but not least, our scheme and the scheme of Ref.[26] don't contain any TTP, while the scheme of Ref.[32] requires to introduce a TTP. Meanwhile, we analyze the theoretical performance and the results are listed as time complexities in Table 2, where the symbols E, S, V, Exp, H and P are respectively used to denote the data encryption, signature generation, signature verification, exponentiation in G1, hash computation and pairing calculation. Moreover, n and l respectively represent the total number of the data blocks and the number of the transferred/deleted data blocks. For simplicity, we ignore the communication overhead and other calculations, such as multiplication and addition.

5 Simulation results

We simulate our scheme and previous schemes [26,32] with the OpenSSL library and the PBC library on the same Linux machine equipped with 4 G main memory and Intel(R) Core(TM) i5-4590 processors that running at 3.30GHz. Moreover, we assume that $k = 20$, $m/n = 29$.



In encryption phase, we increase the file from 1MB to 8MB with a step for 1MB, and the number of the data blocks is fixed in 8000, then the time cost comparison is shown in Fig.5. We can find that the time cost of the three schemes will increase with the size of the encrypted data. However, the growth rate of our scheme is relatively lower than that of the scheme of Ref.[32], and almost the same with the scheme of Ref.[26]. Note that the time cost of our scheme is less than that of the other two schemes because the scheme of Ref.[26] needs much more hash computations to generate encryption keys, and the scheme of Ref.[32] needs more encryption operation to generate the MAC. Hence, we think our scheme is more efficient to encrypt the file. In storage phase, the computation overhead comes from storage proof generation and storage result verification. Fig.6 shows the time cost of storage proof generation. We find that the time of our scheme is much less than that of Yang et al.'s scheme of Ref.[26], and the growth rate of Yang et al.'s scheme of Ref.[26] is relatively higher than that of our scheme. Hence, our scheme is more efficient to generate the storage proof. Then the data owner checks

the storage result, and Fig.7 shows the performance comparison. We can find that the overhead of our scheme is much less than that of Yang et al.'s scheme of Ref.[26], because our scheme only needs to execute some hash calculations and a signature verification operation. But Yang et al.'s scheme of Ref.[26] needs to execute plenty of bilinear pairing computations. Finally, the data owner wants to delete the transferred data from cloud A, and we fix $n = 400$, then the performance evaluation is presented in Fig.9. The time overhead of Hao et al.'s scheme of Ref.[32] is almost constant. However, the time cost of our scheme and Yang et al.'s scheme of Ref.[26] will increase with the number of deleted data blocks, and the growth rate of Yang et al.'s scheme of Ref.[26] is relatively higher. Meanwhile, Yang et al.'s scheme of Ref.[26] costs much more time when the deleted data blocks are more than 20. So, we think that our scheme is more efficient to delete the transferred data blocks.

6 Conclusions and Future Work

In cloud storage, the data owner does not believe that the cloud server might execute the data transfer and deletion operations honestly. To solve this problem, we propose a CBF-based secure data transfer scheme, which can also realize verifiable data deletion. In our scheme, the cloud B can check the transferred data integrity, which can guarantee the data is entirely migrated. Moreover, the cloud A should adopt CBF to generate a deletion evidence after deletion, which will be used to verify the deletion result by the data owner. Hence, the cloud A cannot behave maliciously and cheat the data owner successfully. Finally, the security analysis and simulation results validate the security and practicability of our proposal, respectively.

Future work Similar to all the existing solutions, our scheme considers the data transfer between two different cloud servers. However, with the development of cloud storage, the data owner might want to simultaneously migrate the outsourced data from one cloud to the other two or more target clouds. However, the multi-target clouds might collude together to cheat the data owner maliciously. Hence, the provable data migration among three or more clouds requires our further exploration.

References

- [1] C. Yang and J. Ye, "Secure and efficient fine-grained data access control scheme in cloud computing", *Journal of High Speed Networks*, Vol.21, No.4, pp.259–271, 2015.
- [2] X. Chen, J. Li, J. Ma, et al., "New algorithms for secure outsourcing of modular exponentiations", *IEEE Transactions on Parallel and Distributed Systems*, Vol.25, No.9, pp.2386–2396, 2014.
- [3] P. Li, J. Li, Z. Huang, et al., "Privacy-preserving outsourced classification in cloud computing", *Cluster Computing*, Vol.21, No.1, pp.277–286, 2018.
- [4] B. Varghese and R. Buyya, "Next generation cloud computing: New trends and research directions", *Future Generation Computer Systems*, Vol.79, pp.849–861, 2018.
- [5] W. Shen, J. Qin, J. Yu, et al., "Enabling identity-based integrity auditing and data sensitive information hiding for secure cloud storage", *IEEE Transactions on Information Forensics and Security*, Vol.14, No.2, pp.331–346, 2019.
- [6] R. Kaur, I. Chana and J. Bhattacharya J, "Data deduplication techniques for efficient cloud storage management: A systematic review", *The Journal of Supercomputing*, Vol.74, No.5, pp.2035–2085, 2018.
- [7] Cisco, "Cisco global cloud index: Forecast and methodology, 2014–2019", available at: <https://www.cisco.com/c/en/us/solutions/collateral/service-provider/global-cloud-index-gci/paper-c11-738085.pdf>, 2019-5-5.
- [8] Cloudsfer, "Migrate & backup your files from any cloud to any cloud", available at: <https://www.cloudsfer.com/>, 2019-5-5.
- [9] Y. Liu, S. Xiao, H. Wang, et al., "New provable data transfer from provable data possession and deletion for secure cloud storage", *International Journal of Distributed Sensor Networks*, Vol.15, No.4, pp.1–12, 2019.
- [10] Y. Wang, X. Tao, J. Ni, et al., "Data integrity checking with reliable data transfer for secure cloud storage", *International Journal of Web and Grid Services*, Vol.14, No.1, pp.106–121, 2018.

Secure Message Communication Protocol For Warship Establishment

Arivumathi.V, CSE, MRK Institute of Technology
Jothika.S, CSE, MRK Institute of Technology
,Keerthana.S, CSE,MRK Institute of Technology
Ramalingam.S, CSE, MRK Institute of Technology

Abstract

Eliminate the Secure Message occurred by the two or more Warship communicating via optimal relay with centralized router using Warship network. The overall delay is reduced with increase in throughput. This project studies the Detection where detecting the dropper node. (Warship) is a important of wireless communication under Secure Message computing concept that describes a future where everyday physical objects will be connected to the Internet and be able to identify themselves to other Warship. It is the network of physical Warship, vehicles, buildings and other items embedded with electronics, software, sensors, actuators, and network connectivity that enable these objects to collect and exchange data. We also propose the application of discriminant analysis as a classification technique to select secure connections to improve the security of the DTN architecture.

User Choice-Based Alpha Numerical Random Password Generator For Securing the Data Assets

M.Saleth Reena ,CSE, SACET
Z.Asmathunnisa AP/CSE , SACET

Abstract

The users of computer technology and internet are increasing day by day. As the users are growing , the need for security is also felt very much. The data assets and other valuable facts are stored in the computer systems. One of the way to safe guard the data assets is to have a proper authorization method to access the data. This is achieved by user identification and password mechanism. The selection of password is important, since the entire authorization is dependent on the password. There is a wide range of password generator available through internet. However, they are not secure being generic in nature. Many users face problem in remembering complex passwords thereby increasing the probability of using older passwords. In this paper, a new technique is presented in which random complex passwords are generated from the choice of alphabets and numbers given by user. User can also decide the number of unique complex passwords required from the combination entered, thus making it more reliable and easy to remember as the passwords are generated from the choice of alphabets and numbers given by user as input. The password need to be strong enough to avoid brute force attack and other attacks. Here we discuss a method of generating random passwords, which are strong enough to combat the attacks.

1 Introduction

Password is a sequence of character string used to authenticate personal identity of user and to provide or refuse the access to system resources. The password is not only denying any access to the system from unauthorized person, but also prevent users who are previously logged in from doing unauthorized process in system. Security risk from unauthorized entry involves more than the risk to a single user via their system account[1]. User ID and password combination is the one of the simplest forms of user authentication. Password is a secret word, which is used to authorize the user to particular system or particular application. The identity of the user is tested using the password. If the passwords are not strong or easily guessable, the intruders can attack the system and attack the data assets.

Password is indispensable and inevitable one in numbers, and special characters, prohibited elements such as own name, D.O.B., address, telephone number. The aim of this paper is to provide an Automated Password Generator Model by specifying an algorithm to generate passwords for the protection of computer resources, which provides basic security criteria for the design, implementation, and use of passwords. The algorithm uses random numbers to select the characters that form the random passwords. The generated password is protected through encryption and decryption mechanism.

The length and diversity contribute to the size of the domain set containing all possible, that increases the difficulty of brute force detection [1]. They are minimum length, required categories such as upper and lower case, numbers, and special characters, prohibited elements such as own name, D.O.B., address, telephone number. The most difficult task is to remember the complex passwords thereby increasing the probability of user using older passwords. In this paper, a new technique is presented in which random complex passwords are generated from the choice of alphabets and numbers given by user. User can also decide the number of unique complex passwords required from the combination entered, thus making it more reliable and easy to remember as the passwords are generated from the choice of alphabets and numbers given by user as input. It is always easier to remember passwords resulting from the combinations given by user.

Users of High-Tech Devices such as tablets, smartphones always face a problem of unauthorized access. This illegitimate access leads to loss of user's important data and access to his/her private information. The effect of this leakage in access is worse in case the private data includes bank account details resulting in monetary loss. "Brute Force" attack is used by most of the attackers to guess users' password. Commonly used and simple passwords are easier to crack facilitating the invader to have control and access of users' device. A complex password is difficult to guess and is less susceptible to hackers' attack. Passwords are users' way of proving their authorization for the use of computing device. In case of multiple users operating a single computing device, each user has their own unique password to prove their authenticity. The generated password is protected through encryption and decryption mechanism.

Guessing attacks have had major business implications, such as a 2009 incident in which a vandal guessed a Twitter executive's password and was able to leak all of the company's internal documents [2]. Because of the scenario of widespread re-use of passwords across sites [3], an emerging attack model is to compromise accounts by a guessing attack against a low-security website and attempt to re-use the credentials at critical websites [4]. The length and diversity contribute to the size of the domain set containing all possible, that increases the difficulty of brute force detection [1]. Most organizations specify a password rules that form the requirements for the composition and usage of passwords. They are minimum length, required categories such as upper and lower case, which contain upper-case letters, lower-case letters, and numbers. They have highlighted that random passwords have several benefits over user-chosen passwords mainly security and confidentiality. DICEWARE generator produces random lists of words. This is based on the concept of memorization and the mental connection required to remember the password.

The following section of paper is organized as: Section 2 contains the Related works, Section 3 represents the proposed technique; Section 4 represents the results of proposed technique and section 5 concludes the paper.

2 Related Works

Art Conklin, Glenn Dietrich, Diane Walz [1] have discussed about conceptual model of password-based security across multiple systems connected by user activity. They have showed a light on user authentication with examples of user ID and password combination, one of the simplest forms of user authentication, smart card system where a user typically has an ID, a password, and also a time-generated passkey from the smart card which changes every 60 seconds. They have also discussed about human cognitive ability in remembering passwords, potential risks in weak passwords. According to them, adherence to password rules does produce passwords that are more difficult to break. They also recognized the problem of remembering it. Adherence to system rules produces passwords that are more difficult to discover.

Manoj Kumar Singh [5], proposed a method to exploit the artificial neural network to develop the more secure means of authentication, which is more efficient in providing the authentication. He discussed about architecture of neural Network, learning rule, target definition and process, which will apply for authentication. He has highlighted that neural network with intrusion detection capability can handle the challenge associated with password and authentication.

Michel D. Leonhard and V.N. Venkatakrishnan [6] analyzed three random password generation algorithms namely ALPHANUM, DICEWARE, and PRONOUNCE3. They used the metrics such as security, memorability and affinity to find out, which of the three methods produces best passwords. They used six character length random password, today's communication process and provides security to user's data Kamini H. Solanki and Chandni R. Patel [8] introduced new type of symmetric key cryptographic algorithm to improve the security of data. They have also used bit manipulation for encryption and decryption. The character is converted to ASCII and then converted to binary digits. The binary digits are complemented. The key constant 10 is multiplied with the complemented binary digit and the result is converted to hexadecimal value. They have proposed this algorithm to design and implement a new algorithm to address this issue of cost effectiveness to encrypt a small amount of data.

3 Proposed Work

In order to reduce the risk of password being cracked, the following points are taken care of:

- Short passwords are always easier to guess. Therefore, it's even mandatory for most of the companies to have to have long password with high complexity. Our technique allows the user to choose length of
- password to be generated.
- Longer and complex the password, more tedious job it is for the attacker to crack.
- Passwords must have blend of lower case and upper case letters, numbers, commas, and various signs. However, in our proposed technique, user is given the choice to enter digits, letter and special symbols. This makes it easier for the user to remember the password as it is generated out of letters, digits and special characters entered by user.
- It is always recommended to use different password for different devices. This reduces chance of single point of failure, i.e. if password of one machine is compromised, authentication of machines having different password still remains secure. In the mechanism proposed, users are given different complex passwords out of combination entered by them.

3.1 Proposed technique consists of following phases:

- User is asked for the choice of password to be generated among Complex password or PIN password.
- The second input from user is about the length of password required, i.e. basically number of characters in the password the user wants.
- Next input specifies the number of different password user wants to be generated of length specified in the above step.
- In this step, the user is asked to input letters, digits or special characters of his/her choice.
- Out of the characters input by user in the above step, combination of different complex passwords is generated.
- The maximum number of different pins that can be generated depends upon the length of pin required. Suppose a user enters 4 different numbers for a 4-digit PIN password. In this case, maximum number different PINs mathematically possible are $4!$ i.e. 24

3.2 Random Password Generator

Random password generator is to produce random password with high security. Generally, random passwords have various benefits over user-chosen password where it enhances security and confidentiality. The new methodology has been created to generate random password which consists of both upper & lower case letter and digits from 0 to 9, with fixed length. The alphanumeric is a simple algorithm that generates random password with predetermined length. The password generator algorithm selects a random character form random character list and forms the password, which is combination of numbers, lower & upper-case letters.

The total length of the password is 12. This algorithm produces the password with the combination of randomly selected lower-case character, upper-case character and numbers. The entire alphabet size is 62 [$10+26+26=62$], which indicates 10 digits (0 to 9), 26 upper-case letters and 26 lower-case letters. There are 62 possibilities of occurrence of each character in password. So the number of possible passwords is:

$$62 \times 62 \times 62 \times 62 \times 62 \times 62 \times 62 \times 62 \times 62 \times 62 \times 62 \times 62 = 62^{12}$$

3.3 Procedure

Step 1: Start the process

Step 2: Create random character list with numbers, upper & lower-case letters.

Step 3: Password must be in fixed length of 12.

Step 4: Create Random Password Generator method to generate the password.

Step 5: Random Password Generator chooses any of the three character set.

Step 6: The index position of any one of the characters from the random character set is returned.

Step 7: Append the characters selected through the index, one by one.

Step 8: Print the password.

Step 9: End.

4 Experimental Study

The concept is well experimented and demonstrated through the software program. Alpha-Numeric Random Password Generator Algorithm is tested by generating password for the users of a browsing centre. When the new users are registered in the browsing centre, all the details are stored in the server and the password is generated and sent to the user through a message. At each login, the users can use the randomly generated passwords. This provides security to the regular customer of a browsing centre, to safely maintain his/her work in the server based environment. Whenever the user is logging on to the system, he/she has to submit the respective user name and password. Password that is entered by the user is always being in the form of a plaintext but the information which is stored in the database is an encrypted form of the plain text. Hence, the plain text is converted between encrypted and decrypted form accordingly while comparing the user entered password and already stored password. The security measure is increased by storing the password using the encrypting and decryption method proposed in this paper.

4.1 Results And Discussion

The following were the results.

WELCOME TO SECURE PASSWORD GENERATOR

SELECT THE PASSWORD TEMPLATE:

1 for COMPLEX PASSWORD

2 for PIN PASSWORD

1

Enter the length of password required

6

Enter the no of diff. passwords

After getting the desired information, user is asked to input the characters of his/her choice out of which they want to the password to be generated. Fig 2 depicts the same.

Enter the length of password required

6

Enter the no of diff. passwords

3

Enter the Letters/ Numbers / Special Characters out of which you want your password to be generated

K@MALPR3ETS1NOH

As depicted in Fig 3, three different random passwords out of characters entered by user (Fig 2) are generated.

Your desired password:

1 : MR83NA

2 : 88RE15

3 : 8@EMNH

5 Conclusions

The password generated using alpha-numerical random password mechanism that was illustrated above is practical and can be used with great results. When the password is selected manually, most of the time, the users select the password that are related to himself or herself and related to any of the event. This gives the space for the intruders to deploy various attacks in breaking the passwords. The random generated passwords avoid this particular situation. One of the drawbacks could be the difficulty in memorizing the randomly generated password. But when comparing the security achieved through the randomly generated password, it is much preferable than the manually chosen password. The encryption and decryption standard provided here also strengthens the security measures. Since, the encryption and decryption standards are simple, it is cost effective. The above done work also creates awareness and interest to start exploring this field more.

References

- [1] Art Conklin, Glenn Dietrich, Diane Walz, "Password-Based Authentication: A System Perspective", Proceedings of the 37th Hawaii International Conference on System Sciences – 2004.
- [2] NikCubriloic, The Anatomy of the Twitter Attack, TechCrunch, July2009.
- [3] Thorsten Brantz and Alex Franz, The Google Web 1T 5-gram corpus, Technical Report LDC2006T13, Linguistic Data Consortium, 2006.
- [4] Mike Bond, Comments on authentication, [ww.cl.cam.ac.uk/~mkb23/research/GrdsureComments.pdf](http://www.cl.cam.ac.uk/~mkb23/research/GrdsureComments.pdf), 2008.
- [5] Manoj Kumar Singh, "Password Based a Generalize Robust Security System Design using Neural network", IJCSI-International Journal of Computer Science Issues, Vol. 4, No. 2, 2009.
- [6] Michael D. Leonhard, V. N. Venkatakrishnan, "A Comparative Study of Three Random Password Generators", IEEE EIT 2007 Proceedings.
- [7] Ayushi, "A Symmetric Key Cryptographic Algorithm", International Journal of Computer Applications, Volume 1 – No. 15, 2010.
- [8] Kamini H. Solanki, Chandni R. Patel, "New Symmetric Key Cryptographic algorithm for Enhancing Security of Data", International Journal of Research in Computer Engineering and Electronics, volume 1, issue 3, Dec 2012

Blind Assistance System with Voice Enabled and Real-Time Object Detection

S. Sri Ram, S. Syed Thameem P.A. Yokesh

Mrs E.Indhuma

Department of Computer Science Engineering
St. Anne's College Of Engineering And Technology

Abstract

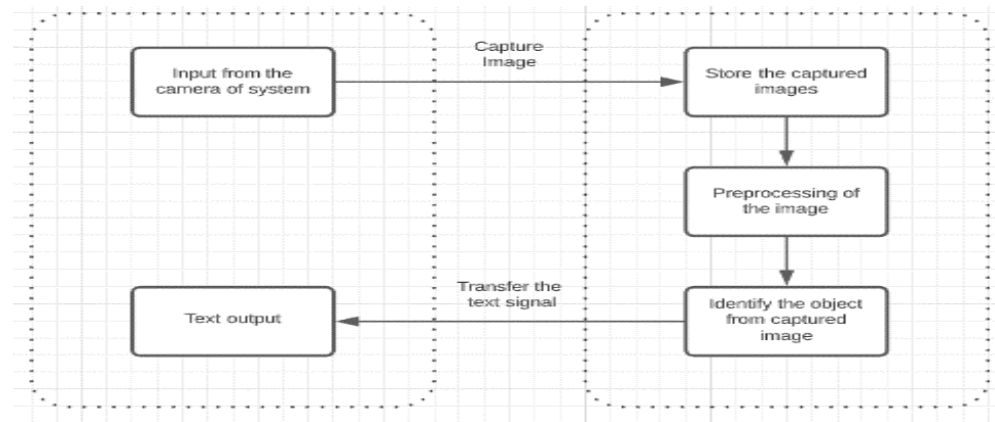
Real-time object detection is a difficult operation since it requires more computing power to recognize the object in real time. However, the data created by any real-time system is unlabeled, and effective training frequently necessitates a huge quantity of labelled data. Single Shot Multi-Box Detection is a quicker detection approach for real-time object detection, based on a convolution neural network model proposed in this paper (SSD). The feature resampling stage was eliminated in this work, and all calculated results were merged into a single component. Still, a light-weight network model is required for places with limited processing capability, such as mobile devices (eg: laptop, mobile phones, etc). In this suggested study, a light-weight network model called MobileNet is adopted, which uses depth-wise separable convolution. The usage of MobileNet in conjunction with the SSD model increases the accuracy level in detecting real-time household objects, according to the results of the experiments.

Keywords: Object Detection, TensorFlow object detection API, SSD with MobileNet.

1. Introduction

In today's advanced hi-tech environment, the need for self-sufficiency is recognised in the situation of visually impaired people who are socially restricted [3]. Visually impaired people encounter challenges and are at a disadvantage as a result of a lack of critical information in the surrounding environment, as visual information is what they lack the most [1]. The visually handicapped can be helped with the use of innovative technologies. The system can recognise items in the environment using voice commands and do text analysis to recognise text in a hard copy document. It may be an effective approach for blind persons to interact with others and may aid with their independence. Those who are wholly or partially blind are considered visually impaired. According to the World Health Organization (WHO), 285 million people worldwide suffer from vision impairment, 39 people are blind, and around 3% of the population of all ages is visually impaired [1][4]. Visually impaired people go through a lot and encounter a lot of difficulties in their daily lives, such as finding their way and directions, as well as going to places they don't go very often. In existing system (Fig.1.), system take surrounding information with help of webcam and then store the captured images. These images under goes preprocessing step and then identify the objects from the captured image and after that system will give output in text format [1][3].

2. Flow Chart Of Existing System

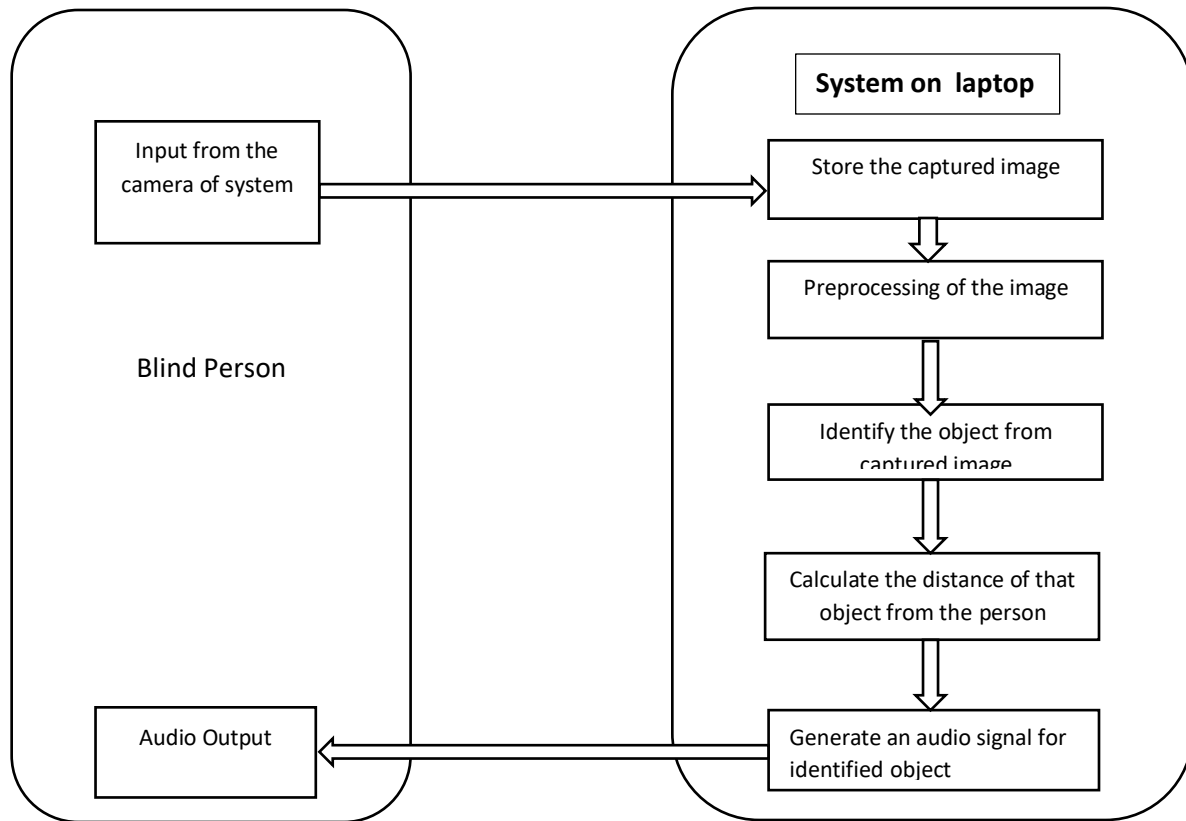


3. Working

Visually challenged people, on the other hand, cannot readily go outside for work. They are completely reliant on others. As a result, when they wish to walk outside, they will want assistance [12]. Our system's (Fig.2.) proposed design is based on the recognition of objects in the environment of a blind person. The proposed object/obstacle detection technology works in such a way that it requires various steps from frame extraction to output recognition. To detect items in each frame, a comparison between query frame and database objects is performed [3][8]. We present a system for recognizing and locating objects in photographs and videos. An audio file carrying information about each object detected is activated. As a result, both object detection and identification are addressed at the same time.

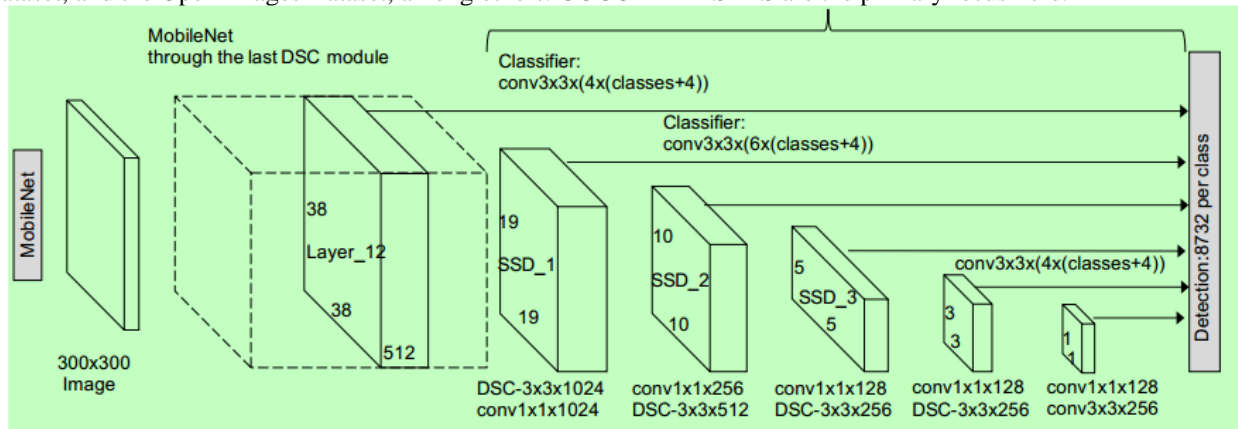
4. Methodology

- 1] The system is set up in such a way where an system will capture real-time frames.
- [2] The Laptop Based Server will be using a pre-trained SSD detection model trained on COCO DATASET. It will then test and the output class will get detected with an accuracy metrics.
- [3] After testing with the help of voice modules the class of the object will be converted into a default voice notes which will then be sent to the blind victims for their assistance.
- [4] Along with the object detection, we have used an alert system where approximate will get calculated. If that Blind Person is very close to the frame or is far away at a safer place , it will generate voice-based outputs along with distance units.



5. Tensor Flow

TensorFlow APIs were used to implement it. The benefit of using APIs is that they give a collection of common operations [5][9]. As a result, we don't have to write the program's code from start. They are both helpful and efficient, in our opinion. APIs are time savers since they give us with convenience. The TensorFlow object detection API is essentially a mechanism for building a deep learning network that can solve object detection challenges [5][11]. Their framework includes trained models, which they refer to as Model Zoo [3]. This contains the COCO dataset, the KITTI dataset, and the Open Images Dataset, among others. COCO DATASETS are the primary focus here.



Architecture of SSD

6 SSD

The SSD consists of two parts: an SSD head and a backbone model. As a feature extractor, the backbone model is essentially a trained image classification network. This is often a network trained on ImageNet that has had the final fully linked classification layer removed, similar to ResNet [3][1]. The SSD head is just one or more convolutional layers added to the backbone, with the outputs read as bounding boxes and classifications of objects in the spatial position of the final layer activations [3]. As a result, we have a deep neural network that can extract semantic meaning from an input image while keeping its spatial structure, although at a lesser resolution. In ResNet34, the backbone produces 256 7x7 feature maps for an input picture. SSD divides the image into grid cells, with each grid cell being in charge of detecting things in that region [1][7]. Detecting objects entails anticipating an object's class and placement inside a given region.

7 MobileNet

This model is based on the MobileNet model's idea of depthwise separable convolutions and generates a factorised Convolutionsv [7]. The depthwise convolutions are created by converting a basic conventional convolution into a depthwise convolution. Pointwise convolutions are another name for these 1 * 1 convolutions. These depthwise convolutions apply a general single filter based notion to each of the input channels for MobileNets to work. These pointwise convolutions use 1 * 1 convolution to combine the depthwise convolutions' outputs. Both filters, like a typical convolution, combine the inputs into a new set of outputs in a single step [1][7]. The depthwise identifiable convolutions partition this into two layers — one for filtering and the other for mixing. This approach of factorization has the effect of dramatically lowering computing time and model size.

8 Voice Generation Module

Following the detection of an object, it is critical to inform the person on his or her way of the presence of that object. PYTTSX3 is a crucial component of the voice generation module. Pyttsx3 is a Python conversion module for converting text to speech [8]. This library is compatible with Python 2 and 3. Pyttsx3 is a simple tool for converting text to speech. This technique works in the following way: everytime an item is identified, an approximate distance is calculated, and the texts are displayed on the screen using the cv2 library and the cv2.putText() function. We utilise Python-tesseract for character recognition to find buried text in an image. OCR recognises text content on images and encodes it in a format that a computer can understand [7]. The text is detected by scanning and analysing the image. As a result, Python-tesseract recognises and "reads" text encoded in images. These texts are also linked to a pyttsx.

As an output, audio commands are generated. "Warning: The object (class of object) is too close to you," it says if the thing is too close. And if the object is at a safe distance, a voice is generated that states, "The object is at a safe distance." This is accomplished using libraries like as pytorch, pyttsx3, pytesseract, and engine.io.

Pytorch is a machine learning library first and foremost [7][8]. Pytorch is primarily used in the audio field. Pytorch aids with the loading of the voice file in mp3 format.

9 Image-Processing:

Image processing is a technique for performing operations on a picture in order to improve it or extract relevant information from it [6].

"Image processing is the study and manipulation of a digital image, notably in order to increase its quality," says the fundamental definition of image processing.

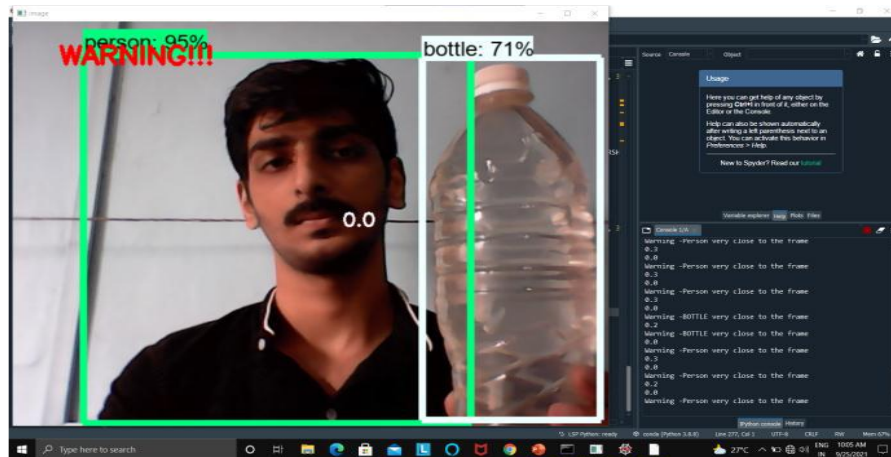
9.1 OPENCV:

OpenCV is a free, open-source computer vision library. This library includes functions and algorithms for motion tracking, facial identification, object detection, segmentation and recognition, and a variety of other tasks [7]. This library allows you to edit images and real-time video streams to meet your specific needs.

9.2 What is COCO?

The image dataset was built with the objective of improving image recognition, therefore COCO stands for Common Objects in Context. The COCO dataset offers demanding, high-quality visual datasets for computer vision, with the majority of the datasets containing state-of-the-art neural networks [12]. There are a total of 90 predefined objects in this data set.

10 Result



11 Conclusion & Feature

In this research, we attempted to recognise an object that was displayed in front of a webcam. TensorFlow Object Detection API frameworks were used to test and train the created model. Reading a frame from a web camera generates numerous problems, so a good frames per second solution is required to reduce Input / Output concerns [3]. As a result, we focused on threading methodology, which considerably improves frames per second and hence greatly reduces processing time for each item. Despite the fact that the application accurately identifies each thing in front of the webcam, it takes roughly 3-5 seconds for the object detected box to move over the next object in the video.

Using this study, we will be able to recognise and track objects in a sports field, allowing the computer to learn deeply, which is a Deep Learning application.

12 References

- [1] U. A. Hvidtfeldt, M. Ketzel, M. Sørensen et al., “Evaluation of the Danish AirGIS air pollution modeling system against measured concentrations of PM_{2.5}, PM₁₀, and black carbon,” *Environmental Epidemiology*, vol. 2, no. 2, 2018.
- [2] Y. Gonzalez, C. Carranza, M. Iniguez et al., “Inhaled air pollution particulate matter in alveolar macrophages alters local pro-inflammatory cytokine and peripheral IFN production in response to mycobacterium tuberculosis,” *American Journal of Respiratory and Critical Care Medicine*, vol. 195, p. S29, 2017.
- [3] L. Pimpin, L. Retat, D. Fecht et al., “Estimating the costs of air pollution to the National Health Service and social care: an assessment and forecast up to 2035,” *PLoS Medicine*, vol. 15, no. 7, Article ID e1002602, pp. 1–16, 2018.
- [4] F. Caiazzo, A. Ashok, I. A. Waitz, S. H. L. Yim, and S. R. H. Barrett, “Air pollution and early deaths in the United States. Part I: quantifying the impact of major sectors in 2005,” *Atmospheric Environment*, vol. 79, pp. 198–208, 2013.
- [5] B. Holmes-gen and W. Barrett, *Clean Air Future, Health and Climate Benefits of Zero Emission Vehicles*, American Lung Association, Chicago, IL, USA, 2016.
- [6] US Environmental Protection Agency (US EPA), “Criteria air pollutants,” *America’s Children and the Environment*, US EPA, Washington, DC, USA, 2015.
- [7] CERN, *Air Quality Forecasting*, CERN, Geneva, Switzerland, 2001.
- [8] G. E. Box and D. A. Pierce, “Distribution of residual autocorrelations in autoregressive-integrated moving average time series models,” *Journal of the American statistical Association*, vol. 65, no. 332, pp. 1509–1526, 1970.
- [9] C. L. Hor, S. J. Watson, and S. Majithia, “Daily load forecasting and maximum demand estimation using ARIMA and GARCH,” in *Proceedings of the 2006 International Conference on Probabilistic Methods Applied to Power Systems*, pp. 1–6, IEEE, Stockholm, Sweden, June 2006.
- [10] L. Y. Siew, L. Y. Chin, P. Mah, and J. Wee, “Arima and integrated arfima models for forecasting air pollution index in shah alam, selangor,” *He Malaysian Journal of Analytical Science*, vol. 12, no. 1, pp. 257–263, 2008.
- [11] J. Zhu, “Comparison of ARIMA model and exponential smoothing model on 2014 air quality index in yanqing county, Beijing, China,” *Applied and Computational Mathematics*, vol. 4, no. 6, p. 456, 2015
- [12] T. M. Mitchell, “Machine learning,” in *Proceedings of the IJCAI International Joint Conference on Artificial Intelligence*, Pasadena, CA, USA, July 2009.

VIDEO COMPRESSION

Mrs. Z. Asmathunnisa AP/CSE, St. Anne's CET
B.Dhivagar, CSE , St. Anne's CET
K.Rajesh, CSE, St. Anne's CET
P.A.Vasanth, CSE, St. Anne's CET

Abstract

Data Compression is a technique of reducing the amount of space data occupies, to ease the process of storage and communication. The fundamental process of compression involves using a well drafted technique to convert the actual data into the compressed data (smaller size). Depending upon how well a compression technique works and how much data can be regenerated from the compressed data given by a certain technique, the technique is classified as either as a lossy data compression technique or lossless data compression technique. Compression is the process of modifying, encoding or converting the bits structure of data in such a way that it consumes less space on storage disk. It enhances reducing the storage size of one or more data instances or elements. The technique of data compression can save storage capacity, speed up file transfer, and decrease costs for storage hardware and network bandwidth. The Compression techniques enables sending a data object or file quickly over a network or the Internet and in optimizing physical storage resources. Different methodologies have been defined for this purpose. There is a complete range of different data compression techniques available both online and offline working such that it becomes really difficult to choose which technique serves the best. A data compression algorithm developed in this article consumes less time while provides more compression ratio as compared to existing techniques. In this paper we represent a MPEG compression algorithm to compress the video files.

Keywords: *lossless compression, lossy compression, storage, MPEG.*

1 Introduction

The video data compression has wide implementation in computing services and solutions, specifically data communications. The video data compression works through several compressing techniques and software solutions that utilize data compression algorithms to reduce the data size. Data compression technique, also called compaction, the process of reducing the amount of data needed for the storage or transmission of a given piece of information, typically by the use of encoding techniques. Today, data compression is important in storing information digitally on computer disks and in transmitting it over communications networks.

Also compressed files are much more easily exchanged over the internet since they upload and download much faster. We require the ability to reconstitute the original file from the compressed version at any time. Data compression is a method of encoding rules that allows substantial reduction in the total number of bits to store or transmit a file.

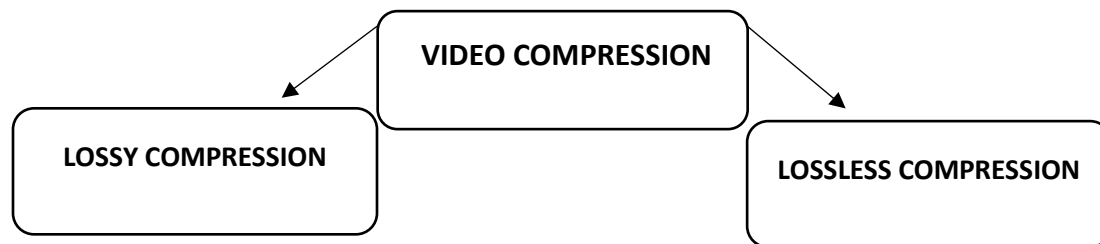
Compression technologies have been an enabler for the broadcast industry starting with the analogue television. Ever-increasing data from image and video capture require methods and techniques to reduce the amount of data to be transported or stored. Nearly over the last four decades MPEG Motion Pictures Expert Group - developed MPEG-1, MPEG-2, MPEG-4 and MPEG-H video compression standards. A given codec standard is developed with contribution from many researchers over a considerable time. ISO/MPEG and ITU have harmonised and standardised them. The following sections discuss briefly the process, advancements, trends and challenges.

For video coding standards, the core problem has remained the same over the years: reduce the size of stored or transmitted video data as much as possible while keeping the visual quality as close as possible to the original video. The convention when it comes to video coding standards has been to only define the bitstream format (syntax) and the decoder but not the encoder. This allows for cross-industry compatibility of the most critical component i.e. the decoder and at the same time. It allows for innovation and flexibility in the design of the encoding process, for example, meeting requirements of latency and availability of computational resources.

1.1 Types of Video Compression

Compression changes the original format of the video into a format supported by the video player. The video codec determines the format of the video. There are two mainly two types of video Compression:

- Lossy Compression
- Lossless Compression



1.1.1 Lossy Data Compression

Lossy compression involves eliminating some data permanently, especially for perceptual coding based on human colour perception. This method allows compressing the file to smaller sizes or low bit rate. However, the compression removes some data permanently, which affects the quality of the reconstructed image or video.

1.1.2 Lossless Data Compression

Lossless compression is a class of data compression that allows the original data to be perfectly reconstructed from the compressed data with no loss of information. Lossless compression is possible because most real-world data exhibits statistical redundancy. By contrast lossy compression permits reconstruction only of an approximation of the original data, though usually with greatly improves compression rates (and therefore reduced media sizes).

2 LITERATURE REVIEW

This section involves the Literature survey of various techniques available for video compression and analyzing their results and conclusions.

1: G.Suresh, P.Epsiba, Dr.M.Rajaram, Dr.S.N.Sivanandam “**A Low Complex Scalable Spatial Adjacency Acc-Det Based Video Compression Method**”,2010 proposed a video compression approach which tends to hard exploit the temporal redundancy in the video frames to improve compression efficiency with less processing complexity. Produces a high video compression ratio. Many experimental tests had been conducted to prove the method efficiency especially in high bit rate and with slow motion video. The proposed method seems to be well suitable for video surveillance applications and for embedded video compression systems.

2: Tzong-Jer Chen, Keh-Shih Chuang “**A Pseudo Lossless Image Compression Method**”,2010 present a lossless compression which modifies the noise component of the bit data to enhance the compression without affecting image quality. Data compression techniques substantially reduce the volume of the image data generated and thus increase the efficiency of the information flow. Method is information lossless and as a result, the compression ratio is smaller.

3: Qiang Liu, Robert J. Sclabassi, Mark L. Scheuer, and Mingui Sun “**A Two-step Method For Compression of Medical Monitoring Video**”2010 present a two-step method to compress medical monitoring video more efficiently. In the first step, a novel algorithm is utilized to detect the motion activities of the input video sequence. Then, the video sequence is segmented into several rectangle image regions (video object planes), which contain motion activities restricted within these windows. In the second step, the generated video object planes are compressed.

4: Raj Talluri, , Karen Oehler, Thomas Bannon, Jonathan D. Courtney, Arnab Das, and Judy Liao “**A Robust, Scalable, Object-Based Video Compression Technique for Very Low Bit-Rate Coding**” 1997 describes an object-based video coding scheme (OBVC) this technique achieves efficient compression by separating coherently moving objects from stationary background and compactly representing their shape, motion, and the content. In addition to providing improved coding efficiency at very low bit rates, the technique provides the ability to selectively encode, decode, and manipulate individual objects in a video stream. Applications of this object-based video coding technology include videoconferencing, video telephony, desktop multimedia, and surveillance video.

5: Ian Gilmour, R. Justin Dávila “**Lossless Video Compression for Archives: Motion JPEG2k and Other Options**” 2011 algorithm is clearly for end-user distribution through narrow bandwidths, and where no subsequent re-coding or re-purposing is required. The optimisation of image quality within individual frames allows true lossless data-reduction for applications such as archiving, where no loss of image quality is acceptable.

6: Yu cel Altunbasak, A. Murat Tekalp, and Gozde Bozdagi “**Two-Dimensional Object-Based Coding Using A Content-Based Mesh And Affine Motion Parameterization**” 1995 present a complete system for 2-D object-based video compression with a method for 2-D content-based triangular mesh design, two connectivity preserving affine motion parameterization schemes, two methods for temporal mesh propagation, a polygon-based adaptive model failure detection/coding scheme, and bitrate control strategies.

7: Raj Talluri “**A Hybrid Object-Based Video Compression Technique**” 1996 describes a hybrid object-based video coding scheme that achieves efficient compression by separating coherently moving objects from stationary background and compactly representing their shape, motion and the content. In addition to providing improved coding efficiency at very low bit rates.

3 Algorithm

The MPEG Compression

The MPEG compression algorithm encodes the data in 5 steps

First a reduction of the resolution is done, which is followed by a motion compensation in order to reduce temporal redundancy. The next steps are the Discrete Cosine Transformation (DCT) and a quantization as it is used for the JPEG compression; this reduces the spatial redundancy (referring to human visual perception). The final step is an entropy coding using the Run Length Encoding and the Huffman coding algorithm.

Step 1: Reduction of the Resolution

The human eye has a lower sensibility to colour information than to dark-bright contrasts. A conversion from RGB-colour-space into YUV colour components help to use this effect for compression. The chrominance components U and V can be reduced (subsampling) to half of the pixels in horizontal direction (4:2:2), or a half of the pixels in both the horizontal and vertical.

The subsampling reduces the data volume by 50% for the 4:2:0 and by 33% for the subsampling:

$$|Y| = |U| = |V|$$

$$4:2:0 = \frac{|Y| + \frac{1}{4}|U| + \frac{1}{4}|V|}{|Y| + |U| + |V|} = \frac{1}{2}$$

$$4:2:0 = \frac{|Y| + \frac{1}{2}|U| + \frac{1}{2}|V|}{|Y| + |U| + |V|} = \frac{2}{3}$$

MPEG uses similar effects for the audio compression, which are not discussed at this point.

Step 2: Motion Estimation

An MPEG video can be understood as a sequence of frames. Because two successive frames of a video sequence often have small differences (except in scene changes), the MPEG-standard offers a way of reducing this temporal redundancy. It uses three types of frames:

I-frames (intra), P-frames (predicted) and B-frames (bidirectional).

The I-frames are “key-frames”, which have no reference to other frames and their compression is not that high. The P-frames can be predicted from an earlier I-frame or P-frame. P-frames cannot be reconstructed without their referencing frame, but they need less space than the I-frames, because only the differences are stored. The B-frames are a two directional version of the P-frame, referring to both directions (one forward frame and one backward frame). B-frames cannot be referenced by other P- or Bframes, because they are interpolated from forward and backward frames. P-frames and B-frames are called inter coded frames, whereas I-frames are known as intra coded frames.

Step 3: Discrete Cosine Transform (DCT)

DCT allows, similar to the Fast Fourier Transform (FFT), a representation of image data in terms of frequency components. So the frame-blocks (8x8 or 16x16 pixels) can be represented as frequency components. The transformation into the frequency domain is described by the following formula:

$$F(u, v) = \frac{1}{4} C(u)C(v) \sum_{x=0}^{N-1} \sum_{y=0}^{N-1} f(x, y) \cdot \cos \frac{(2x+1)u\pi}{2N} \cdot \cos \frac{(2y+1)v\pi}{2N}$$

$$C(u), C(v) = 1/\sqrt{2} \text{ for } u, v = 0$$

$$C(u), C(v) = 1, \text{ else}$$

$$N = \text{block size}$$

The inverse DCT is defined as:

$$f(x, y) = \frac{1}{4} \sum_{u=0}^{N-1} \sum_{v=0}^{N-1} C(u)C(v)F(u, v) \cos \frac{(2y+1)v\pi}{16} \cos \frac{(2x+1)u\pi}{16}$$

The DCT is unfortunately computational very expensive and its complexity increases disproportionately ($O(N^2)$). That is the reason why images compressed using DCT are divided into blocks. Another disadvantage of DCT is its inability to decompose a broad signal into high and low frequencies at the same time. Therefore the use of small blocks allows a description of high frequencies with less cosine terms.

The first entry is called the direct current-term, which is constant and describes the average grey level of the block. The 63 remaining terms are called alternating-current terms. Up to this point no compression of the block data has occurred. The data was only well-conditioned for a compression, which is done by the next two steps.

Step 4: Quantization

During quantization, which is the primary source of data loss, the DCT terms are divided by a quantization matrix, which takes into account human visual perception. The human eyes are more reactive to low frequencies than to high ones. Higher frequencies end up with a zero entry after quantization and the domain was reduced significantly

$$F_{QUANTISED} = F(u, v) \text{ DIV } Q(u, v)$$

Where Q is the quantisation Matrix of dimension N. The way Q is chosen defines the final compression level and therefore the quality. After Quantization the DC- and AC- terms are treated separately. As the correlation between the adjacent blocks is high, only the differences between the DC-terms are stored, instead of storing all values independently. The AC-terms are then stored in a zig-zag-path with increasing frequency values. This representation is optimal for the next coding step, because same values are stored next to each other; as mentioned most of the higher frequencies are zero after division with Q

Step 5: Entropy Coding

The entropy coding takes two steps: Run Length Encoding (RLE) and Huffman coding . These are well known lossless compression methods, which can compress data, depending on its redundancy, by an additional factor of 3 to 4.

MPEG video compression consists of multiple conversion and compression algorithms. At every step other critical compression issues occur and always form a trade-off between quality, data volume and computational complexity. However, the area of use of the video will finally decide which compression standard will be used. Most of the other compression standards use similar methods to achieve an optimal compression with best possible quality

4 Future Enhancement

In Near future we are going to create a new algorithm either by combining a newly created algorithm with the existing one creating a hybrid system or else a standalone algorithm with a high compressing ratio and less loss of quality compared to the existing system which will be more effective.

5 Conclusion

The advantages of compression are reduction in storage hardware usage , data transmission time and communication bandwidth -- and the resulting cost savings. The compressed file also requires less time for transfer, and it consumes less network bandwidth than an uncompressed file.

References

- [1] Raj Talluri, Member, IEEE, Karen Oehler, Member, IEEE, Thomas Bannon, Jonathan D. Courtney, Member, IEEE, Arnab Das, and Judy Liao “A Robust, Scalable, Object-Based Video Compression Technique for Very Low Bit-Rate Coding”, IEEE TRANSACTIONS ON CIRCUITS AND SYSTEMS FOR VIDEO TECHNOLOGY, VOL. 7, NO. 1, FEBRUARY 1997.
- [2] G.Suresh, P.Epsiba, Dr.M.Rajaram, Dr.S.N.Sivanandam “A LOW COMPLEX SCALABLE SPATIAL ADJACENCY ACC-DCT BASED VIDEO COMPRESSION METHOD”, 2010 Second International conference on Computing, Communication and Networking Technologies.
- [3] Tarek Ouni, Walid Ayedi, Mohamed Abid “New low complexity DCT based video compression Method”, 2009 IEEE.
- [4] K.Uma, P.Geetha palanisamy, P.Geetha poornachandran “Comparison of Image Compression using GA, ACO and PSO techniques” , IEEE-International Conference on Recent Trends in Information Technology, ICRTIT 2011.
- [5] Tzong-Jer Chen, Keh-Shih Chuang “A Pseudo Lossless Image Compression Method”, 2010 3rd International Congress on Image and Signal Processing.
- [6] Nasir D. Memon, Khalid Sayood “Asymmetric Lossless Image Compression”, 2011IEEE
- [7] S.L. Lahudkar and R.K. Prasad “Real Time Video Compression implemented using adaptive block transfer/ motion compensation for lower bit rates” Journal of Engineering Research and Studies E-ISSN0976-7916.

Automation Using Iot In Greenhouse Environment

Jasmine Medona .A, CSE, St.Anne's college of Engineering and Technology, Anguchettypalayam.

Abstract

Green house is generally a building of small or large structures. The structure of the green house is made of walls and the translucent roof, with the capability of maintaining the planned climatic condition. It ensures the growth of plants that requires a specified level of soil moisture, sunlight, humidity and temperature. The green house systems available are human monitored systems that entail the continuous human visit causing distress to the worker and also decrease in the yield if the temperature and the humidity are not properly and regularly maintained. This paves way for the concept of the green house automation. The green house automation formed by the incorporation of the Internet of things and the embedded system addresses the problem faced in the green house and provides with the automated controlling and monitoring of the green house environment replacing the undeviating administration of the farmers. This paper also proposes the automation using internet of things in green house environment by using the Netduino 3 and employing the sensors for the sensing the moisture, temperature, sunlight and humidity, to enhance the production rate and minimize the discomfort caused to the farmers.

Keywords: *Green House, Automation, Internet of Things, Netduino 3, Atmospheric sensors*

1 INTRODUCTION

Due to the unexpected climatic changes that occur due to the global warming, human causes and many other natural causes such as the earth tilt, ocean currents etc. Growth of the seasonal crops such as the millets, beans, cotton and sugar cane gets affected causing a decrease in the production rate of those crops. So in order to maintain a proper climatic condition by perfectly controlling the temperature humidity, soil moisture and the luminous entailed by the crops the green house is preferred in most places. Green house structured with transparent sheets all over maintains perfect climatic conditions under the human monitoring. It requires a constant and periodic human monitoring to control the temperature, light intensity, soil moisture and the humidity to retain the required climatic condition that is entailed for the crop growth. It serves as protection against the climatic changes to extend the season for the growing the crops.

Despite the green house being very beneficial for the farmers as it increase the yield of the crops and production rate; it causes a discomfort for the farmers as they have to keep a periodic check on the green house by making regular visits and failure to maintain the perfect climatic conditions will result in the destruction of the crops and the production rate. The fig.1 below shows the general green-house for growing crops under human surveillance.

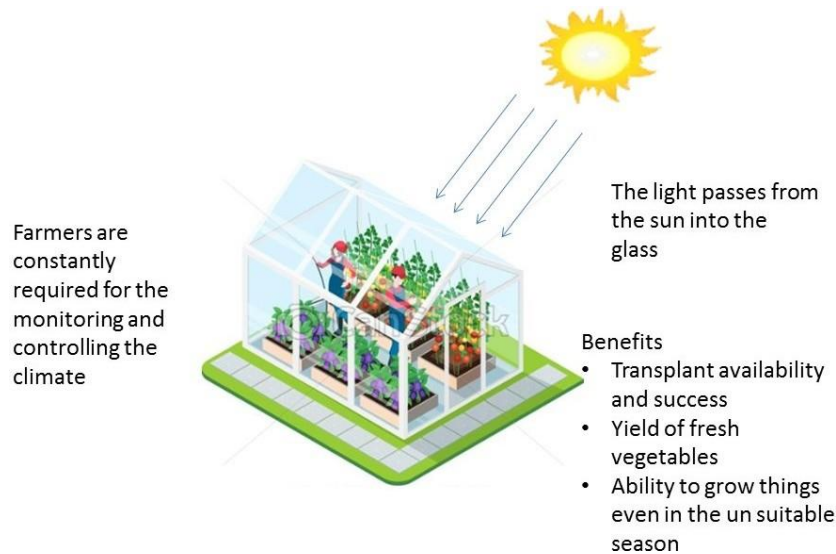


Fig.1 Structure of Green House

But the emergence of the sensors and the internet of things have changed the situation of the green-house. It has brought in the automation into the controlling and the surveillance of green-house by employing the sensors, internet of things and the embedded technology.

The paper puts forward the structure of the green house embedded with the internet of things, sensors and the Netduino 3 Wi-Fi to enable an automated monitoring and controlling in the green house.

The remaining of the paper is organized with the related works in the section 2. Proposed work in section 3, Results and Discussion in section. 4. and conclusion in section 5.

2 RELATED WORKS

The Internet of things have become the heart and soul for a wide range of applications by enabling a connectivity between the all the tangible things that are enabled with internet connection. The author Sreekantha et al [1], presents the literature survey on the internet of things for the online crop monitoring. He describes that the IOT enables an effective and an easy production of the crop, increasing the profits of the farmers. The Sensors also play a vital role in the monitoring of the crop growth by gathering information about the growth and sending them to the farmer's mobile devices for implementing the corrective measures. Suma, et al [2] the author strives to enhance the interest towards the agriculture by proposing an IOT based smart agriculture by providing a "remote control monitoring for sensing of the moisture, temperature, intruder, security and the leaf wetness using the GPS module" Yoon et al [3] the paper is about the farm system that is made smart by employing the low power blue tooth and communication module of low power wide area network. The controlling and the monitoring functions for the farm system is done by employing the MQ telemetry Transport" causing a progress in the agricultural IOT development. Vatari, et al [4], the author initiates a green-house environment combining the IOT and the Cloud, to control the system and enable the information to be stored respectively. Linlin et al [5], the implementation of the intelligent green-house environment is developed by the author using the internet of things, sensor and the infrared cameras Vimal et al [6], the author utilizes the Arduino based framework for the automated controlling and the monitoring of the environmental changes in a green-house Ferrandez et al [7].

3 PROPOSED WORK

To overcome the draw backs in the existing system, the proffered system uses the sensors to monitor the temperature, humidity, moisture and the light, the sensors are connected to the input pins of the Netduino and the output from the Netduino is given to the motors and the relays to regulate the flow of the climatic condition. Based on the threshold value set for the temperature, moisture, humidity and the light the Netduino operates the driver circuit to regulate the flow of the of the air and the temperature. The Wi-Fi connectivity in the Cloud enables to transmit the information gathered from the sensors to the cloud and gets stored in the cloud data base. The information stored in the cloud is regularly transmitted to the farmer’s mobile device over the internet to initiate a remote monitoring. This enables to elude the human to machine interaction and provides a machine to machine interaction.

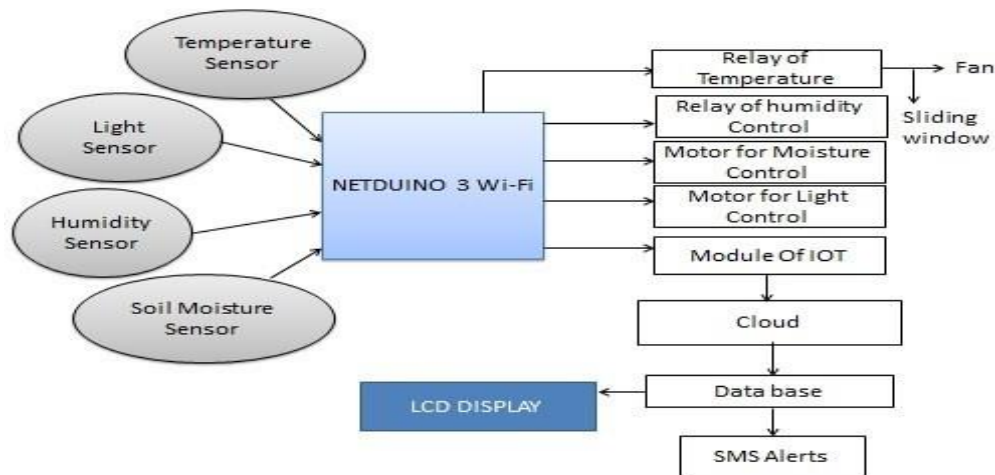


Fig .2 Proposed Structure

The proffered internet of things platform provides an automated form of green- house environment enabling a significant connections among the people and the tangible things around, it allows a real time information gathering, analysis, processing and meditation employing the social networking that are connected through an application interface that is open source to aid variety of platforms. The system put forward for providing the automated controlling and monitoring gathers and conveys the sensor information using the Google cloud IOT core, to have an anywhere and a anytime access of the information that are sensed in the green house, this would enable production rate increase and be beneficial for the farmers reducing the weariness in them.

HARDWARE USED

3.1.1 NETDUINO 3 Wi-Fi

The Netduino is open source hardware, and ensures the execution of the application that was constructed with the Dot Net frame work. The Netduino is capable of and are utilized in constructing any connected thing. It resembles the conception of the Arduino. The Netduino is more effective and provides a robust hardware. The Netduino is the vital core of our this project, it is a single board, built with the Cortex-M4 @168Mhz, flash memory of 1408 KB, RAM of

164+ KB , inbuilt Wi-Fi, Bluetooth connectivity and has network connectivity with 802.11b/g/n with SSL /TLS 1.2 support. It is powered with the built in USB adapter and accepts input voltage of 5V to 12V. The steps to run the Netduino initiates with the installation of the Netduino on the SD card Slot, the python programming is done on the windows platform. The programming of the Netduino and the application programming are run simultaneously using the XMING .



Fig .3 Netduino 3 Wi-Fi

3.1.2 Soil moisture sensor

The automated system utilizes the YL69 moisture sensor to sense the moisture in the soil. The soils moisture sensor is powered by the operating voltage of 3.3v to 5v and current of 35mA. The tow electrodes found in the moisturizer are placed in contact with the soil. Initially when it is placed into the soil the voltage fluctuates, an increase in the voltage is found if the soil moisture is less and voltage decrease with the increase in the soil moisture. [4, 5, 6, 9]

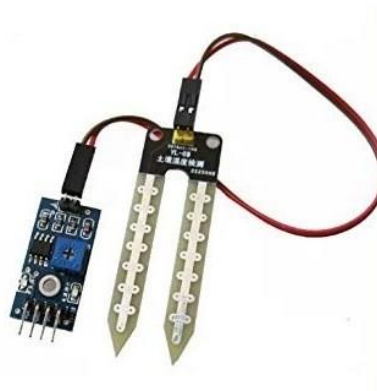


Fig. 4 Moisture Sensor

3.1.3 Humidity and temperature sensor

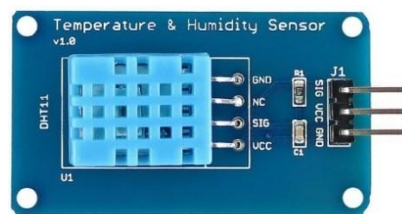


Fig.5 Temperature and Humidity Sensor (DTH11)

It is a digital sensor to monitor and gather information about the temperature and humidity that is prevailing in the green house. It is operated in the voltages of the 3 to 5 volts with the maximum current of 2.5mA. Range for the temperature is fixed to zero degree to fifty degree and the humidity percentage is set in between 20 to 80 percentages. The thermistor present inside engages a negative temperature coefficient and component to sense the humidity to identify the moisture content in the air.

3.1.4 Light sensor

This enables an incorporated control of the green house environments; GL5528 detects the light intensity of the environment. It is powered by the input voltage of 5V. The output voltage of the light sensor changes based on the light intensity whenever the light intensity increases the voltages sensed at the output is very high and when the intensity of the light decreases the output voltage decreases.



Fig.6 Light Sensor

Along with the sensors the motor driver circuit IC L293D along with the coolers and the sliding windows are set to assist the motor to run and retain the temperature for regulating the air flow within the green house.

4 Results and Discussion

The hard ware setup of the proffered system consisting of the Netduino 3 Wi-Fi, temperature sensor, moisture sensor humidity sensor, motors used along with the coolers and the sliding window is given below in Fig.7



Fig .7 Hardware Setup

The fig.8 below is the snapshot of the result visualized by employing the automated greenhouse system that is equipped with the coolers, sliding windows and the sensors. The fig.9 below is the SMS Alerts transmitted to the user on regular intervals.



Fig .8 Results Acquired



Fig.9 SMS Alert

5 Conclusion

The automated system for the green house management (control and monitoring) in the paper is done by employing the sensors of temperature, moisture, humidity and light for the monitoring of the environmental changes and the Netduino to regulate the driver circuits to maintain the normal climatic conditions within the green house. The remote monitoring and the control of the green house is enabled in the system using the IOT platform and the cloud services that store the information and sends the regular SMS alters to the farmer about the room conditions. The Wi-Fi connectivity in built in the Netduino enables an easy information transfer to the cloud. The Google Cloud IOT core used in the system enables the conveyance of the information gathered about the green house to the farmers. The

proffered system using the Netduino ensures production increase and a stress reduction for the farmers providing a capable automated system for green house management with a SMS alters to the users.

6 References

- [1] Sreekantha, D. K., and A. M. Kavya. "Agricultural crop monitoring using IOT-a study." In *2017 11th International Conference on Intelligent Systems and Control (ISCO)*, pp. 134-139. IEEE, 2017.
- [2] Suma, N., Sandra Rhea Samson, S. Saranya, G. Shanmugapriya, and R. Subhashri. "IOT based smart agriculture monitoring system." *International Journal on Recent and Innovation Trends in computing and communication* 5, no. 2 (2017): 177-181.
- [3] Yoon, Chiyurl, Miyoung Huh, Shin-Gak Kang, Juyoung Park, and Changkyu Lee. "Implement smart farm with IoT technology." In *2018 20th International Conference on Advanced Communication Technology (ICACT)*, pp. 749- 752. IEEE, 2018.
- [4] Vatari, Sheetal, Aarti Bakshi, and Tanvi Thakur. "Green house by using IOT and cloud computing." In *2016 IEEE International Conference on Recent Trends in Electronics, Information & Communication Technology (RTEICT)*, pp. 246-250. IEEE, 2016.
- [5] Linlin, Qin, Lu Linjian, Shi Chun, Wu Gang, and Wang Yunlong. "Implementation of IOT-based greenhouse intelligent monitoring system." *Transactions of the Chinese Society for Agricultural Machinery* 46, no. 3 (2015): 261- 267.
- [6] Vimal, P. V., and K. S. Shivaprakasha. "IOT based greenhouse environment monitoring and controlling system using Arduino platform." In *2017 International Conference on Intelligent Computing, Instrumentation and Control Technologies (ICICT)*, pp. 1514-1519. IEEE, 2017.
- [7] Ferrández-Pastor, Francisco, Juan García-Chamizo, Mario Nieto-Hidalgo, Jerónimo Mora-Pascual, and José Mora- Martínez. "Developing ubiquitous sensor network platform using internet of things: Application in precision agriculture." *Sensors* 16, no. 7 (2016): 1141.
- [8] Zhao, Ji-chun, Jun-feng Zhang, Yu Feng, and Jian-xin Guo. "The study and application of the IOT technology in agriculture." In *2010 3rd International Conference on Computer Science and Information Technology*, vol. 2, pp. 462-465. IEEE, 2010.
- [9] Muthupavithran, S., S. Akash, and P. Ranjithkumar. "Greenhouse monitoring using internet of things." *International Journal of Innovative Research in Computer Science and Engineering* 2, no. 3 (2016).
- [10] Mekala, Mahammad Shareef, and P. Viswanathan. "A Survey: Smart agriculture IoT with cloud computing." In *2017 international conference on microelectronic devices, circuits and systems (ICMDCS)*, pp. 1-7. IEEE, 2017.

Drowsiness Detection of Driver by using Transfer Learning of Deep Learning

N.Kanishya ,Cse, *Krishnasamy College of Engineering and Technology*
B. Ranjani, Cse, *Krishnasamy College of Engineering and Technology*
A.Reshma, Cse, *Krishnasamy College of Engineering and Technology*
V.Sindhu, Cse, *Krishnasamy College of Engineering and Technology*
P.M.Kamatchi. Cse, *Krishnasamy College of Engineering and Technology*

Abstract

This project presents the development of an ADAS (advanced driving assistance system) focused on driver drowsiness detection, whose objective is to alert drivers of their drowsy state to avoid road traffic accidents. In a driving environment, it is necessary that fatigue detection is performed in a non-intrusive way, and that the driver is not bothered with alarms when he or she is not drowsy. Our approach to this open problem uses sequences of images that are 10 s long and are recorded in such a way that the subject's face is visible. To detect whether the driver shows symptoms of drowsiness or not, two alternative solutions are developed, focusing on the minimization of false positives. The first alternative uses a recurrent and convolutional neural network, while the second one uses deep learning techniques to extract numeric features from images, which are introduced to Transfer Learning. The accuracy obtained by both systems is similar: around 70% accuracy over training data, and 65% accuracy on test data. However, the Transfer Learning stands out because it avoids raising false alarms and reaches a specificity (proportion of videos in which the driver is not drowsy that are correctly classified) of 95%.

Keywords: ADAS; drowsiness; deep learning; convolutional neural networks; recurrent neural networks; Transfer Learning; computer vision

1. Introduction

Drowsy driving is the dangerous combination of driving and sleepiness or fatigue. This usually happens when a driver has not slept enough, but it can also happen because of untreated sleep disorders, medications, drinking alcohol, or shift work.

No one knows the exact moment when sleep comes over their body. Falling asleep at the wheel is clearly dangerous but being sleepy affects your ability to drive safely even if you don't fall asleep. Drowsiness:

- Makes you less able to pay attention to the road.
- Slows reaction time if you must brake or steer suddenly.

For this work, our premise is the following: a camera mounted on a vehicle will record frontal images of the driver, which will be analyzed by using artificial intelligence(AI) techniques such as Deep Learning.

For this work, our premise is the following: a camera mounted on a vehicle will record frontal images of the driver, which will be analyzed by using artificial intelligence (AI) techniques such as Deep Learning.

Thus, the main novelty of this work is the use of a non-intrusive system that is capable of detecting fatigue from sequences of images, which at the moment is an open problem. In most of the available works, the experimental methodology consists of extracting and classifying individual frames from each video and verifying whether the classification is correct or not, but that approach does not consider the intrinsic relationship between consecutive images, and their measures of false positives are less reliable. Currently, there are few works that test the systems on complete videos and count the number of alarms emitted during each video (which is necessary when evaluating the number of false alarms raised during a period of time). Therefore, the proposals presented in this paper can be considered a starting point for the design of such systems.

An important concept related to CNNs is transfer learning. This technique consists of using a model that was previously trained to solve a different problem on a similar domain (e.g., detecting dogs in images), and use it to solve a new problem (e.g., detecting cats). The idea is to create a new CNN in which the first layers correspond

to the lower layers of the pre-trained model and the upper layers are new layers adapted and trained to solve the new proposed problem. In this way, the knowledge acquired by the pre-trained model serves as a starting point for the new model. This technique is especially useful to generate accurate models with a small amount of data, where it would not be feasible to train a model from scratch, and, on the other hand, it is useful to reach high accuracy with few training epochs.

In this context, we propose two different solutions to approach the fatigue detection problem:

1. The first one is focused on using deep learning to analyze a sequence of images of the driver.
2. The second one uses a combination of AI and deep learning techniques called Transfer Learning to extract the important features from the image and, after that, the obtained data are evaluated whether the driver is drowsy or not.

2. Existing System

To address the above difficulties, in this study, we consider deep convolutional neural networks (CNNs). CNNs have developed rapidly in the field of machine vision, especially for face detection. Viola and Jones and Yang et al. pioneered the use of the AdaBoost algorithm with Haar features to train different weak classifiers, cascading into strong classifiers for detecting faces and nonhuman faces. In 2014, Facebook proposed the DeepFace facial recognition system, which uses face alignment to fix facial features on certain pixels prior to network training and extracts features using a CNN. In 2015, Google proposed FaceNet, which uses the same face to have high cohesion in different poses, while different faces have low coupling properties. In FaceNet, the face is mapped to the feature vector of Euclidean space using a CNN and the ternary loss function. In 2018, the Chinese Academy of Sciences and Baidu proposed PyramidBox, which is a context-assisted single-lens face detection algorithm for small, fuzzy, partially occluded faces. PyramidBox improved network performance by using semisupervised methods, low level feature pyramids, and context-sensitive predictive structures. CNN-based face detection performance is enhanced significantly by using powerful deep learning methods and end-to-end optimization. In this study, we combine eye and mouth characteristics and use a CNN rather than the traditional image processing method to realize feature extraction and state recognition and the necessary threshold is set to judge drowsiness.

The primary contributions of this study are summarized

- (1) The Transfer Learning, which is based on a state recognition network, is proposed to classify eye state (i.e., open or closed). In machine vision-based fatigue driving detection, blink frequency are important indicators for judging driver drowsiness. Therefore, this paper proposed a convolutional neural network that recognizes the state of the eyes to determine whether the eyes are open or closed. The Transfer Learning can reduce the influence of factors such as changes in lighting, sitting, and occlusion of glasses to meet the adaptability to complex environments. A method is developed to detect driver fatigue status. This on MTCNN, and the state of eyes is determined by Transfer Learning. Binocular images (rather than monocular images) are detected to obtain abundant eye features. For a driver's multipose face area, detecting only monocular's information can easily cause misjudgment. To obtain richer facial information method combines multiple levels of features by cascading two unique CNN structures. Face detection and feature point location are performed based, a fatigue driving recognition method based on the combination of binocular and mouth facial features is proposed, which utilizes the complementary advantages of various features to improve the recognition accuracy.

Since the average blink duration ranges from 100 to 400 ms , in this work, a frame rate of 10 FPS is used, which is enough to detect blinks and avoid overloading the system. This way, 600 frames are evaluated every time a new frame is captured by the camera. To do this, the system stores the previous 599 frames, so that a full sequence of 60 s is analyzed at each instant.

As mentioned in Section, this work proposes two alternative solutions to estimate drivers' drowsiness. The first alternative uses a recurrent and convolutional neural network, while the second one uses AI and deep learning techniques to extract numeric features from images, and then introduces them into a fuzzy system. However ,both solutions follow the same process Structure which consists of three phases: Preprocessing ,analysis ,and Alarm activation Figure 1 shows the three different phases.

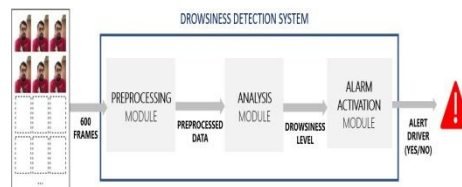


Figure1: System Overview

Preprocessing

As previously mentioned, before sending the image to the recurrent CNN, we crop and preprocess the original frame at the *preprocessing module*. To avoid that the model is affected by possible noise, the first step is to apply a Gaussian blur to the original image. Blurring images is a common technique used to smooth edges and remove noise from an image, while leaving most of the image intact.

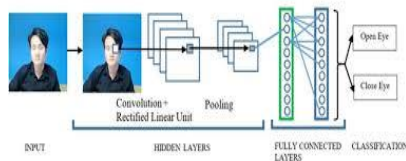


Figure 2 Preprocessing

Analysis

The analysis module uses a recurrent and convolutional neural network to estimate the drowsiness level of the driver. The CNN is based on the EfficientNetB0 architecture , which presents a lightweight model that is highly precise. Smaller models are processed faster, and EfficientNetB0 presents the smallest model of the EfficientNet series. Since the differences in accuracy are not significant in our domain when upgrading to a superior model, we consider EfficientNetB0 to be the most adequate model for this case, where the model needs to quickly obtain a prediction. This way, we perform transfer learning on this model by using previously trained weights that have great performance in recognizing objects on images from the ImageNet dataset .

Alarm Activation

To calculate whether the ADAS has to alert the driver or not, the system based on fuzzy logic performs the same process as that of the system that uses a recurrent CNN.

Flowchart

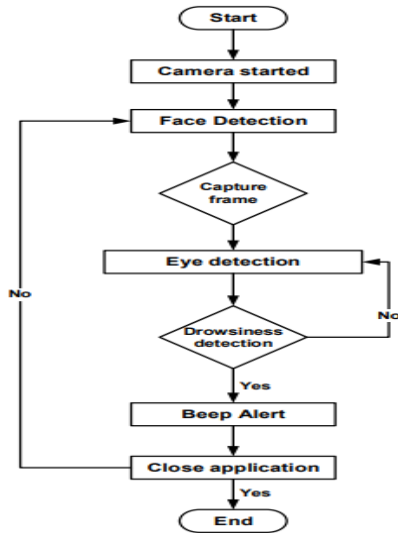


Figure 3 Flowchart

4 Conclusions

In this paper, two different implementations for a driver drowsiness detection system are proposed, where deep learning plays an important role. These systems use images of the driver to identify fatigue symptoms, but instead of predicting whether a driver is tired or not from a single image, in this work, a full sequence of 10 s is used to determine whether the driver is tired or not over the last minute.

5 References

1. Dinges, D.F. An overview of sleepiness and accidents. *J. Sleep Res.* **1995**, *4*, 4–14. [[CrossRef](#)]
2. Dawson, D.; Reid, K. Fatigue, alcohol and performance impairment. *Nature* **1997**, *388*, 235. [[CrossRef](#)]
3. Williamson, A.M.; Feyer, A.M.; Mattick, R.P.; Friswell, R.; Finlay-Brown, S. Developing measures of fatigue using an alcohol comparison to validate the effects of fatigue on performance. *Accid. Anal. Prev.* **2001**, *33*, 313–326. [[CrossRef](#)]
4. Soares, S.; Monteiro, T.; Lobo, A.; Couto, A.; Cunha, L.; Ferreira, S. Analyzing Driver Drowsiness: From Causes to Effects. *Sustainability* **2020**, *12*, 1971. [[CrossRef](#)]
5. Pouyanfar, S.; Sadiq, S.; Yan, Y.; Tian, H.; Tao, Y.; Reyes, M.P.; Shyu, M.L.; Chen, S.C.; Iyengar, S.S. A Survey on Deep Learning: Algorithms, Techniques, and Applications. *ACM Comput. Surv.* **2018**, *51*, 1–36. [[CrossRef](#)]

Hybrid Key Splitting scheme for Secure Datasharing on prevention of Cyber Security

A.Nandhini., D. sowmiya., S. Subalakshmi
MS. S. T. Preethi
UG-student, Assistant Professor
Department of Computer Science and Engineering.
MRK Institute of Technology

Abstract

The capability of selectively sharing encrypted data with different users via public cloud storage may greatly ease security concerns over inadvertent data leaks in the cloud. A key challenge to designing such encryption schemes lies in the efficient management of encryption keys. The desired flexibility of sharing any group of selected documents with any group of users demands different encryption keys to be used for different documents. However, this also implies the necessity of securely distributing to users a large number of keys for both encryption and search, and those users will have to securely store the received keys, and submit an equally large number of keyword trapdoors to the cloud in order to perform search over the shared data. The implied need for secure communication, storage, and complexity clearly renders the approach impractical. In this paper, we address this practical problem, which is largely neglected in the literature, by proposing the novel concept of key aggregate searchable encryption (HYBRID) and instantiating the concept through a concrete HYBRID scheme, in which a data owner only needs to distribute a single key to a user for sharing a large number of documents, and the user only needs to submit a single trapdoor to the cloud for querying the shared documents. The security analysis and performance evaluation both confirm that our proposed schemes are provably secure and practically efficient

Keywords: *Green House, Automation, Internet of Things, Netduino3, Atmospheric sensors*

AI Based Transport System In RealTime Traffic Monitoring With Machine Learning

B.Harine, E.Premalatha, S.Sivaranjani, S.Sneha, R.Vijayabharathi,
Department of CSE,MRK Institute of Technology

Abstract

In This project proposes a Machine Learning approach to sense the Intelligent Transportation Systems network. It uses Machine Learning to describe the status of the changeable objects in the Intelligent Transportation Systems network sensed by the system, and adopts a block centralized storage structure to organize the routing table, which reduces redundant information and makes full use of routing space and historical routing information for network sensing. This project offloads a large part of the rerouting computation at the vehicles, and thus, the re-routing process becomes practical in real-time., traffic data have been generating exponentially, and we have moved towards the big data concepts for transportation. Available prediction methods for traffic flow use some traffic prediction models and are still unsatisfactory to handle real-world applications. This fact inspired us to work on the traffic flow forecast problem build on the traffic data and models. It is cumbersome to forecast the traffic flow accurately because the data available for the transportation system is insanely huge.

1 Introduction

Internet of Things (IoT) is a system of devices connected to the internet with ability to collect and exchange data from user or environment with no human intervention. Intelligent transportation system It allows safe and free flow traffic. It uses GPS equipped devices. VANET share the message from vehicles which are placed in same region. It can be connected vehicle to vehicle, vehicle to infrastructure and infrastructure to infrastructure. The dependency of traffic flow is dependent on real-time traffic and historical data collected from various sensor sources, including inductive loops, radars, cameras, mobile Global Positioning System, crowd sourcing, social media. Traffic data is exploding due to the vast use of traditional sensors and new technologies, and we have entered the era of a large volume of data transportation. Transportation control and management are now becoming more data-driven. [2], [3]. However, there are already lots of traffic flow prediction systems and models; most of them use shallow traffic models and are still somewhat failing due to the enormous dataset dimension.

2 Background

Intelligent Transportation system (ITS) is adopted in world congress held in Paris, 1994. the ITS has used the application of computer, electronics, and communication technology to provide traveller information to increase the safety and efficiency of the road transportation systems. The main advantage of ITS is to provide a smooth and safe movement of road transportation. It's also helpful in the perspective of environment-friendliness to reduce carbon emission. It provides many opportunities for automotive or automobile industries to enhance the safety and security of their travellers [6].

Irrespective of vehicles increases on roads, the traffic also increases. And the available road network capacity is not feasible to handle this heavy load. There are two possible approaches to resolve this issue. The first one is to make new roads and new highway lanes for the smooth functioning of vehicles. It requires extra lands and also the extensive infrastructure to maintain it, and due to this, the cost of expenditure also high. Sometimes many problems came into the network like in the urban area. This land facility is not available for the expansion of the roads and lanes. The second approach uses some control strategies to use the existing road network efficiently. By using these control strategies, the expenditure also reduces, and it is cost-effective models for the government or the traffic managers. In this control, strategies identify the potential congestions on the roads, and it is directed to the passengers to take some alternative routes to their destinations.

3 Implementation And Results

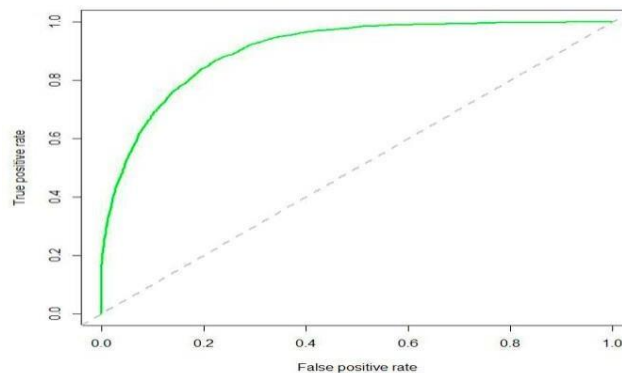
We have applied and tested different machine algorithms for achieving higher efficiency and accurate results. To identify classification and regression we have used a Decision Tree Algorithm (DT). The goal of this method is to

predict the value of the target variables. Decision tree learning represents a function that takes as input a vector of attributes value and returns a "Decision" a single output value. It falls under the category of supervised learning algorithm. It can be used to solve both regression and classification problem. Data mining is the process of analyzing, predicting and discovering interesting knowledge and hidden patterns from large amounts of data stored in repositories, such as databases and data warehouses [4]. This process includes statistical models, mathematical algorithms, and machine learning methods [4]. Using data mining technology in traffic management provides a powerful analysis and processing function of mass traffic data and directs drivers and systems to make better decisions. Knowledge mining and discovery is an emerging area in traffic management systems focuses on using and analyzing large amount of traffic data to be used for traffic control, route guidance, or route programming. Gap filling is an event that occurs when the driver tries to position his vehicle into the available gaps in the road section ahead. The proposed model uses area occupancy, relaxation time, and the relative speed of vehicles. Field data from an arterial road in Chennai city in India were used to validate and evaluate their proposed model. The evaluation results showed that their proposed model generates results that are comparable with those from few existing generalized multi-class models. Estimating the traffic flow based on traffic video analysis is another method that was proposed by Hung et. al. in [20]. The authors used the captured videos from a surveillance camera mounted in a cross road to detect moving vehicles and control the traffic flow. In addition, they used the traffic flow as input for automatic timing for the traffic light accordingly. The authors used background subtraction and Gaussians model to detect and trace vehicles and then synchronized in a given time period to eliminate the shadow from the sunlight or street light. The authors used Vietnam as a context, which include a mixed flow of motorbikes with other transport means, to evaluate the proposed system.

3.1 EVALUATION MATRIX FOR DIFFERENT MACHINE LEARNING ALGORITHMS

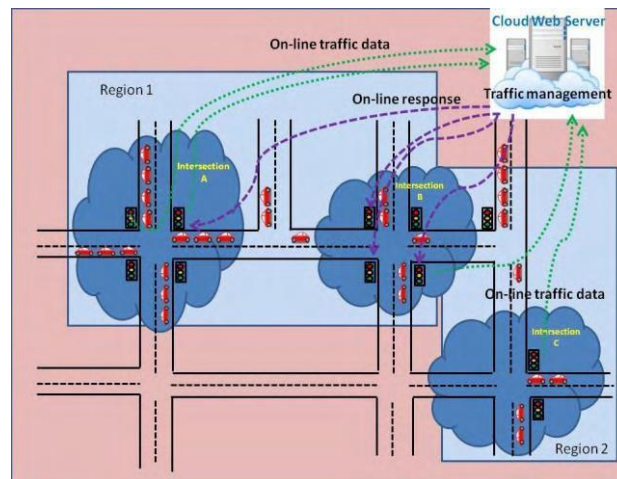
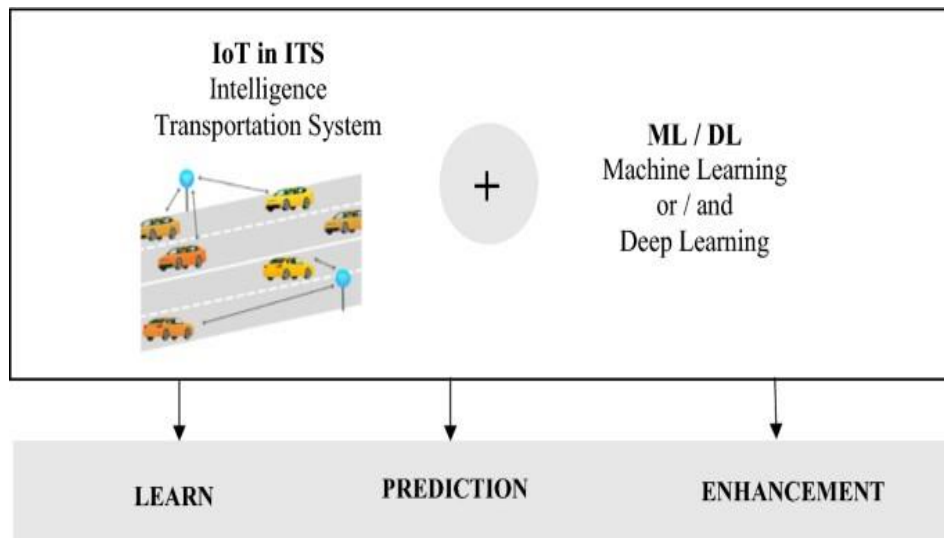
Algorithm	Accuracy	Precision	Recall	Time
Decision Tree	88%	88.56%	82%	108.4sec
SVM	88%	87.88%	80%	94.1sec
Random Forest	91%	88.88%	82%	110.1sec

Fig. 1. ROC curve for Decision Tree Algorithm
ROC Curve



4 Estimation And Predicting Of Real Time Travel Time

Throughput, travel time, safety, fuel consumption, emission, reliability, and traffic density are considered as the primary measures of quantifying traffic congestion on roadways other than signalized intersection [3]. The prediction of real-time traffic density could be done based on: 1) Aerial Photography loop detector, 2) Data driven approach using linear model, linear regression, ANN, k-NN, pattern matching, PCA, nearest neighbor approach, Kalman filtering, clustered neural network, wavelet neural network, k-NN and Linearly Sewing Principle Components, and 3) Image processing techniques. Jithin *et al.* in [3] used the k-Nearest Neighbor (kNN) and Artificial Neural Network (ANN) as machine learning techniques to estimate the travel time and traffic density. The authors used the available data collected every five minutes from automatic sensors as input to estimate the target travel time and density. The evaluation results showed promising results in terms of Mean Absolute Percentage Error (MAPE) in Indian



5 Conclusion

The proposed AI-based traffic control system for emergency vehicles using the Machine Learning Routing Protocol (MLRP) is simulated using Network Simulator 2 and performance metrics are analyzed as transmitted packet, packet retrieved, packet transmission ratio, average throughput and residual energy average. • In order to monitor road traffic and smooth flow of emergency vehicles, the AI based system is introduced. approaches that focused on the traffic light signals. Our future work will focus on proposing a new traffic management approach.

In future we can use a novel Grid-based On-road localization system with the help of RSU, where vehicles with and without accurate High end GPS signals self-organize into a Satellite VANET, exchange location and distance information and help each other to calculate an accurate position for all the vehicles inside the network.

REFERENCE

- [1] (Mar. 2015). *TomTom*. Accessed: Oct. 11, 2018. [Online]. Available: <https://corporate.tomtom.com/news-releases>
- [2] D. Schrank, B. Eisele, and T. Lomax, “TTI’s 2012 urban mobility report powered by INRIX traffic data,” Texas A&M Transp. Inst. and Texas A&M Univ. Syst., Texas, TX, USA, Tech. Rep. 1, 2012.
- [3] J. Raj, H. Bahuleyan, and L. D. Vanajakshi, “Application of data mining techniques for traffic density estimation and prediction,” *Transp. Res. Procedia*, vol. 17, pp. 321–330, Dec. 2016.
- [4] S. Sundaram, S. S. Kumar, and M. D. Shree, “Hierarchical clustering technique for traffic signal decision support,” *Int. J. Innov. Sci., Eng. Technol.*, vol. 2, no. 6, pp. 72–82, Jun. 2015.
- [5] S. Anand, P. Padmanabham, A. Govardhan, and R. H. Kulkarni, “An extensive review on data mining methods and clustering models for intelligent transportation system,” *J. Intell. Syst.*, vol. 27, no. 2, pp. 263–273, 2018.
- [6] J. Zhang, F.-Y. Wang, K. Wang, W.-H. Lin, X. Xu, and C. Chen, “Data-driven intelligent transportation systems: A survey,” *IEEE Trans. Intell. Transp. Syst.*, vol. 12, no. 4, pp. 1624–1639, Dec. 2011.
- [7] J. Lopes, J. Bento, E. Huang, C. Antoniou, and M. Ben-Akiva, “Traffic and mobility data collection for real-time applications,” in *Proc. 13th Int. IEEE Annu. Conf. Intell. Transp. Syst.*, Madeira, Portugal, Sep. 2010, pp. 216–223.
- [8] K. Miller, M. Miller, M. Moran, and B. Dai, “Data management life cycle,” Texas A&M Transp. Inst., College Station, TX, USA, Tech. Rep. 1, Mar. 2018.
- [9] Z. Diao *et al.*, “A hybrid model for short-term traffic volume prediction in massive transportation systems,” *IEEE Trans. Intell. Transp. Syst.*, vol. 20, no. 3, pp. 935–946, Mar. 2019.

GREEN ENERGY HARVESTING FROM RADIO FREQUENCY TO DIRECT CURRENT

E. Elakiya, Department of ECE, Student, MRKIT

S. Heera, Department of ECE, Student, MRKIT

T. Pavithra, Department of ECE, Student, MRKIT

S. Sathya Moorthy, Department of ECE, Assistant Professor, MRKIT

Abstract

The energy harvesting from external ambient sources e.g., wind, solar, vibration, heat, radio frequency (RF) are emerging as promising alternative to existing energy resources. In recent years, the huge proliferation of RF mobile communication in developing country like India has made RF energy harvesting as an attractive solution to the dramatically increasing energy needs. Energy harvesting is the process of electronically capturing and accumulating energy from a variety of energy sources deemed wasted or otherwise said to be unusable for any practical purpose. Wireless sensors and the potential of energy harvesting to provide power for the life of these devices. The greatest potential, however, lies in a new class of devices that will be battery free and thus enable applications that would have been prohibitively expensive due to the maintenance cost of eventual and repeated battery replacement. This project deals with the harvesting of energy based on the RF source here the power is transfer from the antenna, there by using the impedance matching is done. Hence this project deals with the harvesting of energy based on the RF source here the power is transfer from the antenna, there by using the impedance matching is done so that to gain more power from tower and the rectifier circuit convert an incoming RF signal to DC signal that is fed into battery and an efficient rectification improves the output power.

KEY WORDS: Green Energy Harvesting technology, dual path, power conversion efficiency, reconfigurable, RF to DC power converter, RF energy harvesting.

1. INTRODUCTION

In recent years, radio frequency (RF) energy harvesting has become an intensive area of research for remote powersupply of wireless sensors/devices in the Internet of Things (IoT), radio frequency identification (RFID) systems and biomedical implanted devices by eliminating the need for battery and its limited lifetime. Depending upon batteries as reliable energy source for wireless sensors/devices impose several constraints including regular charging and maintenance of the batteries due to their limited lifetime and their replacement in harsh environments. An RF-DC converter in an RF energy harvesting system scavenges the electromagnetic energy from ambient sources (mobile phone and environment) and converts into DC voltage for power supply of wireless sensor/devices.

Fig. 1 shows a block diagram of an entire far-field wireless power transfer (WPT) system which consists of a RF power source connected to a transmitting antenna, a radio channel, and a receiving antenna connected to an RF energy harvester. The receiving antenna receives the incoming RF energy and forwards it to an impedance matching circuit which ensures the maximum power transfer from the receiving antenna to an RF-DC power converter. The RF-DC converter rectifies the incoming RF energy and converts into the output DC power. Finally, an energy storage component (capacitor or battery) is used to store the output DC voltage.

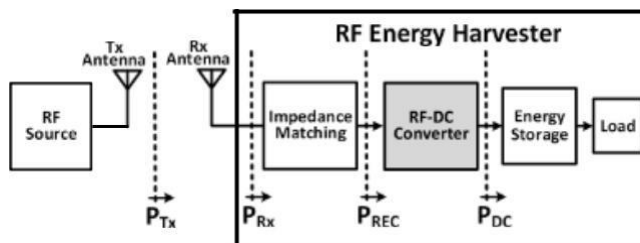


FIGURE 1. Block diagram of a far-field wireless power transfer system.

The performance of the RF-DC converter, being the main component in RF energy harvesting system, can be evaluated by its power conversion efficiency (PCE) and sensitivity. The PCE is the ratio of power, harvested by the RF-DC converter, delivered to the load to the RF input power while sensitivity is the minimum input power required to generate DC voltage at the output. The PCE of the RF-DC converter can be expressed as:

$$\eta = P_{out}/P_{in} = -V^2_{out}/R_L * P_{in} \times 100\% \quad (1)$$

.In a far-field WPT system, the performance of an RF energy harvester is strongly affected by several factors. For example, limited signal strength received at the input of the RF energy harvester due to path loss, the unpredictable attenuations in the signal strength over distance from the power source, presence of hurdles/obstacles between the RF energy harvester and the power source, antenna orientation, and transmission medium in which the RF energy harvester is utilized. As a result, the overdrive voltages generated by the RF voltage levels are not large enough for the rectifying devices to have low conduction losses even after boosted by the impedance matching circuit. Consequently, the RF energy harvester fails to harvest the maximum possible energy and its performance degrades. Therefore, designing a high performance RF energy harvester over a wide input power range is a major challenge, especially at low input power levels.

A number of threshold voltage compensation techniques for the rectifying devices have been proposed in order to increase the efficiency of the RF energy harvesters. Technology-based techniques use Schottky diode or HSMS diodes to implement the rectifier circuit. The drawbacks of these techniques are high production cost that is caused by the additional fabrication steps and integration with the standard CMOS integrated circuits. Circuit-based techniques including active/passive circuits are alternatively used for threshold voltage (V_{th}) compensation of transistors used as rectifying devices. The active circuit reported in requires external battery that results in increased cost and maintenance. On contrary, passive techniques generally do compensation of threshold voltage of the rectifying devices by using additional circuitry. An adaptive threshold voltage compensated scheme proposed in uses auxiliary transistors to control gate-source voltage of the rectifying devices.

Authors in implement maximum power point tracking (MPPT) technique selecting optimum number of rectifier stages to maintain high PCE over wide input power range. A differential CMOS rectifier used in implements a reconfigurable circuit that reconfigure the stages from parallel to series and vice versa based on the RF power level. A hybrid threshold voltage compensated scheme used in employs PMOS transistors as rectifying devices in all rectifier's stages except in first stage in order to eliminate the need of NMOS triple-well transistors. Author in reports a dual-band rectifier implementing an Internal threshold voltage compensation technique. A differential crosscoupled rectifier reported in compensates the threshold voltage of the rectifying devices and minimises their leakage current. A self-compensation scheme used in consists of triple-well NMOS transistors in order to provide individual body biasing. A self-biasing circuit described in provides DC biasing voltage by using off-chip impedance resistive network. Author in presents a threshold voltage compensation circuit where passively generated compensated voltage stored on the capacitor is applied to gate-source terminal of the rectifying devices. However, differential circuits require a PCB balloon for conversion of single-ended to differential or differential antenna which result in additional cost and large area on the PCB board. Authors in report a cascaded rectifier using dynamic threshold voltage cancellation (DVC) technique in combination with the internal threshold voltage cancellation (IVC) technique to efficiently compensate threshold voltages of the rectifying devices. Most of the circuit solutions proposed in the literature have been designed to produce maximum PCE at a specific input power level and failed to harvest RF energy at wide low input power range. This paper presents a reconfigurable RF-DC converter that harvests the maximum possible RF energy and maintains high PCE over wide low input power range. The proposed circuit demonstrates superior performance to the published state-of-the-art work. This paper is organized as follows. Section II describes the working principle of the proposed reconfigurable RF-DC converter. Section III explains the circuit description of the sub-blocks of the proposed architecture. Sections IV depicts the measurement results. Section V finally concludes the paper.

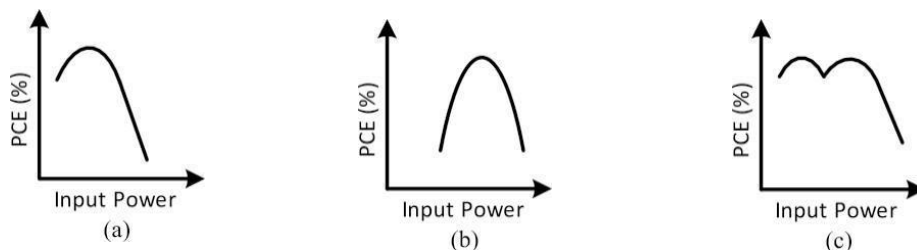


FIGURE 2. Conventional rectifier's performance (a) at low power, (b) at high power, and (c) reconfigurable rectifier's performance

BLOCK DIAGRAM

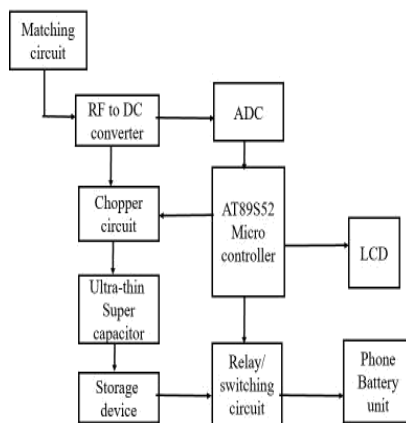


FIGURE 3. Block diagram of the proposed reconfigurable RF-DC power converter.

2. PROPOSED RECONFIGURABLE RF-DC CONVERTER

Fig. 2 presents the conceptual idea applied in the proposed reconfigurable circuit. Fig. 2(a) and (b) display the PCE of a conventional single-path power converter that is optimized to operate efficiently at low input power and high input power, respectively. It is clear that the high-PCE can only be achieved over a narrow input power range for the single-path rectifier. On the contrary, Fig. 2(c) depicts a high PCE graph of the reconfigurable circuit. This high PCE, over wide input power range, is achieved by combining both graphs of Fig. 2(a) and (b).

Fig. 3 shows block diagram of the proposed reconfigurable RF-DC converter. The proposed scheme is composed of two identical rectifier blocks, three MOSFET switches (SW1, SW2 and SW3), a comparator, and an inverter. The switches are used to reconfigure the proposed circuit and are controlled by the output of the comparator and the inverter. The transistors used in the proposed architecture are low threshold voltage (LVT) of general purpose (GP). Fig. 4 presents the working principle of the proposed circuit. Fig. 4(a) shows the series-path operation of the proposed circuit for low input power range. The comparator compares output voltage (VO_{UT}) of the proposed circuit to a reference voltage (V_{REF}). As long as the VO_{UT} is lower than the V_{REF}, the comparator gives low-voltage “VCMP L” and the inverter gives high output “H”. This mechanism turns-on the switch SW1 and turns-off the switches SW2 and SW3 to allow the two identical rectifier blocks to operate in series with each other. This increases the harvested power at the output and eventually increases the PCE of the proposed scheme at the low input power range. Fig. 4(b) represents parallel-path operation of the proposed circuit for high input power range. When VO_{UT} becomes higher than the V_{REF}, the comparator produces high-voltage “VCMP H” and inverter produces low voltage “L”. This process turns-off the switch SW1 and turns-on the switches SW2 and SW3 to allow the two identical rectifier blocks to operate in parallel with each other. This increases the PCE of the proposed scheme at high input power level. Consequently, the overall PCE of the proposed reconfigurable circuit is extended and improved over extended input power range.

3. CIRCUIT DESCRIPTION: RF-DC CONVERTER DESIGN

Fig. 5 presents circuit description of one of the rectifier blocks used in the proposed reconfigurable power converter scheme. The rectifier circuit used in the proposed scheme is similar to the rectifier proposed in. The rectifier circuit employs internal threshold voltage cancellation (IVC) technique for threshold voltage (V_{th}) compensation of the transistors used as rectifying devices. The main rectification body is composed of one NMOS transistor (M_n) and two PMOS transistor's (M_{p1} and M_{p2}). An auxiliary block is made-up of two PMOS transistors, namely M_a and M_b, which are referred as back-compensated transistor and forward compensated transistor, respectively. The width of M_n is chosen 7 μm while widths of M_{p1} and M_{p2} are set to be 14 μm each. The widths of M_a and M_b are selected to be 1 μm each, and channel lengths of all the transistors are set to be minimum. The value of both coupling capacitor (C_{in}) and auxiliary capacitor (C_{aux}) are chosen 2 pF. The transistors M_a and M_b reduce V_{th} of forward-biased transistors and minimize the reverse leakage current of the reverse-biased transistors in the main rectification chain, respectively. During positive phase of input power, as shown in Fig. 5(a), the back-compensated transistor M_a reduces V_{th} of the forward-biased transistors (M_{p1} and M_{p2}), and increases harvested power in the main rectification chain. The forward-compensated transistor M_b remains turned-off as its source-gate voltage (V_{sg}) lies below V_{th}. During negative phase of input power, as shown in Fig. 5(b), the rectifying devices M_{p1} and M_{p2} are reversed-biased, and V_{sg} of M_b is larger than its V_{th} to turn it on. This reduces source-gate voltages (V_{sg1} and V_{sg2}) of transistors (M_{p1} and M_{p2}) to zero, respectively, and consequently minimizes the leakage current in the rectification chain.

The auxiliary capacitor, C_{aux} , stores some charge which is lost during reversed-biased condition. Indeed, the voltage drop (V_{aux}) across capacitor C_{aux} is obtained from both forward and reverse conduction and can be written as:

$$V_{aux} = C_{aux} \times (Q_{fwd} + Q_{rev}) \quad (2)$$

By applying the Kirchhoff Voltage Law (KVL) in Fig. 5.

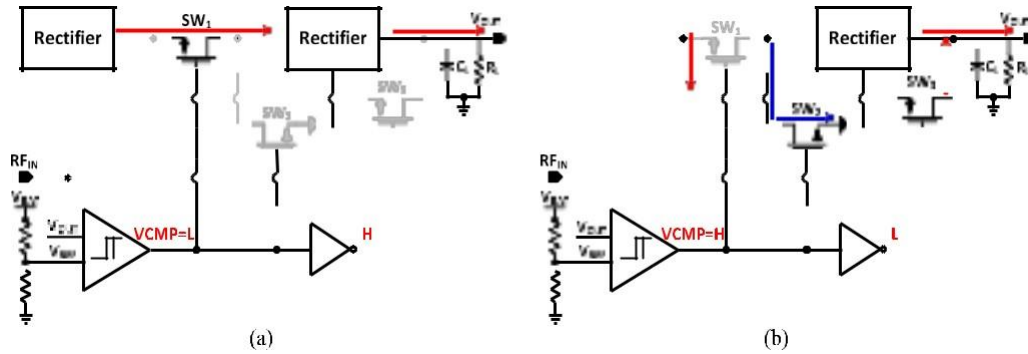


FIGURE 4. Rectifier circuit with (a) positive phase operation, and (b) negative phase operation.

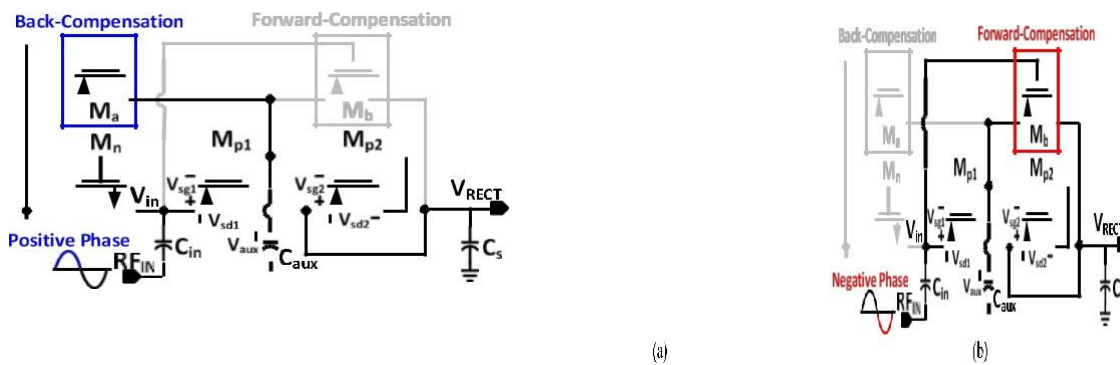


FIGURE 5. Rectifier circuit with (a) positive phase operation, and (b) negative phase operation.

$$V_{in} = V_{sg1} + V_{aux} \quad (3)$$

where V_{in} is the peak RF input amplitude. The output DC voltage (V_{RECT}) of the rectifier can be written as:

$$V_{RECT} = V_{in} - V_{sd1} \quad (4)$$

where V_{sd1} is the source-drain voltage of the M_{p1} . By replacing V_{in} of Eq. (3) in Eq. (4), V_{RECT} can be written as:

$$V_{RECT} = -V_{sd1} + V_{sg1} + V_{aux} \quad (5)$$

Similarly,

$$V_{RECT} = V_{sg2} + V_{aux} \quad (6)$$

By subtracting (6) from (5), it can be written as:

$$V_{sd1} = V_{sg1} - V_{sg2} \quad (7)$$

The V_{sg2} of the M_{p2} increases as long as the output voltage (V_{RECT}) of the rectifier increases. When the V_{sg2} is equal to the threshold voltage of the M_{p2} , the M_{p1} enters the saturation region. As a result, the proposed circuit compensates the effect of threshold voltage and improves the PCE and output.

Due to limited harvested power from ambient environment, power consumption must be taken into account when design low-power adaptive control circuit (ACC). The ACC consists of a common-gate input comparator, an inverter and three switches comparator is the key circuit of the ACC. Fig. 6 displays the circuit diagram of the common-gate input comparator having same structure as described in [15]. The comparator compares the output voltage (V_{OUT}) of the proposed circuit to the reference voltage (V_{REF}) and controls the switches (SW1, SW2 and SW3) in order to reconfigure the proposed circuit depending upon the input power level. At low input power conditions, the current consumption of the comparator is exponential and is negligible. Moreover, high voltage devices with low-current conduction are used in the comparator to avoid extra current consumption at high input power conditions.

4. MEASUREMENT RESULTS:

The proposed reconfigurable RF-DC converter is fabricated in a standard 180 nm CMOS technology. Fig. 7(a) presents the chip microphotograph of the proposed circuit having an active die area of $340 \mu\text{m} \times 310 \mu\text{m}$, excluding the pads. Fig. 7(b) depicts the measurement setup to check the performance of the proposed circuit. The fabricated chip is wire-bonded on a PCE board. A single-tone sinusoidal signal operating at 902 MHz is generated by Agilent E4438C signal generator to test the chip. An Oscilloscope, Tektronix TDS 2024B, and a digital voltmeter are used to record the output DC voltage. An off-chip pi-matching circuit is implemented onto the PCB board to match the input impedance of the proposed circuit to 50Ω and reflection co-efficient S_{11} is calculated. The net input power that is given to the chip is calculated after excluding the transmission losses and the reflection losses.

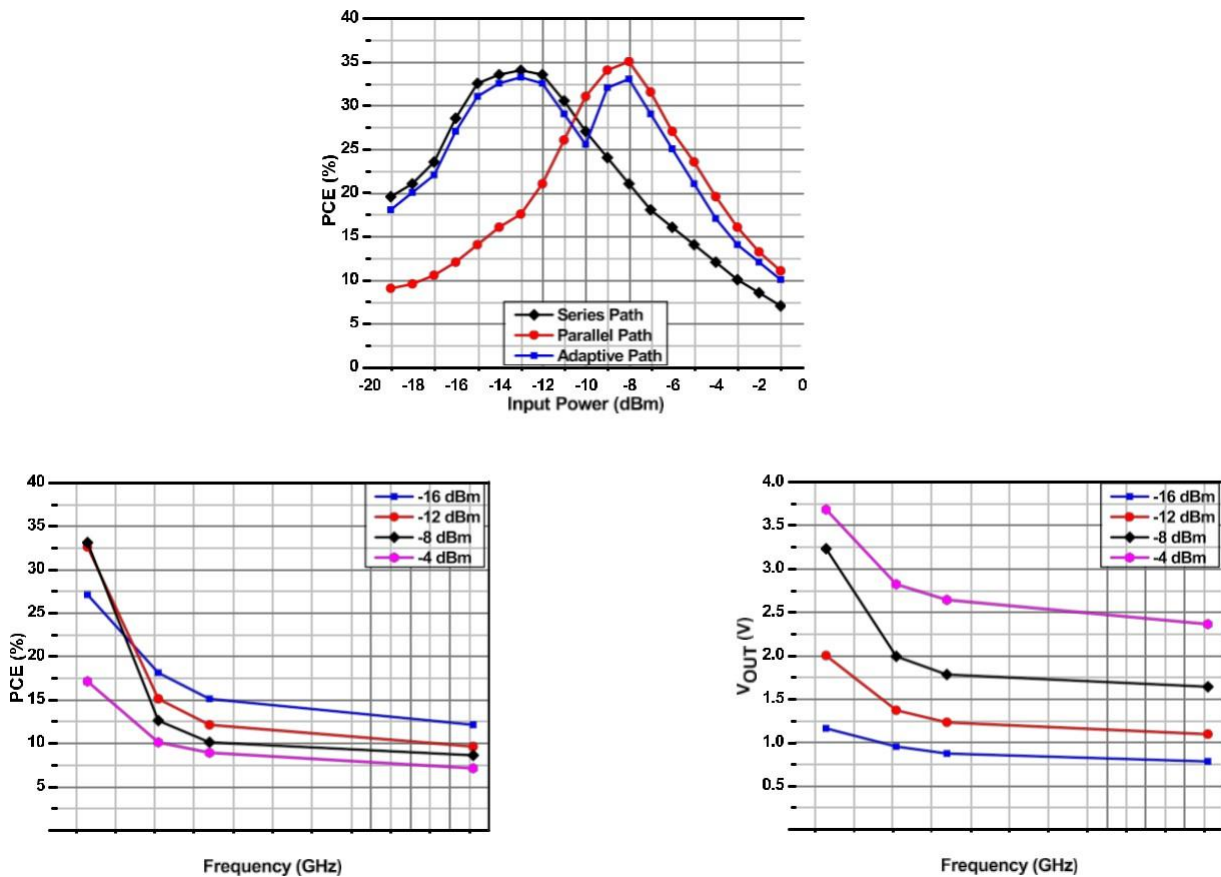


FIGURE 7. Measurement results of the proposed circuit versus frequency for 200 k Ω load. (a) PCE, and (b) output DC voltage..

5. CONCLUSION

In this paper, a reconfigurable RF-DC converter operating at 902 MHz frequency to efficiently harvest radio frequency energy is presented. The proposed architecture uses a dual-path, a series (low-power) path and a parallel (high-power) path, to maintain high PCE over extended input power range. The adaptive control circuit activates the series path or the parallel path based on the input power level to maximize the harvested power at the output. Despite of process variations of the switches, the proposed circuit still achieves better PCE over extended input power range. The proposed scheme has been designed and fabricated in 180 nm CMOS technology. The measurement results show that the PCE of the proposed scheme is above 20% from 18 dBm to 5 dBm with peak measured PCE of 33% at 8 dBm. The proposed circuit obtains 20.2 dBm sensitivity for 1 M load while producing 1 V output DC voltage.

6. REFERENCES

- [1] J. Qian, C. Zhang, L. Wu, X. Zhao, D. Wei, Z. Jiang, and Y. He, "A passive UHF tag for RFID-based train axle temperature measurement system," in Proc. IEEE Custom Integr. Circuits Conf. (CICC), San Jose, CA, USA, Sep. 2011, pp. 1–4.
- [2] D. Bouchouicha, F. Dupont, M. Latrach, and L. Ventura, "Ambient RF energy harvesting," in Proc. Int. Conf. Renew. Energies Power Qual., Granada, Spain, Mar. 2010, pp. 2–6.
- [3] M. H. Ouda, M. Arsalan, L. Marnat, A. Shamim, and K. N. Salama, "5.2-GHz RF power harvester in 0.18- μ m CMOS for implantable intraocular pressure monitoring," IEEE Trans. Microw. Theory Techn., vol. 61, no. 5, pp. 2177–2184, May 2013.
- [4] H. Jabbar, Y. Song, and T. Jeong, "RF energy harvesting system and circuits for charging of mobile devices," IEEE Trans. Consum. Electron., vol. 56, no. 1, pp. 247–253, Feb. 2010.
- [5] K. Finkenzeller, RFID Handbook: Fundamental and Applications in Contactless Smart Cards and Identification. Sussex, U.K.: Wiley, 2003.
- [6] A. Costanzo and D. Masotti, "Smart solutions in smart spaces: Getting the most from far-field wireless power transfer," IEEE Microw. Mag., vol. 17, no. 5, pp. 30–45, May 2016.
- [7] P. S. Yedavalli, T. Riihonen, X. Wang, and J. M. Rabaey, "Far-field RF wireless power transfer with blind adaptive beamforming for Internet of Things devices," IEEE Access, vol. 5, pp. 1743–1752, 2017.
- [8] T. Le, K. Mayaram, and T. Fiez, "Efficient far-field radio frequency energy harvesting for passively powered sensor networks," IEEE J. Solid-State Circuits, vol. 43, no. 5, pp. 1287–1302, May 2008.
- [9] M. Xia and S. Aissa, "On the efficiency of far-field wireless power transfer," IEEE Trans. Signal Process., vol. 63, no. 11, pp. 2835–2847, Jun. 2015.
- [10] X. Lu, P. Wang, D. Niyato, D. I. Kim, and Z. Han, "Wireless networks with RF energy harvesting: A contemporary survey," IEEE Commun. Surveys Tuts., vol. 17, no. 2, pp. 757–789, 2nd Quart., 2015.
- [11] U. Karthaus and M. Fischer, "Fully integrated passive uhf rfid transponder ic with 16.7- μ minimum rf input power," IEEE J. Solid-State Circuits, vol. 38, no. 10, pp. 1602–1608, Oct. 2003.
- [12] C. R. Valenta and G. D. Durgin, "Harvesting wireless power: Survey of energy-harvester conversion efficiency in far-field, wireless power-transfer systems," IEEE Microw. Mag., vol. 15, no. 4, pp. 108–120, Jun. 2014.
- [13] T. Umeda, H. Yoshida, S. Sekine, Y. Fujita, T. Suzuki, and S. Otaka, "A 950-MHz rectifier circuit for sensor network tags with 10-m distance," in Proc. IEEE Int. Solid-State Circuits Conf., San Francisco, CA, USA, Dec. 2005, pp. 34–51.

IOT APPROACH TO VEHICLE ACCIDENT DETECTION AND LIVE LOCATION TRACKING

K.Mohanapriya¹, Department of ECE, VRS college of Engineering and Technology-Villupuram
G.Indumathi², Department of ECE, VRS college of Engineering and Technology-Villupuram

ABSTRACT

In today's daily life vehicle holds an important place in everyone's life. Each day millions of peoples use personal and public transport system to reach their location on time. Among these, roadways transport is one of the major transport systems used by commuters. Thousands lose their valuable life in vehicle accidents everyday due to the traffic, road condition and speed. Reasons behind it may vary but most of the cases comes from drink and drive habits. By using GPS antenna and latest technological concept of IoT, accident can be immediately reported, reduced and human life can be saved; by connecting different kinds of sensors to different parts or position of vehicle. In-tern by making these sensors to communicate with the hospital immediate treatment can be given to the injured person during accident. In this paper, we have designed and implemented by connecting to different sensors to vehicle, which notifies the registered members whenever accident takes place. Using the GPS exact location will be sent to registered user, local control room and hospital. In this proposed system tilt sensor is used to detect the accident caused due to tilting, Alcohol sensor to monitor the driver, vibration sensor to detects the accident if there is a hard vibration of vehicle due to road condition and Ultrasonic sensor is used for notifying if vehicle is too close to some other vehicle or obstacles.

Keywords- Accident detection, Arduino, GPS, IoT, sensor, Vehicle.

1.INTRODUCTION

The development in technology is increasing every day and it is solving our problems of daily life with minimum effort and short span of time. As the access to internet is getting easier, number of internet-based devices is also increasing exponentially. These developments are converting our world into a smart and better world. In this era, all beings are somehow dependent on the internet to fulfill our daily necessities. Using maps to reach our destination faster, to order food online, to purchase medicines online, every platform is now connected with internet. Thus, area acquired by internet in our daily life is increasing day by day. To increase people safety which in-tern helps to avoid and controls many accidents. To notify the family members, Local control room and Hospital about the accident along with the accurate location. By embedding various sensors to the different parts of vehicle and by designing vehicle-to-vehicle communication system.

1.2.EXISTING SYSTEM

The primary impact of this work was to reduce the waiting period for accident victims to receive medical assistance and be rescued from a catastrophic vehicle accident. The conceptual idea of achieving this was by accommodating sensors and a microcontroller in a vehicle to compute the displacement of the vehicle. The system was developed using a vibration sensor to determine the collision impact of an accident and a gyro sensor to determine the x-y displacement of the vehicle. When an accident occurs, the instantaneous coordinates of the vehicle will be captured using a GPS module and transmitted to the emergency response department via a GSM module. The coordinates are visualized on a registered mobile phone at the emergency response department and mirrored to a desktop's Push bullet application. With that, necessary emergency response units can be deployed to the accident location. So, it will take delay in time.

LIMITATIONS IN EXISTING SYSTEM

The vehicle tracking system uses the GPS module to get geographic coordinates at regular time interval, which misleads to proper location of the accident place. Hard to find the Accident location using geo-coordinates. Accident Message will be sent to single contact only. Mobile should be present at the user's side so that information about the accident can be shared and necessary actions can take place.

PROPOSED SYSTEM

This study includes the implementations of IoT in the field of automotive sector. It is developed on IoT platform using the help of existing embedded system of vehicles. Sensors and actuators are used to get the data and controller is used to perform the instructions based on the data received from the sensors. Benefits of implementing this concept are: safety of passengers can be achieved by locking the ignition system of the vehicle if the driver is drunk. If an accident took place, location of accident can be easily found using Google Maps. GSM module will send a text alert to relatives of the passengers and concerned authorities along with the live link.

GPS antenna is used to receive the stronger satellite signal hence to minimize the loss of signal when vehicle is in motion. This helps to get accurate location of the accident. In this system, Universal Asynchronous Receiver/Transmitter (UART) protocol is used to get the data from the GPS. UART transmit data received from GPS antenna to Microcontroller through the data bus. Since it is asynchronous clock signal is not required to synchronize transmitting UART and Receiving UART, but baud rate has to be matched. Tilt, Ultrasonic Vibration sensors and produces the output. When an accident occurs, one of the sensors get triggered then the location will be sent through the GPS module along with passengers information to the respective contacts. The proposed system architecture shows how the components are connected with each other. The flowchart of the system is shown in the Fig,1.5.1

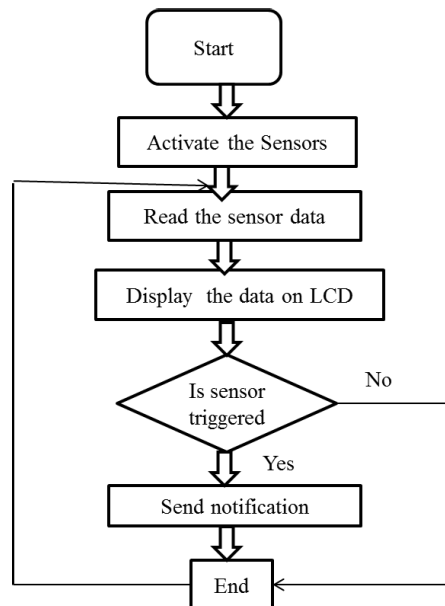


Fig 1.5.1 Flowchart of proposed System

ADVANTAGES OF PROPOSED SYSTEM

- GPS- Live location sharing using IOT.
- Distance limit alert.
- Accident SMS alert to Police, Ambulance, registered family members.
- Buzzer alert for obstacles in the road.
- Vibration & Tilting Alert.
- Alcohol Consumption detection.

BLOCK DIAGRAM

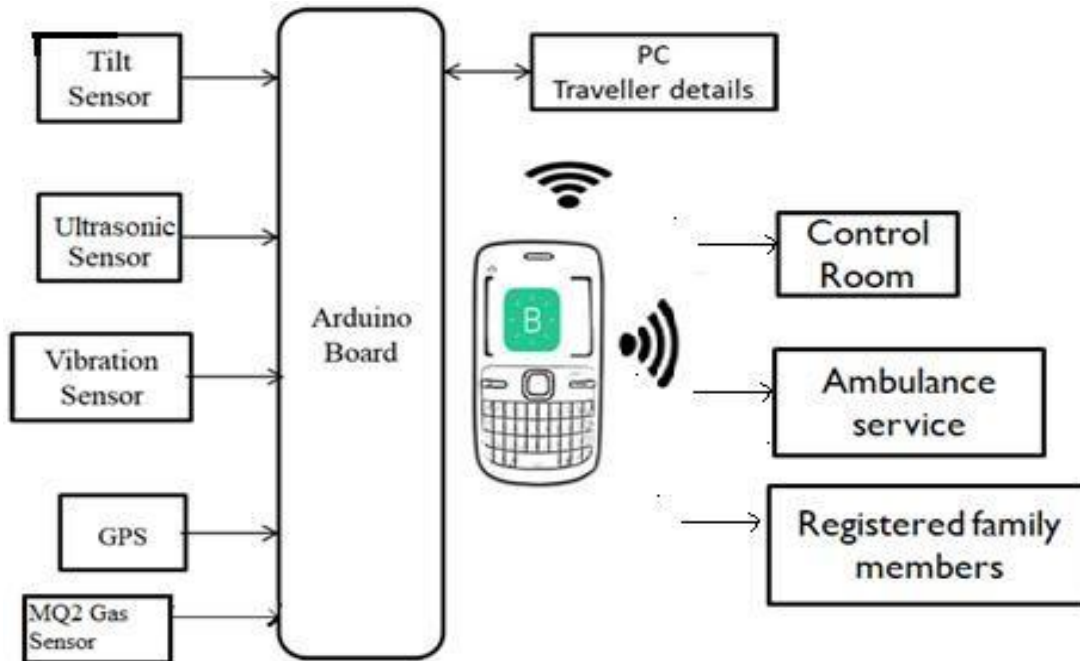


Fig 1.7.1 Block diagram of proposed system

The Block diagram of proposed system is shown in Fig 1.7.1. On the basis of above survey and description, our system includes Tilt sensor, Alcohol sensor, Vibrationsensor and different communication modules like GSM, GPS to find out the exact location of the device.

Alcohol sensor will detect if driver of the vehicle is under the influence of alcohol or not. It is done when driver of vehicle is instructed to blow breathing air using air-blow fan incorporated near driver seat. Mouth air is blown with proper pressure and with proper speed, if he is drunk command to seize the ignition of Engine is sent to the ECU of Vehicle otherwise Engine will start. If vehicle met with an accident during its journey, then sensor values are captured and sent to the registered members indicating that accident of the vehicle has been occurred.

That data consists of live link of the location including the date and time of the accident. There is an option to track the location using Google Maps. Accident alert SMS is also sent to the registered mobile number informing the location and time of Accident. To interface GSM and GPS, serial communication UART protocol is used. Other sensors are interfaced with the help of ADC present on the Arduino. Data is collected and compared with threshold value written in program.

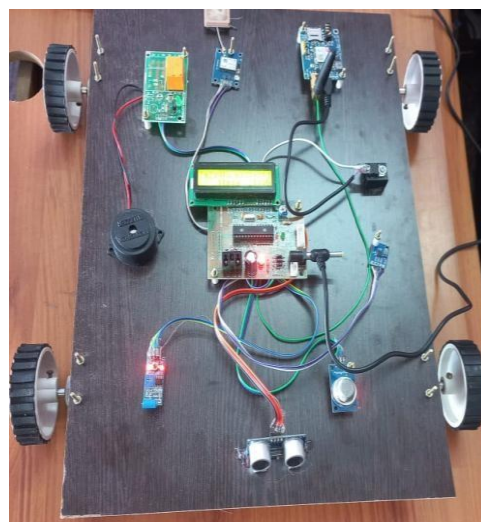
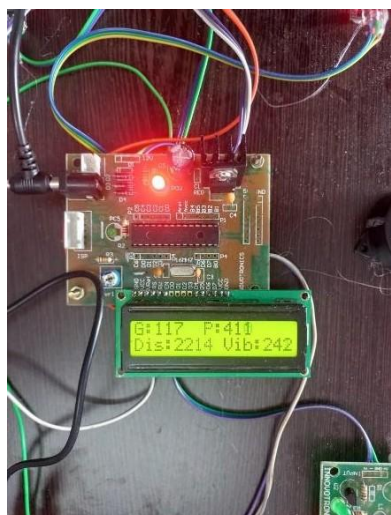
2. CONCLUSION

In this paper vehicle detection system using IOT and live link has been proposed which can be used to detect accident of a vehicle occurred in remote areas.

This proposed system uses tilt sensor and Ultrasonic sensors to detect accident and GSM, GPS modules to locate the exact live location of the vehicle so that rescue team will reach as soon as possible. The live location collected from GPS modem is pushed to web-server so that Google map API can track the location and guides with shortest path possible. As per-safety feature, alcohol sensor is used which detects alcohol presence in driver's body. The system will seize the ignition system of the vehicle if alcohol is detected. By using Ultrasonic Sensor the vehicle which is coming close can also be intimated through buzzer alert. Tilt and Vibration alert also provided depending on the threshold value.

3. RESULT

This system comprises of alcohol sensor, vibration sensor and tilt sensor which gives the safety to the driver of the vehicle. The vibration and Tilt sensors also activated when it reaches above the threshold value and a buzzer alert is provided. Ultrasonic sensor which is attached in the front of the vehicle provides you a distance limit alert between other vehicles. GSM are used to provide the connectivity to web server and users mobile. Google maps API is also incorporated with web server so that real time tracking can be achieved.



4. REFERENCES

- [1] Asad Ali and Mohamad Eid," An Automated System for Accident Detection", 978-1-4799-6144-6/15/\$31.00 ©2015 IEEE
- [2] Md. Syedul Amin, JubayerJalil ,M.B.I.Reaz ,"Accident Detection and Reporting System using GPS, GPRS and GSM Technology", "IEEE/OSA/IAPR ICIEV, 2012
- [3]]Mugila.G, Muthulakshmi.M, Santhiya.K, Prof. Dhivya.P-Smart Helmet System Using Alcohol Detection For Vehicle Protection [International Journal of Innovative Research in Science Engineering andTechnology (IJIRTSE) ISSN: 2395- 5619, Volume -2, Issue -7. July 2016]

5. ACKNOWLEDGEMENT

I am indebted to Mr.G.SADIQ BASHA, Associate Professor, Head of the Department of Electronics and Communication Engineering. I would like to express our gratitude to my guide, Ms.G.INDUMATHI, Assistant Professor, Department of Electronics and Communication Engineering for her constant motivation, direction and guidance throughout the entire course of my Phase I&II project. I thank all the Staff members and Lab technicians of the Department of Electronics and Communication Engineering and V.R.S. College of Engineering and Technology for their support and finally thank the Almighty and our family members who have been a guiding light in all our endeavours.

SMART AND SECURE VOTING MACHINE USING BIOMETRICS AUTHENTICATION

S.ABINANDHINI, Department of ECE, MRK INSTITUTE OF TECHNOLOGY
R.IYSHWARYA, Department of ECE, MRK INSTITUTE OF TECHNOLOGY
S.SUWETHA, Department of ECE, MRK INSTITUTE OF TECHNOLOGY

ABSTRACT

India, considered being one of the largest democratic countries in the world. Besides this country have the largest number of population and a number of politicians in each party. The fate of the country and citizens is in the hand of the political representative of the country, who was chosen by the citizens of the country by voting. This gives an illustration of how much the fundamental right to vote is important. But according to research, in 2014, in common election, in India, only 66.4% of valid citizens cast their votes. This may represent that the voters do not value or care about their right to vote or maybe there is a problem with the voting system. The voting system has a few problems with it. One of the major problems in existing voting system, which is EVM (Electronic Voting Machine), in that the voter cannot verify whether his vote is registered or not and even if it is registered it is not possible to know if it is registered under the correct candidate the voter had cast his vote too. So, in this paper, we propose a system or method which will solve that problem of the current voting system available in India.

Keywords—electronic voting machine, biometrics, GSM, cloud-based database, SMS, double verification.

1. INTRODUCTION

In India, a machine is used in order to cast the votes in the general election which is known as an Electronic Voting Machine (EVM), which is put to use in order to register the votes and compute the votes by the voter of India. In ancient times, papers and boxes were used to elect a leader, that method is known as a paper ballot. That age-old method required more manual labour, energy, workforce, and time. Therefore the process was substituted by the electronic method of voting. Despite the fact of this present day's system is precise and rapid than the earlier method, it requires additional efficiency, manpower, and accuracy. In addition to this, there is a chance of failure in the machine that is presently being used in this country. To reduce these problems in the current polling system, this article suggested an intelligent, smart and protected process of voting.

The core topic of this system is biometrics. There is a big total of populations who are appropriate to vote are called as voters, in India to identify each voter, a unique number is provided with the voter id. Besides, for verification purposes, biometrics traits can be used. A fingerprint is unique to each human being, which provides much better protection than any secret keywords or passes keys. Thus, the biometric concept can provide a better protected system for polling. In EVM there is no module that can confirm if the citizen's vote cast or not. So, the paper is proposed to include an SMS module and GSM module to confirm the vote cast by the voter is registered via a confirmation message to the registered mobile phone. This will improve the consistency and proficiency of the system.

2. EXISTING SYSTEM

In the paper [1] the system consists of fingerprint authentication with connection to the Aadhar card database. If the voter has cast vote already then, the buzzer alarm is activated. If not then the voter can cast his/her vote in EVM.

The issues that are found in the existing systems are that increased costs, single point of failure, and the message does not confirm that the vote is registered for the voter's favourite candidate to whom he/she had cast the votes. There is a possibility that the voter's vote is registered to some other candidate rather than the one who he had cast his vote.

In the paper,[1] the engineering wherein use Global System for Mobile communication(GSM module) in order to accelerate the voting process and to improve the protection of the casting a ballot framework. Utilizing

this component, the voters will receive a message to citizen's cell phone which the voter has effectively chosen the favourite candidate. Therefore the voter can effectively check with no disarray.

At that point, another new innovation utilized in that paper is IOT which is a huge idea. Utilizing the Internet of Thing concept, the votes which are checked may be effectively notified to the aggregate server of the database. The goal of this system is that the selected representative is reported effectively to the voter. As indicated by the topic, no malpractice is permitted at the polling booth. Utilizing the province of IoT and embedded system Technology, they could move the casted ballot information online to the ace server unit. As indicated by the topic, in various areas, many slave frameworks are placed. Every sub-slave framework is connected to the closest Main framework System. All the Sub-Slave framework of the given Main framework system interact with each other effectively.

These Main framework Systems interact with the Main Server. Impeccably made programming would be created as a secure component. In last, after the last voter makes the choice, the result will be announced quickly, which can evade part stock of expense. The proposed flowchart starts with unique mark validation and afterward it contrasts and the government database which contains Aadhar card details and that likewise verify the individual identity if the individual already made the choice or not. In the event that he is as of now thrown, at that point a component makes the alert and the error message shows up and the voter cannot make the choice with the goal that it can maintain a strategic distance from misinterpretations during decisions. In the event that the voter is not as of now made the choice then the EVM catch is empowered with the goal that the voter makes the choice effectively and in the wake of throwing the vote, the person's portable will get a message that he had effectively made the choice with the goal that he can ensure that he has made the choice. At that point, the outcome will be reported when the database gathers all the checked votes utilizing IoT innovation and after that, the procedure stops.

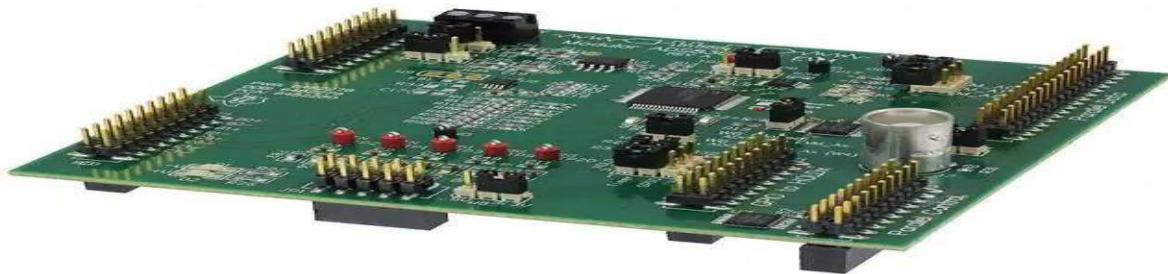


FIG .EVM MODEL KIT BOARD

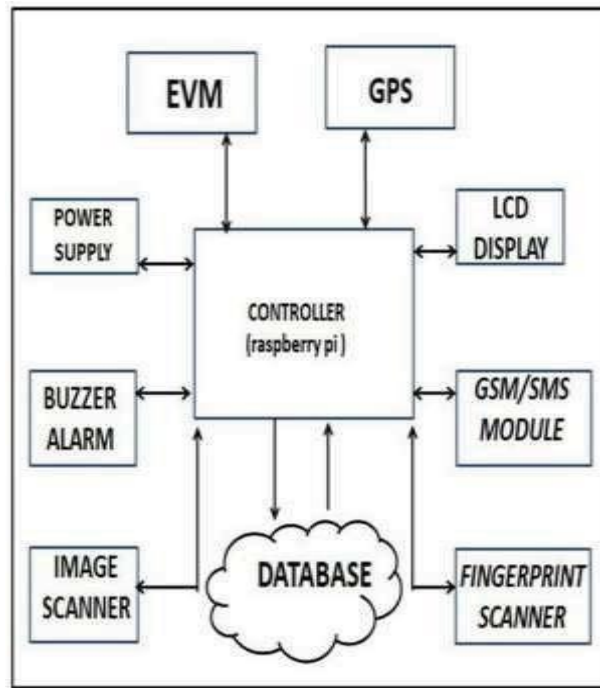
3.PROPOSED SYSTEM

A. PROPOSED IDEA

In this paper, we proposed a system (fig. 1) which includes a GSM module, SMS module, GPS, fingerprint sensor and an image scanner. This makes the system more secure and efficient than the current existing EVM. We use biometrics technology to identify the valid voter from the database which has the voter's details with his fingerprints. With the help of the GSM module and SMS unit, the message is notified to a valid citizen's portable device that he has effectively made the choice. So he can check effectively with no disarray. The given system also involves the Global Positioning System, which provides the Geographical location of the given system is located. The GPS module provided with the system helps in tracking the device in the case of stealing the device from the polling booth. Considering that the cloud is coupled with the system, the system can act as an online system. In this proposed system the flaws of EVM are overcome. This system is much better protected and works with higher

efficiency than the system that is already present. This system includes a database that has a list of the voters who have cast their votes. This list is provided in order to determine the voters one's who wasted their valuable chance to decide the rightful candidate representative and the corresponding steps or measures can be taken regarding these default voters.

Fig. 1. The architecture of proposed system



B. COMPONENT DESCRIPTION

a) *Microcontroller (Raspberry pi)*: It's in a credit card size processor. It can be socket into any computer or laptops with a standard input device. It helps in coding the system and control the devices or modules connect with it. For a miniature of the system, the raspberry pi model 3 B+ is used. The advantages of using a raspberry pi as a microcontroller are low cost, portable, consume less power.

b) *GSM/SMS Modules*: GSM represents Global System for Mobile correspondence which goes about as a modem for versatile correspondence. It is open and digital cellular technology for transmitting voice and provides internet services through air. Later technology was developed and SMS were included in it. SMS stands for Short Message Service. It is a technology that helps to send and receive text or images from sender to receiver(s). The major advantages are international roaming, provides new services, making calls and short message services since it can be supported by GSM modem.

c) *GPS*: GPS stands for Global Positioning System. It is a device that can be used for locating a device or a person with this system. It works as follows when a person or a device has a GPS, it will send the radiation or signal to the satellites around it and when a device or person needs to be located the base station will calculate the data and provide the location. It helps this project in such a way that if the voting machine is stolen or anyone tries to take it away from the polls and try to make changes it can be tracked and located easily rather than the current voting system.

d) *Image scanner*: Image scanner is a kind of scanner that creates an arithmetical illustration of an image for records responsive to a PC. It is also known as an optical scanner. It is an electronic device that can read or scan visuals, manuscript or handwritten manuscript and convert it into an electronic arrangement that the

computer can recognize. In this project, the image scanner will scan the voter id and extract the voter id number from the image and use that image for identification and then further for verification.

e) *Fingerprint scanner:* A fingerprint scanner is a sort of tool that recognizes and validates the fingerprints of a distinct in order to permit or refuse entree to a system or a physical facility. It is a kind of biometric security equipment that functions with the arrangement of hardware and software procedures to detect the fingerprint images of a distinct. It normally operates by initially record fingerprint images of all approved individuals for a specific system or device. These images are held back within a database. The user requesting for access place their thumb on a fingerprint sensor, which senses and provide the duplicate fingerprint of the particular citizen and search for correspondence with the main database and cross-checks with the previously stored images. Solitary if there is an optimistic contest, the individual is permitted for an entrance or access. In this project, fingerprint scanners are used for verification purposes so that the vote's voting procedure can be more secure.

f) *Buzzer:* A signal is a minimal yet achieved module to supplement sound structures to our framework. It is decisively minimal and compacted 2stick development consequently it very well may be just utilized on a breadboard, Perf Board and just as on PCBs which makes this a generally utilized segment in most electronic applications. It is going with a changing circuit to a mood killer or turn on decisively at an important time and required break. In this project, the buzzer is active when there is any error occurs during the voting procedure such as when a voter who already voter try to cast vote again, when the voter id number, as well as fingerprints, does not match, and when any other error occurs.

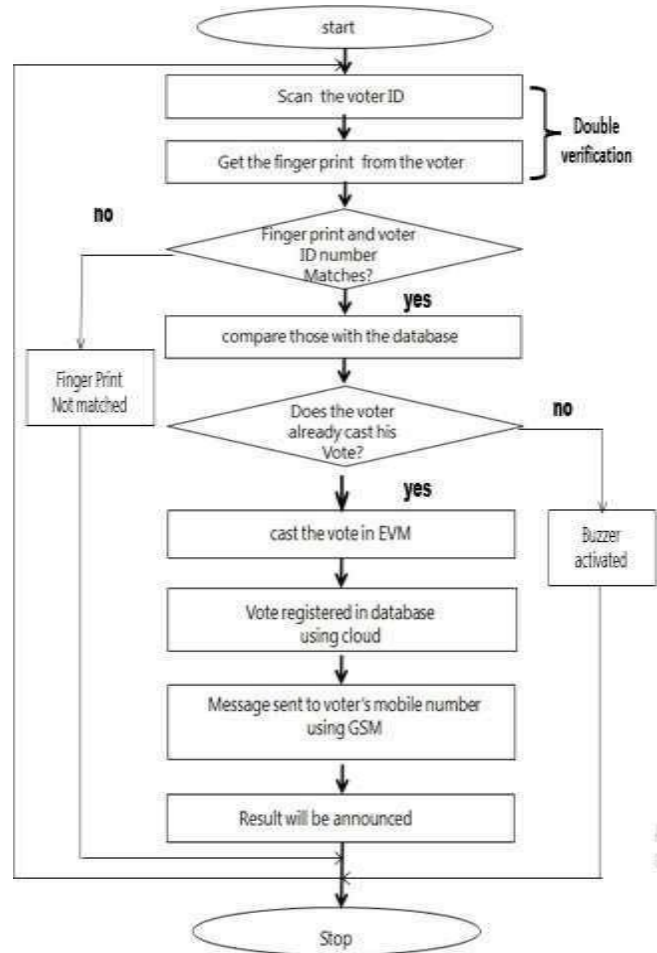
g) *LCD display screen:* LCD is "Liquid Crystal Display". It is a plane piece with a display technology that is usually used in Smartphone's, televisions and system monitors, PC, tablets, and laptops. It does not look any dissimilar than bulky CRT monitors, the manner it functions is considerably altered as well. As an alternative of firing electrons at a glass display, and even it has rear light that deals light to individual pixels structured in a rectangular network. RGB sub-pixel (blue, red, and green) are present in every pixel of LCD which can be spun on whenever required.

The screen is black when all the sub-pixels of the pixel are in the off state. Else if all the sub-pixels of the pixel are in the on state, the screen is turned on. The difference in the level of the RGB (amount of red, green and blue), millions of mixtures of colours can be created. In this project, the LCD display is used to convey the information to the user of the machine that is voters themselves. Such as when the voter who cast his voter already claim to vote again a buzzer is activated and the LCD will display the current voter had already cast his vote beforehand, when the voter id number does not match with the fingerprints scanned that time also it will show the text that there is no match to two inputs and when there is any other error occurs it will show the text correspondence with the error.

h) *EVM:* Electronic Voting Machine, EVM can be described as a machine used for voting and computing votes. It is also known as e-voting. Depending on the specific action or application, voting through electronic means may custom objective electronic voting machines (also called EVM) or systems coupled to the Internet. It may include a range of Internet services, from the fundamental broadcast of tabulated outcomes to completely internet-oriented voting through common linkable household devices. The degree of automation may be restricted to marking a paper ballot, or maybe a widespread system of elect response, vote registering, broadcast to servers, cassette or recording, data encryption and, and the announcement of election outcomes. This project used EVM for the general purpose of the electronic voting machine as mentioned above.

i) *Cloud-based database:* It can be termed or defined as a database that will deliver the data or list of contexts to the client at the request of the client with the permit. Similarly, a database using the cloud can utilize cloud computing to conquer great availability, optimized scaling, effective resource allocation, and multi-tenancy is stated to as Database as a Service (i.e. DBaaS). Still, database using cloud might be old-fashioned similar to the popular SQL Server database, MySQL which also executes on the cloud utilize, natural database based on cloud rises to increase the prepare in order to accurately practice resource of cloud plus promise well scalable in accumulation to obtain ability as well as firmness, for example, Xeround's MySQL which uses Cloud database. It may propose important benefits against the old-fashioned counterparts, including high accessibility, programmed failover and fast automated retrieval from and theoretically better presentation, minimal investment, failure, preservation of in-house hardware and automated on-the-go scaling. Simultaneously, databases of the cloud have their part of possible disadvantages, counting security and private problem and the possibilities of losing, changing or incapability to the data access during some unexpected obstacles

or ruin the cloud database service provider. In this project, the cloud is used to store all the details of voters and their fingerprints. During elections, the votes are recorded in the cloud so retrieval is somewhat considered to be easy and efficient for maintenance purposes also



4.RESULT

After the implementation of the workflow, the output will look as shown in fig 3. This will be helpful to the voter to verify whether his vote is cast or not, along with under which candidate his vote was cast. Additional to it, the corresponding message will be sent only to the registered phone number.

Fig. 3. The sample output of the system



5. CONCLUSION

The proposed system has a double verification for a more secure system. This system uses a cloud database; hence it will be more efficient than the existing system. There is additional GPS in the system, this will prevent the system from theft if the system is stolen it can be located easily and immediately through satellites. Through GSM, we can get a confirmation message about to which candidate the vote got registered to, this way the elector can verify that the voter is pitched to his favourite candidate.

6. FUTURE WORK

In this system, we can add any other devices for better performance. This system can be further improved with any other advanced technology. So that the system can be more efficient, and hence can be more secure and compact.

ACKNOWLEDGEMENT

It is indeed a great pleasure and proud privilege to acknowledge the help and support we received from the positive minds around us in making this end over successful one. First and foremost I express my sincere gratitude to the Almighty. The infrastructural support with all kinds of lab facilities in my Department have been a motivating factor in this completion of project work, all because of our beloved Chairman **Thiru. P. Kathiravan, B.E.**, with great pleasure we take this opportunity to thank him. From the academic side the constant support from our Respected Principal Prof. **Dr. K. Anandavelu, M.E., Ph.D.**, has encouraged us to work hard and attain this goal of completing this project.

Our sincere thanks to our Head of the Department, **Mr. S.SATHYA MOORTHY, M.E.**, who have given us both moral and technical support adding experience to the job we have undertaken.

We thank our Supervisor and Project Co-Ordinator, **R.SIVAPRATHA, M.E.**, who has led us, right from the beginning of the Project and encouraging us most of the time, thereby extracting quality work from us.

We are grateful our Administrative Officer, Manager and Staff Members, We also thank to our Non-Teaching and other Staff Members of our College, who supported and motivated us in all end over to complete this Project. Finally our acknowledgment goes to our Family Members and Friends who extended their excellent support and ideas to make our project successful one.

7.REFERENCES

- a. V. Kiruthika Priya, V. Vimaladevi, B. Pandimeenal, T. Dhivya, “Arduino based Smart Electronic Voting Machine”,International Conference on Trends in Electronics and Informatics, ICEI 2017, pp.641-644.
- b. Dr. Z.A. Usmani , Kaif Patanwala, Mukesh Panigrahi, Ajay Nair, “MULTI PURPOSE PLATFORM INDEPENDENT ON LINE VOTING SYSTEM”, International conference on innovation in Information, Embedded and CommunicationSystems, 2017
- c. Komminist Weldemariam, Andrea Mattioli, Adolfo Villafiorita, ,“Managing Requirements for e-voting Systems: Issues and Approaches Motivated by a Case Study”, First International Workshop on Requirements Engineering for E-Voting Systems,2009
- d. Chunlin Yang, Techshino, “Fingerprint Biometrics for ID Document Verification”, IEEE 9th Conference on Industrial Electronics and Applications (ICIEA), pp.1441-1445, 2014.
- e. Sravya. V, Radha Krishna Murthy,Ravindra Babu Kallam, Srujana B, “A Survey on Fingerprint Biometric System”, International Journal of Advanced Research in Computer Science and Software Engineering ,pp.307-313 Volume II,Issue 4, April 2012.

Implementation of Speed Assistance in Vehicle by using Internet of Things(IoT)

Mohanraj.R, Department of ECE, Student , MRK Institute of Technology, Kattumannarkoil
Sanjay.T, Department of ECE, Student, MRK Institute of Technology, Kattumannarkoil
Yogeshraja.R, Department of ECE, Student, MRK Institute of Technology, Kattumannarkoil
Prithiviraj.K, Department of ECE, Asst Prof., MRK Institute of Technology, Kattumannarkoil

Abstract

This document contains the formatting information for the papers presented at the “International Conference on Recent Developments in Science, Engineering and Technology (ICRDSET - 2022)”. The conference would be held at the St. Anne’s College of Engineering and Technology, Panruti during 2022. Even though the accidents are occur due to driver over speed and rash driving. This project continuously monitor the drivers vehicle speed state to avoid accidents. According to this project when a driver is over speeding, the sensor sense that and sends it to controller. Microcontroller sends the information to the authority person via android app and sends commands to stop the vehicle.

Keywords:

1.Introduction

Smart accident prevention for driver is a project undertaken to increase the rate of safety among drivers. The idea is obtained after knowing that the increasing number of fatal accidents over the years is cause for concern among drivers. This project aims for accident avoidance, safety and security of driver.

2.Existing System

The system takes password input and checks it is correct or not, if it is true then allows driving over speed but if it is false then activating the speed limit function. The speed is senses in form of pulse by op-amp comparator and given to microcontroller which calculates the pulses per sec and display the speed. It also comparers the speed with stored speed limit data and if it is over the speed limit than turn off the relay which is connected with the ignition power supply. So, speed will decrease and when it comes below speed limit than turn on supply and continues

1. Disadvantages of Existing System

- Less security.
- Potentially high payoff.
- Complexity is very high.

3.Proposed System

The proposed system is to design a smart safety system to intimate the authority person when over speeding situation of the vehicle. Most of the times we may not be able to find the driver speed but in order to reduce the accident and fall, first we need to know the condition of each drivers speed limit, then in case of over speeding the information is passed to the authority person via android app using IoT. This system placed a speed sensor to know about the speed of vehicle with the potentiometer. The live monitoring and control of the vehicle is processed by android app connected to the cloud.

4.Methods:

Nineteen volunteers (8 male) were recruited to complete a drive in the simulator equipped with a speed warning system while their eye movements were tracked. Participants had to be able to drive without glasses or contact lenses. The participants' average age was 27.53 years, (SD = 6.32) and they had an average of 9.26 years of experience as licensed drivers (SD = 6.74). They reported an average of 175.95 km driving per week (SD = 170.05). This research complied with the tenets of the Declaration of Helsinki and was approved by the School of Psychology Research and Ethics Committee, University of Waikato. The experiment took place in the University of Waikato fixed-base driving simulator which consisted of a complete automobile (2010 Toyota Prius plug-in) positioned in front of three angled projection surfaces. As has been described in Starkey et al, the centre projection surface was located 2.32 m in front of the driver's eye position with two peripheral surfaces connected to the central surface at 52 ° angles. This configuration produced a 178.2 ° (horizontal) by 33.7 ° (vertical) forward view of the simulated roadway from the driver's position. The vehicle model and the simulator screens were updated at least 100 Hz. The simulator hardware and software was developed by the Transport Research Group. Its validity against on-road performance has been tested in several different kinds of experimental scenarios, including those with a focus on speed choice . Four small infra-red LEDs were placed on the outside of the car windscreen to facilitate calibration and analysis of their eye movements. The simulated speed was displayed in digital form on the dashboard. The speed warning system was implemented as an application on a smart phone attached to the console to 12 cm to the left of the steering wheel. Visually, the display was located 10.6° below, and 29.3° to the left of the driver's forward line of sight. A speed warning was triggered if the driver exceeded the speed limit by 4 km/h for 3 s. Speed warnings consisted of a large speed round (display size of 2.7 in., resolution of 1280 × 720) flashing and beeping until the participant reduced their speed to within 4 km/h of the speed limit. The speed warning app had two modes, passive and active. In the passive mode, the display automatically updated to show the new speed limit after entering a new speed zone. In the active mode, the participants were told to select the new speed limit when they entered a new speed zone (from the small speed limit signs along the bottom of the display screen). If the driver forgot to select the speed, it was automatically updated to the correct speed after 7.0 s.

5.Discussion

The aim of the study was to examine the influence of a speed warning system on drivers' speedometer monitoring, and how drivers respond when they receive a warning. We wanted to see if the presence of a speed warning system would increase the speedometer monitoring, measured as the speedometer glance rate, as would be expected if the system increased drivers' cognitive control over their speed. In addition to such overall effect, we expected to see an increase of speedometer glances after receiving a warning, and possibly decrease of speedometer glances before, if speeding were linked to a momentary lapse of cognitive control over speed. Drivers frequently glanced at the speedometer, but the speedometer glance rates were not different with or without a speed app. Especially, in the 60 km/h speed limit, where the control group exceeded the speed limit most often and where there was most speeding by the control group, the speedometer glance rates were not significantly higher with the system compared to the control. Drivers often looked at the speedometer just before they released an accelerator. This pattern appeared to be more pronounced with a speed warning system, but not statistically significantly so. In other words, there is no indication the warning system would have changed the speedometer monitoring in general. It is also good to note that there was no indication that a speed warning system would lead drivers to complacency, where they would reduce their speedometer monitoring, waiting for the warnings instead.

The speed limit, however, influenced the speedometer glance rates among all groups. The speedometer glance rate was higher in the 60 km/h zone compared to 80 km/h and 100 km/h zones. In the experiment, the 60 km/h segment had a similar road geometry to 100 km/h and 80 km/h segments. The higher speedometer glance rate can be interpreted to reflect increased cognitive control over the speed when the visual cues indicated a higher optimal speed than the speed limit would allow. The situation is analogous to asking drivers to drive slower on the same road. Recarte and Nunes reported that time

spent looking at the speedometer increased three-fold when drivers were asked to drive between 90 and 100 km/h compared to free speed choice on a motorway with 120 km/h speed limit. The time course of speedometer glances relative to the speed warnings indicated that speedometer glance rates decreased 2–7 s before the warnings and started to increase 2 s seconds prior to the warning. Speed started to increase approximately 10 s before a warning was triggered. Within 0–2 s before the warning, the average speed was higher than 0–1 s after the warnings, suggesting that drivers often noticed before the warning that they are going over the speed limit, and therefore glanced at the speedometer and started to reduce their speed, typically by releasing the accelerator. The decrease of speedometer glances prior warnings suggest that a partial explanation for speeding can be a momentary lapse of cognitive control over speeds.

The results also demonstrated that drivers do not only react to speed warnings, but they anticipate them and start speed adaptation before a warning occurs. This suggests that part of the speed reducing the effect of a speed warning system can be that drivers recognize when they are going over the speed limit and try to react by reducing their speed. The analysis of speedometer glances during the speed limit transitions supported the interpretation that the increase in the speedometer glance rate with warnings is related to speed adaptation. Speedometer glance rate started to increase when the average speed profile started to change, and lasted until the transition to the new speed level was finished. Noteworthy, there was no difference between speed transition upwards or downwards.

Regarding the visual distraction of ISA, Starkey et al. already concluded that the speed warning system used in the experiment is unlikely to visually distract the driver, as the number of glances to the speed app was very small, and most of them were with the active system, which required the driver to manually set the current speed limit. In this sense, the speed warnings systems appear to be very different from constantly updating visual eco-driving feedback systems that can attract a significant portion of drivers' visual attention. The further analysis of speedometer monitoring does not suggest that a speed warning system would be very distracting, either. Glances to the speedometer are frequent, but because most of the glances to the speedometer are short, less than 1 s and thus clearly under the recommended 2 s threshold for off-road glances, they are unlikely to distract the driver. However, to minimize any potential distraction, it could be beneficial to avoid giving speed warnings in situations which may require fast response from the driver, e.g. when following a lead vehicle at short distance or when overtaking, because those may trigger drivers to look at the speedometer.

The current results suggest speed warning systems can be especially effective to counteract unintentional speeding caused by inattention over the control of speed. Systems can be also more effective if the drivers are able to predict when a warning would be triggered, enabling them to use available perceptual cues to re-engage their cognitive control even without a warning. A better understanding of the temporal coupling between speedometer glances, speed regulation and speed warnings could be used to design ISA systems adapt to the driver's speed regulation strategies, for example by not issuing a warning if the driver has just glanced the speedometer and it is likely that he/she will release the accelerator soon. Such adaptive designs may increase the user acceptance of ISA systems and help to realize their true potential to improve safety.

6.LIMITATION

The experimental settings have likely affected driver behaviour. Speedometer glance rates in the simulator were up to three times higher than those calculated from data collected on a motorway, without a speed warning system but with an instruction to keep the speed at 90 km/h. The participants were aware that the study was about speed warning systems and had experimenters monitoring their driving, which may have led them to monitor their speed more closely than they usually would. Also, the simulator may not replicate all the perceptual cues which can be used for the control of speed, requiring the drivers to exert more cognitive control over the speed with the help of speedometer glances, further increasing their speedometer glance rates. Inflated speedometer glance rates may have masked differences between the control and speed warning groups. The present study was also limited in the number of participants.

The current results cannot be generalized to intentional speeding, because we would assume that most of

the participants tried to comply with the presented warnings. It would be valuable to check if the observed synchronization of glances and speed warnings would emerge also using naturalistic data with a commercially available ISA system, and if glance patterns could be used to distinguish intentional and unintentional speeding events.

ii. Block Diagram:

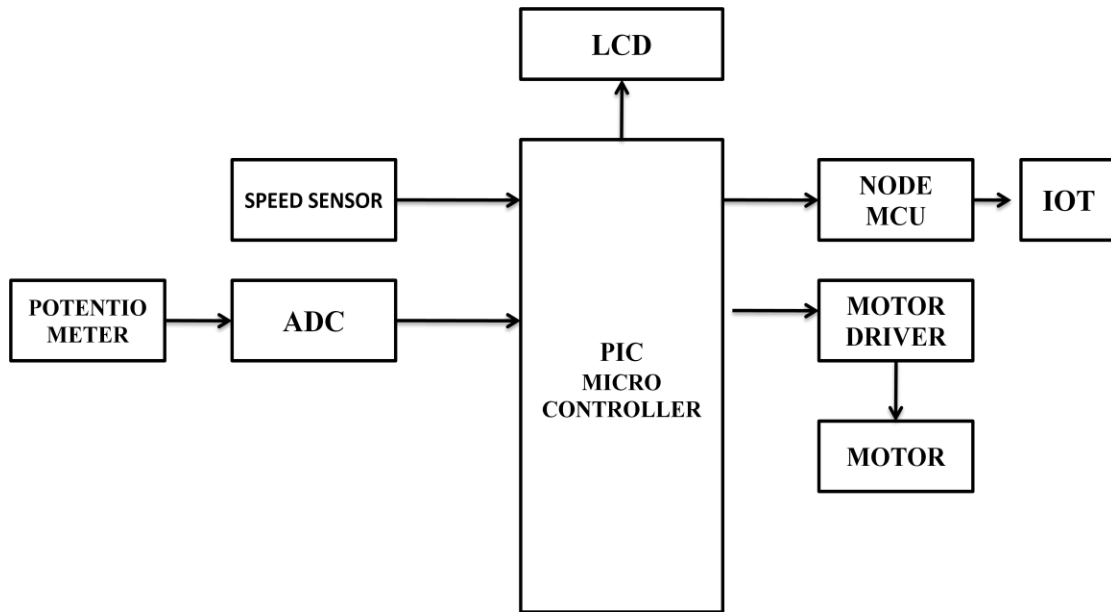


Fig: Block Diagram of Transmitter Section

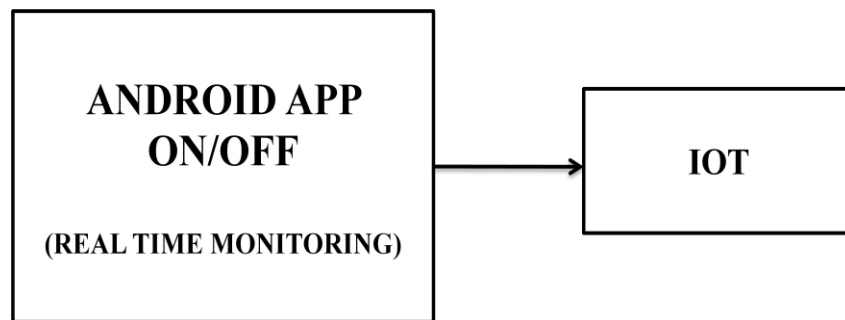


Fig: Block Diagram of Receiver Section

iii. Microcontroller:

PIC16F877a is a 40-pin PIC Microcontroller, designed using RISC architecture, manufactured by Microchip and is used in Embedded Projects. It has five Ports on it, starting from Port A to Port E. It has three Timers in it, two of which are 8-bit Timers while 1 is of 16 Bit.

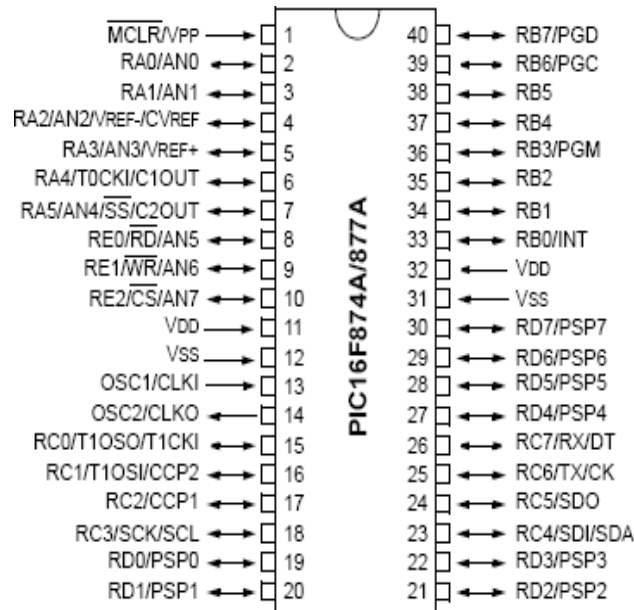


Fig: PIN Diagram of 16F877A

iv. Speed Sensor:

The vehicle speed sensor (VSS) measures transmission/transaxle output or wheel speed. The ECM uses this information to modify engine functions such as ignition timing, air/fuel ratio, transmission shift points, and to initiate diagnostic routines.

v. NODE MCU:

The ESP8266 is the name of a micro controller designed by Espressif Systems. The ESP8266 itself is a self-contained WiFi networking solution offering as a bridge from existing micro controller to WiFi and is also capable of running self-contained applications. This module comes with a built-in USB connector and a rich assortment of pin-outs. With a micro USB cable, you can connect NodeMCU devkit to your laptop and flash it without any trouble, just like Arduino. It is also immediately breadboard friendly.

vi. Specification:

- Current consumption: 10uA~170mA.
- Flash memory attachable: 16MB max (512K normal).
- Integrated TCP/IP protocol stack.
- Processor: Tensilica L106 32-bit.
- Processor speed: 80~160MHz.
- RAM: 32K + 80K.
- GPIOs: 17 (multiplexed with other functions).

vii. DC MOTOR

In any electric motor, operation is based on simple electromagnetism. A current-carrying conductor generates a magnetic field when this is then placed in an external magnetic field, it will experience a force proportional to the current in the conductor, and to the strength of the external magnetic field. As you are well aware of from playing with magnets as a kid, opposite (North and South) polarities attract, while like polarities (North and North, South and South) repel. The internal configuration of a DC motor is designed to harness the magnetic interaction between a current carrying conductor and an external magnetic field to generate rotational motion.

viii. EQUATION

The quantization step in ADC0809/ADC0808 is given by,

$$Q_{\text{step}} = \frac{V_{\text{REF}}}{2^8} = \frac{V_{\text{REF}}(+)-V_{\text{REF}}(-)}{256_{10}}$$

The digital data corresponding to an analog input (V_{in}) is given by,

$$\text{Digital data} = \left(\frac{V_{\text{in}}}{Q_{\text{step}}} - 1 \right)_{10}$$

ix. Conclusions

To improve the safety of drivers. To develop a Smart safety system for driver, And to design a project with features like detecting the driver speed. Speedometer glances can be used as an indicator of cognitive control over driving speed. The current results suggest that before speed warnings the speedometer glance rate may decrease, and after warnings it increases. This indicated the speed warnings re-engage the drivers to cognitive control of speed, which they may have momentarily lost before speeding. Drivers anticipate warnings by increasing their speedometer glance rate and adjusting their speed a couple of seconds before a warning is triggered. The present study did not find evidence that a speed warning system would change the speedometer monitoring in general. The results suggest that warnings can effectively counteract unintentional speeding, caused by momentary inattention over the speed control. Further re- search linking speeding to distractive events and/or mind- wandering could provide direct support for this idea.

x. References

1. Aarts, L., & Van Schagen, I. (2006). Driving speed and the risk of roadcrashes: A review. Accident Analysis and Prevention.
2. Adell, E., Várhelyi, A., &Hjälmdahl, M. (2008). Auditory and haptic systems for incar speed management - A comparative real life study. TransportationResearch Part F: Traffic Psychology and Behaviour.
3. Adell, E., Várhelyi, A., &Hjälmdahl, M. (2008). Auditory and haptic systems for incar speed management - A comparative real life study. TransportationResearch Part F: Traffic Psychology and Behaviour.
4. Charlton, S. G., Starkey, N. J., &Malhotra, N. (2018). Using roadmarkings as a continuous cue for speed

choice. Accident Analysis and Prevention.

- 5.** Engström, J., Markkula, G., Victor, T., & Merat, N. (2017). Effects of cognitive load on driving performance.

ABANDONED BORE WELL RESCUE SYSTEM FOR TODDLERS USING APL DEVICE

R.Aasha, Department of ECE, Student,MRKIT
M.Shylaja, Department of ECE, Student MRKIT
S.Nivedha, Department of ECE, Student MRKIT
T.Karthiga, Department of ECE, Assistant Professor MRKIT

Abstract

Borewells are a common alternative for those in cities where channelled water cannot satisfy everyone's water needs. A few lakh borewells have been dug, and a large number of them have failed to provide water after burrowing. When the bombed ones are revealed, they will become death traps for unsuspecting children who can quickly slip through the 8 to 10 inch deep gaps. Since 2009, more than 40 children have died as a consequence of dropping down borewells, according to the National Disaster Response Force (NDRF), with salvage attempts struggling at least 70% of the time. It's complicated, time-consuming, and risky to save the abducted infant from the borewells. To ensure the safety of the child who fell in bore well a automatic plate lifting system was developed that checks the health and environmental condition around the child and give oxygen according to that. This system will be helpful in rescuing the child from bore well and also send the information to the control unit via GSM. The air temperature is monitored by a temperature sensor, whereas the existence of some poisonous gas is detected by a CO2 sensor. The suggested framework would better shield the infant without adding unnecessary harm to the child.

Keywords - *Automatic plate lifting device , CO2 monitoring, Infrared sensing , Victim thermal sensing ,Automatic oxygen spraying.*

1.Introduction

Borewells are necessary to meet the essential needs of daily life due to water scarcity. The paper belongs to the field of Mine hole and bore well accidents. This is a very hazardous rescue area and the number of accidents in this area too is increasing day by day. This is why a proper rescue system is very much necessary in this area. Mine holes and bore wells are all very narrow and their diameter is very less. So, the entry of a person manually for rescue is not possible all the time. Therefore, we have to adopt other methods that would give the necessary result. And there is no better way to enter such a dangerous place without actually entering such a place. The application of this system can be made effective in deep trenches and other places where a human cannot enter manually. The wells are not properly sealed while they are burrowed. In general, small children will reluctantly collapse into borewells. Another arduous task is ensuring the safety of the child. A simple aim of this paper is to save the child with less time compared to any remaining breathing plans. The extraordinary breakthrough deduced

in this paper is arm waistline convenience. The rest of the paper's references are mentioned below. So, an APL device along with the precision mechanical system enables us to enter such a dangerous place with easy and extract the victim safely.

Related Work

In the existing technique the controlling of a robot to protect the child from the drag opening is constrained by the individual from outside and there's no movable arm breadth robot. The past framework, a huge opening is burrowed close to the drag well until the profundity where the youngster is caught for an all-encompassing time. Indeed, even a little postponement in these assets may decrease the possibility to save loads of the youngster alive. The world close to the drag opening may in some cases contain shakes somewhere inside; all things considered the opportunity to save bunches of the child alive is low and dangerous. Because of less oxygen and no light may cause the significant trouble during the activity of salvage of the child. Till period there's no such single gear for good the kid caught intimate the drag opening. There's no method to safeguard the child. The military individuals are called if this framework doesn't work. It includes huge loads of your time and energy and costly assets which aren't effectively accessible all over. [1] This technique lowers the temperature and allows fresh air to circulate. With infrared waterproof cameras and a flexible high-resolution TV display, imagining the child is feasible. This is a little machine that will go down into the drag well line and purposefully save the youngster's life. This computer will descend the drag well and complete the task. This robot-like machine will keep a body trapped in a bore well alive before an equivalent corridor is exposed, which will fill in a reasonable amount of time and effectively save the youngster's life. [2] Borewell salvage device is a solution for these types of situations. It's easy, cost-effective, and safe. To raise the infant from the borewell, we're using a wiper engine and a wire rope with a cinching component. [3] This computer will descend the drag well and complete the mission. This robot-like system will keep a body trapped in a bore well alive before an equivalent lobby is uncovered, which will fill in time and save the youngster's life methodically. [4] A mechanical arm and a foldable seat were used to securely separate the child from the drag well in this experiment. The child-care device is built in such a manner that the child is never injured, and the robot itself has some pre-treatment to allow the child to keep working before the Procedure is over. To prepare for this mission, the PIC 16F 877A micro controller was used.



Fig. 1. Existing System (no technique to rescue the kid)

Proposed system

Salvage framework has different sensors to gauge the climate inside the opening. Carbon dioxide level is checked, on the off chance that it surpasses certain level, oxygen will be siphoned, and the whole cycle is programmed. Temperature, pressure is likewise estimated for wellbeing of the Toddlers. PIR is utilized to know profundity of the youngster accessibility. Estimated values are moved to PC for observing. In this proposed framework more significance is given for youngster's well being. So Toddlers can be safeguarded securely. We've intended to use the temperature and gas finder to detect the temperature and gas spillage in the particular region.

Rescue system has various sensors to measure the environment CO2 level is monitored, if it exceeds certain level, oxygen will be pumped, the entire process is automatic PIR is used to know depth of the child availability. Measured values are transferred to control unit via GSM for monitoring. In this proposed system more importance is given by passing the information immediately when the child fell by using IR sensor and here it also have APL device to lift the child upward.

PIC Microcontroller

The PIC microcontroller is a CMOS (equal content oxide semiconductor) high-RISC hanging microcontroller that enables companies to exclude law and data transport, allowing for coextensive access to information and data memory. The low force needed to obtain a small chip gauge with a small stick quest is the main benefit of integrating CMOS and RISC. Operating rate DC - 20 MHz The operating voltage is between 4.2 volts to 5.5 volts. If you provide it voltage more than 5.5 volts.

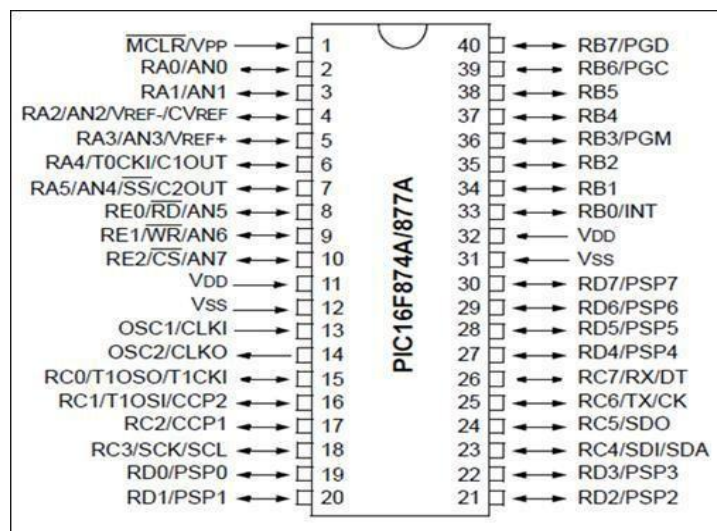


Fig.2. PIC Microcontroller

Temperatures Sensor

The LM35 is a precision IC temperature locator with a yield that is proportional to the temperature (in OC). The identifier information is set, so it isn't subject to oxidation or other strategies. Temperature can be measured more accurately with the LM35. Rather than using an external regulator, this method is more accurate.

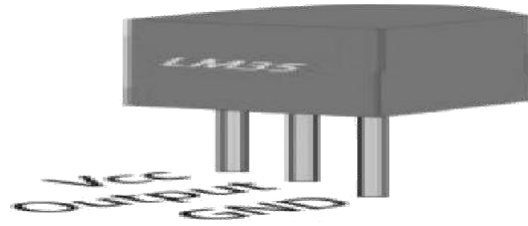


Fig. 3. Temperature Sensor

CO2 Sensor

The presence of Carbon dioxide can be detected and measured using a carbon dioxide sensor. A carbon dioxide sensor measures **gaseous carbon dioxide levels** by monitoring the amount of infrared (IR) radiation absorbed by carbon dioxide molecules. Measuring carbon dioxide is critical in monitoring by indoor air quality.



Fig 4.Co2 Sensor

IR transmitter & Receiver

An infrared transmitter and beneficiary are used to assess the duration of the rope. It's used to find out how far the kid has sunk. For each twist, the duration of the rope is determined.

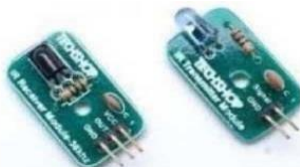


Fig.5. IR transmitter and Receiver

2.APL Device

The APL device is once again used to securely remove the toddlers from the borewell. It is a very effective and time-saving device for quickly growing the without risking significant harm. It, for the most part, guarantees children's wellbeing and decreases the amount of children that perish in boreholes.





3. Block Diagram

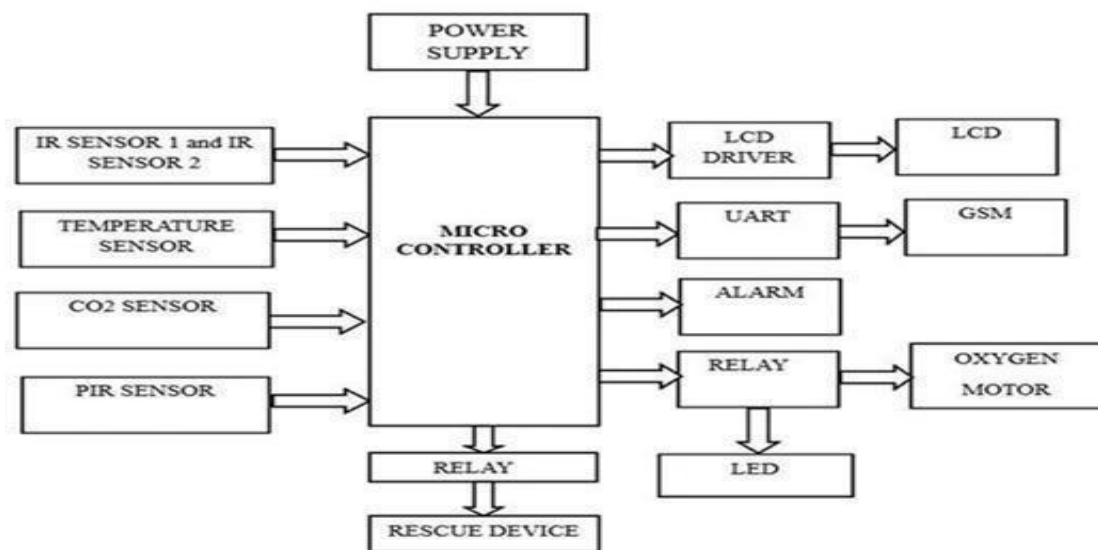


Fig 3.1 Block diagram

4. Result

In this project ideas to save child life from borewells, so the designing of the project kid is more helpful to save the child life. They have fitting lot of sensors and plating device they will be working well with the help of save the child. Below the figure is model kit,





5. Conclusion

Many lives have been lost as a result of falling into the drag well because it consolidates burrowing a pit, which is a repetitive technique. By executing flexible distance through the mechanical system, the proposed framework aims to alleviate these burdens. This task is used to decompose human efforts in order to shield operations from bore wells. When shown up in a different way than normal protocols, it conducts shield activities in less time. The experience included using an air filler to provide oxygen in the absence of air. We will save the presences of youth by completing this mission in a simple manner. In the future, we can use this work in several applications by adding components to this proposed system. Our system is new in innovation in the market it will provide the entrepreneurs with many new ideas and it gives benefits to society.

ACKNOWLEDGMENT

It is indeed a great pleasure and proud privilege to acknowledge the help and support we received from the positive minds around us in making this end over successful one. First and foremost I express my sincere gratitude to the Almighty. The infrastructural support with all kinds of lab facilities in my Department have been a motivating factor in this completion of project work, all because of our beloved Chairman **Thiru. P. Kathiravan, B.E.**, with great pleasure we take this opportunity to thank him. From the academic side the constant support from our Respected Principal Prof. **Dr. K. Anandavelu, M.E., Ph.D.**, has encouraged us to work hard and attain this goal of completing this project.

Our sincere thanks to our Head of the Department, **Mr.S.SATHYA MOORTHY, M.E.**, who have given us both moral and technical support adding experience to the job we have undertaken.

We thank our Supervisor and Project Co-Ordinator, **T.KARTHIGA., M.E.**, who has led us, right from the beginning of the Project and encouraging us most of the time, thereby extracting quality work from us.

We are grateful our Administrative Officer, Manager and Staff Members, We also thank to our Non-Teaching and other Staff Members of our College, who supported and motivated us in all end over to complete this Project. Finally our acknowledgment goes to our Family Members and Friends who extended their excellent support and ideas to make our project successful one.

Reference

- [1] Dr. C.N. Sakhale, 2D.M. Mate 3Subhasis Saha, Tomar Dharmpal, Pranjit Kar, Arindam Sarkar, Rupam Choudhury, Shahil Kumar, “An Approach to Design of Child Saver Machine for Child Trapped in Borehole “, International Journal of Research in Mechanical Engineering, October-December, 2013, pp. 26-38.
- [2] K. Saran¹, S. Vignesh², Marlon Jones Louis have discussed about the project is to design and construct a “Bore-well rescue robot” (i.e., to rescue a trapped baby from bore well), International Journal of Research in Aeronautical and Mechanical Engineering, Boar well rescue robot, pp. 20-30 April 2014
- [3] G. Nithin, G. Gowtham, G. Venkatachalam and S. Narayanan, School of Mechanical Building Sciences, VIT University, India, Design and Simulation of Bore well rescue robot– Advanced, ARPN Journal of Engineering and Applied Sciences, pp. MAY 2014
- [4] B. Bharathi¹, B. Suchitha Samuel, M. Tech (Embedded systems) in Geethanjali College of Engineering and Technology, Cheeryal (V),Keesara (M), R R Dist, India have discussed about Design and Construction of Rescue Robot and Pipeline Inspection Using ZigBee, International Journal of Scientific Engineering and Research (IJSER), pp. September 2013.
- [5] Prof. J.P. Ajith Kumar have discussed about Design Robot for Bore well Rescue Robot for bore well rescue offers a solution to these kinds of situations, timeis@ficci.com.

IOT BASED IMPLEMENTATION OF RIVER WATER FLOW AND WATER QUALITY MONITORING FOR PICO HYDRO POWER PLANT

P.PARUTHI ILAM VAZHUTHI1, Assistant professor ,ECE Department
V.HEERA, Assistant professor ,UG Student ECE Department
VRS College of Engineering and Technology ,Arasur

Abstract

Pico hydro could be a inexperienced energy that victimization little watercourse to come up with electricity while not wishing on any sources of non-renewable energy. This energy offers a inexperienced theme that's reliable, economical and cost-efficient. The problem that unremarkably emerged is that the uncertainty of water debit. This could cause the harm of the Pico hydro power station instrumentation which additionally results in arrive the watercourse path. watercourse water that is employed as drink for the folks today watercourse water affected thanks to direct discharge of commercial effluents and domestic wastages into the watercourse. This contaminated water harms the setting that affects the health of individuals and causes the destruction of water system and water shortage state of affairs. To boot unhealthy water quality results in inefficient processes and will increase maintenance efforts in power station. The planned system is intended to watch the water flow, pH scale level of water in power station unit and to avoid arrive watercourse path by fixing sensors across the watercourse path through on web of Things (IoT) . This project could give to boost the agricultural folks normal that live saround the Pico power station.

Keywords: IOT, Pico power plant, River monitoring

1 INTRODUCTION

Pico hydro could be a hydro-electric that capable of manufacturing a most output power up to 5 kilowatts. Electricity generated by Pico-hydro is extremely helpful particularly to a rural community village that has roughly thirty homes that have little electricity consumption, as an example, fluorescent lights and television or radio. Pico-hydro is additionally able to upgrade the living standards of individuals in poor countries and in rural areas wherever it's trouble some for the government to line up the transmission grid line. Nowadays, the analysis works and innovation in developing this inexperienced technology is extremely encouraging. This effort provides several edges in terms of capability, efficient, the scale of the look, and installation compared to alternative larger hydro. Currently, several developing countries chop-chop have implementing the Pico-hydro generation system thanks to anxiety of the fossil fuels shortage and therefore the volatile of oil costs. Moreover, Picohydro system has become one in every of the foremost people's selections as a result of seventieth of the Earth's surface is roofed by water. However, while not a decent generating system, it'll not be economical and thanks to that, it's vital to possess a decent rotary engine system that may utilize all theon the market water power. Stream watershed refers to a part of land that features rivers and alternative streams that may be wont to hold, save, and drain the downfall off to the lakes, bays, or ocean naturally. Relating to watersheds, the upstream space incorporates a strategic perform , particularly as a geographical region, conservation space, and buffer for areas below like little rivers. A stream could be a long and large water stream that flows unceasingly from upstream (source) to downstream (estuary).

1.1 INTERNET OF THINGS:

One in every of the advanced technologies nowadays is IOT. Basically, IOT technology has been found since the Nineteen Nineties. The primary device used IOT technology for turning on and off remotely over the net was a cake toaster. In 2000, the enormous company of LG created a wise icebox that has its capability to work out whether or not or to not fill the food things hold on.

Those build the IOT gaining vital interest from researchers thanks to its potential for science and information exchange.

.Now, in every round twenty years since Kevin choreographer introduced the IOT in a international organizationITU report, the IOT became capable of showing intelligence observation, managing, tracking, or positioning some explicit system. IOT technology could be a construct during which the device will transfer information over a web network while not requiring human-and pc interaction. In alternative words, the user (human) doesn't got to managementor monitor Associate in Nursing object or device directly by their hand. The management and observation method may be done remotely via a wise phone, PC, or laptop. Recently, IOT has been wide utilized in several topics; a number of them are in sensible looking system, for saving current, for college group action system, etc. IOT has been conjointly significantly utilized in the sphere of small-scale electrical power like the Pico hydro powerhouse. Pico hydro is one in every of the choice energy sources with comparatively little mechanical energy that may be wont to give current in remote areas.

2. EXISTING SYSTEM

Within the existing system style a water flow observation (WAFLOW-MT) device supported the web of Things (IoT). This device might facilitate the technicians at the Pico hydro station in observation the speed of water flow at the watercourse in order that the water debit is recorded all the time. No integration of station and watercourse path unit observation.

2. LIMITATIONS OF EXISTING SYSTEM:

- No integrated unit of hydro station and watercourse observation system squaremeasure on the market.
- Solely monitor the speed of water within thestation
- Water quality parameters cannot be thought of like pH scale level within the watercoursewater.
- It cannot be monitor the water level within the station. It should cause the fatal accident for the Pico hydro station.

3. PROPOSED SYSTEM

During this planned system is observation the water quality and water level beside water flow of the ability plant & monitor the watercourse water levels within the revive path for avoiding flood at any circumstances .This system consists of two units like station unit and watercourse path unit. 1st unit isstation unit , the observation method is completed over the web network by applying the IoT construct.

Water level device, water flow device and pH scale level device square measure wont to monitor the water quality of the reservoir. The desired sensors connected within the system square measure usedbecause the main computer file that may be transferred to the actual web site. After, the information collected are often utilized by the user or technician at the Pico hydro station. The second unit is watercourse path unit, this can be enforced to live the breadth and depth of the watercourse path for avoiding floods beside of the watercourse path. Numerous device units square measure deployed in over the route of the watercourse, All the device unitscollect the readings of breadth and depth of the methods and transferred the information in multi hop fashion to observation unit.

4. DESIDN AND IMPLEMENTATION

In general, this technique contains two parts: 1st, the look that relates to the hardware system and also the second, the look that focuses on the software system of the system. In hardware system the microcontroller acts because the main brain of the system. Arduino UNO R3 was elect because the mainprocessor thanks to its easiness, flexibility, tiny and lightweight, low-cost, and robust. So as to gather the information of the water flow device, level deviceand pH scale device . The water flow works by mensuration what proportion liquid has rapt through its pin wheel. Level water level thanks to seasonal unsteady water levels as a result of the unit won't generate power once there's deficient water and can't power-up the turbine; the water flow device measures what proportion water has rapt through; the pH scale device measures the hydrogen-ion activity in water totake care of the sturdiness of the system over-time. These sensors are then generates pulses that square measure regenerate into digital information. The digital information collected is then sent to the microcontroller. The microcontroller calculates the information so sends it to the ESP8266 IoT module. The ESP8266 module could be a self-contained SoC (system on chip) with associate integrated TCP/IPprotocol that has the potential to attach to the web network. This module can incessantly send the information over the web to the net server. All the electronic elements within the system square measure battery-powered by the freelance power offer that includes a battery and moveable cell for self-charging.

In software system half the event of program code are often conducted by mistreatment the Arduino software system IDE the software system starts by initializing method. This method sets all variables employed in the program associated with the microcontroller pin addressing and a few initial planned worth. The program continues by obtaining the information from the water flow module. the mostcontroller processes the collected information and sends it to the network through the IoT module. This method can never be stopped unless the most switch of the system is converted. The information is then received by factor Speak net server. Factor Speak is associate open IOT platform that permits the user to gather, visualize, and analyze live information streams within the cloud.

4.1 BLOCK DAIGRAM OF POWER PLANT UNIT:

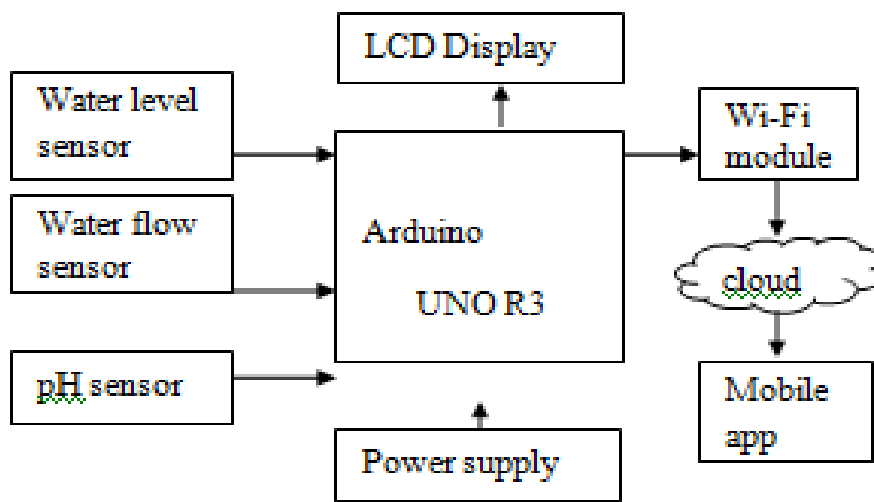


Fig:1.1Block diagram of Power Plant Unit

5..HARDWARE DESCRIPTION

ARDUINO UNO MICROCONTROLLER

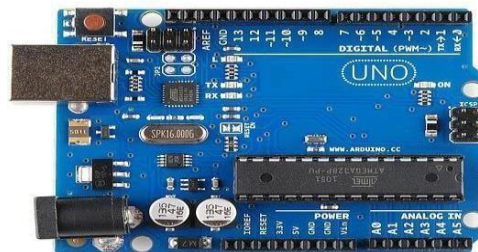


Fig:1.3 Arduino Uno microcontroller board

Arduino is a microcontroller board based on the ATmega328P. It has 14 digital input/output pins (of which 6 can be used as PWM outputs), 6 analog inputs, a 16 MHz quartz crystal, a USB connection, a power jack, an ICSP header and a reset button. It contains everything needed to support the microcontroller. Arduino Software (IDE) were thereference versions of Arduino, now evolved to newer releases. The Uno board is the first in a series of USB Arduino boards, and the reference model for the Arduino platform; for an extensive list of current, past or outdated boards see the Arduino index ofboards

PH Sensor:

A pH Meter could be a device used for potentiometric measurement the pH, that is either the concentration or the activity of gas ions, of associate solution. it always contains a glass conductor and a chloride reference conductor, or a mix conductor. pH meters area unit} typically wont to measure the pH of liquids, although special probes area unit} generally wont to measure the pH of semi-solid substances

Water Flow Sensor

Flow sensor is used to measure the flow of water through the flow sensor. This sensor basically consists of a plastic valve body, a rotor and a Hall Effect sensor. The pinwheel rotor rotates when water / liquid flows through the valve and its speed will be directly proportional to the flow rate. The Hall Effect sensor will provide an electrical pulse with every revolution of the pinwheel rotor.

Water Level Sensor

Water Level sensors in the main wont to monitor and regulate levels of a specific free-flowing substance at intervals a contained area. These substances are typically liquid, however, level sensors additionally, wont to monitor some solids like small-grained substances. Level sensors wide used industrially, as level acts as a very important watching parameter.

WI-FI MICROCHIP ESP8266

The ESP8266 WiFi Module is a self contained SOC with integrated TCP/IP protocol stack that can give any microcontroller access to your WiFi network. The ESP8266 is capable of either hosting an application or offloading all Wi-Fi networking functions from another application processor. Each ESP8266 module comes pre-programmed with an AT command set firmware. The ESP8266 module is an extremely cost effective board with a huge, and ever growing, community.

6. SOFTWARE DESCRIPTION

Arduino IDE

IDE stands for "Integrated Development Environment": it is a politician computer code introduced by Arduino.cc, that's in the main used for redaction, assembling and uploading the code within the Arduino Device. the majority Arduino modules ar compatible with this computer code that's associate open supply and is instantly accessible to put in and begin assembling the code on the go.

Arduino IDE is associate open supply computer code that's in the main used for writing and assembling the code into the Arduino Module.

Thingspeak

Thing Speak is IoT Cloud platform wherever you'll be able to send device knowledge to the cloud. you'll be able to additionally analyze and visualize your knowledge with MATLAB or alternative computer code, as well as creating your own applications. The factor Speak service is operated by maths Works. so as to sign on for factor Speak, you want to produce a replacement maths Works Account or log in to your existing maths Works Account.

7. HARDWARE RESULT

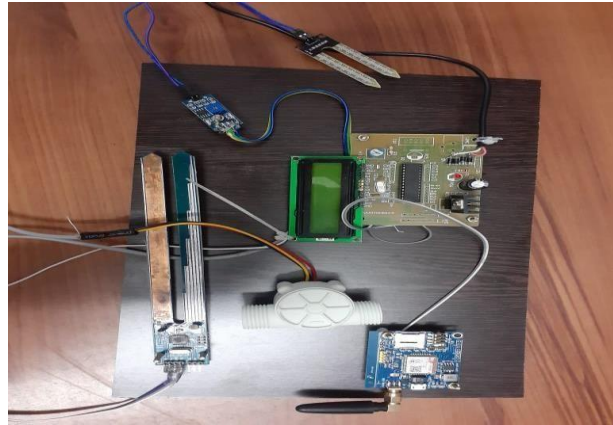


Fig: 1.4 Result of power plant unit

8. SIMULATION RESULT

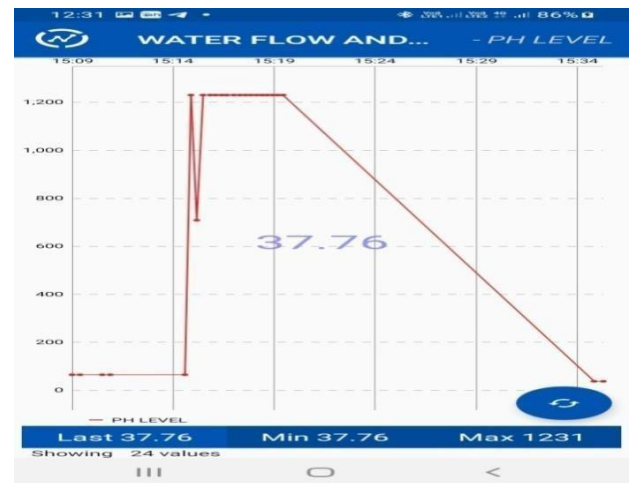
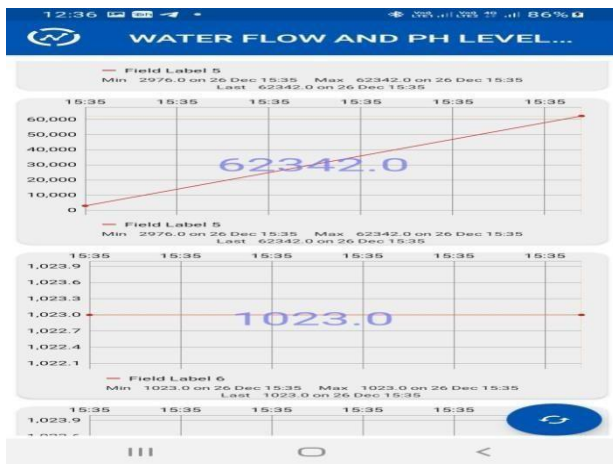


Fig:1.5 Monitoring result of power plantunit

CONCLUSION

The planned Pico hydro powerhouse watching system will monitor the water Flow, water level and pH level of water all the time and therefore the collected knowledge store the cloud. hold on knowledge will simply access the mobile application. additionally, the collected knowledge will be downloaded thus it will be then simply went to analyze the potential issues associated with the unstable water flow speed and water level that will risk the Pico hydro powerhouse and observe a flood and provides a early intimation to near living folks. additionally we tend to collected the pH level of water in real time it thus we tend to might get the acidity associated pH scale values unceasingly thus it's useful for determine the hurt things within the watercourse water to produce pure drinkable to the folks and save the water system it's an automatic watching system thus it doesn't want folks on duty. The system has smart flexibility and therefore the real time watching system is economical and low in value. For the primary section of the project, Water quality watching unit is completed, the device readings has been collected through associate humanoid application for simple maintenance of pico powerhouse. In second section of the project ,many device units are enforced to finish the project.

FUTURE SCOPE

In future, It will increase the water quality parameters like cloudiness, temperature, DO, electrical conduction by addition of multiple sensors to produce a clean drinkable and safe the water system. Another major issue for the ability plant is floating stuff like plastics, medical wastes, leaves within the watercourse water blocks the wheel rotation of powerplant and have an effect on the cultivation within the water and it can not be drinkable water for folks. thuswe tend to style a floating garbage removing system in water surface to tackle the pollution and keeping the water surface clean.

REFERENCES

- [1] Putra, I. S. (2016). Studi Pengukuran Kecepatan Aliran pada Sungai Pasang Surut. *Infoteknik*, 16(1), 33-46.
- Supangat, A. B., Indrawati, D. R., Wahyuningrum, N., Purwanto, P., & Donie, S. (2020).
- [2] Suresh, P., Daniel, J. V., Parthasarathy, V., & Aswathy, R. H. (2014, November). A state of the art review on the Internet of Things (IoT) history, technology and fields of deployment. In 2014 International conference on science engineering and management research (ICSEMR) (pp. 1-8). IEEE. <https://doi.org/10.1109/icsemr.2014.7043637>
- [3] Chin, J., Callaghan, V., & Allouch, S. B. (2019). The Internet-of-Things: Reflections on the past, present and future from a user-centered and smart environment perspective. *Journal of Ambient Intelligence and Smart Environments*, 11(1), 45-69. <https://doi.org/10.3233/ais-180506>
- [4] Hussien, N., Ajlan, I., Firdhous, M. M., & Alrikabi, H. (2020). Smart Shopping System withRFID Technology Based on Internet of Things. *International Journal of Interactive Mobile Technologies (iJIM)*, 14(04), 17-29. <https://doi.org/10.3991/ijim.v14i04.13511>
- [5] Alrikabi, H., Alaidi, A. H., & Nasser, K. (2020). The Application of Wireless Communication in IOT for Saving Electrical Energy. *International Journal of Interactive MobileTechnologies (iJIM)*, 14(01), 152- 160. <https://doi.org/10.3991/ijim.v14i01.11538>.
- [6] Mrabet, H., Moussa, A. A. (2020). IoT-School Attendance System Using RFID Technology. *International Journal of Interactive Mobile Technologies (iJIM)*
- [7] Fortaleza, B. N., Juan, R. O. S., & Tolentino, L. K. S. (2018). IoT-based pico-hydro power generation system using Pelton turbine. *Journal of Telecommunication, Electronic and ComputerEngineering (JTEC)*, 10(1-4), 189-192.
- [8] Moreno, C., Aquino, R., Ibarreche, J., Pérez, I., Castellanos, E., Álvarez, E., ... & Edwards, R. M. (2019). RiverCore: IoT device for river water level monitoring over cellular communications. *Sensors*,19(1), 127.

Form Monitoring by Augmented Reality Using Underground Sensor Network

S.ABINAYA, Department of ECE, Student,
R.BAVADHARINI, Department of ECE, Student
V.KALKI, Department of ECE, Student
S.RAMAPRIYA, Department of ECE, Assistant professor MRKIT

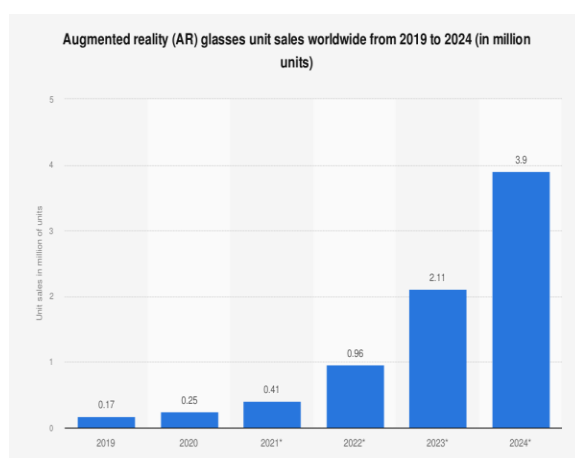
Abstract

Augmented reality (AR) are rapidly becoming increasingly available, accessible and importantly affordable, hence their application into agriculture to enhance the medical use of data is certain. AR promise to provide the infrastructure for novel applications. Farmers are regularly on the lookout for technologies that will enhance their cultivating environment. They are often the adopters of technologies that allow their field to offer a Agriculture experience. The continuing enhancement of the agriculture environment in the digital age has led to a number of innovations being highlighted as potential disruptive technologies in the workplace. Here the soil quality is monitored and the conditions are continuously sends to the farmer in augmented reality technology.

Keywords: *Wireless technology, potential disruptive Technology, Moisture, Humidity and NPK sensor.*

1.INTRODUCTION

Augmented Reality is technology that we could human being superimpose virtual content (images, sounds, text) over a real –global environment. In an augmented reality, farmers can visualize the whole farm in a one dashboard. It is used to monitor the overall production quality and detect the moisture, Ph, Nitrogen, phosphorus and potassium (NPK), Temperature, Humidity. This is used to training new farmers. AR can permit new farmers to get acquainted with agricultural system through immersive e-getting to know environment. Irrigation process is the rural method of managed quantity of water to land to help growing of crop. Agriculture is the largest water use at global level Irrigation of agricultural lands accounted for 70% of the water used worldwide. In numerous growing international locations, irrigation represents as much as 95% of all water uses, and performs a main position in food manufacturing and food security. Irrigation of sprinkler other name is water sprinkler device is used to irrigate (water) from land in automation method and also pumping motor is used to pump water in lower to a higher level, suddenly moisture is decreasing pumping motor help to moisture the land. It is very useful to agriculture. The NPK is called soil nutrient speed meter is find the level of nitrogen, phosphorus and potassium in the soil can be used to identify and thus the soil condition can be easily and systematically assessed. A temperature sensor is used to measure the temperature level. There are different types of temperature sensor available in market. Each temperature sensor using different technology is and principles to take the temperature measurements. Types of temperature sensors such as Thermostat, RTDs, thermocouples, temperature probes.



The framework is aimed towards integrators of operator support equipment who wants to be able to quickly assess how high they should prioritize ARSG compared to alternative ways to improve production. It is used by answering 15 questions about a production case, with 5 potential follow-up questions in total. The questions have predefined answers and generate a normalized score, indicating how suitable ARSG is as an operator support tool. Depending on which quartile the score landed in, one of four general descriptions of the case suitability was generated. This first version of the framework received positive feedback, but a limitation of the framework is that it does not provide deeper motivations or practical guidance in how ARSG are suitable or not suitable for a case.

Related work

In the existing method, the signals can be transmitted in the form of analog data at the transmitter and can be converted to digital form at the receiver. These transmitter signals are transfer in the form of electromagnetic waves. In mobile communication the voice turns into a digital signal with the help of MEMS sensor and this digital data transmits in the form of zeros and ones using electromagnetic waves. When EM waves are used for communication through soil it cannot penetrate through soil due to various compositions of soil like red, black cotton soil etc. When these waves are used for data transmission in soil there will be loss in data because of high diffraction. When there is increase in transmission distance there will be high path loss and high attenuation.

In this proposed method, the real time data can be obtained from the soil and transmitted. And here the data can be transmitted in the form of text or image format through augmented reality as a medium. A huge number of multiplesensors implemented in the sensor networks can be utilized in the process of reducing the loss in measurements or the channel utilization. Here the NPK sensor is used to monitor the wealth of the soil, humidity and moisture sensor is for monitor the water intake of plants in the soil.

AR is the addition of artificial information to one or more of the senses that allows the user to perform tasks more efficiently. We propose a system inwhich important information for the farmers are displayed on semi-transparent glasses included in an AR-headset and therefore are mixed with the real-world view

System architecture

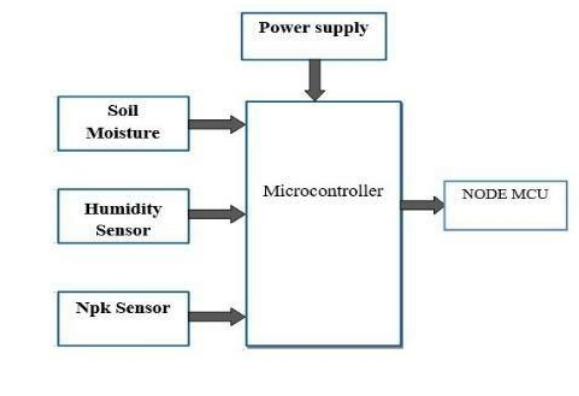


Figure 1 shows the transmitter side of the proposed system,

Augmented Reality is a technology that we could human being superimpose virtual content (images, sounds, text) over a real –global environment. In an augmented reality, farmers can visualize the whole farm in a one dashboard.

It is used to monitor the overall production quality and detect the moisture, Ph,Nitrogen, phosphorus and potassium (NPK), Temperature, Humidity. This is used to training new farmers . AR can permit new farmers to get acquainted with agricultural system through immersive e-getting to know environment.

Irrigation process is the rural method of managed quantity of water to land to help growing of crop. agriculture is the largest water use at global level ,Irrigation of agricultural lands accounted for 70% of the water used world wide. In numerous growing international locations, irrigation represents as much as 95% of all water uses, and performs a main position in food manufacturing and food security.

Irrigation of sprinkler other name is water sprinkler device is used to irrigate (water) from land in automation method and also pumping motor is used to pump water in lower to a higher level, suddenly moisture is decreasing pumping motor help to moisture the land. It is very useful to agriculture.

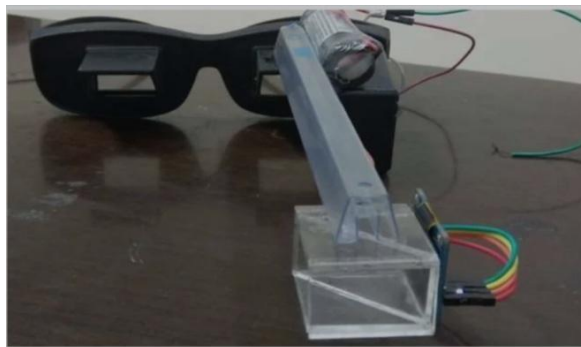


Figure 2 shows the Receiver side of the proposed system,

The NPK is called soil nutrient speed meter is find the level of nitrogen, phosphorus and potassium in the soil can be used to identify and thus the soil condition can be easily and systematically assessed. It is used monitor the wealth of soil.

A temperature sensor is used to measure the temperature level. There are different types of temperature sensor available in market. Each temperature sensor using different technology is and principles to take the temperature measurements. Types of temperature sensors such as Thermistor, RTDs, thermocouples, temperature probes. The soil moisture temperature conductivity sensor is ideal for soil moisture monitoring, scientific studies, agricultural irrigation, greenhouses, flowers and vegetables, grassland and pastures, soil quick testing, plant cultivation, and a variety of other applications. The soil moisture temperature conductivity sensor is ideal for soil moisture monitoring, scientific studies, agricultural irrigation, greenhouses, flowers and vegetables, grassland and pastures, soil quick testing, plant cultivation, and a variety of other applications.

2.Methodology

The method used in this paper is a combination of twomethods: a “method triangle” and “five iterative steps” [16].Lings and Lundell [17] presented three perspectives on amethod:method-in-concept,method-in-tool,andmethod-in-action.ThiswasconceptualizedbyThorvald~~etal~~. [16]asa “method triangle.” According to Lings and Lundell [17],thethod-in-conceptisasocialconstructofhowthestake-holders understand the method. They further state that themethod-in-tool occurs when the method-in-concept is real-ized, and the method-in-action consists of different method-in-tools, used in particular contexts. Both social and technicalissues need to be addressed in order to transform a method-in-concept into a method-in-action. Lings Another method development process, presented by Bland-ford and Green, consists of five iterative steps in a life cycleapproach[18].Thorvald~~etal~~. [16]combinedthethod triangle with the five iterative steps of Blandford and Green[18],seeFig.1.Thiswasdonetoclarifythestepsofmethoddevelopment.Whencombinedlikethis,thefirststepfocuse on the method-in-concept, followed by a focus on both themethod-in-concept and method-in-tool in steps two to four.Stepfive,finally,isthethod-in-action[16] Palmarini~~etal~~. [15]describedaprocessforchoosingan AR system for maintenance. They found that surveys,questionnaires,andcasestudiesweresuitablevalidationpro-cesses. Their case studies compared the choices of expertsand non-experts using the process developed [15]. In thisstudy,iterationcasestudieswillbeused. Expertswilluse the tool and discuss the recommendations it presents in theircases.Thiswillprovideinsightintohowwelltherecommen-dationscomparetotheviewsofexperts.

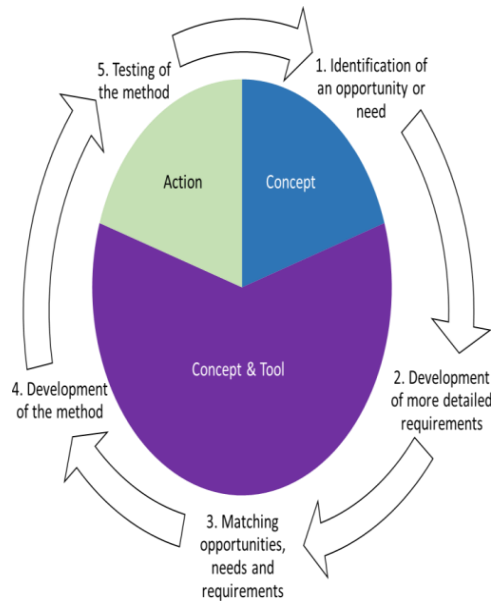


FIGURE 3.

1.3 Focus groups

create ARSG or AR-interfaces.

There are five characteristics of focus group interviews: “(1) a small group of people who (2) possess certain characteristics, (3) provide qualitative data (4) in a focused discussion (5) to help understand the topic of interest” [23, p. 6]. According to [24], it is not useful to provide a universal sample size recommendation for focus groups, and ultimately, saturation will be determined during data collection. They do, however, argue that the parameters they identified can help to guide in identifying and justifying sample sizes a priori. The parameters are study purpose, type of codes, group stratification, groups per strata, type of saturation, and degree of saturation. By analyzing 40 focus groups, [25] found that at least 80% of all themes are likely to be captured with a sample size of two to three focus groups, and 90% of the themes are likely to be identified with three to six focus groups. In traditional focus groups, participants congregate at a specific location.

2 Experimental Result

The experimental results show that the augmented reality using an underground sensor network is used to monitor the wealth of soil for moisture, temperature, and NPK (nitrogen, phosphorous, and potassium) and to visualize the wireless augmented reality glass. It avoids plenty of wiring and PC.



3 .Conclusions

Augmented reality technology has proven to be one of the top innovations opening up new growth points for businesses around the world. Analysts predict that the AR market will reach \$198 billion in 2025. This year, the number of mobile AR users is expected to reach 3.5 billion. According to Deloitte Research, augmented reality and AI will transform the traditional healthcare business model by offering AR/MR enabled hands-free solutions and 1A-based diagnostic tools. For example, Microsoft HoloLens 2 can provide information to the surgeon while allowing them to use both of their hands during the procedure. With the continued restrictions associated with Covid-19, the use of augmented reality solutions is becoming increasingly important to address issues such as the complexity of remote patient support and the increased burden on hospitals. This includes both telesurgery solutions and mental health apps that are helping people to maintain psychological balance during these difficult times. AR technology can also improve telemedicine solutions that are on the rise right now. Features such as drawing and annotating on the 3D screen can make communication between doctors and patients much easier and clearer. Remote assistance tools can also help clinicians support their patients while reducing

References

- [1] T. P. Caudell and D. W. Mizell, "Augmented reality: An application of heads-up display technology to manual manufacturing processes," in *Proc. 25th Hawaii Int. Conf. Syst. Sci.*, vol. 2, Jan. 1992, pp. 659–669.
- [2] R. Azuma, Y. Baillet, R. Behringer, S. Feiner, S. Julier, and B. MacIntyre, "Recent advances in augmented reality," *IEEE Comput. Graph. Appl.*, vol. 21, no. 6, pp. 34–47, Nov. 2001.
- [3] O. Bimber, "Modern approaches to augmented reality," in *Proc. SIGGRAPH*, 2006, pp. 1–86.
- [4] J. Peddie, *Augmented Reality: Where We Will All Live*. Cham, Switzerland: Springer, 2017, p. 349.
- [5] P. Fraga-Lamas, T. M. Fernández-Caramés, Ó. Blanco-Novoa, and M. Vilar-Montesinos, "A review on industrial augmented reality systems for the industry 4.0 shipyard," *IEEE Access*, vol. 6, pp. 13358–13375, 2018.
- [6] R. Pierdicca, M. Prist, A. Monteriù, E. Frontoni, F. Ciarapica, M. Bevilacqua, and G. Mazzuto, "Augmented reality smart glasses in the workplace: Safety and security in the fourth industrial revolution era," in *Proc. Int. Conf. Augmented Reality, Virtual Reality Comput. Graph.* Cham, Switzerland: Springer, 2020, pp. 231–247.
- [7] A. Syberfeldt, O. Danielsson, and P. Gustavsson, "Augmented reality smart glasses in the smart factory: Product evaluation guidelines and review of available products," *IEEE Access*, vol. 5, pp. 9118–9130, 2017.
- [8] O. Danielsson, M. Holm, and A. Syberfeldt, "Augmented reality smart glasses for operators in production: Survey of relevant categories for supporting operators," *Procedia CIRP*, vol. 93, pp. 1298–1303, Jan. 2020.
- [9] Á. Segura, H. V. Diez, I. Barandiaran, A. Arbelaiz, H. Álvarez, B. Simões, J. Posada, A. García-Alonso, and R. Ugarte, "Visual computing technologies to support the operator 4.0," *Comput. Ind. Eng.*, vol. 139, Jan. 2020, Art. no. 105550.
- [10] M. Campbell, S. Kelly, J. Lang, and D. Immerman, "The state of industrial augmented reality 2019," PTC, Boston, MA, USA, White Paper J13046State-of-AR-WP-EN-0319, 2019.
- [11] *Global Augmented Reality Smart Glasses Market*, Inside Market Rep., Westford, MA, USA, 2020.
- [12] T. Masood and J. Egger, "Adopting augmented reality in the age of industrial digitalisation," *Comput. Ind.*, vol. 115, pp. 1–6, Feb. 2020.
- [13] L. Gong, Å. Fast-Berglund, and B. Johansson, "A framework for extended reality system development in manufacturing," *IEEE Access*, vol. 9, pp. 24796–24813, 2021.
- [14] O. Danielsson, A. Syberfeldt, M. Holm, and P. Thorvald, "Integration of augmented reality smart glasses as assembly support: A framework implementation in a quick evaluation tool," *Int. J. Manuf. Res.*, 2021.
- [15] R. Palmarini, J. A. Erkoyuncu, and R. Roy, "An innovative process to select augmented reality (AR) technology for maintenance," *Procedia CIRP*, vol. 59, pp. 23–28, Jan. 2017.
- [16] P. Thorvald, J. Lindblom, and R. Andreasson, "On the development of a method for cognitive load assessment in manufacturing," *Robot. Comput. Integr. Manuf.*, vol. 59, pp. 252–266, Oct. 2019.
- [17] B. Lings and B. Lundell, "On transferring a method into a usage situation," in *Information Systems Research*. Boston, MA, USA: Springer, 2004, pp. 535–553.

- [18] A. Blandford and T. R. Green, *Methodological Development*. Cambridge, U.K.: Cambridge Univ. Press, 2008.
- [19] O. Danielsson, M. Holm, and A. Syberfeldt, “Augmented reality smart glasses for industrial assembly operators: A meta-analysis and categorization,” in *Proc. 17th Int. Conf. Manuf. Res.*, Belfast, U.K., vol. 9, 2019, pp. 173–179.
- [20] O. Danielsson, M. Holm, and A. Syberfeldt, “Augmented reality smart glasses in industrial assembly: Current status and future challenges,” *J. Ind. Inf. Integr.*, vol. 20, p. 10, Dec. 2020.
- [21] M. Tremblay, A. Hevner, D. Berndt, and S. Chatterjee, “The use of focus groups in design science research,” in *Design Research in Information Systems*, vol. 22. Boston, MA, USA: Springer, 2010, pp. 121–143.
- [22] D. W. Stewart, P. Shamdasani, and D. W. Rook, *Focus Groups*, 2nd ed. Thousand Oaks, CA, USA: SAGE Publications, 2007. Accessed: Apr. 14, 2021. [Online]. Available: <https://methods.sagepub.com/book/focus-groups>
- [23] R. A. Krueger, *Focus Groups: A Practical Guide for Applied Research*. Newbury Park, CA, USA: Sage, 2014.
- [24] M. M. Hennink, B. N. Kaiser, and M. B. Weber, “What influences saturation? Estimating sample sizes in focus group research,” *Qualitative Health Res.*, vol. 29, no. 10, pp. 1483–1496, Aug. 2019.
- [25] G. Guest, E. Namey, and K. McKenna, “How many focus groups are enough? Building an evidence base for nonprobability sample sizes,” *Field Methods*, vol. 29, no. 1, pp. 3–22, Feb. 2017.
- [26] D. W. Stewart and P. Shamdasani, “Online focus groups,” *J. Advertising*, vol. 46, no. 1, pp. 48–60, Jan. 2017.
- [27] R. H. Von Alan, S. T. March, J. Park, and S. Ram, “Design science in information systems research,” *MIS Quart.*, vol. 28, no. 1, pp. 75–105, 2004

MILITARY ROBOT FOR SURVEILLANCE AND PROTECTION SYSTEM

Ajay.K, Department of ECE, Student
Gokul Raj.R, Department of ECE, Student
Santhosh Kumar.S, Department of ECE, Student
Venkatesan.G, Assistant Professor, Department of ECE

Abstract

To ensure the border security in our nation. We are replacing robots to secure the borders and to identify the unknown person in our border. It will send the information alert to the military base station with the use of MATLAB image processing to identify unknown person that are not encoded image the robot.

Keywords: PIR sensor, Ultrasonic sensor, video surveillance, Dc motor, Matlab Image processing.

1 Introduction

Borders demarcate the geographic boundaries of a political territory. Borders are critical to a state security and carve out its physical place in the international system. Insecure borders can ultimately jeopardize stability and increase the likelihood of conflict. Post-conflict countries rarely have a robust border security systems, which is especially important for preventing spoilers from destabilizing the state. Borders can either be prosperity-generating as cooperating states. Fragile states need to protect themselves internally and engage internationally through the legitimate transfer of goods, peoples and services.

2 Working Procedure

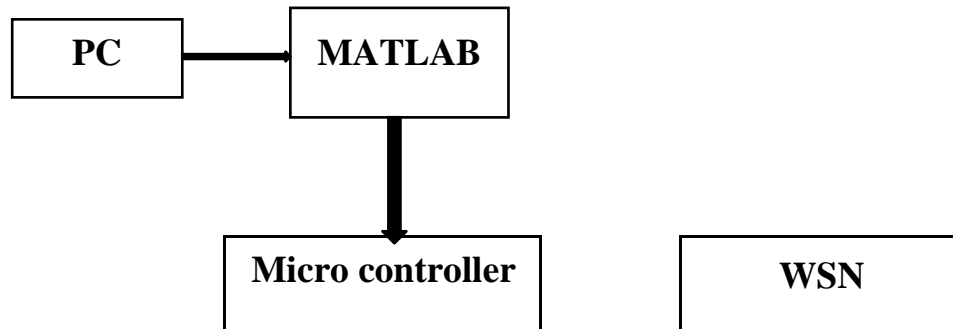
The field of Surveillance system is entirely well popular. More number of researches has been carried out in navigational procedures and circuitry system of wireless surveillance robots. A common motivation is usage of a camera on the robot in order to receive live video stream at receiver. Several research works are done so far on surveillance system. Some innovative research works have also been successfully carried out. Various authors discussed about various aspects of different types of observing activities and tracing applications. An examination team in DRDO has done a shared research work where they have suggested and applied intrusion detection in large secure place using ad-hoc wireless sensor network.

- Emerging technologies have metamorphosed the nature of surveillance and monitoring applications. Sensory data collected using the gadgets still remains unreliable and poorly synchronized. Surveillance system covers only a particular direction.
- Not possible to turn to a particular direction based on priority.
- The output is stored in hard disk with help of DVR, which requires more disk space.
- The systems do not have conference features.
- Security to access the robot is lacked and thus anybody nearby can access the robot.

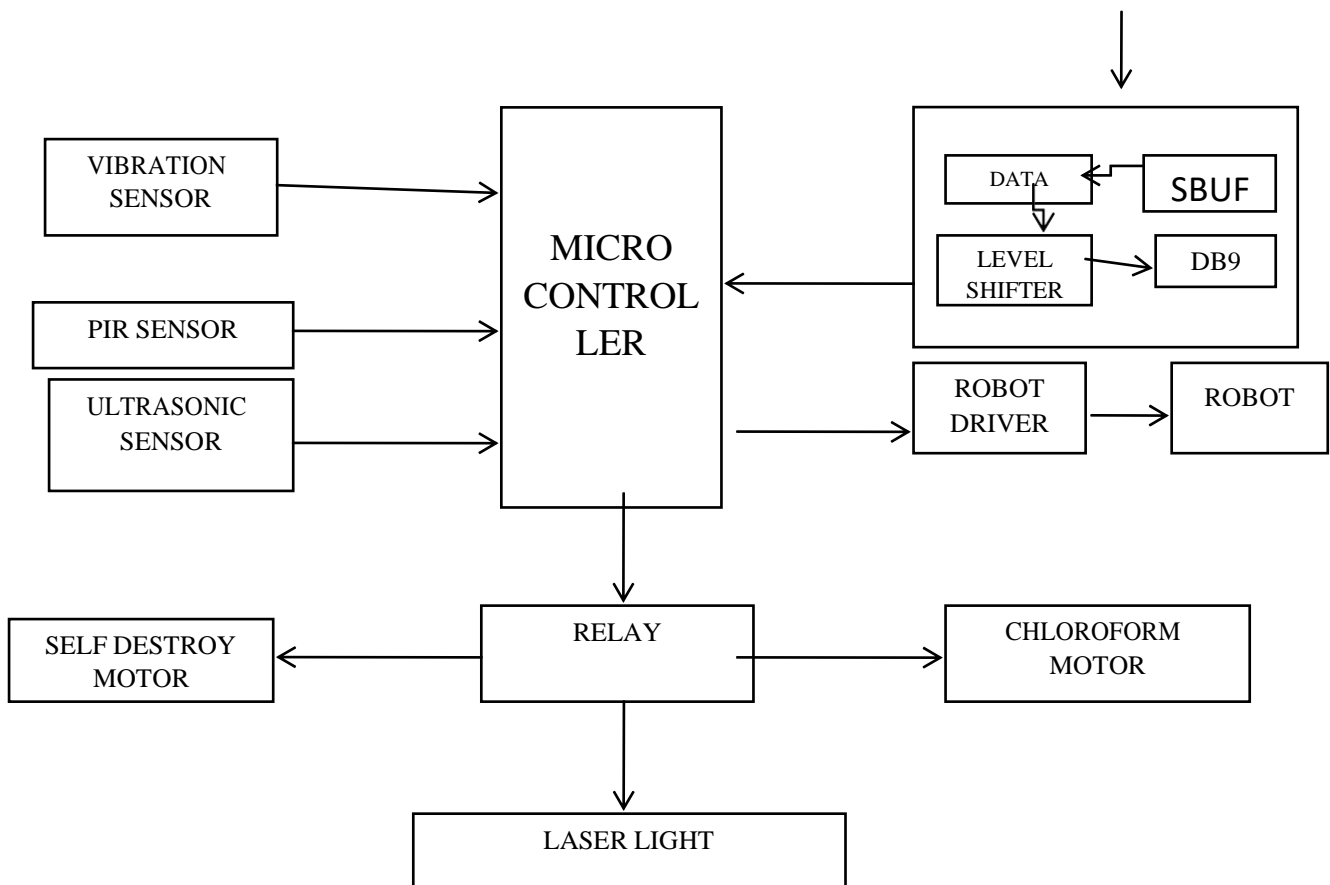
3 Proposed System

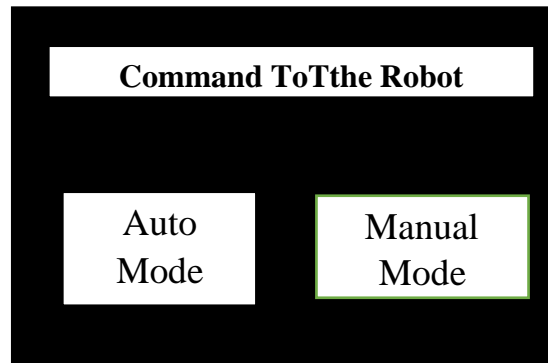
The proposed system of our project is to monitor by using robots. The image processing will done by using the MATLAB. The information will be transmitted through the WSN Transmitter. The control will be mode of operation are automatic and manual mode in robot section, robot monitors the boundary compare with the information from the WSN receiver. If any intruder is found then the robot will automatically send the messages to base station .Ultrasonic sensor used to find the obstacle and if anyone attack the robot then it will get self destructed.

Block Diagram (Transmitter)



Block Diagram (Receiver)





Receiver Section

When an intruder is detected, the robot receives a notification from the sensor network. Then, the client also receives a warning message from the robot and even he/she can watch the video output of the triggered zone from a mounted camera. Moreover, the client can control the web camera remotely through the web application which was implemented using web RTC and Node.js. Intruder detection was done with back ground subtraction method. OpenCv python image processing library was used to detect the motion.

Robot is controlled itself when a target or a destination location is indicated. According to the indicated target, an optimum path is planned using a Navigation Stack. Once the relevant velocities are published for the wheels through sabre toothed motor controller to the Arduino micro-controller, the robot moves according to the provided commands. LIDAR was used to retrieve the sensor readings of the surrounding while the robot is moving. The sensor readings will be used to localize the robot in a specified area. The main function of the Navigation Stack is to produce a safe path for the robot to execute by processing data from odometry, sensors and surrounding map.

4 Conclusion

The aim of this system is to monitor by using robots and to detect the obstacle and if anyone attack the robot then the robot will get destructed. The conclusion is that the proposed system is completed successfully. The motion of the robot is being controlled manually using a webpage. According to the movement, we could control the wheel and hence the movement of the robot through the webpage by using PC. The input given to the webpage is sent through the internet and desired movement occurs at the robot end.

5 Reference

- [1] G. Csaba, L. Somlyai and Z. Vámosy, "Mobil robot navigation using 2D LIDAR, 2018 IEEE 16th World Symposium on Applied Machine mIntelligence and Informatics (SAMI), 2018, pp. 000143-000148.
- [2]E. Herranz, A. Llamazares, E. Molinos and M. Ocaña, "A comparison of SLAM algorithms with range only sensors," 2014 IEEE International Conference on Robotics and Automation (ICRA), 2014, pp. 4606-4611.
- [3] M. Faisal, H. Mathkour and M. Alsulaiman, "Smart mobile robot for security of low visibility environment," 2015 5th National Symposium on Information Technology: Towards New Smart World (NSITNSW). 2015 2015, pp. 1-6.
- [4] G. Hu, S. Huang, L. Zhao, A. Alempijevic and G. Dissanayake, "A robust RGB-D SLAM algorithm," 2012 IEEE/RSJ InternationalConference on Intelligent Robots and Systems, 2012, pp. 1714-1719.

“Bus Tracking System for Visually Impaired Person”

Ms.K.Santhini-UG Student-ECE, V.R.S. College of Engineering and Technology,
Ms.G.Gayathri-UG Student ECE, V.R.S. College of Engineering and Technology,
Mr.V.Thiyagarajan-Associate Professor, V.R.S. College of Engineering and Technology.
Mr.G.Sadiq Basha- Associate Professor, V.R.S. College of Engineering and Technology

Abstract

There are many techniques which are used for navigating the visually challenged people, navigation in real time traffic is the main problem. Objective of the project is to provide a solution with the aid of wireless sensor networks (WSNs). ZigBee system is used for indicating the presence of blind person in the bus station. Voice module and APR9 600 audio play back systems are used to update and inform the blind person about the bus arriving and reaching destinations and to guide him as to what he has to do next. Microcontroller analysis the information provided and generates the corresponding bus number. ZigBee transceiver sends the bus number and announced in the microphone attached with the system. The system is connected with GPS which indicates the destination given. Audio output is generated by the voice synthesizer. The expected outcome of the project is to obtain an easy navigation system for people with visually impaired.

Keywords: APR9600, ARM7, GPS, Voice module, ZigBee.

1. Introduction

Works essentially through the smooth trade of merchandise, administrations, and brotherhood. Be that as it may, data and assets are made most promptly accessible to the eye. The societal frame work and trade system are intended to streamline the opportunity, working, and delight in located individuals- confronting the visually impaired with rejection from this system Society. The world is loaded with risks and ponders which society accepts the utilization of vision to maintain a strategic distance from or appreciate. Being visually impaired limits their exposures to these marvels and expands their risk to the perils. More undermining than being cut off from business and societal trade is the contrary condition of general world awareness in regards to visually impaired individuals. Mainstream thinking has dependably fought that visual deficiency drives specifically to lack and insufficiency. Our point is to add to making their lives ordinary in the little way that we can. As indicated by the measurements and predicts of the WHO upgraded in 2014,285 million individuals are assessed to be outwardly disabled around the world: 39 million are visually impaired and 246 have low vision. Each outwardly impeded individual countenances diverse difficulties taking into account their particular level of vision. With the ascent of different backing based associations, all the more outwardly disabled individuals have been given the chance to instruction and numerous different means.

However, the issues of route for the visually impaired are still exceptionally mind boggling and troublesome particularly when they strolled down in road furthermore explore to inaccessible spots by open transport framework. Blind people might be unwilling to move openly and easily or, out of anxiety, society limits development of the visually impaired person. Deliberate, self-coordinated development is viewed as one of the all the more difficult ranges confronted by visually impaired individuals. While absence of sight is regularly remunerated by improving different faculties, social boundaries and systems of over insurance frequently hamper the perceptual advancement and improvement of useful development in visually impaired individuals.

Guide puppies and strolling sticks take into consideration a free method for navigation, however they are restricted in new situations. RFID is doable and financially savvy however it is more appropriate for indoor correspondence as it were. Likewise it gives stand out way correspondence and a short range of identification. For open air correspondence, all the blind people trust that the guide route offices can manage them like an ordinary individual, and ensure that they are constantly advantageous and safe out and about. The motivation behind this project is to reduce the troubles confronted by blind person when taking city transports, using interactive wireless communication system.

2. Motivation

To use technology for the welfare of the society which includes visually challenged people. The project outcome is indirectly related to the —Digital India concept which is introduced by Govt. of India. Smart city concept is also in its development stage which aims to bring about change in public transportation system. Thus the project is present day concept and hence supports innovation of the current/existing system.

3. Existing System

Consider the case of blind how he confronts the accompanying issues, when utilizing open transport, Trip arranging –finding a stop/station –finding a passage way to the station-exploring inside the station finding the right stage and holding up spot-knowing when the right vehicle arrives - finding a vehicle passageway -installment – finding a seat - withdraw on right stop –exploring inside the station-finding the way out of the station – finding the destination.

The vast majority of these assignments are paltry for the located, yet exceptionally troublesome for the outwardly debilitated. There are situations when a visually impaired individual has spent a few hours on the transport stop, since he couldn't perceive entry of the right vehicle. What's more, present framework has taking after disadvantages.

Manual operation

Monitoring relies upon driver

Alertness of the system is less

System is unsafe

4. Problem Statement

With expansion in movement and populace of the city areas the blind people confront a great deal of obstacles while venturing out starting with one point then onto the next. Because of this most of the blind people are compelled to stay inside and abandon their objectives and dreams as it might include driving from one spot to different spots and in this way costing them their profession/future. This anticipate archives the configuration and usage of a safe visually impaired route framework for the blind people to help them in going from their present area to their craved destination.

5. Proposed System

To conquer the drawback so available accessible assistive gadgets, we propose a Wireless sensor system framework with ZigBee for blind identification in the bus station and installed framework for giving the bus information, lastly GPS for destination sign. Proposed system has following features.

Safety concerns for blinds

Automatic operation

Continuously quick monitor

High alert system.

6. Scope of the Proposed System

Blind can undoubtedly get the data about transport to achieve destination, so travelling makes simple to him.

Can travel autonomous of any persons need.

User-friendly interactions with the user.

Easy to use.

Audio and vibration alert.

Voice based input for destination target.

This is not limited to just visually impaired individual it likewise helps senior individual.

Communication is given between the visually impaired and driver if there should be an occurrence of any crisis.

7. Block Diagram

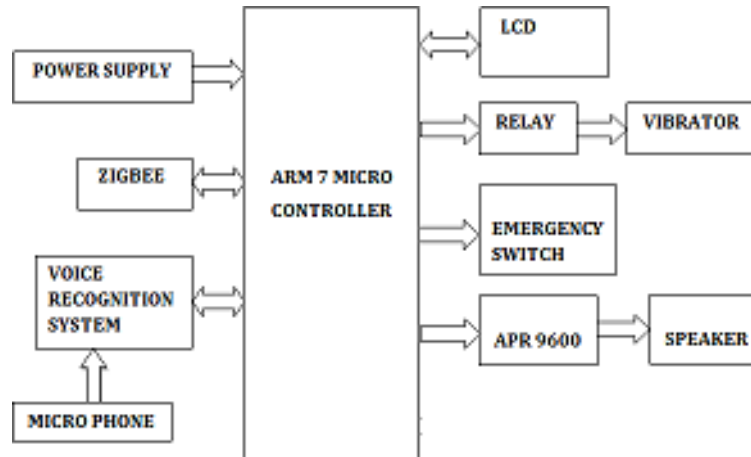


Fig 1: Blind Unit

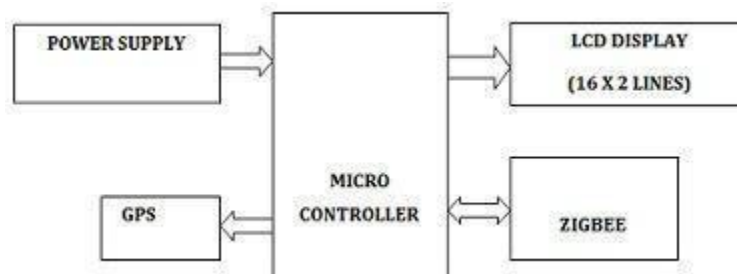


Fig 2: Bus Unit

8. Working Description

Stage1: Acquisition of bus arrival information

The ZigBee in the blind module receives the signal which is transmitted by the ZigBee in the bus module within the 30meters range. So that the blind person can easily get the information about bus arrival.

Stage2: Intake of the destination to be travelled by the blind person

The blind person gives an audio input of the destination he wishes to reach to the system.

Stage3: Reception of information by the bus

The blind person gives the input about destination to the voice module V2 and voice module translates the voice of blind person to text and sends it to microcontroller.

Stage4: Processing of bus information

Once the got signal changed over to text, it should be matched with the destination database present on the bus module so that the framework can illuminate the blind person if that bus is heading off to his wanted destination and in the event that he ought to take that specific user wait for the next one.

Stage5: Audio output for blind interaction

Once they got signal has been decoded ,the information is utilized to encourage the sound interface .A voice playback module is interfaced for redesigning the individual about different information, for example, getting on and off the transport. In this anticipate GPS is utilized for the visually impaired individual to understand that his stop has arrived .At the point when the transport contacts the visually impaired individual's wanted destination he is again educated by his module that he ought to get off the transport.

At the point when the blind module is turned ON, the ARM7 controller is initialized. The system waits for the ZigBee to establish the communication. The APR9600 plays that the bus has arrived loudly and also vibration alert for the blind upon the reception of the signal from the ZigBee on bus module. Now the system waits for the blind to give the destination as voice input. All of the above processes are displayed on the LCD.

Once the bus module is turned ON it gets initialized and if it is in range of the user module ZigBee the nit establishes connection and receives the data that is input from the blind person and the 8051 compares it with the database present on it. It sends back acknowledgement back to the user whether the bus goes to the destination or not.

9. System Design model

Software Designing:

The modules are required to be programmed for the operation. In this is project, Embedded C programming language is used by utilizing KEIL μ vision software. This is popular software that helps in creating embedded C programs, source code editing and debugging, compiling, execution can be done in one single environment. Developed program is dumped into the microcontroller memory by the programmer by the help of Flash Magic software.

Hardware Design module:

Every single operation ought to be controlled. For the control activities, microcontrollers are utilized. ARM7 and 8051controller are used in the blind and bus module respectively. ARM Board-LPC214X is a breakout board for LPC2148, ARM7TMDI based microcontroller. The LPC2148 microcontrollers depend on a 32-bit ARM7TDMI-S CPU with embedded trace support and real time emulation, which join the microcontroller within stalled flash memory. Since the bus module does not require a32- bit controller as it doesn't have the more number of functions as the blind module, 8051uC is utilized rather than another arm7 to spare expense without trading off on the usefulness. The Intel 8051 is a 8-bit microcontrollerwhich implies that most accessible operations are constrained to 8 bits. There are 3 essential "sizes" of the 8051: Short, Standard, and Extended. The Short and Standard chips are regularly accessibleinDIP(double in-line bundle) structure, yet the Extended 8051 models frequently have an alternate structure figure, and are not "drop-in perfect". To have the communication between the both modules, ZigBees are utilized. ZigBee gives remote RF correspondence .It Works on IEEE 802.15.4 standard and has low power utilization and has a scope of 30 meters which is appropriate for this application. The destination is given as contribution to the arm 7controller through voice module. There are different voice modules accessible like V1, V2, V3. Contrasted with V1,V2 is easy to control .But just serial information or yield of V1, V2 has other helpful approaches to control and yield the outcome. APR9600 is a sound recorder IC with playback limit for 60 seconds. It is utilized as a part of this anticipate to overhaul and advise the blind person about the bus arriving and achieving destinations and to guide him with reference to what he needs to do next. Vibrator is a small brushless DC motor and it is utilized asa part of this anticipate to give vibration alarm. This is one of the undeniable advantages with cellular telephones, you can get warnings when the gadget is in your pocket without upsetting those around user .GPS permits recording or making areas from spots on the earth and helping user explore to and from those spots. Here it is used to recognize the destination. Global Positioning System (GPS) satellites telecast signals from space that GPS recipients, use to give three-dimensional area (scope, longitude, and elevation)in addition to exact time

.GPS receivers gives solid situating, route, and timing administrations to overall users on a ceaseless premise in all climate, day and night, anyplace on or close to the Earth. GPS receivers can secure GPS signals from 65 stations of satellites and yield position information with high exactness into a great degree testing situations and under poor sign conditions because of its dynamic antenna and high sensitivity. LCD is utilized here to show the operations which are occurring .A LCD is a little minimal effort show. It is easy to interface with a microcontroller due to an installed controller (the dark blob on the back of the board). This controller is standard crosswise over numerous presentations (HD 44780) which implies numerous microcontrollers (counting the Arduino) have libraries that make showing messages as simple as a solitary line of code. Thus it is essential gadget in inserted framework. It offers high adaptability to user as he can show the required information on it.

10. Conclusion

With this proposed scheme, a visually impaired person can successfully travel from his location to his desired destination using a bus independently without any hassle.

11. Future scope

This system can further be improved by using GSM to provide communication between blind and his/her relatives in case of any emergency about more realistic location of his arrival and destination.

12. Results

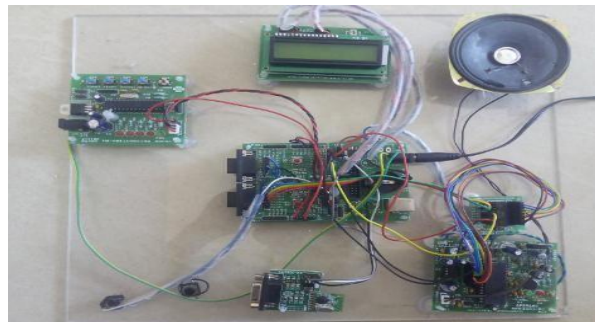


Fig.3: Blind Module

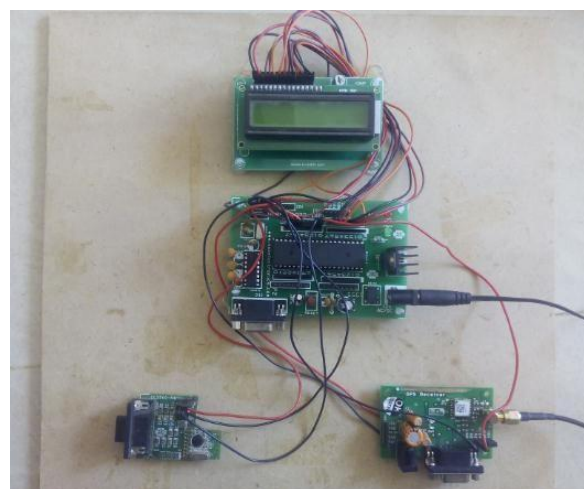


Fig.4: Bus Module

13. References

- [1] Olivier Venard, Geneviève Baudoin, Gérard Uzan, —Field Experimentation of the RAMPE Interactive Auditive Information System for the Mobility of Blind People in Public Transport:Final Evaluation| Intelligent Transport Systems Telecommunications,(ITST),2009 9th International Conference, Oct. 2009.
- [2] Syed Rizal Alfam Wan Alwi, Mohamad Noh Ahmad, —Survey on Outdoor Navigation System Needs for Blind People, IEEE Student Conference on Research and Development (SCORED), 2013, pp.144-148.
- [3] DavorVirkes, KarmenNenadic, Diana ZerecVirkes, —Positioning systems for mobility of the blind, overview and analysis,46th International Svmposium Electronics in Marine, ELMAR- 2004, 16-18 June 2004.
- [4] Zadar, Croatia Passenger BUS Alert System for Easy Navigation of Blind, 2013 International Conference on Circuits, Power and Computing Technologies [ICCPCT-2013]
- [5] MounirBousbia-Salah, AbdelghaniRedjati, Mohamed Fezari, MaamarBettayeb, —AN ULTRASONIC NAVIGATION SYSTEM FOR BLIND PEOPLE, IEEE International Conference on Signal Processing andCommunications (ICSPC 2007), pp.1003-1006.
- [6] Jin Liu, Jingbo Liu, Luqiang Xu, WeidongJin, —Silicon Eyes: GPS-GSM based Navigation Assistant for Visually Impaired using Capacitive Touch Braille Keypad and Smart SMS Facility, IEEE paper 2013.
- [7] Mohsin Murad, Abdullah Rehman, Arif Ali Shah, Salim Ullah, Muhammad Fahad, Khawaja M. Yahya, —RFAIDE – An RFID Based Navigation and Object Recognition Assistant for Visually Impaired People, IEEE paper, 2011.
- [8] Adrien Brilhault, Slim Kammoun, Olivier Gutierrez, Philippe Truillet, Christophe Jouffrais, —Fusion of Artificial Vision and GPS to Improve Blind Pedestrian Positioning, IEEE paper, 2011.
- [9] Bin Ding, Haitao Yuan, Li Jiang, XiaoningZang, —The Research on Blind Navigation System Based on RFID.

Audio Data Transmission on Light Using Li-Fi Technology

Raju S S¹, Assistant Professor, Department Of ECE,AKT MCET

Bhuvanitha K², Student , Department Of ECE,AKT MCET

Anupriya K³, Student,Department Of ECE,AKT MCET

Deivanai E⁴ ,Student,Department Of ECE,AKT MCET

Abstract

In a world of wireless technology, the number of devices accessing the internet is growing every second. Most of the devices use wireless communication to access internet for sharing data, this has unfortunately led to an increase in network complexity, shortage of wireless radio bandwidth and an increased risk of interference of radio frequencies. Li-Fi technology is used to transmit the data using Visible light communication by using light-emitting diodes. Signals are transmitted from one system to another by using LED as a Li-Fi transmitter and photodiode as a Li-Fi receiver. This is a much more secure method of transmission compared to existing technologies. Noticeable Light Communication (VLC) has increased extraordinary enthusiasm for the most recent decade because of the quick improvements in Light Emitting Diodes (LEDs) manufacture. Adequacy, durable and long life expectancy of LEDs make them a promising private lighting hardware and also an option shabby and quick information exchange gear. Also the data transmission rate is very high around few Gbps. This project describes and implements the design of Li-Fi audio transmission system.

Keywords: Li-Fi, Data Transmission, VLC, NS-3, TCP, UDP.

I. INTRODUCTION

In today world, communication between the devices are much common. Radio wave spectrum is very small part of spectrum available for communication. Wi-Fi and Bluetooth are currently the two prominent short range wireless technologies. But with increase in advanced technology and number of user the network becomes overloaded which results in failure to provide high data rate. Visible light acts as rival to the present wireless radio frequency communication by achieving larger bandwidth and high data rate. Because with larger frequency spectrum it is possible to provide a larger portion of the bandwidth to each user to transfer information. A switching LED can be improbably causing annoyance, but data can therefore be encoded in the light by varying the rate at the LEDs switch on and off to provide various strings of 1's and 0's.

The use of fast pulses of light to transfer data without physical connection such method is called as Visible light communication (VLC). The LEDs can be switched ON and OFF very fast which is not noticeable by human eye thus the light source appear to be constantly on. When these signals transmitted to the receiver via the wireless channel, the photo diode will convert these optical signals to electrical signals and the original information will be recovered..

2. EXISTING SYSTEM

The existing Wireless communication makes use of electromagnetic waves for communication system. For instance, the deployment of Wi-Fi obviously brings several important benefits. Because it is very convenient that numbers of equipment connect to each other using wireless networks. Home- based Wi-Fi enabled device helps you to connect PC, game console or laptop. There are no boundaries if you are using Wi-Fi, you can move from one room to another or even away from home you have the liberty to access internet within the range of radial distance. Wi-Fi hotspots concept is getting popularity among business communities and mobile workers. For this reason ISPs are consolidating Wi-Fi switches to numerous spots for the scope of wide range.

3. IMPLEMENTATION

On the basis of visible light communication technology, the advanced technology called Li-Fi provide dual function of visible light LED for illumination and data transmission. Li-Fi is very latest version of Wi-Fi which uses visible light in place of radio waves. Hence, visible light data transmission rate have higher speed than other broadband. It overcome the problem related with Wi-Fi, because Li-Fi has wider network area so traffic handling capacity improved and it is cheaper than Wi-Fi.

The VLC system is compared with other wireless communication system that are in current use like LAN and Wi-Fi. LAN is available in very short range and it is not mobile. And Wi-Fi has low traffic handling capacity as number of user increases Wi-Fi becomes unable to achieve user's need. Li-Fi offers significant capability to resolve this problem compared with Wi-Fi. It transmits data by switching LEDs on and off rapidly by changing light intensity which is not detected by human eye.

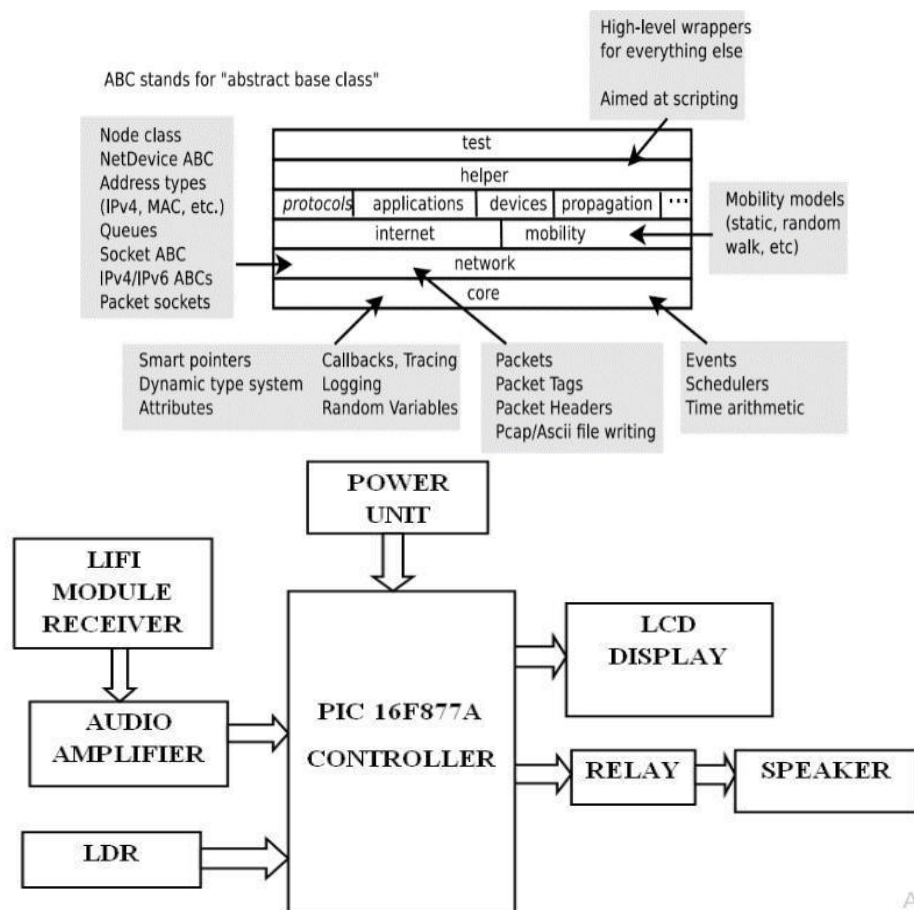
The data transmission rate is about 10Gbps by using white bright LED. The indoor visible light communication uses visible light spectrum to provide high rate data transmission which at the same time used as energy efficient illumination. In this way, the idea of the dual function of communication and illumination offers opportunity for efficient cost reduction and carbon footprint reductions.

4. PROPOSED SYSTEM

The proposed system consists of a transmission section and a receiver section. The transmitter section consists of an APR, Li-Fi transmitting module, MIC and the receiver section consists of a Li-Fi receiving module, PIC microcontroller, an amplifier, speaker and a transformer.

Transmitter Section

In the process of voice communication through the visible light on the transmitter side, voice is used as the input signal. This signal is converted to an electrical signal through a microphone. The transmitted data will be digitized then the digital signal drives the LED by using on-off-keying (OOK) modulation. LED, turning led ON for ones and OFF for zeros. Hence, the transmission data rate has to be so high that it eliminates the flicker and perceive as a constant light source to human eye. LED, turning led ON for ones and OFF for zeros



Li-Fi Receiver:

The data of ones and zeros from the LED source absorbed by the photo detector and equivalent electrical signal is produced. This signal is demodulated and then amplified by audio amplifier. Light intensity is absorbed by LDR. Based on the intensity of the light, microcontroller detects the error and minimizes using PWM error minimization technique. The error controlled audio signal comes out using speaker

5. CONCLUSION

This technology is still under research and surely it will be a breakthrough in communication. It assures data speed of 100gbps which is entirely greater than radio waves. The scope of this Li-Fi technology is ultimately greater. As Li-Fi provides secured, low cost, easy data transmission and provides reliable communication, It can be used in industrial, medical, military applications. Li-Fi is still in its beginning stages, but improvements are being made rapidly, and soon this technology will be able to be used in our daily lives. It is intended that this research will provide the starting steps for further study. In spite of the research problems it is our belief that the VLC system will become one of the most promising technologies for the future generation in optical wireless communication.

6. REFERENCES

- [1] Asad Ali and Mohamad Eid, "An Automated System for Accident Detection", 978-1-4799-6144-6/15/\$31.00 ©2015 IEEE
- [2] Md. Syedul Amin, Jubayer Jalil, M.B.I. Reaz, "Accident Detection and Reporting System using GPS, GPRS and GSM Technology", "IEEE/OSA/IAPR ICIEV, 2012
- [3] Mugila.G, Muthulakshmi.M, Santhiya.K, Prof. Dhivya.P-Smart Helmet System Using Alcohol Detection For Vehicle Protection [International Journal of Innovative Research in Science Engineering and Technology (IJIRTSE) ISSN: 2395- 5619, Volume –2, Issue –7. July 2016]

Design and Fabrication of Optimized Railgate Control and Obstacle Detection using Wireless Protocol

Jeevanandam.V, Department of ECES tudent

Manikandan.R, Department of ECE, Student

Mohamed Akshith.M, Department of ECE, Student

Thivagar.T, Assistant Professor, Department of ECE

MRK Institute of Technology, Kattumannarkoil, Anna University, Chennai

Abstract

It has been noted that lot of fatalities of lives occur everyday due to manually operated railgates. This is due to un manned gates of crossing zones. This paper presents the design and implementation of automatic railgate control and obstacle detection for developing countries. This project was carried out using parallel monitoring architecture along with IR sensor, PIR sensor, DC motor and LCD. This project is a combination of old technology with recent wireless technology and analytics to provide the best possible service to the nation.

Keywords: Automatic Railgate System, Real Time Monitoring, Automatic Train Stop and Rail Gate Automation.

1 Introduction

Railways are the largest mode of connectivity and transport inside a country. Poor maintenance of level crossings and railway bridges by the authorities, among other issues, contributed to the rise in rail accidents. To reduce the accidents in the level crossings by using parallel monitoring architecture. This project is a combination of old technology with recent wireless technology and analytics to provide the best possible service to the Nation.

2 Proposed System

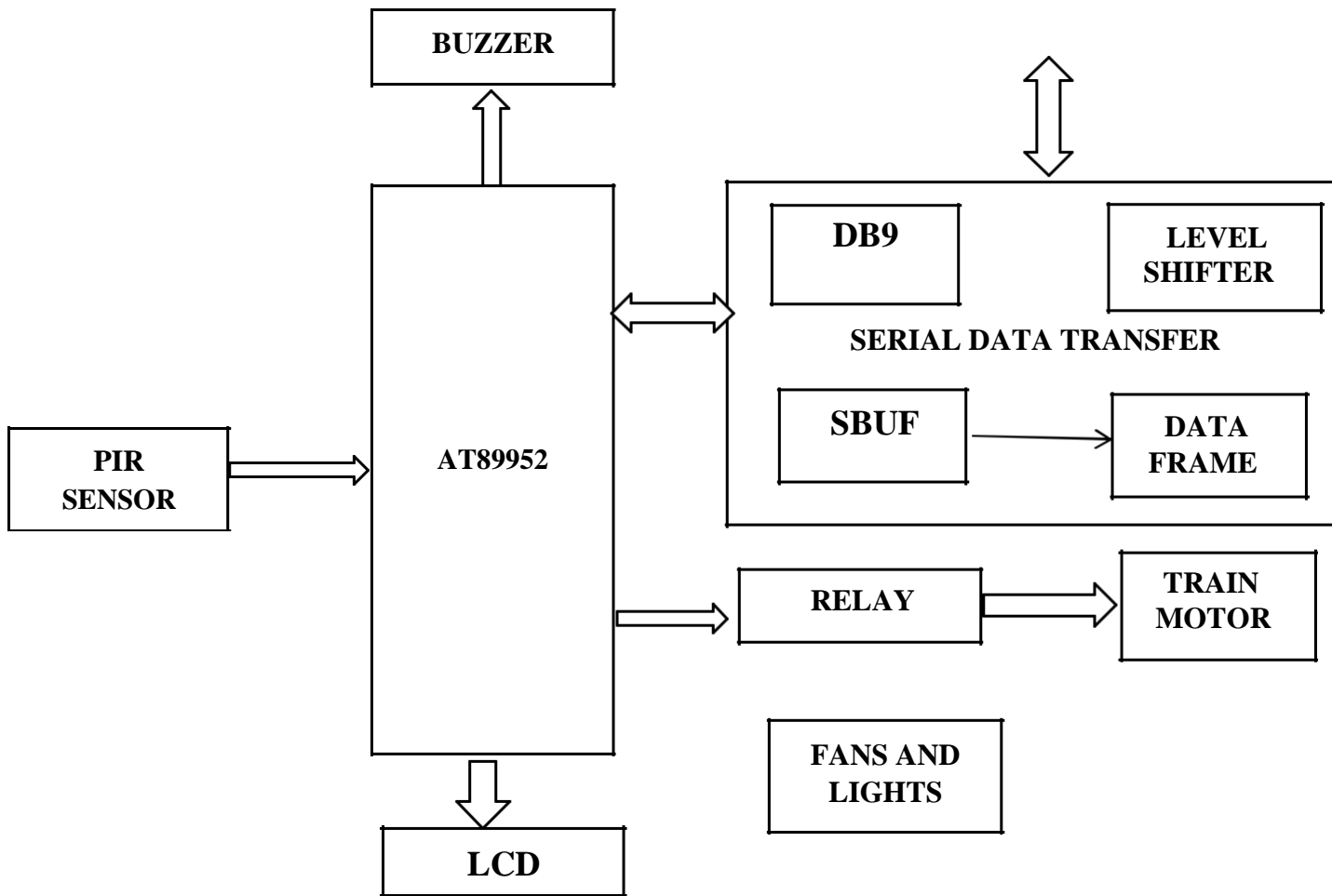
In this system, it has architecture similar to most modern train control systems, with the addition of parallel monitoring hardware. The new system is designed to meet requirements such as data acquisition, data transmission, data processing and alarm control. Here we use two section. We are using PIR sensor and ultrasonic sensor to monitor human crossing and obstacle detection in the train section. The gate section having IR sensor and gate motor to detect if any person crosses the gate. Our system is designed in such a way that minimal human contact is required, avoiding all kinds of human error. High Efficiency makes it extremely reliable, gaining the trust and reliability of such service users in our country.

3 Design Process

This process includes two sections namely the Train section and the Gate Section.

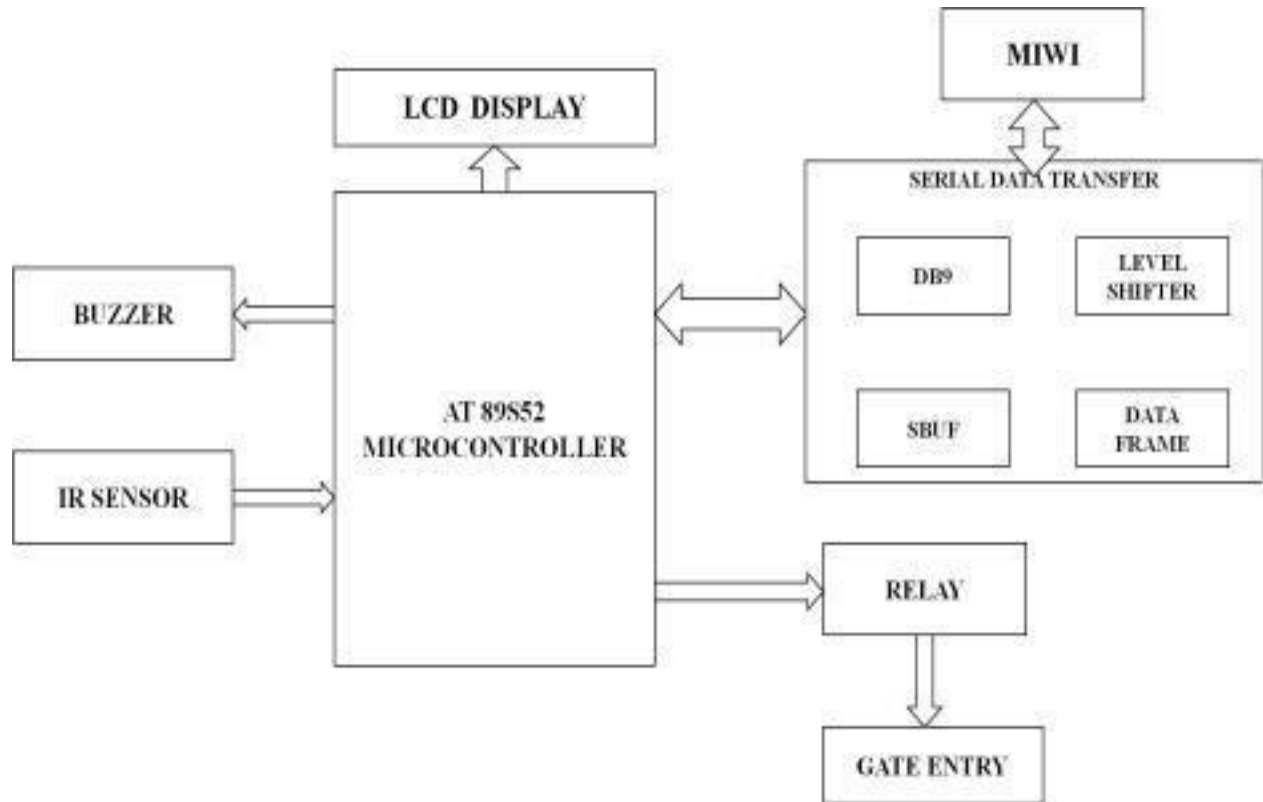
Train Section

In the train section, we use PIR sensor to monitor whether any human crosses the track within a specified range. The microcontroller is connected with PIR sensor. The information are monitored by the control unit and it also have the automation facility to fans and lights. It receives signals from the gate section and runs by the command of gate section.



4 Gate Section

The gate section has IR sensor and gate motor connected with microcontroller. If any person crosses the gate, the buzzer will be turned on. The information of arrival time is transmitted and received using MIWI.



5 Conclusion

An automatic railgate control system and the real time monitoring is done using parallel monitoring architecture. This project will save many human lives in the rail crossing gates across cities and towns. This will help to reduce such accidents across the gates and will alert the humans by the alarm.

6 Reference

1. Kuraish Bin Quader Chowdry, Md.Abdur Razzak, Moshiur Rahman Khan on "Automation of Rail Gate Control with Obstacle Detection and Real Time Tracking in the Development of Bangladesh Railway",2020
2. Jeff Cicolani on "Beginning Robotics with Raspberry Pi and Arduino",2018.
3. E.Amarnatha Reddy,K.Srinivas Rao on "A Secure Railway Crossing System using IOT ",2017.
4. M.Siva Ramkumar, "Unmanned Automated Railway Level Crossing System using Zigbee",2017.
5. Alexandra Simic, Milena Milosevic on "Driver Monitoring Algorithm for Advanced Driver Assistance System",2016
6. B.Brailson Mansingh,S.R.Vignesh Kumar on "Automation in Unmanned Rail Crossing",2015.

CASCADE ATTENTIVE REFINENET FOR BLOOD VESSELS SEGMENTATION OF DIABETIC RETINOPATHY

M. Abinesh ,(Electronics and Communication Engineering, St.Anne's colleges of engineering and technology
P. Ravichandiran,(Electronics and Communication Engineering,,st.annes colleges of engineering and technology
Mrs.D.Umamageshwari,,Electronics and Communication Engineering, st.annes colleges of engineering and
,technology

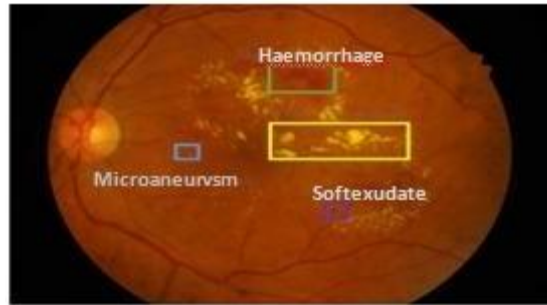
Abstract

Diabetic retinopathy is the leading cause of blindness in working population. Blood vessel segmentation from fundus images helps ophthalmologists accurately diagnose and early detection of diabetic retinopathy. However, the task of Blood vessels segmentation is full of challenges due to the complex structure, the various sizes and the interclass similarity with other fundus tissues. To address the issue, this paper proposes a cascade attentive RefineNet (CARNet) for automatic and accurate Blood vessel segmentation of diabetic retinopathy. It can make full use of the fine local details and coarse global information from the fundus image. CARNet is composed of global image encoder, local image encoder and attention refinement decoder. We take the whole image and the patch image as the dual input, and feed them to ResNet50 and ResNet101, respectively, for down sampling to extract Blood vessel features. The high-level refinement decoder uses dual attention mechanism to integrate the same-level features in the two encoders with the output of the low-level attention refinement module for Multiscale information fusion, which focus the model on the Blood vessel area to generate accurate predictions. We evaluated the segmentation performance of the proposed Kaggle and DDR data sets. Extensive comparison experiments and ablation studies on various data sets demonstrate the proposed framework outperforms the state-of-the-art approaches and has better accuracy and robustness.

Keywords · Diabetic retinopathy · Blood vessels segmentation RefineNet · Attention fusion

1. INTRODUCTION

Early diagnosis is crucial in many sight-threatening diseases like glaucoma, hypertension and diabetic retinopathy which cause blindness among working age people [1], [2]. Therefore retinal image analysis has become one major diagnosis method in modern ophthalmology. Retinal image analysis typically involves in blood vessel segmentation, optical disc segmentation and fovea segmentation for detecting and analyzing any abnormalities [3], [4]. The contrast enhancement is one mandatory step in any of the related image analysis approaches [1]–[6]. The main challenge of any contrast enhancement algorithm is finding a method to regulate the amplification according to the illumination variations over the image [7]. A typical solution is applying a homomorphism filter to normalize the illumination. However, some contrast enhancement techniques such as contrast limited adaptive histogram equalization (CLAHE) [8] and local normalization (LN)[9] have the capability of analyzing the local illumination and regulate the amplification to bring the final outcome up to an acceptable level of quality. CLAHE is able to handle the illumination variation by doing local histogram equalization and also can regulate the amplification of the details. However, it introduces a box-shaped artifact which may cause to suppress some details and also it amplifies some undesirable details.



2. DATA PREPROCESSING AND AUGMENTATION:

We subtract all the images by the local average color to highlight effective details on the fundus image, and the readers can turn to the competition report from the champion of the Kaggle competition. We also apply some commonly used data augmentation strategies for both patches and the entire images, including randomly crop with scale=(0.9, 1.1), ratio=(0.9, 1.1), random horizontal and vertical flip ($p=0.5$), and random rotation with the rotate degree range in (0, 180). Training details: The lesion attention generator is pre-trained with the patches from IDRid dataset. To train the final framework in an end-to-end manner, the gradients are only back propagated from the abnormal shortcut to fine-tune the lesion attention generator. The grade information from the shortcut can be more directly transmitted through the shortcut than from the deep grading net.

Although great progress has been made in the task of lesion segmentation, it is still full of challenges. The main reasons are as follows. (1) The proportion of lesions (e.g., MA) in the high-resolution fundus image is so small that is easily confused as noises. (2) The structure of the lesion is complex, and various kinds of lesions have differences in shape, size, colour and brightness. (3) The colour, contour and texture of tissues on the retina (e.g., blood vessels and optic disc) are similar to those of lesions, which are prone to false-positive results. (4) The appearance of the retinal images varies due to differences in the camera system and light source intensities. (5) The tissue pigmentation in fundus images of patients of different races varies greatly, which increases lesion segmentation difficulty [6]. Specifically, compared with the fundus images of white people and yellow people, the retinal pigmented epithelium of black people contains more melanocytes, which forms the most outer layer of the retina. Compared with the light-colored retina, the darker retina obscures some lesions and vascular changes

Recently, convolutional neural networks (CNNs) have become widespread in many fields of real life [7–11], numerous deep learning-based methods have been presented for lesion segmentation of DR. The existing methods [12–17] for lesion segmentation of DR are categorized into encoder–decoder structures and non-encoder–decoder structures. On the one hand, due to the high resolution of fundus images and GPU memory limitations, works [12–15] first cropped the original image into patches or resized and input them into U-Net and its variants for lesion segmentation. However, patch images lack global information, and the deconvolution operation cannot preserve the detailed information of small lesions, such as MA, which makes generating accurate predictions difficult. On the other hand, considering that different types of lesions are inconsistent in size and scale, algorithms [16,17] fed the full image to VGG or ResNet to extract the contextual information and used a 1×1 convolution operation to fuse multiscale feature maps.

However, tutes without excessively consuming computing resources is crucial for accurate multi-lesion segmentation of DR images. To address the above issues, this paper proposes a cascade attentive RefineNet (CARNet) for multiple lesion segmentation. CARNet adopts a dual-input encoder–decoder structure and trains in an end-to-end manner. The input is the whole image and the patch image, and the output is the segmentation result of four lesions. The proposed model includes the whole image encoder, patch image encoder and attention refinement decoder. First, the whole images and the patch images are sent to ResNet50 and ResNet101, respectively, for down sampling to extract features. Second, the deep features of the fourth residual block in ResNet50 and ResNet101 are simultaneously fed to the bottom-level attention refinement module (ARM) to fuse the global and local features. Third, the feature maps from the same level in the two encoders and the output of the previous ARM are fed to the current ARM to fuse multiscale lesion features. Finally, the fused feature maps of the top-level ARM are sent to the dense sigmoid layer to obtain the final Blood vessel segmentation results. We evaluate the proposed CARNet on three public data sets, i.e., IDRid [18], E-Ophtha [19] and DDR [20]. Experimental results show that our method has good robustness and accuracy. It not only overcomes the interference of similar tissue and noise but also

reserves the fine details of the lesion area without overloading GPU memory usage. To the best of our knowledge, this is the first study to apply attentive RefineNet for multi-lesion segmentation from DR images.

3. Existing method

Traditional methods

Traditional methods for lesion segmentation are grouped into four categories: region growing methods [21], thresholding algorithms [22], mathematical morphology approaches [23] and machine learning-based methods [24]. Wu et al. [21] first preprocessed the original fundus image to make the MAs clearer, then used the region growing method to locate the MA candidate areas, and extracted dimensional features to feed to AdaBoost, Bayesian net and k-nearest neighbour (KNN) classifiers to segment MA from fundus images. Long et al. [22] combined fuzzy Cmeans clustering with a dynamic threshold to determine the candidate HE regions, extracted the texture features from fundus images, and finally fed them into the support vector machine (SVM) classifier for automatic HE detection. Colomer et al. [23] extracted granulometric profiles and local binary patterns (LBP) to calculate the morphological and texture features of the fundus images and then used Gaussian processing, random forest and SVM for EX, MA and HE segmentation on the DIARETDB1 [25] and E-Ophtha_EX [19] data sets. Amin et al. [24] first applied the Gabor filter for image enhancement, then extracted geometric and statistical features from the candidate lesion area, and finally adopted Bayesian net, KNN and SVM for EX detection on the DIARETDB1 and E-Ophtha EX data sets. However, the performances of the above methods are easily limited by the brightness and contrast of the fundus images. Therefore, the robustness is poor and inefficient for meeting the need for clinical screening.

Deep learning methods

In recent years, deep learning algorithms [12–17,26–29] have shown outstanding performance and outperformed traditional methods in Blood vessel segmentation. The existing methods can be classified into two types: encoder–decoder and nonencoder–decoder structure. Zhou et al. [26] proposed a semi-supervised collaborative learning model based on attention mechanism to realize lesion segmentation and DR classification. They combined U-Net with the Xception module to generate segmentation masks for four kinds of lesions. Foo et al. [13] presented MTUnet for Blood vessel segmentation and DR classification on the IDRiD and SiDRP14–15 [30] data sets. They replaced the encoder with a VGG16 network and passed the skip connection to the decoder before each max-pooling operation. Furthermore, transposed convolution instead of the usual upsampling operation is used in the decoder. Yang et al. [14] proposed a two-stage network for lesion detection (e.g., EX, HE and MA) and DR grading.

The original fundus images are divided into patches overlapping grid and input into the local network to generate weighted lesion maps, and then the weighted lesion maps are fed to the global network to classify the DR severity. Sambyal et al. [15] developed an improved U-Net framework for MA and HE segmentation. The model adopts ResNet34 as the encoder and applies the upsampling operation of periodic shuffling convolution to realize the rapid convergence of the network. However, periodic shuffling with subpixel convolution is suitable for the super-resolution task. In summary, the deconvolution operation in the encoder–decoder framework cannot recover the low-level features lost after downsampling, which makes generating accurate high-resolution segmentation results difficult. Guo et al. [16] modified VGG16 and proposed L-Seg, using a multiscale feature fusion approach and a multichannel bin loss function to address the issues of small lesions that are difficult to accurately segment and class imbalances, respectively.

The goal of this study was to create a Blood vessel segmentation method from DR images that overcomes the limitations of traditional algorithms and deep learning approaches. Therefore, a cascade attentive RefineNet is proposed in this paper to realize automatic multi-lesion segmentation of DR images.

4. Proposed method

Mathematical Approach

Let $T = \{(X, Y)\}$ denote the training set, where $X = \{x_i, i = 1, \dots, m\}$ denotes the original fundus image, $Y = \{y_i, i = 1, \dots, m, y_i \in (0, 1)\}$ denotes the lesion label, and m denotes the number of images in the training set. Each original image corresponds to a maximum of four labels due to different types of lesions in fundus images.

Before inputting the segmentation network, we crop each training image and the lesion mask (x_i, y_i) into n patches $p = \{(x_k, y_k), k = 1, \dots, n\}$. In my paper, we take the whole images and the patch images as dual inputs and train the segmentation model by minimizing the difference between the predictions and ground-truth masks. Our goal is defined as:

Preprocessing

We perform necessary preprocessing on the original image for lesion enhancement and data augmentation before training the proposed network. First, all images are uniformly resized to 1024×1024 due to inconsistent image size in different data sets, and the inner circle of retina is appropriately cropped and filled into squares to remove zero-pixel areas. Second, the original fundus images are cropped into patches with a resolution of 1024×1024 . Third, due to the differences in illumination and contrast between fundus images, we use contrast-limited adaptive histogram equalization (CLAHE) to enhance the contrast between the lesion area and the background, as shown in Fig. 2. Finally, data augmentation operations are performed on the original image because of the limited number of image samples. (1) Scaling randomly by a factor of $[0.8, 1.2]$ in a step of 0.1. (2) Rotating randomly within the range of $[0, 360^\circ]$ in a step of 60° . (3) Translating the original image from -50 pixels to 100 pixels in 30-pixel steps vertically and horizontally.

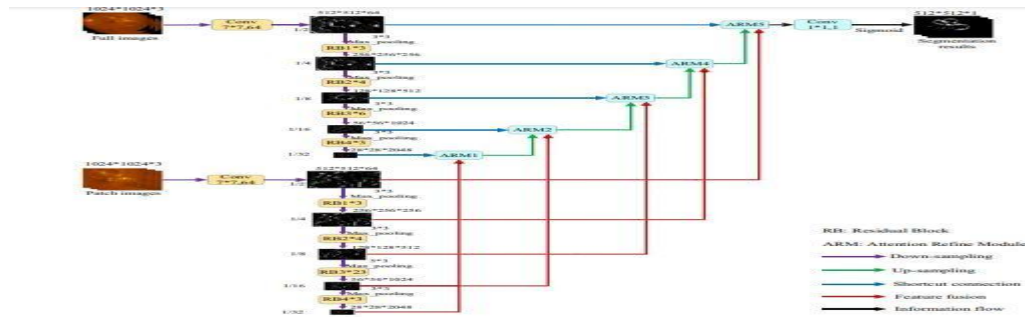
Deep residual network

The whole image encoder Enc_{whole} and patch image encoder Enc_{patch} use ResNet50 and ResNet101, respectively, to extract multiscale contextual features from full images and patch images. The encoding process of Enc_{whole} and Enc_{patch} can be expressed as

$$F1_w, F2_w, F3_w, F4_w = Enc_{whole}(x_i),$$

$$F1_p, F2_p, F3_p, F4_p = Enc_{patch}(x_k), \quad (2)$$

where F_w and F_p represent the encoding features of the whole image and the patch image in different hidden layers, respectively. Both ResNet50 and ResNet101 [35] are composed of four residual blocks, and the resolution of the output image after each residual block is reduced to $1/4$ of the original image. The structure of residual block is shown in Fig. 4.



Which includes three convolutional layers, two batch normalization (BN) layers and three rectified linear unit (ReLU) layers. ResNet introduces a residual block through skip connection to improve the information flow, and it consists of multiple shallow networks to speed up network convergence.

Attention refinement module

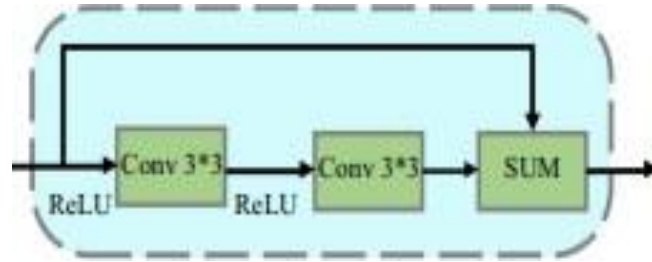


The decoding process of the attention refinement module is formulated as

$$S_j = \text{Dec}_{\text{ARM}}(F_j^w, F_j^p), j = 1,$$

$$S_j = \text{Dec}_{\text{ARM}}(F_j^w, F_j^p, S_{j-1}), j = 2, 3, 4, 5, (3)$$

where S_j indicates the predictions of the j th ARM, and S_5 denotes the final segmentation results. Figure 5 shows the framework of the proposed ARM, which includes RCU, AFB and CRP. The arrows in different colours represent input features of various types. First, the whole image features, the patch image features and the output features of the previous ARM are input into the RCU to extract multiscale features. Second, the feature maps of three RCUs are integrated into the AFB to locate the lesion area. Third, the fused attention features are fed to the CRP to capture contextual features in a larger image area. Finally, the outputs of the pooling operation are fed to the RCU to obtain the final prediction



5. Implementation details

All experiments were performed on an Ubuntu 18.04 system with an NVIDIA GeForce RTX 2080Ti graphics card with 11 GB of RAM. The framework was implemented based on the PyTorch platform. We used ResNet pretrained on ImageNet [37] as the backbone of the encoder. We applied the stochastic gradient descent (SGD) method to train the model for rapid convergence. Moreover, we used the multilearning strategy to update the learning rate. The batch size was set to 4, and the initial learning rate, momentum and weight decay were set to 10^{-4} , 0.9 and $2e^{-3}$, respectively. The learning rate was the

Evaluation metrics

We adopted sensitivity (Sen), specificity (Spe), accuracy (Acc) and Dice to evaluate the segmentation performance of various networks. The evaluation metrics are calculated as follows:

$$\text{Sen} = \text{TP} / \text{TP} + \text{FN}, (8)$$

$$\text{Spe} = \text{TN} / \text{TN} + \text{FP}, (9)$$

$$\text{Acc} = 1/2 (\text{sen} + \text{spe}), (10)$$

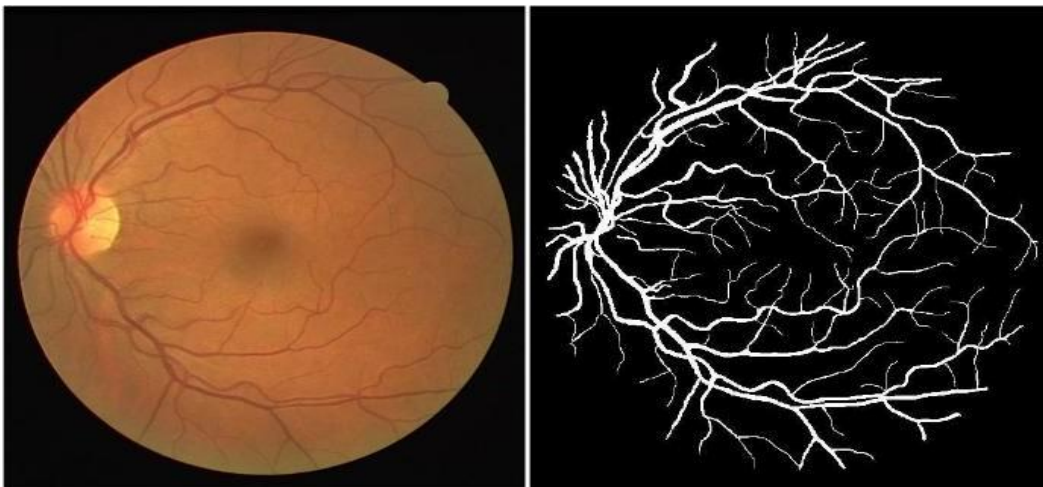
$$\text{Dice} = 2\text{TP} / 2\text{TP} + \text{FN} + \text{FP}, (11)$$

6. Proposed network Result

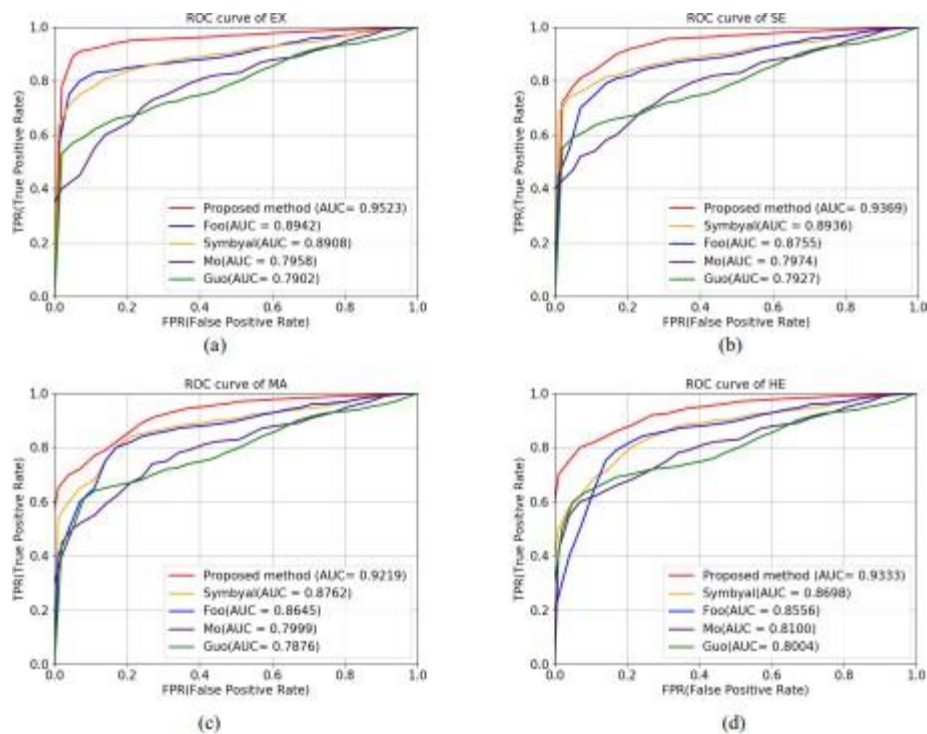
$$\text{Acc} = 0.9652$$

$$\text{Sen} = 0.9582$$

$$\text{Spe} = 0.9489$$



ROC curves of the four lesions segmentation on the IDRiD data set



7. Conclusion

This paper proposes a cascade attentive RefineNet to realize automatic and accurate multi-lesion segmentation of DR images. The framework consists of three parts: the whole image encoder, the patch image encoder and the attention refinement decoder. First, the dual input of the whole image and the patch image are input into ResNet50 and ResNet101, respectively, to extract the features of multi-size fundus images. Then, the features of the same level in the two encoders and the output of the previous attention refinement module are fed to the current attention refinement module to fuse multiscale context features of lesions and obtain the final segmentation results. We evaluate the segmentation performance on fundus images from mixed races, Caucasian and Mongolian race. Comprehensive experimental results demonstrate the superiority and effectiveness of our CARNet over state-of-the-art networks. It can overcome the interference of similar fundus tissue and noise and fully use coarse-grained global features and fine-grained local details to achieve precise segmentation of multiscale lesions.

8. References

1. TingDSW, CheungGCM, WongTY (2016) Diabetic retinopathy: global prevalence, major risk factors, screening practices and public health challenges: a review. *Clin Exp Ophthalmol* 44(4):260–277
2. YauJWY, RogersSL, KawasakiR, LamoureuxEL, KowalskiJW, BekT, ChenS-J, DekkerJM, FletcherA, GrauslundJetal (2012) Global prevalence and major risk factors of diabetic retinopathy. *Diabetescare* 35(3):556–564
3. Salamat N, Missen SMM, Rashid A (2019) Diabetic retinopathy techniques in retinal images: a review. *Artif Intell Med* 97:168–188
4. Stolte S, Fang R (2020) A survey on medical image analysis in diabetic retinopathy. *Med Image Anal* 64:101742
5. VarunG, LilyP, MarcC, MartinCS, DerekW, ArunachalamAN, SubhashiniV, KasumiW, TomM, JorgeCetal (2016) Development and validation of a deep learning algorithm for detection of diabetic retinopathy in retinal fundus photographs. *Jama* 316(22):2402–2410
6. Asiri N, Hussain M, Al-Adel F, Alzaidi N (2019) Deep learning based computer-aided diagnosis systems for diabetic retinopathy: a survey. *Artif Intell Med* 99:101701

7. GuoJ, YiP, WangR, YeQ, ZhaoC(2014)Featureselectionforleast-squaresprojectiontwinsupportvectormachine. *Neurocomputing*144:174–183
8. YuY, GaoY, WangH, WangR(2018)Jointuserknowledgeandmatrix factorization for recommender systems. *World Wide Web*21(4):1141–1163
9. Zheng H, Wang R, Ji W, Zong M, Wong WK, Lai Z, Lv H(2020) Discriminative deep multi-task learning for facial expression recognition. *InfSci*533:60–71.

IoT- Based intelligent aquaculture monitoring system for fish farming

Radhakrishnan.R¹, Balabasker.S²

Electronics and Communication Engineering

St. Anne's College of Engineering and Technology, Panruti

ABSTRACT

As current human Population is 7.7 billion and growing day by day hence food demand is also increasing accordingly. Fish is a rich source of vitamins, minerals, protein, nutrients and micronutrients. It is an important part of consumer's diet especially in poor and underdeveloped countries. It is a big challenge for farmer to fulfill market demand with healthy sea food. Aquaculture is a tool to fill gap between of sea food supply and demand. Use of controlled environment production of aquaculture has been increased to a significant level but losses huge due to manual equipment and management failure. Farmers need real time and accurate information to monitor and maximize production potential. Farmers are using traditional techniques and procedures for the aquaculture. By following traditional approach, farmer measure and monitors the water quality, water level, oxygen level and stress level of the aquaculture manually. In this study, we proposed an Internet of Things (IoT) based smart aquaculture model that will measure water quality (pH, water level, temperature, turbidity and motion detection of fish) for aquaculture. In this work uses low cost and short range wireless sensors network module to monitor and control aquaculture in real-time. Water recycling mechanism also proposed to reduce the amount of aquatic waste materials. By using this system parameters of water are monitored continuously using a serial port which reduces internet consumption, transmitted data regularly with small latency with error free and ensures survival of aquatic life also ensures the quality of growth and increases the economic benefits of aquaculture. The system also detects the movements of fish in the pond.

Keywords: Aquaculture, Internet of things (IoT), PH, Turbidity, Water quality Monitoring,

1.INTRODUCTION

Aquaculture also called aqua-farming, breeding, raising, harvesting of fish, seaweed, algae and many other organisms. It is also defined as breeding species which develop in the aquatic environment under controlled conditions. Aquaculture is one of most reliable and low environment impact process producing high quality protein for humans. This process is more efficient than other forms of agriculture because of higher food convergence. Aquaculture has become famous all over the world. Farmer faces a lot of problems like water rescors, manualtesting of water, sudden climate change, no government interest etc. Unlike daily monitoring of aquaculture behavior and health of thousand individual manually testing is very difficult. Some other problems like inappropriate management technique, water quality, improper record keeping, poor site selection. Traditional water quality monitoring cannot change the dynamic of aquaculture water quality monitoring and also achieved a fixed point monitoring. The aqua farmer presently in depend on manual testing for water parameters.This leads in increase the death rate of fish, decrease the growth rate of the fish, and one of major drawback is more time consumption. Fish pond operators face the challenge of constant monitoring of the water and water changing in such a way that quality is compromised. The model proposed in this work will assist the fish farmers in monitoring fish ponds using IoT. Integrating sensor and internet technology in combination with a user-

friendly interaction interface smartphone application, desktop application, and web services to provide real-time monitoring of fish ponds; system database contributes significantly to reducing the risk of losses and improving efficiency. GSM modem is also used which reduces internet consumption. Internet is the main issue while former in the field area. Internet is used when former open their Android application or web application otherwise GSM modem send the message when parameters crosses the threshold range. Proposed system using water filtration plant to improve the water quality. By using the proposed system, we will increase the productivity of the fish, reduce the cost, minimize loss and increase the survival of aquatic life. There are vast opportunities to improve the fish farming. Water quality is a key to success and also has direct impact on production of fish yield, among all farms of aquaculture for all species most important parameters are Temperature, PH, dissolved oxygen, turbidity. Water quality is an important factor for aquaculture and drinking water treatment plants and other related industries because polluted water not only claim losses of aquatic products but also face significant human health threats. These parameters (temperature, turbidity, PH, Dissolved oxygen) are most important for aquatic life and each fish required suitable growth environment.

To achieve the best quality production, we must use the IoT (i.e. sensors, controlling system, telecommunication system, mobile devices and solar system).

In this paper, we discuss multiple sections as a first step, introduction to the topic of aquaculture, what problems exist in this field, how to solve them, and the benefits. In which we discuss a range of works on aquaculture systems and what are the opportunity in this field, and which of these will be addressed in this work. The Methodology chapter presents the proposed system and a detailed description of the hardware or software. The features, some photographs and the results obtained using the system are shown in Experimental Results. We're reflecting on this job in conclusion. For this task, we suggest the next phases of future work and present the advantages.

2.LITERATURE REVIEW

In the start Conventional methods were adopted for monitoring the water quality, the samples of the water would be taken from the water and sent to the chemical laboratory for analyzing hazardous material. The drawback in the system is all the processing were being executed manually like measurements, maintenance and controlling of the system etc. On the other hand, manual system was time consuming. Some of the previous studies discussed the water monitoring models like culture models and forecasting models and integrated models but these systems had not ability of online monitoring, real time communication data collection. So we can say that these models are not good for fish monitoring but, IoT is one of the fast- growing technologies of recent decades. The purpose of IoT is identifying, monitoring, tracking, locating the things telecommunication and interconnectivity between devices. The invention of new sensors technologies, wireless telecommunication technology, data transmission technology, many devices are made for real time monitoring in remote areas The growth of aquatic life is effected by the water quality variation which have been discussed in many studies. Mostly studies used a lot of sensors but management of these sensors are costly but most papers concentrate on few forms of sensors such as PH, DO, Temperature, Turbidity, water level, and suggested the solutions of the problems because all parameters are not nursery to monitor these parameters (PH, DO, Temperature, Turbidity, water level) are dependent on each other if one parameter

unstable cause of other variable unstable that why we are choosing these parameters. Proposed architecture uses different sensors (Temperature, PH water level, Turbidity, Motion detection). These sensors are configured with Arduino Uno for sensing and observing measurements in aquatic environment. The previous proposed approaches by authors used cloud database for the storage of output data which makes the architecture costly by maximum consumption of internet, to overcome this consumption Computer system acts like a server host to compute and manage the output values generated through sensors are easily managed and the necessary data could be retrieved by user by consuming minimum cost of internet. Local database helps the former for analytics and take pro-active measures when its needed. Most of models using focus on sending the sensor data but in our model we also provide pro-resolution if parameter crosses the limits that listed in below Table 1 and also discuss the factor that effect the fish growth. Our main focus is reducing internet consumption. In the field areas internet is main problem we reducing internet consumption also using GSM modem for sending the message if internet is not available, and also using Android application, desktop application for the formers. **Physical Water Quality Parameters of Aquaculture Water structure varies with the climate patterns but how the water is being used. The goal of good management of the fish culture is to control this structure in order to produce the best results.**

Temperature.

Temperature is the most important element and has a strong influence on biological and chemical processes. The values of chemical and biological reaction increased for each 10°C increases in temperature. This is a fact that fish are cold blooded animals that adapt their temperature depending on the weather around them. Temperature is based on the fish species but temperature is controlled and maintain according to right range. Higher temperature accelerates the metabolism of the fish feeding and respiration increases, and there is a general also movement increases because temperature vary according to depth of water. If the temperature increases the need of dissolved oxygen demanded.

Turbidity.

The second physical element is turbidity. The color of water suggests that what kind of turbidity is. If the water color is clear that means low biological output so fish do not live well in it because it is not fertile enough. If the color is green, it's because of algae and if the color is brown, it's because of clay. Muddy water is also not good for fish, because fish can have gills that blocked the clay particles causing the fish to die. Greenish water indicates that over generation of planktons [16]. The presence of these suspended particles in varying amounts is responsible for water turbidity.

Water Level.

The third one is water level. The variation in fish pond water levels affect the behavior of the fish. Fish have a tendency of moving to specific areas of the pond where they can feed and relax. When the water level for the area shrinks, then is likely to cause competition for survival among the fish.

3.3PH.

There is another parameter for quality check of water is pH for the fish survival is between 6.5–8.5. Fish growth rate is slowing down and also stressed in water if pH

is less than 6.5 than death of the fish is almost confirmed at pH 4.0 and greater than 11.0. PH is also called hydrogen potential, Night time respiration can cause the oxygen depletion for the fish. PH voicing whether the water is acidic or fundamental in response. During photosynthesis, the marine plant and phytoplankton remove carbon dioxide from the water; The pH of the water rises during the day and decreases during the night. In a day time, low heap alkalinity has a PH level of 6 to 8 but in the night time development of phytoplankton development is increases the PH level is also increases up to 10 or more. PH changes in pond water affected through carbon dioxide and ions .

3.4 Dissolved Oxygen.

DO is the prime concern for water quality and that determines the growth health size of the fish population. Dissolved oxygen should be in between 5-12 ppm. Oxygen comes from two resources first comes from photosynthesis and second diffusion from the air. At this harmful level, total concentrations of dissolved gas in water should not exceed 110 per cent. Oxygen problem occur when consumption of respiration exceeds as a result fish feeding increased water temperatures can also contribute to a decrease in the DO content, as it cannot retain O₂. But dissolved oxygen (DO) level is crosses the limit, however, it can cause a disease of the gas bubble which can kill fish. If too small, it will allow bacteria to infect fish easily.

Parameters	Range	Solution (if parameters cross the range)
PH	6.5 ~ 8.5	(Caco ₃) calcium carbonate 0.05/letter calcium carbonate 0.05/letter calcium carbonate 0.05/letter calcium
Temperature	5C-35C	Pumping freshwater into the
Turbidity	Less than 25mg/l (TSS)	Change the water/Recycle the water
Motion detection	//	Detect the motionof fish

MATERIAL AND METHOD

Required Hardware and Software

Sensors.

Arduino analog pH sensor (SEN0161) referred to in Fig. 1. is used to measure the pH of the water. PH-sensor is specifically suited for Arduino series and features easy communication and integrated functions. To attach the sensor to Arduino it needs a BNC connector. This PH sensor has a range of 0-14. It is ± 0.1 PH accurate at a standard temperature of 25- 30°C and running temperature range from 0 to 60 °C The water can only be fed to a few sections of the sensor. Reliability of the pH sensor will last a half of year if the water is clear, and a month for high turbidity water.



Fig. 1. FT1 SENSOR.

We have also used turbidity sensor, for measuring turbidity rate or opacity, the Arduino gravity turbidity sensor senses water quality. The sensor uses measuring light transmission and the dissipation rate to distinguish dissolved particles in water, that differs in water with total suspended solids (TSS) (displayed in the Fig. 3. A turbidity monitor responds by transmitting a laser rays into the water for analysis. Any suspended particles would then disperse the light. The sum of the reflected light is used to identify particle density within the water.



Fig. 3. Turbidity sensor.

Proposed model also used water level sensor. This sensor contains SONAR to measure the distance of an object, just as the bats do. This guarantees high non- contact detection of the range with great accuracy and accurate readings from 2 cm to 400 cm or 1 to 13 feet in an easy to use kit. The water is measured using a water level sensor Fig. 4. This sensor functions by transmitting sound waves at frequencies that are too high for detection by humans. They also wait to see the sound reflected backwards and measure distance depending on the correct time. This is closely related to whether the radar measures the time it would take for an object to return to a radio wave. The module sensing the water level uses an ultrasonic emitting transmitter to ultrasonicreceiver. The tone of it wave reflection time is translated to depth of the surface.



Fig. 4. Water level sensor.

Microcontroller: Arduino Uno Fig. 8. used as Microcontroller. Arduino is a microcontroller kit which is free software, focused on the Atmega328P Microcontroller board created by Arduino.cc. The board has combination of 14 digital and 6 analog input / output pins that can communicate with different boards and other circuits, 16 MHz ceramic resonator and also reset button and forwards the data to the system using serial port and save into system data Base.

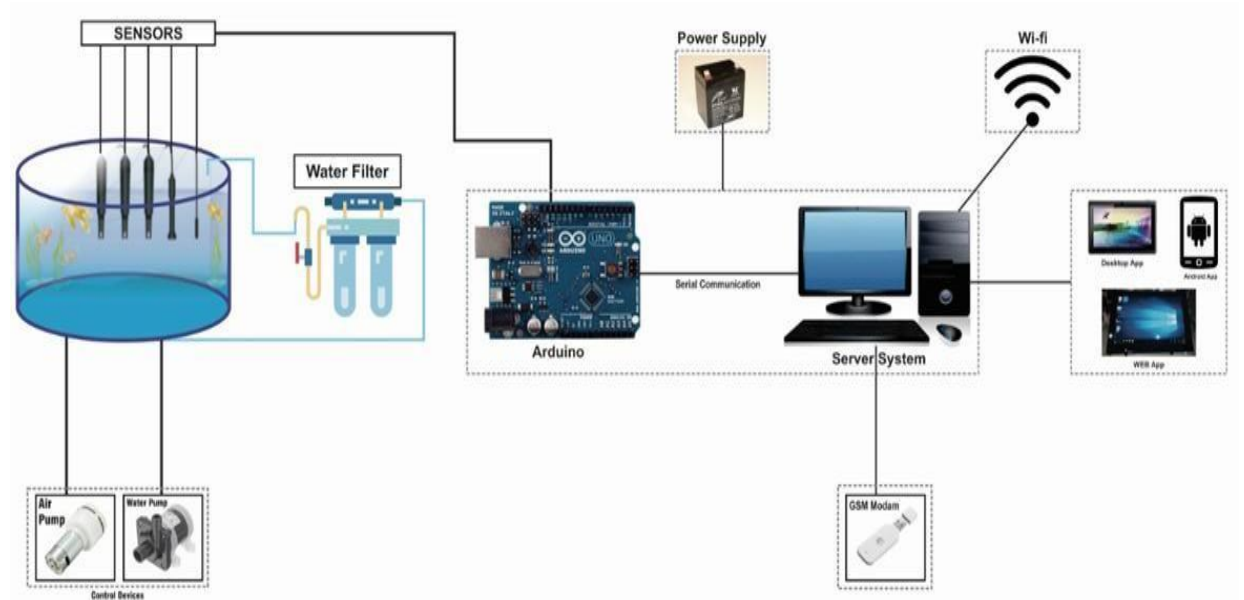


Server. The server analyzes the data received and acts predefined conditions.

Applications. The Mobile App, desktop App, and web provides a means of viewing data on the different applications Server and provides decision making and interface to the user.

Actuators. The actuators act upon the aquaculture environment based on instructions received from the IoTsystem.

The proposed model primarily focuses on the continuous monitoring of parameters of water quality from time to time, to take inhibitory measures for avoiding the actual damages in inhospitable environment. Proposed architecture uses different sensors (Temperature, PH water level, Turbidity, Motion detection). These sensors are configured with Arduino Uno for sensing and observing measurements in aquatic environment. Arduino Uno a low cost small computer board used as controller hub comprises with various analog and digital pins and operated with Arduino IDE software for interaction with computer system with controller using serial port. The previous proposed approaches by authors used cloud database for the storage of output data which makes the architecture costly by maximum consumption of internet, to overcome this consumption Computer system acts like a server host to compute and manage the output values generated through sensors are easily managed and the necessary data could be retrieved by user by consuming minimum cost of internet. This model provides us facility to avoid periodic computation of data and internet cost of uploading. The proposed desktop application provides directly view to analyze the measurements and daily basis reports. For remote monitoring android application and web based application are proposed with interactive GUI (Graphic User Interface) provides services for a user to monitor the aquatic field. Motor pump and air pump is also working automatically using actuator relays. Proposed an embedded with GSM modem in provide services as system alert which sends the notification to farmer if the aquatic pond is in critical condition. Moreover, advantage of GSM is when farmer does not have internet then this alert notification helps in emergency condition with feasible solution. Water filtration plant is coming in to play when turbidity level is high and worked until when level of turbidity comes into normal range and saves the water also.



Block Diagram

4.RESULTS AND DISCUSSION

As already discuss that farmer using traditional method and techniques and also use the forecasting models to measures the water quality parameters. In our model we reduce internet consumption and also creating a cost effective model and cannot use cloud database because of internet consumption but some of studies uses a cloud database [22]. Some of the models are cost efficient [23] but it cannot fulfill the demand of water quality because system use less amount of sensor. The main objective of this system is to provide real time monitoring using GSM, android app, desktop application. In this system using a serial port, the advantage of serial port is transmitted data regularly with small latency and also error free. The proposed model has been applied in an aqua pond and the tests were obtained from different sensors for 24 hours. The following are the plots collected for varying quality of water parameters about time.

FUTURE SCOPE

In near future we are expecting to use upgraded sensors and collection of more data that can be used for big data and analytics or to develop some AI algorithms for process optimization.

5.REFERENCES

- [1]. Garcia, M., S. Sendra, G. Lloret, and J. Lloret. (2011). "Monitoring and control sensor system for fish feeding in marine fish farms". *IET Communications*, (5), PP. 1682-1690,.
- [2]. Sung, W.T., J.H. Chen, and H.C. Wang. (2014).

Remote fish aquaculture monitoring system based on wireless transmission technology. In Proceedings of the *IEEE international conference on information science, electronics and electrical engineering ISEEE*, PP. 540- 544.

[3]. Dzulqornain, M. I., M. U. H. Al Rasyid, and S. Sukaridhoto. (2018). Design and development of smart aquaculture system based on IFTTT model and cloud integration, in Proceedings of the MATEC Web of Conferences. EDP Sciences PP. Page 01030.

[4]. Raju, K. R. S. R., and G. H. K. Varma, (2017). Knowledge based real time monitoring system for aquaculture using IoT, in Proceedings of the IEEE 7th *International Advance Computing Conference (IACC)*. *IEEE*, PP. 318-321.

[5]. Sj, A., and E. Ng. (2015). Aquaculture Sentinels: Smart-farming with Biosensor Equipped Stock. *Journal of Aquaculture Research & Development* 07.

[6]. Wei, Y., Q. Wei, and D. An. (2020). “Intelligent monitoring and control technologies of open sea cage culture: A review”. *Computers and Electronics in Agriculture*, pp. 169:105119.

Design and Implementation of Microcontroller Based vehicular Smart Helmet for Safe Journey using sensors

B. Arunkumar¹ S. Durai Raj², V.Venkatesan³

Assistant Professor^{1,2,3}, Department of ECE, St. Anne's College of Engineering and Technology, Panruti

Abstract

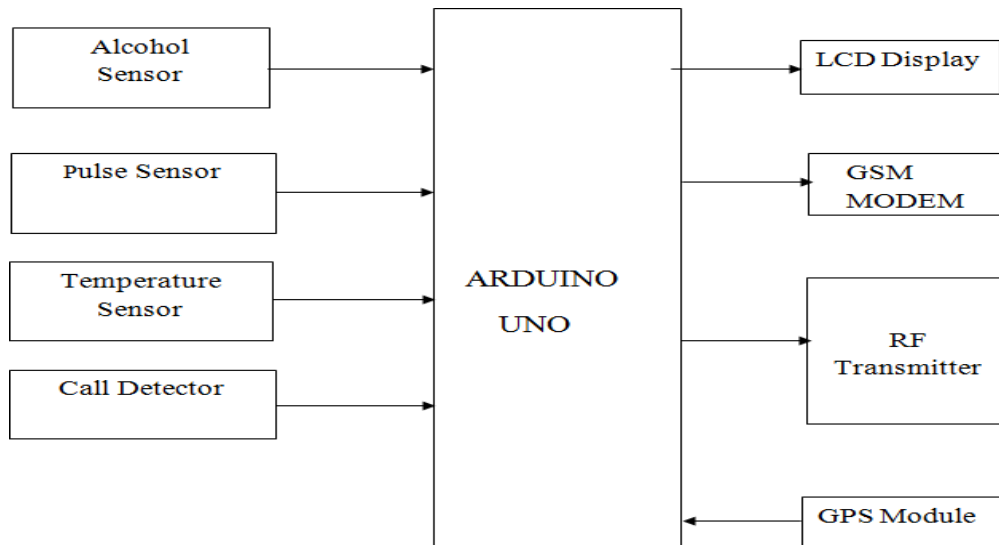
A smart helmet is a special idea which makes motorcycle driving safer than before. This is implemented using GSM and GPS technology. Many times we hear the cases of bikes getting stolen from parking area or sometimes we forgot to remove the keys from bike by mistake. In these cases it is really difficult to get the bike back. This project is designed to solve this purpose. Main concept behind this project is of a bike security system using a password entered through keypad. This system turns on the Buzzer when wrong password is entered for 3 times. User can change this password anytime he/she wish using a keypad. If the rider wears the helmet then only the bike will be turn on. The working of this smart helmet is very simple, vibration sensors are placed in different places of helmet where the probability of hitting is more which are connected to microcontroller board. So when the rider crashes and the helmet hit the ground, these sensors sense and gives to the microcontroller board, then controller extract GPS data using the GPS[8] module that is interfaced to it. When the data exceeds minimum stress limit then GSM module automatically sends message to ambulance or family member. The RF is used for start the two wheeler firstly it checks whether the driver is drunk end or not if drunken it will not allow to start two wheelers. Here a circuit which detects when a call is incoming in a mobile phone by means of a flashing LED. It can detect even when the calling mobile phone and the engine is automatically turn off.

Keywords: Alcohol Sensor, GSM, GPS, Microcontroller, Pressure Sensor, Smart helmet, Vibration Sensor

1. Introduction

The thought of developing this project comes to do some good things towards the society. Day by day the two wheeler accidents are increasing and leads to loss of many lives[6]. Accord to a survey of India there are around 698 accidents occurring due to bike crashes per year. The reasons may be many such as no proper driving knowledge, no fitness of the bike, fast riding of bike, drunken and drive etc[14]. Sometime the person injured, the accident may not be directly re possible for the accident, it may be fault of rider, but end of the day it's both the drivers involved in the accidents who is going to suffer[12]. If accidents are one issue, lack of treatment in proper time is another reason for deaths. According to the survey India 698 accidents occur per year, nearly half the injured people die due to lack of treatment in proper time. The many reasons for this such as late arrival of ambulance, no persons at place where the accident occur to give information to the ambulance or parents. This is a situation we observe our day to day life, a thought of finding some solution to resolve this problem come up with this idea of giving the information about accident as soon as possible and in TIME....!!!! Because after all time matter is a lot, if everything is done in time, at least we can save half the lives that are lost due to bike accidents. Considering three major factors for avoiding the accident causes such as I. Make wearing the helmet compulsory. II. Avoid drunk and drive. III. If person met with an accident, no one is there to help him. Simply leaving or ignoring the person he may die. In such situation, informing to ambulance or family members through mobile to rescue him for an extent. The idea of this work is to give information about the rider wearing the helmet or not, whether the rider drunken or not and also, he met with an accident it gives an information about location where he is met with an accident through GSM module to mobile numbers family members, so I have chosen GSM technology to give the information by sending SMS, using GSM module which has SIM card slot to place the SIM and send SMS[8]. Sending SMS alone can't help the driver, if we send an SMS saying that accident had occurred where the ambulance will come without knowing the location of the accident. So to trace out the location where exactly accident occur using GPS module, and gives to microcontroller, then it sends the SMS which contains the latitude and longitude of an area to family members mobile numbers For this we use GPS module to extract the location of the accident, the GPS data will contain the latitude and longitude values using which we can find the accurate position of the accident place[16].

2. PROPOSED SYSTEM



In this system Arduino UNO is used. When the system is switched on, LED will be ON indicating that power is supplied to the circuit [19]. The RF is used for starting two wheeler first it checks whether the driver is drunken end or not if drunken it will not allow starting two wheelers.

The small voltage of ignition of the two wheeler is grounded. In normal condition when the helmet is wearied the pressure sensor is senses pressure and the RF transmitter radiates the FM modulated signal [8]. The RF receiver is connected with the two wheeler which receives the radiated signal and activate the relay. The relay is remove the ignition wire from the ground and connected with the starter switch now the two wheeler will start. When driver met with accident vibration sensor sends message to microcontroller [1]. The GPS receives the location of the vehicle that met with an accident and gives the information back. This information will be sent to a mobile number through a message. This message will be received using GSM modem present in the circuit[2].The message will give the information of longitude and latitude values. Using these values, the position of the vehicle can be estimated.



Fig: 1.2.Alcohol Detection using Sensors

3.Accident detector

To run the GPS and GSM module, microcontroller is a very user friendly device which can be easily interfaced with any sensors or modules and is very compact in size. Now some of the thoughts in our mind, how will send the SMS using the GSM module by keeping the GPS location in the SMS which is obtained from the GPS module. But when should all this is done? When accident occurs, how will the microcontroller detect the accident? This can be done by using a vibration sensor which is placed in the helmet.



Fig: 1.3. No Alcohol Consumed

The vibration sensor is placed in the helmet such that it detects vibrations of the helmet. When the rider crashes, the helmet hits the ground and the vibration sensor detects the vibrations that are created when the helmet hits the ground and then the microcontroller detect the accident occurrence and it will send an SMS containing information about the accident and location of accident using GSM and GPS modules. Alcohol sensor sense the alcoholic content whether the rider drunken or not, if he drunken bike will not start showing as alcohol detected on LCD display. Use of pressure sensor, gives the whether the rider wear the helmet or not. If he not wears the helmet again bike will not start and intimate to rider to wear the helmet.

LCD (Liquid Crystal Display) screen is an electronic display module and find a wide range of applications. A 16x2 LCD display is very basic module and is very commonly used in various devices and circuits. These modules are preferred over seven segments and other multi segment LEDs. The reasons being LCDs are economical easily programmable have no limitation of displaying special & alphanumeric characters A 16x2 LCD means it can display 16 characters per line and there are 2 such lines.

4. Vibration Sensor

This sensor buffers a piezoelectric transducer. As the transducer is displaced from the mechanical neutral axis, bending creates strain within the piezoelectric element and generates voltages.

5. Hardware Software Description

The Aurdino Uno is an open-source microcontroller board based on the Microchip ATmega328P microcontroller and developed by Arduino.cc. The board is equipped with sets of digital and analog input/output (I/O) pins that may be interfaced to various expansion boards (shields) and other circuits. The board has 14 digital I/O pins (six capable of PWM output), 6 analog I/O pins, and is programmable with the Arduino IDE (Integrated Development Environment), via a type B USB cable. It can be powered by the USB cable or by an external 9-volt battery, though it accepts voltages between 7 and 20 volts. It is similar to the Arduino Nano and Leonardo. The hardware reference design is distributed under a Creative Commons Attribution Share-Alike 2.5 license and is available on the Arduino website. Layout and production files for some versions of the hardware are also available. The word "uno" means "one" in Italian and was chosen to mark the initial release of Arduino Software. The Uno board is the first in a series of USB-based Arduino boards; it and version 1.0 of the Arduino IDE were the reference versions of Arduino, which have now evolved to newer releases. The ATmega328 on the board comes preprogrammed with a bootloader that allows uploading new code to it without the use of an external hardware programmer.



Fig.1.4. Arduino UNO

While the Uno communicates using the original STK500 protocol, it differs from all preceding boards in

that it does not use the FTDI USB-to-serial driver chip. Instead, it uses the Atmega16U2 (Atmega8U2 up to version R2) programmed as a USB-to-serial converter. The capability to field/update the application firmware makes a wide range of applications possible.

6. LCD display

When Vibration Sensor Alarm recognizes movement or vibration, it sends a signal to either control panel. Developed a new type of Omni-directional high sensitivity Security Vibration Detector with Omni-directional detection.

Flashing LED: It can detect even when the calling tone of the device is switched-off^[10]. It must place a few centimeters from the voltage is doubled by C2 & D2 in order to drive reliable sound less than 200µs. Sensitivity of this circuit depends on the sensor coil type. L1 can be made by winding 130 to 150 turns of 0.2 mm. enameled wire on a 5cm diameter former. Remove the coil from the former and wind it with insulating tape, thus obtaining a stand-alone coil^[9].



Fig.1.5 Display showing Ignition OFF

7. GSM Modem SIM 300

Designed for global market, SIM300 is a Tri-band GSM/GPRS engine that works on frequencies EGSM 900 MHz, DCS 1800 MHz and PCS1900 MHz. SIM300 provides GPRS multi-slot class10 capability and support the GPRS^[8] coding schemes CS-1, CS-2, CS-3 and CS-4. With a tiny configuration of 40mm x 33mm x 2.85 mm, SIM300 can fit almost all the space requirement in your application, such as Smart phone, PDA phone and other mobile device.

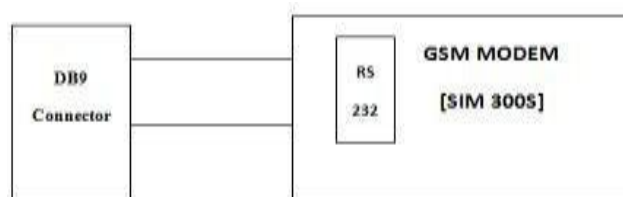


Fig: 1.6. GSM communication

8. EMS (Enhanced Messaging Service)

Besides the data size limitation, SMS has another major drawback -- an SMS message cannot include rich-media content such as pictures, is the abbreviation for European Telecommunications Standards Institute. Now the 3GPP(Third Generation animations and melodies. EMS (Enhanced Messaging Service) was developed in response to this. It is an application-level extension of SMS. An EMS message can include pictures, animations and melodies. Also, the formatting of the text inside an EMS message is changeable. For example, the message sender can specify whether the text in an EMS message should be displayed in bold or italic, with a large font or a small font.

The drawback of EMS is that it is less widely supported than SMS on wireless devices. Also, many EMS-enabled wireless devices only support a subset of the features defined in the EMS specification. A certain EMS feature may be supported on one wireless device but not on the other.

9. Call detector

Here a circuit which detects when a call is incoming in a mobile phone by means of a flashing LED. It can detect even when the calling mobile phone, so that its sensor or coil L1 can detect the field emitted by the phone receive during an incoming call working^[17]. The sensor coil L1 detects the signal and the detected signal is amplified by transistor Q1 and drives the mono stable input pin of ICI. The IC's output

A commercial 10mH miniature inductor, usually sold in the form of a tiny rectangular plastic box, can be used satisfactorily but with lower sensitivity. ICI must be a CMOS type; only these devices can safely operate at 1.5V supply or less.

10. Results and Discussion:



Fig:1.7 Circuit Diagram



Fig: 1.8 Output Display

Here a circuit which detects when a call is incoming in a mobile phone by means of a flashing LED. It can detect even when the calling mobile phone and the engine is automatically turn off. This system is cost effective, so we can implement easily. It must may be also implement in all driven system. It is more effective.

Conclusion

As the concluding part of this project, I would like to say that-- "Without proper action at proper time, danger awaits us with a bigger face." We must act on time when a person is injured. We must take care of person the way it is meant. Otherwise, a valuable life might be lost. We need to understand how precious lives of people are and what importance first-aid carries in saving these precious lives. This may be useful to each and every person in day to day life and they will never be afraid of the vehicle thefts. By this project people come to existence that our country is developing and they move forward the leg with full of daresness in their minds. If this project imparts this idea in even one person, I would think that the project will be successful.

REFERENCES

- [1] IEEE standard for local and metropolitan area networks: Overview and architecture. IEEE Std 802-2001 (Revision of IEEE Std 802-1990), pages 1–48, February 2002.
- [2] S. H. Ahmed, G. Kim, and D. Kim. Cyber physical system: Architecture, applications and research challenges. In Proc. of 2013 IFIP Wireless Days (WD), November 2013.
- [3] I. F. Akyildiz, W. Su, Y. Sankarasubramaniam, and E. Cayirci. A survey on sensor networks. IEEE Communications Magazine, 40(8):102–114, August 2002.
- [4] A. Al-Fuqaha, M. Guizani, M. Mohammadi, M. Aledhari, and M. Ayyash. Internet of things: A survey on enabling technologies, protocols, and applications. IEEE Communications Surveys Tutorials, 17(4):2347–2376, Fourth quarter 2015.
- [5] I. Andrea, C. Chrysostomou, and G. Hadjichristofi. Internet of things: Security vulnerabilities and challenges. In Proc. of 2015 IEEE Symposium on Computers and Communication (ISCC), July 2015.
- [6] Wang Wei, Fan Hanbo— "Traffic Accident Automatic Detection and Remote Alarm Device" 978-1-4244-8039-5/11/2011 IEEE.

- [7] “Automatic traffic accident detection and alarm system” International Journal of Technological Exploration and Learning (IJTEL) Volume 1 Issue 1 (August 2012).
- [8] “Automatic accident notification system using GSM and GPS modems with 3g technology for video monitoring” International Journal of Emerging Trends in Electrical and Electronics (IJETEE) Vol. 1, Issue. 2, March-2013.
- [9] A. P. Athreya and P. Tague. Network self-organization in the internet of things. In Proc. of 2013 IEEE International Conference on Sensing, Communications and Networking (SECON), June 2013.
- [10] L. Atzori, A. Iera, and G. Morabito. The internet of things: A survey. *Computer Networks*, 54(15):2787–2805, October 2010.
- [11] L. Atzori, A. Iera, G. Morabito, and M. Nitti. The social internet of things (siot) when social networks meet the internet of things: Concept, architecture and network characterization. *Computer Networks*, 56(16):3594 – 3608, November 2012.
- [12] S. Azadegan, W. Yu, H. Liu, A. Sistani, and S. Acharya. Novel antiforensics approaches for smart phones. In Proc. of 2012 45th Hawaii International Conference on System Science (HICSS), 2012.
- [13] P. Baronti, P. Pillai, V. W. C. Chook, S. Chessa, A. Gotta, and Y. F. Hu. Wireless sensor networks: A survey on the state of the art and the 802.15.4 and zigbee standards. *Computer Communications*, 30(7):1655–1695, May 2007.
- [14] J. Belissent. Getting clever about smart cities: New opportunities require new business models. Technical report, Forrester Research, Novemer 2010.
- [15] M. V. Bharathi, R. C. Tanguturi, C. Jayakumar, and K. Selvamani. Node capture attack in wireless sensor network: A survey. In Proc. of 2012 IEEE International Conference on Computational Intelligence Computing Research (ICCIC), December 2012.
- [16] F. Bonomi, R. Milito, J. Zhu, and S. Addepalli. Fog computing and its role in the internet of things. In Proc. of the First Edition of the MCC Workshop on Mobile Cloud Computing, August 2012.
- [17] C. Bormann, A. P. Castellani, and Z. Shelby. Coap: An application protocol for billions of tiny internet nodes. *IEEE Internet Computing*, 16(2):62–67, March 2012.
- [18] A. Botta, W. de Donato, V. Persico, and A. Pescap. On the integration of cloud computing and internet of things. In Proc. of 2014 International Conference on Future Internet of Things and Cloud (FiCloud), August 2014.
- [19] N. Bressan, L. Bazzaco, N. Bui, P. Casari, L. Vangelista, and M. Zorzi. The deployment of a smart monitoring system using wireless sensor and actuator networks. In Proc. of 2010 First IEEE International Conference on Smart Grid Communications, October 2010.
- [20] Z. Cai, Z. He, X. Guan, and Y. Li. Collective data-sanitization for preventing sensitive information inference attacks in social networks. *IEEE Transactions on Dependable and Secure Computing*, 2017.

Microfluidic Syringe Pump

R. Sineka,UG Student ,Department of ECE, St. Anne's College of Engineering and Technology, Panruti
Dr. S. Anita,Assoc.prof., Department of ECE, St. Anne's College of Engineering and Technology, Panruti.

Abstract

Syringe pumps are widely used in microfluidics research since they are easy to use and enable fast setup of microfluidic experiments. A syringe pump is a small positive displacement pump used to gradually dose precise amounts of fluid for use in chemical and biomedical research. The key issue is how to make the flow of the syringe pump with very high accuracy and precision. The syringe pump has a stepper motor that drives the lead screw, which in turn moves the pusher block where the syringe plunger is fixed. The stepper motor drives the piston with a desired flow rate, it is controlled by the micro controller and the user interface collects the input data such as volume of drug and infusing time, depending on that flow rate is calculated. The microcontroller ESP32 that interfaces input and output components which controls the syringe pump.

Keywords: *syringe pump, microfluidics, micro controller, and stepper motor*

1 Introduction

In several international studies it was verified that the infusion techniques are a technology with underestimated risks due to several influence factors, namely the use of very small flow (300 ml/min) in premature babies, multi pump administration with the use of several administration lines and the individual variables of the different drugs. At present, microfluidic syringe pump system are needed in the medical, sensor industries and in research purpose. The microfluidic syringe pump will be used in the area where accuracy and precision are very important. Traceability and conformity of measurements are needed to improve the measuring instrument so that it meets the specifications and supports the quality system in the industry or other fields related to the tool [1]. Error and uncertainty associated with the measurement of flow-rate depending on the conditions of the infusion pump and the type of components used. The gravimetric method commonly used for standard calibration in laboratories [2].

Based on the design that has been made, to reduce errors and uncertainties of the components, Lead screw with spring coupler is used for the mechanical efficiency. The spring coupler creates a smooth gliding surface for the screw, thereby reducing friction and lead screw that transform rotary or turning movements into linear movements. The motor that used this microfluidic syringe pump system has been designed and made using a stepper motor as an actuator to drive the lead screw. Because the linear thread used to move the needle has a width pitch, the clock must be divided so that the speed is appropriate. Motor speed adjustment is done by dividing the hours that will be sent to the motor. Therefore, the DRV8825 micro stepping motor driver is used. It is designed to operate bipolar stepper motors in full-, half-, quarter-, eighth-, sixteenth- and thirty second-step modes, with an output drive capacity of up to 45 V and ± 2.2 A [3].

2 Requirements and Specification

The syringe pump should be programmable, user friendly, safe use and should have battery backup and comprehensive alarm system. Self-test the device when it is powered on. This power-on self-test includes tests of all critical processors, circuit circuitry, indicators, displays and alarm functionality, the simple monitoring of current through light-emitting diodes (LEDs) as they are turned on and off. If currents fall outside the acceptable range, a fault is indicated. The rate of injection depends on the syringe diameter and the adjusted flow rate of the pump. High or even low injection dosages of a specific drug can be dangerous for living cells. Plastic syringes manufactured by different companies are not identical; therefore, pumps are adjustable to work with different syringe models. Universal clamp is used for all types of syringe models to fit. The DRV8825 Stepper motor driver makes interfacing with a microcontroller super easy as you only need two pins to control both the speed and the direction of the stepper motor.

Principle Flow Operation

Syringe is placed within the pump designed to support it, filled with the prescribed fluid. The piston is fitted within a receptacle and the instrument is programmed for that syringe either manually or automatically. The type of infusion pump used to generate flow is the piston syringe pump whose volume is generated from displacement of the piston inside the cylinder and flow (Q) is determined by volume divided by time (Δt) when the piston displaces. That means the flow generated is proportional to the speed of the piston [2].

$$V = \lambda \cdot \theta \cdot \frac{FM}{D} \quad (1)$$

Where :

V: Velocity of piston (mm/s)

λ : Linear thread characteristic (mm/angle)

θ : Characteristic steppers motor (angle/clock)

F: Frequency (clock/s)

M: Driver mode ($1, \frac{1}{2}, \frac{1}{4}, \frac{1}{16}, \frac{1}{32}$)

D: Frequency divider

In this system the value of λ , θ , F and M are constant).

The Volumetric flow rate (Q) of a fluid is defined as the volume of fluid that is passing through a given cross sectional area per unit time.

$$Q = \frac{V}{t} = \frac{Ad}{t} = A \frac{d}{t} = Av \quad (2)$$

where:

F: Flow-rate (ml/s)

A: Cylinder and Piston Area (mm^2)

Liquid Density Calibration

In the process of testing the flow-rate system on the syringe system, it must be known the volume of liquid that comes out of the syringe. The liquid used is water, therefore the water used must be known for its density to get its volume. Water density testing is done by taking volume and mass data from the water used. To find out the mass of water used a digital scale PTS 02 with accuracy 0.01g. Meanwhile, to find out the volume of injection used. Measurement of density is done repeatedly so that the density value obtained is close to the ideal value of the density of water and also to avoid large error values. Measurement of density is done by measuring the volume of water that comes out of the injection every 1mL and measuring the weight of the water that comes out of the injection.

Flow Rate Calibration

This calibration is carried out to ensure the stepper motor can work well and ensure the clock and degree of the stepper motor are in accordance with the stepper motor datasheet. The calibration performed on this stepper motor is done by comparing the output degrees of the stepper motor with the clock value given to this stepper motor. Calibration of the syringe is done to ensure the fluid flow-rate that comes out of the syringe pump has the same data as the input. Syringe pump calibration is done by adjusting the clock divider value on the motor from 10 to 1000 by first adjusting the micro stepping resolution value in the DRV8825 driver and recording the flow-rate value generated from each clock divider value. From the data obtained, a linear regression between volume and time is then performed. Where the result of this linear regression is the flow-rate value for each divider. For

the generated program to be automatic, a function must be sought to connect the input and output variables. Where the input variable is debit and the output is the divider.

Gravimetric Calibration

Gravimetric method commonly used for standard calibration in laboratories [2]. The gravimetric method is the primary method used to determine flow by measuring mass of liquid released from a particular instrument. The instrument used here is the syringe pump. The equation to determine the volume of syringe is given by ISO/FDIS 8655-1.

$$\Delta V_{20} = \frac{\Delta m}{\rho_b} \frac{\rho_b - \rho_u}{\rho_a - \rho_u} [1 - \beta_s (T_s - 20)] \quad (3)$$

ΔV_{20} : Volume of syringe at 20 (mL)

Δm : Mass reading of water (gram)

ρ_b : Density of weight that calibrate the balance, 8.0 g/cm³

ρ_a : Density of water (g/cm³)

ρ_u : Density of air (g/cm³)

β_s : Thermal coefficient of plastic (°C⁻¹)

T_s : Syringe temperature (°C)

3 System Architecture

The system consists of electronic boards and mechanical parts. The electronic boards are a controller board and driver boards. The mainboard is controlled by ESP32 microcontroller, while the motor driver boards are controlled by DRV8825 micro stepping motor driver. Microcontroller interfaces with the input device Rotary encoder and optical end-stop switch, which helps to stop the stepper motor. The input collected from the encoder is displayed in the LCD display. Block diagram of the microfluidic syringe pump system is shown in Fig. 1.

Electrical design

In the electrical design of the system, there are DRV8825 micro stepping motor drivers, the driver is controlled by ESP32 as a controller. The direction of movement can be adjusted by the direction input in the motor driver. A syringe mechanism was used to serve as the fluid reservoir for infusion. It uses an endless worm thread to position the plunger, managing in this way the liquid movement. The user interface was programmed to display the menu for selection of the fluid volume and initiation of the infusion process. This system is controlled by a stepping motor where the rotation of the motor is transmitted to the endless thread, that is stopped by the Optical end-stop switch and spring is used to push the plunger with a constant force, necessary for a stable infusion pressure. This type of infusion generates a continuous high precision flow.

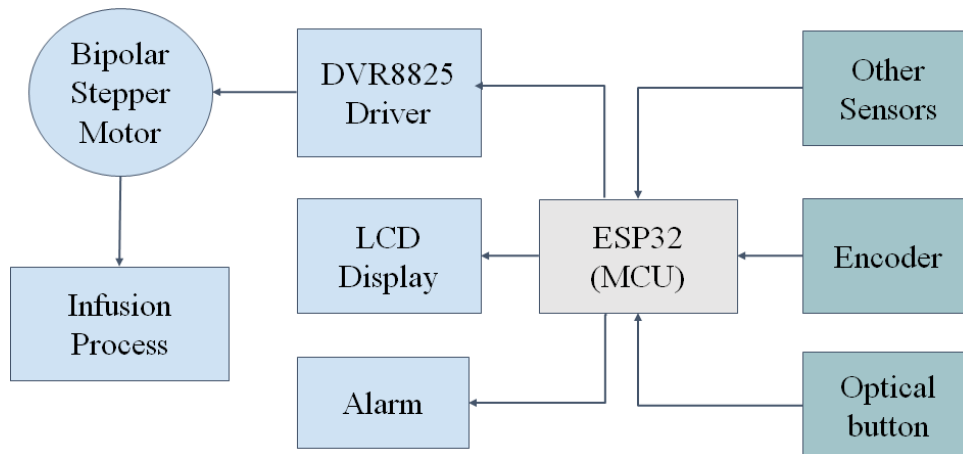


Figure 1: Microfluidic Syringe Pump system block diagram

Mechanical design

There are several components used to design the mechanics of this system including NEMA 17 stepper motor, spring coupler, lead screw, 3D printed parts. NEMA 17 was chosen because it has enough torque to move the injection where there is a liquid with a certain thickness. Lead screw used in this system which will change the rotational motion into linear motion. This lead screw has a long-threaded shaft with spring coupler that serves to hold the load that serves to withstand excessive pressure and weight. By using this mechanical system, the resulting mechanical efficiency will be better. In addition, with this system errors due to tool components will be fewer. The main advantages in choosing a lead screw are that they can be easily controlled, highly accurate in microns, the ease of running at high speeds, and are highly efficient. The 3D printed parts with NEMA 17 stepper motor is shown in the figure 2.

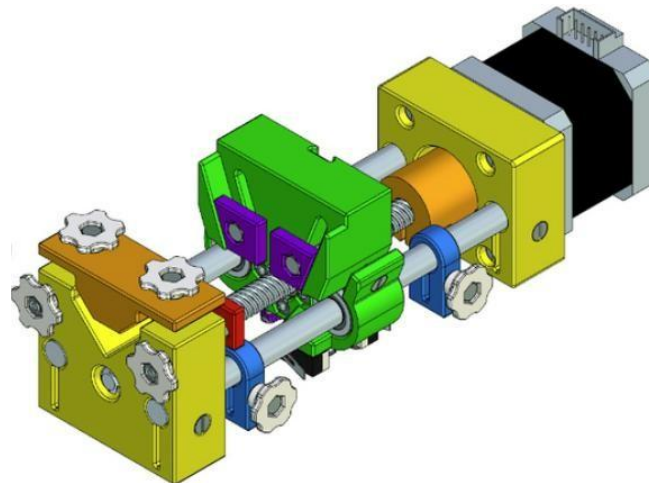


Figure 2: mechanical setup with 3D printed parts with NEMA 17 stepper motor, spring coupler, lead screw and two optical switches.

4 Implementation and Testing

The proposed micro fluidic syringe pump systems have been successfully realized and implemented. Each of the mechanical and electrical systems that have been made can function properly in accordance with the proposed design. In making a syringe pump, the mechanical principle works by converting rotational motion from a stepper motor into a straight motion via the screw iron connected to the motor. The mechanical system greatly influences the success of the syringe pump developed. In the driving section, there are three irons, which are mounted on the bottom with a plain and threaded type.

The initial test is done to find out that every full rotation of the stepper motor will shift the injector pusher as far as 1 mm. At first, the injection is filled with a volume of 3 ml, marking the starting position; then, the pusher is slowly slid until the volume that comes out is 1 ml. The driver can move (forward/backwards) because there is already a simple program uploaded to ESP32 to run the driver manually without setting the flow rate and timer values.

Validation of the Calibration

The results show that there is almost no difference between the measured flow rate and the calibration flow rate. The equation of the line obtained from the calibration and test results is matched. Table I shows the test results for each calibrated flow rate where the biggest error is 3.24 percent. The smallest flow rate that can be generated is 0.0043 mL/second.

Table 1: FLOW-RATE MEASURED

S. No.	Flow rate input (ml/s)	Flow rate		
		Divider Calibration	Divider test	Error
1	0.4292	10	9.996641129	0.034
2	0.2145	20	19.99660058	0.017
3	0.1423	30	30.1332795	0.444
4	0.1071	40	40.02513579	0.063
5	0.0859	50	49.8884992	0.223
6	0.0715	60	59.91791246	0.137
7	0.0613	70	69.86704302	0.190
8	0.0533	80	80.32838243	0.410
9	0.0475	90	90.11038522	0.123
10	0.0427	100	100.2094377	0.209
11	0.0213	200	200.2844039	0.142
12	0.0142	300	299.5267477	0.158
13	0.0106	400	400.0320026	0.008
14	0.0085	500	497.3887093	0.522
15	0.0071	600	593.7184587	1.047
16	0.0061	700	689.0374147	1.566
17	0.0053	800	790.5763301	1.178
18	0.0048	900	870.7767328	3.247
19	0.0043	1000	969.0861518	3.091
20		Average		0.674

5 Conclusions

Microfluidics applications demand accurate control and measurement of fluid flow and volume within the micro channel. In this study, a system of a microfluidic syringe pump was designed and realized. This system is equipped with controlling flow-rate of the fluid using micro stepping from the motor driver and dividing the clock value of the program so that the flow-rate of the system can reach microfluidics. The syringe pump can work in a volume range of 0.01–60.00 ml with the lowest flow rate resolution of 0.10 ml h⁻¹, and with an error value of less than 2%.

6. Acknowledgement

This research was carried out with financial aid support from ISMO Bio-photonics Private Limited, Indian Institute of Technology Research Park, incubation cell.

7. References

- [1] Rahmat Nur Fajri, Arief Sudarmaji, Zaadit Taqwa, *Design and Calibration of a microfluidic Syringe System for Nanofiber Electrospinning, International seminar on Intelligent Technology and its Application, 2020.*
- [2] Sirenden, Bernadus H Ghufron Zaid, and Prawito Prajitno, "Development of volumetric micro-flow calibration system using FPGA for medical application," 21st IMEKO World Congress on Measurement in Research and Industry. 2015.
- [3] Surya, Asian J. Pharm. Clin, Ocular drug delivery system using open-source syringe pump. Res., 11(6), 152–157, V. et al. (2018). <https://doi.org/10.22159/ajpcr.2018.v11i6.24151>
- [4] Amir Supriyanto, Rani Anggriani, Sri Wahyu Suciayati, Arif Surtoto, Junaidi and Sutopo Hadi, A Control System on the Syringe Pump Based on Arduino for Electrospinning Application, Journal of Physical Science, Vol. 32(1), 1–12, 2021.
- [5] DRV8825 datasheet – Texas Instrument. Available: <https://www.ti.com/lit/gpn/drv8825>

Design and Analysis of Multi-Patient Monitoring System Using Cloud Computing

V. Ramya, Department of ECE, St. Anne's College of Engineering and Technology
G. Seetha Lakshmi, Department of ECE, St. Anne's College of Engineering and Technology
R. Radhakrishnan AP/Department of ECE, St. Anne's College of Engineering and Technology.

Abstract

This paper presents the design and implementation of a health monitoring system using the Internet of things (IoT). In present days, with the expansion of innovations, specialists are always looking for innovative electronic devices for easier identification of irregularities within the body. IoT-enabled technologies enable the possibility of developing novel and non-invasive clinical support systems. this paper presents ahealth care monitoring system. In particular, COVID-19 patients, high blood pressure patients, diabetic patients, etc., in a rural area in adeveloping country, such as Bangladesh, do not have instant access to health or emergency clinics for testing. Buying individual instruments or continuous visitation to hospitals is also expensive for the regular population. (e system we developed will measure a patient's body temperature, heartbeat, and oxygen saturation (SpO2) levels in the blood and send the data to a mobile application using Bluetooth. (e mobile application was created via the Massachusetts Institute of Technology (MIT) inventor app and will receive the data from the device over Bluetooth. (e physical, logical, and application layers are the three layers that make up the system. (e logical layer processes the data collected by the sensors in the physical layer. A 95 percent confidence interval with a 5 percent maximum relative error is applied to all measurements related to determining the patient's health parameters. (e use of these devices as support tools by the general public in a certain situation could have a big impact on their own lives.

Keywords: SpO2, Pulse Sensor, LM35 Sensor, Arduino IDE

1 Introduction

IoT devices are profoundly utilized in the clinical area. In this paper, the research is about an IoT-based health monitoring system. In particular, for COVID-19 patients, high blood pressure patients, hypertension patients, diabetic patients, etc., in a country territory, in rural areas, the number of doctors is not exactly the same as in urban areas. Medical equipment is not readily available in rural areas, except for government medical canters. The percentage of patients in these clinics is greater than that in government medical facilities. Similarly, the equipment has, for the most part, ended. As a result, if an emergency situation arises, this hardware component will send a report to the physicians or medical professionals as soon as possible. IoT devices are widely used in the medical sector. And the technology we are talking about is a patient health monitoring system that uses the IoT. A sensor in this health monitoring system will collect information about the patient's health condition. It is smaller in size, faster, and more affordable. This system can be used to measure the oxygen saturation level, heart rate, and temperature of the human body and display the results on a web-based platform. The physical, logical, and application layers are the three layers of the system. It is a multiparameter monitoring system that will monitor oxygen saturation level, heart rate, and temperature simultaneously. The term "IoT" was first referenced by Kevin Ashton in 1998.

2 Literature Survey

Existing System:

The system used for health monitoring is the fixed monitoring system, which can be detected only when the patient is in hospital or in bed. In existing system, patient needs to get hospitalized for regular monitoring of the patient. The existing systems are measuring the health parameters of the patient and send it through zig bee, Bluetooth protocol etc., These are used for only short-range communication to transfer the data. Not all the time the doctor can fetch these details.

PROPOSED SYSTEM:

The system which we prefer to develop would not only help in monitoring the health of the patient. The main idea of the system is to transmit the information through the webpage to continuous monitoring of the patient over internet. Such a system would continually detect the important body parameters like temperature, pulse rate and oxygen level it against predetermined range set and if these values cross the specific limit, it would immediately alert the doctor. In this system microcontroller is used to transmit the data. It is connected to IoT which provides information to doctor or caretaker. The data of the patient's health is stored in the cloud.

3Material

This system's structure is depicted. Here, patients will measure their pulse rate and SpO2 using the max30100 sensor and body temperature using the Lm35 sensor, and patients can see measurement data in the mobile app and LCD display. (e data will be shown in the mobile app with the help of a Bluetooth module that will receive data from the Arduino and save it in the cloud. From there, the data will be transferred into the mobile application, and the patients can view the measurement of the health parameters. After measuring the physiological vital data of the human body, it will be sent to the Arduino UNO, which will process the analog data into digital. After that, the data via Bluetooth module will appear on the mobile application. Measured data from the human body can be seen on the LCD display as well.

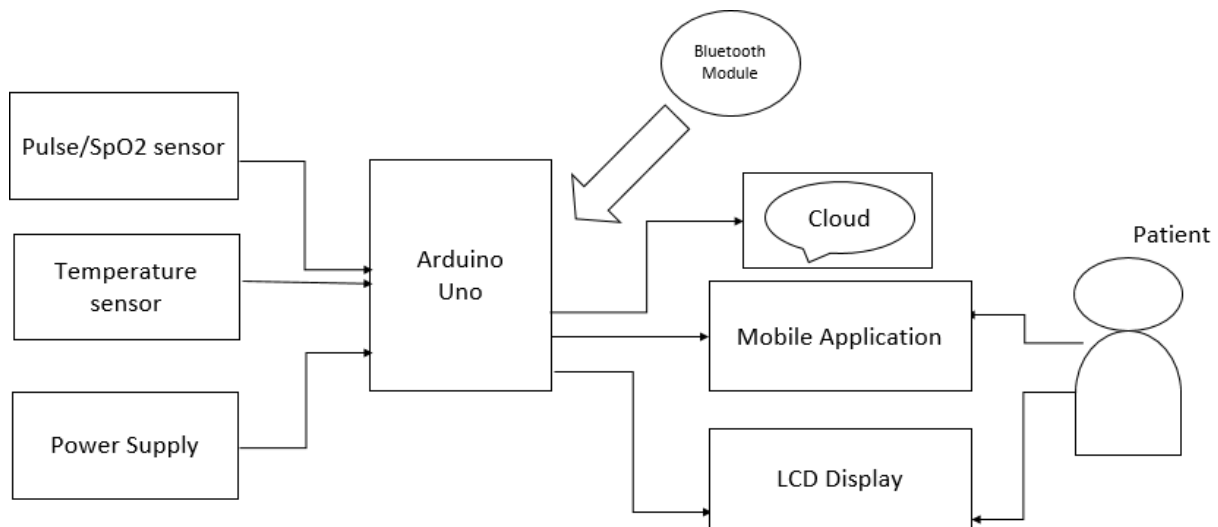


Figure 1: Block Diagram of Proposed System

4 Hardware Design

This health monitoring system consists of sensors and a microcontroller. We used the Arduino Uno as the microcontroller, and the sensors are MAX30100 (pulse rate and SpO2 measurement sensor) and LM35 (body temperature measurement sensor). And there are more components we are using, such as an HC-05 (Bluetooth module), to connect the Arduino with the mobile application and LCD display. All the needed components for the health monitoring system are described in the circuit diagram for the system. An Arduino Uno microcontroller, two sensors (MAX30100 and LM35), a 16 × 2 I2C LCD display, and a Bluetooth module make up the circuit. The whole system is powered by 5V. (e microcontroller (Arduino Uno) is connected to the computer using a USB (Universal Serial Bus) that sends commands to the device. The circuit was designed on an online circuit designing app called circuit. Is the prototype of the whole health monitoring system. In the connections between the sensors, Bluetooth module, and microcontroller are shown, as is the connection between the microcontroller and a device using a USB. Also, the data is received in the mobile application, and the serial monitor of the Arduino IDE is

shown in Figure 3. The circuit is mainly made with an Arduino Uno and two sensors that can measure three human body parameters. A 5 V power supply powers the sensors, LCDdisplay, and microcontroller. The microcontroller is connected to a laptop using a USB that sends commands to the sensors. There is also a Bluetooth module that helps mobile applications read data from the system.

Arduino Mega

Arduino Mega the Arduino Mega 2560, a microcontroller board based on the ATmega2560, which consists of 54 digital input/output pins, 16 analog inputs, 4 UARTs (Hardware serial ports), a 16 MHz crystal oscillator, a USB connection, a power jack, an ICSP header, and a reset button. It is provided with everything needed to support the microcontroller, by simply connecting it to the computer with a USB cable or power it with AC-to-DC adapter or battery to get started. The Mega is compatible with most shields designed for the Arduino Duemilanove or Decimal.



Figure 2: Arduino Mega

SPO2

SpO₂ also known as oxygen saturation, is a measure of the amount of oxygen-carrying haemoglobin in the blood relative to the amount of haemoglobin not carrying oxygen. Our body needs blood with certain level of oxygen to function efficiently. MAX30102 is a Bio-Sensor module which is an integrated Pulse oximeter and Heart rate monitor. This module integrates a red LED and an infrared LED, Photo detector, optical components, and low-noise electronic circuitry with ambient light suppression. This is a wearable device and can be worn on fingers, earlobes, and wrist. I2C Compatible communication interface is used to transmit the obtained values to the Arduino Mega 2560 to calculate the Heart Rate and Blood Oxygen level. Main Parameters: o LED peak wavelength: 660nm/880nm. o LED power supply voltage: 3.3~5V. o Detection signal type: light reflection signal (PPG). o Output signal interface: I2C interface Communication. o interface voltage: 1.8~3.3V~5V (optional). o Board assembly hole size: 0.5 x 8.5mm. Pin Description: VIN: main power input terminal 1.8-5V 3-bit pad: Select the pull-up level of the bus, depending on the pin master voltage, select 1.8v or 3_3v (this terminal contains 3.3V and above) SCL: the clock connected to the I2C bus; SDA: data connected to the I2C bus; INT : Interrupt pin of the MAX30102 chip; RD: RED LED ground terminal of MAX30102 chip, generally not connected; IRD: The IR LED ground of the MAX30102 chip is generally not connected; GND: Ground wire.



Figure 3: SpO₂

LM35 Temperature Sensor:

LM35 is a Precision IC Temperature sensor, the output of which is directly proportional to temperature (in °C). The temperature measurement using the LM35 is more accurate than using thermistor. The sensor is sealed such that it is not subjected to oxidation. The self-heating to air is comparatively less and doesn't cause more than 0.1 °C temperature rise in still air. The temperature range which the sensor can operate is from -55 °C to 150 °C. For every °C rise/fall in ambient temperature the output voltage varies by 10mV, i.e., its scale factor is 0.01V/ °C.

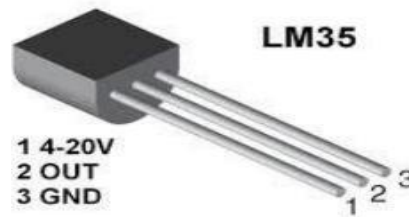


Figure 4: LM35 Temperature Sensor

Pulse Sensor

The Pulse sensor used detects the heartbeat by the method of a Photoplethysmography (PPG). PPG illuminates the skin optically and measures the pulse as a change of resistance to the blood flow in the skin. The sensor could be connected to the finger/earlobe. Since, the heart pulse is detected, heart rate and Inter Beat Interval (IBI) are calculated alongside.



Figure 5: Pulse Sensor

5 Software Requirement

The Arduino Integrated Development Environment - or Arduino Software (IDE) - contains, a message area, a text console, a text editor for writing code, a toolbar with buttons for common functions and a series of menus. It connects to the Genuine hardware and Arduino to upload programs and communicate with them.



Arduino IDE Programming

6 Result and Analysis



7 Conclusion and Future Work

This design and implementation of a health monitoring system using IoT are presented in this study. This IoT-based device allowing users to determine their health parameters, which could help regulate their health over time. Eventually, the patients could seek medical assistance if the need arises. They could easily share their health parameter data instantly within one application with the doctor. As we know, the IoT is now considered one of the most desirable solutions in health monitoring. It makes sure that the parameter data is secured inside the cloud, and the most important thing is that any doctor can monitor the health of any patient at any distance. The paper is about an IoT-based health monitoring system using Arduino that has been developed. The system will measure a patient's body temperature, heartbeat, and the SpO2 levels in the blood and send the data to an app via Bluetooth. This information is also transmitted to the LCD panel, allowing the patient to see their current health state quickly. Elderly patients, asthma patients, COPD patients, patients with chronic diseases, COVID-19 patients, and diabetic patients will be able to keep their health in check over time with the help of the system we developed.

8. References

- [1] A. Sharma, A. K. Sing, K. Saxena, and M. A. Bansal, “Smart health monitoring system using IoT,” *International Journal for Research in Applied Science and Engineering Technology*, vol. 8, no. 5, pp. 654–658, 2020.
- [2] M. MacGill, “What should my heart rate be?,” 2021, [https:// www.medicalnewstoday.com/articles/235710](https://www.medicalnewstoday.com/articles/235710).
- [3] Minnesota Department of Health, “Pulse oximetry and COVID-19,” 2020, <https://www.health.state.mn.us/diseases/ coronavirus/hcp/pulseoximetry.pdf>.
- [4] N. S. M Hadis, M. N. Amirnazarullah, M. M. Jafri, and S. Abdullah, “IoTbased patient monitoring system using sensors to detect, analyse and monitor two primary vital signs,” *Journal of Physics: Conference Series*, vol. 1535, pp. 1– 12, Article ID 012004, 2020.
- [5] J. Wan, M. A. A. H. Al-awlaqi, M. S. Li, M. O. Grady, and X. Gu, “Wearable IoT enabled real-time health monitoring system,” *EURASIP Journal on Wireless Communications and Networking*, vol. 298, pp. 1–10, 2018

Design of GaAs Based Low Noise Amplifier For 5G Frond-End System

K.Kaveri, Department of ECE, ,St.Anne's College of Engineering and Technology
P.Sivasakthi, Department of ECE, ,St.Anne's College of Engineering and Technology
M.Sahinipiriya, Department of ECE, ,St.Anne's College of Engineering and Technology

Abstract

In radio receivers amplification is most important functionality. The low noise amplifier is the chief design in the radio receiver architecture. The CMOS technology has drawback of highest noise figure, small gain and less linearity and it cannot be applied for long range communication. In this paper the amplifier is designed in a GaAs Pseudomorphic High Electron Mobility Transistor (PHEMT) technology which has larger bandgap differences. The design is GaAsPHEMT process at 50nm technology. The simulation are done using ADS Software and parameters like noise figure and gain are measured and compared

Keywords: LNA, ADS software, pHEMT, Noise figure, Forward gain

1 Introduction

Recent years the 5G communications systems are popular because of huge data rate, economical, high reliable small size. These all parameters are possible by chosen technology and selected band frequency. The preferable band frequencies for 5G IS SUB- 6 GHz and mm wave frequencies. Usually the mm wave frequencies are suitable for military applications. For 5G systems required many process steps for design and implementation to increase data rate, high reliable. Increase the coverage area the transceiver required better sensitivity and more dynamic range.

The most important block in any receiver is LNA. The LNA can play an important role in the entire performance of receiver. The most important parameter in any LNA design and its performance forward gain S_{21} , Input and output matching network Noise Figure, linearity, IIP3, OIP3 and 1dB compression point. The CMOS technology has drawback of highest Noise Figure, Small gain and less linearity. But low cost and better system integration [1] – [2]. The GaAs, pHEMT process of technology of compound semiconductor (III –IV group periodic table components) process has Low Noise, high linearity advantages. This is widely used in industry as well as academic fields [3]. In order to meet requirements the all existing published work papers authors suggested that different topologies and technology processes. In reference [4] the authors suggested the current reuse technology with cascaded inter stage resonance is demonstrated for the design of LNA, but design is restricted for 5.2 GHz frequency with minimum substrate resistance. Similarly in gm boosting with current reuse technique is implemented. Similarly in reference [6] a 5.7 GHz differential mode LNA is designed. In this proposed LNA a wideband low noise, high linearity GaAs pHEMT technology with two stage common source transistor cascaded current reused technique with enhanced matching network at inter stage.

Low Noise Amplifier

A low-noise amplifier (LNA) is an electronic amplifier that is used to amplify signals of very low strength, usually from an antenna where signals are barely recognizable and should be amplified without adding any noise, otherwise important information might be lost. LNAs are one of the most important circuit components present in radio and other signal receivers. Analog Devices low noise amplifiers cover the frequency range from DC (IF) to RF Microwave and W-Band (95 GHz). These MMIC-based designs cover various gains and bandwidths with noise figures as low as 0.7 dB. Our low noise amplifiers offer some of the lowest noise and highest linearity available in the industry. Many of the designs offer a self-biased topology, and are internally matched to 50 ohms. They are used in a wide range of applications including telecom, instrumentation, and military/aerospace. All Analog Devices low noise amplifiers are fully specified over frequency, temperature, and supply voltage.

2 Proposed Design

The two stages cascaded common source (cs) current reused topology the bias current is shared in two stages, so that the power consumption is reduced. The different types of current reuse topologies are shown in figure below.

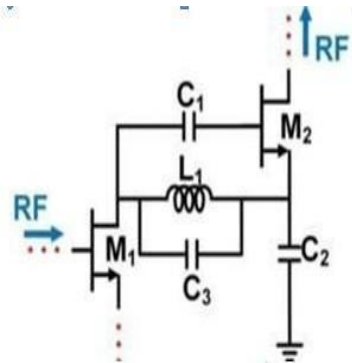


Figure 1: Different Current reused topologies a) Resistive

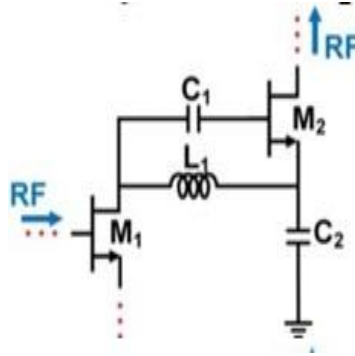


Figure 2: Different Current reused topologies b) Inductive

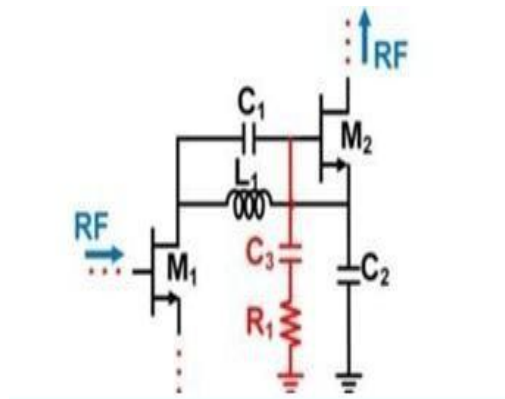


Figure 3: Different Current reused topologies c) LC Resonant based

From fig. 1.a resistance inter stage current reuse network reduces the voltage, but its noise characteristics increased the power consumption. Fig 1.b due to inductance the chip size will increase and it occupies large area, fig 1.c it also occupies more area but increases the gain. Fig 1.d the proposed two stages cascaded enhanced inters stage matching RC network helps to increases the gain, stability and return losses. The inter stage network can play an important role for better performance of the proposed wideband LNA design.

Table1: Proposed Values in wideband LNA design

PARAMETER	DESIGNED VALUE
M ₁	8 × (0.75 μm)
M ₂	8 × (0.75 μm)
C _{in}	100.0 pF
C _{out}	100.0 pF
R _b	2.0 kΩ
L _{dd}	18.0 nH
V _{bias1}	0.6 V
V _{bias2}	3.0 V
V _{DD}	5.0 V
I _{DD}	60.0 mA

The proposed wideband LNA design schematic is shown in figure 2. An enhanced mode GaAs pHEMT process of 50nm technology achieved a better performance of parameters especially high linearity and Noise figure.

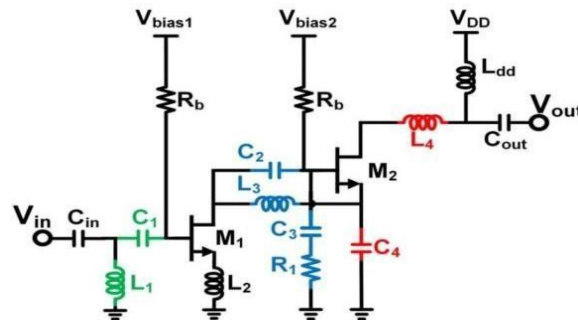


Figure 4: The proposed topology

The depletion mode required a negative power supply. So it is replaced with enhanced mode, to provide negative supply to depletion mode the number of components are increased so that chip size will increased. Hence the enhancement mode pHEMT transistor is chosen with gate width of 75 μm and number of figures are 8 for both stages in order to get better noise and linearity performance and also with 5v,60ma current supply. In the schematic Cin, Cout and Ldd are the external connections. The L1 and C1 is used as a input matching network. The source degenerated inductor is used for better input matching, so that decrease the Noise. The output matching is achieved by L4 and C4 at the M2 transistor of source terminal. The RC network at the gate of transistor M2 is to increase stability and also improves the return losses. The inductor to be chooses in small size in order to reduce the chip size

3 Simulation Results

The post simulated results are achieved the better performance by EM simulator of Agilent ADS software. The proposed wideband LNA micrograph is shown in figure 3 and the occupied area of 0.64mm². The proposed wideband LNA achieved better performance with single power supply 5V and it dissipates 300 mW. The S₂₁, S₁₁ and S₂₂ parameters are simulated and shown in figure 4. A stable flat forward gain (S₂₁) 16dB is achieved and shown in figure 5. The input / output return losses are less than -1dB in the frequency range of 1.5GHz -5.5GHz. The reverse isolation is less than -25dB is achieved in the required band. The post layout simulation are shown figure in figure 5.

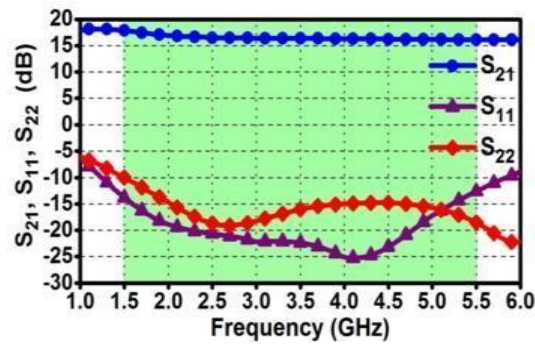


Figure 5: Simulation results of S21, S11 and S22

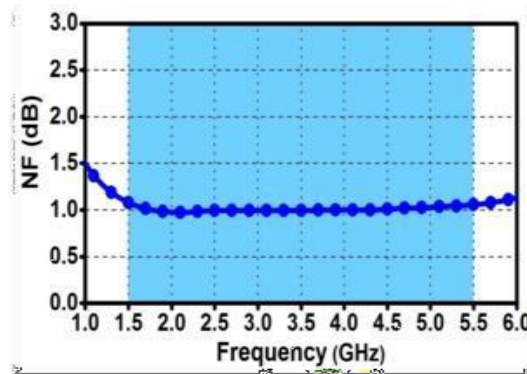


Figure 6: Simulation result of Noise Figure

Table: 2 Comparison of Parameters with proposed design

			MT		
Freq (GHz)	2 – 4.5	2.5 -5.0	3.5	1.5 - 2.7	1.5 - 5.5
BW (GHz)	2.5	2.5		1.2	4.0
Gain (dB)	17.2	17	16.7	17.5	16
NF (dB)	2.9	3.0	1.8	0.75	1.0
Chip Area	2.25	1.5		1.948	0.64

4 Conclusion

The proposed Ga As pHEMT process of wideband LNA is performed and evaluated at 50nm using current reuse topology. The design is achieved better performance for all the parameters to propose for 5G front end systems. An inductor based inter stage matching network improved the bandwidth. The RC cascade series network is connected at second stage is performed the better return losses and stability of the system by choosing transistor size and its biasing provided better Noise Figure. The Simulation result at post layout process forward gain of 16dB flat and Noise Figure achieved 1dB at a wideband width of 1.5GHz to 5.5GHz. The linearity achieved a +40dbm and OIP3 is achieved 20dbm at 1dB compression point. The chip size including pad is 0.64mm².

5. References

- [1] H. L. Kao, C. S. Yeh, C. L. Cho, B. W. Wang, P.-C. Lee, B. H. Wei, and H. C. Chiu, "Design of an S-band 0.35 μm AlGaIn/GaN LNA using cascode topology," in IEEE DDECS Symp. Dig., April, 2013

- [2] K. Kang *et al.*, "A 60-GHz OOK receiver with an on-chip antenna in 90nm CMOS," *IEEE J. Solid-State Circuits*, vol. 45, no. 9, pp. 1720–1731, Sep. 2010.
- [3] Y. Yu, H. Liu, Y. Wu and K. Kang, "A 54.4–90 GHz Low-Noise Amplifier in 65-nm CMOS," *IEEE Journal of Solid-State Circuits*, vol. 52, no. 11, pp. 2892–2904, Nov. 2017
- [4] H. Morkner, M. Frank, and D. Millicker, "A high performance 1.5 dB low noise GaAs PHEMT MMIC amplifier for low cost 1.5-8 GHz commercial applications," in *IEEE Microwave Millimeter-Wave Monolithic Circuits Symp. Dig.* pp.13–16, 1993.
- [5] C. Y. Cha and S. G. Lee, "A 5.2-GHz LNA in 0.35 μm CMOS utilizing inter-stage series resonance and optimizing the substrate resistance," *IEEE J. of Solid-State Circuits*, vol. 38, pp. 669-672, Apr.2003.
- [6] Y. Y. Peng, X. Y. Wang, F. Y. Ma, and W. Q. Sui, "A low power S-band receiver using GaAs pHEMT technology," in *IEEE 13th ISIC Symp. Dig.*, Dec., 2011.

REMOTE HEALTH MONITORING SYSTEM FOR VISUALLY IMPAIRED

D.Delisiya, Department of ECE, St. Anne's College of Engineering and Technology
K.Kavitha Department of ECE, St. Anne's College of Engineering and Technology
B.Arunkumar, Asst.prof./Department of ECE, St. Anne's College of Engineering and Technology.

Abstract

There are some visually impaired people throughout the world. Some of them may be around us. The Visually impaired person finds difficulty while performing day to-day life tasks. The main challenge faced by blind people is they feel very difficult to get immediate help from other people when they are unhealthy or in panic condition. Mostly the blind people rely on their caretaker and family doctor whom they cannot accommodate them all the time. Hence there is a need to develop a system that will assist the blind person to automatically inform the care taker and the family doctor if he/she is in danger or in unhealthy condition. Most of the already existing system is expensive and no cost-effective approach is available to automatically intimate the emergency information toknown to blind person caretaker and the family doctor during panic condition. The proposed idea is to provide a suitable device with a Virtual assistant system for the visually impaired person. The proposed system consists of a heart rate sensor, temperature sensor, GSM modem, GPS module interfaced to the Arduino controller.

1.INTRODUCTION

In this fast-growing world, the number of people affected by vision loss is increasing [1]. According to a recent World Health Organization (WHO) report on blindness and visual impairment, globally, over 2.2 billion people suffer from vision impairment or blindness. The total inability to see while impaired visually or with low vision is a severe reduction in vision that cannot be treated using standard glasses or contact lenses and reduces a person's ability to function at certain or all tasks. As per the data collected and observations made in [3], approximately 65% of the visually impaired travel five or more times a week, which is an unexpected result (shown in Fig.1). Most of these people belong to the working class of society. The frequency of head level accidents who are blind and legally blind (partially blind people who have vision 20/200 or less) as shown in Fig.2. The main challenge faced by blind people is that they feel very difficult to get immediate help from therecaretaker or family doctor when they are unhealthy or in panic condition In the existing system the alert is given only to the blind person. This information is not made known to blind person caretaker and the family doctor in different locationas there is no provision in the existing system to monitor the health condition of blind people continuouslyand send the report to their caretaker and family doctor if they are unhealthy or in the panic condition in real-time. The proposed idea is to provide a suitable device with a real-time health monitoring system for the visually impaired

The proposed system consists of a heart rate sensor, temperature sensor, pulse sensor GSM modem, and GPS module interfaced with the Arduino controller. The Arduino controller continuously monitors the blind person. If the blind person is panicking, or abnormal the system will automatically detect the condition using a heart rate sensor, pulse sensor, and temperature sensor and send the alert message to the caretaker of the blind person and his family doctor's mobile using a GSM modem. The blind person could also get help manually from his caretaker in an emergency situation by pressing the panic button interfaced with the system. If the person presses the panic button the system will send an alert message to the caretaker's mobile phone. The location of a blind person can be tracked using a GPS module.

2.LITERATURE SURVEY

There have been work and research in order to design smart wearable devices to help blind people techniques. In the paper titled" IOT Enable Real-Time Remote Health Monitoring System (IEEE Journal on 2020)" by IOT Enable Real-Time Remote Health Monitoring System (IEEE Journal on 2020) by AnaganiVenkata Mohan Siva Sainadh,Jeevan Sarwat Mohanty, Sushirutan ,bop ,Gudauta Vishnu Tea ,Rose PreetKaurBhopal" Node MCU and cloud computing technique were used to send message which is costly and complex. Inthis Various technique in Remote health Monitoring system have been explained. In the paper titled "Mobile Health in Remote patient Monitoring for chronic Diseases: Principle ,Trends, and Challenges(IEEE Journal on 2021) by Nora E1-rashidy,shakarE1-sappah,S.M.Riazul Islam ,Hazen M.E1-bakry and SamirAbdulrazak" Zigbee module, cloud

server mobile Applications is used to send and receive message. In this Challenges in Health Monitoring system is done.

These methods have two main flaws. Firstly, given that carrying a stick is already a liability, adding sensors and IoT devices to it increases its weight and hinders its balance. The goal here should be to make the visually impaired independent of these sticks. Secondly, interpreting the actuator signals on a stick can be a difficult task.

3. PROPOSED METHODOLOGY

The proposed idea is to provide a suitable device with a real-time health monitoring system for the visually impaired person. The proposed system consists of a heart rate sensor, temperature sensor, pulse sensor, GSM modem, and GPS module interfaced with the Arduino controller. The Arduino controller continuously monitors the blind person. If the blind person is panicking, or abnormal the system will automatically detect the condition using a heart rate sensor, pulse sensor, and temperature sensor and send the alert message to the caretaker of the blind person and his family doctor's mobile using a GSM modem. The blind person could also get help manually from his caretaker in an emergency situation by pressing the panic button interfaced with the system. If the person presses the panic button the system will send an alert message to the caretaker's mobile phone. The location of a blind person can be tracked using a GPS module.

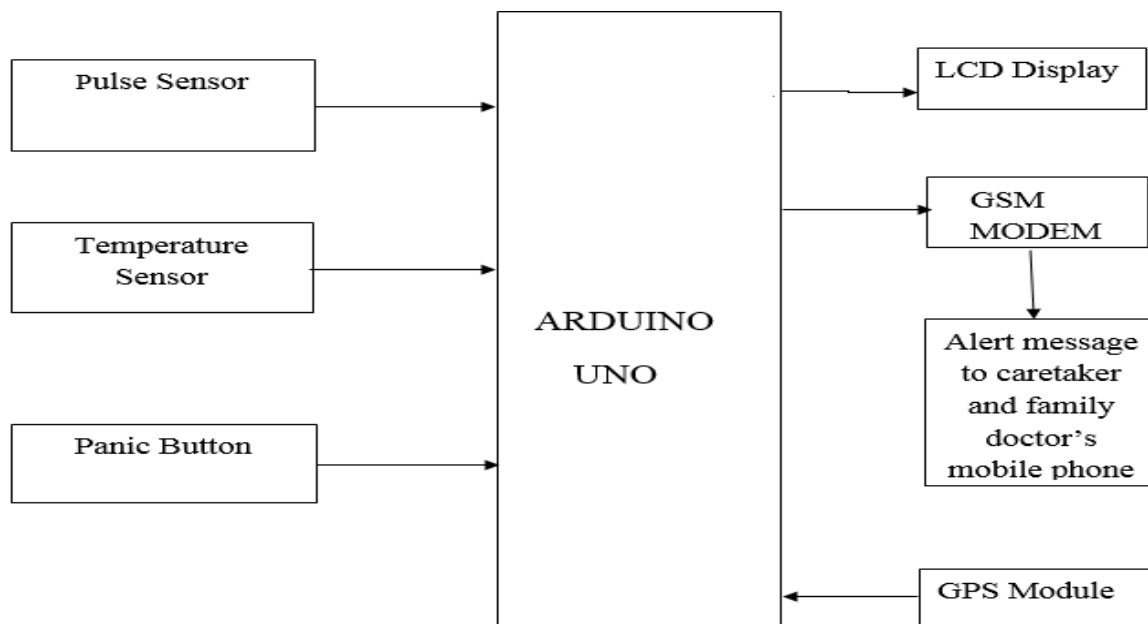


Figure 1. Block Diagram of Proposed System

4. WORK FLOW

- Interfacing Temperature sensor, Pulse sensor, Heart rate sensor with Arduino UNO.
- Programming Arduino UNO to read the sensor values and to check for the threshold condition.
- Interfacing GSM modem and Programming Arduino UNO to send the emergency information to caretaker's mobile and family doctor's mobile.
- Interfacing GPS module and Programming Arduino UNO to track the blind person location.

5. TECHNICAL DETAILS

5.1 Temperature sensor

LM35 is a temperature sensor that outputs an analog signal which is proportional to the instantaneous temperature. The output voltage can easily be interpreted to obtain a temperature reading in Celsius. The advantage of LM35 over thermistor is it does not require any external calibration. The LM35 device does not require any external calibration or trimming to provide typical accuracies of $\pm 1/4^{\circ}\text{C}$ at room temperature and $\pm 3/4^{\circ}\text{C}$ over a full -55°C to 150°C temperature range.

- Operates from 4 to 30 volts.
- Suitable for remote application.
- Less than 60 μA current drain.

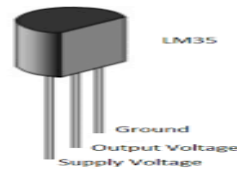


Figure2: Temperature sensor

Heart rate sensor



Figure3: Heart rate Sensor

Sensor would be an IR LED and the detector would be any photo Detector like a photo Diode. 5 v input and lighting based analog signal convert to digital signal values. An optical heart rate sensor measures pulse waves, which are changes in the volume of a blood vessel that occur when the heart pumps blood.

ARDUINO UNO PINOUT

- A0 – Temperature Sensor
- A1 – Heart Rate Sensor
- Gnd – Ground
- Vcc – Power Supply 5V
- Connecting wires

The Arduino Uno is an open-source microcontroller board based on the Microchip ATmega328P microcontroller and developed by Arduino.cc. The board is equipped with sets of digital and analog input/output (I/O) pins that may be interfaced to various expansion boards (shields) and other circuits.



Figure 4: Arduino Uno

GSM MODULE: (SIM800L)

- Power input – 3.4 V to 4.5V
 - Operating Frequency – EGSM900 and DCS1800
 - Transmitting Power Range – 2W for EGSM900 and 1W for DCS180
 - Data Transfer Link – Download: 85.6kbps, Upload: 42.8kbps
- A GSM modem or GSM module is a device that uses GSM mobile telephone technology to provide a wireless data link to a network. GSM modems are used in mobile telephones and other equipment that communicates with mobile telephone networks. They use SIMs to identify their device to the network.



Figure 5: GSM MODULE

GPS MODULE: (NEO 8MN)

- Input supply voltage: 0.5- 3.6 v
 - Sensitivity: 161 dbm
 - 5 v input and lighting based analog signal convert to digital signal values
- GPS modules contain tiny processors and antennas that directly receive data sent by satellites through dedicated RF frequencies. From there, it'll receive timestamp from each visible satellite, along with other pieces of data.

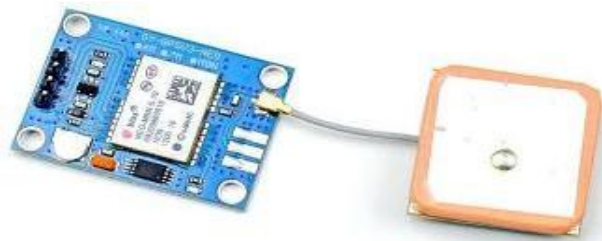


Figure 5:GPS MODULE

6. RESULT

The temperature sensor monitors blind person continuously if the value is beyond the threshold level the information is send to blind person caretaker and family doctor the location of the blind person sends along with the information.

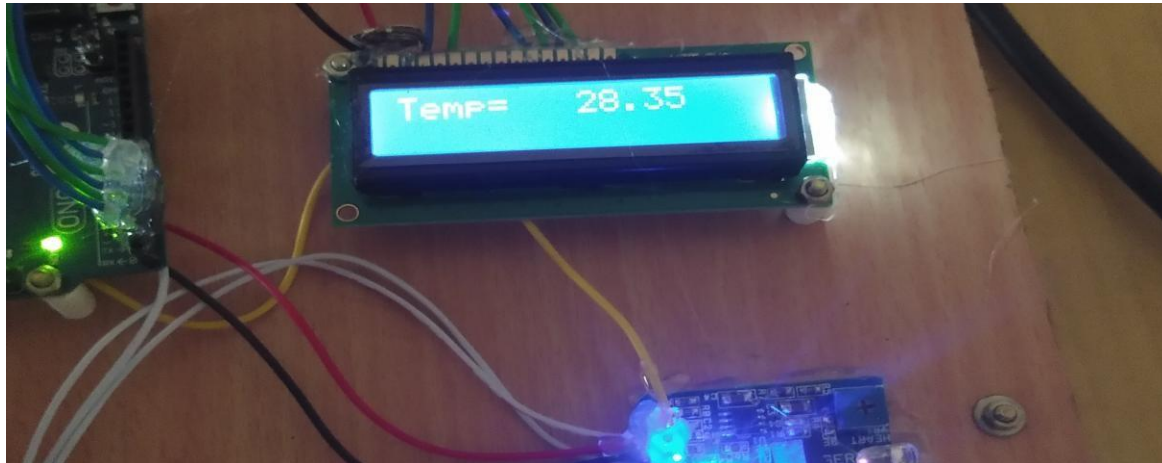


Figure 1 Temperature Output diagram

7. CONCLUSIONS AND FUTURE WORK

The proposed system assures the safety of the visually impaired person. The caretaker of a blind person can do their own work without any worry about the blind person under their care. The proposed system is a low-cost module that could be offered by most blind people. The Arduino controller used here is very faster and they produce reliable output.

This project can be extended using IoT technology in which the real time data. Can be collected from blind person and it can be maintained in cloud storage that can be used for future issues if arises.

8. REFERENCE

- [1] Anagama Venkata Mohana Siva Sainath, Jeevan Sarwat Mohanty, Sutratman. B.P, Gudauta Vishnu Tea, Rose n Preet Bhopal Lovely Professional University IEEE 2020.
- [2]. Nora E1-rashidy, Shaker E1`-sappagh, Sambrailo Islam, Hazem M.E1-Bakry and Samir Abdulrazak IEEE 2021 November
- [3]. Parihar, Y. Singh. "Internet of Things and Node cu." Revest de Technologies Emergences -Investigacion Innovadora 6: pp.1085-1088, 2019.
- [4]. F. Ivies. Calculating geographic distance: concepts and methods. In Proceedings Of the 19th Conference of Northeast SAS User Group, 2006.

SALINE LEVEL MONITORING SYSTEM USING LORA TECHNOLOGY

R.Preethi, Electronic and communication Engineering, St. anne's college of engineering and technology
G.Parameswari, Electronic and communication Engineering, St. anne's college of engineering and technology
S.Krishna Dharshini, Electronic and communication Engineering, St. anne's college of engineering and technology
Mr. S.Balabaker/ASP, Electronic and communication Engineering, St. anne's college of engineering and technology

Abstract

Beyond Multiple treatments available in the hospital, saline therapy is one of the hospital's essential treatments. When saline is catered to the patients, it has to be monitored by a doctor, a caretaker, or a nurse. But due to the busy schedule, negligence, and inattentiveness of doctors and nurses in monitoring the saline level lead to critical conditions like the reverse flow of patients' blood into the saline tube. This acute condition harms patients highly and even leads to death in many hospitals. Hence, the system is designed to remotely control and monitor the saline level using LoRa (long-range) technology. The proposed system continuously monitors the weight of the saline bottle with the help of the load sensor, and it is converted into the saline level. This is the first time the LoRa technology has been deployed in the medical sector

Keywords:

Arduino uno Board, LCD Display, RA02 LoRa module(433Mhz), Loadcell with HX711 Amplifier module, solenoid valve

1 INTRODUCTION

Every human life has infinite value. Therefore, their lives must be protected in all the ways possible and it should not be taken for granted. The active living of human life is threatened by various factors due to the amplified death rate. It is mandatory to protect the lives of the people. In recent years, there is a rapid growth in the medical sector due to the technological advancements which assures speedy recovery of patients in the hospitals. Beyond multiple treatments available in hospitals, Saline Therapy is one of the most important treatments that many patients receive. So, when saline is catered to the patients, it has to be monitored by a doctor, a caretaker, or a nurse. But due to the busy schedule, negligence and inattentiveness of the doctor and nurse in monitoring the saline level leads to critical conditions like reverse flow of patients' blood into the saline tube. This critical condition harms a patient too highly and even leads to death in many hospitals. Hence, the system is designed to control and monitor the saline level remotely by using Lora (Long Range) Technology. It is a low power wide area network where the saline level is observed up to 10km range. The proposed system continuously monitors the weight of the saline bottle with the help of a load sensor and it is converted into saline level. The saline level reaches a threshold limit (10% of saline) it automatically switches off the flow with the help of the solenoid valve connected to the saline bottle. The notification is also sent to the person in charge with the help of the Lora Module (Ra-02). The system utilizes the wide area with low power and offers high accuracy even in the remote area where the internet is not available. This is the first time the Lora technology is deployed in the medical sector.

2 EXISTING SYSTEM

The system eliminates nurses' continuous visual monitoring of the patient from distinct places. The entire project works on the principle of Beer-lambert's law. The amount of transmitted light from the LED to the photodiode depends on the saline bottle's electrolyte. The voltage across the photodiode is monitored every millisecond. Threshold levels of voltage are calibrated on Arduino Uno by programming. Blynk application receives and sends data through mobile. The change in threshold level activates the alarm at the nurse station at the 100 ml mark. However, at the 50 ml mark, a message will be sent to the nurse station as well as a saline tube is clamped through a solenoid plunger to prevent it from air embolism. Table Below is the briefing of the actions taken.

3 PROPOSED SYSTEM

The proposed system is designed to control the saline level automatically using Low power long-range technology called LoRa. The Load cell sensor is connected to the weight sensor amplifier module (HX711) which is used to measure the weight of the saline bottle. The measured weight is sent to the microcontroller (Arduino UNO R3) module. The weight grams are converted into milliliters (indicates saline level) and transmitted to the receiver module using RA02 LoRa Module. When the shared value is less than 750ml, 500ml, or 250ml, the notification will be sent to the doctor/nurse. In addition, the LCD module will display the current level of saline, and the buzzer will notify it. When the level is reduced below 100 ml, the solenoid valve connected to the saline tube is closed; thereby, the critical condition like the reverse flow of patients' blood into the saline tube is eliminated.

4 WORKING PRINCIPLE

Transmitter

The load cell is used in this work as a weight sensor. The rated load of this load cell is 10 kg with a maximum working voltage of 15v DC. It is placed on the intravenous medical pole. The saline bottle is suspended on the load cell. This strain gauge load cell converts the saline weight into an electrical signal and then sent to the weight amplifier module(HX711) before going to the microcontroller. The weight sensor module (HX711) is an integrated circuit with an amplifier and precision 24-bit analog to digital converter designed for weight scale. This weight sensor amplifier module is placed between the load cell and the Arduino to amplify the signal from the load cell and then convert them from the analog signal digital signal for the microcontroller Arduino Uno R3 is an open-source microcontroller used as a central processing and programming unit for receiving input information from the input switches and load cell and then sending an instruction to the LoRa module, buzzer and LCD display. The LoRa module acts as a transceiver. This module becomes a transmitter when it transfers data from the microcontroller to the mobile phone used in LoRa (without internet).

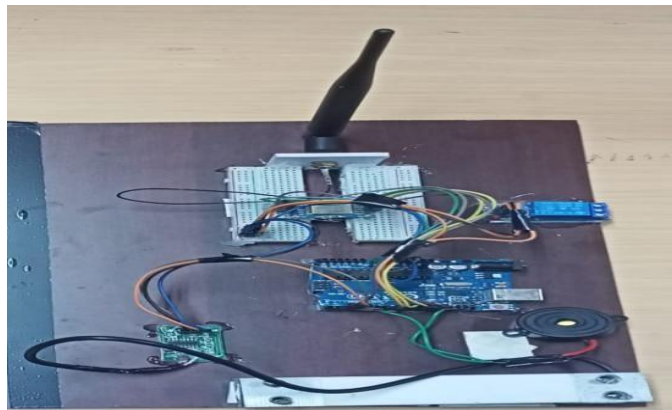
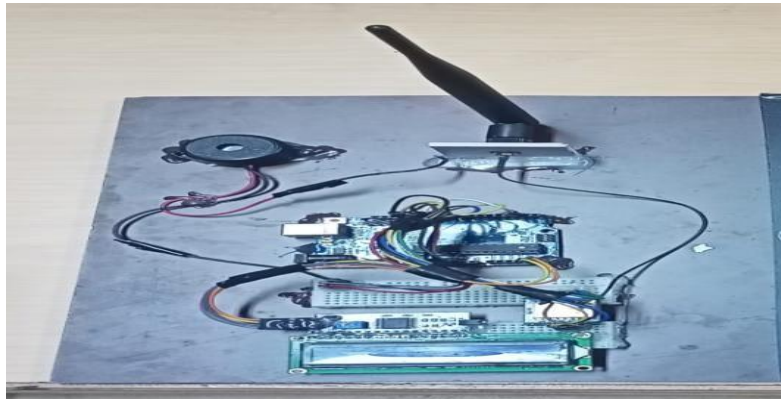


Figure4.1

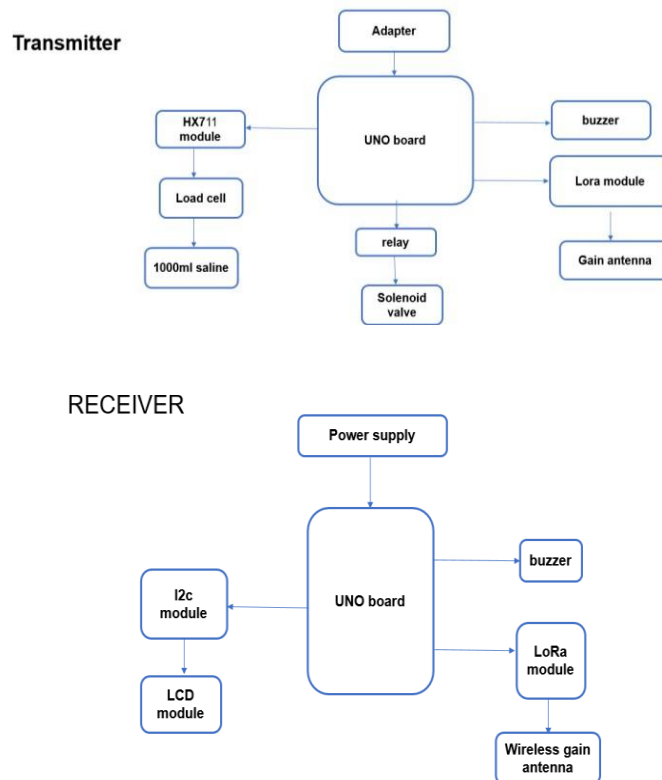
Receiver

A liquid crystal display(LCD) is utilized in the developed system to display the current volume value, instruction messages, input setting volume, and alert messages. The buzzer is an audio signaling device used to give an alarm to the medical staff and caretakers when the saline volume reaches the pre-defined critical value. LCD is used to display the value of the current volume, instruction, input setting volume and alert message. In this solenoid valve system, we interface the load sensor, Lcd, and keypad and measure fluid weight in ml. The relay and the solenoid valve will be used to verify the functionality, then the hall will flow. Sensor and intel, outel will verify the flow rate for the different flow rate causes. Then it will display all the information on the Lcd screen, and it sends all the data to the mobile phone through the Lora module.

Figure4.2



5. BLOCK DIAGRAM



6. TECHNICAL DETAILS

RA02 Lora module long range wireless module 433Mhz

LoRa stands for long range radio and is mainly targeted for M2M and IOT network. To send the data successfully from a transmitter to a receiver without the internet.



Figure6.1

Arduino UNO module

The arduino uno board is a microcontroller based on the ATmega328. It has 14 digital input/output pins in which 6 can be used as PWM outputs, 6 analog inputs, a power jack and reset button.



Figure6.2

8. CONCLUSION

In conclusion, the saline monitoring system was successfully deployed. This system is able to indicate the current saline volume in the bottle. When the level of saline reaches the pre-defined critical volume, the medical staff or caretakers will be notified by the alarm from the buzzer and an alert message will be sent to the medical staff via the application on the mobile phone using LoRa technology. This developed system can provide advantages on low power consumption and without internet. It can be reused for the next saline bottle.

9. FUTURE SCOPE

The saline level is controlled and monitored using Lora Technology to protect the active living of human lives. The proposed work could be extended with more features using Lora Technology. The wireless messages can be sent to doctors and nurses about the saline droplet rate. Smart health systems using Lora technology can be implemented, which gives information about body temperature, blood pressure, heart rate and also the pulse rate.

10. References

- [1]. Dr. Karunakar Pothuganti, Associate Professor, Computer Science Engineering, Mai Nefhi College of Engineering, Eritrea.
- [2] Mihir Tilak, Darshan Bhor, Dept. of Biomedical Engineering, Vidyalankar Institute of Technology, Mumbai, India.
- [3]. Kriti O., Jatin P. and Gouri B., "IoT based saline level monitoring system", Journal of Science and Technology, vol. 06, special issue 01, August 2021, pp. 125-130

DESIGN OF FAST FULL ADDER BY EXPLORING XOR AND XNOR GATES

R.Manju, Electronic and communication Engineering, St. anne's college of engineering and technology
k.vijayalakshmi, Electronic and communication Engineering, St. anne's college of engineering and technology
V.venkatesan/AP, Electronic and communication Engineering, St. anne's college of engineering and technology

Abstract

In this paper, circuits for fast full adder and simultaneous full adder functions are proposed. The proposed circuits are highly optimized in terms of the power consumption and delay, which are due to low output capacitance and low short-circuit power dissipation. The power consumed by the full adder is not therefore reduced by optimizing the design NOR gates. Simulation results are performed in tanner tool . These circuits are designed to have high speed and less power consumption compared to existing circuits. This is possible due to low output capacitance. Each one of the proposed full adder circuit has its own advantages of speed, power consumption and driving ability. From results, proposed circuits are found to be better than existing circuits. The novel structures of XNOR gate are proposed for the design of fast full adders with low power, high speed and less PDP. The proposed hybrid full adder has superior speed against other full adder circuits with less number of transistors.

Keywords: 2T (2 Transistors), 3T, 8T, XNOR and PDP.

I. INTRODUCTION

The need for small chip circuits, power consumption and speed vital factors should be taken into consideration while choosing the VLSI design with high performance. A basic arithmetic operation heavily demanded in VLSI design such as multiplier and accumulator, microprocessor, digital signal processing applications, so the system performance will be affected by the performance of full adder. A full adder is essential in arithmetic operation such as division, subtraction, addition and multiplication. The main block of the full adder circuit is the XOR/XNOR gate, as the XOR/XNOR gate consumes more power. The power consumed by the full adder is therefore reduced by optimizing the design of the XOR / XNOR gates. These can be used in a variety of multipliers, such as Vedic, Wallace, Array, etc. Simulation results are performed in Cadence Virtuoso tool 45-nm CMOS technology with 0.45V supply voltage.

The novel structures of XOR / XNOR gate are proposed for the design of hybrid full adders with low power, high speed and less PDP. The proposed HFA-14T has superior speed against other full adder cells with less number of transistors. Present day ever increasing number of compact applications requires low power. Power is one of the superior assets a designer tries to rescue when designing a system. Each full adder circuit has its own excellence regarding speed, power consumption, PDP (power delay product). PDP exhibited by full adder would affect the system's overall performance. The main block of the full adder circuit is XOR/ XNOR gate, because XOR/ XNOR gate consumes more power. So, the power consumed by the full adder is reduced by optimum design of XOR/ XNOR gates.

2. VLSI DESIGN CYCLE

The invention of the transistors by William B.Shockley, Walter H.Brattain and John Bardeen of Bell Telephone Laboratories drastically changed the electronics industry and paved the way for the development of the Integrated Circuit(IC) technology.VLSI circuit are present everywhere ,our computer ,our car, our brand new state-of-the-art digital camera, the cell-phones ,and what we have all this involves a lot of expertise on many fronts within the same field. All modern digital designs start with a designer writing a hardware description of the IC in the Verilog /VHDL.RTL description is done using HDLs. This RTL description is simulated to test functionality. From here onwards we need the help of EDA tools. RTL description is then converted to a gate-level netlist using logic synthesis tools.The design process of producing a package VLSI chip physically follows various steps which are popularly known as VLSI design cycle. This design cycle normally represented by a flowchart below. The various step involved in the design cycle.

- a) System specification: The specification of the system to be designed is exactly specified in this step. It consists performance, functionality, and the physical dimensions of the design. The choice of fabrication technology and design technique is also considered. The end results are specifications for the size, speed, power, and functionality of the VLSI system to be designed.
- b) Functional design: In this step, behavioral aspects of the system are considered. The outcome is usually a timing diagram or other relationships between sub-units. This information is used to improve the overall design process to reduce the complexity of the subsequent phases.
- c) Logic design: In this step, the functional design is converted into a logical design, using the Boolean expressions. These expressions are minimized to achieve the smallest logic design which conforms to the functional design. The logic design of the system is simulated and tested to verify its correctness.
- d) Circuit design: This step involves conversion of Boolean expressions into a circuit representation by taking into consideration the speed and power requirements of the original design. The electrical behaviour of the various components is also considered in this phase. The circuit design is usually expressed in detailed circuit diagram.
- e) Physical design: In this step, the circuit representation of each component is converted into a geometric representation. This representation is set of geometric patterns which perform the intended logic function of the corresponding component. Connections between different components are also expressed as geometric patterns.
- f) Design verification: In this step, the layout is verified to ensure that the layout meets the system specifications and the fabrication requirements. Design verification consists of design rule checking (DRC) and circuit extraction DRC is a process which verifies that all geometric patterns meet the design rules imposed by the fabrication process.
- g) Fabrication: This step is followed after the design verification. The fabrication process consists of several steps like, preparation of wafer, deposition, and diffusion of various, materials of the wafer according the layout description. A typical wafer is 10cm in diameter and can be used to produce between 12 and 30 clips is mass produced, prototype is made and tested.
- h) Packaging, testing, and debugging: in these steps, the clip is fabricated and diced in fabrication facility. Each chip is then packaged and tested to ensure that it meets all the design specifications and that it functions properly.

3. FULL ADDER DESIGN

The proposed design of XNOR gate is shown in Figure 2. It consists of 3 transistors as one pMOS and two nMOS. The Out terminal is connected to drain of all transistors. When $ab=00$, nMOS M2 is OFF and pMOS M1 is ON on account of higher gate voltage than the corresponding threshold. As pMOS is strong '1' device it will pass complete logic "high" signal at the output. When $ab=01$, nMOS M2 is OFF but nMOS M3 becomes ON. As nMOS is strong "0" device, it will pass complete logic "low" signal at the output. When $ab=10$, both nMOS M2 and pMOS M1 are ON. As mobility of nMOS is nearly three times higher than pMOS, it will drive the output ignoring the effect of ON pMOS transistors which results into complete zero output. When $ab=11$, both nMOS transistors are ON and only nMOS will be responsible for driving the output. Table 1 describes the performance of proposed 3T XNOR gate.

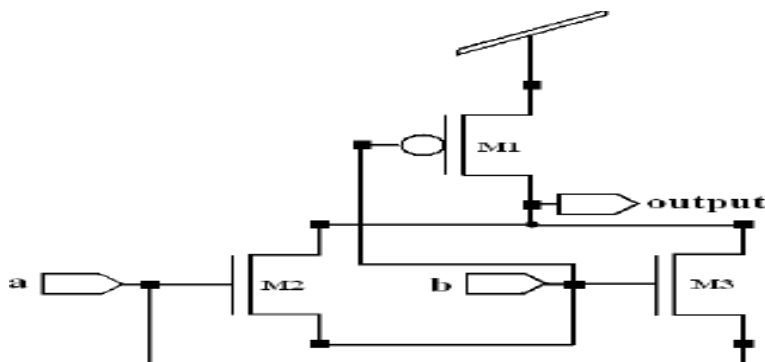


FIGURE: 2 Proposed 3T XNOR Gate

a	b	Expected Output	Obtained Output
0	0	1	1.00
0	1	0	0.00
1	0	0	0.15
1	1	1	1.00

Performance Table 1 :3T XNOR GATE

The output of first stage is simply the XNORing of the input „a“ and „b“. For generation of the sum output, the output of the first stage is further XNORed with „cin“. The output of the first stage is used as a selector circuit for the carry output. When the output of the first stage i.e is “0”, the carry output is equal to the carry in i.e. „cin“. When the output of the first stage i.e is “1”, the carry output is equal to the input „a“. This is important for the complex circuit design. This circuit reduces the overall PDP at varying input voltages and operating frequencies and also improves the temperature sustainability. The average power consumption in VLSI circuits is expressed as sum of three components as shown where Pswitching represents the average switching power consumption, Pshort-circuit represents short circuit power consumption and Pleakage represents leakage power consumption. The average power consumption is given by simulations are carried out for power, power-delay product at varying supply voltages, temperatures and frequencies. Figures Shows through 11 reveal that the proposed 8T full adder cell proves its superiority in terms of power consumption, power delay product at various input voltages and frequencies, and temperature sustainability over the existing 8T full adder.

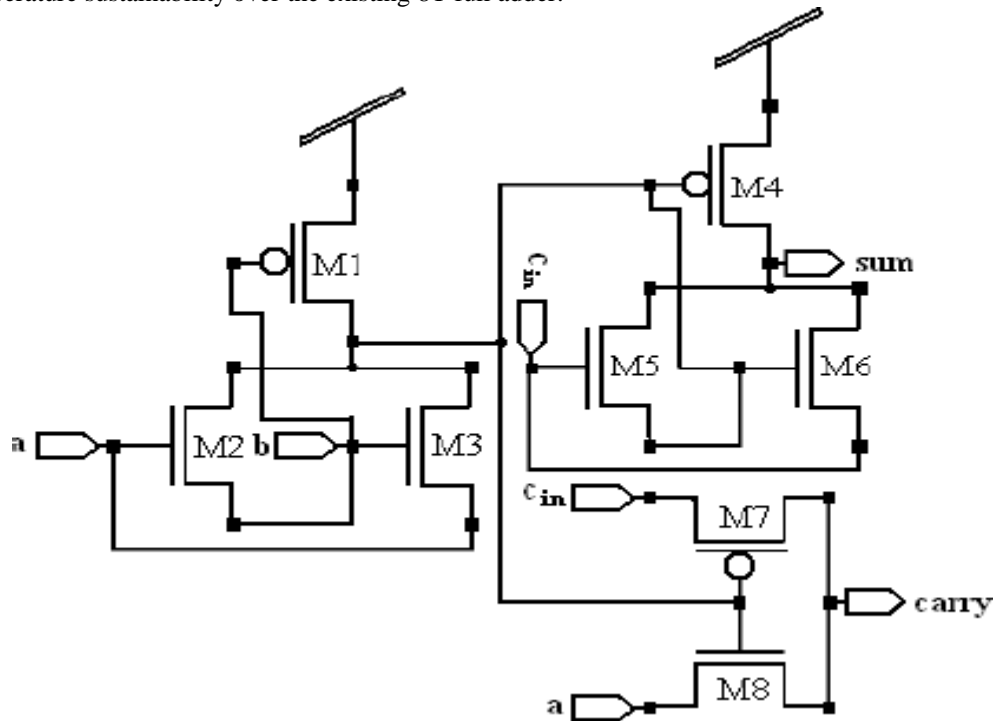


FIGURE:3. Schematic Circuit Diagram for Proposed Hybrid Full Adder

4. SIMULATION AND COMPARISON

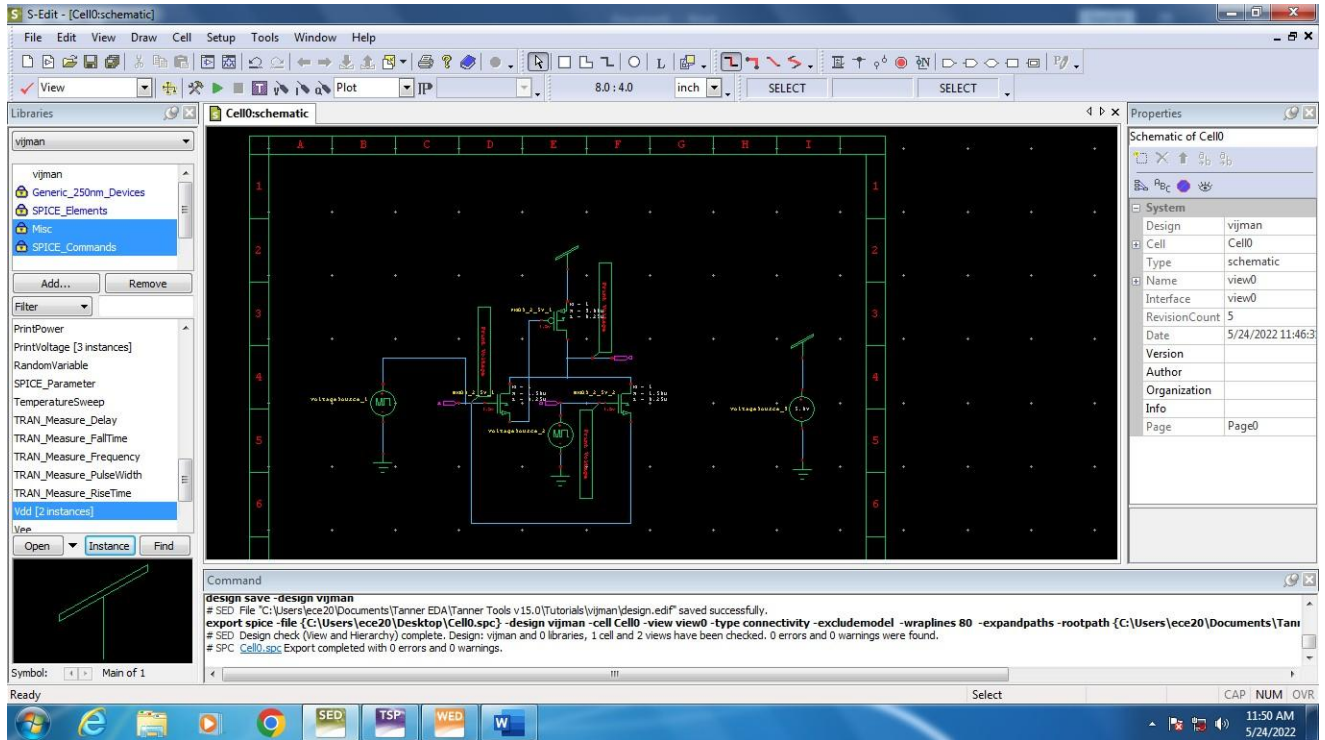


FIGURE:4 SIMULATION OF XNOR GATE



FIGURE 5: Simulation Output Waveform of Xnor Gate

All schematic simulations have been performed on Tanner EDA tool at 45nm technology with input voltage ranging from 0.6V to 1V in steps of 0.1V. To establish an impartial testing environment both circuit have been tested on the same input patterns which covers all combinations of the input stream. In order to prove that proposed design is consuming low power along with better performance, simulations are carried out for power, power-delay product at varying supply voltages, temperatures and frequencies. That the proposed 8T full adder cell proves its superiority in terms of power consumption, power delay product at various input voltages and frequencies, and temperature sustainability over the existing 8T full adder.

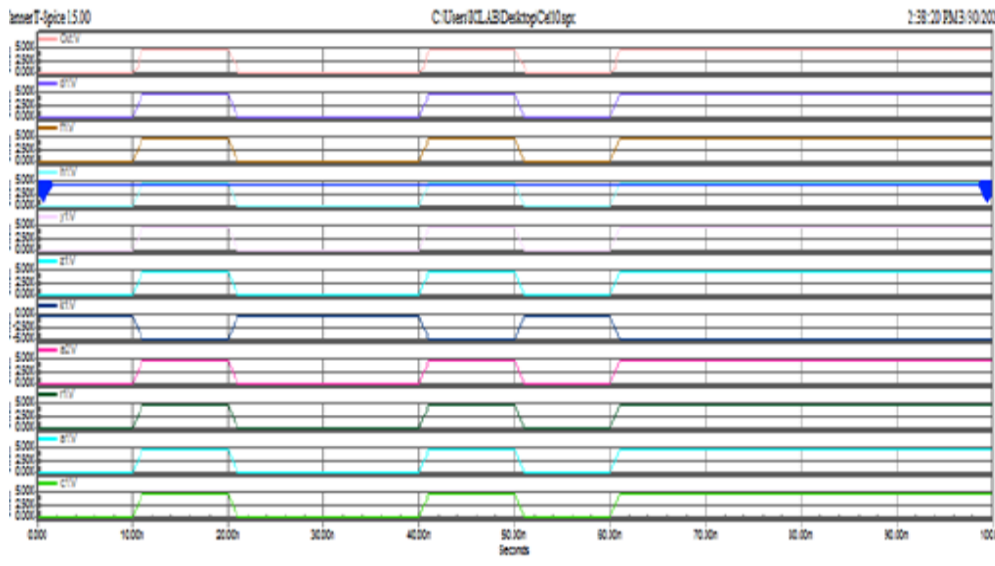


FIGURE 6: INPUT AND OUTPUT WAVEFORM 8T FULL ADDER

TABLE.2.COMPARISON OF HYBRID FULL ADDER CIRCUITS

Full Adders	No. of Transistors	Power (nW)	Delay (ns)	PDP (nJ)
HFA-20T	20	0.134	3010	403.3
HFA-B-26T	26	0.283	3012	852.3
HFA-NB-26T	26	0.228	3010	686.2
HFA-22T	22	0.146	3000	438
HFA-19T	19	0.139	1010	140.3
HFA-14T	14	0.129	3087	398.2
HFA-12T	12	0.147	1011	148.6
HFA-8T	08	0.135	0999	131.7

5. CONCLUSION

The proposed 8T adder has been designed and simulated on Tanner EDA tool at 45nm technology. The proposed 8T 1-bit full adder is found to give better performance than the existing 12T full adder. It has been tested to have better temperature sustainability and significantly less power and power-delay product at various input voltages and frequencies. It gives 82% improvement in threshold loss than the existing 8T full adder.

6. REFERENCES

[1] PygastiJuveria, K. Ragini, "Low Power and high Speed Full Adder using new XOR and XNOR Gates"International Journal of Innovative Technology and Exploring Engineering (IJITEE)

- [2] H. Naseri and S. Timarchi, "Low-Power and Fast Full Adder by Exploring New XOR and XNOR Gates," IEEE Trans. Very Large Scale Integrated Systvol. 26, no. 8, pp. 1481–1493, Aug.2018, doi:10.1109/TVLSI.2018.2820999.
- [3] N. E. H. Weste and D. M. Harris, "CMOS VLSI Design: A Circuits and Systems Perspective", vol. 53, no. 9.2013.
- [4] N. Zhuang and H. Wu, "A New Design of the CMOS Full Adder," IEEEJ. Solid-State Circuits, vol. 27,no. 5, pp.840–844, 1992,doi:10.1109/4.133177.
- [5] P.Kumarand R. K. Sharma, "Low voltage high performance hybrid full adder," Eng. Sci. Technol. an Int. J., 2015,doi:10.1016/j.jestch.2015.10.001.
- [6] H. T. Bui, Y. Wang, and Y. Jiang, "Design and analysis of low-power 10-transistor full adders using novel XOR- XNOR gates," IEEE Trans .Circuits Syst. II Analog Digit. Signal Process.,vol.49,no. 1, pp.25–30,2002,doi:10.1109/82.996055.

High Speed Gate Level Synchronous Full Adder Designs

V.Venkatesan¹ Arunkumar², sahinipriya³

Assistant Professor^{1 2 3}, Department of ECE, St. Anne's College of Engineering and Technology, Panruti

Abstract

Addition forms the basis of digital computer systems. Three novel gate level full adder designs, based on the elements of a standard cell library are presented in this work: one design involving XNOR and multiplexer gates (XNM), another design utilizing XNOR, AND, Inverter, multiplexer and complex gates (XNAIMC) and the third design incorporating XOR, AND and complex gates (XAC). Comparisons have been performed with many other existing gate level full adder realizations. Based on extensive simulations with a 32-bit carry-ripple adder implementation; targeting three process, voltage and temperature (PVT) corners of the high speed (low Vt) 65nm STMicroelectronics CMOS process, it was found that the XAC based full adder is found to be delay efficient compared to all its gate level counterparts, even in comparison with the full adder cell available in the library. The XNM based full adder is found to be area efficient, while the XNAIMC based full adder offers a slight compromise with respect to speed and area over the other two proposed adders. Key-Words: - Combinational logic, Full adder, High performance, Standard cells, and Deep submicron design.

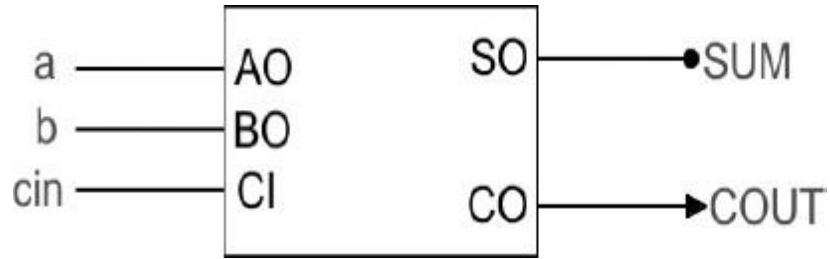
1. Introduction

A binary full adder is often found in the critical path of microprocessor and digital signal processor data paths, as they are fundamental to almost all arithmetic operations. It is the core module used for many essential operations like multiplication, division and addresses computation for cache or memory accesses and is usually present in the arithmetic logic unit and floating point units. Hence, their speed optimization carries significant potential for high performance applications. A 1-bit full adder module basically comprises of three input bits (say, a, b and cin) and produces two outputs (say, sum and cout), where 'sum' refers to the summation of the two input bits, 'a' and 'b', and cin is the carry input to this stage from a preceding stage. The overflow carry output from this stage is labeled as 'cout'. Many efficient full custom transistor level solutions for full adder functionality have been proposed in the literature [1] – [10], optimizing any or all of the design metrics viz. speed, power and area. In this paper, our primary focus is on realizing high performance full adder functionality using readily available off-the-shelf components of a standard cell library [11]. Hence, our approach is semi-custom rather than being full custom.

This article primarily focuses on the novel design of full adders at the logic level and also highlights a comparison with many other existing gate level solutions, from performance and area perspectives. The inferences from this work may be used for further improvement of full adder designs at the transistor level. Apart from this, this article is also intended to provide pedagogical value addition. The remaining part of this paper is organized as follows. Section 2 describes the various existing gate level realizations of a 1-bit binary full adder. The three newly proposed full adder designs are mentioned in section 3. Section 4 gives details about the simulation mechanism and results obtained. Finally, we conclude in the next section.

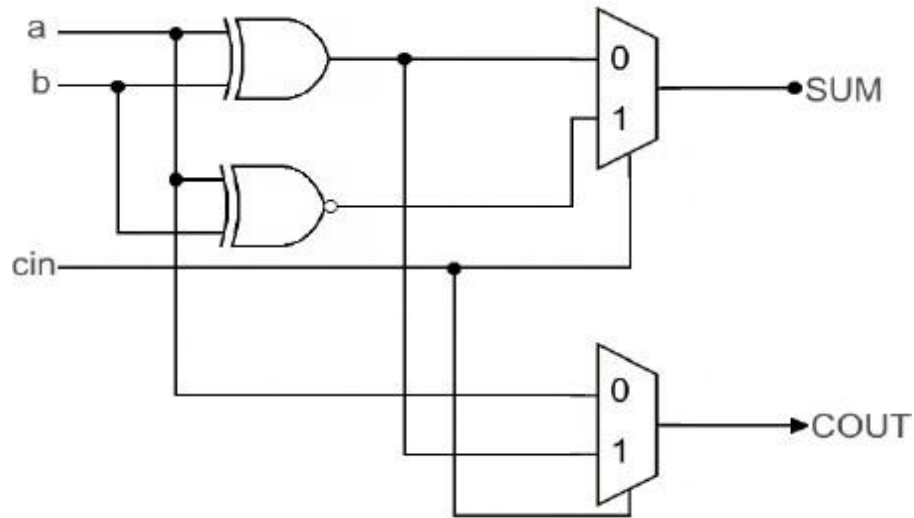
2. Library's full adder cell

The internal details of the full adder cell, which forms a part of the commercial library [11], could not be commented upon in this article and so only the block schematic of the same is given below in fig. 9. The inputs and outputs are listed therein.



Fig;1Black Box Model Of The Library's Full Adder Cell

3. Centralized full adder design



Gate level centralized full adder design

4. XNM FULL ADDER

Three full adder designs are proposed in this work. The first design employs only XNOR gates and 2:1MUXes. However, one of the two non-inverting 2:1MUXes has an inverted input. This design is portrayed by fig. 10 and shall be referred to as XNM based full adder. The second design employs XNOR, AND, NOT, inverted input 2:1 MUX and complex gates (XNAIMC based full adder), as shown in figure. The complex gate used is the AO12 cell, which performs the function, $f = xy + z$, where 'x' and 'y' are the inputs to the AND logic and 'z' is the separate input to the OR logic.

The last adder design is a refinement of the full adder design mentioned in section 2.2, in that, the AND gate of the second half adder module and the OR gate associated with the carry output are replaced by a single complex gate, namely AO12 cell. This design, referred to as XAC based full adder.

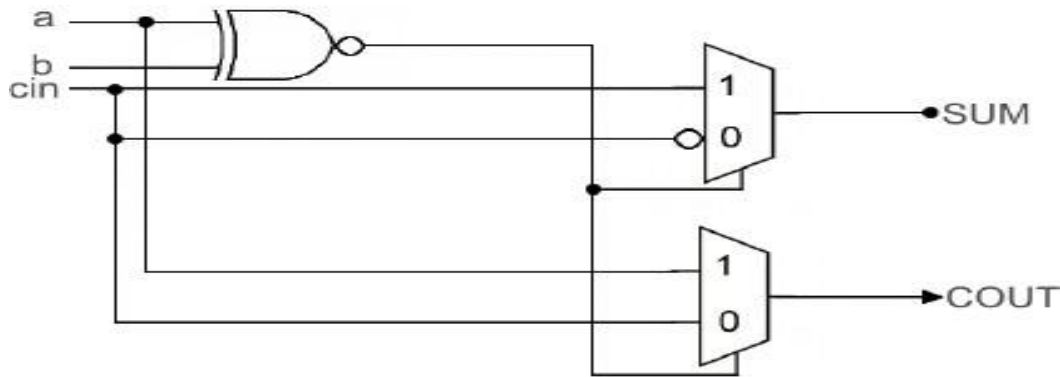


Fig 2. proposed xnm full adder

Amongst all the other gate level full adders, the XAC based full adder realization was found to be the fastest. This is substantiated by the maximum operating speed values, highlighted in figures. The expressions for the *sum* and *carry* outputs of the XAC based full adder are as follows.

The Boolean product term, $(a \oplus b) \cdot cin$ in (4), has been implemented by the complex gate, AO12 cell.

$$sum = (a \oplus b) \oplus cin$$

$$cout = a \cdot b + (a \oplus b) \cdot cin$$

5.Simulation Method and Discussion of Results

29.3% more area increase over it. The various 1-bit full adder realizations mentioned previously, were all described in cell level VerilogHDL, so that the physical implementation would be in exact conformity with the logical description. They were then instantiated to implement a 32-bit RCA, consisting of a series cascade of 32 full adder stages. The simulations were performed targeting a nominal case (typical case), best case and worst case PVT corner of the 65nm STMicroelectronics bulk CMOS process [11]. The simulation results purely reflect the performance and area metrics of the combinatorial adder logic and do not consider any sequential components. This sets the tone for a fair comparison of various full adder designs. The library has been inherently optimized for low power applications. The library corresponding to a supply voltage of 1.10V with low V_t was chosen, for which all the different process corner specifications exist. Static timing analysis and cells area estimation were done within the Synopsys PrimeTime environment. All the adder's inputs have the driving strength of the minimum sized inverter in the library, while their outputs possess fanout-of-4 (FO-4) drive strength. Appropriate wire loads were selected automatically for timing evaluation purpose. Tabular columns 2, 3 and 4 depict the performance of various full adder modules for 32-bit addition, based on a ripple carry adder (RCA) topology.

Table reports the area measure for different 32-bit RCAs. The percentage figures mentioned within brackets highlight the percentage increase in the design metric for the other adders in comparison with the optimal adder. We find that the proposed XAC based full adder features the least critical path (or least data path) delay amongst all other adders and the percentage figures for all other adders indicate their relative delay degradation compared to the proposed XAC based full adder for 32-bit addition. It is evident that the full adder present in the library suffers delay degradation over the proposed XAC based full adder, on an average, across all the three process corners by 36.9%. However, the commercial library's full adder cell was found to occupy the least area in comparison with all other adders, with the next best area-efficient adder suffering from at least 1.33x increase in cells area in comparison with it; the proposed XAC based full adder reporting

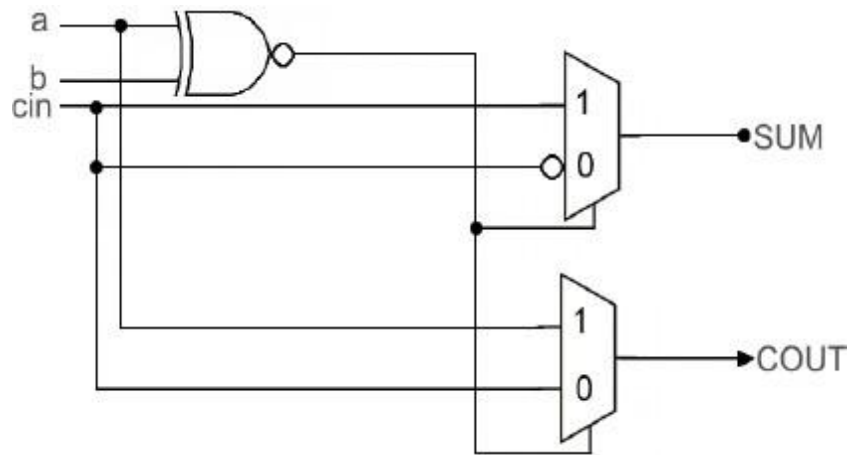


fig 3: Proposed XNM based full adder

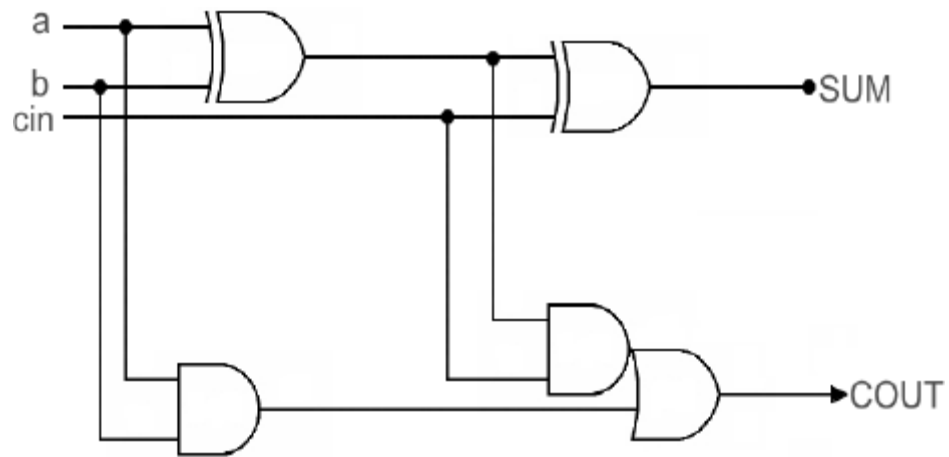


fig 4 :Proposed XAC based full adder

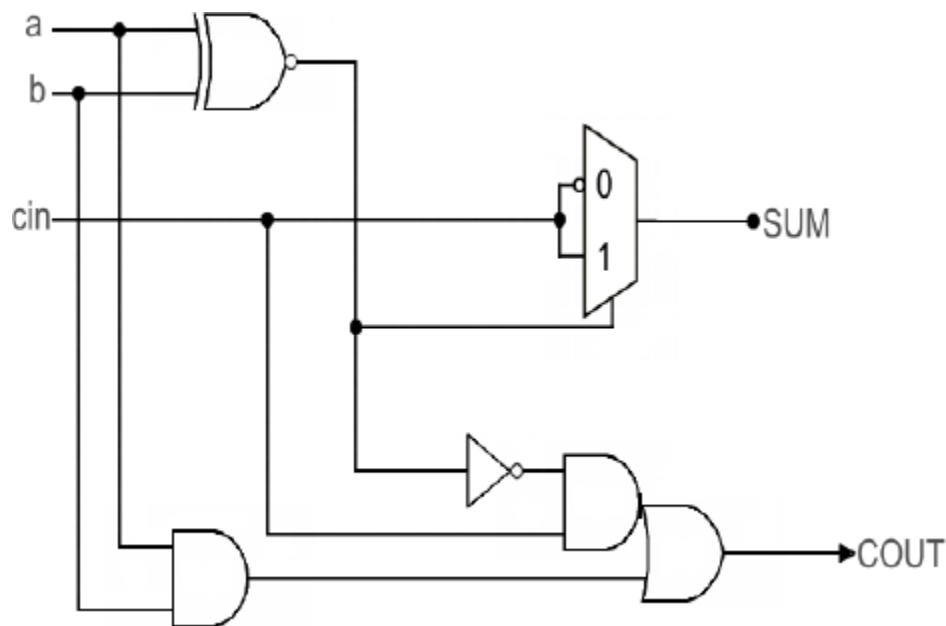


figure 5:Proposed XNAIMC based full adder

Though the proposed XNM based full adder reports the least area measure among the proposed adders, in line with those corresponding to XNOR-XNOR and XOR-XOR based full adder designs, it comes at the expense of an increase in the delay metric over the proposed XAC based full adder by 21.3%, on an average, considering all the targeted PVT corners. The maximum data path delay of the proposed XNAIMC based adder is somewhat close to the proposed XAC based adder, but it occupies 10.7% more area than the latter realization. It might be interesting to note that the classical full adder (constructed using two half adder modules) reports increase in worst case delay over the proposed XAC based full adder by a whopping 45.5%, on an average, when considering all the process corners.

In terms of the operating frequency, this translates to a similar ratio of speed advantage for the proposed XAC based adder over the conventional full adder design, with respect to all the PVT corners considered. This is in addition to the fact that the proposed XAC based full adder features 12.5% lesser area consumption than the classical full adder.

It is clearly evident that the proposed XAC based full adder exhibits the highest operating frequency amongst all the other adders, including the other two proposed adders. Among all the other gate level adders (i.e. excepting the proposed adders), the XNOR-XNOR based full adder design is faster. Nevertheless, the proposed XAC based adder reports an improvement in speed over the XNOR-XNOR based adder by 16.9%, 14.6% and 18.9% across the typical, best and worst case library corners respectively. In comparison with the commercial library based full adder, the proposed XAC based adder is found to be speed efficient by 36.9%, on an average, across all the three process corners. The above observations clearly emphasize the role played by complex gates in effecting high speed solutions, whilst minimizing area occupancy.

**Experimental results corresponding to a nominal case PVT corner for 32-bit addition
(V_{dd} = 1.10V, T_{Junction} = 25°C)**

Design style	Critical path delay (ns)
Minimized SOP based full adder design [12]	5.41 (82.77%)
Half adders based full adder design [13]	4.28 (44.59%)
Full adder design embodying logic sharing [14]	5.78 (95.27%)
MUXes based full adder design [4]	3.73 (26.01%)
XNOR-XNOR based full adder design [7] - [9]	3.46 (16.89%)
XOR-XOR based full adder design [7] - [9]	3.50 (18.24%)
Centralized full adder [8] [9]	3.75 (26.69%)
Shannon's theorem based full adder [10]	5.17 (74.66%)
Commercial library's full adder [11]	4.11 (38.85%)
Proposed design – XNM based full adder	3.59 (21.28%)
Proposed design – XNAIMC based full adder	3.12 (5.41%)
Proposed design – XAC based full adder	2.96

6. Conclusions

Three novel gate level full adder designs have been presented in this work: XNM, XNAIMC and XAC based full adders. Amongst these, the XAC based full adder achieves the highest speed, while the XNM based full adder occupies the least area. The XNAIMC based adder is somewhat closer to the XAC based adder with respect to delay. It is worth noting that the proposed XAC based full adder is faster than even the full adder cell present in a commercial standard cell library. Apart from advancing fundamental research in data path element designs, this research article encompasses considerable pedagogical value. It is anticipated that the inferences from this work are likely to facilitate better transistor level solutions for full adder functionality compared to those which currently exist.

Design of Rectangular Patch 4×4 Array For Satellite Communication

R.Sandhiya ,ECE , St Anne's College of Engineering And Technology.
S.Selva praveena ,ECE ,St Anne's College of Engineering And Technology.
Mr.S.Durai raj .AP, ECE ,St Anne's College of Engineering And Technology.

Abstract

This work presents the design and implementation of a micro strip patch array antenna with 4x4 element operates on a frequency of 12 GHz for satellite communication .The main element of this arrangement is a rectangular patch antenna design on the RT/Duroid 5880 substrate.Rogers duroid, in which ϵ_r is 2.2 and height is 1 mm. The RT/duroid 5880 has a long industry presence of providing high reliability materials with superior performance.Based on the design results the micro strip patch array antenna with 4x4 element with achieve high efficiency, gain, VSWR and Return loss (S11) by which is simulate and optimize using High Frequency simulation structure software (HFSS 15.0 version).

Keywords: Microstrip Patch Array Antenna (MPAA), Satellite Communication, Bandwidth, HFSS.

1 Introduction

In any wireless communication field, the antenna is a primary need . The antennas are equipments used for connecting two or more devices by means of wireless medium connection. It is used for radiating or receiving radio waves by using air. Microstrip antennas have attracted a lot of attention due to rapid growth in wireless communication area. A microstrip antenna in its simplest configuration is shown in fig 1[5]. Figure 1: Microstrip Patch Antenna There are a lot of shapes of micro strip patch antenna that are usually square, rectangular, circle, triangle etc. For mobile communication, it requires small antennas dimensions at low cost and low profile. Microstrip patch antennas full fil all those requirements and they have been designed for use in wireless communication systems and satellite communication as well. The most significant advantage of antenna arrays is that the direction of maximum radiation can be changed and thus they can be used in beam scanning capabilities . The proposed antenna may find applications in wireless local area network . Today patch microstrip array antennas are probably the most widely used type of antennas due to their low volume, low cost, light weight. In satellite communication, there are a lot of types of antennas, the most common of which is Microstrip patch array antenna .

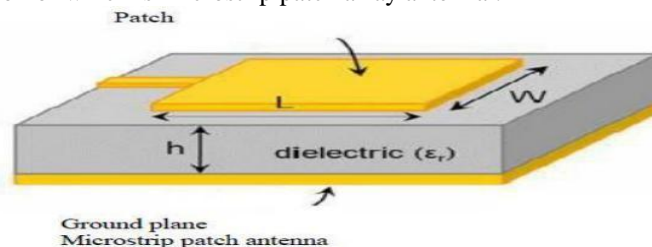


Figure 1: Microstrip Patch Antenna [5]

2 Antenna Design Methodology

Following are the parameters used to design the antenna.

W : The width of patch antenna

L : The length of the patch antenna

λ_0 : The Wavelength

f_0 : The operating frequency

ϵ_r : With dielectric const

ΔL : Length extension

ϵ_{eff} : Dielectric constant effective

h : Height of the substrate

W_g : Width of ground

L_g : Length of ground

C : Velocity of light

The steps involved in the design of microstrip patch antenna are as follows:

Step 1: The width of the micro strip patch antenna is calculated by eqn (1)

$$W = c/2f\sqrt{(\epsilon_r+1)/2} \quad (1)$$

Step 2: Calculation of Effective dielectric constant given by eqn (2)

$$\epsilon_{eff} = \epsilon_r + 1/2 + \epsilon_r - 1/2 * 1/\sqrt{1+12/w} \quad (2)$$

Step 3: Calculation of the Effective length as given by eqn (3)

$$L_{eff} = C/2f0\sqrt{\epsilon_{eff}} \quad (3)$$

Step 4: Calculation of the length extension given by eqn (4)

$$\Delta = 0.412 h (\epsilon_{eff} + 3) (w + 0.264) / (\epsilon_{eff} - 0.258) (w + 8) \quad (4)$$

Step 5: Calculation of actual length of patch

$$L = L_{eff} - 2 \Delta L \quad (5)$$

Step 6: Ground plane Measurements is presented by eqn (6-7)

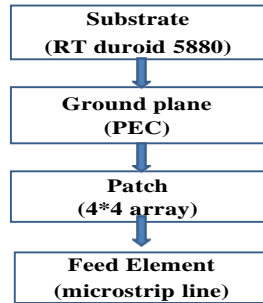
$$L = L + 6 \quad (6)$$

$$W_g = W + 6 \quad (7)$$

In this section, the structure of an array antenna designed to operate at 12 GHz for satellite communication has been presented. The antenna has 16 elements of 4x4 array using the line feeding. The ground of antenna has dimension of 23 x 12.03 mm². The substrate material is RT/Duroid 5880 because of its availability in the market. Several methods are used to enhance the bandwidth, for example by changing the height of substrate to allow many applications to be used with a single antenna. The flow chart for the simulation of the microstrip patch antenna is presented in Figure 2. The first step in design of microstrip patch antenna is selection of frequency, followed by selection of substrate material. Next step is to design the array antenna and later on produce the simulation results. If the result produced does not meet the desired specification, then some parameters need to be changed for the design of an array antenna. If the results produced meet the desired specification, then it must be tested in the laboratory and then shall be passed to the fabrication process. Once the antenna has been fabricated the results obtained from the physical antenna shall be compared with the

simulation results to see the variation in the simulated and physical antennas

DESIGN FLOW DIAGRAM



8

Desing flow diagram

The dimensions of the single rectangular patch have been calculated using the equations from step 1 to step 5. The patch has been optimized for an input impedance of 50-ohm using HFSS for designing and simulation. The results of the simulation will be viewing down. The dimensions of the 4x4 array antenna used in this design are being presented in table 1. Figure 3 illustrates the 4x4 patch array antenna in HFSS software.

Table 1:4×4 Array Antenna Dimensions

w	17mm	Leff	6.98 mm
h	1 mm	L	6.03 mm
εreff	3.198	Lg	12.03
ΔL	0.475	wg	23

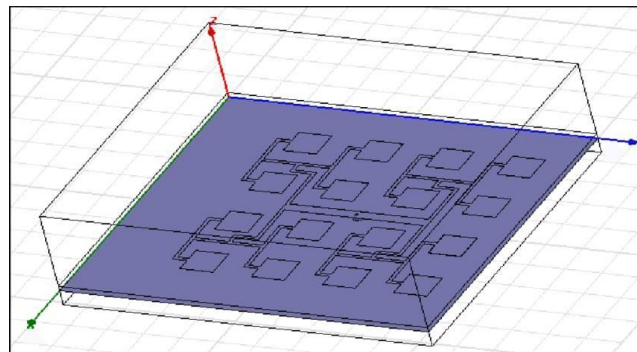


Figure 3: 4x4 patch array antenna in HFSS

3 Results And Discussion

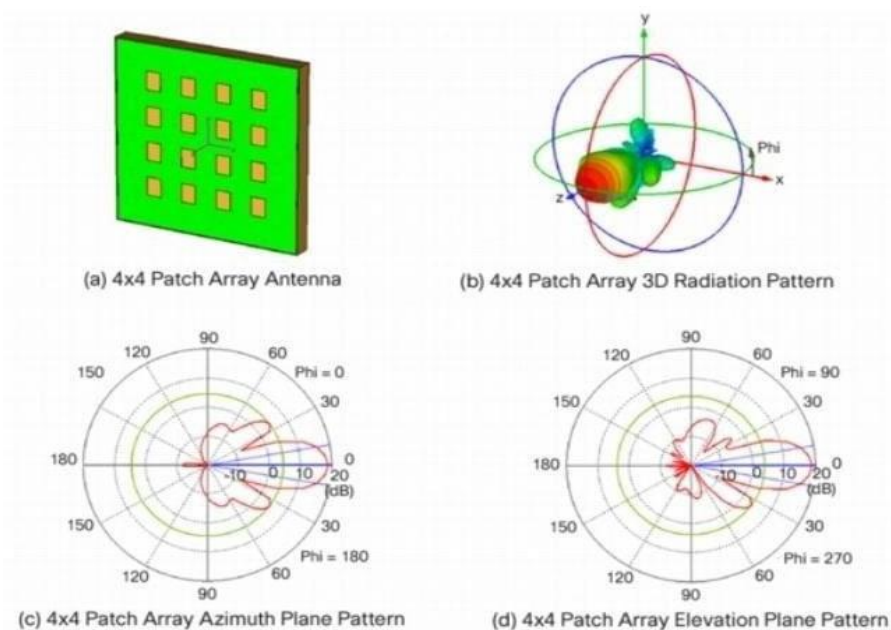
The results obtained from the design of the microstrip patch array antenna for the proposed approach has been discussed in this section. The microstrip patch array antenna has been designed using HFSS software and the simulation has also been done using the same software. The S11 or Return Loss of 4X4 patch array antenna has been illustrated in Figure 5.

The return loss of the proposed antenna known as 4x4 patch array antenna has been reported as -32.33 dB, which means the power transmitted got losses around 0.05% at the operating frequency equal to 11.79 GHz. When we consider the return loss at -10 dB, we have the lowest frequency around 11.4954 GHz and the highest frequency around 12.1890 GHz, so the bandwidth at -10 dB can be calculated as

$$B = FH - FL \text{ GHz}$$

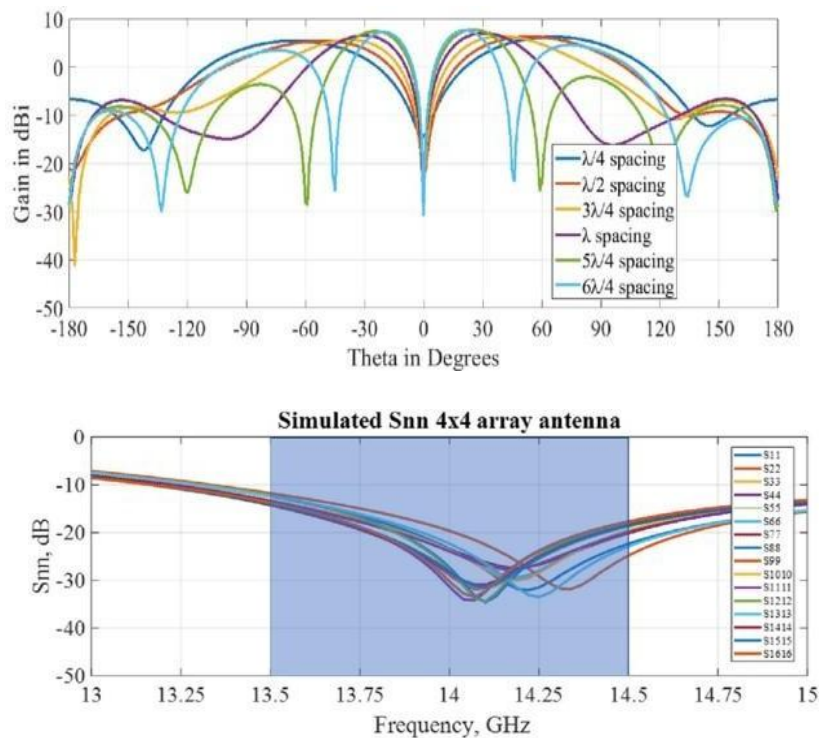
$$B = \frac{FH - FL}{FC} \times 100 \%$$

Where, FH is the higher frequency, FL is the lower frequency and FC is the central frequency. By above equation, we can easily find the values of the Bandwidth. Thus the bandwidth for the proposed microstrip patch antenna is found to be $B = 0.6936$ GHz or $B = 693.6$ MHz and $B = 5.9 \%$. Therefore, this antenna can be used in several applications. The gain and the Directivity of the proposed antenna can be found by using their respective graphs and for the proposed microstrip patch antenna the gain has been obtained as $G = 8.98$ dB and $D = 10.83$ dB. The most advantage of microstrip patch array antenna is the improvement of the parameters of the antenna like gain, bandwidth, etc. [7] The obtained efficiency of the microstrip patch antenna has been $\epsilon = G D$, so $\epsilon = 83 \%$. For a good antenna, the average value of the efficiency is around 50 to 60%. So this antenna is an efficient one. Figure 6 and 7 illustrate Gain of 4 x 4 patch array antenna and Directivity of 4 x 4 patch array antenna.



4 Conclusion

In this work, authors have proposed design of a micro strip patch array antenna for satellite communication having 23 x 12.03 mm dimensions. For the proposed design the feeding line gives good control, gain and bandwidth and a very good return loss results. This proposed micro strip patch array antenna 4x4 operates at 12 GHz has a bandwidth equal to 693.6 MHz (5.9 %), a gain equal to 8.98 dB, directivity equal to 10.83 dB and finally an efficiency equal to 80.01 %. This array antenna is suitable for X-band and KU-band applications.



5 Reference

1. C. A. Balanis, Antenna theory: analysis and design (John Wiley & Sons,2005).
2. Mrs.Devashree S. Marotkar, Dr. Prasanna Zade "Bandwidth Enhancement of Microstrip Patch Antenna using Defected Ground Structure" in IEEE, International Conference on Electrical, Electronics, and Optimization Techniques (ICEEOT), Nagpur, 2016, pp. 1712-1716
3. Mohini Narendra Naik and H. G. Virani "Design and Simulation of Array of Rectangular Slotted Microstrip Patch Antenna with Improved Bandwidth for WLAN" in IEEE International Conference on Internet of Things and Applications (IOTA), Pune, India, 22 Jan - 24 Jan, 2016, pp. 40-45.
4. Ali W. Azim, Shahid A. Khan, Zeeshan Quamar, K.S Alimgeer and S.M Ali "Current Distribution in Microstrip patch antenna Arrays" International Journal of Future Generation Communication and Networking, 2011, vol. 4, no. 3.
5. Neha Gupta and Devraj Gangwar "Survey on Microstrip Antenna" in IJEMR International Journal of Engineering and Management Research, 2017, vol.7, no.2, pp. 189-193
6. Atser A. Roy, Joseph M. Môm, Gabriel A. Igwue "Enhancing the Bandwidth of a Microstrip Patch Antenna using Slots Shaped Patch" in American Journal of Engineering Research (AJER), Nigeria, 2013, vol. 2, no. 9, pp. 23-30
7. Jagadeesha S, Bharatraj M, Madhusudhana.K, Chintesh "E-Shaped microstrip antenna array with improved gain for wireless applications" in IJEE, Ujire, 2014, vol. 6, no. 1, pp. 46-52
8. D. M. Pozar, "Microstrip antennas", in Proceedings of the IEEE, 1992, vol. 80, no. 1, pp. 79- 91
9. Aaron K Shackelford, K-F Lee, and KM Luk. "Design of small-size wide-bandwidth Microstrippatch antennas", in IEEE Antennas and Propagation Magazine, 2003, vol. 45, no. 1, pp. 75-83

Optimal Placement and Sizing of Distributed Generator Based on Multi Objective Particle Swarm Optimization

A. Richard Pravin, Assistant Professor, Department of Electrical and Electronics Engineering
J. Aarthiroja, UG student, Department of Electrical and Electronics Engineering
M. Eswari, UG student, Department of Electrical and Electronics Engineering
S.Sivapriya, UG student, Department of Electrical and Electronics Engineering
St. Anne's College of Engineering and Technology,
Panruti, Tamil Nadu, India

Abstract

To solve the problems of environmental pollution and energy consumption, the development of renewable energy sources becomes the top priority of current energy transformation. Therefore, distributed power generation has received extensive attention from engineers and researchers. However, the output of distributed generation (DG) is generally random and intermittent, which will cause various degrees of impact on the safe and stable operation of power system when connected to different locations, different capacities, and different types of power grids. Thus, the impact of sizing, type, and location needs to be carefully considered when choosing the optimal DG connection scheme to ensure the overall operation safety, stability, reliability, and efficiency of power grid. This work proposes a distinctive objective function that comprehensively considers power loss, voltage profile, pollution emissions, and DG costs, which is then solved by the multi objective particle swarm optimization (MOPSO). Finally, the effectiveness and feasibility of the proposed algorithm are verified based on the IEEE 33 bus and 69-bus distribution network.

1 Introduction

With the rapid development of the world's electric power industry, the total amount of social electricity consumption has risen sharply over the last decade (Yang et al., 2016; Yang et al., 2017; Zhang et al., 2021). Under the traditional grid framework, the power sector mainly builds large centralized power sources such as nuclear power stations, large hydropower stations, and coal-fired power stations and then expands into a large-scale power system (Yang et al., 2019a; Yang et al., 2019b; Yan, 2020). However, its disadvantages are also increasingly prominent (Li et al., 2020; Xi et al., 2020), in particular, highly centralized power supply is gradually difficult to meet the flexibility requirements of power grid operation, and the failure of important power supply nodes seriously affects the overall reliability of power grid's power supply. Moreover, long-distance transmission is also under serious power loss and security problems (Mehleri et al., 2012; Wang et al., 2014; Yang et al., 2018).

To overcome the negative impact of the aforementioned problems, the concept of distributed generation (DG) was put forward in the 1980s (Gopiya Naik et al., 2013; Yang et al., 2015). DG has an extremely important influence on the planning and operation of the distribution network (Sara et al., 2020; Yang et al., 2020; Ali and Mohammad, 2021). Also, proper access of DG in distribution network can effectively enhance the power quality, reduce the active power loss, improve the voltage distribution, and boost the overall economy and flexibility of the power network operation (Abdurrahman et al., 2020; Bikash et al., 2020; Suresh and Edward, 2020). As the end of power network, the stability and efficiency of distribution network directly affect its overall efficiency (Surajit and Parimal, 2018; Bikash et al., 2019). Therefore, the location and sizing of distributed power generation have become an important research content of power grid planning.

The problem of location and sizing of DG is to optimize its installation point and sizing to maximize the benefits under the constraints of satisfying the given investment and system operation (Kumar et al., 2019; Nagaballi and Kale, 2020). With the increasing requirements for power system reliable operation, the problem of DG location and constant sizing has developed from a single-objective problem that only considers the minimum network loss to multi objective optimization problem that comprehensively considers voltage quality, current quality, and environmental factors. Quadratic programming method, genetic algorithm, and other methods have been applied to solve such multi objective location and constant volume problem. These methods all need to set weights to transform the multi objective problem into a single-objective problem for proper solutions (Murty and Kumar, 2015); however, these weights are often difficult to determine in actual operation.

Besides, the solution of a large number of planning models is relatively complicated, while the selection of the algorithm directly affects the choice of planning schemes (Aman et al., 2014; Nezhad Pashaki et al., 2020; Zeng and

Shu, 2020). At present, the solving algorithms mainly include mathematical optimization and metaheuristic algorithm (Doagou - Mojarrad et al., 2013; Satish et al., 2013; Sultana et al., 2016).

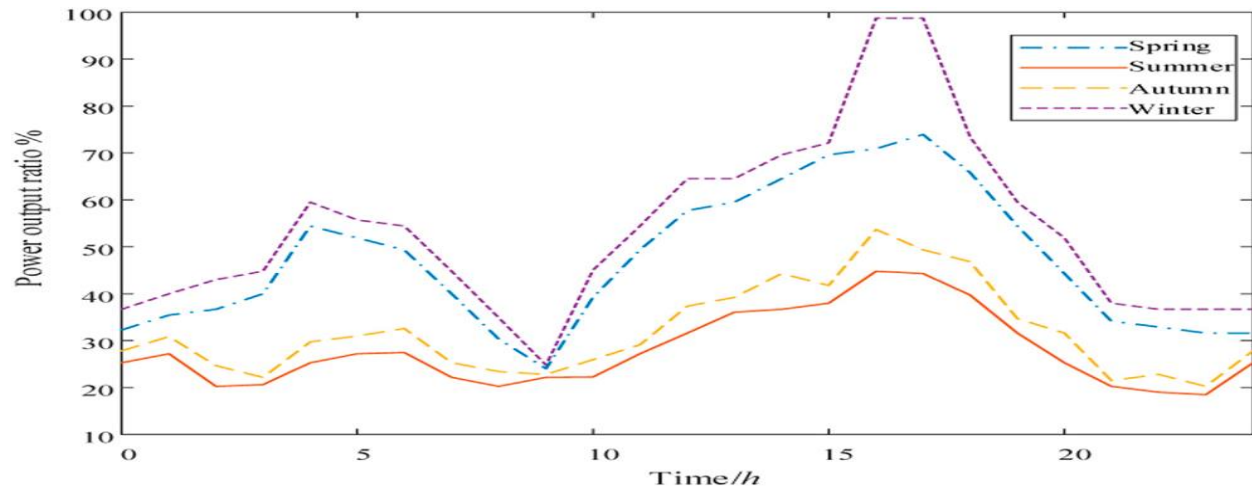


Figure 1| Annual output curve of wind turbine

Mathematical optimization algorithm owns relatively low computational efficiency and is only suitable for small-scale distribution networks. Thus, metaheuristic algorithm has received much attention and application in recent years (Aman et al., 2012; Pabu and Singh, 2016; Iqbal et al., 2018). Literature (Chandrasekhar and Sydulu, 2012) adopts genetic algorithm (GA) to optimize the new load nodes for expansion plan of distribution network, and then simulated annealing algorithm is utilized to optimize the generated single plan, which considerably reduces the load size of DG connected to the distribution network and the influence of power flow of the distribution network. Literature (Aman et al., 2013) proposes an improved particle swarm optimization algorithm based on hybrid simulated annealing method to optimize the location and sizing of distributed power sources. However, the convergence speed of the aforementioned algorithms is relatively slow, and the result is prone to local optimal solutions.

Therefore, an objective function comprehensively considering power losses, voltage profile, pollution emission, and DG cost is proposed in this work, and MOPSO is utilized to solve it. Finally, the proposed method is validated via an IEEE 33-bus and 69-bus distribution network to verify its effectiveness. Then, the Pareto front result is given.

The remaining of this paper is organized as follows: Mathematical Optimization Model of DG Planning develops the objective function. In Multi objective Particle Swarm Optimization Algorithm, multi objective particle swarm optimization (MOPSO) is described. Comprehensive case studies are undertaken in Case Studies. At last, Conclusion summarizes the main contributions of the paper.

2 Mathematical Optimization Model of DG Planning

2.1 Load and DG Power Output Timing Model

2.1.1 Wind Turbine Output Timing Model

The output power of wind turbine mainly depends on wind speed, which can be expressed by the following piecewise function (Velasquez et al., 2016):

$$P(v) = \begin{cases} 0, & (v \leq v_{ci} \text{ or } v \geq v_{co}) \\ P_r \frac{v-v_{ci}}{v_R-v_{ci}}, & (v_{ci} \leq v \leq v_R) \\ P_r, & (v_R \leq v \leq v_{co}) \end{cases}, \quad (1)$$

where $P(v)$ is the power output of the wind turbine; v_{ci} denotes the entry wind speed; v_{co} is the cut-out wind speed; v_R means rated wind speed; P_r represents the rated output power. The wind turbine output curve is modeled according to the mean seasonal wind speed, and the output curve is shown in Figure 1 (Sara et al., 2020).

2.1.2 Photovoltaic System Output Timing Model

The output power PPV of the photovoltaic (PV) system can be approximated by (Velasquez et al., 2016)

$$P_{pv} = P_{stc} \frac{I_{r,t}}{I_{stc}} [1 + \alpha_T (T_t - T_{stc})], \quad (2)$$

where Pstc means the output power of the PV system when the solar radiation intensity Istc 1000W/m2 and the temperatureTstc _ 25°C; Ir,t denotes the radiation intensity during actual operation; αT represents the power temperature coefficient of the PV system; Tt is the actual operating temperature of the photovoltaic power supply. In addition, the output curve of the PV system obtained by fitting the irradiance of typical days in all seasons is shown in Figure 2 (Sara et al., 2020).

2.1.3 Load Timing Model

The load size shows certain regularity due to people's living habits. Figure 3 shows the typical load curve of residents in all seasons (Velasquez et al., 2016).

2.2 Objective Function

2.2.1 Power Losses

The power losses index takes into account the total active power loss of 96 h in four typical days, which is established as follows (Velasquez et al., 2016):

$$\min f_1(x) = \sum_{t=1}^T \sum_{i=1}^n \sum_{j=1}^n A_{ij} \cdot (P_i P_j + Q_i Q_j) + B_{ij} \cdot (Q_i P_j - P_i Q_j), \quad (3)$$

$$\begin{cases} A_{ij} = \frac{R_{ij} \cdot \cos(\delta_i - \delta_j)}{V_i V_j} \\ B_{ij} = \frac{R_{ij} \cdot \sin(\delta_i - \delta_j)}{V_i V_j} \end{cases}, \quad (4)$$

where Pi and Qi are the active power and reactive power injected into node i, respectively; Rij represents the resistance of the transmission line connecting the ith node with the jth node; N means the number of nodes in the distribution network; Vi and δi are the voltage and angle of node i, respectively; T is the number of simulation periods; the value is 96.

2.2.2 Voltage Profile

Reasonable access of DG to the distribution network can effectively improve the voltage profile. Therefore, this work adopts the total voltage deviation of 96 h in four typical days to measure the optimization effect, and the voltage profile index is established as follows (Ali and Mohammad, 2021):

$$\min f_2(x) = \sum_{t=1}^T \sum_{i=1}^n (V_{DG,i} - V_{rated})^2, \quad (5)$$

where VDG, i is the voltage of the ith node after DG is configured in the distribution network and V rated is the rated voltage with a value of 1 p.u.

2.2.3 Pollution Emission

In order to reduce the emission of polluting gases, this work adopts the pollution emission considering carbon dioxide, sulfur dioxide, and nitrogen compounds as follows (Ali and Mohammad, 2021):

$$\min f_3(x) = \sum_{t=1}^T \sum_{i=1}^n P_{DG,i} \cdot \eta_{i,k} \cdot (e\omega_{CO_2} \cdot AE_{pi,CO_2} + e\omega_{SO_2} \cdot AE_{pi,SO_2} + e\omega_{NO_x} \cdot AE_{pi,NO_x}), \quad (6)$$

where PDG, i is the rated active power output of the I th DG; ηi, k means the output efficiency of the ith DG at time t; k denotes the number of DG in the distribution network; AEpi,co2, AEpi,so2, and AEpi,NOx are, respectively, the mass of carbon dioxide, sulfur dioxide, and nitrous oxide released by unit power output of the ith DG. In addition, ewCO2, ewSO2, and ewNOX are the weight coefficients among different gases, and their values are 0.5, 0.25, and 0.25, respectively.

3 MOPSO Algorithm

3.1 Particle Swarm Optimization Algorithm

Particle swarm optimization is a heuristic algorithm that mimics bird foraging, which can conduct intelligent guidance optimization through cooperation and competition among particles (Doagou-Mojarrad et al., 2013). Suppose a population has m particles, each particle has an N -dimensional variable, and the position and flight speed of the i th particle in the k th iteration are $X_{ki} = [x_{ki,1}, x_{ki,2}, \dots, x_{ki,n}]$ and $V_{ki} = [v_{ki,1}, v_{ki,2}, \dots, v_{ki,n}]$, respectively. Through evaluating the fitness value of the objective function, the individual optimal position $P_{ki} = [p_{ki,1}, p_{ki,2}, \dots, p_{ki,n}]$ and the population optimal position $G_{ki} = [g_{ki,1}, g_{ki,2}, \dots, g_{ki,n}]$ of each particle are determined, and the velocity and position of particle i in the next iteration are determined by (Doagou-Mojarrad et al., 2013)

$$\begin{cases} v_{ij}^{k+1} = \omega \cdot v_{ij}^k + c_1 r_1 \cdot (p_{ij}^k - x_{ij}^k) + \\ c_2 r_2 \cdot (g_{ij}^k - x_{ij}^k) \quad j = 1, 2, \dots, n \\ x_{ij}^{k+1} = x_{ij}^k + v_{ij}^{k+1} \end{cases}, \quad (15)$$

where r_1 and r_2 denote random numbers obeying uniform distribution on the interval (0,1); c_1 and c_2 represent learning factors, both of which are normal numbers. ω is the inertia weight used to balance the global and local optimization capabilities among particles. The value of ω is usually calculated using (Doagou-Mojarrad et al., 2013)

$$\omega = \omega_{max} - \frac{\omega_{max} - \omega_{min}}{K} k, \quad (16)$$

where K is the maximum number of iterations; k is the current iteration times; $\omega_{max} = 0.9$; $\omega_{min} = 0.4$.

3.2 MOPSO Algorithm

In order to constantly update a set of Pareto optimal solutions obtained by MOPSO during iterations, this work designs the historical Pareto optimal solution set and the global Pareto optimal solution set during iterations with the help of archiving technology. Global Pareto optimal solution set holds all Pareto optimal solutions generated during the current iteration. Assuming that a population contains m particles and each particle has N_{obj} objective function value, the global Pareto optimal solution set generated by each iteration is found by the following (Doagou-Mojarrad et al., 2013):

- 1) Let $i = 1$.
- 2) Compare particle x_i with particle x_j for all $j = 1, 2, \dots, m$ and $j \neq i$.
- 3) If j exists so that particle x_j dominates x_i , then particle x_i is marked as the inferior solution.
- 4) If $i > m$, turn to 5). Otherwise, let $i = i + 1$ and turn to (2).
- 5) Remove all marked solutions, and the remaining solutions constitute the global Pareto optimal solution set of this iteration.

Historical Pareto optimal solution set: this solution set is used to hold the Pareto optimal solution throughout the iteration.

$$k_{i,i+1} = \frac{(f_{2,i} - f_{2,i+1}) / (f_{2,max} - f_{2,min})}{(f_{1,i} - f_{1,i+1}) / (f_{1,max} - f_{1,min})}, \quad (17)$$

$$k_{i-1,i+1} = \frac{(f_{2,i-1} - f_{2,i+1}) / (f_{2,max} - f_{2,min})}{(f_{1,i-1} - f_{1,i+1}) / (f_{1,max} - f_{1,min})}, \quad (18)$$

where $k_{i,i+1}$ denotes the normalized slope between the Pareto optimal solution i and its adjacent solution $i + 1$; $k_{i-1,i+1}$ means the normalized slope between the two solutions $i - 1$ and $i + 1$ adjacent to the Pareto optimal solution i . If $k_{i,i+1} > k_{i-1,i+1}$, then the Pareto optimal solution i is close to the ideal Pareto optimal front, and such a solution is retained. If $k_{i,i+1} \leq k_{i-1,i+1}$, it indicates that the Pareto optimal solution i deviates far from the ideal Pareto optimal front, and such a solution is deleted. In addition, the flowchart of MOPSO is given in Figure 4 (Doagou - Mojarrad et al., 2013):

4 Case Studies

As shown in Figure 5 and Figure 6, DG planning research on an IEEE 33-bus and 69-bus distribution network is carried out to verify the effectiveness of the proposed method, including PV system (two nodes installed), wind turbine (two nodes installed), fuel cell (one node installed), and microturbine (one node installed). It is worth noting that fuel cell and micro-gas turbine can carry out power output stably. When PV system and wind turbine are used together, the defect of fluctuating output power can be well compensated. In addition, in four typical days, the total active power loss of the network is 4061.87 kW, while the total voltage deviation is 66.1991 p.u. and the proposed method was coded in MATLAB 2017b.

5 Conclusion

In this work, MOPSO is used to optimize the location and sizing of DG, which contributions are outlined as follows:

1. The objective function with four indexes of distribution network losses reduction index, voltage profile index, environmental emission reduction index, and economic indicators is established to comprehensively optimize the distribution network.
2. Based on an IEEE 33-bus and 69-bus distribution network, it is effectively verified that MOPSO has strong global searching efficiency and high convergence speed. Also, it can effectively avoid falling into local optimum under complex objective function.
3. Four types of DG, PV station, wind turbine, fuel cell, and microturbine are installed, and the connection of microturbine and fuel cell can stabilize the instability of PV station and wind turbine. The experimental results show that the power losses of the distribution network optimized by MOPSO decrease by 51.91%, and the voltage profile is also significantly improved. In future studies, more advanced solution algorithms and multiobjective decision-making method will be devised to solve this problem.

Reference

- [1] Abdurrahman, S., Sun, Y. X., and Wang, Z. H. (2020). *Multi-objective for Optimal Placement and Sizing DG Units in Reducing Losses of Power and Enhancing Voltage Profile Using BPSO-SLFA*. *Energ. Rep.* 6, 1581–1589. doi:10.1016/j.egy.2020.06.013
- [2] Ali, A., and Mohammad, K. S. (2021). *Optimal DG Placement in Power Markets from DG Owners' Perspective Considering the Impact of Transmission Costs*. *Electric Power Syst. Res.* 196, 107218. doi:10.1016/j.epsr.2021.107218
- [3] Aman, M. M., Jasmon, G. B., Bakar, A. H. A., and Mokhlis, H. (2013). *A New Approach for Optimum DG Placement and Sizing Based on Voltage Stability Maximization and Minimization of Power Losses*. *Energ. Convers. Management* 70, 202–210. doi:10.1016/j.enconman.2013.02.015
- [4] Aman, M. M., Jasmon, G. B., Bakar, A. H. A., and Mokhlis, H. (2014). *A New Approach for Optimum Simultaneous Multi-DG Distributed Generation Units Placement and Sizing Based on Maximization of System Loadability Using HPSO (Hybrid Particle Swarm Optimization) Algorithm*. *Energy* 66, 202–215. doi:10.1016/j.energy.2013.12.037
- [5] Aman, M. M., Jasmon, G. B., Mokhlis, H., and Bakar, A. H. A. (2012). *Optimal Placement and Sizing of a DG Based on a New Power Stability index and Line Losses*. *Int. J. Electr. Power Energ. Syst.* 43 (1), 1296–1304. doi:10.1016/j.ijepes.2012.05.053

Cost Saving on Micro Grid Operation using Grey Wolf Optimization Algorithm

K.Sriram, Assistant Professor, Department of Electrical and Electronics Engineering
B.Anbumani, UG Student, Department of Electrical and Electronics Engineering
S.KalaiPriyan, UG Student, Department of Electrical and Electronics Engineering
C.Naveenkumar, UG Student, Department of Electrical and Electronics Engineering
St.Anne's College of Engineering and Technology

Abstract

As a result of today's rapid socioeconomic growth and environmental concerns, higher service reliability, better power quality, increased energy efficiency and energy independency, exploring alternative energy resources, especially the renewable ones, has become the fields of interest for many modern societies. In this regard, MG (Micro-Grid) which is comprised of various alternative energy sources can serve as a basic tool to reach the desired objectives while distributing electricity more effectively, economically and securely. In this paper an expert multi-objective AMPSO (Adaptive Modified Particle Swarm Optimization algorithm) is presented for optimal operation of a typical MG with RESs (renewable energy sources) accompanied by a back-up Micro-Turbine/Fuel Cell/Battery hybrid power source to level the power mismatch or to store the surplus of energy when it's needed. The problem is formulated as a nonlinear constraint multi-objective optimization problem to minimize the total operating cost and the net emission simultaneously. To improve the optimization process, a hybrid PSO algorithm based on a CLS (Chaotic Local Search) mechanism and a FSA (Fuzzy Self Adaptive) structure is utilized. The proposed algorithm is tested on a typical MG and its superior performance is compared to those from other evolutionary algorithms such as GA (Genetic Algorithm) and PSO (Particle Swarm Optimization).

1 Introduction

In recent years, the application of alternative energy sources such as wind, biomass, solar, hydro and etc. has become more widespread mainly due to needs for better reliability, higher power quality, more flexibility, less cost and smaller environmental footprints. On the other hand, DGs (Distributed Generations) such as PV (photovoltaics), micro-turbines, fuel cells and storage devices are expected to play an important role in future electricity supply and low carbon economy [1,2]. However, high penetration of DGs into the grid environment will bring new challenges for the safe and efficient power system operation. These challenges can be partially addressed by MG (Micro-Grid) which is defined as an aggregation of DGs, electrical loads and generation interconnected among themselves and with distribution network as well [2e5]. In this regard, the methodologies applied to manage and control the operation of MGs are going through continuous changing in order

MG, in its whole vision, is an exemplar of a macro-grid in which local energy potentials are mutually connected with each other as well as with the L.V utility and make a small-scaled power grid. In such a network, DGs are exploited extensively both in forms of renewable (e.g., wind and solar) and non-conventional (MT (microturbine), fuel cell, diesel generator) resources because these emerging prime movers have lower emission and the potential to have lower cost negating traditional economies of scale [42]. In addition to DGs, storage options are also used widely to offset expensive energy purchases from utility or to store energy during off-peak hours for an anticipated price spike. In a typical MG, DERs generally have different owners handle the autonomous operation of the grid with the help of Local Controllers (mc or MGLC) which are joined with each DER and mcc or MGCC (Micro-Grid Central Controller). Moreover, the CCU (Central Control Unit), which is a part of the MGCC, does the optimization process to achieve a robust and optimal plan of action for the smart operation of the MG. The raw input data to this unit includes the amount of load inside the grid and the powers generated by the nonscheduled DGs typically based on RESs (Renewable Energy Sources) and the output information involves the optimal set points for DGs in terms of suitable ON/OFF states and required active and reactive powers for supplying the load while keeping the node voltages within the range specified by Norm EN 50160 [43].

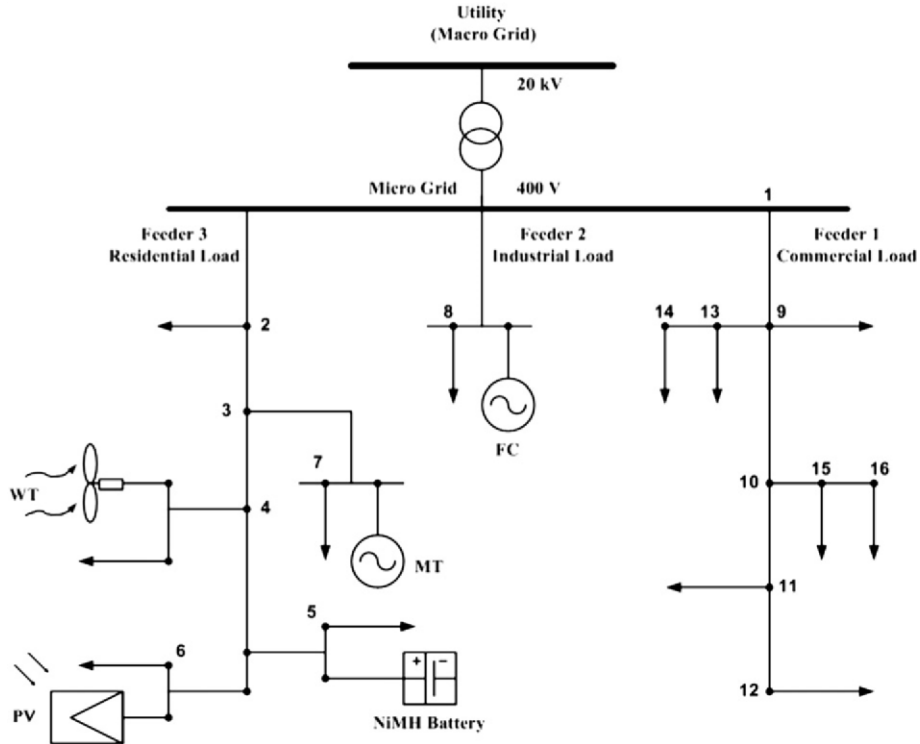


Fig. 1. A typical L.V micro-grid.

2 Simulation results

In this part of the work the proposed AMPSO algorithm is implemented to solve the multi-operation management problem for a typical MG as shown in Fig. 1. Since the two conflicting objectives (cost and emission) must be taken into account and minimized simultaneously, a set of optimal solutions known as Pareto-optimal will be obtained for the mentioned problem. Regarding a Pareto-optimal set, there is a strong need to find the extreme points of the trade-off front and this can be easily done by solving the operation management problem with respect to each objective function separately. Moreover, to get better insight to the extreme points, the problem is solved in three different cases including the main case, where all the units are dispatched regarding their real constraints, the second case in which both RESs (WT and PV) act at their maximum output powers (Max-Renw) and the third case in which the utility can exchange energy with the MG infinitely (Inf-Eneg.Exch). The main reason for selecting such cases is originated from the background knowledge of authors from power market planning and practical considerations in DG management. For the entire cases, the load demand within the MG for a typical day comprises one primarily residential area, one industrial feeder serving a small workshop and one feeder with light commercial consumers which is equivalent to a total energy demand of 1695 kwh for the mentioned day as shown in Fig. 7. The real-time market energy prices for the examined period of time are considered as Table 4. For allocation of optimal set points to the units through the entire case studies, all DGs are considered to be “ON” or in state “1”, thus there will be no start-up or shut-down cost for the mentioned units.

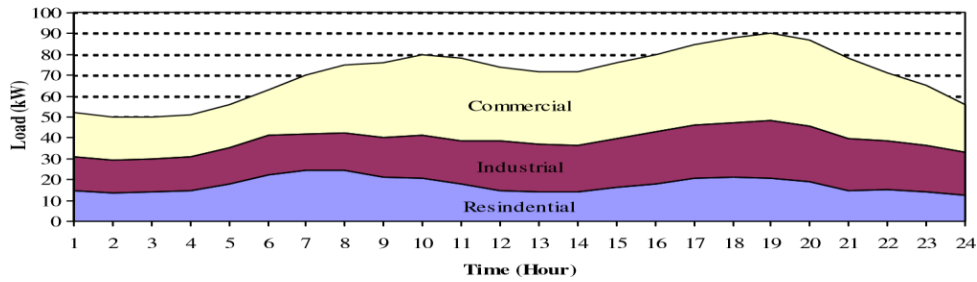


Fig. 7. Daily load curve in a typical Micro-Grid.

Table 4 generation limits of the DGs are given in Table 5. The bid coefficients in cents of Euro (Vct) per kilo-Watt hour (kWh) as well as emissions in kilogram per MWh for DGs are given in Table 6. In the same table, start-up/shut-down costs where applicable are presented. To simplify our analysis, all units in this paper are assumed to be operating in electricity mode only and no heat is required for the examined period. The maximum power outputs obtained from RESs are also estimated for a day ahead using an expert prediction model and neural networks which is out of the scope of this paper and will be presented in future works. Such predicted values are shown in Fig. 8 and tabulated in Table 7 for WT and PV correspondingly. Beyond what has been said, to verify the accuracy of the proposed approach and to make it valid, the authors try to compare the proposed method against an analytical optimization method proposed by Palanichamy et al. [52,53] (see Appendix A).

Table 5 Installed DG sources.

ID	Type	Min power (kW)	Max power (kW)
1	MT	6	30
2	PAFC	3	30
3	PV	0	25
4	WT	0	15
5	Bat	30	30
6	Utility	30	30

Table 6

Bids & s of the DG
emission source s

ID	Type	Bid (Vct/kWh)	Start-up/shut-down cost (Vct)	CO ₂ (kg/MWh)	SO ₂ (kg/MWh)	NO _x (kg/MWh)
1	MT	0.457	0.96	720	0.0036	0.1
2	PAFC	0.294	1.65	460	0.003	0.0075
3	PV	2.584	0	0	0	0
4	WT	1.073	0	0	0	0
5	Batt	0.38	0	10	0.0002	0.001

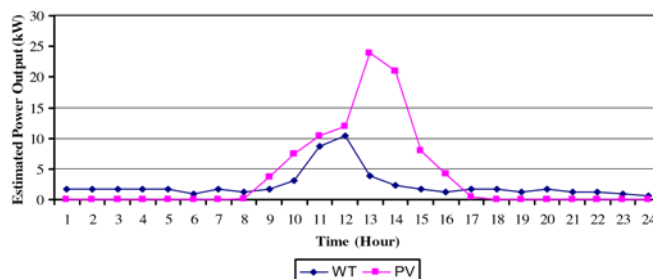


Fig. 8. Forecasted power outputs from RESs.

Table 7 Forecasting output of WT & PV.

h	WT (kW)/installed (kW)	PV (kW)/installed (kW)
1	0.119	0
2	0.119	0
3	0.119	0
4	0.119	0
5	0.119	0
6	0.061	0
7	0.119	0
8	0.087	0.008
9	0.119	0.150
10	0.206	0.301
11	0.585	0.418
12	0.694	0.478
13	0.261	0.956
14	0.158	0.842
15	0.119	0.315
16	0.087	0.169
17	0.119	0.022
18	0.119	0
19	0.0868	0
20	0.119	0
21	0.0867	0
22	0.0867	0
23	0.061	0
24	0.041	0

3 First scenario (Main Case)

In the first scenario it's assumed that all DGs with related characteristics produce electricity within the MG and additional demand or surplus of energy inside the grid is exchanged with the utility from the point of common coupling (PCC). All the units including the macro-grid (utility) can operate just within their power limits while satisfying the needed constraints. Performance evaluation of several optimization algorithms along with their best results in the case of each objective is presented in Tables 8 and 9. In these tables, all the evolutionary optimization methods including the GA, PSO, FSAPSO, CPSO-T (Chaotic PSO based on Tent equation), CPSO-L (Chaotic PSO based on Logistic equation), AMPSO-L (Adaptive Modified PSO based on Logistic equation) and AMPSO-T (Adaptive Modified PSO based on Tent equation) are compared for 20 random trials for both objective functions. For better understanding of the AMPSO performance, the convergence characteristics of AMPSO-L against the standard PSO algorithm for the best solution and in the case of each objective are shown in Figs. 9 and 10 separately. Likewise, the best optimal power allocations to the DGs using the proposed algorithm (AMPSO-L) are presented in Tables 10 and 11 regarding each objective function solutions for both objectives indicates that the proposed AMPSO-L algorithm not only demonstrates a better performance but also presents a faster convergence characteristic. Moreover, the statistical indices of average and standard deviation confirm another advantage of the proposed algorithm in optimization process.

4 Second scenario (Max-Renw)

In the second scenario it's assumed that RESs (WT & PV) are exploited at their available maximum power outputs during each hour of the day and the rests of DGs including MT, PAFC, NiMH Battery and the utility act as in the main case. Again, the entire optimization schemes are applied to the optimization problem and corresponding results are recorded. Tables 12 and 13 show brief comparisons from the performances of the mentioned algorithms regarding each objective for 20 trials. Similarly, the result of economic power dispatch using the proposed approach is indicated

in Table 14. It should be mentioned that the results of environmental power dispatch don't vary greatly among the scenarios mainly due to the fact that all RESs (which have the lowest emissions) are utilized up to their extremes during the examined period. Regarding the second scenario, it's again observed that the proposed algorithm allocates optimal power set points to the DGs appropriately while keeping small diversity in finding the optimal solutions during different trials in the case of each objective. It's also investigated from Table 14 that the operating cost of the MG increases greatly in comparison with the main case and demonstrates a growth of %75.5 in related cost. In other words, although higher penetration of RESs into the grid environment results lower emission, it imposes higher cost of operation.

5 Third scenario (Inf-Eneg.Exch)

In the last scenario, it's supposed that the utility behaves as an unconstrained unit and exchanges energy with the MG without any limitation while the rests of DGs and their related characteristics remain unchanged. Similar to the previous scenarios, all the optimization algorithms are implemented to solve the economic dispatch problem and the simulation results are gathered correspondingly as shown in Tables 15 and 16. The best performance of AMPSO-L in scheduling of the units for a day ahead and in terms of cost objective is also shown in Table 17. Once again, it's observed that the proposed algorithm can solve the optimization problem successfully while maintains small variations in finding optimal solutions considering both objectives. Moreover, the numerical results of Table 17 indicate that allocation of optimal powers to DGs regarding an unlimited power exchange situation ends in a reduction of %42.45 in operation cost of the MG in comparison with the main case. It's also notable that in the third scenario the utility takes the lead in supplying the load inside the grid during the first hours of the day while purchasing energy in bulk amount from the MG during the peak times. From an economical point of view, WT and PV start-up when shortage of power generation occurs inside the grid or there is a need for more energy export to the macro-grid. Likewise, other DGs such as FC, MT and NiMH-Battery adjust their generation set points according to load levels during each hour of the day in an economical manner.

It's observed from Fig. 11 that the non-dominated solutions achieved by the proposed AMPSO-L algorithms are well distributed over the Pareto front although the one from standard PSO lacks this feature. Similarly, through comparison of results obtained by CPSO-T, CPSO-L, FSAPSO and PSO it's concluded that hybrid PSO approaches (e.g., FSAPSO or CPSO) improve the capability of a classic PSO in finding non-dominated solutions to a high extent although there are slight differences between their corresponding performances. It's also important to mention that the performances obtained by the AMPSO-L methods outweigh the ones from other algorithms both in terms of non-dominated solutions and diversity of them along the Pareto front as shown in Fig. 13.

6 Conclusion

In this paper, an expert multi-objective Adaptive Modified PSO (AMPSO) optimization algorithm is proposed and implemented to solve the multi-operation management problem in a typical MG with RESs. A CLS approach is applied to find the best local solutions within the search space and a FSA mechanism is utilized to adjust PSO parameters when they are needed. Moreover, a fuzzy clustering approach is used to control the size of repository for non-dominated solutions. To evaluate the performance of the proposed algorithm several test cases are introduced and the simulation results are gathered subsequently. The numerical results indicate that the proposed method not only demonstrates superior performances but also shows dynamic stability and excellent convergence of the swarms. The proposed method also yields a true and well distributed set of Pareto-optimal solutions giving the system operators various options to select an appropriate power dispatch plan according to environmental or economical considerations.

Tables A.3eA.5 provide the dispatch results of the proposed and the classical methods in the case of economic dispatch, emission dispatch and combined economic and emission dispatch with transmission losses, respectively. For the entire test cases the load demand is fixed to 900 MW. As observed from numerical results, the proposed AMPSO not only demonstrates better results in the case of each single objective but also outweighs in optimal power dispatch regarding both objectives compared to the conventional analytical methods mentioned in Refs. [52,53]. The Pareto-fronts of AMPSO algorithm in the case of both objectives is also shown in Fig. A.2 for the mentioned test system. As an example, it's observed that by applying AMPSO to optimal power dispatch problem the total cost reduces about 1.02 (\$/h) in comparison with the one proposed in Ref. [52] and about 0.93 (\$/h) compared to the Ref[53] regarding the cost objective. Likewise, the net emission inside the grid reduces 0.15 (kg/h) and 0.8 (kg/h) by using the AMPSO algorithm in comparison with Refs. [52,53] considering emission objective solely.

References

- [1] Ayres RU, Turton H, Casten T. *Energy efficiency, sustainability and economic growth*. Energy 2007;32(5):634e48.
- [2] Sanseverino ER, Di Silvestre ML, Ippolito MG, De Paola A, Re GL. *An execution, monitoring and replanning approach for optimal energy management in micro grids*. Energy 2011;36(5):3429e36.
- [3] Niknam T, Zeinoddini Meymand H, Doagou Mojarrad H. *An efficient algorithm for multi-objective optimal operation management of distribution network considering fuel cell power plants*. Energy 2011;36(1):119e32.
- [4] Houwing M, Ajah AN, Heijnen PW, Bouwmans I, Herder PM. *Uncertainties in the design and operation of distributed energy resources: the case of microCHP systems*. Energy 2008;33(10):1518e36.
- [5] Pearce JM. *Expanding photovoltaic penetration with residential distributed generation from hybrid solar photovoltaic and combined heat and power systems*. Energy 2009;34(11):1947e54.
- [6] Hawkes AD, Leach MA. *Cost-effective operating strategy for residential microcombined heat and power*. Energy May 2007;32(5):711e23.
- [7] Dali M, Belhadj J, Roboam X. *Hybrid solarewind system with battery storage operating in grid-connected and standalone mode: control and energy management e experimental investigation*. Energy 2010;35(6):2587e95.
- [8] Pouresmaeil E, Montesinos-Miracle D, Gomis-Bellmunt O, Bergas-Jané J. *A multi-objective control strategy for grid connection of DG (distributed generation) resources*. Energy 2010;35(12):5022e30.
- [9] Sayyaadi H, Babaie M, Farmani MR. *Implementing of the multi-objective particle swarm optimizer and fuzzy decision-maker in exergetic, exergoeconomic and environmental optimization of a benchmark cogeneration system*. Energy 2011;36(8):4777e89.

A 129-level Asymmetrical Cascaded H-Bridge Multilevel Inverter with Reduced Switches and Low THD

A. Annai Theresa, Assistant Professor, Department of Electrical and Electronics Engineering
P. Vivethitha, UG student, Department of Electrical and Electronics Engineering
K. Srilekha, UG student, Department of Electrical and Electronics Engineering
M. Nivetha, UG student, Department of Electrical and Electronics Engineering
St. Anne's College of Engineering and Technology
Panruti, Tamil Nadu, India

Abstract

The multilevel inverter is a power conversion device which uses multiple dc sources to provide required alternating current level. It can be used for medium to high power applications. This paper presents a 129 level asymmetrical cascaded H bridge multilevel inverter with reduced switching components and higher THD. The proposed inverter uses multiple dc sources with voltage ratio 1:1:2:4:8:16:32. The proposed inverter uses voltage reference technique to control the switching components of the topology. The comparative analysis of 129 level ASCHBMLI and conventional inverter topologies have been presented. The main advantages of the proposed topology is lower switching components, lower losses, and lower THD without the need of filter. MATLAB/SIMULINK software is used to perform simulation and analyse the performance of the proposed topology.

Keywords: *Multilevel Inverter (MLI), Asymmetrical Cascaded H Bridge Multilevel Inverter (ASCHBMLI), Cascaded H Bridge (CHB), MATLAB, Total Harmonic Distortion (THD).*

1 Introduction

The basic function of Inverters is to convert DC electricity to AC electricity, for uses in either stand-alone systems or to connect dc source to AC grid. The Multilevel inverters are power electronic method to generate multiple level AC voltages from multiple medium voltage, dc sources. The multilevel inverters were first invented in 1979, as a three level MLI. It gained popularity due its high-power capability and lower THD, lower electromagnetic interference. Due its vast applications, including FACTS drives, VAR control, HVDC, renewable systems etc., MLIs are popular. today more commercial products are based on MLIs. Thus, there is increased efforts in developing multilevel inverters by changing its topology to obtain superior performance, decreased switching losses, lower THD, lower components requirement etc. There are several topologies having distinctive features. Fig.1 shows different multilevel topologies.

The Multilevel inverters are classified into 3 basic types:

- A. Diode clamped multilevel inverter
- B. Flying capacitor multilevel inverter
- C. Cascaded multilevel inverter

The diode-clamped multilevel inverter consists of clamping diode to generate multiple voltage levels through different phases to the capacitors which are connected in series. It requires $(n-1)$ main dc link capacitors and $(n-1)(n-2)$ diodes, where 'n' is number of levels required. Some of the advantages of Diode clamped multilevel inverter are that it has high efficiency for fundamental frequency, it can be used for high voltage back-to-back inter-connection or an adjustable speed drive. However, diode clamped MLI suffers from various limitations.

The maximum output voltage obtained is limited to one half of input DC voltage. The number of diodes required is quadratically equal to number of levels, thus it requires a large number of diodes to generate high number of levels, disturbed charge balance for more than three levels etc.

The Flying capacitor (FC) topology uses a large number of capacitors of equal value. The topology requires a total number of $(n-1)(n-1)/2$ capacitors per phase and $(n-1)$ main bus capacitors. The main advantage of the Flying capacitor topology is that the phase redundancy is achievable for balancing voltage levels of capacitors. The flying capacitor topology suffers from high switching losses, limited output voltage, requirement of large number of capacitors, complex start-up etc.

The advantages of this topology is modular design which makes the manufacturing of inverter, quicker and cheaper than other alternatives. The Cascaded H-Bridge inverters (CHB) are further classified into two categories. Symmetrical CHBMLI uses dc sources of equal magnitude (1:1:1:1:1:1). Hence it requires more dc sources to get higher levels. Asymmetrical CHBMLI uses dc sources of unequal magnitude in the order of (1:1:2:4:8:16:32).

The proposed topology uses 7 dc sources with dc source voltage ratio of 1:1:2:4:8:16:32 and uses voltage reference switching technique is used generate 129 level AC voltage. The design, simulation, and performance are analyzed and presented.

2 Proposed Topology

2.1 Schematic Diagram of Proposed Topology

In conventional MLI topology, the number of levels depends on number of dc sources. In the proposed topology, high level voltage output can be obtained keeping number of dc sources required low. The schematic diagram of the proposed 129 level ASCHBMLI is shown in the Fig 1. The proposed topology consists of fourteen switches, five dc sources. The switches can be MOSFET or IGBT power semiconductor devices. The proposed topology consists of two parts, a h bridge circuit and a level switching circuit. The H-bridge circuit functions as a polarity changing circuit. It changes polarity for every half cycle. In the Fig 1, the switches S7, S8, S9, S10 make up h-bridge circuit. To get positive polarity, S7, S9 are switched on together while S8, S10 are turned off. To get negative polarity, S7, S9 are switched off and S8, S10 are on. The switches, S1, S2, S3, S4, S5, S6 make up level generating circuit. This circuit generates multiple dc output voltage levels based on switching sequences.

The switching sequence is generated by a switching control unit which uses voltage reference switching technique to generate switching pulses, There are 129 different operating modes to generate 129 different output voltage levels for the proposed 129 level ASCHBMLI topology.

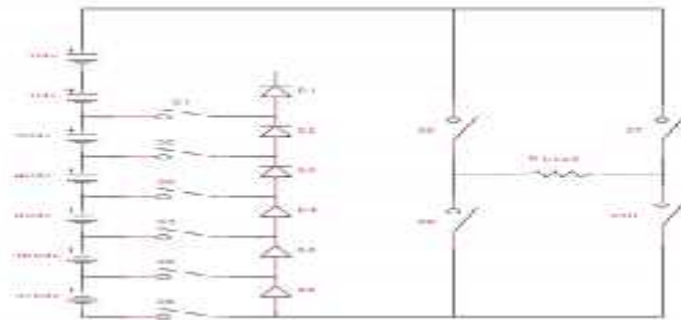


Fig 2. Proposed single phase 129 level ASCHBMLI topology

2.1 Comparative Analysis of Proposed Inverter with Other Topologies

The comparative analysis of different topologies with the proposed topology is given in the table 1. The different parameters compared are number of switches, dc sources, capacitors, diodes. Where, n is the number of levels.

TABLE 1: Comparison of different topologies.

Inverter Topologies	NPC	FC	CHB	Proposed Topology
Number of levels	n	n	n	n
Number of DC sources	1	1	$(n-1)/2$	$\log_2(n-1)$
Number of switches	$2(n-1)$	$2(n-1)$	$2(n-1)$	$\log_2(n-1)+3$
Number of Diodes	$(n-2)(n-1)$	-	-	$\log_2(n-1)$
Number of Capacitors	n-1	$(n-2)(n-1)/2$	-	-

From the table 1, it can be proved that proposed topology can generate 129 level output voltage with lesser number of DC sources, capacitors, power diode. The lesser number of components required reduces the switching losses of the system, reduces the system size, and makes the system cheaper.

2.2 Control Strategy

The switching sequence and the obtained voltage levels of the proposed topology is shown in the table 2 and table 3. The switches S1, S2, S3, S4, S5, S6 are controlled to supply different voltage levels and switching sequence for them is given in the table 2 and H-bridge switches S7, S8, S9, S10 are controlled to reverse polarity and its switching sequence is given in table 3. The switching sequence has 64 positive levels, 64 negative levels with only one '0' level in the output.

The switching control unit provides gate signals to the switches to control the switching states of the circuit. The control strategy is done by a voltage reference technique. In this technique, switching control unit will change the switching angles by comparing a reference signal, the switching pulses are generated by comparing absolute sine wave with multiple DC offset voltages.

The comparator unit compares the absolute sine signal with DC offset values to generate binary values 0 or 1. The comparator outputs are 0, when reference signal is lesser than DC offset and 1, when reference signal is greater than DC offset. If the comparator outputs is 1 at that time, switching angle is achieved.

TABLE 3: Switching States for polarity changing h-bridge inverter

Voltage Polarity	Conducting Switches			
	S7	S8	S9	S10
Positive	1	0	1	0
Negative	0	1	0	1

The switching pulses for the operation of proposed 129 level ASCHBMLI is given the Fig 3

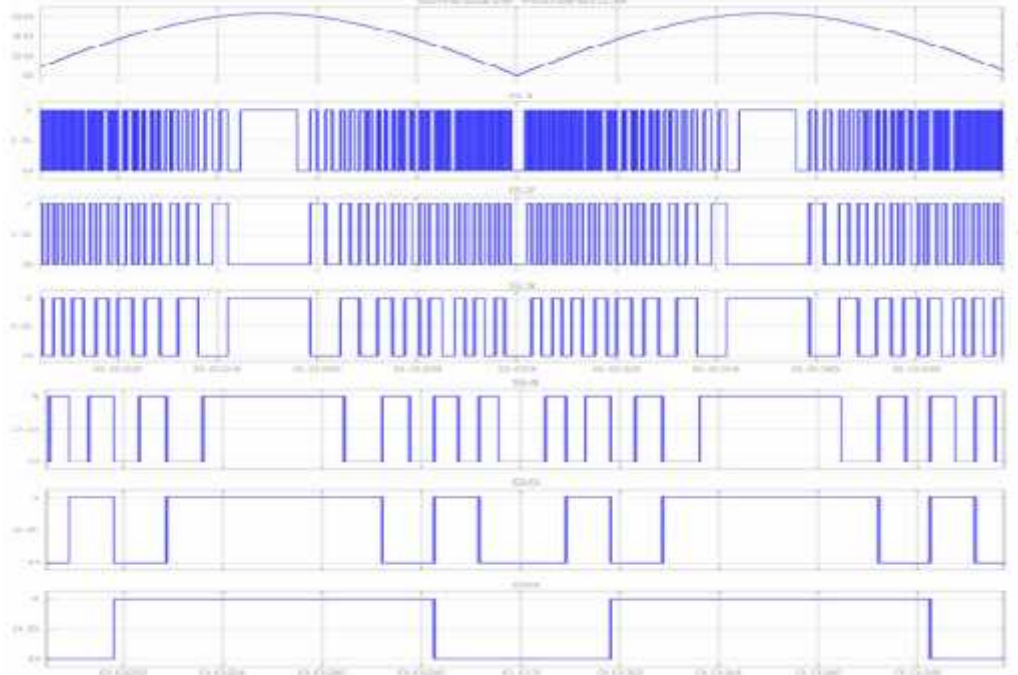


Fig 3. Switching pulse pattern for proposed inverter

3 Simulation and Results

The proposed topology is simulated in MATLAB/SIMULINK software, and performance of the topology in different loading conditions is studied in simulation of topology. Fig 4. shows Simulink model. The output voltage and current waveforms, value of THD and output power is measured. The value of different dc voltage sources are chosen in the ratio of 1:1:2:4:8:16:32 and the value of resistor during

resistive load condition is 45 Ω and during RL loads, the resistors and inductors are 45 Ω and 10mH respectively.

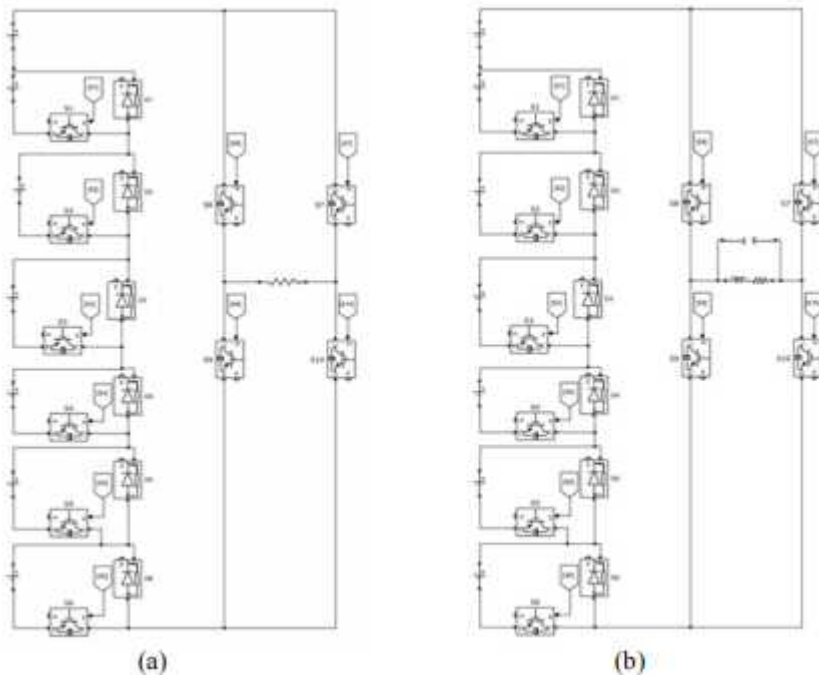


Fig 4. Simulink model of the 129 level multilevel inverter for (a) R Load (b) RL Load

The DC sources in the simulation are of voltage magnitude 5Vdc, 10Vdc, 20Vdc, 40Vdc, 80Vdc, 160Vdc. The inverter generates output voltage of maximum voltage magnitude of 310V and minimum voltage magnitude of -310V. The switches used are IGBT which have fundamental operating switching frequency of 50 Hz. A capacitor of 1.2 μ F is connected in parallel to RL load to reduce the spikes.

The output waveform of 129 level inverter for R Load and R-L Load is given in the Fig 5 and Fig 6 respectively. The peak positive output current is found to be 6.88 A for R load and R-L load

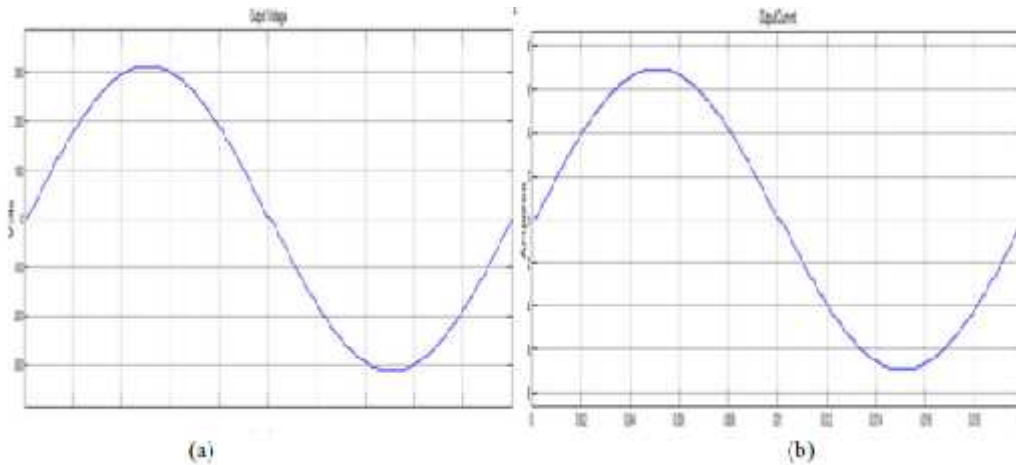


Fig 5. (a) Output voltage waveform (b) Output current waveform for R Load

The Fast Fourier Transform (FFT) is used to calculate the Total Harmonic Distortion of the proposed converter for different loads. The FFT analysis is done for output voltage waveform and current waveform.

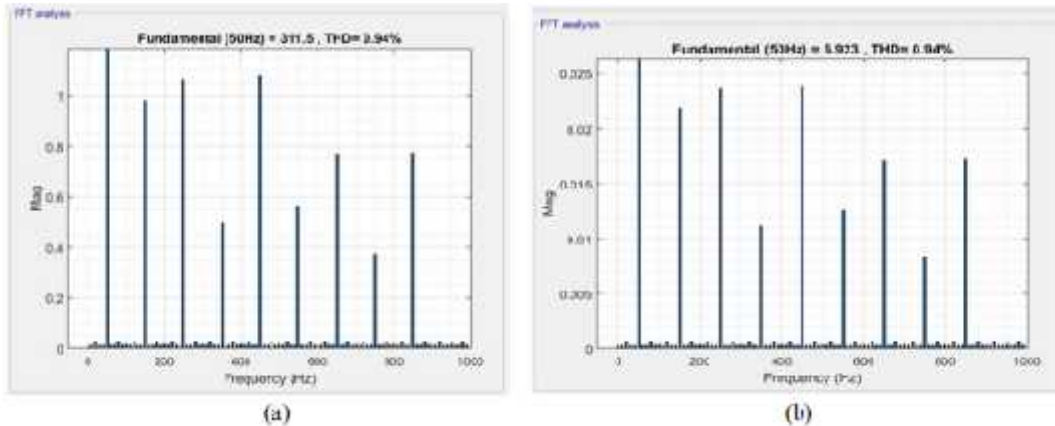


Fig 7. (a) Output voltage THD analysis for R Load (b) output current THD analysis for R Load

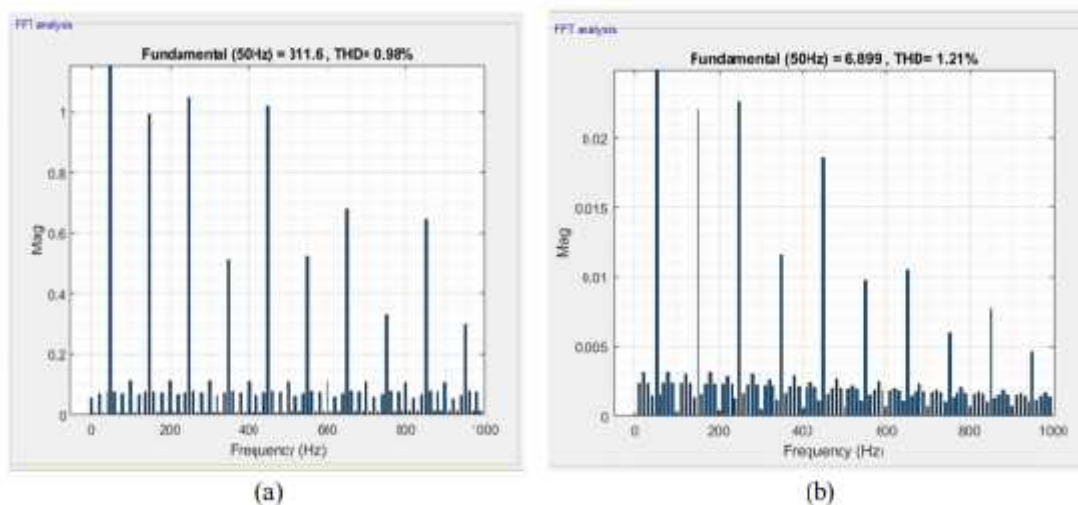


Fig 8. (a) Output voltage THD analysis for RL Load (b) output THD analysis for RL Load

4 Conclusion

The simplified and reduced component cascaded H bridge inverter topology is proposed. The topology produces 129 level output voltage using less switches and lower THD value. The proposed topology has THD value of 0.94 % for voltage wave forms for R load and 0.98% for RL Load which is very less and within IEEE standards. For output currents, the FFT analysis gives THD values of 0.94 % and 1.21 % for R and RL loads respectively. The proposed inverter has output power measured to be 1072W. Due to low THD values and good power capacity, the proposed inverter is suitable for medium to high voltage applications.

References

- [1] Kamaldeep Arjun Tyagi, Himanshu "A New Multilevel Inverter Topology with Minimal Power Electronics Component" 3rd International Conference on Recent Developments in Control, Automation & Power Engineering (RDCAPE), 978-1-7281-2068-3/19/\$31.00 ©2019 IEEE pp-687-692, 2019
- [2] Ponkumar, S.; Rivera, M.; Kamroon, F.; Kumar, S.G. "Realization of cascaded multilevel inverter". In Proceedings of the 2017 CHILEAN Conference on Electrical, Electronics Engineering, Information and Communication Technologies (CHILECON), Pucon, Chile, 18–20 October 2017; pp- 1–7.
- [3] Chacko S. and Thomas J., "THD analysis of multilevel inverter with different loads, International Journal of Advanced Research in Electrical, Electronics and Instrumentation Engineerin" g. Vol-3, No-5, pp-200-201.

- [4] Gautam Shivam Prakash, "Novel H-bridge Based Topology of Multilevel Inverter with Reduced Number of Devices", IEEE Journal of Emerging and Selected Topics in Power Electronics, 10.1109/JESTPE.2018.2881769 ,pp-1-10.2018
- [5] M. Vijayakumar, S. M. Ramesh, "Component Count Reduced, Filter less H-Bridge Multilevel Inverter with Series and Parallel Connected Switches", Journal of Circuits, Systems and Computers, doi:10.1142/S0218126621500523 pp-1-38.

Monitoring the Microgrid using IoT

J.Ramesh, Assistant Professor, Department of Electrical and Electronics Engineering
C.Boobathi, Department of Electrical and Electronics Engineering
K.Mohanraj, Department of Electrical and Electronics Engineering
R.Rasu, Department of Electrical and Electronics Engineering
St.Anne's College of Engineering and Technology
Anguchettypalayam, Panruti,

Abstract

The current microgrid power management system is undergoing a significant and drastic overhaul. The integration of existing electrical infrastructure with an information and communication network is an inherent and significant need for microgrid classification and operation in this case. Microgrid technology's most important features: 1) Full duplex communication; 2) Advanced metering infrastructure; 3) Renewable and energy resource integration; 4) Distribution automation and complete monitoring, as well as overall power system control. A microgrid's communication infrastructure is made up of several hierarchical communication networks. Microgrid applications can frequently be found in numerous aspects of energy consumption. Because it provides a spontaneous communicational network, the Internet of Things plays a fundamental and crucial role in Microgrid infrastructure. This paper covers the deployment of a comprehensive energy management system for microgrid communication infrastructure based on the Internet of Things (IoT). This paper discusses microgrid operations and controls using the Internet of Things (IoT) architecture. Microgrids make use of IoT-enabled technologies, in conjunction with power grid equipment, which are enabling local networks to provide additional services on top of the essential supply of electricity to local networks that operate in parallel with or independently of the regional grid. Local balancing, internal blockage management, and request for support marketplace or grid operator activities are examples of auxiliary services provided by the microgrid that can add value to each end-user and other true stakeholders. Different technologies, architectures, and applications that use IoT as a key element with the main purpose of preserving and regulating innovative smart microgrids in accordance with modern optimization features and regulations are designed to update and improve efficiency, resiliency, and economics.

1 Introduction

For the US Department of Energy, the Microgrid Exchange Collection, an ad hoc collection of research and deployment specialists, created the following widely recognized definition: "A microgrid is a collection of interconnected loads and distributed energy resources that operate as a single controllable entity in relation to the grid and are contained within well-defined electrical boundaries. A microgrid may connect to the grid and disconnect from it, allowing it to function in grid-connected and island modes [1] Three prerequisites are included in this description: 1) The microgrid's neighborhood can be separated from the rest of the distribution system; 2) The resources linked to a microgrid are managed by one another rather than by remote resources; 3) The microgrid can operate whether or not it is connected to the larger grid. There is no mention of the scale of distributed energy resources or the technologies that will or should be implemented in the definition [2].

For balancing local loads and achieving economic advantages, microgrids have specific control needs and techniques. According to the agreement, microgrid controllers must have the following functional characteristics: Present the micro grid to the utility grid as a single self-contained entity capable of providing frequency control (similar to a synchronous generator system); avoiding power flow exceeding line ratings; regulating voltage and frequency within acceptable bounds during islanding; dispatching resources to ensure energy balance; islanding smoothly; safely reconnecting and resyncing [3].

Microgrids can be regulated in the same way as the main grid, that is, using a three-level hierarchical control system. Primary and secondary frequency and voltage regulation are typically performed by a Microgrid Central Controller (MGCC) that sends explicit instructions to distributed energy resources, or in a decentralized manner, such as CERTS, where each resource responds to local conditions [4].

Furthermore, microgrids typically include a tertiary control layer to enable economic and optimization operations for the microgrids, which is primarily focused on managing battery storage, distributed generation scheduling and dispatch, and managing electricity import and export between the microgrid and thus the utility grid. In two European microgrids, one on the Greek island of Kythnos and the other in the German "Am Steinweg" project, hierarchical control systems that regulate electricity inside a microgrid and mediate exchanges with the main grid are installed using a "multi-agent system" method. Increasingly, microgrid research and development is that concentrates on adding intelligence to optimize operational controls and market participation [5]

The ability of microgrids to improve the resiliency and reliability of “critical facilities” such as transportation, communications, beverage and waste treatment, health care, food, and emergency response infrastructure has been the main driver of microgrid development in the United States. The Northeastern United States is one of the main areas of activity, where aging infrastructure and regular extreme weather events have caused billions of dollars in damages in recent years. As a result, states are looking at the possibility of expanding microgrids beyond essential facilities to service entire towns, and they’ve started sponsoring demonstration projects [6]. The “New York Prize”, a \$40 million competition to assist towns on the path from feasibility studies to implementation, is the most famous example of state backing for community microgrids. States in the United States are also considering microgrids as a method to swap out retiring generating capacity and ease congestion in the transmission and distribution system [7].

Figure 1 shows the general components for microgrid system. Several storage systems, Non-renewable power sources and renewable power sources have been used as energy sources.

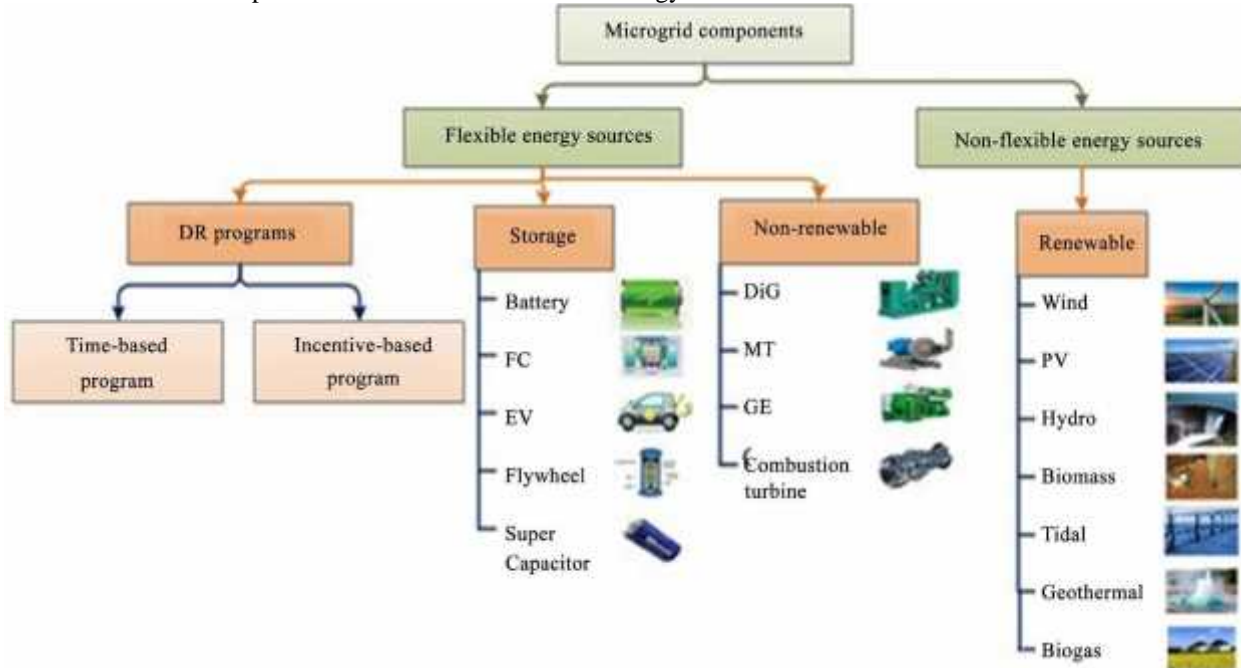


Figure 1. Components of Microgrid.

More important drivers of microgrid activity have been climate change and the necessity to incorporate increasing volumes of renewable electric energy generated into the grid. Climate scientists have also concluded that, by 2050, human society must reduce the proportion of electricity produced by burning fossil fuels from 70% to under 20% to avoid a global average temperature rise exceeding 2°C above pre-industrial levels, which is currently accepted as the threshold between “safe” and “dangerous” climate change. Decentralized, intermittent, and non-dispatchable energy resources are scaling up to fill this gap, making them difficult to incorporate into a grid intended for a one-way flow of power from centralized produced plants to consumer demands. Patchy renewables combined with co-located as well as flexible loads and storage technologies in microgrids allows for local supply and demand balancing, making broad renewable deployment more feasible. To the distribution utility, each microgrid appears as a small power producer or consumer, with the ability to change or vary the net load profile in ways that benefit the main grid the greatest [8]. Microgrid fuel savings and subsidiary grid services are key components of the business case in both locations, despite many disparities in the importance assigned to durability and exhalation. With the support of IoT, new research is being compiled to build microgrids using advanced analytical techniques in order to optimize these advantages over a broad marginal range of parameters, including land usage, water consumption, employment, CO emissions, investment expenses, and energy cost [9]. Microgrids are defined by the International Council on Large Electric Systems as an electricity distribution system that contains loads and distributed energy resources such as distributed generators, spontaneous storage devices, or controllable loads that will operate in a controlled and coordinated manner, either while connected to the main power network or while islanded in a telecommunications network. Following Figure 2, here the overall microgrid system is shown with a vivid diagram.

2 Operation of Microgrid

The Internet of Things (IoT) is allowing businesses to construct smart grids, also known as microgrids, at a lower cost. Organizations can make better use of their power by leveraging this option to disconnect and function on the grid or in island mode. Due to the high integration technique of fashionable technology within a microgrid system, it's difficult to properly operate all the diversity of devices placed during a microgrid using a logically coordinated way. Possible ranked management of microgrids is mentioned. The operational characteristics and classifications of a microgrid area unit are completely different from rate with smaller generation inertia, total variable power generation thanks to RES integration, low fault currents once islanded, and so on. The first management in this framework is for dominant decigram units to have virtual inertias and regulate output electrical phenomena. Secondary management is in charge of correcting the first management loop's steady-state frequency and voltage magnitude mistakes [11]. Superior management is established for facility energy management based on a variety of factors. Such as microgrid stability, environmental issues and concerns, and so on. As a result, in order to achieve strong coordination of this ranking system, a centralized microgrid management method is being developed, in which three controllers are primarily used to control; Microgrid central controller, DER distributed controllers, and Distribution management system DCs work at the device level in the primary and secondary management area units, which are designed to ensure that each DER operates correctly. In microgrids, there are two levels of inertia, which means that each DC must be rapid and dependable in order to keep voltages, frequencies, and power flows within acceptable tolerances and to adjust in real-time to unknown and variable hundreds and network conditions [12]. The microgrid's facility management is decided at the MGCC level of tertiary management based on information from DERs active facility, load demand, and storage requirements. The inter-change of power and energy references or setpoints sent to the DERs and hundreds is enabled by a 2-method communication between the Microgrid management criteria and the DCs, while each individual DC ensures that the facility reference from the central management level is reached. Overall microgrid demands and stabilizing needs are appropriately met at the DMS level. As a result, the MGCC is primarily responsible for microgrid facility optimization, as well as the best management strategies to be conferred in the following section and area unit produced during this entity [13]. Figure 3 shows microgrid operation.

3 Control of Microgrids

Voltage and frequency regulation, real and reactive power control, load forecasting and scheduling, microgrid monitoring, protection, and black start are all part of microgrid control. Primary voltage and frequency regulation, as well as primary real and reactive power control, are all part of the local control and protection level for each local generation and energy storage unit. Distributed generation, energy storage devices, distributional network and loads, as well as hierarchical network control and management, make up an IOT-based Microgrid. Power electronic interfaces and control strategies are utilized to integrate energy from DG to grid. Different works have shown a tendency to employ different techniques to ease network stability control utilizing IOT in this regard. A microgrid can operate in two modes: Grid-connected and Island mode. Both of these modes are requiring in different control mechanisms. Control methods can be classified into two types: Those that involve communication and those that do not. This paper is a brief overview of microgrid control techniques such as Power Quality Control, Energy Management Systems, Optimal Load Scheduling, and Multi-Objective Optimization [14].

3.1. Power Quality Control

The demand for higher power quality has risen as the spectrum of electronic gadgets and LEDs has expanded exponentially. Microgrids are well suited to providing greater power quality since they have the ability to regulate frequency, voltage, and cargo on a domestic level, as well as a quick-responding energy storage system. [15]. Harmonic interferences that emerge as a result of grid-to-star panel connections are decreased by converting the system to an autonomous microgrid. Harmonics created in a microgrid's high-voltage supply electrical converter (VSI) largely based renewable energy supply are filtered using specifically built frequency selective filters. These frequency selective filters are made up of three parts, each of which is a space-vector quantity [16]. By constructing a DC microgrid with a cogeneration system for each house, a residential complex is provided with high-quality electricity and a constant supply. Adjusting the number of co-generation units running will affect the overall power output that is shared across residences. Super capacitors were chosen as the energy storage system in this system. In a very set of grid-interfacing system, the quality series-parallel structure is customized. The series parallel structure, for example, is used to connect the utility grid with a local grid or microgrid. These designs have been compared to

traditional series-parallel systems and microgrid linked systems, demonstrating their versatility [17]. Figure 4 shows the series parallel structure applied for coupling the utility grid and a local grid/micro-grid.

Microgrids will function in both grid-connected and autonomous modes, with management variables that are fundamentally different in each mode. For the best operation of the system to work in two modes, completely separate management methods must be utilized. Two management loops are provided to a microgrid operating in autonomous mode. The PI controllers' inner loop, which is supplied with power and voltage, rejects these high-frequency disturbances and reduces the output filter, avoiding resonance with the external network. The outer loop manages droop by sharing the grid's elemental real and reactive powers with micro-sources [18]. With the goal of improving system stability, an optimization problem is designed for style controllers, filters, and power sharing coefficients. To obtain the best parameters, the particle swarm optimization (PSO) rule is used. Adapting a droop control strategy for the main interconnecting device improves facility sharing between AC and DC in a hybrid microgrid. To improve power sharing by improving droop control features, an adaptive virtual electric resistance management technique is used [19].

By designing a flexible AC distribution system device, an attempt is made to optimize power quality and resiliency of the total facility to which the microgrid is attached. The device style employs a model predictive management rule that optimizes both steady state and transient state management problems separately, reducing process time [21]. The most significant downside of FACTS devices is their high cost. This is frequently overcome by misusing information-based sensible parks. To eliminate voltage imbalance and improve current limitation, a prophetic controller is used in this model. Using a decentralized management strategy, the distributed energy sources are protected against overloading. The MPC is raised using the droop approach in order to create a coordinated operation with rapid dynamic responsiveness [22].

A three-stage hierarchical control system architecture is proposed in the system. Here, the three control levels are:

- 1) Local micro source controllers and load controllers;
- 2) Microgrid system central controller;
- 3) Distribution management system.

3.2. Energy Management Systems

The most important building component of a microgrid to reap all of its benefits is a cost-effective and optimal energy management system. For the most efficient functioning of microgrids, researchers have devised a variety of methodologies and tactics. A MG's Energy Management System (EMS) could be a sophisticated machinecontrolled system largely focused on resource schedule optimization: It can optimize the management of distributed power and energy storage devices within the microgrid thanks to superior information technology. A planning problem's premise is to accurately state load and supply data; a comparative study of wind speed statements is discussed [26].

Intelligent algorithms are used to make recommendations about how devices and systems should be operated for optimal performance. It is proposed to develop an optimum generation planning model for virtual stations (VPP) that takes into account the degradation price of energy storage systems. Because of its manageable and schedulable behavior, the energy storage system is an essential component of a microgrid for flexible dispatch. Following a thorough investigation into the effects of degradation price on optimal VPP planning, it was discovered that day-ahead market rates move significantly less, and batteries with lower degradation prices are sent more frequently by the VPP. A microgrid's energy storage system's capability and size are optimized jointly. The improvement issue considers a variety of practical restrictions. The issue has been fixed piece by piece to save machine time and complexity [27].

A probabilistic model using a revised scenario-based decision-making methodology is used to achieve optimal day-ahead programming of electrical and thermal energy resources. The demand response-aware concurrent energy and reserve programming paradigm has been mentioned. Modeling uncertainty in operational problem solving makes the planned outcomes more realistic. By installing an intelligent energy management system that supports close to correct generating power interpretation and optimum power flow, costs are successfully minimized [28].

The storage states and frequency of renewable energy systems were taken into account using an intelligent technique. In addition, a distributed Intelligent Energy Management System is used to reduce the operational costs of a microgrid based on a model electrical phenomenon. The Fuzzy Adjustive Resonance Theory (ART) map neural network is used to construct a heuristics-based forecast of PV generation as part of the improvement theme. To mimic the unpredictable character of a microgrid, affine arithmetic is used. The random weight trade-off particle swarm improvement algorithmic software lowers the price. To meet operational limits and unpredictable energy demand, the best energy management approach for energy storage is created as a Mixed-Integer Linear Improvement downside (MILP) [29]. The primary goal is to reduce the system's price function, while the secondary goals are to meet customer demand and ensure safety. Before discussing improvement, there is a storage strategy in which the energy state of the

storage system is pre-determined, and another storage strategy in which the storage energy state is defined when a multi-objective improvement problem gives a set of answers. A competent in nursing must select one of them based on his experience and background. The design and operation of a microgrid are multi-objective improvements that have been optimized. By using fuzzy satisfaction-maximizing methods, the multi-objective improvement problem is reborn as a single improvement problem. The resurrected disadvantage is victimization MILP [30].

For power mercantilism, an attempt is made to model associate in nursing energy mercantilism system. The model has two stages: The planner and the short-time equalization mechanism. The Planner envisions the programming of many predefined activities in order to achieve partial demand aspect management and obtain statistics on ability usage. The Planner also calculates background usage and projects the ability to produce energy from renewable sources. In a Short-Time Equalization System, a multiagent, distributed system manages governable sources to achieve power balance in a short period of time. When the energy management problem of two cooperative microgrids is addressed, a new idea of energy cooperation is planned. The improvement is initially obtained via an off-line manner. Associate in nursing on-line improvement methodology is produced to support the solutions obtained for energy collaboration [31].

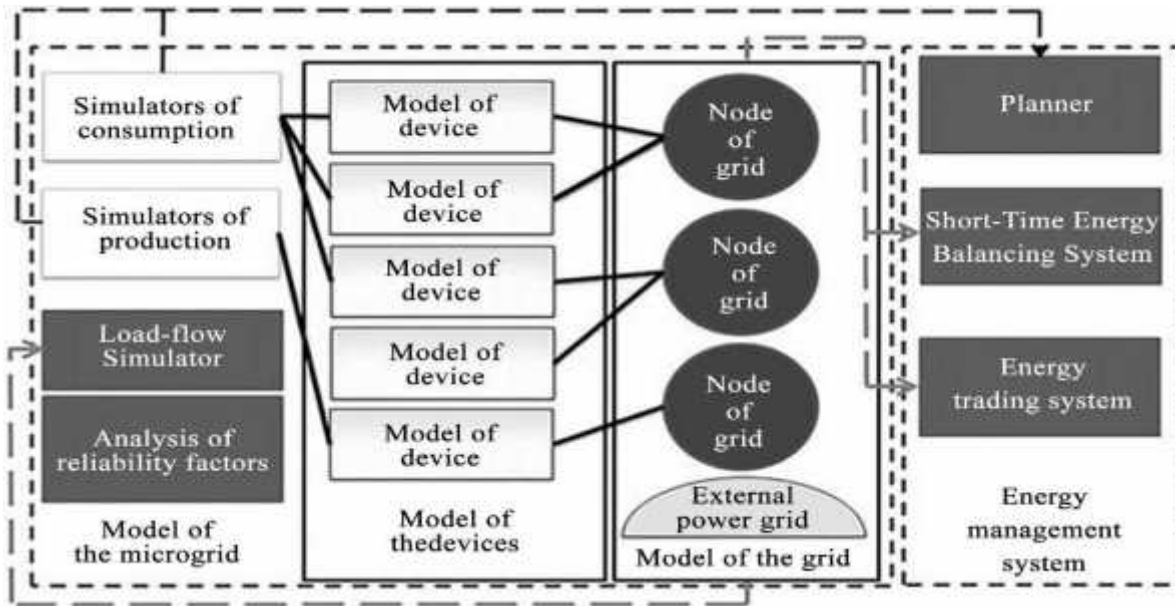


Figure 2. The general structure of two stage optimization system.

4 Conclusion

An expanded outcome for IoT-based microgrids will aid us in the use of electronic power energy in the near future. Microgrids with IoT will distribute renewable energy resources in each grid in a way that is both compatible and comprehensive. Many different improvement techniques and intelligent improvement algorithms will be required in the area unit, each with its own set of benefits and drawbacks. If we can use IoT to operate microgrids, the adaptability will be greatly improved. In the near future, the procedure will require more improvements. Because this procedure is entirely reliant on wireless commands, the cost of connecting gear will be significantly reduced. Microgrids will also be more appealing to people all around the world.

Acknowledgements

Avoid the stilted expression, “One of us (R. B. G.) thanks...” Instead, try “R. B. G. thanks”. Do NOT put sponsor acknowledgements in the unnumbered footnote on the first page, but here. Authors would like to thank the Department of Electrical and Computer Engineering of North South University.

References

- [1] Mohan, V., Suresh, R., Singh, J.G., Ongsakul, W. and Madhu, N. (2017) Microgrid Energy Management Combining Sensitivities, Interval and Probabilistic Uncertainties of Renewable Generation and Loads. *IEEE Journal on Emerging and Selected Topics in Circuits and Systems*, 7, 262-270. <https://doi.org/10.1109/JETCAS.2017.2679030>
- [2] De Leone, R., Giovannelli, A. and Pietrini, M. (2016) Optimization of Power Production and Costs in Microgrids. Springer-Verlag, Berlin. [32] Chen, J., et al. (2018) Optimal Sizing for Grid-Tied Microgrids with Consideration of Joint Optimization of Planning and Operation. *IEEE Transactions on Sustainable Energy*, 9, 237-248. <https://doi.org/10.1109/TSTE.2017.2724583>
- [3] Radziszewska, W. and Nahorski, Z. (2016) Microgrids and Management of Power. In: *Challenging Problems and Solutions in Intelligent Systems*, Springer, Cham, 161-178. https://doi.org/10.1007/978-3-319-30165-5_8 [34] Kondoro, A., Dhaou, I.B. and Tenhunen, H. (2020)
- [4] Enhancing the Security of IoT-Enabled DC Microgrid Using Secure-MQTT. 2020 6th IEEE International Energy Conference (ENERGYCon), Tunis, 28 September-1 October 2020, 29-33. <https://doi.org/10.1109/ENERGYCon48941.2020.9236448>
- [5] Rahbar, K., Chai, C.C. and Zhang, R. (2018) Energy Cooperation Optimization in Microgrids with Renewable Energy Integration. *IEEE Transactions on Smart Grid*, 9, 1482-1493. <https://doi.org/10.1109/TSG.2016.2600863>
- [6] Kerdphol, T., Qudaih, Y., Watanabe, M. and Mitani, Y. (2016) RBF Neural Network-Based Online Intelligent Management of a Battery Energy Storage System for Stand-Alone Microgrids. *Energy, Sustainability and Society*, 6.

Power Loss Reduction and Voltage Profile Improvement Using Optimal Placement of FACTS Devices

M.Prema Latha, Assistant Professor, Department of Electrical and Electronics Engineering
S.Kannan, UG Student, Department of Electrical and Electronics Engineering
G.Sampathkumar, UG Student, Department of Electrical and Electronics Engineering
K.Surendhar, UG Student, Department of Electrical and Electronics Engineering
St. Anne's College of Engineering and Technology, Panruti.

Abstract

The crucial role of an electric power system is to generate sufficient electricity to meet customer demands with an acceptable level of reliability in an economic manner. In recent years, Flexible AC Transmission Systems (FACTS) devices have been widely used to increase power system operation flexibility and controllability to meet this need. This paper presents an application of Differential Evolution (DE) to optimise the allocation of a Thyristor Controlled Series Capacitor (TCSC), a Static Var Compensator (SVC), and Unified Power Flow Controller (UPFC), as example FACTS devices. The objective of the research was to reduce power losses and improve the voltage profile in an IEEE 30-bus test system. The system performance was assessed with and without each FACTS device under different scenarios of load increase at up to 150% of the base case. The results obtained are encouraging in terms of reassessing electrical restructuring.

1 Introduction

Electric power production and distribution companies are constantly looking for new industrial technologies to contribute to improving energy supplies to consumers that can overcome the problems of increased demand for electric power and the disruption of recent fuel price increases. In recent years, many of these companies have increased their interest in the use of FACTS device technologies, which offer an effective way to improve the stability, reliability and capability of electric power transmission systems in traditional networks without the need to establish new transmission lines [1]. FACTS devices make power flow in transmission systems more flexible by controlling the active and reactive power flows in the transmission lines. The flow of electrical energy in AC transmission lines depends on the size of the wire, the line's intrinsic resistance, and the phase angle between the transmitting and receiving ends of the transmission line [2]. However, although the addition of FACTS devices generally improves the performance of electric power transmission networks, it also adds several technological and economic complications in terms of control, maintenance, and costs [3]. Identifying the optimal location and sizing of FACTS devices may, however, help address these issues, and thus a significant amount of research has been conducted to identify the best use of FACTS devices.

In [4], modelling of the best location for the installation of FACTS devices in an electric power transmission network was discussed, while in [5], FACTS devices were added to power systems suffering from congestion due to overloads; in that case, the locations and sizing of the FACTS devices were determined based on those factors considered to be most sensitive based on the nature of the load. In [6], an adaptive genetic algorithm was used to determine the best allocation of various types of FACTS devices, with the aim of that study being to reduce costs by reducing system losses. Researchers in [7] addressed increasing power transmission capacity by applying PSO technology to reducing system losses and improving line voltage, while in [8], the researchers sought to reduce system losses by adding various types of FACTS devices to power transmission systems. It was thus deduced that the economic cost of adding these devices was offset by a reasonable percentage reduction in total energy losses. In [9], the performance of a power transmission system without the use of FACTS devices and with several types of such device was compared. An artificial intelligence technique was used to determine the best location and size for the relevant FACTS devices, which reduced losses and improved the voltage profile; in addition, the economic costs were calculated in each case and compared with those for the system without FACTS devices.

The current work is divided into several parts as follows: in section 2, a brief overview of FACTS technologies and types is presented, while in section 3, the basic principles of the DE improvement method are reviewed. The methodology used in this study is presented in section 4 and the results of the study are reported in section 5. Finally, these results are discussed in section 6.

2 FACTS Devices

The integration of FACTS devices with transmission systems offers many benefits, including increased transmission system reliability, increased transient and dynamic stability in a network, reduced loop fluctuations, increased supply quality to sensitive loads, increases in the fixed limits of transmission lines, and some environmental benefits [10].

FACTS devices are generally classified according to their purpose or according to their connection to the network; this means that they may be series controllers, shunt controllers, combined series-shunt controllers. Depending on their technological features, they are also divided into two generations: the first generation uses Thyristor ignition gate controls (TCR), while the second generation uses ignition semiconductors and portal-controlled extinction (GTO, IGBTs, MCTS, IGCTS, etc.). The primary difference between the two generations is the latter's ability to facilitate reactive active exchange energy and power generation [11].

Three main FACTS devices, identified by their method of connection with the transmission networks, were analysed and studied as shown in Figure 1. The serial controllers were used in cases of disturbed voltages, with series voltage injected at the connection point to correct the voltage level. In the shunt controllers, an electric current is injected into the contact point to compensate for active power throughout the system, while in combined series-shunt controller FACTS devices, the electric current is injected at the shunt portion of the controllers and the series voltage is injected at the serial portion in the same controller [12]. The FACTS devices discussed in this paper are thus

TCSC (Thyristor Controlled Series), which uses a series of capacitor modules running in parallel with a thyristor (TCR). The TCR controls the capacitive reactance smoothly and over a wide range, and the two-way thyristor pairs operate continuously to introduce inductive reactance on the line according to their instructions. This type of device is used to control line overloads.

SVC (fixed VAR compensator), which is a device used to improve high-voltage electricity transmission lines by providing fast acting reactive energy. SVCs regulate voltage and increase the stability of the system. SVCs also have no moving parts other than separate circuit breakers. Previously, power compensation was done by adding a large number of capacitors simultaneously; the SVC instead uses the reactors to consume VAR from the system if the load is reactive, thus controlling the system voltage as the banks switch capacitor automatically.

UPFC (Unified Power Flow Controller), which is one of the most widely used types of FACTS device in terms of transmission systems. These have the ability to set bus voltages within the required levels, controlling the transmission line reactance and phase angle between two buses independently. The UPFC controls these three parameters by including a control voltage in phase, a square voltage, and shunt compensation. The use of this type of device thus offers major advantages in terms of the dynamic operation of transmission lines based on its real-time and dynamic control compensation for AC power transmission systems

3 Differential Evolution Techniques

Several artificial intelligence techniques may be used to identify optimal solutions to nonlinear problems. One of these techniques is the Differential Evolution (DE) technique, which is based on optimising random parameter algorithms [13]. Storn and Price laid down the basic principles of this innovative method for solving nonlinear optimisation problems in 1995, creating a less random approach to achieving the required results as compared to classical methods, and thus increasing efficiency. The DE method is generally used initially to find the optimum point in a D-dimensional parameter space. The first operation of the DE algorithm is the creation of an initial population (NP) of D-dimensional parameter vectors. Each vector in this population is randomly initialised within certain limits for each parameter.

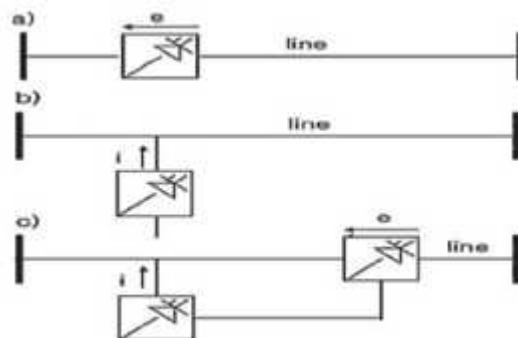


Figure 1. Block diagram of various types of FACTS devices: a) series controller, b) shunt controller, and c) combined series-shunt controller.

The vectors of the current generation are known as the target vectors, which are then mutated to produce donor vectors, a process implemented by randomly selecting three vectors from the population, with the scaling of any two of the vectors applied to the third vector. The new trial vectors are then generated using exponential or binomial crossover methods, and a comparison is made between the trial vector and the target vector to allow selection of the best vector to transfer to the next generation based on a pre-set fitness value. Figure 2 represents the basic stages used in the DE method.

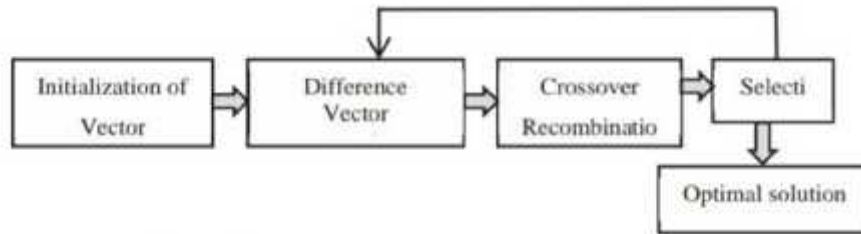


Figure 2. Basic stages of the DE method.

The algorithm thus creates a random population of size (NP) and a floating point for each solution, allowing each individual to act as a candidate solution, as in Equation 1.

$$P^{(G)} = [X_1^{(G)}, \dots, X_i^{(G)}, \dots, X_{NP}^{(G)}]$$

The DE method preserves the population $P^{(G)}$ in each generation (NP) for each nominee solution (X_i). A nominee solution (X_i) is an integer value within the D-dimensional vector that depends on decision parameters (D), as given in equation 2.

$$X_i^{(G)} = [X_{1,i}^{(G)}, \dots, X_{j,i}^{(G)}, \dots, X_{D,i}^{(G)}], i = 1, \dots, N_p, j = 1, \dots, D \quad (2)$$

4 The Proposed Approach

After installing FACTS devices in the most appropriate location in an electric power transmission lines, the entire system must maintain acceptable limits of active and reactive power. These limitations are described in equations 3 to 5 [14].

$$P_{ni}^{min} \leq P_{ni} \leq P_{ni}^{max} \quad (3)$$

$$Q_{ni}^{min} \leq Q_{ni} \leq Q_{ni}^{max} \quad (4)$$

$$V_i^{min} \leq V_i \leq V_i^{max} \quad (5)$$

To achieve the objective of this research, which is to reduce the total losses of the system and improve the profile of the voltage, action steps as outlined in Figure 3 were applied.

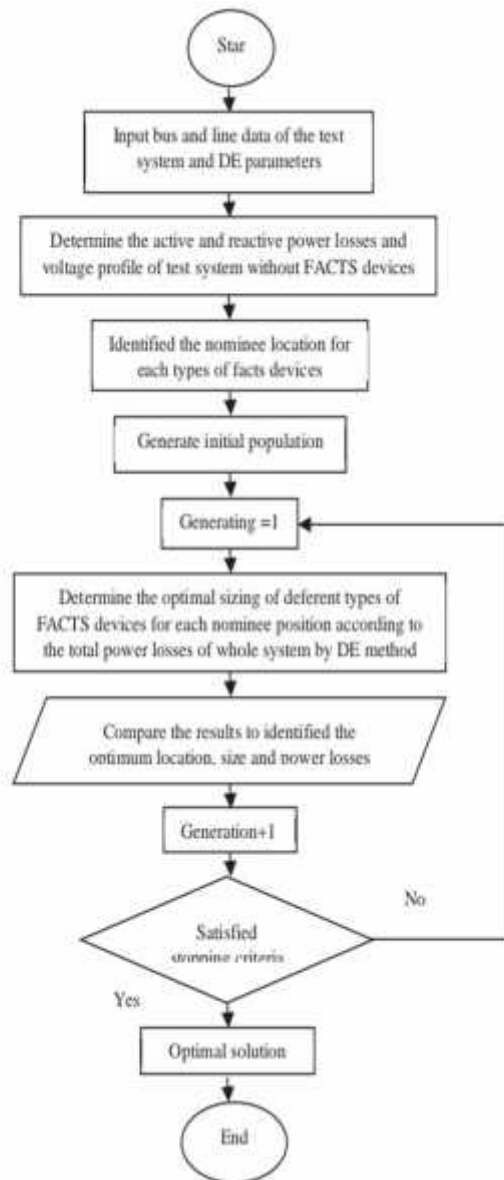


Figure 3. Flowchart of action steps

5 Results

5.1 Optimal location

The active and reactive electrical energy of the IEEE 30 test system was calculated based on the power flow for each transmission line (41 lines) using the Newton-Raphael method; the transmission lines with the highest levels of active and reactive power were thus identified as candidate sites for the initial installation of FACTS devices. The total load of the test system was increased in three steps (100%, 125%, and 150%) from the base case by increasing the total load connected to the slack bus.

The lines 6, 7, and 4 have the highest active power flows in the system. These lines are connected between buses 2-6, 4-6, and 3-6, respectively; these lines are thus nominees for UPFC devices. Transmission lines 41, 25, and 18 have the largest reactive power flows, making them candidate locations for the installation of TCSC devices. To find the best locations to install SVC devices, the busses connected to the ends of the transmission lines that have the second-highest reactive capacities were identified. From Table 1, lines 27, 26, and 9 have the second highest reactive power flows in the test system, making buses 17, 7, and 2 the best locations for the proposed device. Table 1 shows the nominee buses and lines for the various types FACTS devices.

Table 1. Nominee locations for various FACTS devices

Type of FACTS	Candidate position		
	1 st position	2 nd position	3 rd position
UPFC	Line 6 (2-6)	Line 7 (4-6)	Line 4 (3-4)
TCSC	Line 41 (6-28)	Line 25 (10-20)	Line 18 (12-15)
SVC	Bus 17	Bus 7	Bus 21

5.2 Optimum size

To determine the optimum size of the UPFC, TCSC, and SVC devices, the DE optimisation method was applied with the parameters shown in Table 3. The total power losses of the test system with the FACTS devices added were then calculated. The data for the test system were taken from [15], where an IEEE 30-bus test system consisting of six generating units and 41 transmission lines was developed and tested. The total power losses of the system from that work are thus 17.5280 MW and 68.8881 MVar.

Table 3. DE Parameters

Differential valuation parameters	
Variable Size D*5	15
Maximum Generation (Gen max)	100
Crossover Probability (Ω_c)	0.9
Mutation probability (Ω_m)	0.2
Initial size range	0-10

Table 4 illustrates the power losses in the test system with the relevant UPFC devices. Line 4, between buses 3-4, is clearly the optimum location for a UPFC device of 9.854 MW, as this causes the total active and reactive power losses of the test system to become 15.755, 16.198, and 16.743 MW and 61.227, 62.516, and 62.854 MVar, respectively, when the test system is increased by 100%, 125%, and 150%.

Table 4. Power losses of the test system with UPFC devices.

UPFC Location	UPFC Size MW	Total losses Loading 100%		Total losses Loading 125%		Total losses Loading 150%	
		MW	MVar	MW	MVar	MW	MVar
Line 6 (2-6)	9.8624	15.817	61.457	16.201	62.544	16.761	62.874
Line 7 (4-6)	9.7851	15.921	61.389	16.311	62.672	16.788	62.911
Line 4 (3-4)	9.8546	15.755	61.227	16.198	62.516	16.743	62.854

Table 5 illustrates the results of the test system with TCSC devices. Here, line 41, connected between busses 6-28, is the optimal placement of a device of 9,640 MW, whereby the total active power losses of the test system become 15.531, 15.764 and 15.934 MW, while the reactive power losses become 63.560, 63.865, and 64.706 MVar during successive load increases

Table 5. Power losses of the test system with TCSC devices.

TCSC Location	TCSC Size MW	Total losses Loading 100%		Total losses Loading 125%		Total losses Loading 150%	
		MW	MVar	MW	MVar	MW	MVar
Line 41 (6-28)	9.640	15.531	63.560	15.764	63.865	15.934	64.706
Line 25 (10-20)	9.476	15.592	63.578	15.772	63.893	16.247	64.844
Line 18 (12-15)	9.600	15.603	63.564	15.816	64.101	16.312	64.937

It is clear that bus 21 is the optimal location for an SVC device of 9,720 MW. The total test system active and reactive power losses are then 14.897, 15.674, 15.864 MW, and 62.015, 63.278, and 64.214 MVar, respectively, with the various different loadings.

As shown in Figure 4, the voltage profile of the whole test system is improved significantly after the installation of all different types of FACTS devices. However, the SVC device achieves the best improvement in the voltage profile of the test system.

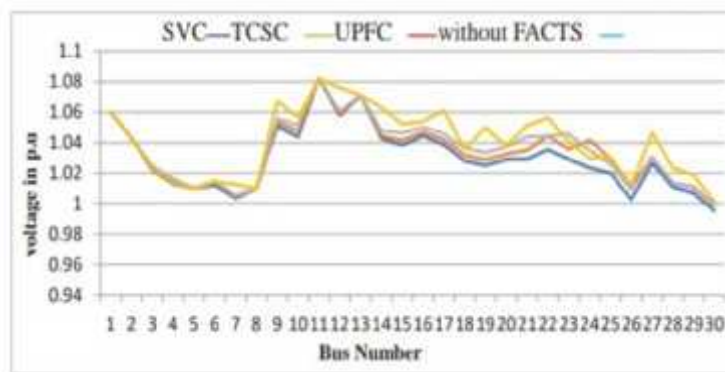


Figure 4. Comparison of voltage profiles.

6 Conclusion

In recent years, there has been an increase in interest from electric power generation and distribution companies in FACTS devices, which can provide tremendous technological advantages when used correctly. In this research, three basic types of FACTS devices with different total loads were studied in order to assess their improvement of the performance of a test system. The addition of UPFC devices in the optimum location (line 4) reduced the active and the reactive losses of the system to 15.755, 16.198, and 16.743 MW and 61.227, 62.516, and 62.854 MVar, respectively, while the installation of TCSC devices in transmission line 44 reduced the losses to 15.531, 15.764, and 15.934 MW for active power and 63.560, 63.865, and 64.706 MVar for reactive power. Bus 21 was found to be the best place to install an SVC device, with total active and reactive power losses of 14.897, 15.674, and 15.864 MW and 62.015, 63.278, and 64.214 MVar, respectively, with varying loads.

References

- [1] Akpeke, N. E., Muriithi, C. M., & Mwaniki, C., "Contribution of FACTS devices to the transient stability improvement of a power system integrated with a PMSG-based wind turbine". Engineering, Technology & Applied Science Research, 9(6), 4893-4900, 2019.
- [2] Lal, D. K., & Barisal, A. K., "Comparative performances evaluation of FACTS devices on AGC with diverse sources of energy generation and SMES", Cogent Engineering, 4(1), 1318466, 2017.
- [3] D.J.Gotham and G.T.Heydt, "Power Flow Control and Power Flow Studies for system with FACTS Devices,"IEEE Trans on Power System, Vol 13, No 1, February 1998.

- [4] Gerbex, S., Cherkaoui, R., & Germond, A. J. (2001). Optimal location of multi-type FACTS devices in a power system by means of genetic algorithms. *IEEE transactions on power systems*, 16(3), 537-544.
- [5] Singh, S. N., & David, A. K., "Optimal location of FACTS devices for congestion management", *Electric Power Systems Research*, 58(2), 71-79, 2001.
- [6] Radu, D., & Besanger, Y., "A multi-objective genetic algorithm approach to optimal allocation of multi-type FACTS devices for power systems security", In 2006 IEEE Power Engineering Society General Meeting (pp. 8-pp). IEEE, June 2006.
- [7] Gaur, D., & Mathew, L., "Optimal placement of FACTS devices using optimization techniques: A review", In 3rd International Conference on communication Systems, IOP Conference Series, Material Science and Engineering (pp. 1-16), March 2018.
- [8] Bhattacharyya, B., & Kumar, S., "Loadability enhancement with FACTS devices using gravitational search algorithm", *International Journal of Electrical Power & Energy Systems*, 78, 470-479, 2016.
- [9] Aghaebrahimi, M. R., Golkhandan, R. K., & Ahmadnia, S., "Localization and sizing of FACTS devices for optimal power flow in a system consisting wind power using HBMO. In 2016 18th Mediterranean Electrotechnical Conference (MELECON) (pp. 1-7). IEEE, April 2016.
- [10] Malatji, E. M., Twala, B., & Mbuli, N., "Optimal placement model of multi- type FACTS devices in power system networks on a limited budget", In 2017 IEEE AFRICON (pp. 1296- 1300). IEEE, September 2017.
- [11] Malatji, E. M., Twala, B., & Mbuli, N., "Comparison of Different Optimal Placement Models of FACTS Devices in Power System Networks on a Limited Budget", In 2019 7th International Conference on Smart Grid (icSmartGrid) (pp. 108-112). IEEE, December 2019.
- [12] Chirantan, S., Swain, S. C., Panda, P. C., & Jena, R., "Enhancement of power profiles by various FACTS devices in power system", In 2017 2nd International Conference on Communication and Electronics Systems (ICCES) (pp. 896-901). IEEE, October 2017.
- [13] Caraffini, F., & Kononova, A. V., "Structural bias in differential evolution: A preliminary study", In AIP Conference Proceedings (Vol. 2070, No. 1, p. 020005). AIP Publishing LLC, February 2019.
- [14] Elmitwally, A., & Eladl, A., "Planning of multi-type FACTS devices in restructured power systems with wind generation", *International Journal of Electrical Power & Energy Systems*, 77, 33-42, 2016.
- [15] Barrows, C., Bloom, A., Ehlen, A., Ikäheimo, J., Jorgenson, J., Krishnamurthy, D., ... & Staid, A., "The IEEE reliability test system: A proposed 2019 Update", *IEEE Transactions on Power Systems*, 35(1), 119-127, 2019

A Novel Circuit for Battery Charging and Motor Control of Electric Vehicle

V. Balaji, Assistant Professor, Department of Electrical and Electronics Engineering
K. Bhuvaneshwaran, UG student, Department of Electrical and Electronics Engineering
M. Muralikrishnan, UG student, Department of Electrical and Electronics Engineering
V. Vijay, UG student, Department of Electrical and Electronics Engineering
St. Anne's College of Engineering and Technology

Abstract

A new method of battery charging and motor controlling of an electric vehicle (EV) is disclosed in this paper. The entire system consists of two major divisions, those are, EV charger and motor controller, which determine the arrangement of the battery, acting as load or source, and the motor that comes into action during the driving mode. Both the charging and motor control can be performed by two separate highly efficient DC-DC converters named as TA converter which is a Buck-Boost by its nature. While charging a battery it is necessary to make the charging process effective. Microcontroller employs to control all parameter of EV in all conditions. When the motor draws over current, the invented circuit will be tripped through the microcontroller. The supply for the charger will be either from the renewable source or rectified output from the grid.

Keywords : *Electric Vehicle, DC-DC Converter, PI & Hysteresis Controller*

1 Introduction

In the current world the technologies and equipment's are improving in a fast-accelerating speed. However, the wasteful emission from these equipment's is a humongous problem towards the society and Environment. Also, nowadays fuel consumption is at its peak. Time will come when the natural resources will be exhausted. Many vehicle manufacturing companies have already started working on hybrid electric vehicles to avoid the foreseeable future to some extent. An EV is a gift to the nature observing the rate of increase in pollution caused due to various human activities. Several new topologies were designed with different gain and variation in voltage range. LUO converter provides complex model with a high gain converter [8]. Some other non-isolated converters such as CUK, SEPIC can provide multiple drawbacks to buck-boost converters and can't provide positive output voltage as well [9, 4]. Maksimovik and Cuk suggested a converter having a gain of $\frac{D^2}{(1-D)^2}$, which is able to operate only in buck mode because of the clamping diodes D1 and D2 [9]. P. N. Ekemezie suggested that Compared to conventional dc-dc converters, two-switch buck-boost converter is more efficient because of low voltage stress across the switches [5]. A transformer less buck-boost converter with a voltage gain square time of conventional Buck-boost converter has been purposed by Shan Miao which has a drawback that it carries negative inductor current [7]. Markel and Simpson addressed with various operational approaches the battery capacity and energy needs for grid powered parallel Hybrid Electric Vehicles (HEVs) [10]. Bauml and Simic developed a sequence of hybrid simulations of electric vehicles using the language of simulation Modelica [11]. Divya and Jacob purposed a possible potential scenario in the sense of power device systems for the battery developments and the electric hybrid vehicles [12]. A two switch non isolated Buck-Boost converter which has a better performance than the conventional Buck-Boost Converter also known as TA converter has been purposed by Tapas Kumar Mohapatra and Asim Kumar Dey [2, 3]

Here the authors are attempting to use an efficient Buck-Boost Converter (BBC) i.e. the TA converter which is a new topology of BBC, for the purpose of charging the batteries and controlling the motor current of an EV, which has a gain $\frac{D^2}{(1-D)^2}$ [1, 2 and 3]. This BBC also provides a positive output voltage and positive inductor current that is not generated by other BBCs. This converter can provide the required output voltage for any range of input voltage variation. As most of the EVs are designed using 12 volt rated batteries and the voltage rating of available

Solar plates fluctuating between 6 to 30 volts, a Buck-boost converter is suitable to use as a charger for the EV batteries. As TA converter overcomes almost all the drawbacks of other buck boost converters and charging the batteries of EV with motor current controller to control the output current to PMDC motor. Hysteresis current control technique is one of the robust control techniques and also provides several benefits as suggested by [6]. So, hysteresis current control is implemented as current control technique. Hardware testing of both the

EV charger and motor controller circuit has been performed with proper control techniques using DSP board. The article is organized as following. Section-II contains brief discussion of TA converter along with its circuit diagram. Section-III contains how TA converter can be operated as Battery charger. Section-IV contains how TA converter can be operated as motor current controller. In section-V & VI the simulation and hardware results are Discussed.

2 Dc-Dc Buck-Boost (TA) Converter

A DC-DC converter is an electrical power converter that changes the output level of a DC source voltage to another. Applications vary from very low (small batteries) to very high (high-voltage transmission) power.

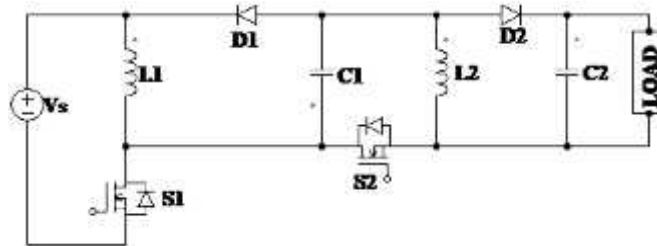


Fig 2.1: Schematic diagram of new Buck-Boost (TA) Converter

When both the switches are ON (act as short circuit), the diodes are reverse biased (act as open circuit) and current will flow through the path 'VS L1 S1 VS' and 'C1 S2 L2 C1'.

$$V_{L1} = V_s \Rightarrow L_1 \frac{dI_{L1}}{dt} = V_s \Rightarrow \frac{dI_{L1}}{dt} = \frac{V_s}{L_1} \quad [1]$$

$$V_{L2} = V_{C1} \Rightarrow L_2 \frac{dI_{L2}}{dt} = V_{C1} \Rightarrow \frac{dI_{L2}}{dt} = \frac{V_{C1}}{L_2} \quad [2]$$

$$V_0 = V_{C2} \quad [3]$$

When both the switches are OFF (act as open circuit), the diodes are forward biased (act as short circuit) and current will flow through the path 'L1 C1 D1 L1' and 'L2 D2 C2 & Load L2'.

$$V_{L1} = -V_{C1} \Rightarrow L_1 \frac{dI_{L1}}{dt} = -V_{C1} \Rightarrow \frac{dI_{L1}}{dt} = \frac{-V_{C1}}{L_1} \quad [4]$$

$$V_{L2} = -V_{C2} \Rightarrow L_2 \frac{dI_{L2}}{dt} = -V_{C2} \Rightarrow \frac{dI_{L2}}{dt} = \frac{-V_{C2}}{L_2} \quad [5]$$

$$V_0 = V_{C2} \quad [6]$$

By equating the average inductor voltage to Zero, we get

$$V_0 = \frac{D^2}{(1-D)^2} \times V_s$$

3 Battery Charger

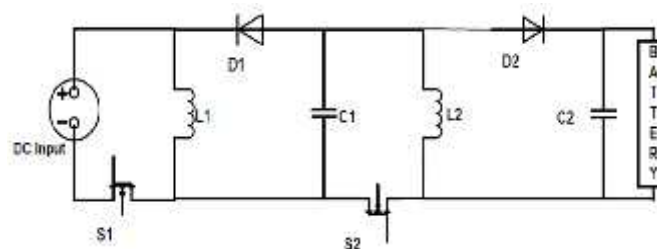


Fig.3.1 Battery Charger using DC-DC converter

The above charger circuit with the control technique is applicable for solar charger as the solar panel output is obtained as DC voltage. If solar supply is not available then can go for AC supply. However, in case of

charging the battery from direct AC supply, need to add a rectifier circuit to first convert the supply AC voltage to DC and then feed it to the DC-DC converter to charge the battery effectively and efficiently. The rectified voltage is measured and multiplied with the PID controller output, and the product is compared with the inductor current, which results in an error that produces a variable frequency pulse when passed through a hysteresis band. This pulse is fed to circuit-driven switching devices. The pulse frequency depends upon the user's setting of the hysteresis band. This control technique allows the Continuous Conduction Mode (CCM) converter to work.

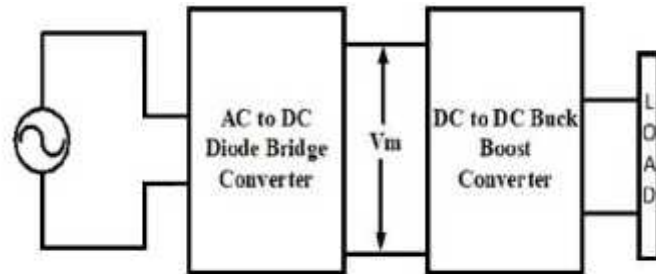


Fig.3.2 Battery Charger using AC-DC converter

4 Motor Current Controller

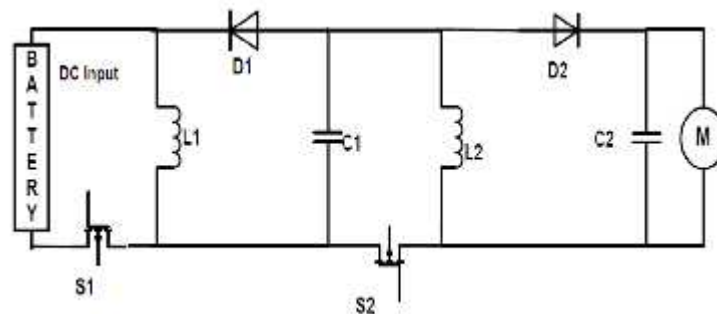


Fig.4.1 Motor current controller using DC-DC converter

The used PMDC motor can take maximum 19A as the input current. Hence, have planned to design a converter which can provide a constant 12.5A current to the motor at rated and higher load. During light load, the output current remains same, while the output voltage increases. For designing the appropriate controller, make use of an accelerator having an output of 0-12.5A, which will vary the output current supplied to the motor, according to the accelerator position. For the control purpose, compare the accelerator output with the inductor current and the resulting error is passed through a hysteresis band, generating a pulse, which in result is supplied to the switch.

5 Hardware Implementation

The DSP F28377S board was used to give pulse to driver circuit. In case of solar charger a PID controller with ePWM and ADC block in the Simulink design has been used. By following user guide of DSP F28377S, pin no. 40 as PWM output, pin 20 as ground and pin 27 as ADC output, are selected. For operation of AC-DC charger use for PID controller with GPIO, ADC blocks, MATLAB function (For HCC) in the Simulink design. By following user guide of DSP F28377S, pin no. 40 as GPIO output, pin 20 as ground and pin 27 as ADC-A0 (output voltage), pin 28 as ADC-B0 (input voltage) and pin 26 as ADC-B2 (inductor current), are selected. The P and I parameters are selected by using optimization technique in the MATLAB interface.

All the parameter values involved in the research for EV battery charger and Motor controller are given in the Table I and Table II respectively.

Table I: Parameters used for EV Battery charger

Input voltage variation for solar charger	10V to 20V (DC)
Input voltage variation for charger taking supply from AC source	12V to 40V (AC)
Output voltage	14 V (DC)
Charging current of battery	3A/Hr
Inductances used in DC-DC converter	10mH each
Capacitance used in DC-DC converter (C_1 and C_2)	100 μ F and 13600 μ F
Controllers used	PI and Hysteresis
PI control parameters	P=0.145, I=10

Table II: Parameters used for Motor Current Controller

Input voltage	24V (DC)
Nominal voltage of motor	24V (DC)
Current rating of motor	19A (DC)
Power Rating of motor	250W
Inductances used in DC-DC converter	10mH each
Capacitance used in DC-DC Converter (C_1 and C_2)	100 μ F and 13600 μ F
Controller used	Hysteresis
Accelerator rating	5V

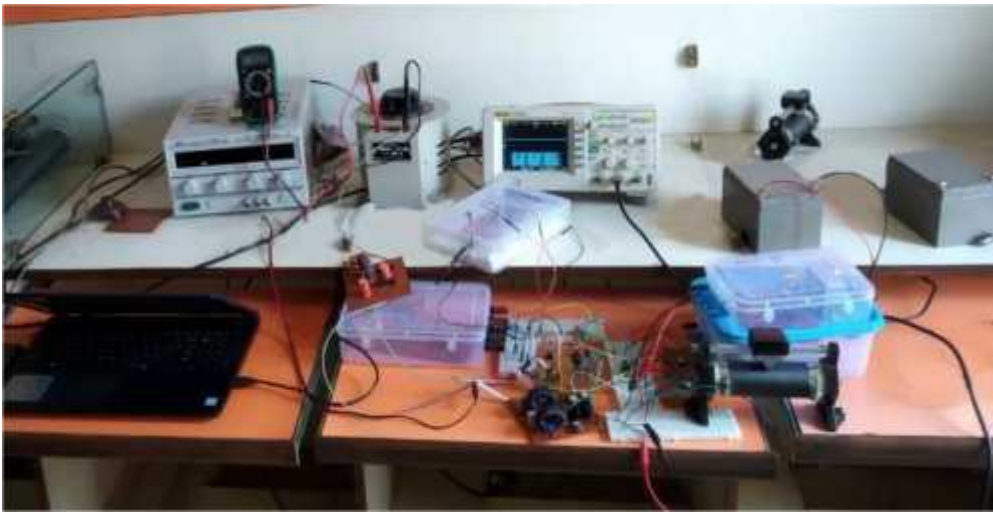


Fig 6.1.a: Hardware setup for AC-DC Battery Charger

In case of motor current controller Firstly, the I_{actual} is sent to the ADC of the DSP, where the I_{actual} is converted from analog format to digital format for digital operation in DSP. A hysteresis band of hysteresis width of 0.2 is generated, using the I_{ref} as the reference value. At this instant the switching frequency is 3.4 KHz.

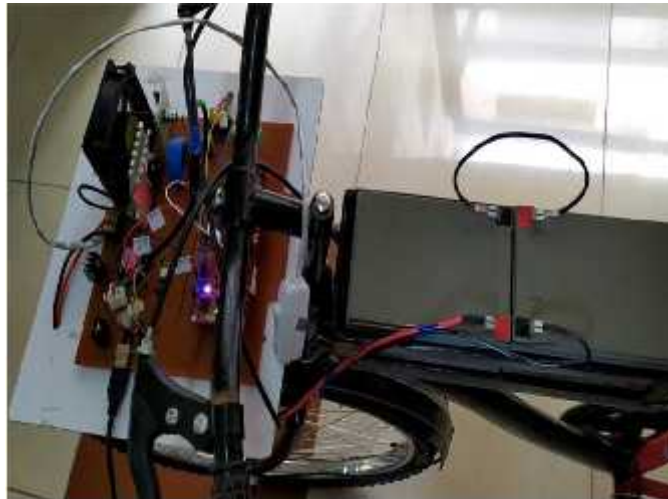


Fig.6.2.a: Hardware setup for Motor Current Controller



Fig.6.2.b: Setup when the cycle is in running condition

The targeted speed of the designed EV is 30 km/hour as the motor current controller is designed for maximum current of 12 ampere. The targeted speed can be improved by increasing the motor current controller rating.

6 Conclusion

From the hardware implementation for battery charger it is observed and it can be concluded that the designed circuit can provide the desired output i.e. 14V DC for an input variation from 30V to 40V AC. From the simulations and hardware operations for motor current controller, observe and conclude that designed circuit is able to operate in the entire three conditions i.e. Normal load, under load and Over load perfectly. When the motor current is less than 12.5 ampere, the vehicle is in running condition and when the motor current just exceeds 12.5 ampere the circuit become automatically trip by DSP microcontroller. All the performances of both battery charger and Motor current controller can be extended by changing the parameters if possible.

References

- [1] Prateek Kumar Sahoo, Ashish Pattanaik, Sagar Kumar Champati and Tapas Kumar Mohapatra, "EV battery charging with input Power Factor correction using a Buck-boost converter", Springer, 2020
- [2] Tapas Kumar Mohapatra, Asim Kumar Dey, Krushna Keshab Mohapatra, and Binod Sahu. "A novel non-isolated positive output voltage buck-boost converter". World Journal of Engineering 16, no. 1 (2019): 201-211.
- [3] Tapas Kumar Mohapatra, Asim Kumar Dey, Krushna Keshab Mohapatra, and Binod Sahu. "A novel non-isolated positive output TA converter", IEEE, 2019
- [4] B. Singh, B. N. Singh, A. Chandra, K. Al-Haddad, A. Pandey, and D. P. Kothari, "A review of single phase improved power quality AC DC converters", IEEE Trans. Ind. Electron., vol. 50, no. 5, pp. 962- 981, Oct. 2003.
- [5] P. N. Ekemezie, "Design of A Power Factor Correction AC-DC Converter", IEEE Conference Publications [Accessed March 10, 2010].

Wireless Power Transmission System

J.Arul Martinal, Assistant Professor, Department of Electrical and Electronics Engineering
A.Pieorex, UG Student, Department of Electrical and Electronics Engineering
A.Arockiaraj, UG Student, Department of Electrical and Electronics Engineering
I.Kavinilavan, UG Student, Department of Electrical and Electronics Engineering
D.Vijaykumar, UG Student, Department of Electrical and Electronics Engineering
St.Anne's College of Engineering and Technology
Anguchettypalayam, Panruti, India

Abstract

This wireless power transfer (WPT) system with repeater coils for multiple loads. Every two repeater coils form a repeater unit where one is used to receive power from its preceding unit and other transmits power to subsequent unit. Each load is connected to a repeater unit and multiple loads can be powered with several repeater units. The two coils in the same repeater unit or both bipolar ones, which are placed perpendicularly so that the magnetic coupling between them can be eliminated. In order to obtain independent power control of all the loads, the series –parallel – series (SPS) compensation method is adopted for each repeater unit. With a proper resonant condition proposed in this paper, the constant load current can be obtained for all the loads when neglecting the coils parasitic resistances. Also we utilize the solar power in our project. An experimental setup has been constructed and the effectiveness of the proposed multiload WPT system is validated by the experimental.

Keywords: *wireless power transmission; resonance; efficient power transmission; high frequency; design of winding; coupling factor.*

1 Introduction

In the early 20th century, the great scientist Nikola Tesla dedicated to transport the power without wire. On the other hand, specific embodiments implicated unfortunately large electric fields [1]. Subsequently the wireless power transmission concept has become the most trending topic throughout the world. There are many applications using the wireless power technology. Many sensor networks and cellular networks also use the same principle as of wireless transmission. There are many approaches to adopt this. On the application of wireless power transmission some issues and initiatives are noticed in Japan although specific forum imitated in order to concentrate achievements in the new business area [2]. The overview of recent development in this field like Electrodynamic induction, Electrostatic induction and Evanescent wave coupling clearly discussed [3]-[6]. At the same time the review highlighted the merits, demerits and cost. The performance of induction resonance principle compared with inductive coupling principle for wireless transmission systems. After noticing the problems with old techniques a few more new methodologies are invented [7].

In the wireless power transfer system coupled magnetic resonance plays a vital role because it has lot of advantages compared other methods. But its efficiency drastically decreases in the point of distance. To overcome this problem frequency tracking methods introduced [8]. Every method has its own advantages and disadvantages, after analyzing the all approaches one of the researchers introducing the wireless power transfer system based on inductive coupling technology for electric car battery charger. From the experiment they observed that to transfer wireless power resonant inductive coupling method is more efficient as compared to other methods [9]. Author T.Imura introducing maximizing air gap technique with help of electromagnetic induction principle to improve the efficiency. Here they are introducing Neumann formula with equivalent circuits and performance are found to be good [10]-[13].

In this paper, a new high frequency resonant inductive coupling method is proposed. Design of the HFWPT system is to be operated at resonance frequency of 50 kHz. It can be expected that the high frequency resonance coupling will improve the efficiency of transmission allowing one to transmit at lesser frequency which is nearly in a range of few kHz range. The performance of HFWPT is observed satisfactory to maintain the output voltage as required by changing the coupling coefficient.

2 Design of Wireless Power Transmission System

2.1 Designing

This design includes two sections

- Sending end

- Receiving end

Initially from the side of sending end ac power is given to the first full wave rectifier which converts two directional ac into a single directional dc. This dc supply is given as input to the inverter which converts dc to ac. The frequency of the output ac from the inverter is increased by changing the switching frequency of the inverter gate pulses. The time intervals of switching intervals are calculated based on the frequency as it is required. Hence frequency is inversely proportional to the time period would decrease i.e., for increasing the frequency of the output ac switching time interval is reduced and for decreasing the frequency of the output the switching time interval is increased. Further, parameters for the transmitter and receiver coils are calculated. The inductance of the coil and resonant frequency is calculated as follows. The calculation of required frequency of the ac output from the inverter in this project is as follows.

$$f = 1/T$$

Here the frequency $f=50\text{ kHz}$ and $T=20\mu\text{s}$.

Fig.1. depicts the schematic diagram for the wireless power transmission showing sending end and receiving end side of the system.

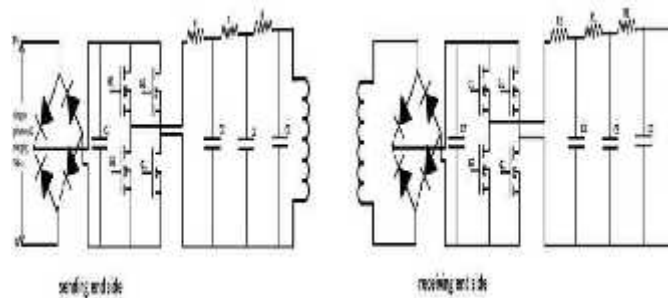


Figure 1. Schematic diagram for wireless power transmission system

2.2 Inverter

In this project, one of the major works is changing the frequency it is done by using inverter. Solar power inverters are made popular because of wireless power transmission [14]- [16]. The gating pulses giving to switches and working the inverter is very difficult because the switching frequency is high. For low values of frequency there is no difficulty with the MOSFET turning OFF process. But as the frequency increases the MOSFET does not turn OFF as quickly as possible. It is happened because of presence of junction capacitance present in the MOSFET. In order to make successful operation of inverter there should be a delay time between the turning OFF and turning ON times of two MOSFETs. Even though the MOSFET can operate at high frequency but while applying it in full bridge inverter circuit there should be some delay time has to provide in the circuit as shown in Fig.2.

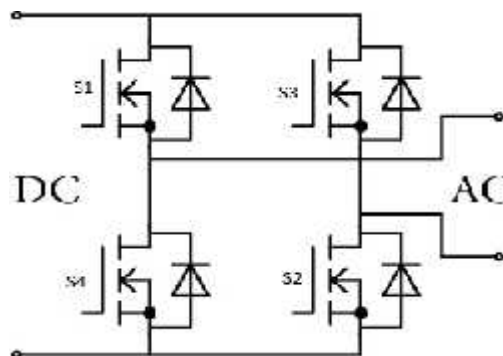


Figure 2. Simple inverter circuit

The switches S1, S2 are switched ON at one time and S3, S4 are switched at other time. The delay time after S1, S2 OFF and to turn ON S3, S4 is chosen $2\mu\text{s}$.

2.3 Square to Sine wave Converter

The output of inverter is square wave and it has to be change to sine wave. For this 3 step RC ladder circuit is used as shown in Fig.3.

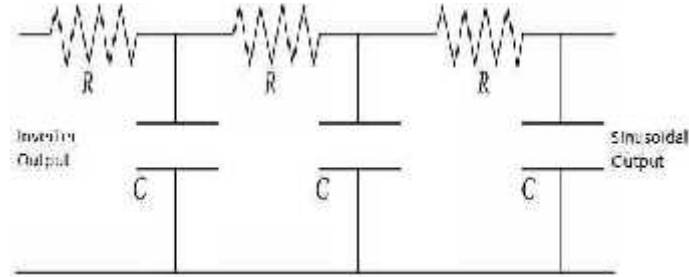


Figure 3. Square to sin wave converter

The values of RC should be chosen properly for proper output sine wave. The RC network can be replaced with a LC network to minimize losses thereby increase in efficiency.

3 System Components

All the components are chosen in accordance with the project requirement as shown in the Table I.

Table I: Experimental Values

S.no	Name	Specification	Qty
1	MOSFET	IRF640	8
2	Resistor	50	6
3	Capacitor	240pF	3
4	Diode	FR306	8
5	Capacitor	6pF	3
6	Optocoupler	TLP250	8
7	Pulse generator	Arduino	2

Diodes FR306 are used for rectification and capacitor is used for filtering purpose. Arduino and opto coupler forms the gate driver circuits to the MOSFETs [17]-[19].

4 Experimental Results

The output of rectifier is shown in Fig.4. it is very close to ideal dc source. Ripple content in the output is being minimized with the help of filters.

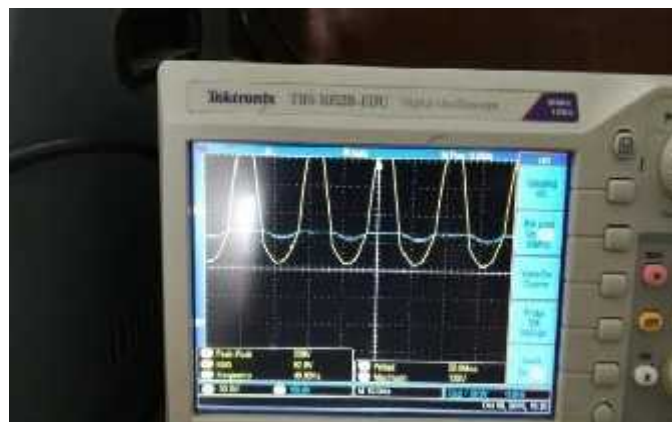


Figure 4. Rectifier output

After the application of filter also the output is not a pure dc. But we have given it as a source to the inverter. The final view of the circuit is shown in the Fig.5.

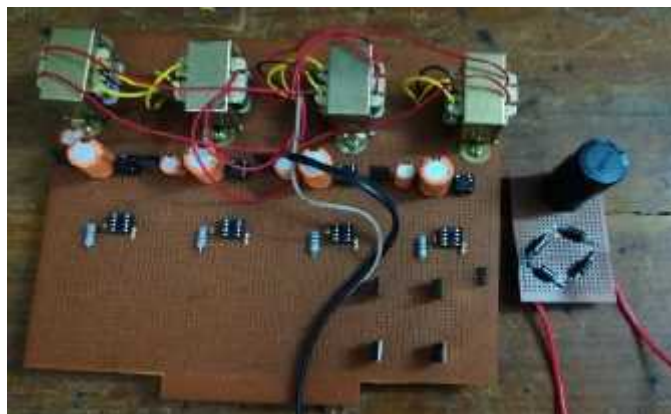


Figure 5. Hardware setup of rectifier and inverter

The above figure shows the actual model of this project and here in the 8 pin base to put the opto coupler. All the wiring is done in the back side of the PCB [20].

The main difficulty in the design of inverter is increasing frequency. To increase frequency switching frequency has to be varied. While doing the project the opto couplers are damaged due to operating them at high frequency. Then at beginning some MOSFET's are fried due to internal capacitance effect. This problem is overcome by providing dead time between switching. Finally the total project is finished and the major part of our proposed work is completed. Sinusoidal output at increased frequency is shown in Fig.6.

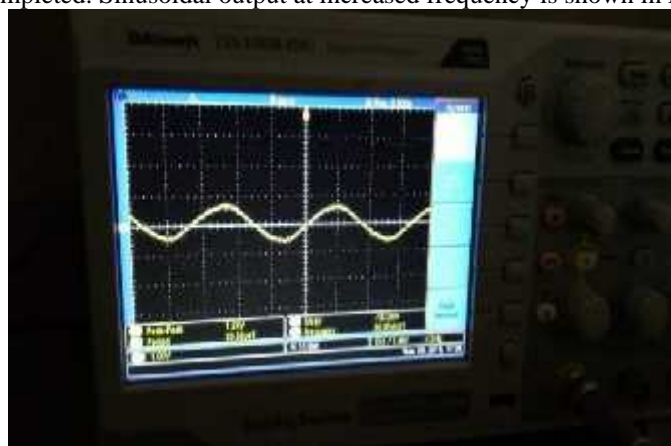


Figure 6. Sinusoidal output at increased frequency

5 Conclusion

The concept of new high frequency wireless power transfer system (HFWPT) is presented. The efficacy of the system is improved with resonant inductive coupling method. Electric cars are the present trend of automobiles which will be charged through wirelessly. In certain biomedical implants in body research is occurring in the field of charging them wirelessly rather than replacing them. Use of wireless power in harsh environments like drilling, mining, also in situations where it is impossible to lay wires wireless power transfer finds its applications. Now a day's drone-based business is fast growing and it can expect wireless power could help to charge those drone-based systems. Hence the high frequency resonant inductive coupling increases the efficiency of the system it will be very useful for the next generation.

References

- [1] N.Tesla, U.S.patent 1,119,732 (1914).
- [2] Ali Agcal, Selin Ozcira and Nur Bekiroglu (June 29th 2016). Wireless Power Transfer by Using Magnetically Coupled Resonators, Wireless Power Transfer - Fundamentals and Technologies, Eugen Coca, IntechOpen, DOI: 10.5772/64031.

- [3] H. Shoki, "Issues and initiatives for practical use of wireless power transmission technologies in japan," 2011 IEEE MTT-S International Microwave Workshop Series on Innovative Wireless Power Transmission: Technologies, Systems, and Applications, Uji, Kyoto, 2011, pp. 87-90, doi: 10.1109/IMWS.2011.5877097.
- [4] Sagolsem Kripachariya Singh, T. S. Hasarmani, and R. M. Holmukhe, "Wireless transmission of electrical power overview of recent research & development," International Journal of Computer and Electrical Engineering, vol.4, no.2, pp.207-211, April 2012.
- [5] Chunbo Zhu, Kai Liu, Chunlai Yu, Rui Ma and Hexiao Cheng, "Simulation and experimental analysis on wireless energy transfer based on magnetic resonances," 2008 IEEE Vehicle Power and Propulsion Conference, Harbin, 2008, pp. 1-4, doi: 10.1109/VPPC.2008.4677400.
- [6] P.T. Stephy, A. Anbarasan, "PV system with neutral point clamped inverter for suppression of leakage current and harmonics based fuzzy controller," International Journal of Advanced Engineering Research and Science, vol.1, no.6, pp.36-41, Nov.2014.
- [7] T. Rohith, V. S. Samhitha and Mamatha I, "Wireless transmission of solar power using inductive resonant principle," 2016 Biennial International Conference on Power and Energy Systems: Towards Sustainable Energy (PESTSE), Bangalore, 2016, pp. 1-6, doi: 10.1109/PESTSE.2016.7516535.
- [8] Z. Yan, Y. Li, C. Zhang and Q. Yang, "Influence factors analysis and improvement method on efficiency of wireless power transfer via coupled magnetic resonance," in IEEE Transactions on Magnetics, vol. 50, no. 4, pp. 1-4, April 2014, Art no. 4004204, doi: 10.1109/TMAG.2013.2291861.
- [9] G. Buja, M. Bertoluzzo and K. N. Mude, "Design and experimentation of WPT charger for electric city car," in IEEE Transactions on Industrial Electronics, vol. 62, no. 12, pp. 7436-7447, Dec. 2015, doi: 10.1109/TIE.2015.2455524.
- [10] T. Imura and Y. Hori, "Maximizing air gap and efficiency of magnetic resonant coupling for wireless power transfer using equivalent circuit and neumann formula," in IEEE Transactions on Industrial Electronics, vol. 58, no. 10, pp. 4746-4752, Oct. 2011, doi: 10.1109/TIE.2011.2112317.
- [11] Anbarasan P., Ramkumar S. and Thamizharasan S, "A new three phase reduced switch multilevel dc-link inverter for medium voltage applications," 2015 IEEE International Conference on Electrical, Computer and Communication Technologies (ICECCT), Coimbatore, 2015, pp. 1-4, doi: 10.1109/ICECCT.2015.7225962.
- [12] A. Subramanian and G. Ravi, "Multi-type facts placement for loss minimization using biogeography based optimization," Archives of Electrical Engineering, 2012, vol. 61 ,no 4, pp.517-531, DOI: 10.2478/v10171-012-0040-0.
- [13] Agcal A., Bekiroglu N. and Ozcira S., "Examination of efficiency based on air gap and characteristic impedance variations for magnetic resonance coupling wireless energy transfer", J. Magn. 2015;20(1):57– 61. doi:10.4283/JMAG.2015.20.1.057.
- [14] M. Kaliamoorthy, S. Himavathi and A. Muthuramalingam, "DSP based implementation of high performance flux estimators for speed sensorless induction motor drives using TMS320F2812," 2006 India International Conference on Power Electronics, Chennai, 2006, pp. 104-109, doi: 10.1109/IICPE.2006.4685350.
- [15] Sandirasegarane Thamizharasan, J. Baskaran and S.Ramkumar, "A new cascaded multilevel inverter topology with voltage sources arranged in matrix structure," Journal of Electrical Engineering & Technology, 2015, vol.4, no.4, pp. 1552-1557.
- [16] V Krishnakumar, V Kamaraj and S Jeevananthan, " Random pulse width modulation technique for performance improvement of multilevel inverter brushless dc motor drive," Australian Journal of Basic and Applied Sciences, 2015, vol.9, no.16, pp. 162-171.
- [17] S.Sheik Mohammed, and K.Ramasamy and T.Shanmuaganatham, "Wireless power transmission-A next generation power transmission system," International Journal of Computer Applications, 2010, vol.1, no.13, pp. 100-103.
- [18] M fareq, M fitra and M Irwanto, "Low wireless power transfer using inductive coupling for mobile phone charger," Journal of Physics: Conference Series, Volume 495, 2014 International Conference on Science & Engineering in Mathematics, Chemistry and Physics (ScieTech 2014), 13–14 Jan 2014, Jakarta, Indonesia.
- [19] B. L. Cannon, J. F. Hoburg, D. D. Stancil and S. C. Goldstein, "Magnetic resonant coupling as a potential means for wireless power transfer to multiple small receivers," in IEEE Transactions on Power Electronics, vol. 24, no. 7, pp. 1819-1825, July 2009, doi: 10.1109/TPEL.2009.2017195.
- [20] J. Wang et al., "Lateral and angular misalignments analysis of a new PCB circular spiral resonant wireless charger," in IEEE Transactions on Magnetics, vol. 48, no. 11, pp. 4522-4525, Nov. 2012, doi: 10.1109/TMAG.2012.2196980.

Solution to Combine Economic and Emission Dispatch Problem using Adaptive Particle Swarm Optimization Algorithm

M.Gnanaprakash, Research Scholar, Department of Electrical and Electronics Engineering
S.P.Mangaiyarkarasi, Assistant Professor, Department of Electrical and Electronics Engineering
R.Vijayakumar, UG Student, Department of Electrical and Electronics Engineering
S.Sathishkumar, UG Student, Department of Electrical and Electronics Engineering
University College of Engineering, Panruti, Tamil Nadu. India.

Abstract

In India Electrical Energy is generated mainly Coal based Thermal Power stations and hydro Electric Power Stations. The main aim of power generating company is to provide good quality and reliable power to consumers at minimum cost. The problem of Combined Economic and Emission Dispatch deals with the minimization of both fuel cost and emission of pollutants such as oxides of Nitrogen and Oxides of Sulphur. In our power system the emission is major problem created that's why in now a days we move from green energy source or renewable energy such as Sunlight, Wind, Tides, Wave, and Geothermal Heat Energy. The Emission constrained Economic Dispatch problem treats the emission limit as an additional constraint and optimizes the fuel cost. In this paper we optimize the Combined Economic and Emission Dispatch problem by Adaptive particle swarm optimization (APSO). The proposed APSO Algorithm has been successfully implemented is to IEEE 30 bus system. The simulation result are found the effective algorithm for Combined Economic and Emission Dispatch problem

Keywords: *Emission Dispatch, APSO, Economic Dispatch and Optimization algorithm*

1 Introduction

Since an engineer is always concerned with the cost of products and services, the efficient optimum economic operation and planning of electric power generation system have always occupied an important position in the electric power industry. A saving in the operation of the system of a small percent represents a significant reduction in operating cost as well as in the quantities of fuel consumed. The classic problem is the economic load dispatch of generating systems to achieve minimum operating cost. Traditional algorithms like lambda iteration, base point participation factor, gradient method, and Newton method can solve this ELD problems effectively if and only if the fuel-cost curves of the generating units are piece-wise linear and monotonically increasing. Practically the input to output characteristics of the generating units are highly non-linear, non-smooth and discrete in nature owing to prohibited operating zones, ramp rate limits and multi-fuel effects. Thus the resultant ELD becomes a challenging non-convex optimization problem, which is difficult to solve using the traditional methods.

2 Literature Survey

Economic dispatch (ED) is an optimization problem where optimal generation for each generator is determined to minimize total fuel costs, subject to equality constraints on power balance and inequality constraints on power outputs. Moreover, transfer losses, generation rate changes and line flows may also be considered.

A variety of techniques may be used to solve ED problems; some are based on classical optimization methods, such as linear or quadratic programming [1]-[2], while others use artificial intelligence or heuristic algorithms. Classical techniques are highly sensitive to a selection of the starting point and often converge to a local optimum or even diverge altogether. Linear programming methods are generally fast and reliable but use piecewise linear cost approximation which reduces accuracy. Non-linear programming methods, on the other hand, have convergence problems and often result in very complex algorithms. Newton based algorithms suffer from difficulties associated with handling a large number of inequality constraints [3].

More recently, heuristic search techniques – such as particle swarm optimization (PSO) [4]–[6] and genetic algorithm (GA) [7] – have also been considered in the context of ED. In addition, differential evolution algorithms were implemented to solve the ED problem [8]–[10]. Differential evolution (DE) is a stochastic search based method, which can present a simple structure, convergence speed, versatility, and robustness. However, DE fast convergence might lead the direction of the search toward a local optimal and premature solution. Finally, the use of harmony search (HS) method to find the global or near global solution for the ED problem can be found in [11]-[12]. HS is considered as a stochastic random search method, which does not need any information about the derivative. Nevertheless, HS has some insufficiencies associated with the premature convergence in its performance. A combined Particle Swarm Optimization and Sequential Quadratic Programming (PSO–SQP) algorithm was developed in [13], where PSO is the main optimizer and the SQP is used to fine tune the PSO

solution. However, since SQP is a gradient dependent method, its application to non-continuous, non-differentiable and multimodal problems, such as ED, might not lead to an optimal solution.

An increasing international concern about environment also affects the field of power generation where environmental issues are addressed directly. In another hybrid approach [14], the Differential Evolution (DE) and the Sequential Quadratic Programming (SQP) were combined into a single algorithm and used on 13 and 40 thermal units whose incremental fuel cost functions contain the valve point loading effect. In [15] the authors combined three evolutionary methods to solve a fuzzy modelled Unit Commitment Problem (UCP). The three methods are Tabu Search (TS), Particle Swarm Optimization (PSO) and Sequential Quadratic Programming (SQP) (referred to as a hybrid TS–PSO–SQP). TS is used to solve the combinatorial sub-problem of the UCP.

In [16], the modified sub gradient (MSG) and the harmony search Sequential (HS) algorithms were combined into a single algorithm and used on 3, 5 and 6 thermal units whose incremental fuel cost functions contain the valve point loading effect. In [17] the authors to solve Unit Commitment Problem through modified group search optimizer (MGSO) method. Samir Sayah and AbdellatifHamouda [18] discusses the non convex economic dispatch problems through a hybrid DE based on PSO.

Direct Search methods, in contrast to more standard optimization methods, are often called derivative-free as they do not require any information about the gradient (or higher derivative) of the objective function when searching for an optimal solution. Therefore Direct Search methods are particularly appropriate for solving non-continuous, non-differentiable and multimodal (i.e. multiple local optima) optimization problems, such as the economic dispatch. The main objective of this study is to introduce a new Adaptive Practical swam optimization (APSO) [19] in the context of power system economic dispatch problem with a valve-point effect. The results are obtained from an IEEE 30 bus 5 machine system solved with different methods in the literature. The resulting optimal solution values are compared with the solution values in the literature and the results are discussed.

3 Adaptive PSO

PSO is a population based probabilistic mechanism designed using swarm-intelligence. Swarm intelligence, also referred to as collective intelligence, is twined on socio-psychological principles and offers insights into social behaviour, in addition to contributing to engineering applications. It describes a coordinated behaviour of decentralized self-organised systems

3.1 Adaptive Adjustment of PSO parameters

There are three tuning parameters $w^{(t)}$, τ_1 and τ_2 that greatly influence the PSO algorithm performance. The inertia weight $w^{(t)}$ is used to control his impact of the previous history of velocities on the current velocity. A large inertia weight $w^{(t)}$ facilitates global exploration while a smaller inertia weight tends to facilitate local exploration to fine-tune the current search area. Suitable selection of inertia $w^{(t)}$ can provide a balance between global and local optimum points

4 Problem Description

The main objective of ELD is to minimize the total generation cost of the power system within a defined interval. The basic ELD considers the power balance constraint apart from the generating capacity limits. However, a practical ELD must take a variety of practical operating conditions into consideration to provide the completeness for the ELD problem formulation. These include transmission losses, valve-point effects, prohibited operating zones, ramp rate limits and spinning reserve etc.

4.1 Objective Constraints

4.1.1 Equality constraints

Power balance is equality constraint. In other word, the total power generation must cover the total demand (PD) and total real power loss in transmission lines (Ploss). The condition of equality constrain can be expressed as:

$$\sum_{i=1}^N P_i - P_D - P_{loss} = 0 \dots\dots\dots (9)$$

where, PD is the total load of consumers and PLoss is the total transmission network losses. Loss of transmission network is expressed as a quadratic function of the generators' power outputs as shown in.

$$P_L = \sum_{i=1}^{ng} \sum_{j=1}^{ng} P_i B_{ij} P_j + \sum_{i=1}^{ng} E_{0i} P_i + B_{00} \quad \dots\dots (10)$$

where, Bij is the ijth element of the loss coefficient square matrix. B0i and B00 are the ith element of the loss coefficient vector and the loss coefficient constant, respectively.

4.2 Generation Capacity Constraints

For unflinching operation, the generator outputs and bus voltage constraints by lower and upper limits as follows:

$$P_i^{min} \leq P_i \leq P_i^{max}, Q_i^{min} \leq Q_i \leq Q_i^{max}, V_i^{min} \leq V_i \leq V_i^{max} \quad \dots\dots (11)$$

where Pimin is the minimum loading limit below which it is uneconomical to operate the unit and Pimax is the maximum output limit. Eq. (4.20) shows minimum and maximum domain for reactive power and voltage magnitude of the ith transmission line, respectively

4.3 Line flow constraints

One important constrain of EED problem is determinate of constrain of Line, because any line have a limit capability for current power, the limit can checking after load flow for power system. Therefore, this paper discussed the solution of EED problem with line flow constraints through the application of supposed algorithm. It's constrains can be modeled by:

$$|P_{L,k}| \leq P_{L,k}^{max}, k = 1, 2, \dots, L \quad \dots\dots (12)$$

where PLf,k is the real power flow of line k; PmaxLf ,k is the power flow upper limit of line k and L is the number of transmission lines .

4.4 Prohibited operating zone constraints

Faults in the generators themselves or in the associated auxiliaries such as boilers, feed pumps, etc., may cause instability in certain ranges of generator power output. Consequently, discontinuities are produced in cost curves corresponding to the prohibited operating zones. So, there is a quest to avoid operation in these zones in order to economize the production. The prohibited operating zones constitute the following constraint for ED.

$$P_j \begin{cases} P_{jz} & P_j & P_j^{Lz} \\ P_j^{Uz-1} & P_j & P_j^{Lz} \\ P_j^{Uz} & P_j & P_j \end{cases} \quad j = 1, 2, \dots, N_g \quad (13)$$

where PjLBz and PjUBzare lower and upper bounds of the zth prohibited zone of unit j; z is the index of prohibited zones.

4.5 Environmental objective

The atmospheric pollution caused by the fossil fired generator contains sulfur oxides (SOx), nitrogen oxides (NOx), carbon dioxide (CO2) and so on. For simplicity, the total emission of these pollutants is expressed as a sum of a quadratic and exponential function.

$$\min E = \sum_{i=1}^N [a_i + b_i P_i + \gamma_i P_i^2 + \eta_i \exp(S_i P_i)] \quad \dots\dots (14)$$

4.6 Generator operation and ramp limit constraints

$$P_i^{min} \leq P_i \leq P_i^{max}, \max(P_i^{min}, P_i^D - DR_i) \leq \min(P_i^{max}, P_i^O + UR_i) P_i \in \Lambda_{oi} \quad \dots\dots\dots (15)$$

where P_i min and P_i max are lower and upper bounds for power outputs of the i th generating unit

4.7 System spinning reserve constraints

Spinning reserve is the amount of synchronized generation that can be used to pickup source contingencies or load increase. The available system reserve should be at least equal to the system requirement to overcome contingencies. The system spinning reserve constraint can be formulated as follows:

$$\sum_i S_i \geq S_R \quad \dots\dots\dots (15)$$

With
 $S_i = \min\{(P_i^{\max} - P_i), S_i^{\max}\}, \forall_i \in (\Omega - \Psi)$
 $S_i = 0, \forall_i \in \Psi$

where S_i is the spinning reserve of unit i ; S_R is the system spinning reserve requirement; S_i^{\max} is the maximum spinning reserve contribution of unit i ; Ω is the set of all online units and Ψ is the set of units with prohibited zones. Note that for unit with prohibited operating zones, these zones strictly limit the unit to regulate system load because load regulation may result in its falling into a certain prohibited operating zones. As a result, a unit which has prohibited operating zones does not contribute spinning reserve to the system.

5 Result & Discussion

The proposed method (PM) has been tested on IEEE 30 bus test system comprising six generating units with a net load demand of 283.4 MW. The fuel cost coefficients with generator limits are given in Table 1. The emission coefficients are given in Table 2. The B-loss coefficients in per unit on a 100 MVA base are given in Table 3. The simulation is performed for two test cases and the results of PM are compared with that of the existing methods of EM1, EM2 and EM3, presented in references [26]

The proposed method (PM) has been tested on IEEE 30 bus test system comprising six generating units with a net load demand of 283.4 MW. The fuel cost coefficients with generator limits are given in Table 1. The emission coefficients are given in Table 2. The B-loss coefficients in per unit on a 100 MVA base are given in Table 3. The simulation is performed for two test cases and the results of PM are compared with that of the existing methods of EM1, EM2 and EM3, presented in references [24], [25] and [26].

Table 1 Generator Fuel Cost Coefficients and Generation Limits for six-unit system

Gen No	Fuel cost coefficients					Generation limits Per Unit	
	<i>a</i>	<i>b</i>	<i>c</i>	<i>d</i>	<i>e</i>	P_G^{\min}	P_G^{\max}
1	100	200	10	15	6.283	0.05	0.50
2	120	150	10	10	8.976	0.05	0.60
3	40	180	20	10	14.784	0.05	1.00
4	60	100	10	5	20.944	0.05	1.20
5	40	180	20	5	25.133	0.05	1.00
6	100	150	10	5	18.48	0.05	0.60

In case-1, the cost function is modelled as a quadratic, considering only a_i, b_i, c_i and in case-2, the cost function is modelled as a quadratic summed with a sine term to incorporate the valve-point effect, considering a_i, b_i, c_i, e_i, f_i . The best fuel cost and the optimal generations obtained by the PM for ELD, which minimises the fuel cost alone, are given in Table 4. It is clear from these results that the PM without valve point effect provides better fuel cost than that of other methods. However, it should be noted that the results for test case-2 offers solution with higher fuel cost.

Table 2 Emission Coefficients for six-unit system

Gen No	Emission coefficients				
	r	s	x	\langle	E
1	6.49	-5.554	4.091	2.0e-4	2.857
2	5.638	-6.047	2.543	5.0e-4	3.333
3	4.586	-5.094	4.258	1.0e-6	8
4	3.380	-3.550	5.326	2.0e-3	2
5	4.586	-5.094	4.258	1.0e-6	8
6	5.151	-5.555	6.131	1.0e-5	6.667

Table 3 Results of Best Fuel Cost (ELD)

Method	Without Valve Point				With Valve Point
	EM1 [24]	EM2 [25]	EM3 [26]	PM	PM
P_{G1}	0.1168	0.1245	0.1086	0.1280	0.0994
P_{G2}	0.3165	0.2792	0.3056	0.2701	0.3624
P_{G3}	0.5441	0.6284	0.5818	0.5550	0.4834
P_{G4}	0.9447	1.0264	0.9846	1.0051	0.8736
P_{G5}	0.5498	0.4693	0.5288	0.4543	0.6642
P_{G6}	0.3964	0.3993	0.3584	0.4452	0.3900
Best Fuel Cost	608.245	608.147	607.807	606.48	626.88
Emission	0.21664	0.22364	0.22015	0.22069	0.21392

Table 4 Results of Best Emission (MED)

Method	Without Valve Point				With Valve Point
	EM1 [24]	EM2 [25]	EM3 [26]	PM	PM
P_{G1}	0.4113	0.3923	0.4043	0.3712	0.3788
P_{G2}	0.4591	0.4700	0.4525	0.4664	0.3932
P_{G3}	0.5117	0.5565	0.5525	0.5641	0.4994
P_{G4}	0.3724	0.3695	0.4079	0.3648	0.5343
P_{G5}	0.5810	0.5599	0.5468	0.5223	0.5734
P_{G6}	0.5304	0.5163	0.5005	0.5783	0.4864
Fuel Cost	647.251	645.984	642.603	647.93	659.34
Best Emission	0.19432	0.19424	0.19422	0.19463	0.19567

Table 5 Best Compromise Solutions (EED)

Method	Without Valve Point				With Valve Point
	EM1 [24]	EM2 [25]	EM3 [26]	PM	PM
P_{G1}	0.2699	0.2227	0.2594	0.17612	0.14088
P_{G2}	0.3885	0.3787	0.3848	0.28187	0.34414
P_{G3}	0.5645	0.5560	0.5645	0.54078	0.67557
P_{G4}	0.6570	0.7147	0.7030	0.76962	0.83970
P_{G5}	0.5441	0.5500	0.5431	0.65018	0.49042
P_{G6}	0.4398	0.4424	0.4091	0.44568	0.39797
Fuel Cost	618.686	615.097	616.069	612.34	639.64
Emission	0.19940	0.20207	0.20118	0.20742	0.21105

The best emission and the optimal generations obtained by the PM for MED, which minimises the emissions alone, are given in Table 5. It is obvious from these results that the PM without valve point effect provides better emission than that of other methods. However, it should be noted that the results for test case-2 offers solution with higher emission.

6 Conclusion

An adaptive PSO based method for EED is presented. The method considers convex and no convex type of fuel cost characteristics besides considering emission function. The method adaptively adjusts the inertia weight and acceleration coefficients and provides better results. The method is suitable for practical implementation.

References

- [1] R.B. Adler, R.Fischl (1977), "Security constrained economic dispatch with participation factors based on worst case bus load variations", IEEE Transaction on Power Apparatus Systems, Vol: 96, No.1, pp:347–56.
- [2] R.T. Bui, S.Ghaderpanah (1982), "Real power rescheduling and security assessment". IEEE Transaction on Power Apparatus Systems, Vol: PAS 101, No.1, pp:2906–2915.
- [3] R.K.Pancholi, K.S.Swarup (2004), "Particle swarm optimization for security constrained economic dispatch", International conference on intelligent sensing and information processing, (IEEE Cat. No. 04EX783), Chennai, India; pp: 7–12.
- [4] L. Dos Santos Coelho, V.C.Mariani (2008), "Particle swarm approach based on quantum mechanics and harmonic oscillator potential well for economic load dispatch with valve-point effects". Energy Conservation and Management, Vol: 49, No.1, pp: 3080–3085.
- [5] T.Niknam (2010), "A new fuzzy adaptive hybrid particle swarm optimization algorithm for non-linear, non-smooth and non-convex economic dispatch problem", Applied Energy, Vol: 87, No.pp:327–329.
- [6] J.Cai, X.Ma, L.Li, P.Haipeng (2007), "Chaotic particle swarm optimization for economic dispatch considering the generator constraints". Energy Conservation and management, Vol:48, No.1, pp:645–53.
- [7] H.K.Youssef, K.M.El-Naggar (2000), "Genetic based algorithm for security constrained power system economic dispatch", Electrical Power System Research ,Vol:53, No.1, pp:47–51.
- [8] L.D.S.Coelho, V.C.Mariani (2007), "Improved differential evolution algorithms for handling economic dispatch optimization with generator constraints", Energy Conservation and management , Vol:48, No.1,PP:1631–1639.
- [9] N.Noman , H. Iba (2008), "Differential evolution for economic load dispatch problems", Electrical Power System Research , Vol:78, No.1, pp:1322–1331.
- [10] L.D.S.Coelho, R.C.T.Souza, V.C. Mariani (2009), "Improved differential evolution approach based on cultural algorithm and diversity measure applied to solve economic load dispatch problems", Mathematical Computation and Simulation, Vol.79, pp:3136–3147.
- [11] M.Fesanghary, M.M.Ardehali (2009), "A novel meta-heuristic optimization methodology for solving various types of economic dispatch problem" Energy, Vol.34, No.1, pp: 757–766.
- [12] L.D.S.Coelho, V.C.Mariani (2009), "An improved harmony search algorithm for power economic load dispatch", Energy Conservation and maPnagement , Vol:50, No.1, pp:2522–2536.
- [13] T.A.A.Victoire, A.E.Jeyakumar, (2004), "Hybrid PSO-SQP for economic dispatch with valve-point effect", Electrical Power System Research, Vol:71, No.1, pp:51–59.
- [14] L.S.Coelho, V.C.Mariani, (2006), "Combining of chaotic differential evolution and quadratic programming for economic dispatch optimization with valve-point effect", IEEE Transaction on Power Systems, Vol:21, No.1, pp:989–996.
- [15] T.A.A.Victoire, A.E.Jeyakumar (2006), "A tabu search based hybrid optimization approach for a fuzzy modelled unit commitment problem", Electrical Power System Research, Vol: 76, No.1, pp:413–425.
- [16] C. Yas, S. Ozyon (2011), "A new hybrid approach for nonconvex economic dispatch problem with valve-point effect", Energy, Vol.36, No.1, pp: 5838–5845.
- [17] K. Zare, M. T. Haque, E. Davoodi (2012), "Solving non-convex economic dispatch problem with valve point effects using modified group search optimizer method", Electric Power Systems Research, Vol: 84, No.1,pp:83– 89.
- [18] S. Sayah, A. Hamouda (2013), "A hybrid differential evolution algorithm based on particle swarm optimization for nonconvex economic dispatch problems", Applied Soft Computing, Vol: 13, No.1,pp: 1608–1619.
- [19] G.W Yan. and Z.J. Hao (2013), "A Novel Optimization Algorithm Based on Atmosphere Clouds Model", International Journal of Computational Intelligence and Applications, Vol: 12, No. 1, pp:1-16.
- [20] Lianbo M, Kunyuan H, Yunlong Z, Hanning C and Maowei H, A Novel Plant Root Foraging Algorithm for Image Segmentation Problems, Mathematical Problems in Engineering, Volume 2014, pp: 1-16, 2014.
- [21] J. Yuryevich, K. P. Wong (1999), "Evolutionary programming based optimal power flow", IEEE Transaction on Power Systems, Vol:12, No.4, pp:1245–1250.
- [22] M. A. Abido (2002), "Optimal power flow using tabu search algorithm", Electrical Power Components and Systems, Vol. 30, No.1, pp. 469-483.
- [23] W. Ongsakul, and P. Bhasaputra (2002), "Optimal power flow with FACTS devices by hybrid TS/SA approach", Electrical Power and Energy Systems, Vol. 24, No. 10, pp. 851-857.
- [24] W. M. Lin, F. S. Cheng, M. T. Tsay (2002), "An improved tabu search for economic dispatch with multiple minima", IEEE Transaction on Power Systems, Vol:127, No.4, pp:108–112.

Design of Efficient Electric Motorcycle Using Brushless DC Motor

A. Sundarapandiyan, Assistant Professor, Department of Electrical and Electronics Engineering
St. Anne's College of Engineering and Technology

Abstract

Transportation is a tool that human needs from the past until now; it is an essential device in human life. Along with the development of transportation in this world, more and more energy used to come from fossil energy, which is limited, and the number of its availability decreases over time. Therefore, we must preserve the environment and limit the use of fossil energy. The solution to overcome the use of fossil energy is to replace the consumption of energy, mainly used by vehicles, by consuming electrical energy in the means of transportation. Electric vehicles are an excellent solution to keep the environment, aside from reducing the use of fossil energy. Electric vehicles do not produce waste substances or, in other words, emissions that are not produced so that the surrounding air is not contaminated with pollution like waste substances generated by vehicles using fossil energy. Also, electric vehicles can be categorized as energy-saving vehicles. It is our purpose in this study to design an efficient electrical motorcycle prototype, which can be accelerated up to 40 km/h and operational cost ten times less than the usual petrol vehicle with more efficiency.

Keywords — *Electric Motorcycle, BLDC, Controller PWM*

1 Introduction

At this time humans rely heavily on fossil fuels that provide at least three severe threats: (1) depletion of known petroleum reserves, (2) instability/price increases due to higher demand rate of production the oil itself, and (3) greenhouse gas (mainly CO₂) pollution caused by the burning of fossil fuels. The development of an environmentally friendly renewable fuel implementation needs to get serious attention worldwide. One way to reduce the use of fossil fuels is to use electricity stored in batteries for vehicles including electric motorcycles [1]. This way, a motorcycle can be enhanced for security [2,3] and automation like IoT [4].

Here in this study, electrical energy in the battery is used as a source of electrical energy in electric motors. The purpose of this study is to design an electric motorbike with 5 kW BLDC motor (7 HP) is expected to drive up 130 km/h with cruises up to 230 km and then use Li-ion batteries or Sodium Silicate. We studied the amount of the cost needed in one trip and also to analyze the battery power that can be stored and how long the motor can work.

2 Material and Methods

A. Electric Current Direction

An electric current is a flow of electricity that flows through a conductor or conductor in a closed circuit. The electric current flows from the positive pole to the negative pole within a closed circuit. The direction of the electric current is opposite to the electron current from the negative pole to the positive pole on a closed circuit. When an electric current flows in a particular direction; at the same time, the electron flows in the opposite direction.

B. Ohm's Law

Ohm law is used because the electric current flowing through a conductor always directly proportional to the potential difference applied. A conductor follows the ohms law said that if the resistance value is not depending on the magnitude and polarity of the potential difference applied to it.

C. Definition of System

A system built is a comprehensive system to design an efficient motorcycle. A whole system is a collection of all the components in which each component interacts with each other, where each component to another component has a reciprocal interaction [5]. The power used in electric motorcycles is the electric motor, which is reduced to the roller chain through the gears. This reduction is made to transfer the power that is on the electric motor to the gears to roller chain that can drive the motorcycle.

D. Basic Forms Electric Motorcycles

The shape of the electric motorcycle will be designed and built using the basic framework of CB100 Motorcycle. It is because spare parts that are used are not too many that it reduces the weight of the motorcycle and make it more efficient in use. It is also accessible to a raft and secure release of electronic devices in pairs. At the time of the assembly process of the electric motorcycle, there is not too much change required to keep the authenticity of the components and maintain the motorcycle model CB100.

E. Brushless DC Motor (BLDC)

BLDC motor is the most commonly used electric vehicle of medium speed grade. This motor is no longer using Brush since motor coil acts as a rotor, on a permanent magnet BLDC. As a transfer point, when the BLDC phase motor execution requires the Hall sensor to help to know the location of the magnetic position. BLDC motor is required to use the controller to rotate because it requires the data processor provided by the hall sensor, as seen in Figure 1.

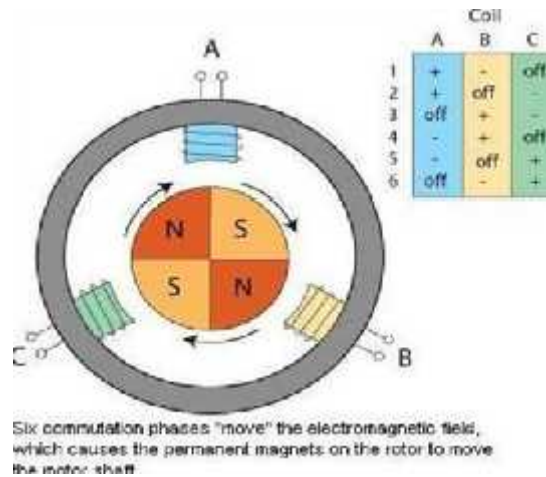


Fig. 1. BLDC Motor Scheme

The advantages of BLDC motor are excellent torque, considered to be high efficiency, have excellent durability in the longer usability, can work optimally on all ranges of rpm rotation, and also BLDC motor is the best in low-rotation work [6]. At the other hand, BLDC motor weakness includes the required controller, which must be controlled by Pulse Wide Modulation and degree of phase hall sensor; Top speed is limited, the power-weight ratio is low, not ideal in high power, max 30KW power and also not ideal in high voltage (V max equals to 200V).

Examples of the use of BLDC Motor are on middleclass electric vehicles, such as electric motorcycles and electric bicycles, as seen in figure 2. Also, fan computers and electric helicopter motor toys use BLDC motors. The motors have several loops on the dynamo to provide a more uniform torque, and the magnetic field is generated by an electromagnetic arrangement called a field coil. In understanding a motor, it is essential to analyze what the motor load is, which refers to the output of torque at the required speed.

F. Research methods

The design of the tool was done in the Energy Conversion laboratory, and retrieval was implemented on Denai-Street Lapangan Merdeka. The research flow diagram is shown in figure 3 below. To perform the test, the following tools are required: electric motorcycles, BLDC motor, PWM, Voltmeter, Ampere meter, 48-volt source battery, charger 48 volts, and potentiometer.



Fig 2. BLDC motor hub

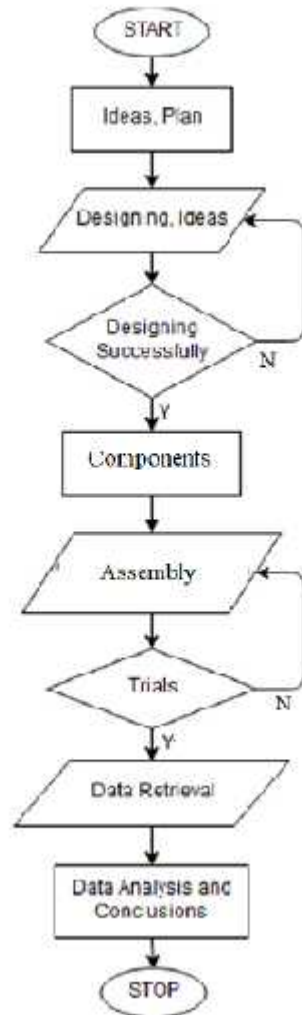


Fig. 3. Flowchart of the design process BLDC

(a) P WM (Pulse Width Modulation) / Controller:

This motor control circuit is made using the principle of PWM (Pulse Width Modulation). The PWM regulates the speed of the motor using a square wave whose pulse width is modulated, resulting in a varying average voltage. This technique provides ease in setting the motor speed, without much energy wasted [7]. The output of Pulse Width Modulation is a square wave, as shown below. If T_{on} is a high output period (V_{max}), while T_{off} is a low output period (zero volts). The full-wave period then defined as follows:

$$T_{Total} = T_{on} + T_{off}$$

Duty Cycle is defined as:

$$D = \frac{T_{on}}{T_{Total}}$$

The output voltage varies according to the duty cycle as follows:

$$V_{out} = D \times V_{in}$$

$$V_{out} = \frac{T_{on}}{T_{Total}} \times V_{in}$$

From the above equation, if $T_{on} = 0$, then $V_{out} = 0$ and will increase with the increase of T_{on} . The maximum output will be achieved at $T_{on} = T_{Total}$ that is equal to V_{in}

(b) Mechanical System:

The planned mechanical system consists of:

- The framework of the motorcycle that is the holder of the shaft and motor made of iron with a thickness of 2.5 mm
- Belt or chain transmission is a device that connects the BLDC motor pulley with a rotating wheel pulley with the number of front gigs 33 and rear 45
- The ratio of DC motor pulley with wheel turning pulley is 4: 3. With motor pulley motor drive that is using BLDC motor with the speed which is controlled using the PWM circuit.

3 Results and Discussion

From the result of research hence obtained that the costs incurred to make one unit of the efficient electric motorcycle are relatively low that does not include the manufacturer. The total weight of the vehicle was found at 71.5 Kg.

The specification of electrical motorcycles is as follows:

-) Power : 350Watt
-) Magnet Size : 35mm
-) Phase Angle : 120 degrees
-) Battery : 48v11Ah, weight 15,5 kg
-) Range : 10 km
-) Charging Time : 3 hours
-) Top Speed : 35 – 40 km/h
-) Sensor : Brake level
-) Motor : Brushless gearless hub motor
-) Controller : 48v11Ah, 350 watt,
-) Weight : 0,2 kg
-) 3 Power Speed Switch: 1-2-3

In designing this motorcycle, some things need to be calculated; among them is the driving force, namely:

(a) The Twisted Moment:

$$MP = \frac{60 \times P}{2 \times 3,14 \times n}$$

$$MP = \frac{60 \times 350}{2 \times 3,14 \times 400}$$

$$MP = 8,359 Nm.$$

(b) The power generated by an electric motor to drive the vehicle:

$$P_{out} = W \times V$$

$$= 25,84 \times 9,72.$$

$$= 251,16 watt.$$

(c) The efficiency of machine work:

$$\eta = \frac{P_{out}}{P_{in}} \times 100\%$$

$$= 71,76\%.$$

In designing the electric motorcycle, we have to know first the properties of the vehicle, because many things that can affect the nature of electric motorcycles, such as the condition of the road, the type of machine used, and situations that affect the obstacles when the motorcycle is running.

(d) Aerodynamic Resistance: Aerodynamic resistance is a barrier in the natural electric motorcycle due to the friction of the air. The magnitude of aerodynamic resistance (R_a) can be expressed in the following equation:

$$R_a = 0,5 \cdot c \cdot d \cdot A \cdot V^2 \cdot \rho$$

$$R_a = 0,5 \cdot 0,9 \cdot 1 \cdot (9,72)^2 \cdot 1,175 = 49,95 N$$

(e) Rolling resistance: The resistance caused by the electric motorcycle due to the change of shape that occurs on the tires and the road surface. The amount of rolling resistance (R_r) can be expressed in the following equation:

$$R_r = C_r \cdot W_t = 0,008 \cdot 1,338 = 10,7 N$$

(f) Resistivity: Resistance is in the natural electric motorcycle on the way up. The magnitude of the climb resistance (R_g) can be expressed in the equation as follows:

$$R_g = W_t \cdot \sin \phi = 1,338 \times \sin 0,50 = 11,67$$

For vehicles traveling at constant speeds, usually, the total resistance of the vehicles is traction force. Where the traction force that occurs on an electric motorcycle is:

$$\text{Traction Force (F)} = R_a + R_r + R_g = 49,95 + 10,7 + 11,67 = 72,32 N$$

Giving that in motor power it can be:

$$P_{motor} = F \cdot V = 72,32 \cdot 9,72 = 702,95 watt$$

(g) Calculation of Round Motor: Motor rotation can be obtained by calculating the rotations on the transmission wheel axle of BLDC Motor. Known that

- Gear on motor; $Z1 = 33$ T and $D1 = 10$ cm
- Gear on wheels; $Z2 = 45$ T and $D2 = 14$ cm
- D wheels = 56 cm
- $N1 = 400$ rpm

From the data above, then on each round can be done calculation as follows:

$$\frac{N2}{N1} = \frac{D1}{D2}$$
$$N2 = \frac{N1 D1}{D2} = \frac{400 \cdot 10}{14} = 285,71 \text{ rpm.}$$

From the results of testing and discussion of data obtained, it can be concluded that funds needed to assemble an electric is quite low. The total weight of electric motorcycles is 1.338 N consisting of weight of rider 637 N and weight of electric motorcycle 701 N.

Energy consumption spent on a 10 km trip is 0.499 kWh. The cost for a journey as far as 10 km spends money of Rp.516 or equal to only Rp 5.160 per 100 km. It is more efficient than the usual petrol vehicle that cost Rp 8.000 per 10-15 km (a liter), or 15 times more efficient.

4 Conclusion

In this study, we were succeeded in designing an efficient electrical motorcycle prototype with a scale of the laboratory, which can be accelerated up to 40 km/h and operational cost 15 times less than the usual petrol vehicle with more efficiency. This result is quite promising to be implemented on an industrial scale to support reducing fossil energy use.

References

- [1] Buntarto, "Sepeda Motor Listrik", Pustaka Baru Press, Yogyakarta, 2016.
- [2] Siregar, Baihaqi, Chairul Saleh Nasution, Dani Gunawan, Sawaluddin Sawaluddin, Ulfi Andayani, and Fahmi Fahmi. "Security Device for Motorcycle Using Smartphone Android with Promini." In 2nd International Conference on Statistics, Mathematics, Teaching, and Research IOP Publishing, IOP Conf. Series: Journal of Physics: Conf. Series, vol. 1028, p.012049. 2018.
- [3] Siregar, Baihaqi, Syahril Efendi, Cethi Setiawan, and Fahmi Fahmi. "RFID Wristband for Motorbikes Real-Time Security System." In 2019 3rd International Conference on Electrical, Telecommunication and Computer Engineering (ELTICOM), pp. 116-119. IEEE, 2019.
- [4] Fahmi, F., F. Nurmayadi, B. Siregar, M. Yazid, and E.Susanto. "Design of Hardware Module for the Vehicle
- [5] Condition Monitoring System Based on the Internet of Things." In IOP Conference Series: Materials Science and Engineering, vol. 648, no. 1, p. 012039. IOP Publishing, 2019.
- [7] Rangkuti, H.; Harahap, R.; Suherman, . and Yusmartato, "Compares Design of the 3 KW with 350 Watt Electric Motor Cycle", in Proceedings of the 7th International Conference on Multidisciplinary Research - Volume 1: ICMR, ISBN 978-989-758-437-4. 2018.
- [8] Zuhail, "Dasar Teknik Tenaga Listrik dan Elektronika Daya", Penerbit Gramedia, Jakarta, 1995.
- [9] Chapman and Stephen J, "Electric Machinery Fundamentals," McGraw Hill Companies, New York, 1999.

Electrical Motor Topologies for Aircraft Propulsion

V. C. Eugin Martin Raj, Assistant Professor, Department of Electrical and Electronics Engineering
St. Anne's College of Engineering and Technology

Abstract

This paper provides the state-of-the art in aircraft electrical propulsion (AEP). Initially, the limitations of on-board energy storage devices are highlighted and contextualised. The definitions of useful measures for determining the suitability of motor design, namely specific power and motor torque per unit rotor volume (TRV), are discussed and relevant examples are provided. The classifications of motors used for terrestrial vehicle applications are reviewed and their limitations highlighted regarding their suitability to AEP applications. A discussion on motor configurations for aerospace applications is provided which includes: synchronous motor stator winding configurations; axial flux motor configurations and the causes of energy losses. Additionally, the topologies and performance characteristics of existing aerospace motor technologies are examined. It was concluded that electrical motors provide an ideal means for achieving aircraft propulsion and that higher motor speeds are likely to be required for future commercial aircraft motor designs.

Keywords : *aircraft electrical propulsion, BLDC, unmanned aircraft, rim driven fan, RDF, specific power, TRV, slotless windings*

1 Introduction

The comparatively low energy storage capacity of electrical aircraft is the only serious obstacle to the development of successful zero-emission flight. Although it is not the aim of this paper to discuss on-board electrical energy storage; it is first considered important to offer a contextual reference to the present feasibility of electrical propulsion for aircraft.

Various methods of electrical energy supply already exist to provide on-board power for propulsion. Fig. 1 provides an indication of power and energy densities of state -of-the-art electrical storage technologies. In [1] existing battery, solar cell, ultra-capacitor and fuel cell technologies are described alongside operational hybrid aircraft and future High-Temperature Superconducting (HTS) systems. HTS technology is becoming increasingly feasible with recent advances in material sciences [2],[3]. Likewise, high -powered metal-air battery technologies, such as lithiumair, offer the potential to equal and surpass the energy release capabilities of hydro-carbon fuels.

Fig. 1 provides an overview of theoretical specific energies of batteries compared with gasoline. Fig. 2. Shows Ragone chart comparing specific energy and power values for electrical storage technologies. At the time of writing, the energy density of practical Lithium-Ion batteries is about 200 Wh/kg whereas Jet-A1 (AvTur) kerosene has an energy density of 11.95 kWh/kg [2]. This is some sixty times greater than is achievable for electrical flight. Thus, it is restricting present aircraft applications to light weight, low speed and short duration flights such as light aircraft, paragliders, unmanned (autonomous) aircraft and model aircraft. Regardless of the means of on-board electrical energy supply, Aircraft Electrical Propulsion (AEP) is likely to bring about the most significant change to the topology of the electric motor for over a century. This paper presents a review of existing motor technologies for aircraft propulsion.

Two useful measures for determining the suitability of a motor design for a particular application are its Specific

Power (kW/kg) and its Torque per unit Rotor Volume (TRV: kNm/m³). The former provides an indication of performance regarding power to weight and allows a comparison to be made between electric motor performance and that of Internal Combustion Engines (ICE). Table I provides an approximate comparison of Specific Power

values for traditional forms of vehicle engines. The latter, TRV (refer to Table II), is a useful guide for designers in sizing an electrical machine as it provides an indication of the effectiveness of the electromechanical energy conversion of motor design. It can be calculated as follows [4]:

$$TRV = \frac{T}{V_{rotor}} = \frac{\pi}{\sqrt{2}} \times k_{rel} \times A \times B = 2\sigma_{rotor}$$

$$T = \frac{\pi^2}{4\sqrt{2}} \times k_{rel} \times A \times B \times D^2 \times L_{stk}$$

$$V_{rotor} = \frac{\pi D^2 L_{stk}}{4}$$

$$\sigma_{rotor} = \frac{T_{rotor}}{Area} = B \times A$$

where T is the motor torque (Nm); V_{rotor} is the rotor volume (m³); D is the rotor diameter (m); k_{w1} is the fundamental winding factor; L_{stk} is the axial active length (m); A is the electric loading: number of ampere-conductors per metre around the stator surface that faces the airgap; B is the magnetic loading: the average flux density over the rotor surface (Tesla); and τ mean is the shear stress on the rotor (N/m²).

A variety of technical characteristics are used to classify motor types. Some sources broadly categorise motors as either AC or DC machines [5] whereas others draw a fundamental distinction between whether they have axial or radial flux topologies [6]. In an overview of electric machine technologies [7] an extensive range of existing and

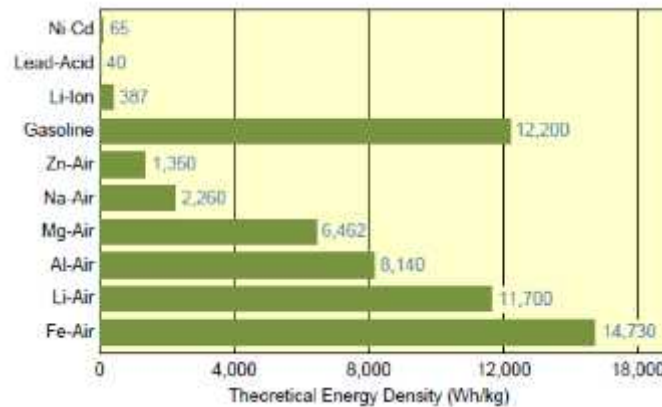


Fig. 1. Theoretical specific energies (Wh/kg) of batteries compared to gasoline [1].

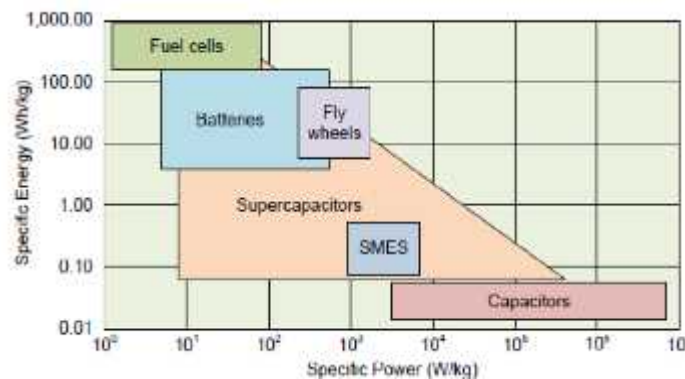


Fig. 2. Ragone chart comparing specific energy and power values for electrical storage technologies [1].

emerging motor concepts is provided, and these are initially categorised as brushed or brushless types. Another method of classification is based on whether the motor operation is synchronous or asynchronous. Fig. 3 shows a typical overall classification of motors used in modern electrical vehicle (EV) traction applications. The automobile sector has seen extensive development in EV motor technology over the past two decades. Over which time, it has become evident, that even though manufacturers' initial development specifications have been similar at the outset of an EV design. Their resultant traction motor solutions have often varied. The Nissan LEAF motor, for example, is based on a Brushless DC (BLDC) permanent magnet motor design, whereas the Tesla model S motor is based on a copper rotor Induction Motor (IM). EV motors also vary considerably in the arrangement of their windings and their cooling provisions. In a comparative study [8] of different electric motors for EVs it was concluded that although induction motor technology was more mature, robust and less costly.

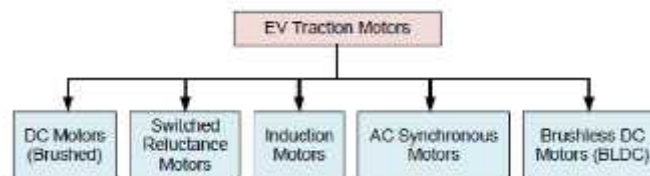


Fig. 3. Classification of motor types used in EV applications

Permanent magnet synchronous motor motors provided less pollution, less fuel consumption and better power to volume ratios. Until recently, electric motors in aerospace applications were mainly used to power on-board systems rather than being the primary method of propulsion. Over the past 20 years, the civil aerospace industry

has concentrated efforts on developing More Electric Aircraft (MEA) technologies embodied by the Boeing 787 and Airbus 350 aircraft [9].

Large (15 kW) axial flow fans are used to recirculate air within the air-conditioning systems for civil airliners such as the Airbus A330 aircraft. Similarly, four 100 kW singlestage centrifugal compressors are used to pressurise the Boeing 787 fuselage. Electrically powered hydraulic and fuel pumps are common to many large aircraft designs, and electric motors incorporated in nose landing gear allow for more efficient ground taxi operations at airports [10].

2 Motor Configurations for Aerospace Applications

BLDC motor designs are currently the most commonly used for small unmanned AEP. They are very similar in design to synchronous AC motors with the primary difference being in the shape of their back-EMF waveform and rotor position sensing: BLDC motors have trapezoidal back-EMF waveforms; whilst synchronous AC machines generate sinusoidal shapes. Common BLDC configurations have the following characteristics and are more suitable for power drive applications that can withstand some torque ripple [8]:

- Full pitched and concentrated windings (generate trapezoidal back-EMF).
- Higher Power Density.
- Low cost Hall effect probes for motor commutation control.

There are two types of synchronous AC motors, namely wound-field (rotor) and permanent magnet [11]. The wound-field type requires brushes to provide an electrical current to the rotor. In common with brushed DC motor configurations, wound rotor AC machines are considered undesirable for aerospace applications on the grounds of their reduced component reliability and susceptibility to arcing. However, wound-field SMs (WFMSMs) potentially have a future in HTS aerospace applications [3]. Permanent magnet (PM) AC synchronous motors are suitable for aerospace applications and considered preferable to BLDC motors for high speed applications as they offer better control and extended field weakening capabilities. AC synchronous motor operations have the following characteristics:

- Distributed and fractional-slot windings for sinusoidal back-EMF (providing smoother operation)
- Better control and extended field weakening capabilities (for high frequency control)
- High cost shaft encoder to control stator currents.

Induction motors (IMs) are used extensively in terrestrial applications and offer a simplicity of construction combined with low costs compared with BLDC machines as their construction requires no expensive rare-earth magnets. Stator windings for induction motors are identical to those of synchronous machines; however, IMs do not match PM machines for power density. IMs also experience performance restrictions due to thermal limitations imposed by rotor induction heating effects.

A. Rotor and Stator Configurations

Stator windings are categorised as either concentrated or distributed types. BLDC motors typically have concentrated stator windings, with conductor wires wound around salient iron pole pieces. In contrast, most PM synchronous motors have distributed windings with stranded or hairpin conductor coils housed in slots evenly distributed around the stator. Both of these winding types are susceptible, in varying degrees, to generating cogging and ripple torque effects owing to variations in their magnetic circuit reluctance [12]. For aerospace applications it is desirable to minimise any sources of noise, vibration and harshness (NVH) and increased attention is being given to slotless (airgap winding) BLDC motor configurations. In [13] a design method for a small-sized brushless DC motor double-layered, short pitched hexagonal winding is provided, which offers an advantage of omitting endwindings and their associated losses. The design and analysis of a lightweight motor for aerospace applications is presented in [14],[15], which achieves high power density, zero cogging torque and low torque ripple using a rotor magnet Halbach array arrangement. Halbach arrays improve airgap flux concentration and offer the future potential to delete the rotor iron from motor designs although not from their stator [16]. Various slotless winding patterns are presented including, helical, basket, skewed (Faulhaber), rhombic, straight (with end turns), ringed and pancake forms.

B. Axial Flux Motor Configurations

Although the majority of motors are radial flux machines, axial flux PM motors attract much attention for traction and aerospace propulsion applications [21]. A comparison of the power density of axial machines is provided in [22] concluding that the axial machines analysed have higher power density when compared with IM machines.

Unfortunately, this study does not provide a like for like comparison of BLDC technologies. Although, a similar comparison of axial and radial BLDC configurations [23] concludes that the axial flux machines have much higher torque to mass ratios than radial flux machines.

C. Energy Losses

The efficiency of aerospace electric motors and their associated controllers are critical to the success of commercially viable AEP systems. BLDC motors and their associated electrical speed controllers (ESCs), used for hobby build and small unmanned aircraft projects, commonly have unit efficiencies under 80%. However, commercial AEP projects target efficiencies above 95% for motors and controllers alike. Thermal management of the power chain is critical to achieving these aims, and much effort is spent in reducing armature currents and controller switching frequencies. High DC line voltages e.g. >500VDC, allow for a significant reduction in current supply to stator windings, thus minimising the I²R losses.

Motor cooling circuits, either liquid or forced air, can further enhance motor efficiencies. Advances in solid-state Silicon Carbide IGBT switching technologies have improved motor control performance as highlighted in a recent study [24], and for high altitude aircraft operations the high voltage DC (HVDC) motor transmission lines are susceptible to corona energy discharge losses [25]. An excellent performance analysis of electric motor technologies is provided in the White Paper produced by Motor Design Ltd. of the UK [26].

3 Overview of Existing Aerospace Motor Technologies

Table III provides an overview of a range of existing aerospace motor technologies sourced online from supplier literature. Some of the aircraft listed below are still in the development phase having not yet flown. A graphical assessment of the achievable performance of these motors is provided in Fig. 4, in which motor powers have been plotted against motor speeds. It can be seen that the lower speed motors have high power applications because greater torque is required to turn large propellers. Such is the case for the magniX magni500, which is used to power the electrical version of the DHC-2 Beaver and also the Cessna Grand Caravan shown in Fig. 5.

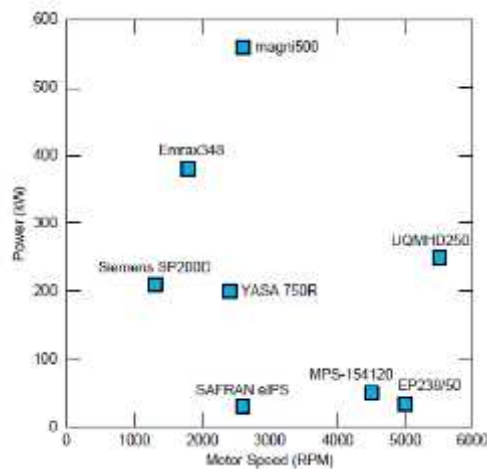


Fig. 4. Motor Powers versus Speed.

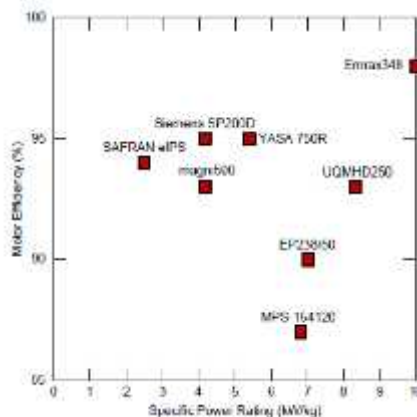


Fig. 5. Comparison of the Specific Powers and Efficiencies of the motors.

Lower motor speeds permit direct coupling of propellers and provide a weight saving that would otherwise be incurred by a reduction gearbox. Aircraft with propellers exceeding 1m in length are normally required to rotate at speeds of less than 3000 RPM to avoid performance degradations owing to sonic airflow conditions at the propeller tips. The CityAirbus (Fig. 6), is powered by eight Siemens SP200Ds which rotate at a relatively slow 1300 RPM. Conversely, the MPS 154120 and the EP 238/50 motor characteristics shown in Fig. 4, indicate motors having high rotational speeds >4000 RPM and relatively low torque characteristics. These motors have typical applications on large homebuild UAV drones and powered paragliders respectively and are readily available to purchase as off-the-shelf equipment. Interestingly the UQM Technologies motor uniquely indicates relatively high rotational speed and power characteristics.

This motor drive system was adapted from a terrestrial vehicle application for the Rutan Long ESA aircraft in a one-off AEP speed record attempt. It shows that the higher output power motors also have higher efficiencies in the range of 93% to 95%. These motors are exclusively liquid cooled and are synchronous permanent magnet types with slotted distributed windings. The lower efficiency motors have efficiencies in the range of 88% to 90% and are air cooled, BLDC permanent magnet types with concentrated windings. Interestingly, a high specific power value does not necessarily indicate good motor efficiency. The air-cooled motors indicating very good specific power values of about 7 kW/kg.

4 Conclusion

An overview of the state-of-the-art in motor topologies for AEP has been conducted, and it has been concluded that electrical motors provide an ideal means for achieving aircraft propulsion. Fan and propeller load (torque) characteristics increase gradually with rotor speed which makes them ideal for electrical motor drive applications. The operational ranges of fan and propeller speeds also permit simple, lightweight direct-drive connections to be achieved and with reference to Table III. It can be seen that the specific power values for existing AEP motor technologies range between 4 and 10 kW/kg placing them between high-performance piston engine and jet engine technologies when correlated with Table I values. It was further concluded that existing AEP motors rotate at relatively low speed ranges of 1300 to 5000 RPM when compared with civil aircraft turbo-fan engines which typically rotate between 5000 and 7000 RPM. Indicating a limitation in attainable fan efflux velocities and ultimately AEP achievable aircraft speeds. A deduction that is evidenced by the low speed aircraft applications on which current AEP motor technologies are implemented. This also suggests that higher fan and motor speeds are likely to be required for future high speed aircraft designs. To this end, development work is already underway on rim driven fan (RDF) technologies that offer the potential of high efficiency and efflux velocities. The importance of high TRV values (refer to Table II) was also realised when considering the flat disc-like, liquid cooled motor topologies evidenced by the images of the high performance motors.

References

- [1] R.C. Bolam, Y. Vagapov, and A. Anuchin, "Review of electrically powered propulsion for aircraft," in Proc. 53rd Int. Universities Power Engineering Conference (UPEC-2018), Glasgow, UK, 4-7 Sept. 2018, pp. 1-6.
- [2] C.A. Luongo, P.J. Masson, T. Nam, D. Mavris, H.D. Kim, G.V. Brown, M. Waters, and D. Hall "Next generation more-electric aircraft: A potential application for HTS superconductors," IEEE Trans. on Applied Superconductivity, vol. 19, no. 3, pp. 1055-1068, June 2009.
- [3] K. Kovalev, J. Nekrasova, N. Ivanov, and S. Zhurzhev, "Design of all-superconducting electrical motor for full electric aircraft," in Proc. Int. Conf. on Electrotechnical Complexes and Systems (ICOECS), Ufa, Russia, 21-25 Oct. 2019, pp.1-5.
- [4] M. Rosu, P. Zhou, D. Lin, D. Lonol, M. Popescu, F. Blaabjerg, V. Rallabandi, and D. Staton, *Multiphysics Simulation by Design for Electrical Machines, Power Electronics and Drives*. Piscataway, NJ:IEEE Press; Hoboken, NJ: Wiley, 2018.
- [5] H.W. Beaty, and J.L. Kirtley, *Electric Motor Handbook*. New York: McGraw-Hill, 1998.
- [6] D.G. Dorrell, M. Hsieh, M. Popescu, L. Evans, D.A. Staton, and V. Grout, "A review of the design issues and techniques for radial-flux brushless surface and internal rare-earth permanent-magnet motors," IEEE Trans. on Industrial Electronics, vol. 58, no. 9, pp. 3741-3757, Sept. 2011.
- [7] C. Liu, "Emerging electric machines and drives — An overview," IEEE Trans. on Energy Conversion, vol. 33, no. 4, pp. 2270-2280, Dec. 2018.
- [8] N. Hashemnia, and B. Asaei, "Comparative study of using different electric motors in the electric vehicles," in Proc. 18th Int. Conf. on Electrical Machines, Vilamoura, Portugal, 6-9 Sept. 2008, pp. 1-5.
- [9] W. Cao, B.C. Mecrow, G.J. Atkinson, J.W. Bennett, and D.J. Atkinson, "Overview of electric motor technologies used for more electric aircraft (MEA)," IEEE Trans. on Industrial Electronics, vol. 59, no. 9, pp. 3523-3531, Sept. 2012.
- [10] B. Sarlioglu, and C.T. Morris, "More electric aircraft: Review, challenges, and opportunities for commercial transport aircraft," IEEE Trans. on Transportation Electrification, vol. 1, no. 1, pp. 54-64, June 2015.
- [11] Hughes, and B. Drury, *Electric Motors and Drives: Fundamentals, Types and Applications*, 5th ed. Kidlington: Newnes, 2019.

- [12] Mujianto, M. Nizam, and Inayati, "Comparison of the slotless brushless DC motor (BLDC) and slotted BLDC using 2D modeling," in Proc. Int. Conf. on Electrical Engineering and Computer Science (ICEECS), Kuta, Indonesia, 24-25 Nov. 2014, pp. 212-214.
- [13] J. Seo, J. Kim, I. Jung, and H. Jung, "Design and analysis of slotless brushless DC motor," IEEE Trans. on Industry Applications, vol. 47, no. 2, pp. 730-735, Mar.-Apr. 2011.
- [14] M.S. Islam, R. Mikail, and I. Husain, "Slotless lightweight motor for aerial applications," IEEE Trans. on Industry Applications, vol. 55, no. 6, pp. 5789-5799, Nov.-Dec. 2019.
- [15] Tessarolo, M. Bortolozzi, and C. Bruzzese, "Explicit torque and back EMF expressions for slotless surface permanent magnet machines with different magnetization patterns," IEEE Trans. on Magnetics, vol. 52, no. 8, pp. 1-15, Aug. 2016, Art. no. 8107015.
- [16] N. Borchardt, and R. Kasper, "Analytical magnetic circuit design optimization of electrical machines with air gap winding using a Halbach array," in Proc. IEEE Int. Electric Machines and Drives Conference (IEMDC), Miami, FL, USA, 21-24 May 2017, pp. 1-7.
- [17] M. Nagrial, J. Rizk, and A. Hellany, "Design and performance of permanent magnet slotless machines," in Proc. 18th Int. Conf. on Electrical Machines, Vilamoura, Portugal, 6-9 Sept. 2008, pp. 1-5.
- [18] F. Magagna, and D. Peroni, "New technologies: Aluminium Litz wire," Bagnoli, Italy, De Angeli Prodotti S.r.l., 2017. [Online]. Available: http://www.deangeliprodotti.com/en/system/files/LITZ_WIRE_aluminium_high_frequencies_2017.pdf
- [19] M. Iorgulescu, "Study of single phase induction motor with aluminium versus copper stator winding," in Proc. Int. Conf. on Applied and Theoretical Electricity (ICATE), Craiova, Romania, 6-8 Oct. 2016, pp. 1-5.
- [20] S. Ayat, R. Wrobel, J. Baker, and D. Drury, "A comparative study between aluminium and copper windings for a modular-wound IPM electric machine," in Proc. IEEE Int. Electric Machines and Drives Conference (IEMDC), Miami, FL, USA, 21-24 May 2017, pp. 1-8.
- [21] F. Giulii Capponi, G. De Donato, and F. Caricchi, "Recent advances in axial-flux permanent-magnet machine technology," IEEE Trans. on Industry Applications, vol. 48, no. 6, pp. 2190-2205, Nov.-Dec. 2012.
- [22] S. Huang, J. Luo, F. Leonardi, and T.A. Lipo, "A comparison of power density for axial flux machines based on general purpose sizing equations," IEEE Trans. on Energy Conversion, vol. 14, no. 2, pp. 185-192, June 1999.
- [23] N. Balkan Simsir, and H. Bulent Ertan, "A comparison of torque capabilities of axial flux and radial flux type of brushless DC (BLDC) drives for wide speed range applications," in Proc. IEEE Int. Conf. on Power Electronics and Drive Systems, Hong Kong, 27-29 July 1999, vol. 2, pp. 719-724.
- [24] R. Ghosh, "Performance analysis of a silicon carbide IGBT for SVM PWM induction motor drive applications," in Proc. Devices for Integrated Circuit (DevIC), Kalyani, India, 23-24 March 2017, pp. 522-526.
- [25] X. Bian, L. Wang, Y. Liu, Y. Yang, and Z. Guan, "High altitude effect on corona inception voltages of DC power transmission conductors based on the mobile corona cage," IEEE Trans. on Power Delivery, vol. 28, no. 3, pp. 1971-1973, July 2013.
- [26] J. Goss, "Performance analysis of electric motor technologies for an electric vehicle powertrain," Wrexham, UK, Motor Design Ltd., White Paper, 2019. [Online]. Available: <https://www.motor-design.com/wp-content/uploads/2019/06/Performance-Analysis-of-Electric-Motor-Technologies-for-an-Electric-Vehicle-Powertrain.pdf>
- [27] R.C. Bolam, and Y.Vagapov, "Implementation of electrical rim driven fan technology to small unmanned aircraft," in Proc. Int. Conf on Internet Technologies and Applications, Wrexham, UK, 12-15 Sept. 2017, pp 35-40.

PERFORMANCE ENHANCEMENT STUDY FOR SINGLE SLOPE SOLAR DESALINATION PLANT

M. Kavitha, Department of Mechanical Engineering, MRK Institute of Technology
K. Anandavelu, Department of Mechanical Engineering, MRK Institute of Technology
K. Thiruvagasamoorthy, Department of Mechanical Engineering, MRK Institute of Technology

Abstract

The global imbalance between supply and demand for fresh water is being created by population growth, economic expansion, and global warming. Fresh water must be discovered, and the most likely sources are the world's vast oceans and seas, which can be distilled using a variety of means, including solar energy. The majority of existing desalination units are powered by fossil fuels. Multi-effect evaporation, multi-stage flash distillation, thin film distillation, reverse osmosis, and electro dialysis are all energy intensive and have high running costs. The usage of conventional energy sources (hydrocarbon fuels) to power these devices, on the other hand, has a negative environmental impact.

Solar distillation is a particularly appealing and straight forward technique among other distillation methods, and it is particularly well suited to small-scale units in areas where solar energy is abundant. The basic concept of harnessing solar energy to turn salty, brackish or contaminated water into potable water is actually fairly simple. Water evaporates when it is kept in a closed container in the open air. A solar still's purpose is to collect evaporated water by condensing it on a cool surface. Solar radiation is employed to speed up the evaporation process.

The ultimate goal of most solar distillation research is to enhance the distillate yield from the solar still. This is accomplished by either raising the water temperature or lowering the temperature of the condensing cover. As a result, any new strategy should be able to efficiently achieve one of the two goals.

The goal of this research is to improve the productivity of a solar desalination plant by (i) increasing the temperature difference between water and glass, (ii) reducing heat losses from the still by using energy storage materials inside the basin, and (iii) studying other parameters such as water depth. The same design parameters are used to manufacture two single slope single basin solar desalination machines. On the single slope solar distillation system, several experimental studies were undertaken to improve productivity with various parameters such as the effect of water depth and energy storage materials.

Keywords: *Solar, desalination, Distillation, Solar still, Slope, brackish and basin*

1. Importance of water for humanity

In earlier days, when the population was small and people lived near water resources, the average consumption of water used to be 15 to 25 liters per person per day. This has however increased to 75 to 100 liters per person per day in the twenty first century. Fresh water, which was available from rivers, lakes and ponds in plenty, is becoming scarce because of industrialization and population explosion. Moreover, these potable water sources are being polluted constantly by industrial wastes and sewage. It is said that presently more than 2000 million people do not get potable water, which leads to many diseases and stops development (Garg and Prakash 2000). Looking at the scarcity and large demand of fresh water, the United Nations on November 10, 1980 declared the years between 1981 and 1990 as the decade of water supply and sanitation. Many U.N. organizations like UNDP, WHO and the World Bank are now actively involved throughout the world in promoting projects concentrating on the supply of fresh water for drinking purposes.

The Government of India too has accorded a top priority to drinking water supply and in order to meet the challenge, has set up a technology mission, known as Rajiv Gandhi National Drinking Water Mission (RGNDWM). The mission functioning under the department of Rural Development is responsible for water management and its scientific application. In India, a huge quantum of national revenue allocated for providing basic infrastructure are not effectively used, thus failing to yield the desired outcome. RGNDWM has developed technologies suitable for water resources development. A wide spread knowledge of scientific practices among the common people, in particular village level functionaries, helps in preventing wastage of water. Vital benefits such as sustained supply of potable water have been realized in drought prone areas

after adopting a scientific approach. The approach makes it possible, (i) to optimize water use so that it can be made available in desired time and space, (ii) avoid wastage and (iii) make it economically viable.

2. Water resources in arid areas

At least eighty arid and semi-arid countries, where 40% of the world's population live, have serious periodic droughts. Some of the highest population growth rates are found in arid countries, many of which are already experiencing severe water scarcity. Areas likely to face increased water shortage include much of Northern Africa, parts of India and Mexico, Northern China, much of the Middle East, parts of the Western United States, North eastern Brazil and the former Central Asian Republics of Soviet Union.

Hydrologists regard that countries whose renewable fresh water availability on an annual per capita basis exceeds about 1700 m³, will suffer only occasional or local water problems. At this threshold, countries begin to experience periodic or regular water stress. When fresh water availability falls below 1000 m³/year per person, countries experience chronic water scarcity in which the lack of water begins to hamper economic development and human health and well being. When renewable fresh water supplies fall below 500 m³ per person, countries experience absolute scarcity. In 1990, 335 million people living in about 28 countries experienced water stress or scarcity (Table 1.1). By 2025, from 46 to 52 countries will fall into these categories, and the number of people in such countries could be as low as 2.782 billion or as high as 3.29 billion, depending on the rate of population growth over the next two decades (Chaibi 2000).

Table 1.1 List of countries affected by shortage of water (Chaibi 2000)

Countries	Annual renewable fresh water available, m ³ per capita	Annual withdrawals m ³ per capita	Population growth rate from 1990-2025, %	Annual desalination production, m ³ per capita
Water scarce countries				
Kuwait	15	358	30	154
Djibouti	26	13	163	0.17
Malta	110	152	22	85
U.A.Emirates	142	1109	75	203
Libya	185	852	183	13
Qatar	194	529	71	179
Bahrain	198	423	87	78
Barbados	195	117	18	--
Singapore	221	141	22	0
Yemen	243	202	193	0
Saudi Arabia	306	949	171	40
Jordon	327	179	169	0
Oman	460	566	208	15.7
Israel	461	447	75	--
Tunisia	463	348	66	1.33
Burundi	655	16	144	0
Algeria	711	288	107	2.34
Kenya	770	76	170	0
Cap Verde	789	70	113	5.25
Rwanda	840	102	193	0
Egypt	927	880	78	0.4
Water stresses countries				
Morocco	1117	407	89	0
Cyprus	1213	285	28	9.43
South Africa	1317	327	92	0.43
South Korea	1452	--	16	--

Poland	1467	--	14	--
Malawi	1500	87	160	0
Somalia	1700	94	169	0

3. Reasons for Opting Solar Still

Distillation process is considered as one of the simplest and widely adopted techniques for converting seawater into fresh water. One of the main advantages of the distillation process is that it requires heating only up to 130 - 135°C, which can be supplied from solar energy or other cheap fuels. The desalination processes such as multistage flash evaporation, reverse osmosis, electro dialysis, ion-exchange, phase change and solvent extraction are energy intensive, expensive and uneconomical for small quantities of fresh water.

On the other hand, the use of conventional energy sources (hydrocarbon fuels) to drive these technologies has a negative impact on the environment. However, solar stills are particularly suitable for developing countries and especially for remote rural areas because they have great economic advantage over other distillation processes with low operating and maintenance costs. In addition to this, their daily operation and routine maintenance is simple, and above all the solar energy is abundant, everlasting, cost free, pollution free and available on site. Because of the simplicity of the apparatus design, requirement of fresh water, and free thermal energy, work in the field of solar distillation has been in progress for more than one hundred years. The main drawback of the solar desalination systems is that it requires large installation areas and high initial investment. However, this is an appropriate solution for remote areas and small communities in arid and semi-arid regions with lack of potable water.

Solar distillation process has been developed in different countries all over the world like Australia, Greece, Spain, West Indies and India. There are various categories of solar stills namely basin solar stills, solar collector still, multiple condensing cover still, wick type solar still, vertical solar still etc. of which more than 90 percent of all functioning stills are of the basin type. The details about classification and functions of various solar distillation systems are explained in the next chapter. Although solar distillation at present cannot compete with oil fired desalination in large central plants, it has potential to become a viable technology in near future, when oil supplies stops.

4. Principle of Solar Still

In the hydrologic cycle, nature utilizes solar energy for converting saline water into fresh water by solar heating of water from oceans, lakes, rivers and other large bodies of water. Vapor is being continuously generated and transported by wind to distant places, which gets condensed and precipitated in the form of rain or snow at cooler regions. This is schematically shown in Figure 1.1. This natural process is the basic principle of basin type solar still.

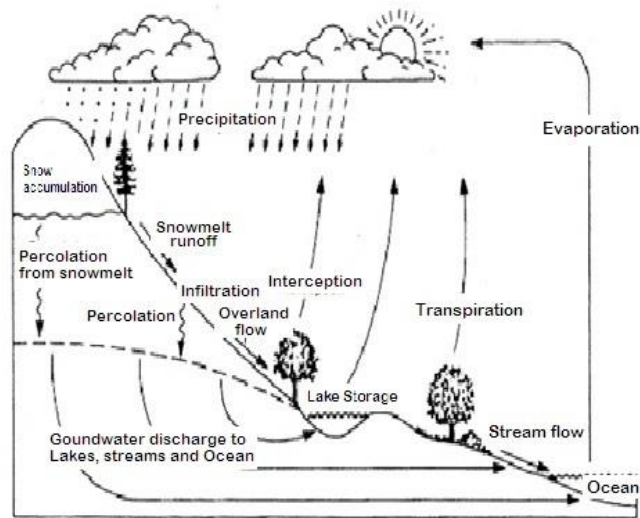


Figure 1.1 Hydrologic water cycle

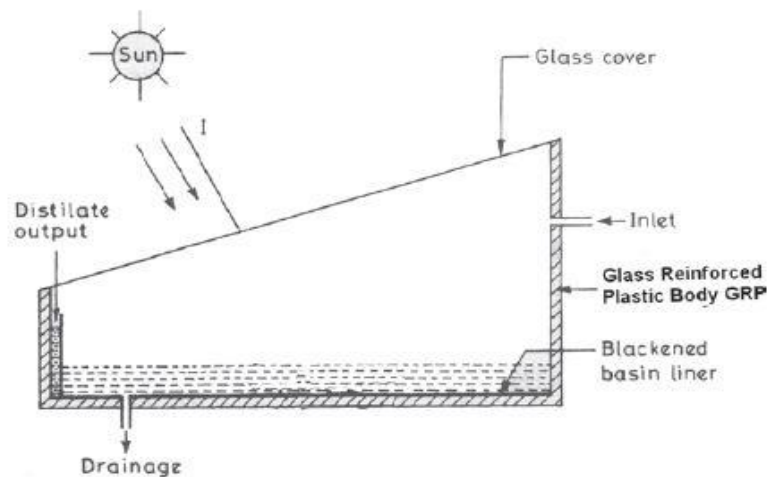


Figure 1.2 Simple solar still

In solar distillation process, sun's energy in the form of short electromagnetic waves passes through a clear glazing surface such as glass. Upon striking a darkened surface, this light changes wavelength, becoming long waves of heat, which is added to the water in a shallow basin below the glazing. As the water heats up, it begins to evaporate. The warm vapor rises to a cooler area. Almost all impurities are left behind in the basin. The vapor condenses onto the underside of the cooler glazing and accumulates into water droplets or sheets of water. The combination of gravity and the tilted glazing surfaces allows the water to run down the cover into a collection trough, where it is channeled in to storage. The schematic arrangement of simple solar still is shown in Figure 1.2.

5. Benefits of Solar Distillation

- Solar distillation could benefit developing countries in several ways, for example, Solar energy is abundant, everlasting, cost free and pollution free and available on site.
- Solar distillation can be a cost effective means of providing four basic human needs i.e. clean water for drinking, cooking, washing and bathing.
- Solar distillation generally uses less energy to purify water than other methods.
- It can foster cottage industries, animal husbandry, or hydroponics for food production in areas where such activities are now limited by inadequate supplies of pure water. Fishing could become important on desert seacoasts where no drinking water is available for fisher men.

- Solar distillation will permit settlement in sparsely populated locations, thus relieving population pressures in urban areas.
- Solar stills, operating on sea or brackish water, can ensure supplies of water during a time of drought.
- The daily operation and routine maintenance is simple.
- No skilled labor is required.
- The potential to use local materials.
- No energy costs.
- Not subject to fuel supply interruptions.
- In residential installations, no subsequent costs for delivering water to the end user.

References

1. Zhenyuan Xu, Lenan Zhang, Lin Zhao, Bangjun Li, Bikram Bhatia, Chenxi Wang, Kyle L. Wilke, Youngsup Song, Omar Labban, John H. Lienhard, Ruzhu “Ultrahigh-efficiency desalination via a thermally-localized multistage solar still” *Energy Environ. Sci.*, 2020, 13, 830, DOI: 10.1039/c9ee04122b
2. Farel H Naptitupulu, A. Halim Nasution, Himsar Ambarita” Exergy analysis of double slope passive solar still” *Material Science and Engineering* 725 (2020) 012005 doi:10.1088/1757-899X/725/1/012005
3. T. Arunkumar K. Vinothkumar Amimul Ahsan R. Jayaprakash and Sanjay Kumar “Experimental Study on Various Solar Still Designs” Volume 2012, Article ID 569381, 10 pages doi:10.5402/2012/569381
4. G. M. AYOUB and L. MALAEB “Developments in Solar Still Desalination” *Critical Reviews in Environmental Science and Technology*, 42:2078–2112, 2012, DOI: 10.1080/10643389.2011.574104
5. Aboul-Enein S., El-Sebaï A.A. and El-Bialy E. (1998), ‘Investigation of a single-basin solar still with deep basins, *Renewable Energy*’, Vol. 14, Issues 1-4, pp. 299-305.
6. Abu-Hijleh B.A/K. (1996), ‘Enhanced solar still performance using water film cooling of the glass cover’, *Desalination*, Vol. 107, Issue 3, pp. 235-244.
7. Akash B.A, Mohsen M.S., Osta O and Elayan Y. (1998), ‘Experimental evaluation of a single-basin solar still using different absorbing materials’, *Renewable Energy*, Vol. 14, Issues 1-4, pp. 307-310.
8. Ashokkumar, Anand J.D. and Tiwari G.N. (1991), ‘Transient analysis of a double slope-double basin solar distiller’, *Energy Conversion and Management*, Vol. 31, Issue 2, pp. 129-139.
9. Badran O.O. and Abu-Khadar M.M. (2007), ‘Evaluating thermal performance of a single slope solar still’, *Heat and Mass Transfer*, Vol. 43, pp. 985-995.
10. Bahadori M.N. and Edlin F.E. (1973), ‘Improvement of solar stills by the surface treatment of the glass’, *Solar Energy*, Vol. 14, Issue 3, pp. 339-352
11. Chaibi M.T. (2000), ‘An overview of solar desalination for domestic and agriculture water needs in remote arid areas’, *Desalination*, Vol.127, Issue 2, 1, pp. 119-133.
12. Dhiman N.K. and Tiwari G.N. (1990), ‘Effect of water flowing over the glass cover of a multi-wick solar still’, *Energy Conversion and Management*, Vol. 30, Issue 3, pp. 245-250.
13. Dunkle R.V. (1961), ‘Solar water distillation: the roof type still and multiple effect diffusion still’. *International Developments in Heat Transfer, ASME Proc. International Heat Transfer, Part V, University of Colorado*, p. 895.
14. Dutt D.K, Ashokkumar, Anand J.D and Tiwari G.N. (1993), ‘Improved design of a double effect solar still’, *Energy Conversion and Management*, Vol. 34, Issue 6, pp. 507-517.
15. El-Bassouni A.A. (1993), ‘Factors influencing the performance of basin-type solar desalination units’, *Desalination*, Vol. 93, Issues 1-3, pp. 625-632.
16. El-Haggar S.M. and Awn A.A. (1993), ‘Optimum conditions for a solar still and its use for a green house using the nutrient film technique’, *Desalination*, Vol. 94, Issue 1, pp. 55-68.
17. El-Sebaï A.A., Aboul-Enein S., Ramadan M.R.I. and El-Bialy E. (2000), ‘Year-round performance of a modified single-basin solar still with mica plate as a suspended absorber’, *Energy*, Vol. 25, Issue 1, pp. 35-49.
18. Garg H.P. and Prakash J. (2000), ‘Solar Energy: Fundamental and applications’, Tata McGraw-Hill Publications Company Limited, New Delhi, pp. 176-190.
19. Gomkale S.D. (1988), ‘Operational experience with solar stills in an Indian village and their contribution to the drinking water supply’, *Desalination*, Vol. 69, Issue 2, pp. 177-182.
20. Gomkale S.D. and Datta R.L. (1973), ‘Some aspects of solar distillation for water purification’, *Solar Energy*, Vol. 14, Issue 4, pp. 387-392.
21. Headley O.StC. (1973), ‘Cascade solar still for distilled water production *Solar Energy*’, Vol. 15, Issue 3, pp 245-

252,

22. Howe E.D. and Tleimat B.W. (1977), 'Fundamentals of water desalination', Solar Energy Engineering by Sayigh A.A.M., Academic Press, New York, pp. 431-264.
23. Lawrence S.A. and Tiwari G.N. (1990), 'Theoretical evaluation of solar distillation under natural circulation with heat exchanger', Energy Conversion and Management, Vol. 30, Issue 3, pp. 205-213.
24. Malik M.A.S., Tiwari G.N., Kumar A. and Sodha M.S. (1982), 'Solar Distillation', Pergamon Press, UK.
25. Mohammed Farid and Faik Hamad (1993), 'Performance of a single-basin solar still', Renewable Energy, Vol. 3, Issue 1, pp 75-83.
26. Mukherjee K. and Tiwari G.N. (1986), 'Economic analyses of various designs of conventional solar stills', Energy Convergent and Management, Vol. 26, Issue 2, pp. 155-157.
27. Nafey A.S., Abdelkader M., Abdelmotalip A. and Mabrouk A.A. (2001), 'Solar still productivity enhancement', Energy Conversion and Management, Vol. 42, Issue 11, pp. 1401-1408.
28. Phadatare M.K. and Verma S.K. (2007), 'Influence of water depth on internal heat and mass transfer in a plastic solar still', Desalination, Vol. 217, Issues 1-3, pp. 267-275.
29. Rahim NHA. (2003), 'New method to store heat energy in horizontal solar desalination still', Renewable Energy, Vol. 28, pp. 419-433.
30. Rai S.N. and Tiwari G.N. (1983), 'Single basin solar still coupled with flat plate collector', Energy Conversion and Management, Vol. 23, Issue 3, pp. 145-149.
31. Rai S.N., Dutt D.K. and Tiwari G.N. (1990), 'Some experimental studies of a single basin solar still', Energy Conversion and Management, Vol. 30, Issue 2, pp. 149-153.
32. Sakthivel M. and Shanmugasundaram S. (2008), 'Effect of energy storage medium (black granite gravel) on the performance of a solar still', International Journal of Energy Research, Vol. 32, Issue 1, pp. 68-82.
33. Sanjeevkumar and Tiwari G.N. (1998), 'Optimization of collector and basin areas for a higher yield for active solar stills', Desalination, Vol. 116, Issue 1, pp. 1-9.
34. Tayeb A.M. (1992), 'Performance study of some designs of solar stills', Energy Conversion and Management, Vol. 33, Issue 9, pp. 889-898
35. Tiwari G.N., Mukherjee K., Ashok K.R. and Yadav Y.P. (1986), 'Comparison of various designs of solar stills', Desalination, Vol. 60, Issue 2, pp. 191-202.

Conclusions

- The average consumption of water used to be 15 to 25 liters per person per day, which has increased to 75 to 100 liters per person per day in the twenty first century.
- Water-related diseases are among the most common causes of illness and death, affecting mainly the poor in developing countries. It is necessary to take corrective action to solve water crisis problem.
- The hydrocarbon based fuel technologies for producing drinking water are expensive, uneconomical and makes negative impact on the environment.
- Solar stills are one of the best options as its daily operation and routine maintenance is simple.
- Solar distillation is the best solution for remote areas and small communities in arid and semi-arid regions with lack of water
- Solar energy is abundant, everlasting, available on site, free of cost and pollution free energy.

1 A Brief Review on the Influence of Nanofillers on Composite Efficiency

A.Abinesh, Dept. of Mechanical Engineering, V.R.S. College of Engineering and Technology, Arasur, Villupuram, Jayakrishnan, Dept. of Mechanical Engineering, V.R.S. College of Engineering and Technology, Arasur, Villupuram, Robin Paul, Dept. of Mechanical Engineering, V.R.S. College of Engineering and Technology, Arasur, Villupuram, A.Shanmugarajan, Dept. of Mechanical Engineering, V.R.S. College of Engineering and Technology, Arasur, Villupuram,

Abstract

The use of nanomaterials has a significant influence on the development of many items in today's world. The use of nanofillers in composite products is one form of nanomaterial development idea. This review provides an overview of the production of various nanofillers and their types, as well as the manufacturing of various composite combinations using various nanofillers. The inclusion of these nanofillers as a reinforcement or matrix for composite fabrication has a substantial influence on the composites' mechanical characteristics. A special emphasis is placed on the nanofiller dispersion, which improves the mechanical qualities. Better matrix-reinforcement bonding only increases the characteristic of how nanofillers act in that aspect, which is also explored in this paper. The paper also discusses the dispersion of nanofillers in various polymer matrix composites. The composites' tensile, flexural, and impact characteristics determine their suitability for diverse structural applications, and this paper summarizes how these properties change concerning various nanofillers. This review study also discusses the effects of nanofillers on thermal characteristics and their influence in diverse industries such as automotive, medicinal, sports, and aerospace applications.

Introduction

The present era's technological advancements are focused on the creation of materials using nanotechnology, which has attracted a large number of researchers interested in developing new materials for diverse purposes. The use of nanofillers is one such method originating from nanotechnology. Nanofillers are deposited into different polymer matrices to see how they influence mechanical, thermal, electrical, and moisture resistant qualities. Fillers, which work as a binder to keep the matrix and reinforcement tightly together, first appeared in composites at the turn of the twentieth century. Because the major benefit supplied by nanofillers or particles is the high surface-to-volume ratio, which in turn enhances the filler and matrix binding, they are the ones that find their position as the nano idea grows. The mechanical characteristics are determined by the evenly scattered nanofillers [1]. The adhesion between fillers and matrixes improves with the addition of nanofillers, preventing composite failure in the early stages. Based on early research, this review paper briefly discusses the manufacturing of composites employing nanofillers and their impact on mechanical characteristics. In addition, the correct approach for producing nanofillers composites is highlighted in this paper to solve dispersion concerns.

Nanofiller Composite Fabrication

Nanofillers, such as nanoclays and carbon nanotubes, are used in the early phases of the process. Nanofillers are employed in such a way that the matrix or reinforcement all have dimensions between 1 and 100 nanometers. Nanofillers come in a variety of shapes, including nanoplates in 1D, nanofibers in 2D, and nanoparticles in 3D, depending on the shape. CaCO₃, Silica, and carbon are the most common forms of nanofillers, and research into them is ongoing; nevertheless, Alumina, Magnesium, Silicon carbide, Titanium, and zinc oxide are a few new materials utilized as nanofillers. These are all common nano-filler materials used in composites. Depending on the applications they have chosen, each material has certain unique features in terms of enhancing mechanical, wear, thermal, and

electrical properties. Insitu technique, wet process-sol-gel method, dry process-ball milling, gas impingement, etc., evaporation process-CVD, GVD, and sedimentation process are the most generally accessible methods for making nanofiller based composites.

Different Performance Investigations on Nanofiller Composites

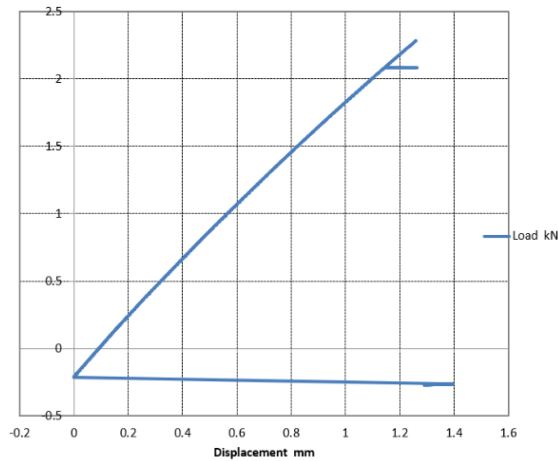
Dilip Kumar, Santharaja. M, Ravindra, et al. [1] conducted experimentation to forecast the optimum combination of factors level, predict the most affecting factors for the test models, and get optimal mechanical characteristics. Tensile tests are performed on test models, with the findings used for experimental and optimum evaluation of mechanical response. The Taguchi analysis using the orthogonal array approach employed the experimental values collected from the tests as input information. The optimal combination of components was predicted from the input data signal to noise ratio and mean value based on the analysis.



Means value plot of Maximum Tensile stress (Source: Dilip Kumar, Santharaja. M, Ravindra, et al.)

Level	GF	NF	AO
1	23.07	23.67	17.87
2	24.72	23.77	25.23
3	25.15	23.86	26.83
4	23.16	24.81	26.17
Delta	2.08	1.14	8.97
Rank	2	3	1

Response Table for Means of Tensile stress (Source: Dilip Kumar, Santharaja. M, Ravindra, et al.)



Tensile test result plot (Source: Dilip Kumar, Santharaja. M, Ravindra, et al.)

The effect of three parameters that are depending on tensile and Young's modulus of hybrid nanocomposite material was examined using the Taguchi technique. Young's modulus of nylon fibre is higher, but the tensile stress value of glass fibre is higher. By raising the proportion over 15% by volume, the glass fibre raises Young's modulus value to 15% by volume fraction and displays a diminishing trend. When the nylon fiber fraction by volume is increased, the trend increases, but when the fraction by volume is increased by over 15%, the trend decreases.



Main effect plots of Young's modulus (Source: Dilip Kumar, Santharaja. M, Ravindra, et al.)

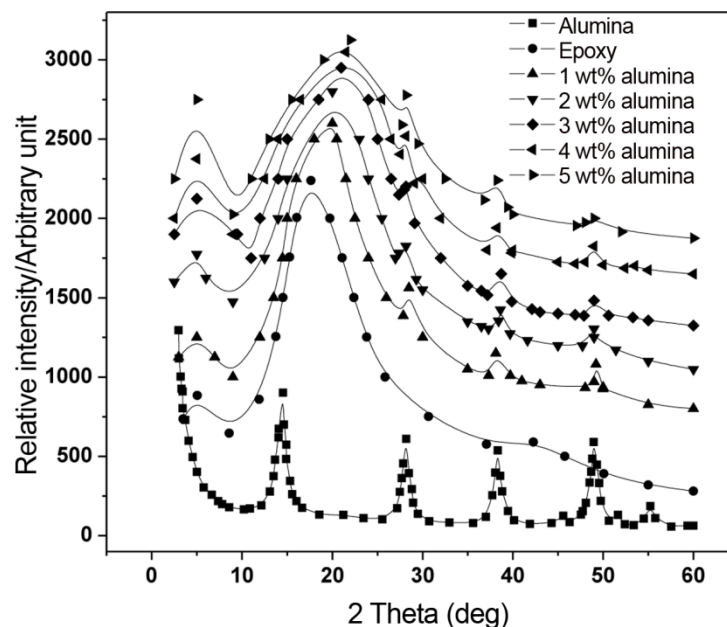
Level	GF	NF	AO
1	4.085	3.942	3.823
2	4.145	4.060	4.107
3	4.138	4.200	4.230
4	4.060	4.225	4.268
Delta	0.085	0.282	0.445
Rank	3	2	1

Response Table for Means of Young's Modulus (Source: Dilip Kumar, Santharaja. M, Ravindra, et al.)

The investigations showed that adding alumina filler materials above 1.0 percent by volume reduces tensile stress values due to increased filler distribution and filler materials dominating the materials. In contradiction Young's modulus increases with increasing nano aluminium oxide percentage but decreases after 1.0 percent by volume fraction.

Akash Mohanty, V.K.Srivastava, et al. [2] investigated the Effect of Alumina Nanoparticles on the Enhancement of Impact and Flexural Properties of the Short Glass/Carbon Fiber Reinforced Epoxy Based

Composites. They used nanocomposites test coupons that were prepared through the open molding route. At an optimum concentration of alumina particles (2 wt%), nanoscale dispersion is obtained, resulting in increased thermal stability, impact strength, flexural modulus, and flexural strength of composites. The largest increase in impact energy was found to be 84 percent when 2 wt % alumina particles were added to the epoxy matrix, 20 % for flexural strength when 3 wt percent was added, and 35 At an optimum concentration of alumina particles (2 wt%), nanoscale dispersion is obtained, resulting in increased thermal stability, impact strength, flexural modulus, and flexural strength of composites. The largest increase in impact energy was found to be 84 percent when 2 wt % alumina particles were added to the epoxy matrix, 20 % for flexural strength when 3 wt% was added, and 35 percent for flexural modulus when 5 wt percent alumina particles were added to the epoxy matrix. There was a 130 % and 170 % increase in flexural strength and a 55 percent and 95 % increase in flexural modulus when 5 wt% short glass/carbon fibres were added to the epoxy. for flexural modulus when 5 wt percent alumina particles were added to the epoxy matrix. There was a 130 % and 170 % increase in flexural strength and a 55 % and 95 % increase in flexural modulus when 5 wt% short glass/carbon fibres were added to the epoxy.



XRD patterns of alumina, epoxy, and their samples from 0 wt%, 1 wt%, 2 wt%, 3 wt%, 4 wt%, and 5 wt% aluminas, scanned from 3 to 60 degrees in a 2θ scan. (Source: Akash Mohanty, V.K.Srivastava, et al.)

In comparison to plain epoxy and fibre reinforced epoxy composites, adding an optimal concentration (2 wt%) of alumina nanoparticles to short glass/carbon fibre reinforced epoxy composites improved impact strength, flexural modulus, and flexural strength. The improvement was due to better stress transfer properties from fibre and

nanoparticles to the matrix, which were attributed to the presence of strong interfacial interactions between both reinforcement and matrix, resulting in greater resistance to fibre pullout than fibre reinforced composites without alumina nanoparticles.

B.M.Rudresh, B.N. Ravi Kumar, D.Madhu, et al. [3] researched the effect of a combination of micro-and nano-fillers on the mechanical, thermal, and morphological behavior of glass–carbon PA66/PTFE hybrid nano-composites. They studied the hybrid glass–carbon fiber–reinforced 80 wt.% PA66–20 wt.% PTFE blend (GC), GC/micro-fillers (MoS₂, SiC, Al₂O₃) (GCM), and GCM/nano-filler (Al₂O₃) (GCN). the material in this research. The melt mix method with the extrusion technique was used for producing the composite. The influence of micro-fillers on the mechanical behavior of micro-composites was discovered through experiments (GCM). The cumulative impact of micro and nano-fillers somewhat degraded the tensile and flexural behavior of nano-composites but increased their impact performance (GCN).

Composites	Temperatures (°C)			ΔH_m (J/g)	Crystallinity (%) (X_c)
	T_o	T_m	T_c		
Hybrid composites(GC)	235.55	249.12	269.24	49.35	25.18
Micro-composites (GCM)	239.37	247.36	269.24	42.27	21.57
Nano-composites (GCN)	236.94	246.56	263.24	39.8	20.34

The heat of fusion of pure crystalline polyamide 66 is 196 J/g

Thermal data of nanocomposites obtained from DSC thermograms (Source: B.M.Rudresh, B.N. Ravi Kumar, D.Madhu, et al)

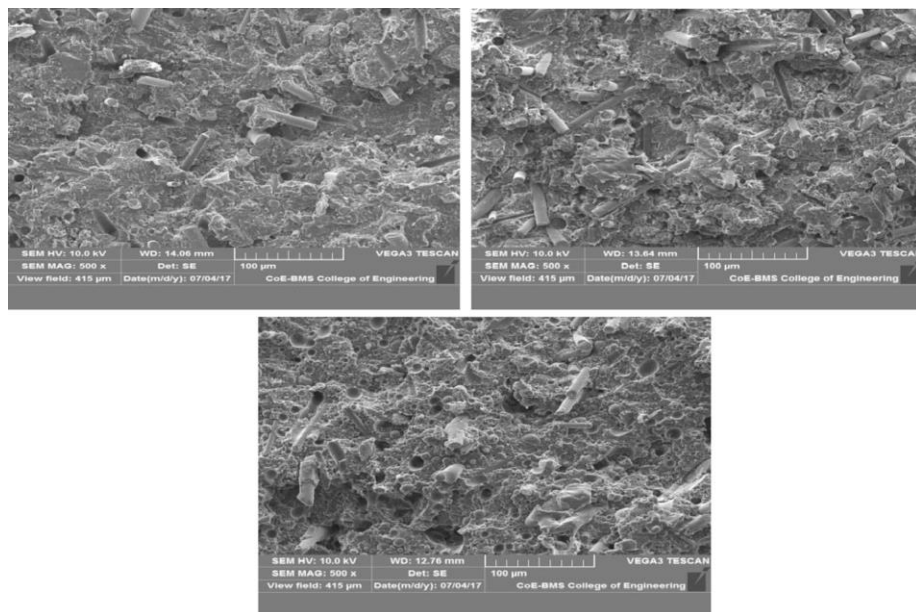
Table 7 The weight loss at different temperatures of nano-composites

Composites	The percentage weight loss at different temperatures (± 2 °C)				
	0%	10%	20%	50%	Maximum
Hybrid composites(GC)	323	431	453	483	624
Micro-composites (GCM)	337	431	451	487	575
Nano-composites (GCN)	342	359	421	515	535

Table 8 Thermal data obtained from TGA thermo grams of micro- and nano-fillers-filled hybrid thermoplastic composites

Composites	Degradation stage and their thermal behavior					
	Stage I			Stage II		
	T_o	T_p	T_c	T_o	T_p	T_c
Hybrid composites(GC)	323.15	472.27	519.11	519.11	554.84	623.86
Micro-composites (GCM)	336.71	464.86	510.48	510.48	524.03	574.56
Nano-composites (GCN)	350.23	494.23	520.45	520.42	550.25	590.42

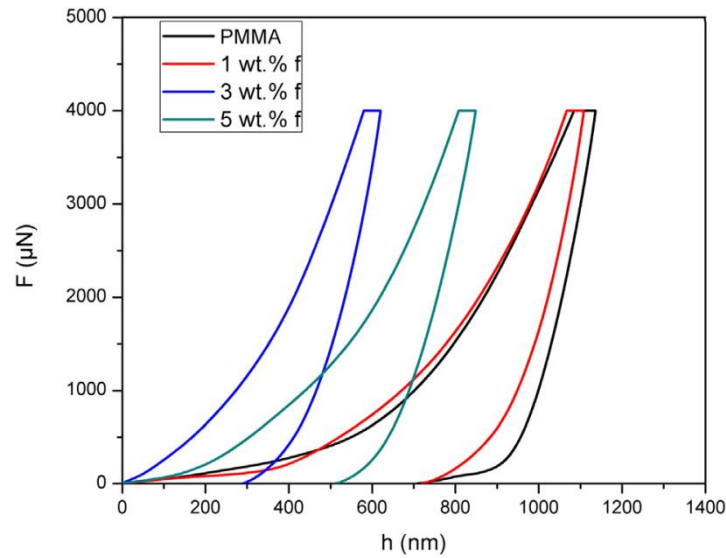
T_o , onset temperature; T_p , peak temperature; T_c , crystalline temperature



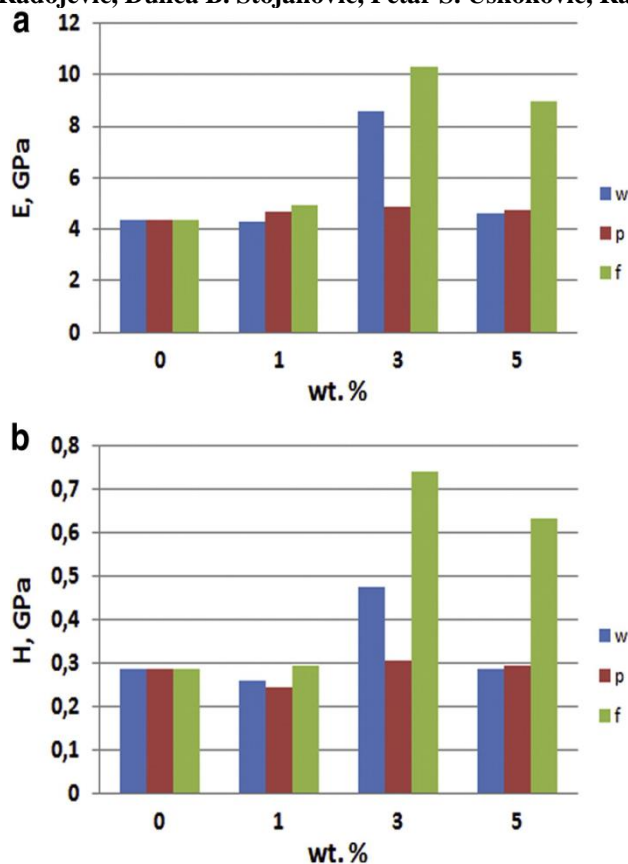
SEM images of the fractured surfaces of nano-composites: a tensile fracture, b flexural fracture, and c impact fracture (Source: B.M.Rudresh, B.N. Ravi Kumar, D.Madhu, et al.)

The synergistic effect of micro- and nano-fillers limited the strength loss of nano-composites at higher temperatures, indicating thermal stability. The broken surfaces also are characterized by fiber breakage, significant deformation, and modest agglomeration of nano-particles in the composite material, according to the morphology investigation using SEM photos. The synergistic action of micro and nano-fillers has reduced the tensile and flexural behavior of nano-composites while significantly increasing their impact strength. Furthermore, due to the synergistic action of fillers, the rigidity of nano-composites is slightly reduced. The effect of micro filler addition has reduced the thermal stability of micro composites. However, due to the combined action of micro- and nano-fillers, little difference in the degree of stability of nano-composites has been found. Due to the synergistic action of fillers, weight loss of nanocomposites at higher temperatures has been slightly prevented. The morphology of nano-composites revealed that mechanical failure is caused by fiber pullout, fiber fracture, the crystalline character of composites, and little filler agglomeration.

Faisal Ali Alzarrug, Marija M. Dimitrijevic b, Radmila M. Jancic Heinemann, Vesna Radojevic, Duiica B. Stojanovic, Petar S. Uskokovic, Radoslav Aleksic, et al. [4] summarized the use of different alumina fillers for improvement of the mechanical properties of hybrid PMMA composites. They have used alumina fillers having several morphologies that were used for reinforcing the PMMA-based composite materials. The fillers used were chemically identical, but morphologically they were spherical nanoparticles, whiskers, and an electrospun composition made up of micro-sized mainly spherical particles and nanofibers. Aluminum chloride hydroxide/PVA/water solution was used to create the electrospun product. The mechanical properties of the composites were investigated using dynamic mechanical analysis (DMA) and nanoindentation after all fillers were added without being treated on the surface. The lowered elastic modulus for the resulting specimens with 3 wt.% electrospun product was 134% of that achieved with the polymer alone, and the hardness was improved to 157.8% when compared to the polymer without any addition, according to the nanoindentation data.



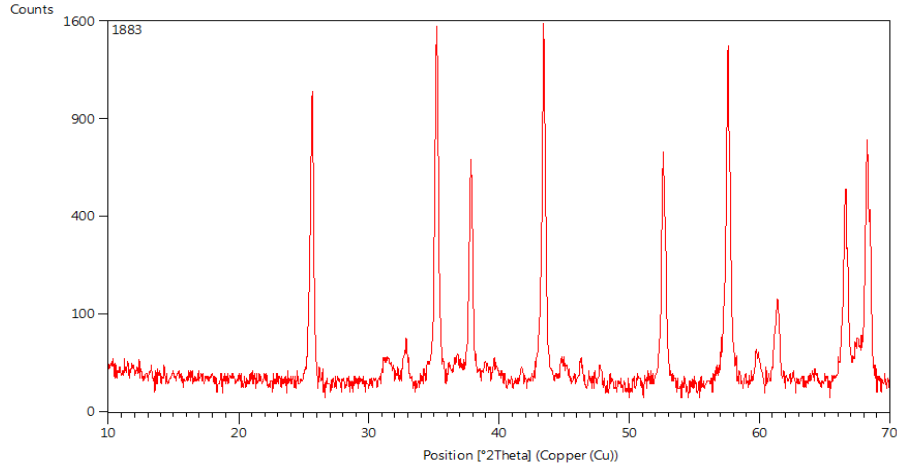
Nanoindentation curves for the best performing specimens were obtained using 1 wt.%, 3 wt.%, and 5 wt.% of electrospun alumina fillers. (Source: Faisal Ali Alzarrug, Marija M. Dimitrijevic b, Radmila M. Jancic Heinemann, Vesna Radojevic, Duiica B. Stojanovic, Petar S. Uskokovic, Radoslav Aleksic et al.)



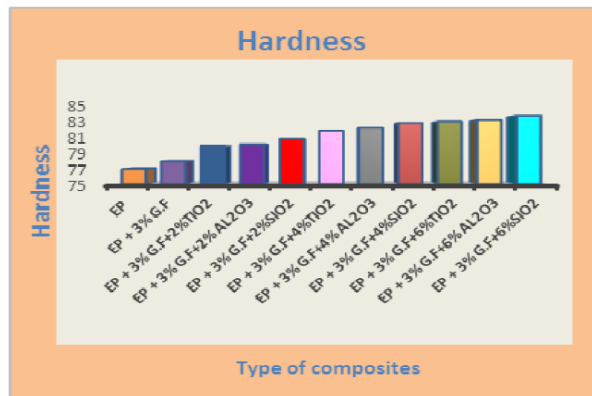
Mean values of reduced elastic modulus and hardness were measured using the nanoindentation technique for specimens containing different fillers. (Source: Faisal Ali Alzarrug, Marija M. Dimitrijevic b, Radmila M. Jancic Heinemann, Vesna Radojevic, Duiica B. Stojanovic, Petar S. Uskokovic, Radoslav Aleksic et al.)

Aseel Basim Abdul-Hussein, Fadhel Abbas Hashim, Tamara Raad Kadhim, et al. [5] studied the Effect of Nano Powder on Mechanical and Physical Properties of Glass Fiber Reinforced Epoxy Composite. To improve the mechanical and physical properties of the glass fiber/epoxy composite, we added Al₂O₃, SiO₂, and TiO₂ nanoparticles to the epoxy matrix. Hand lay-up is used to create the composites. Mechanical parameters such as flexural strength and

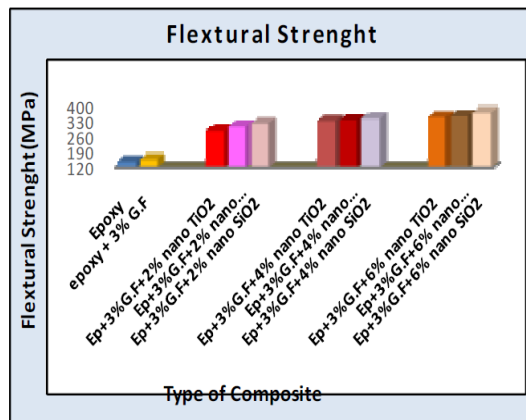
hardness are higher in SiO₂-modified epoxy composites than in other nano modifiers, however, physical properties such as density and water absorption are higher in TiO₂ modified epoxy composites. This could be due to silica's lesser particle size compared to other minerals.



The XED of nanopowder (Source: Aseel Basim Abdul-Hussein, Fadhel Abbas Hashim, Tamara Raad Kadhim, et al.)



The hardness of prepared composite (Source: Aseel Basim Abdul-Hussein, Fadhel Abbas Hashim, Tamara Raad Kadhim, et al.)



Flexural strength of prepared composite. (Source: Aseel Basim Abdul-Hussein, Fadhel Abbas Hashim, Tamara Raad Kadhim, et al.)

Conclusion

Several research works revealed that adding alumina filler materials above 1.0 percent by volume reduces tensile stress values due to increased filler distribution and filler materials dominating the materials, whereas Young's modulus increases with increasing nano aluminium oxide percentage but decreases after 1.0 percent by volume fraction of nano aluminium oxide. At an optimal concentration of alumina nanoparticles (2 wt percent), nanoscale dispersion of alumina nanoparticles is obtained. The greater concentration of alumina nanoparticles (5 wt%) causes alumina nanoparticle aggregation in the epoxy matrix. The inclusion of alumina nanoparticles in the epoxy matrix improves the thermal stability of the epoxy/alumina nanocomposites as well. When 3 wt. percent of an electrospun alumina product with micron-sized particles and nano-sized fibers was added to manufacture the composite, it gave the best performance among those evaluated.

EXPERIMENTAL ANALYSIS OF DIESEL ENGINE USING BIO-FUEL BLENDED WITH ALUMINIUM OXIDE

R.Sasikumar, Dept of Mechanical Engineering, St.Anne's College of Engineering and Technology S.Krishnakumar, Dept of Mechanical Engineering, St.Anne's College of Engineering and Technology D.Manivel, Dept of Mechanical Engineering, St.Anne's College of Engineering and Technology B.Karunakaran, Dept of Mechanical Engineering, St.Anne's College of Engineering and Technology

ABSTRACT

Petroleum products such as petrol and diesels are being used as a fuel to the running of Internal Combustion Engines. Day by day demands for the petroleum products is increasing since its rate of consumption is increasing

INTRODUCTION

Petroleum based fuels plays a conventional energy sources along with increasing demand and also major contributors of air pollutants. The petroleum fuels fulfil energy needs in industrial development, transportation, agriculture sector and other basic requirements. Need alternative fuel for the shortage of fossil fuel The biofuel from the biomass available in large quantity and can be replaced for fossil fuels.The micro algae oil is used as the bio fuel in the direct injection (DI) diesel engine, when the oil extracted by pyrolysis process. An experimental investigation is carried out to analyze the effect of biofuel, the blended fuels to be improving diesel engine performance,emission and properties, where compared to diesel.

OBJECTIVES

The main objective of our project is,To increase the performance and reduce the emission of diesel engine by using bio fuel, blended with aluminium oxide nano particle where compared to diesel.

ALTERNATIVE FUEL

Alternative fuels known as “Non-conventional” or “Advanced fuels” , are any materials or substances that can be used as fuels, other than conventional fuels like fossil fuels (petroleum oil, coal and natural gas) as well as nuclear materials such as uranium and thorium, as well as artificial radioisotope fuels that are made in nuclear reactors.

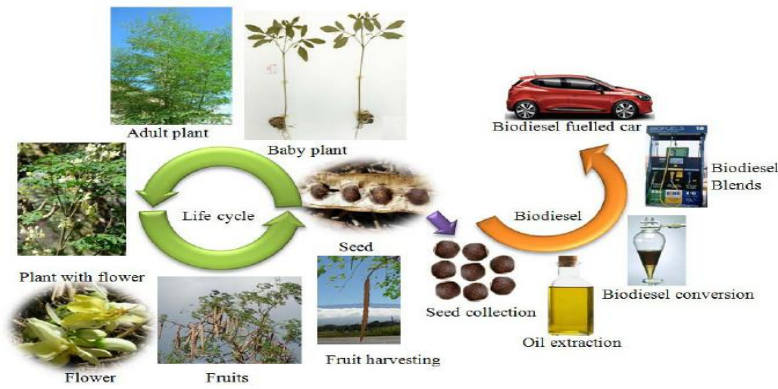
Example

Biodiesel, bioalcohol (methanol, ethanol, butanol), hydrogen , non-fossil methane, non-fossil natural gas, vegetable oil, propane, and other biomass sources.

ENGINE TESTING



BLENDING WITH DIESEL AND SPIRULINA OIL & ALUMINIUM OXIDE NANOPARTICLES



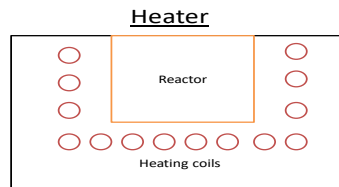
CONSTRUCTION

The pyrolysis setup consists the following parts

1.1 Heater, Reactor, Condenser, Oil collector, Nitrogen cylinder

HEATER

The heater is a U shaped heating element and is made of nicrome wire. Only one heater has 3Kw heating capacity and 240V supply. The heater is inserted outside of reactor in the shape of U.



Specification

Heater

Length (l) = 500 mm
Breath (b)= 500 mm
Depth (h) = 580 mm

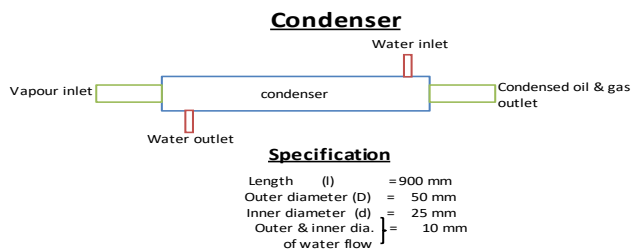
Reactor

Length (l) = 190 mm
Breath (b) = 190 mm
Depth (h) = 300 mm

1.2 REACTOR

The reactor is made of stainless steel material, in the shape of rectangle and the thickness is 10mm. The top side is closed with the help of nuts. The one inlet and outlet are made. Inlet used supply the nitrogen gas and outlet transfer the volatile gases.





1.3 CONDENSER

1.4 The condenser is made up of stainless steel and is connected to the gas liquid separator. The outlet of the reactor is directly connected to the condenser using a stainless steel tube which can withstand high temperature. Another one inlet is connected to the reactor from the nitrogen cylinder. The condenser is firmly connected with help of alloy gasket. Counter flow condenser here selected. The flow of water is directed against the direction of pyrolysis gases. The condensate drips into the gas liquid separator.

1.5 REFERENCE

- [1] Shrivastava R.K, Saxena Neeta, Gautam Geeta, “Air Pollution Due to Road Transportation in India: A review on assessment and reduction strategies”, Journal of environmental research and development, Vol.8 (No.1), 2013.
- [2] T.Subramani, “Study of Air Pollution Due to Vehicle Emission in Tourism Centre”, International journal of engineering research and application, Vol.2 (No.3), 2012.
- [3] Rolvin D’Silva, Binu K.G, Thirumaleshwara Bhat , “Performance and Emission characteristics of a C.I. Engine fuelled with diesel and TiO₂ nanoparticles as fuel additive”, International Conference on Materials Processing and Characterization, 2015.
- [4] A.Selvaganapthy, A.Sundar, B.Kumaraguruban, P.Gopal, “An experimental investigation to study the effects of various nanoparticles with diesel on DI diesel engine, ARPN J.Sci Technol. 3 (1) (January 2013).
- [5] D.Ganesh, G.Gowrishankar, “Effect of Nano -fuel additive on emission reduction in a Biodiesel fuelled CI engine”, Electrical and control engineering conference, 2011.
- [6] M. B. Shafii, F. Daneshvar, N. Jahani, and K.Mobini, “Effect of Ferrofluid on the Performance and Emission Patterns of a Four-Stroke Diesel Engine”, Advances in Mechanical Engineering, 2011.
- [7] Karoon fangsuwannarak and Kittichai Triatanasirichai, “Effect of metalloid compound and bio-solution additive on Biodiesel Engine performance and exhaust emission”, American journal of Applied Sciences, 20 13.
- [8] V.Sajith, C. B. Sobhan, G. P. Peterson, “Experimental Investigations on the Effects of Cerium Oxide Nanoparticle Fuel Additives on Biodiesel”, Advances in Mechanical Engineering, 2010.
- [9] M.A.Lenin, M.R.Swaminathan , G.Kumaresan, “ Performance and emission characteristics of a DI diesel engine with a nanofuel additive”, Fuel ,2013.
- [10] Rakesh Kumar Maurya, Avinash Kumar Agarwal, “Statistical analysis of the cyclic variations of heat release parameters in HCCI combustion of methanol and gasoline”, Applied Energy, 2011.

Electrical Discharge Coating of Aluminum Alloy Using WS₂/Cu Green Compact Electrode

K. Shanmuga Elango, Dept of Mechanical Engineering, St. Anne's College of Engineering and Technology
Arockia Tony Play, Dept of Mechanical Engineering, St. Anne's College of Engineering and Technology
A. Vigneshkumar, Dept of Mechanical Engineering, St. Anne's College of Engineering and Technology
R. Arun Prakash, Dept of Mechanical Engineering, St. Anne's College of Engineering and Technology

ABSTRACT

Aluminium (Al) alloys have been one of the most employed materials in defence applications like torpedoes, manufacture of Missile bodies and parts of automobile such as engine cylinders and pistons, due to their lightweight, high mechanical resistance, good corrosion properties and low cost. Poor wear resistance of the alloys is major constraint for their use particularly when aluminum is in contact with other parts. Keeping in view, improving the antifriction properties of Al-7075 alloy, electrical discharge coating (EDC) was attempted to modify the surface of Al alloy with solid lubricant tungsten disulfide (WS₂). Tungsten disulfide (WS₂) and copper (Cu) powder powders were mixed in the ratio of 60:40 and compacted in the hydraulic press to obtain green compact electrodes. Further it has been used as electrode for EDC technique. In the present work, Response surface methodology (RSM) is used to perform the experiment with different parameter combinations such as discharge current, pulse-on time and pulse-off time on the alloyed characteristics of deposition rate (DR) and electrode wear rate (EWR) were studied. It was found that current has significant parameter on DR and pulse on time was found to be predominant in obtaining higher EWR. Micro structural changes during EDC and composition of materials present on the surface were analyzed through SEM and EDS.

Keywords EDC; Powder metallurgy; DR, EWR.

INTRODUCTION

Electro discharge coating (EDC) is an unconventional coating method developed in recent years. It uses an electrical discharge media to build a hard layer on a metallic work piece. EDC can be used to improve the hardness, wear resistance, corrosion resistance and without causing major changes to the bulk workpiece material. Due to its unique properties, such as light weight and high specific strength, aluminum alloy has rapidly increased its acceptance in industrial applications. It has led to the rapid substitution of ferrous metal materials, mainly in the aviation and automotive fields, with improvements in weight, fuel consumption and performance and efficiency. However, the wear resistance of aluminum alloy is very low [1]. Therefore, surface modification has become very important for improving wear resistance and improving the acceptability of aluminum alloys in industrial environments. In the process of EDM, a spark is activated at the point of the smallest gap between the poles through the high voltage of the positive polarity, which exceeds the dielectric breakdown resistance of the small gap. The insulating effect of the dielectric is important to avoid electrolysis of the electrode during the EDM process melting and vaporisation of the workpiece surface is followed by quick cooling/quenching by the dielectric fluid. Mohanty et al. (2018) used electrical discharge machining to examine the surface alloying of Ti6Al4V using tungsten disulphide powder mixed with dielectric. Surface roughness, material removal rate, and micro-hardness were the responses studied, with voltage, duty factor, and powder particle concentration being the processes. The most important factor affecting the decomposition was the powder concentration. The deposition rate, surface roughness, and recast layer thickness were all influenced by powder concentration[2]. Elaiyaran et al.(2020) examined the ZE41A magnesium alloy, which was deposited using an electrical discharge coating process with a WC-Cu powder metallurgy semi-sintered and sintered electrode. At low compaction loaded partial sintered electrodes, it was revealed that the maximum material migration rate and micro hardness increased as the current and pulse on time increased[3]. Senthil Kumar and Ganesan(2015) used a WC-5

percent Ni P/M sintered electrode to investigate the EDC of EN38 steel. According to the findings, material was deposited on the workpiece at lower values of pulse-on time, pulse-off time, and current, whereas material was removed from the workpiece at higher settings of pulse-on time, pulse-off time, and current. Lower settings allow less electrical discharge energy to be conducted into the machining, whereas higher settings allow more discharge energy to be conducted into the machining, facilitating melting and vaporisation as well as accelerating the enormous impulsive force in the spark gap. When the pulse on time is short, the current is high, and the pulse off time is short, electron flow dominates in the plasma channel, causing the electrode to be bombarded by electrons, resulting in a bigger TWR. TWR drops as the ratio of caution flow in the plasma channel increases with increased pulse-on-time and pulse-off time[4]. Elaiyarsan et al.(2019) has reported studied the ZE41A magnesium alloy was deposited by electrical discharge coating technique with WC-Cu powder metallurgy partial and fully sintered electrode. It was observed that the maximum material migration rate and microhardness increased with increase in current and pulse on time at low compaction loaded partial sintered electrode. A highest microhardness value was achieved at low compaction loaded partial sintered electrode[5]. Using EDC, Rashi Tyagi et al.(2018) successfully deposited solid lubricant WS₂ and Cu green compact electrode onto the surface of mild steel. With a higher proportion of WS₂ content, peak current, and duty factor, the coating thickness increased. Due to the introduction of solid lubricant, the combined effect of duty factor and peak current lowered the micro-hardness of the coating to 44.11HV from 180HV[6]. In a study done, Anusha Roohi Siddique et al.(2019) employed different ratios of WS₂ and brass powder. The coating was produced with a variety of parameter combinations, including composition, voltage, and duty factor, and the coated samples were assessed for metallurgical and tribological characteristics evaluation. It was discovered that increased brass content causes machining and higher WS₂ composition causes coating in the electrode. The maximum material deposition rate was determined to be at a 50:50 mixing ratio, while the 70:30 mixing ratio was found to be the best ideal for a uniform surface. Microhardness was shown to rise considerably when compared to the base material due to the formation of titanium and aluminium oxides. Several studies have been published in the area of EDC that use a powder metallurgy electrode with hard ceramics to change the surface of various materials to improve their surface qualities[7]. Rashed Mustafa et al.(2020) has reported that Powder metallurgical green compact tool (Metal powders of tungsten and copper in a composition of 75%W and 25%Cu) have been selected the compact load plays important role for achieving minimum surface roughness and edge deviation values of the generated pattern[8]. R. Tyagi et al.(2019) studied the EDC of MoS₂+Cu on mild steel substrate. It was found that the high proportion of MoS₂ in mixing ratio (MoS₂: Cu/60:40) tool wear rate and mass transfer rate increases with as the peak current. Moreover, for all the mixing ratios, micro-hardness decreases with increasing current. Also, the Vickers micro-hardness test revealed that the hardness of solid lubricant coating has been reduced (46.83HV0.2–90.44HV0.2) in comparison to mild steel (180HV0.2) due to deposition of solid lubricant [9]. However, reports of EDC with solid lubricants including graphite, polytetra fluoro ethylene (PTFE), molybdenum sulphide, white solids, h-BN, WS₂, and others were scarce, and coating of aluminium with solid lubricants was also uncommon. The wear and friction between two surfaces in relative motion is reduced by tribological components covered with solid lubricants. When components used in space vehicles, such as micro-sized gadgets, are coated with the above-mentioned materials, their tribological qualities deteriorate when they are subjected to high loads and temperatures. Moreover, MoS₂ was discovered to have a good load-bearing capability but loses its tribological capabilities when exposed to temperatures exceeding 400°C. As a result, WS₂ is a suitable solid lubricant for high-temperature applications. It begins to disintegrate in air at 500°C and fully decomposes in vacuum at 2000°C. As a result, in this study, a WS₂ and Cu green compact electrode was created, and an EDC coating was applied on an

Aluminium alloy 7075 to provide a lubricated and wear-resistant surface. This inquiry looked into the effects of different EDC process factors such as applied current, pulse on time, and pulse off time. Experiments were also prepared and carried out utilising face centred cubic design (FCCD), with results such as MRR and TWR being recorded. The paper discusses statistical models for correlating the linear, interaction, and quadratic effects of various EDC factors on DR and EWR in order to achieve controlled EDC.

2. Experimental planning and procedure

2.1 Preparation of the Tool Electrode

For the experimental work, electrode preparation was done with WS₂/Cu in a 60:40 weight percent ratio, with particle sizes of 20 μm. To obtain a more stable body after pressing, Poly Vinyl Alcohol (PVA) was added to WS₂/Cu as a binder. To aid in the homogeneity of the powders, all ingredients are combined in a double cone mixer for 1 hour. The consistency of the completed product, as well as the homogeneous composition throughout the mixed volume, is dependent on proper mixing of the powders. The combination was also crushed for 10 minutes in a hydraulic press with a 150-ton capacity and a 10mm diameter dies and punch constructed of hardened steel at 350 MPa load. The solid green compact is then gently taken from the die and heated in a tubular furnace at 130°C in an argon environment for 30 minutes of heating and 15 minutes of cooling to ensure adequate compact bonding.

3. Detail of Experiment

Electro discharge coating (EDC) was obtained on the surface of an Aluminum alloy 7075 with WS₂/Cu composites made die sink EDM with reverse polarity and immersed in an extremely hydrocarbon dielectric medium. The aluminium alloy 7075 is composed as shown in Table 1. The experiment was carried out with current, pulse on time, and pulse off time as control parameters for a total of 5 minutes. Because of the weak link between particles within the green compact electrode, sparks form when the voltage applied across the gap reaches the edge value, producing melting and chemical reactions between the dielectric and dissolving electrode materials deposited on the workpiece surface. A face-centered composite design is made up of three different components. Three levels of analysis are considered in this study. The method parameters used for the evaluation, such as current pulse on time and pulse off time, are shown in table-2. To calculate the deposition rate (DR) and electrode wear rate (EWR), a digital electronic weighing balance SF400D with a precision of 0.001 g was used. After EDC has been carried out, various defects and morphologies of the surface coated surface was characterized through SEM. To ensure the elements diffused on the coated surface was confirmed by EDS analysis.

Table.1 Chemical composition of Aluminium alloy7075

Zn	Mg	Cu	Cr	Fe	Si	Mn	Tn	OTHERS	Al
5.6	2.5	1.6	0.23	0.50	0.40	0.30	0.20	0.05	BAL

Table.2 Process parameters and their levels

PARAMETERS	Level
------------	-------

	-1	0	+1
Current, Amp (A)	2	3	4
Pulse on time, μs (B)	50	70	90
Pulse off time, μs (C)	5	6	7

4 Result and discussion

4.1 Influence of current on DR

Figure 1 depicts when the current value is increased from 2 to 3A, DR rapidly increases. This is due to the increased creation of spark energy in the machining gap, which is sufficient to crumble the WS_2/Cu electrode and deposit on the surface of the aluminium alloy[11]. The Cu in the electrode absorbs additional heat created during the process, which is then dissipated into the dielectric fluid, and the workpiece cools down. As the temperature rises, less thermal stress is stimulated on the surface, resulting in little or little crack formation. Upon increasing current from 3A to 4A does not result in a significant rise in DR[12]. The reason for this could be that the during high current supply, some pre-deposited layers may be removed and formed irregular deposits piled on the surface with non-uniform morphology.

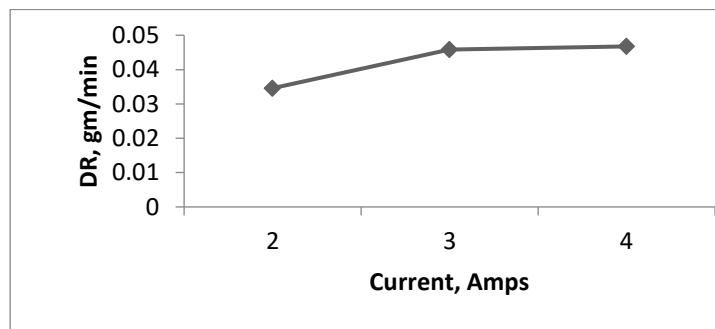


FIGURE 1. Influence of current on DR

4.2 Influence of pulse on time T_{on} on DR

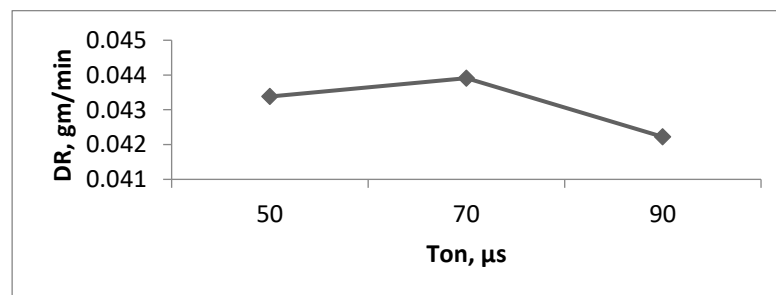


FIGURE 2. Influence of pulse on time on DR

Figure.2 depicts that DR increases with increasing pulse-on time in the beginning, but then decreases, as shown in the graph. At shorter pulse on time intervals of $50\mu\text{s}$ to $70\mu\text{s}$, the plasma density created in each pulse is larger, which would be sufficient to dislodge and melt the electrode diffused on the workpiece's surface[13]. However, when the pulse on time increased from the $70\mu\text{s}$ to the $90\mu\text{s}$, the amount of heat stimulated for each pulse became excessive. As

a result, the coating remained and the pre-deposited layer was partially removed at the same time, becoming rough and brittle, resulting in a drop in DR[14].

4.3 Influence of pulse off time T_{off} on DR

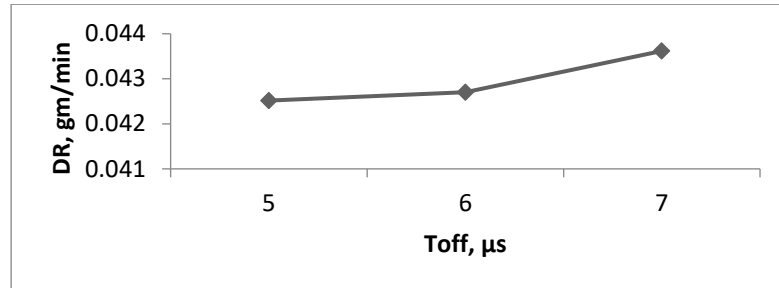


FIGURE 3. Influence of pulse off time on DR

Figure.3 depicts that the variance in pulse off time on the DR. The deposition rate increases as the eroded and molten material is not properly flushed away from the gap and adheres to the surface as spherical globules of varying shape and size multiply over the surface of the workpiece, the formation of globules with varying depends on the strength of the material[15]. In contrast, increasing the pulse off time from $6\mu s$ to $7\mu s$ reduces the spark energy generated, resulting in the formation of a small crater and providing sufficient time for the clearance of melted debris from the gap, resulting in a significant improvement in DR and minimal accumulation of melted in the form of globules[16].

4.4 Influence of current on EWR

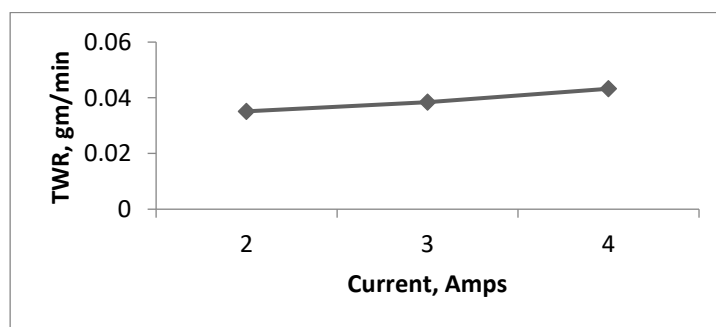


FIGURE 4. Influence of current on EWR

Figure.4 shows that if the current EWR is kept discharged, the EWR raises linearly. Because when the discharge current is increased from 2 to 4amps, more spark energy is created between the gaps, causes more positive ions, flow towards the tool and strike, causing a higher quantity of heat to be generated. As a result, more heat is transported to the electrode, causing the electrode to erode[17].

4.5 Influence of pulse on time T_{on} on EWR

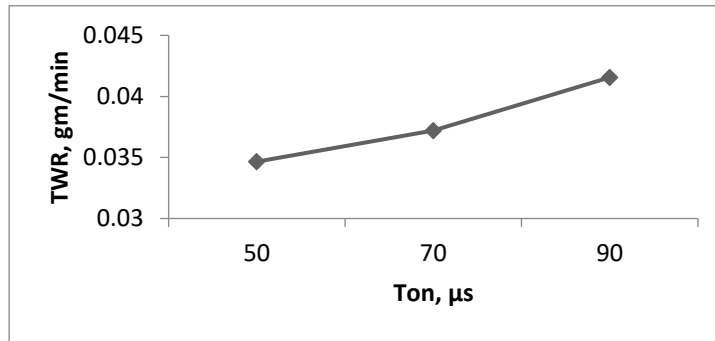


FIGURE 5. Influence of pulse on time on EWR

Figure.5 indicates that EWR increases steadily while increasing the pulse on time $50\mu\text{s}$ to $90\mu\text{s}$ causes, on set of plasma channel supplied adequate amount of discharge energy, as a result number of charged spark frequency occurrence in the gap between electrode and increased, thus completely melt and removed the electrode surface with high impulsive[18].

4.6 Influence of pulse off time T_{off} on EWR

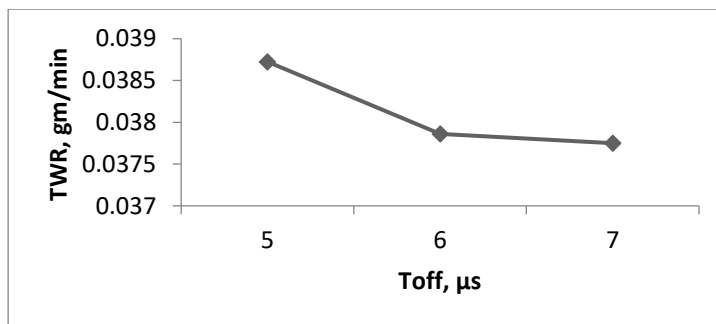


FIGURE 6. Influence of pulse off time on EWR

Figure.6 presents the impact of pulse off time on EWR. The plot shows that the pulse off time increases from $5\mu\text{s}$ to $6\mu\text{s}$, amplifies discharge energy at the tool workpiece interface, increases the temperature in the gap, and generates carbon layer deposits on the electrode surface due to dielectric decomposition, which resists current flow and improves electrode wear resistance[19]. Furthermore, the dielectric fluid is unable to flush alkali out of the electrode. When the pulse off time is increased from $6\mu\text{s}$ to $7\mu\text{s}$, the redundant time lengthens, removing a greater volume of molten debris and produced carbon from the surface, resulting in a modest rise in EWR[20].

5. Energy dispersive spectroscopy (EDS)

To assess the coated characteristics of the workpiece Energy dispersive spectroscopy (EDS) analyses were carried out. It authenticates the presence of electrode materials on the surface of the workpiece during EDC process. Figures.7 depicts different peaks of various elements such as W, Cu, Al, Fe, Mg and S diffused in the surface. It is evident that peaks observed from the figure that the intensity of W peak is comparatively more than that of Cu besides Al, Fe and Mg. The intensity of W peak shows the layer is relatively higher in W followed by Cu, which confirms the deposition of tool material in the deposited layer solid which is very much desirable.

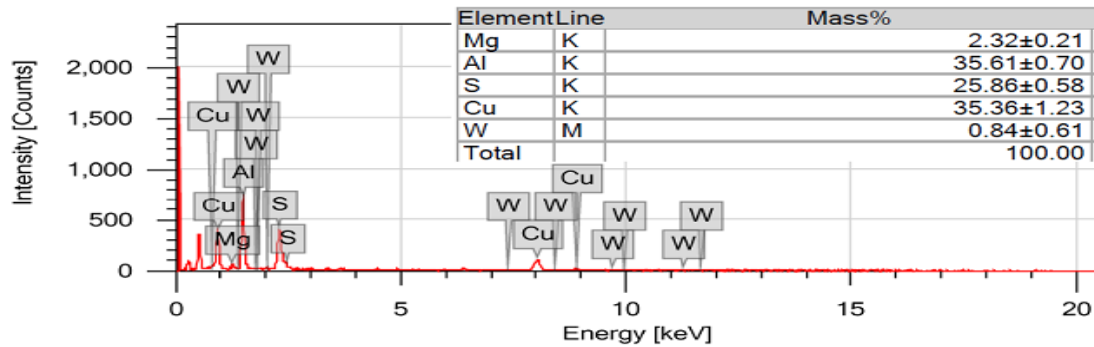


FIGURE 7. EDS result processed at current (2A), T_{on} :50 μ s and T_{off} : 5 μ s

6. Optimization

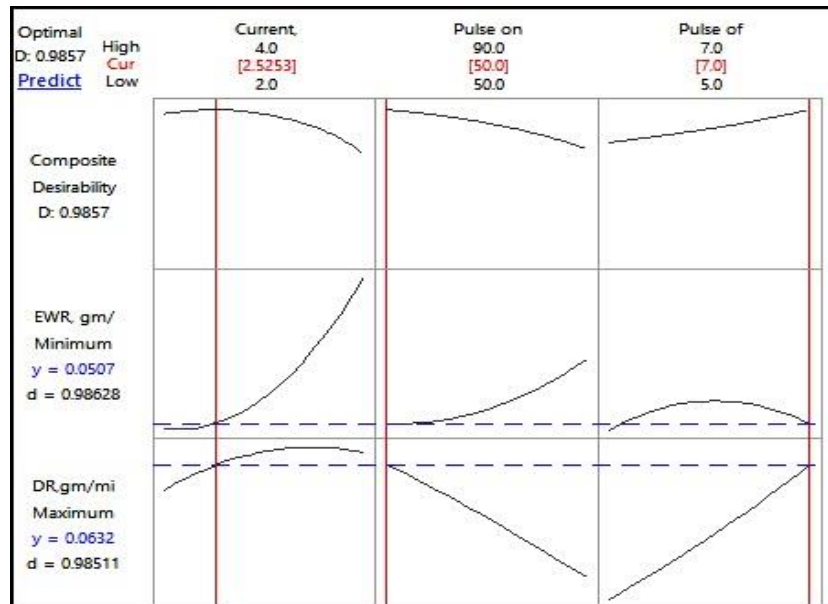


FIGURE 8. Optimization plot for DR and EWR

The process parameters were optimized using the RSM technique. From this table,3 it is clear that run no. 1 (DR and EWR obtained were 0.0631568 gm/mim 0.0506859 gm/min ranks 1 for having produced the optimal responses among all other available combinations. Furthermore, the developed model using the desirability function is used to

the near-optimal solution rather than the available combinations. The final Optimization plot for response is given in Figure .8. The multi-response prediction made by the desirability function suggests a still more optimal parameter condition of T_{on} (50 μ s), T_{off} (7 μ s) and Current (2.52525 amps). This parameter combination yields a maximum response Maximum DR and minimum EWR obtained were 0.0631568 (gm/min) and 0.0506859 (gm/min) respectively.

1.6 Table 3. Process parameters combination for high value of desirability

Solution	Current, Amps	Pulse on time, μ s	Pulse off time, μ s	EWR, gm/min	DR, gm/min	Composite Desirability
1	2.52525	50.0000	7.00000	0.0506859	0.0631568	0.985696
2	2.01924	67.6773	7.00000	0.0519756	0.0527081	0.883196
3	3.32714	50.0010	5.00000	0.0540861	0.0539946	0.864755
4	3.16801	50.0000	5.00000	0.0528658	0.0518099	0.862688
5	3.16444	50.0158	5.63458	0.0553655	0.0555059	0.857272

7. Conclusions

In this research article uses the response surface methodology to study the WS₂ / Cu powder metallurgy electrode discharge coating on an aluminum alloy. From the results, DR can be concluded as current increases with the current. This causes a current to start and process the electrode material and process the strong sparks deposited in the workpiece. Conversely, DR time decreases with high power. This is partially removed with the coating, while the heat in the gap is too high to unload the energy in a high pulse that stimulates the heat in the gap. The shutdown time of the pulse leads to the ionization of the dielectric medium as the removal of fragments melted quickly in the gap. The tool wear rate increases as the current and pulse on time increase, owing to the creation of high temperatures and the subsequent erosion of powder material from the tool electrode. When the pulse off time is increased, the temperature at the interface rises, increasing the formation of carbon through dielectric breakdown, which deposits on the electrode's surface and minimizes tool wear. Optimized parameters were identified in order to attain the maximum DR and minimum EWR. In this research optimized parameters were, 2.52525 A, pulse on time 50 μ s and pulse off time 7 μ s.

REFERENCES :

1. Chen HJ Wu KL and Yan BH 2014 Characteristics of Al alloy surface after EDC with sintered Ti electrode and TiN powder additive *The International Journal of Advanced Manufacturing Technology* Feb **72** 319–332
2. Mohanty et al. (2018) Surface alloying using tungsten disulphide mixed in dielectric in micro-EDM on Ti6Al4V In IOP Conference Series: Materials Science and Engineering
3. Elaiyaran U, Satheeshkumar and Senthilkumar C 2019 Surface modification of ZE41A magnesium alloy using electrical discharge coating with semi sintered electrode *International Journal of Machining and Machinability of Materials* Oct **21** 375– 389
4. Senthilkumar C and Ganesan G 2015 Electrical Discharge Surface Coating of EN38 Steel with WC/Ni Composite Electrode *Journal of Advanced Microscopy Research*.Sep**10** 202–207(6)
5. Elaiyaran U, Satheeshkumar V and Senthilkumar C 2020 Effect of sintered electrode on microhardness and microstructure in electro discharge deposition of magnesium alloy *Journal of the Mechanical Behavior of Materials* Aug **29** 69–76
6. Tyagi R, Das AK and Mandal A 2018 Electrical discharge coating using WS₂ and Cu powder mixture for solid lubrication and enhanced tribological performance. *Tribology International* April **120** 80–92

7. Anusha Roohi Siddique, Shalini Mohanty and Alok Kumar Das 2019 Microelectrical discharge coating of Titanium alloy using WS₂ and Brass P/M electrode *Materials and Manufacturing Processes* Sep **34(3)** 1–14
8. Rashed Mustafa Mazarbhuiya & Maneswar Rahang Reverse EDM process for pattern generation using powder metallurgical green compact tool (2020) *Taylor and Francis*
9. Tyagi R, Mahto N K, Das A K and Mandal A 2019 Preparation of MoS₂+Cu coating through the EDC process and its analysis *Surface Engineering* Jan **36** 86–93
10. Salila Ranjan Dixit, Sudhansu Ranjan Das and Debabrata Dhupal 2019 Parametric optimization of Nd:YAG laser micro grooving on aluminum oxide using integrated RSM-ANN-GA approach [*Journal of Industrial Engineering International*](#). Jan **15** 333–349
11. Abhishek Das and Joy Prakash Misra 2012 Experimental investigation on surface modification of aluminum by electric discharge coating process using tic/cu green compact tool-electrode *Machining Science and Technology, An International Journal*. Dec **16** 601–623
12. Afzaal Ahmed 2016 Deposition and Analysis of Composite Coating on Aluminum Using Ti–B4C Powder Metallurgy Tools in EDM. *Materials and Manufacturing Processes* Mar **31** 467–474
13. Patowari PK, Saha P, Mishra PK 2011 Taguchi analysis of surface modification technique using W-Cu powder metallurgy sintered tools in EDM and characterization of the deposited layer. *Int J Adv Manuf Technol* Oct **54** 593–604
14. Tijo D Kumari S and Masanta M 2017 Hard and wear resistance TiC-composite coating on AISI 1020 steel using powder metallurgy tool by electro-discharge coating process *J Braz. Soc. Mech. Sci. Eng.* May **39** 4719–4734
15. Ankita Sarmah, Siddhartha Kar and Patowari P K 2020 Surface modification of aluminum with green compact powder metallurgy Inconel-aluminum tool in EDM *Materials and Manufacturing Processes* Jun **35** 1104–1112
16. Patowari P K, Mishra U K, Saha P and Mishra P K 2010 Surface modification of C40 steel using WC-Cu P/M green compact electrodes in EDM *International Journal of Manufacturing Technology and Management* Jul **21** 83–98.
17. Orhan Gülcan, İbrahim Uslan, Yusuf Usta and Can Çoğun 2016 Performance and surface alloying characteristics of Cu–Cr and Cu–Mo powder metal tool electrodes in electrical discharge machining *Machining Science and Technology, An International Journal* Oct **20** 523–546
18. Gill A S and Kumar S 2015 Surface alloying of H11 die steel by tungsten using EDM process *Int J Adv Manuf Technol* Dec **78** 1585–1593
19. Senthilkumar C 2019 Optimisation of EDC parameters using TOPSIS approach *International Journal of Machining and Machinability of Materials* Oct **21**.480–492.
20. Gill A S and Kumar S 2016 Surface roughness and microhardness evaluation for EDM with Cu–Mn powder metallurgy tool *Materials and Manufacturing Process*. Jan **31** 514–521.

Analysis of Mechanical Properties of TiC Reinforced Aluminium Alloy Composites

Dr. D.Ommurugadhasan, *Department of Mechanical Engineering, St Anne's College of Engineering and Technology*
M. Arulselvam, *Department of Mechanical Engineering, St Anne's College of Engineering and Technology*
K. Dhinakaran, *Department of Mechanical Engineering, St Anne's College of Engineering and Technology*
A. Krishnaraj, *Department of Mechanical Engineering, St Anne's College of Engineering and Technology*
V. Senthamilselvan, *Department of Mechanical Engineering, St Anne's College of Engineering and Technology*

Abstract

In the present paper, the aluminium alloy i.e. AA 6061-T6 based composites reinforced with different weight fraction of TiC(2-3 μ m) particles (0%, 10%, 15% and 20%) was produced by stir cast technique and the effect of reinforced ratios on the mechanical properties and Tribological behaviour was examined. The test results shows that the increment in weight fraction of reinforcement particles in the matrix metal produced better mechanical properties like hardness, Tensile strength, Impact strength. SEM metallographic images and EDAX analysis evidences the homogenous dispersion of reinforcement in the matrix. The dry sliding wear behaviour shows that wear rate of the casted samples has decreased with the amount of reinforcement added. For the same working conditions wear rate increases with increasing load and with increasing speed.

Keywords: *Metal Matrix Composites, AA 6061-T6-TiC, Mechanical properties, Tribological behaviour, Reinforcement*

1. INTRODUCTION

Metal matrix composite (MMC) is engineered combination of the metal (Matrix) and hard [particle/ceramic (Reinforcement) to get tailored properties. MMC's are either in use or prototyping for the space shuttle, commercial airliners, electronic substrates, bicycles, automobiles, golf clubs, and a variety of other applications. The composites formed out of aluminium alloys are of wide interest owing to their high strength, fracture toughness, wear resistance and stiffness. Metal matrix composites (MMC's) are increasingly becoming attractive materials for advanced aerospace applications because their properties can be tailored through the addition of selected reinforcements [1-2]. In particular, particulate reinforced MMC's have recently found special interest because of their specific strength and specific stiffness at room or elevated temperatures [3]. It is well known that the elastic properties of metal matrix composites are strongly influenced by micro structural parameters of the reinforcement such as shape, size, orientation, distribution and volume fraction [4]. A typical chemical composition of Al 6061 is presented in Table I

Table I CHEMICAL COMPOSITION OF AA 6061-T6

Element	Mg	Fe	Si	Cu	Mn	Ti	V	Al
Weight %	1.08	0.17	0.63	0.32	0.52	0.01	0.02	Remainder

In recent years, the aluminium alloy based MMCs have offered designers many added benefits as they are particularly suited for applications requiring good strength at high temperatures, good structural rigidity, dimensional stability, light weight and low thermal expansion [5-10]. The major advantages of Aluminium Matrix composites (AMCs) include greater strength, improved stiffness, reduced density, improved high temperature properties, controlled thermal expansion coefficient, thermal / heat management, enhanced and tailored electrical performance, improved abrasion and wear resistance and improved damping capabilities [11, 12]. Various types and sizes of reinforcements are used in matrix of Aluminium like SiC, TiC, Al₂O₃, B₄C, TiB₂, TiN, etc. Among these, TiC is a relatively new reinforcement in metal matrix composites and has good properties such as wettability, thermal stability and distribution in Aluminium metal matrix [13-15]. The Al-TiC MMC samples for microscopic examinations were prepared by adopting standard metallographic procedure.

Samples were polished using different size of TiC grit papers of 120, 220, 400, 600, 800, 1000, and 1200, followed by velvet cloth with aluminium paste. The Keller's reagent was used for etching with mixture of 0.5 ml HF, 0.75 ml HCl, 2.5 ml HNO₃ and balance amount of distilled water. The microstructures of the etched sample were examined using Scanning Electron Microscope (SEM) and Compositional test of the sample were carried out using Energy-Dispersive X-ray spectroscopy (EDX)

2. EXPERIMENTAL PROCEDURE

A. Fabrication Process

Batch of 1250 g of aluminium alloy was melted at 660°C using an electrical furnace shown in Fig.1 and reinforcement is preheated at separate muffle furnace in order to make the surface oxidized

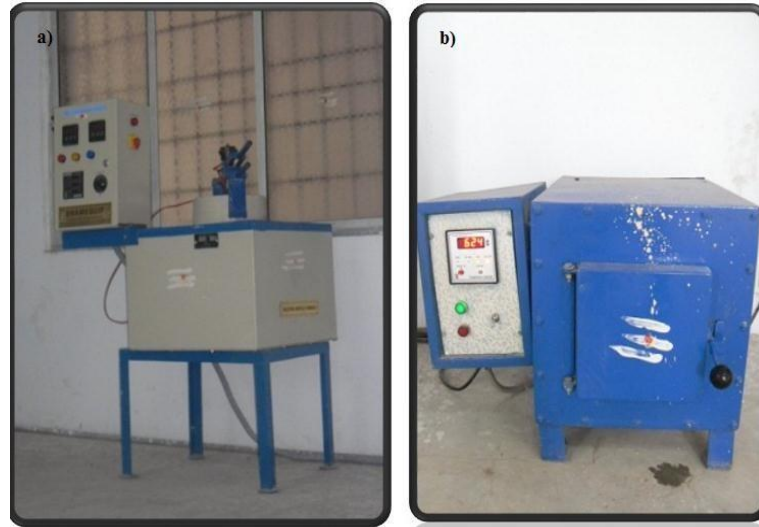


Fig.1 a) Electrical resistance furnace b) Muffle furnace

The melt was agitated with the help of a mechanical stirrer to form a fine vortex. The mixtures of preheated TiC particles with an equivalent amount of K₂TiF₆ flux (with 0.1Ti/TiC ratio) were added at a constant feed rate into the vortex. The process parameters employed are given in Table II

TABLE II PROCESS PARAMETERS OF MODIFIED STIR CASTING

Parameters	Units	value
Spindle speed	RPM	300
Stirring time	min	5
Temperature of melt	°c	920
Preheated temperature of SiC particles	°c	700
Preheated temperature of mould	°c	250
Powder feed rate	g/s	0.8–1.2

Argon gas was supplied into the melt during the operation to provide an inert atmosphere. After stirring the molten mixture, it was poured down into the preheated permanent mould. The AMCs having different weight percentages (0, 10, 15 and 20) of TiC were fabricated by the same procedure. The manufactured procedure of typical AMCs are shown in Fig. 2

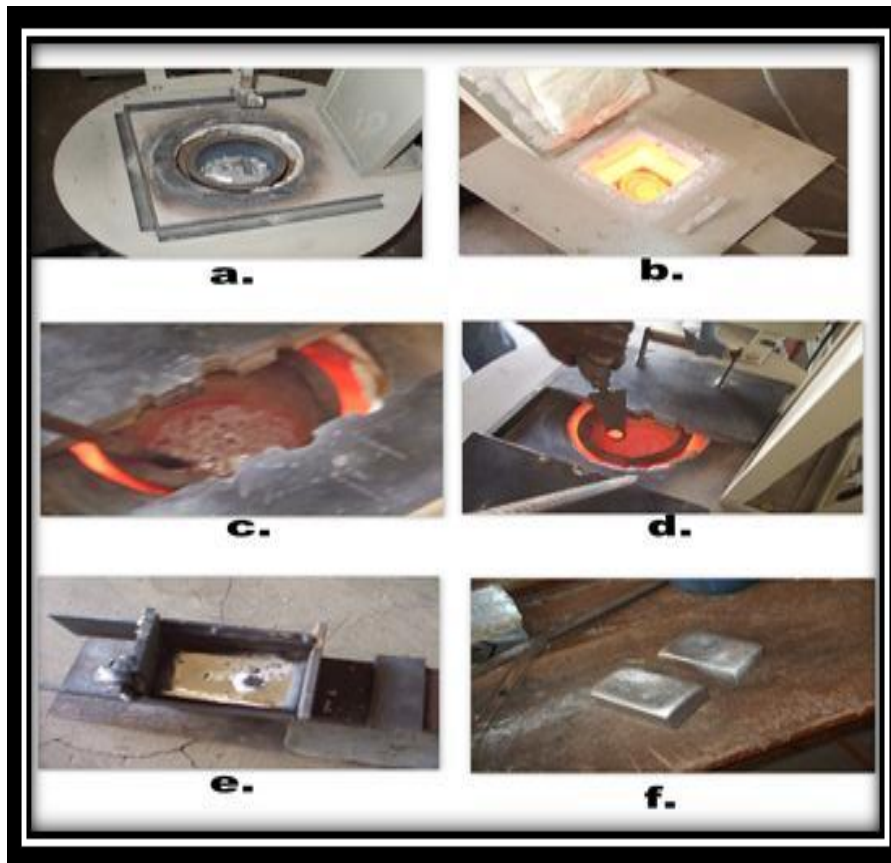


Fig.2 a. Scraps of Al alloy b. Molten Al alloy in liquidus state c. adding of reinforcement. d. Melt at 720°C ready for casting. e. Casted Al poured in mould f. finished cast pieces.

3. MICROSTRUCTURE AND TESTING

The Metallographic study was carried out on the fabricated AMCs using scanning electron. The EDAX analysis, hardness, tensile tests and pin on disc wear test were also carried out. The specimens prepared from the casted AMCs were polished and etched as per the standard metallographic procedure. The microstructures of the specimens were observed using d scanning electron microscope attached with energy dispersive spectroscope (JEOL JSM-6390).

The tensile specimens were prepared as per ASTM E08 standard. The dimensions of the specimen are shown in Fig. 3 the ultimate tensile strength (UTS) was estimated using a computerized Universal Testing Machine (TUE-C-1000), Annamalai University, Chidambaram, Tamilnadu, India.

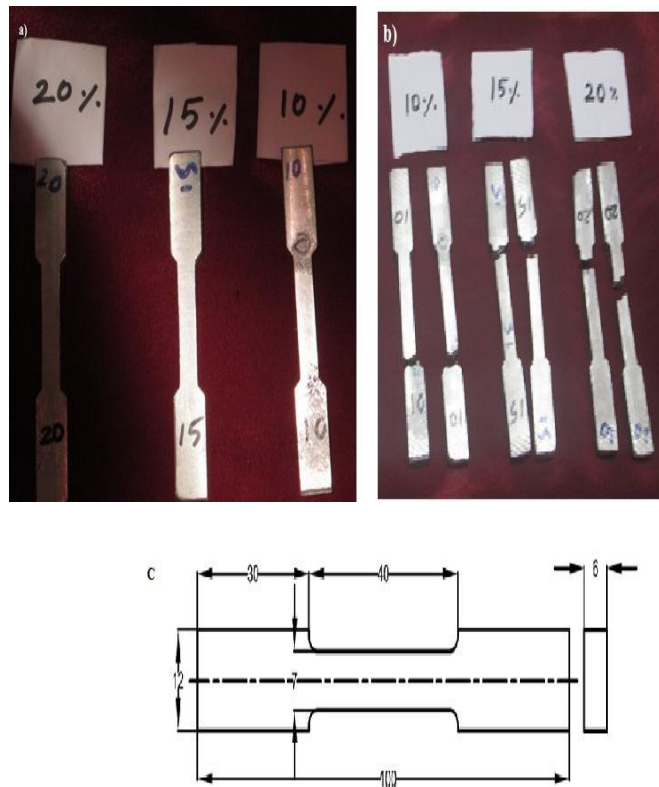


Fig. 3 Tensile specimens of AA6061-TiC composites **a)** before test **b)** After test **c)** Dimensions of tensile Specimen

The hardness was measured at different locations. The microhardness and macrohardness of polished samples was measured using Vickers hardness Tester (Mitutoyo MVK-H1) at a load of 300 g and 500g respectively for 10 seconds.

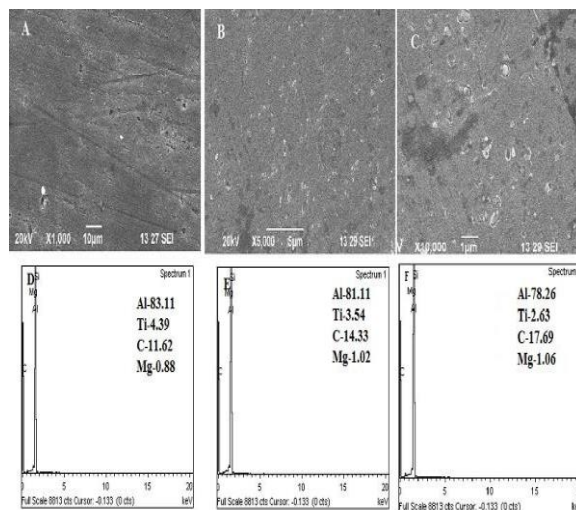


Fig. 4 SEM Micrographs of Cast AA6061-TiC composites **A.** 10% **B.** 15% **C.** 20% **D.** EDX analysis of 10% sample **E.** 15% sample **F.** 20% sample

The SEM photographs are displayed according to their weight percentages. The photomicrographs and EDX analysis of the specimens show that the presence of TiC_p in the matrix

B. Evaluation of Mechanical Properties

The mechanical properties of matrix alloy AA6061 is improved upon TiC incorporation. Fig. 5 shows relation between weight percentage of TiC reinforcement particulates and hardness of fabricated AMCs. It is observed that the micro and macrohardness of AMCs are linearly increasing when the reinforcement particulates increases. Addition of reinforcement particles in the matrix increases the surface area of the reinforcement and the matrix grain sizes are reduced. The presence of such hard surface area of particles offers more resistance to plastic deformation which leads to increase in the hardness of composites. It is reported that [11] the presence of hard ceramic phase in the soft ductile matrix reduces the ductility of composites due to reduction of ductile metal content which significantly increases the hardness value.

The wear volume loss is decreased with the addition of TiC and it is further decreased with the incorporation of Graphite reinforcement. At the initial phase, little change in volume loss was observed for the composites, as the sliding distance increases more change in the wear was observed. The wear resistance of the casted composites is increased compared to the unreinforced alloy at all sliding distances. The drastic decrease in volume loss was observed with the addition of reinforcement content.

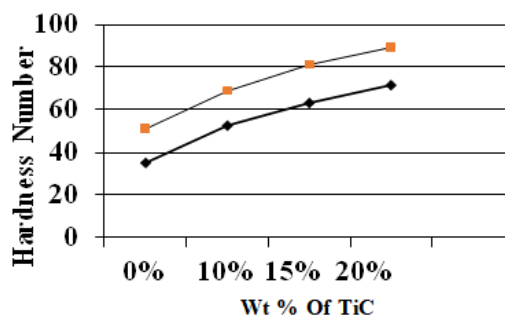


Fig. 5 The effect of amount of TiC particulates on the hardness of MMC

Fig. 6 shows the relation between tensile strength of the fabricated composites and the weight percentage of TiC particulates. It can be inferred that TiC particles are very effective in improving the tensile strength of composites from 181 MPa to 210 MPa. It may be due to the strengthening mechanism by load transfer of the reinforcement [12].

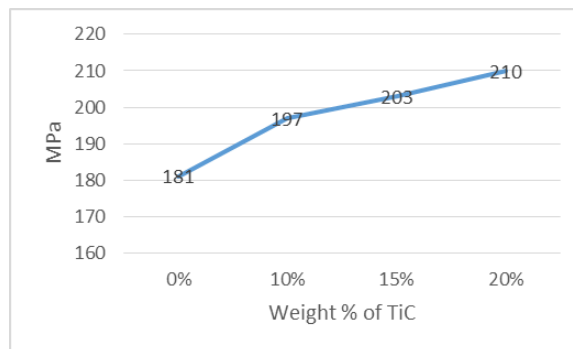


Fig. 6 The effect of amount of TiC particulates on the Tensile strength of MMC

The addition of TiC particles in the matrix induces much strength to matrix alloy by offering more resistance to tensile stresses. It is well known that the thermal expansion coefficient of TiC particle is $4 \times 10^{-6} \text{ } ^\circ\text{C}^{-1}$ and for aluminium alloy is $23 \times 10^{-6} \text{ } ^\circ\text{C}^{-1}$ the thermal mismatch between matrix and the reinforcement causes higher dislocation density in the matrix and load bearing capacity of the hard particles which subsequently increases the composites strength.

Fig. 7 Shows the variation of volume loss with the sliding distance for Aluminium alloy reinforced with TiC and Unreinforced aluminium alloy in as cast condition. It can be observed from that as the sliding distance increases the wear of the composites and alloy also increases. The wear of the unreinforced alloy is more than that of the composites for all sliding distances.

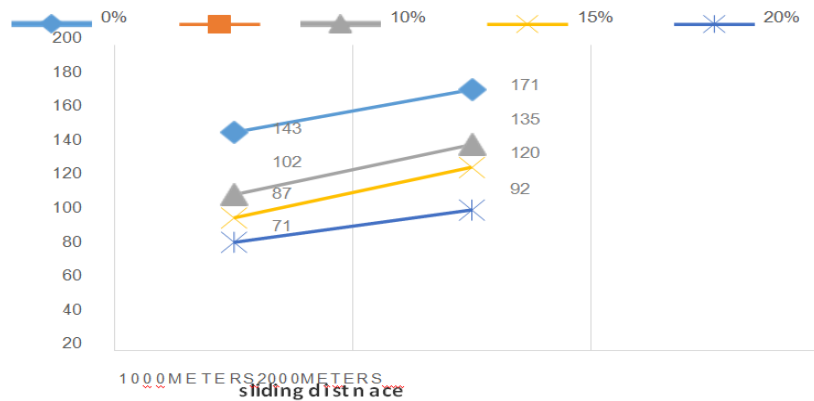


Fig. 7 effect of volume loss with sliding distance

The coefficient of friction (μ) of the samples are shown in Fig.8 where the unreinforced aluminium alloy has a coefficient of friction of 0.78 μ and it is linearly decreasing when the percentage of reinforcement added to it.

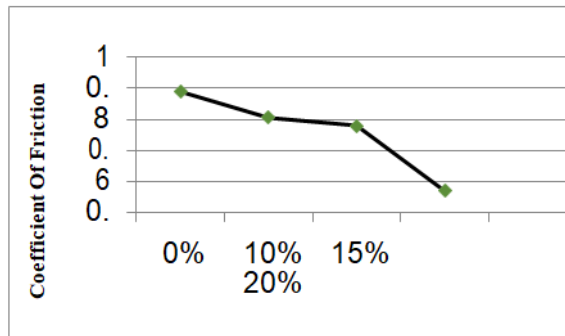


Fig. 8 Co-Efficient of Friction Results

4. CONCLUSIONS

The experimental study reveals following conclusions:

1. The results of study suggest that with increase in composition of TiC, an increase in hardness and tensile strength have been observed.
2. Homogenous dispersion of TiC particles is evidenced by SEM metallographic images and EDX analysis.
3. The micro and macro hardness of the composites were increased from 51 HV to 89.3 HV and 35 VHN to 71.6VHN with respect to addition of weight percentage of TiC particles.
4. The reinforcement of particle has enhanced the tensile strength of aluminium matrix and composites from 181MPa to 210 MPa.
5. The wear rate of the casted (10%, 15% and 20%) samples has decreased with the amount of TiC added

REFERENCES

- [1] Everett, R.K and Arsenault, "R.J. Metal Matrix Composites: Mechanisms and Properties", 1991 (Academic Press, San Diego).
- [2] Kocjak, M.J., Kahtri, S.C., Allison, J.E and Jones, J.W. "Fundamentals of Metal Matrix Composites" (Ed S.Suresh, A.Mortensen and A.Needleman, 1993 (Butterworth- Heinemann, Boston).
- [3] Lloyd, D.J. and Brotzen, F.R." Particle reinforced aluminium and Mg matrix composites". Int. Mater.Rev; 1994, 39, 1-39.
- [4] Sharma, S.C., Girish,B., Kamath, R., and Sathish, B.M., (1999) "Fractography, Fluidity and Tensile Properties of Aluminium/Hematite Particle Composite", *Journal of Materials Engineering Performance*, 8(3): 309-314.

- [5] Sharma, S.C., Seah, K.H.W., Sathish B.M., and Ginish, B.M. (1996) "Effect of Short Glass Fibers on Mechanical Properties of Cast Al6061 Alloy Composites", *Material Design*, **17**(5/6): 245-250.
- [6] Sharma, S.C. (2000) "Albite Particles on the Co-efficient of Thermal Expansion Behavior of the Al6061 alloy Composites", *Metallurgical & Materials Transaction A* 31: 773-780.
- [7] Tjong, S.C., and Ma, Z.Y. "The High-Temperature Creep Behavior of Al Matrix Composites reinforced with SiC, Al₂O₃ and TiB₂ Particles", *Composite Science Technology*, 57(197): 697- 702.
- [8] Akbulut, H., Durman, M., and Yilmaz, F.,(1998) "Higher Temperature Young's Modulus of Aluminium Short Fiber Reinforced Al-SiC MMCs Produced by Liquid Infiltration", *Composite Science Technology*, 14: 299-305.
- [9] M. Singla, D. D. Dwivedi, L. Singh and V. Chawla, "De- velopment of Aluminium Based Silicon Carbide Particu- late Metal Matrix Composite," *Journal of Minerals and Materials Characterization and Engineering*, Vol. 8, No. 6, 2009, pp. 455-467.
- [10] S. B. Boppana and K. Chennakeshavalu, "Preparation of Al-5Ti Mater Alloys for the *In-situ* Processing of Al-TiC Metal Matrix Composites". *Journal of Minerals and Materials Characterization and Engineering*, Vol. 8, No. 7, 2009, pp. 563-568.
- [11] Albiter, C. A. Leon, R. A. L. Drew and E. Bedolla, "Mi- restructure and Heat-treatment Response of Al₂O₃/TiC Composites," *Materials Science and Engineering: A*, Vol. 289, No. 1-2, 2000, pp. 109-115.
- [12] Shen, Y.L., Williams, J.J., Piotrowski, G., Chawla, N. and Guo, Y.L. (2001), "Correlation between tensile and indentation behavior of particle reinforced metal matrix composites: a numerical and experimental study," *Acta Materialia*, Vol. 49 (16), pp. 3219- 3229.
- [13] Lenin S. D., "Development of friction materials through powder metallurgy", Ph.D. Thesis, Indian Institute of Technology Roorkee (INDIA) 2008.
- [14] Nami, H., Adgi, H., Sharifitabar, M., Shamabadi, H., 2010 "Microstructure and mechanical properties of friction stir welded Al/Mg₂Si metal matrix cast composite", *Materials and Design*, Vol.32, pp.976-983.
- [15] Basavarajappa, S., Chandramohan, G., Subramanian, R. and Chandrasekar. "Dry sliding wear behaviour of Al₂219/SiC metal matrix", *Materials Science-Poland*, 2006, 24(2/1), 357-366.

Taguchi optimization of end milling parameters on 316L stainless steel

R. Arokiadass, Dept of Mechanical Engineering, St.Anne's College of Engineering and Technology

S.Daniel, Dept of Mechanical Engineering, St.Anne's College of Engineering and Technology

R.Devendiran, Dept of Mechanical Engineering, St.Anne's College of Engineering and Technology

T.Anbzhagan, Dept of Mechanical Engineering, St.Anne's College of Engineering and Technology

S.Fralick, Dept of Mechanical Engineering, St.Anne's College of Engineering and Technology

Abstract

Meeting predefined quality requirements, enhancing production efficiency with specialised equipment, and sticking to time and cost restrictions are all part of the overall manufacturing problem. Unfortunately, meeting these requirements for certain of a product's quality qualities is difficult. Surface finish is a significant quality attribute. This research examines the direct impacts of three processing parameters on surface roughness (Ra) in 316L stainless steel end milling. Three parameters were used in the experiments: spindle speed, feed rate, and cut depth. The experimental study was conducted using a Taguchi L9 orthogonal design. The Taguchi analysis was utilised to identify the sensitive parameters that have an impact on surface quality.

Keywords: AISI 316L stainless steel, Surface roughness, Main effect plot, SN ratio plot, Optimization

1. Introduction

In industrial processes, end milling is one of the most popular metal removal operations. It is widely utilised in a range of manufacturing industries, including aerospace and automotive, where the creation of slots, pockets, precision moulds, and dies requires high quality. The surface quality has a considerable impact on milling performance, since a high-quality milled surface enhances fatigue strength, corrosion resistance, and creep life [1].

Because of its high mechanical qualities, increased stability and withstand resistance to corrosion, and cost-effective manufacture, AISI 316L is most widely used in biomedical applications, aerospace, and marine[2–4]. Furthermore, as compared to other stainless steels, machining AISI 316L is quite difficult. Because it allows for less intensive martensite formation during metal cutting, making traditional techniques of processing easier[5]. The main advantage of these materials is that traditional machining can be done fast and cheaply. AISI 316L is commonly used to make bioimplants. Because the machined component of a bioimplant could attain very fine surface quality. Surface roughness will cause fatigue cracks, which will lead to corrosion[6].

Researchers have developed a number of techniques to reduce surface roughness and increase metal removal rate. Yang et al [7] focussed on improving the surface finish in face milling operation by the concept of Taguchi. The results predicted the best cutting combination for surface roughness and signal-to-noise ratio. Ghani et al [8] described a procedure for optimising the end milling parameters using Taguchi while execute the machining of steel grade AISI H13 and the outcomes confirm that higher level cutting speed and lower-level feed rate, and depth of cut were the best combinations for obtaining lower resultant cutting force and attain the excellent surface finish.

Gurbuz et al [9] focused on the surface condition of SS316 L and the impact of machining parameters during machining. The results show that when increase the feed and the cutting depth, the surface condition deteriorated; but, when cutting speed was increased, the surface integrity improved. Kadi et al [10] observed the dry turning process of AISI 316L for obtaining low surface roughness. The findings show that major impact registered on surface finish was feed rate.

In conclusion, the mentioned literatures confirmed that the Taguchi approach, when combined with other techniques, can be extremely effective in selecting the best process parameters for a given machining operation. It was found that insufficient research on machining AISI 316L had been conducted. As a result, while cutting AISI 316L, efforts have been made to enhance machining parameters to achieve a minimal Ra. In order to achieve a satisfactory surface quality, this study also attempted to improve end milling settings using the Taguchi method.

2. Experimental Details

The experimental plan, which included three factors and three levels, was created using the Taguchi technique. The input parameters for this analysis were spindle speed (N), feed rate (f), and cut depth (d). Table 1 lists the chemical elements and their compositions found in SS 316L. The levels of these parameters that were chosen for testing were listed in Table 2.

Table 1 Chemical element and its composition of SS 316L

Elements	Cr	Ni	Mo	Mn	Si	P	S	C	Fe
Weight ratio (%)	16.543	11.091	2.043	1.611	0.081	0.035	0.004	0.022	Remaining

Table 2 Selected levels for the chosen process parameters

Sl. No.	Notation	Process parameters	Units	Parameters levels		
				(L ₁)	(L ₂)	(L ₃)
1	N	Spindle speed	RPM	800	1000	1200
2	f	Feed rate	mm/rev	0.2	0.3	0.4
3	d	Depth of cut	mm	0.5	1	1.5

End milling was executed on a CNC milling machine called the "LMW JV Kraft." The importance of selecting this machine is that it can machine all types of materials, soft or hard, with a very fine surface finish and more precision. For machining, an AlTiN PVD coated 4 flute 16mm carbide end mill cutter was employed. The dimensions of the work specimen were 150 mm 50 mm 10 mm. The workpiece's machined length is 150 mm. A contour surface test equipment was used to check surface roughness. The experimental design, which used a L9 orthogonal array, and the findings are shown in Table 3.

Table 3 L₉ Orthogonal array and performance results

Exp. runs	Spindle speed (RPM)	Feed rate (mm/rev)	Depth of cut (mm)	Surface roughness, R_a (μm)	SN ratios R_a (dB)
1	800	0.2	0.5	1.544	-3.77295
2	800	0.3	1.0	1.603	-4.09867
3	800	0.4	1.5	2.227	-6.95440
4	1000	0.2	1.0	1.281	-2.15098

5	1000	0.3	1.5	1.749	-4.85580
6	1000	0.4	0.5	1.698	-4.59875
7	1200	0.2	1.5	1.031	-0.26517
8	1200	0.3	0.5	1.246	-1.91036
9	1200	0.4	1.0	1.701	-4.61409

3. Results and Discussion

3.1 Effects of level of each end milling process parameters on Ra

Figure 1 shows the influence of each parameter's level on Ra . Increased speed reduces surface roughness, as shown in Fig. 1. The chip fractures at a slower speed, exposing the insecure bigger built-up-edge (BUE), resulting in a rough surface. Increased speed lowers roughness by eliminating BUE and chip breakage.

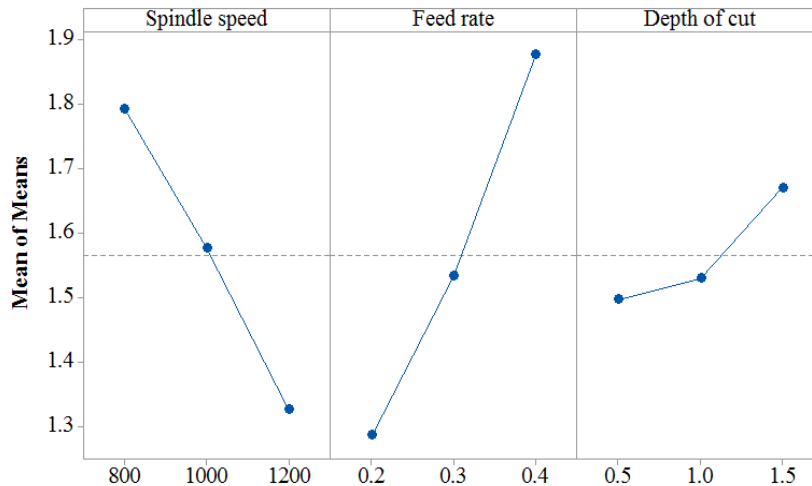


Fig. 1 Plots of main effect for Ra

As shown in Figure 1, Ra becomes more correlated with the feed rate. It shows that when the feed rate rises, the higher tool resistance produced by the workpiece tends to increase the quantity of built-up edges (BUE) on the tool's flank face, resulting in a degraded surface and, as a result, an increase in surface roughness. In addition, as shown in fig. 1, when the depth of cut rises, the Ra tends to rise, owing to the increasing cutting force produced by the increased contact area between the work piece and the tool. As a result, BUE formation is supported, and Ra rises. At $N= 1200$ RPM, $f= 0.2$ mm/rev, and $d= 1.5$ mm, the lowest Ra of 1.031 m has been found.

3.2 Choosing optimum process parameters for Ra

The SN ratios response table and graph created by Minitab 17.0 for surface roughness are shown in Table 4 and Fig. 2. A higher mean S/N implies the smallest difference between desired and actual output. According to Fig. 2, the best range end milling parameters for obtaining minimal Ra were 1200 RPM spindle speed, 0.2 mm/rev feed rate, and 0.5 mm depth of cut (N3- f1- d1).

Table 4 SN ratios responses for Ra

Level	Spindle speed	Feed rate	Depth of cut
1	-4.942	-2.063	-3.427
2	-3.869	-3.622	-3.621
3	-2.263	-5.389	-4.025
Delta	2.679	3.326	0.598
Rank	2	1	3

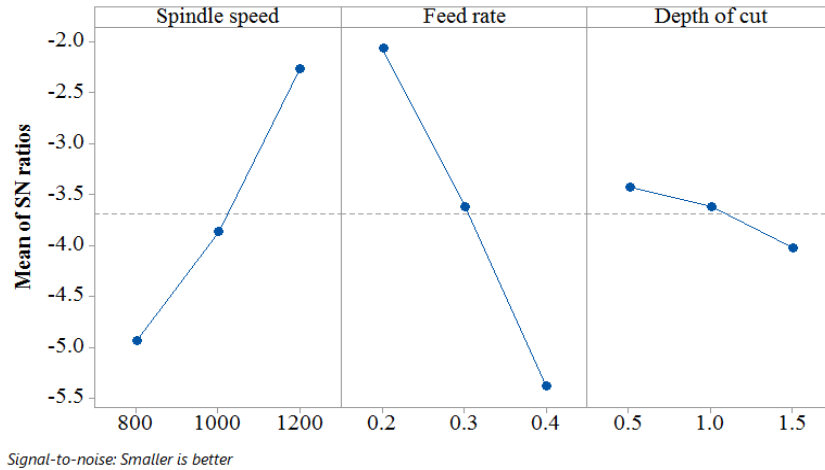


Fig. 2 SN ratios main effects plot for *Ra*

3.3 Validation test

The validation tests were conducted out according to the predicted optimal machining conditions and the test results were presented in Table 5. From the result it was observed that the predicted values improve *Ra* performance. The S/N ratios of predicted and optimized machining conditions for *Ra* was 0.12732dB. The optimum parameter condition reveals that there is a significant improvement in *Ra* when compared to the initial parameter settings.

Table 5 Validation test result for *Ra*

	Initial process parameters	Optimum process parameters	
		Predicted value	Experimental value
Level	$N_2 - f_2 - d_2$	$N_3 - f_1 - d_1$	$N_3 - f_1 - d_1$
Surface roughness (μm)	1.031		0.975
S/N ratio (dB)	-0.26517	-0.37111	-0.39249
S/N ratio (dB) improvement		0.12732	
Reduction of <i>Ra</i> (%)		5.74 %	

7. Conclusions

According to the findings, Taguchi determined optimum cutting conditions for machining AISI 316L stainless steel that significantly reduced the surface roughness: $N = 1200$ RPM, $f = 0.2$ mm/rev, and $d = 0.5$ mm ($N_3-f_1-d_1$). Taguchi-determined optimum cutting condition has been found to result in a 5.74 % decrease in surface roughness.

References

- [1] Sharkawy AB. Prediction of Surface Roughness in End Milling Process Using Intelligent Systems: A Comparative Study. Applied Computational Intelligence and Soft Computing. 2011; 1 – 18. <https://doi.org/10.1155/2011/183764>
- [2] Kang CW, Fang FZ. State of the art bioimplant manufacturing: part 1. Int J Adv Manuf Technol. 2018; 6:20 – 40.
- [3] Godbole N, Yadav S, Manickam R. A review on surface treatment of stainless-steel orthopaedic implants. Int J Pharm Rev Res. 2016; 36 :190–194.
- [4] Kaladhar M. Machining of austenitic stainless steel- a review. Int J Mach Mach Mater. 2012;12: 178 -192.
- [5] Odedeji PB, Abou-El-Hossein K, Liman M. An experimental study of flank wear in the end milling of AISI 316 stainless steel with coated carbide inserts. Journal of Physics: Conference Series. 2017; 843 :1-7.
- [6] Ebara R. Corrosion fatigue crack initiation behaviour of stainless steels. Procedia Eng. 2010; 2:1291–1306.
- [7] Zhang JZ, Chen JC, Kirby ED. Surface roughness optimization in an end-milling operation using the Taguchi design method. Journal of Materials Processing Technology. 2007; 184:233-239.
- [8] Ghani JA, Choudhury IA, Hassan HH. Application of Taguchi method in the optimization of end milling parameters. Journal of Materials Processing Technology. 2004; 145: 84-92.
- [9] Gurbuz H, Seker U, Kafkas F. Investigation of effects of cutting insert rake face forms on surface integrity. Int J Adv Manuf Technol. 2017; 90:3507–3522.
- [10] Kadi RK. Optimization of dry turning parameters on surface roughness and hardness of austenitic stainless steel (AISI 316) by Taguchi technique. J EngFundam. 2015; 2:30–41.

OPTIMIZATION OF MACHINING PARAMETER ON SS316L MATERIAL USING ORTHOGONAL ARRAY METHOD

K.Saravanan, Department of Mechanical Engineering, St.Anne's College of Engineering, Panruti.

M.Sivamanikandan, Department of Mechanical Engineering, St.Anne's College of Engineering, Panruti.

R.Jayakumar, Department of Mechanical Engineering, St.Anne's College of Engineering, Panruti.

ABSTRACT

In this paper, Taguchi techniques are applied to find out the surface roughness, metal removal rate, machinability in milling operation of SS316L. L9 orthogonal array, S/N ratios and ANOVA are used to study the performance characteristics of cutting speed, feed rate and depth of cut as milling parameters with tool flank wear width as response variable. The result of the analysis show that the selected machining parameters affect significantly the tool flank wear width of Tungsten Carbide cutting tool while machining SS316L. And also indicate that the cutting speed is the most influencing parameter out of the three parameters under study. Finally, the results are further confirmed by validation experiments or confirmation run.

Keywords: Taguchi Method, Optimization, Tool flank wear width, S/N ratio.

Introduction

Taguchi method stresses the importance of studying the response variation using the resulting in minimization of quality characteristic variation due to uncontrollable parameter. The metal removal rate was considered as the quality characteristic with the concept of larger better.



The EN8 steel of is mounted on the JV KRAFT vertical milling machine tool and specimens of 10mmx50mmx100mm size are cut.

2 Experimentation

The 12 mm tool was fixed with the help of jaw block in machine. The program was made for cutting operation of the work piece and a profile of 12 mm x 100mm horizontal cut. Each set of experiments was performed at room temperature in a narrow temperature range

Machining parameters

Machining parameters	unit	notation	level		
			-1	0	+1
Spindle speed	rpm	N	800	1000	1200
Feed rate	mm/re v	f	0.2	0.3	0.4
Depth of cut	mm	d	0.5	1	1.5

SN Ratio

Level	speed	feed	doc
1	39.07	38.85	41.54
2	40.87	40.97	40.64
3	42.35	42.47	40.11
Delta	3.28	3.61	1.43
Rank	2	1	3

Response Table for Signal to Noise Ratios

Smaller is better

Level	speed	feed	doc
1	-8.147	-2.906	-7.148
2	-5.449	-6.447	-5.726
3	-4.510	-8.753	-5.232
Delta	3.638	5.847	1.917
Rank	2	1	3

RESULTS AND DISCUSSION

3 Table : Optimization of MRR

S.NO	SPINDLE SPEED(N)	FEED MM/REV	DEPTH OF CUT MM	MRR IN m3/min
------	------------------	-------------	-----------------	---------------

1	800	0.2	0.5	1.44
2	800	0.3	1	3.94
3	800	0.4	1.5	7.53
4	1000	0.2	1	3.60
5	1000	0.3	1.5	7.46
6	1000	0.4	0.5	3.46
7	1200	0.2	1.5	6.23
8	1200	0.3	0.5	2.70
9	1200	0.4	1	7.36

Taguchi method stresses the importance of studying the response variation using the resulting in minimization of quality characteristic variation due to uncontrollable parameter. The metal removal rate was considered as the quality characteristic with the concept of larger better.

5. Conclusions

In the earlier chapters, the effects of process variables on response characteristics (material removal rate and surface roughness) of the computer numerical control (CNC) machining process have been discussed. An optimal set of process variables that yields the optimum quality features to machined parts produced by CNC process has also been obtained.

In this work, an attempt was made to determine the important machining the parameters of steel material for the performance measures like MRR and SR separately in CNC process.

Factors like the depth of cut and the feed rate have been found to play as significant role in rough cutting operations for the maximization of metal removal rate and minimization of surface roughness Taguchi experimental design (L9 orthogonal array) is used to obtain the optimum machining parameters for the maximization of metal removal rate and minimization of surface roughness

6. References

1. SJ. Raykara, D.M. D'Addonab, A.M. Manea, "Multi-objective optimization of high speed turning of Al 707 relational analysis", 9th CIRP Conference on Intelligent Computation in Manufacturing Engineering, Procedia CL) 293 –298
2. P. Jayaramana, L. Mahesh kumar, "Multi-response Optimization of Machining Parameters of Turning AA6063 T-Alloy using Grey Relational Analysis in Taguchi Method", 12th GLOBAL CONGRESS ON MANUFACTURE MANAGEMENT, GCMM 2014, Procedia Engineering 97 (2014) 197 –204
3. Rishu Gupta, Ashutosh Diwedi, "Optimization of Surface Finish and Material Removal Rate with Different Ines for Turning Operation on CNC Turning Center", International Journal of Innovative Research in Science, En Technology, Vol. 3, Issue 6, June 2014
4. Devendra Singh, Vimanyu Chadha and Ranganath M Singari, "effect of nose radius on surface roughness during using response surface methodology". International Journal of Recent advances in Mechanical Engineering (UIN No.2, May 2016
5. Srinivas'athreyal, Dr Y.D. Venkatesh, "Application Of Taguchi Method For Optimization of Process Parameters The Surface Roughness Of Lathe Facing Operation", International Refereed Journal of Engineering and Science (Online) 2319-183X, (Print) 2319-1821 Volume 1, Issue 3 (November 2012), PP.13-19
6. Anoop C A, Pawan Kumar, "Application of Taguchi Methods and ANOVA in GTAW Process Parameters Op Aluminium Alloy 7039", International Journal of Engineering and Innovative Technology (IJEIT) Volume 2, 2013

AN OVER VIEW OF BIOMASS DRYER FOR CASHEW PRODUCT

P.Murugan, Department of Mechanical Engineering, St.Anne's College of Engineering and Technology, Panruti
Dhanushkodi, Department of Mechanical Engineering, Prist University, Vallam.Thanjavur

ABSTRACT

Biomass hybrid dryer is one of the simplest methods used in food and agriculture industries for extracting the moisture contents from the products in less time with good quality of product with and maintain uniform colour. Psychrometrically the psychrometric is important in drying technology as it refers to the properties of water particle mixture which controls drying rate. The temperature and rate at which the liquid vaporization occurs will depend on the concentration of evaporation in the surrounding atmosphere. Biomass drying refers to drying energy methods.. A biomass dryer is a enclosed unit structure to keep the food protected from harm and to preserve product quality. Different types of biomass dryers are available and are generally known as forced convection and natural convection. Biomass dryer more cost efficient than other dryer types. Through this paper we looked at the development of the biomass dryer's architecture and efficiency review

Keywords— *Biomass dryer, natural draft, forced draft, drying time, moisture.*

1. Introduction.

Biomass is one of the main renewable energy sources which are readily available. The energy source supplies are not limited that why it is called as renewable energy and it has much demand in various parts of the world. It is eagerly focusing for the cost effective method of dryers either forced or natural circulation method commonly used for drying. Dryers are utilizing to dry various agricultural products like crop drying, Space heating and product maintaining good quality even studies a few biomass projects in different parts of the world and discusses future. Biomass techniques are available for drying different food products and which has some advantages and disadvantages. This technique is necessary to preserve the food products. The biomass hybrid dryer is one of the most effective methods which have been implemented. There is a lot of awareness growing in the world that the renewable energy is play vital role with extending technology. The developing countries are in need to improving their productivity hence biomass is much acceptable category as an energy saving method in agricultural applications. It is preferred as one of the best among other alternative energy sources and the technology is very good. The biomass hybrid dryers have various applications. Biomass has some benefits in sustainable terms over fossil fuels such as coal petroleum and gas. It does not produce the pollutants but while burning biomass can release carbon dioxide but it is needed to growing plants that why it is balanced. In this review paper, we have reviewed the design modifications applied and development of different types of hybrid biomass dryers. Biomass dryer is not only environmentally friendly but also benefited to utilize both in urban and rural areas for commercial purpose and much more simple compared to other types of dryers. It provides higher drying temperatures as drying takes place in an enclosed cabinet. EERE information center [1] Biomass is one of the most important sources of renewable energy for transport. Biomass is any biological material that has stored sunlight in the form of chemical energy, such as plants, farm crops or residues, urban waste and algae

Tkemaladze et al [2] Economic and political value 'Biomass Action Plan and Multi-Year Plan,' established by the Energy Department of the European Commission. Chum et al[3] the former paper also reviewed the need to reduce emissions of carbon dioxide and focused on raising awareness by increasing the issue of global warming. Biomass renewable energy resource emitted CO₂ during processes of combustion and consumption occurs and results in an rise in atmospheric carbon dioxide in origin. Vegetables use CO₂ and Consecution of other plant degradation processes.

1.1 Comparative Study of various types of dryers with different parameters

There are various types of dryers based on the fuel are available in general it can be classified as follow

1. Biomass dryer: use wood or waste of agricultural product
2. Solar dryer: sun heat only use
3. Electric dryer: based on power avail

From the over view biomass dryer is as easily avail in earth and is low cost than others also used all days include winter days.

s.no	Particulars	Biomass dryer	Solar dryer	Electric dryer
1	Heat energy	From wood/ agricultural waste	From sun heat	From electricity
2	Cost of the fuel cost	Low cost	No cost	Expensive
3	Energy production time	From earth	Sunny days	Minimum hours each days
4	Dryer temp	Up to 100 ⁰ c	Based on sun lights	Same as biomass
5	Capacities	Maximum	minimum	Low
6	Cost of the dryer	Low cost	High cost	moderate
7	Working time	All days	Sunny days only	Only based on supply of power

Table 1. Comparative Study of various dryers with different parameters

2 Biomass dryers: Components and Classification

The following fig show main parts of dryer and each showed briefly in detail it is much useful to understand about the dryer

1. Firing chamber

It is usually show at the bottom at the left direction of the dryer. The firing chamber has a door that should be kept closed when the dryer is working. Therefore the fuel burns well.

2. Duct

This is main part of dryer the duct is generally of made of MS in dryer air which drawn from chamber to dryer

3. Dryer

This is storage place of system the system the size of the dryer according to the capacity of this product. The hot air flows into the drying chamber and this hot air passes through the drying product and eliminates the product's moisture content.

4. Trays

The number of trays in the dryer depends on its size. Stainless steel is the right material to make trays because it does not rust.

5. Thermometer

It is fixed a right placed where provided the chamber. it is main parts of this system because we measure the temperature inside the drying chamber.

2.1 Over View Of Types Of Biomass Dryers

S. .N		Rotary Dryer	Flash Dryer	Ring Dryer	Fluid Bed Dryer	Spray Dryer
1	Purpose	1.Food company	1.Food company	1.Food company	1.Food company 2.Mineral company	1.Food company 2.Madicne

		2.Chemical company 3.Medicine	2.Mineral company 3.Chemical factory	2.Grains	3.Chemical industry 4.Polymer	
2	Design	It had cylinder shell for heating device,output is more than 70%	Spin dryer and also vertical type dryer, average output temp 100kg/hr with 450°C	Air passed via second heated for large amount of product come again to dry.	Hot air passes through distributor plate. supply of air balance more quantity.	Hot air supplied via top of dryer. Final product collect bottom of dryer.
3	Advantages	1. More than 70% of wet remove 2. less Maintenance 3.More capacity	More value of product dryer	1.low time required 2.Remove maximum percentage of wet	1.Drye id more volume of product	1.Fined product output
4	Disadvantages	1.More energy need 2.Minimum output 3.High cost of fuel	1.partly wet remove from the product	1. More time needed.	1.Skilled labor are needed	More area is needed.

Table 2. Comparative Study of different dryers of biomass

Dryer Type	Small Material	Uniform Size	Heat Recovery	Percentage of Fire %	Steam Use
Rotary Dryer	No	No	Difficult	High	Can use steam
Flash Dryer	Yes	No	Difficult	Medium	None
Disk Dryer	No	No	Easy	Low	Saturated steam
Cascade Dryer	No	Yes	Difficult	Medium	None
Superheated Steam Dryer	Yes	No	Easy	Low	Excess steam produced

Table2. Comparative Study of different dryers of biomass

2,2 Working principal of flash dryers

Biomass and hot air normally flow co-currently through the dryer so that the hottest gasses come into contact with

the material, but for materials where temperature is not a concern, the flue gas and solids flow in opposite directions, so that the driest solids are exposed to the hottest gasses with the lowest humidity, but for biomass this exposes the dry material to a high flue gas temperature.

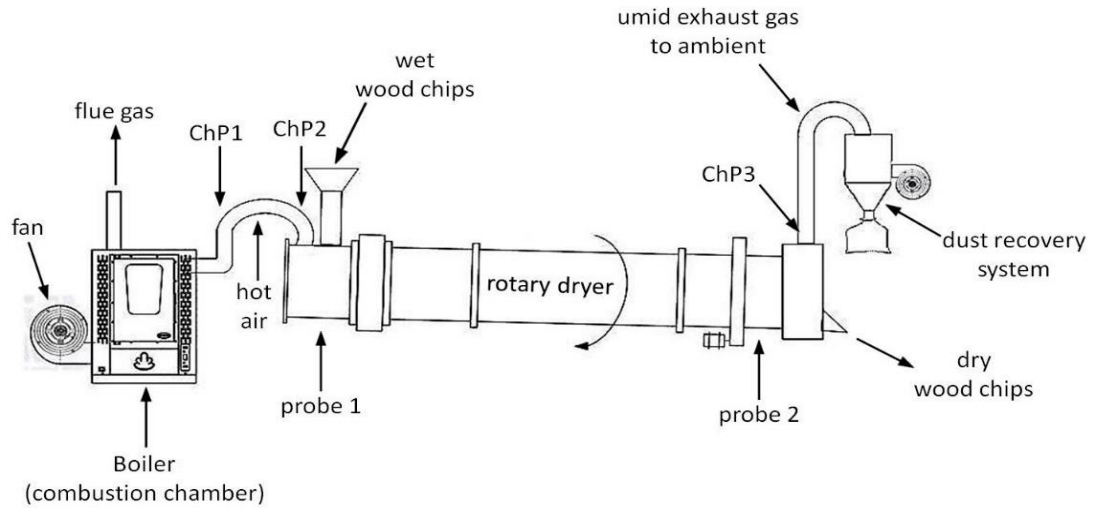


Figure 4 System diagram, and the points



Figure2. Prototype rotary dryer (a); system for recovering dust (b).

In a flash dryer, the solids are mixed with a high-speed hot air stream. The contact of the solids with the air results in a very rapid drying process. The solids and the air are separated, and the gasses continue through the scrubber to the material. Due to the drying time of the flash dryer, the equipment is more compact than the rotary dryer. However, electricity consumption is higher and biomass must pass through a grinder to reduce its size so that it can be suspended in the air stream. Flash dryers have been successfully used for wet materials, such as sludge, to dry most biomass materials, including wood.

3 Recent trends in Biomass dryer

Dhanushkodi et al [4] investigated the energy consumption for drying of cashew nut processing and compare with different processing methods such as electrical, steam and biomass drying. The total energy consumption for 1000 kg the cashew nuts numbered 5866.2 MJ, 5911.69 MJ and 6897.36 MJ. The efficient use of fuel and the drying system based on renewable energy can contribute to a reduction in production costs. The efficient use of fuel and the drying system based on renewable energy have played a vital role in reducing the cost of production. And 95% of energy was used for drying. Energy intensity of cashew processing varied from 1.5 MJ/kg to 3 MJ/kg.

Shafiq Hamid et al [5] investigated about food or conversion of fuel with biomass or agricultural product. Experiment 1 with natural convection and experiments 2, 3 and 4 with forced convection in addition with various numbers of fans. Experiment 2 investigated with one fan, experiment 3 for with two fans and experiment 4 for with three fans. The temperature increased in experiment 3, reaching up to 29°C in the direct dryer and 7°C in the indirect dryer. Both high occurring at 1300. Assisting with fans in increased the temperature of the chamber.

Dhanushkodi1 et al [6] design and developed a biomass dryer system. It was suitable for drying a maximum of 40 kilograms of cashew in a single batch with an air temperature of 65 to 75 ° C and a minimum fuel consumption of 0.5 to 0.75 kg / hr. The biomass dryer can dry the cashew kernel with a moisture content of 9% w.b. Reduced to 3% w.b. within 7 hours. Total efficiency 9.5 percent. Biomass drying was more efficient than sun drying and increased drying rates and time. The dryer performance is also improved by the addition of a solar unit; the system can be operated as a solar biomass hybrid dryer.

Pavane1et al [7] the performance of the hybrid solar biomass dryer was investigated for drying. The average temperature in the dryer was 60.46 ° C with an ambient temperature of 33.23 ° C, solar radiation of 570.65 W / m². Average temperatures in the solar biomass hybrid dryer found to be 55.84 ° C. Average drying rate was 0.2564 to 0.0005 gm/100gm bdm min, respectively. The maximum efficiency of biomass combustor and pyramid shape solar-biomass hybrid dryer was 74.84% and 29.10% The drying was economical because solar energy with biomass energy is freely available. Hybrid dryers protected from rain, insects and dust and dried nutmegs were of high quality compared to shade dried products.

Uthman et al[8] designed and manufactured bio-mass dryer for agricultural products such as groundnut, weight 50 g, 100 g and 150 g, temperature 550C, 600C and 650C. The temperatures of 600C and 650C were much better than the temperature of 550C. The time taken for each sample at different weights and temperatures varies. Therefore, the higher the temperature, the lower the time taken for the groundnut to dry, the higher the weight, the higher the time taken for the groundnut to dry. The higher the temperature, faster the rate of drying. For producers and sellers of groundnuts, a biomass dryer is recommended.

Hamdani et al[9] Performance analysis of the Solar drying unit equipped with biomass-fueled air heaters. The dryer shall consist of a drying chamber with a glass cover and a cross-flow heat exchanger for an air heater using biomass fuel. Initially carried out using solar energy with hot-air produced from biomass combustion and maintained at 40–50 ° C. The overall weight of the fish did not change much, hybrid type fish dryers using solar energy and biomass energy can dry the fish and, if there is no sun, this system operates with biomass energy, which is the extra future of the system.

Augustus Leon et al [10] Thermal performance The air heating system is capable of drying red chilli. The system, combined with an unglazed transpired solar collector, a rock bed and a biomass gasifier stove with a heat exchanger, is used for drying air at a temperature of approximately 60 ° C. And it's 90 m³ / h. The chilli was dried from 76.7 per cent moisture to 8.4 per cent over 32.5 h continuous drying. The dryer reduced the drying time by 66% compared to the open sun. Considering the drying time, reliability and superior quality of the dried product, almost 100% of the drying energy demand from renewable energy sources (solar and biomass energy) has been met.

Sekar et al [11] researchers developed a new drying systems for enrich the quality of products. The energy consumption, and reduce the drying rate. Open sun-drying has certain disadvantages, such as depending on the weather, contamination by dust birds and animals consumes a considerable quantity, slow drying and damage due to strong winds and rain. To overcome this problem, dryers developed in a closed environment, Selection of appropriate drying processes and proper input parameters The most recent progress in the field of drying of agricultural food products, such as new methods , new products and modeling and optimization techniques, has been presented in this review. Challenges and future directions have also been highlighted.

Anand et al [12] investigate huge agricultural wastes used to produces Biomasses. Solar Energy and Biomass companied together used to produce heat and remove the moisture from the vegetables with minimum power consumption. It also have microcontroller to monitor the temperature and humidity. This unit used to investigate onions, garlic, and leafy vegetables. Intelligent solar-biomass dryer is the most effective scenario.

Gaikaar et al [13]. Investigator studied combined solar and biomass energy. The hybrid drying system for fruit and vegetables is becoming popular for increasing the quality of agricultural crops. A prototype solar dryer with a biomass combustor could be designed and developed for use by small-scale rural farmers to dry their harvested fruit and vegetables It focused on various design modifications and enhancement techniques. Hybrid solar dryers did not use any auxiliary equipment and protects the products. This is the simplest and most cost-effective form of dryers.

Boda et al [14] recent innovative techniques used for development of Solar air collector integrated with thermal energy storage, air recirculation, flat plate type nozzle collector, Double hot air pass, finned plate and V-corrugated inside solar air collector, modeling techniques are very important in designing and developing, increasing drying efficiency, analysis and performance to improve shelf life. The solar dryer produces better quality food with a nutritional value that enhances the value of the food and the market value of the product.

Sudhagar Mani et al [15] theoretically and experimentally investigated Biomass drying, reduction of size and compaction. Single pass rotary dryer modeled using different parameters and validated with industrial drying data. The biomass energy was 16% used. The low cost fuels for drying reduce environmental emissions and the energy consumption of grinding biomass is estimated with different burner fuels used. The total energy consumption of the wood pellet plant was between 3 and 3.8 GJ / t depending on the type of fuel burner. Cost of production or coal is the cheapest fuel to be used for the drying of biomass.

Okoroigwe et al [16] Designed a combined solar and biomass dryer with 3 spaced drying trays, Maximum tray temperature of 53 ° C was achieved in combination with solar and biomass heating. Optimal drying rate of 0.0142 kg / hr was achieved, compared to a lower drying rate of 0.00732 kg / h for solar drying and 0.0032 kg / h for biomass drying. The efficiency of agricultural dryers increased, the productivity and economic viability of small and medium-sized enterprises producing and processing agricultural products in developing countries increased.

Stahl et al [17] discussed the different model dryers with quality properties. The amount of volatile hydrocarbons left in saw dust. Low emissions of hydrocarbons and improve the energy content of the saw dust by decreasing air pollution and improve the work environment. If sawdust with 1.4 g terpenes/kg odw dried in the dryer with low emissions, it emitted 0.5 g/kg odw less terpenes than if it was dried in a rotary drum dryer

Martins Ozollapins et al [18] design a Biomass drying was applied to moisture content to develop efficient drying. The drying technology used with composite biomass structure, the highest drying rates, but peat has the lowest. The drying rates increased, drying levels begin to decrease once biomass temperature reaches a certain point. The over 30 percent moisture content and pre-dried in natural drying to prevent high energy consumption. The highest drying rate value at 78 oC temperature with an initial humidity content of 69.7 percent and a layer thickness of 100 mm exceeds 0.79 percent.

Edgars Vigants et al [19] performance analysis of the drying process energy consumption. The energy consumption with and without the air recirculation model for each individual drying cycle. Since this increases the overall consumption of electricity and heat. The increased drying agent flux in the dryer increases the consumption of heat and electricity. The moisture evaporated from the dried material. An increased flux of drying agents in the dryer increases heat consumption and electricity.

Javid Hussain et al [20] investigated three different Hexane Soxhlet (Sox-Hex), Halim (HIP), and Bligh and Dyer (BD) methods have been applied to freeze-dried (FD) and oven-dried (OD) *Chlorella vulgaris* biomass to determine their effectiveness. HIP chose C to one. Recovery of *vulgaris* lipids considering both quality in extraction and toxicity to solvents. It had the largest 20 and 22 percent lipid on FD and OD biomass, 14.8 and 12.7 percent neutral lipid. Correlative models applied to the fatty acid profiles concluded that high content and oleic acids in algal lipids led to balancing the saturated and unsaturated fatty acid ratio and resulted in high-quality biodiesel algae.

Philippe Eliaers et al [21] investigate simulation of vortex chamber based biomass drying Focusing on continuous operation And Combined with multichamber or simultaneous air feeding. The countercurrent to the project considered it to be physically too costly to dry biomass. At the end of the system, higher drying rates pose a risk of overheating the biomass and insufficient air usage with co-current operation.

Matrix Ken et al [22] investigated a sludge-wood waste. The mixture was dried using forced air, and the exothermic metabolic activity of aerobic thermo-philic microorganisms increased. It tracks temperature, moisture, pressure, airflow and overall mass. Losses of moisture and carbon measured for three mixtures of sludge / wood waste. 1:0.5 mixture of sludge / wood waste mass in optimal drying levels, creating favorable conditions and This results in the most effective removal of moisture for critical environmental conditions.

Gebreegziabher et al [23] studied a mathematical model of design and operation of the biomass dryer to Boost the efficiency of combustion, and increased emissions. The task of extracting moisture from biomass, which is

influenced by several factors. Optimum solutions showed the economy was influenced by the size of wood chips. As the size of the wood chips becomes too large, the drying period becomes too long and therefore the dryer size and energy cost increase. The restriction of the minimum heating value without disrupting the atmosphere and the activity of the combustion process when the biomass is too large or too moist

Yuping Liu et al[24] Biomass drying mainly takes place in rotary dryers, good circulation of biomass particles in the fluidized bed without mechanical aids. Initial moisture content of drying high moisture sawdust, in three stages as partial fluidization, complete fluidization with increased drying rate and complete fluidization with reduced drying rate. Given the fast mass and heat transfer rate in the fluidized bed, a high drying rate was achieved. The current fluidized bed dryer has a high drying rate that is similar to a conventional fluidized bed dryer of a binary mixture, but is more compact and requires no separation of biomass from inert parts.

Moreno et al [25] Particles of biomass in southern Chile to understand and optimize the drying process of wood particles in a fluidized bed. The basic density and anhydrous density of the biomass particles was 348 and 395 kg m³. The Langmuir model only predicts the equilibrium moisture well below 10 per cent in the relative humidity range. In an intermediate range of relative humidity up to 40%. So for industrial drying with atmospheric air, the difference is not important. When the biomass particles are dried at temperatures below 187°C they only undergo a change in their mass as a result of the loss of moisture and not as a result of a devolatilisation. The uses of high drying temperatures, the use of high temperatures result in lower specific consumption of energy.

Katarina Rupar et al[26] study focused on the relationship between release of organic compounds and drying of biomass, depending on the raw material, and drying conditions. The drying mediums used while the emissions, hot air and steam, altered the distribution of terpenes compounds between different groups after drying. Biomass drying on "particle level" has shown that the wood drying industry may find this method useful. Special drying medium, biomass diversity and low temperature reducing emissions are useful.

Zabaniotou et al[27] Forest biomass experimental investigation in a rotary dryer has been performed, the experimental panel concerns the influence of air flow rate, temperature, rotation speed and inclination, a mathematical model for drying biomass in a rotary dryer. Rotary dryer as compared to model data and check model validity. In the case of low rotation rate, the final moisture content for the biomass was low. Particulate residence time influenced by the rate of rotation than from the incline of the dryer.

Angelo Del Giudice et al [28] The common type for biomass is rotary dryers. There are several variations of rotary dryers; hot gasses are contacted inside a rotating drum in this type of dryer with biomass material. Lifts the solids inside the dryer with the help of flights. If contamination isn't an issue, hot flue gas can be fed directly into the dryer Fig.1 shows the dryer's schematic view.

CONCLUSION

This paper review the design and performance studied about biomass dryer with advantages and disadvantages, present and past method of different types of drying. We have studied in detail about natural and unnatural convection method of drying suitable for agricultural product, vegetables and fruits with expected quality and lowest cost. Biomass dryer method is better than other drying methods. During fair weather it works well. Biomass has much benefit for the environment than fossil fuels like coal and petroleum. Biomass contains little sulfur and nitrogen, so it does not produce pollutants. It releases carbon dioxide(CO₂) while burning biomass, but uses it to grow plants and remove carbon dioxide from the atmosphere.

References

1. U.S.Department of Energy EERE information center (1-877-337-3463), 'Biomass Basics: The Facts About Bioenergy' , eere.energy.gov/information center.
2. Chum, H., Faaij, A., Moreira, J., Berndes, G., Dhamija, P., Dong, H., Gabrielle, B., Goss Eng, A., Lucht, W., Mapako, M., Masera Cerutti, O., McIntyre, T., Minowa, T., Pingoud, K., 2011. 'IPCC Special Report on Renewable Energy Sources and Climate Change Mitigation', Cambridge University Press, Cambridg.
3. Tkemaladze,G.S,Makhashvili,K.A,2016, Climate changes and photosynthesis
. Ann.Agrar.Sci.14(2).119-126.
4. Dhanushkodi , V. H. Wilson and K. Sudhakar, (2016),'Agricultural Academy ENERGY ANALYSIS OF CASHEW NUT PROCESSING AGRO INDUSTRIES: A CASE STUDY ' ,Bulgarian Journal of Agricultural Science, 22 (No 4) 635–642.
5. Shafiq Hamid, Eqwan M. R, (2017)'Experimental Study of Direct and Indirect Solar Biomass Dryer', Department of Mechanical Engineering, Universiti Tenaga Nasional, Kajang, Selangor, Malaysia, IJSRSET1734118 | Received : 10 August | Accepted : 21 August July- 2017 | July-August-2017 [(3)5: 471-479].
6. S. Dhanushkodi , Vincent H. Wilson and K. Sudhakar, Pelagia , (2015),'Design and performance evaluation of biomass dryer for cashewnut processing ' ,Research Library Advances in Applied Science Research, , 6(8):101-111.
7. D.R. Pavane , Y.P. Khandetod and A.G. Mohod ,(2018) 'Techno-Economics of Pyramid Shape Solar-Biomass Hybrid Drying of Nutmeg ,Int.J.Curr.Microbiol.App.Sci 7(10): 1984-1993.
8. Uthman, F., Balogun, A.L and Onipede, E.A, (2017),'DESIGN, FABRICATION AND TESTING OF A BIOMASS DRYER', TETFUND Sponsored Kwara State Polytechnic Journal of Research and Development Studies Vol. 5. No. 1 June.
9. Hamdani , T.A. Rizal, Zulfri Muhammad,' Fabrication and testing of hybrid solar-biomass dryer for drying fish', Case Studies in Thermal Engineering 12 (2018) 489–496
10. M. Augustus Leon & S. Kumar, (2008) ,'Design and Performance Evaluation of a Solar-Assisted Biomass Drying System with Thermal Storage, Drying Technology: An International Journal, 26:7, 936-947.
11. S.Sekar , M. Purushothaman , S.D. Sekar , Maddela Rama Sharath,' Reddy Recent developments in drying of food products T.N. Valarmathi * , , Kancham Reddy Naveen Kumar Reddy', Materials Science and Engineering 197 (2017) 012037
12. B.A. Anand* , P. Manjunath Babu and B.A. Sunil Raj, 'Intelligent System Based Solar Biomass Hybrid Dryer for Perishable Crops and Leafy Vegetables Int.J.Curr.Microbiol.App.Sci (2018) 7(10): 1701-1707.
13. P. K. Gaikar, Dr. S. R. Kalbande , 'Solar Biomass Hybrid Drying System For Drying Fruits And Vegetables: A Review, International Journal Of Pure And Applied Research In Engineering And Technology
14. M. A. Boda, T. B. Shaikh, S. S. Kale, R. H. Bochare,'Recent Innovative Techniques for Developments of Solar Dryer , International Research Journal of Engineering and Technology (IRJET) Volume: 05 Issue: 12 | Dec 2018.
15. Sudhagar Mani, Shahab Sokhansanj, Adjunct ,Xiaotao , 2005 'Modeling of Biomass Drying and Densification Processes, Conference Paper · January DOI: 10.13031/2013.19928.

16. Okoroigwe E. C. , Eke M. N. and Ugwu H. U, 2013 , 'Design and evaluation of combined solar and biomass dryer for small and medium enterprises for developing countries', International Journal of Physical Sciences, Vol. 8(25), pp. 1341-1349, 9 July.
17. M. Stahl , K. Granström, J. Berghel, R. Renström, 2004 'Industrial processes for biomass drying and their effects on the quality properties of wood pellets', Biomass and Bioenergy 27 ,621–628.
18. Martins Ozollapins, Aivars Kakitis, Imants Nulle, 2014. 'Stalk Biomass Drying Rate Evaluation At Various Layers And Drying Parameters Engineering For Rural Development', Jelgava, 29.-30.05.2014.
19. Edgars Vigants, Girts Vigants, Ivars Veidenbergs, Dace Lauka, Krista Klavina, Dagnija Blumberga, ,2015' Analysis of Energy Consumption for Biomass Drying Process, Environment. Technology. Resources, Volume II, 317-322.
20. Javid Hussain & Yan Liu & Wilson A. Lopes & Janice I. Druzian & Carolina O. Souza & Gilson C. Carvalho & Iracema A. Nascimento & Wei Liao, 2015, 'Effects of Different Biomass Drying and Lipid Extraction Methods on Algal Lipid Yield, Fatty Acid Profile, and Biodiesel Quality, Appl Biochem Biotechnol 175,3048–3057.
21. Philippe Eliaers a , Jnyana Ranjan Pati a,b , Subhajit Dutta a,c , Juray De Wilde, P , 'Modeling and simulation of biomass drying in vortex chambers',. Chemical Engineering Science 123 (2015) 648–664.
22. Matrix Ken M. Frei a , David Cameron b & Professor Paul R. Stuart , 2004 'Novel Drying Process Using Forced Aeration Through a Porous Biomass, Drying Technology Vol. 22, No. 5, pp. 1191–1215.
23. Tesfaldet Gebreegziabher a , Adetoyese Olajire Oyedun b , Chi Wai Hui, T , 2013 'Optimum biomass drying for combustion e A modeling approach', Energy 53 ,67-73.
24. Yuping Liu a , Jianghong Peng b , Yasuki Kansha a , Masanori Ishizuka a , Atsushi Tsutsumi a , *, Dening Jia b , Xiaotao T. Bi b , C.J. Lim b , Shahab Sokhansanj, 2014, 'Novel fluidized bed dryer for biomass drying Fuel Processing Technology 122 ,170–175.
25. R. Moreno, G. Antolí, A. Reyes ,P. Alvarez, 2004 , 'Drying Characteristics of Forest Biomass Particles of Pinus radiata Bio systems Engineering , 88 (1), 105–115.
26. Katarina Rutar, Mehri Sanati, 2003, ' The release of organic compounds during biomass drying depends upon the feedstock and/or altering drying heating medium', Biomass and Bioenergy 25 ,615 – 622.
27. A.A.Zabaniotou,2000, 'Simulation Of Forestry Biomass Drying In A Rotary Dryer, Drying Technology,18(7),1415-1431.

A Review on Recent Development In Design and Energy Enhancement of Flat Plate Hybrid Photovoltaic Thermal (PV/T) Air Collector.

K.Sakthivel, Dept of Mechanical Engineering, Shri Krishnaa College of Engineering and Technology, Pondicherry ,
P.Murugan. Dept of Mechanical Engineering, St. Anne's College of Engineering and Technology, Panruti , S.Dhanushkodi, Department of Mechanical Engineering, PRIST University, Vallam.Thanjavur.

Abstract:

Due to population growth of the present world scenario. The demand *for* electric power and air pollution are also increasing in *the fastest* manner, which causes many problems these include asthma and chronic pulmonary obstructive disease. It can be caused or triggered by rising levels of air pollution. Air pollution is the primary source for breathing ailments in children and the elders, resulting in disease and deaths of around 8.4 million people a year. *However, pollution* is getting a fraction of the global community interest. So we can reduce it and tackle electric energy demand wherever possible. Solar radiation is one natural resource that is readily available without spending our wealth. *It* can be used If it uses effectively it will also increase the national economy. Solar photovoltaic thermal (PVT) collector change over the sun based radiation specifically into power and heat at the same time. *As the solar panel temperature increase*, voltage drop will result extract in the heat being removed from rear side absorber by allowing *the flow* of different sorts of working liquids for example air, fluid, oil and water with Nano fluids. The important reasons extraction of heat from *a PV cell* in order *achieves* better performance and increase the electrical efficiency level. Article reviews historical structure, advancement and execution assessment of different kinds of PV/T collector and *enhanced* performance to meet future energy demand.

Keywords: Solar collector, photovoltaic thermal system, thermal and electrical, design performance Efficiency, collectors, absorber.

1. Introduction

To all the more likely comprehend the present circumstance in India and the eventual fate of the market for sustainable energy. Because of the current grid's rabbit expansion, and the availability of transportation and equipment to look at current energy consumption patterns. Since thermal generation is based on the increase in CO₂ emissions from burning coal, oil and gaseous fuels. This causes environmental damage and global warming. There is also an increase in reliance on imports, which will proceed later on except if the strategy [1] has changed since the 1980s and is still in place India has found some kind of harmony in absolute vitality utilization and creation. This prompted the need to purchase the vitality from outside the nation to gracefully and address the issues of the entire nation [2] India depends predominantly on coal for 57% of all out vitality utilization. Since its area is between the tropics of disease and the equator. India has a normal yearly temperature of between 25 ° C and 27.5 ° C. India has a huge sun oriented potential. The sunniest parts are situated on the south/east coast from Calcutta to Chennai. [3] Power utilization development is relied upon to be the quickest among the rising economies of the world, including India. As indicated by the EIA, the yearly normal increment will be around 4 percent from the year 2002 - 2025. Developing economies are anticipated to dramatically increase their net power utilization, from 4,645 billion kilowatt hours in 2002 to 11,554 billion kilowatt hours in 2025. The first solar collector was built by Swiss scientists in 1767. In 1905, Albert Einstein outlined the photoelectric effects with his theory of relativity. Photovoltaic (PV) systems were installed for 930 megawatts in 2013. Oh, Wolf. M et al [4] Photovoltaic (PV) module has been studied since 1976 and receives only a small percentage of additional energy efficiency. The concept of PVT systems has been developing step by step since the last five decades. However, technology is not much commercialized

2. Concept of Photovoltaic thermal module.

This module transforms direct sun radiation into heat and electrical power by means of photovoltaic effect and improves efficiency by extracting heat from module by utilizing different modification through various techniques, mass flow rate, insulation and working fluids. Sandeep [5] the clear and simplest method of PVT system Fig.1 shows the clear concept of PVT system.

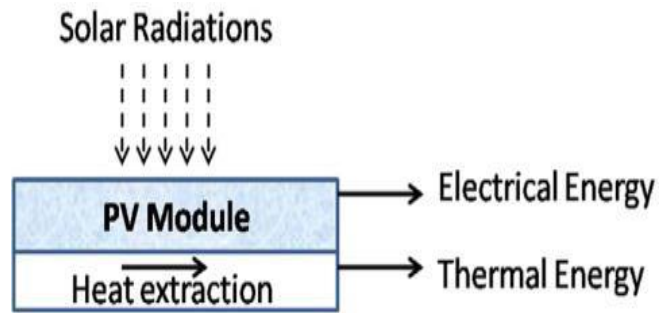


Fig.1 Simple concept of PVT system [5]

2.1 Element of solar panel collector.

Important components of photovoltaic collector

1. At least one glass or plastic transparent layers
2. Absorbing tubes which extract heat.
3. Absorber sheet either straight or modified shapes for example wavy with dark colour.
4. Header is drained and the heat transfer. It is mounted either at top or bottom of the collector.
5. Insulation; reduces heat loss, usually around the collector and the tubes, or at the back.
6. Special frame; holding components from the collector and keeping safe from dust and other factors.

2.2 Types of Solar Collector.

The photovoltaic solar collector / dryer receives solar rays and gathers energy. Could be classified as follows

- A) The type of flat plate without the focus.
- B) Type parabolic drill with line focus.
- C) Central focused parabolic dish.
- D) Centre-focused Fresnel lens.
- E) Heliostats with focused Center receiver.

3. Classification of PVT system (Flat plate concentration)

3.1. Flat plate Collector

FPC is the solar thermal technology which is most commonly used. FPC consists of an enclosure container, a dark colored absorber plate with operating fluid circulation and a transparent cover to enable solar energy to be transmitted into collector. Collector sides and back are typically insulated to lower heat. A warmth move liquid is coursed through the liquid entries of the safeguard to expel heat from the solar system collector.

The flat plate collector Ibrahim et al [6] is divided into the following types namely PVT water, air, water and air combined and nano fluid collector. It can be clearly understood by means of the following Fig.2 It can be further divided according to the working fluid by using different types of material, structure, and absorber size. The absorber assumes an urgent job in diminishing the warmth in photovoltaic module. Like the researchers, the above mentioned fluids were used.

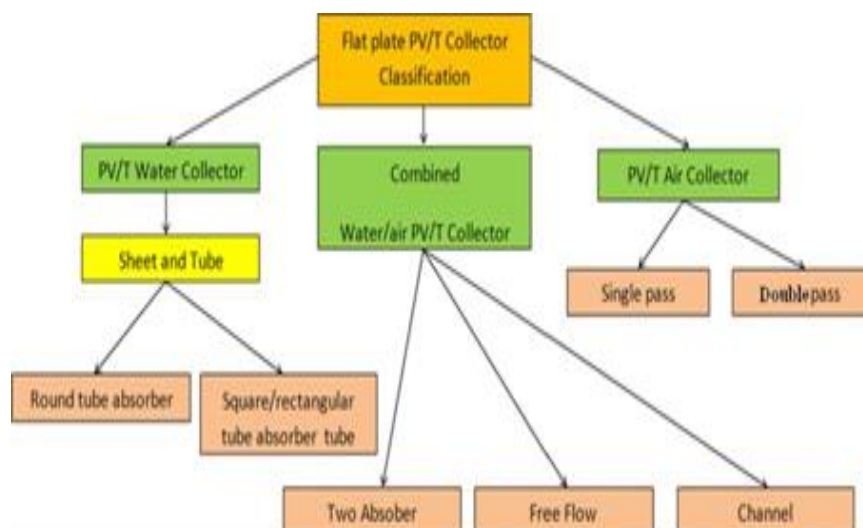


Fig.2.Classification of FPC (PVT) system [6]

4. Conclusions and recommendations

A study on detailed reviews both historical and present trends implemented by the researchers on the performance of solar Photovoltaic thermal technologies, design and analyzed of air base collector with either natural or forced flow, studied and optimized to understand overall development in PVT technology and outcomes can be summarized in the review

- ✓ Photovoltaic panel receive solar radiation from the sun and transformed by photovoltaic effect into electricity, air is used as working fluid to produce heat and to improve electrical energy. It is the simplest method to produce electric energy from solar energy. It also low cost method and no corrosion take place.
- ✓ Business people, Engineers, Industrialist have recently focused their attention on hybrid photovoltaic (PV/T) systems Hence further research and development is needed especially in cost of reduction, design, material, coating, insulation, change of absorber, energy conversion and fabrication and optimal performance level of the collector should be further improved for enhancing electrical and thermal efficiencies on the application of the PV/T air base collector.
 - a) Phase change material (PCM) and
 - b) Implement the novelty design and development of system
 - c) Variety of bionic evaporation cooling techniques can be used as an efficient cooling system and are recommended for further research to improve the cooling effect.
- ✓ Many other innovations are yet to be done on direct and indirect type solar dryers which can fetch more efficient thermal performance.

It would be beneficial to consumers through proper architectural design and configuration and It is not only for the present, because solar power is sure, pure and secure, solar energy will be a medium for the energy needs of the 21st century. This effort will contribute to the global goal of improving the use of renewable energy in residential, industrial and commercial environments.

5. References

1. Solar Electric and Solar Thermal Energy: A Summary of Current Technologies November, 2014 Tayyebatossadat P. Aghaei, Research Associate, Global Energy Network Institute (GENI), www.geni.org
2. Overview of Renewable Energy Potential of India, October 2006. Peter Meisen President, Global Energy Network Institute (GENI) www.geni.org

3. Solar Cells and their Applications Second Edition, Lewis Fraas, Larry Partain, Wiley, 2010, ISBN 978-0-470-44633-1, Section10.2.
4. Wolf. M, 1976,' Performance analyses of combined heating and photovoltaic power system for residences,Energy Conversion,16:79-90.
5. Sandeep. S.Joshi, Ashwinkumar.S, Dhoble,2018,'Photovoltaic thermal system (PVT) Technology review and future trends', Renew. Sustain. Energy Rev.92, 848-882.
6. Ibrahim, A., Othman, M.Y., Ruslan, M.H., Mat, S., Sopian, K., 2011,' Recent advances in flat plate photovoltaic/thermal (PV/T) solar collectors'. Renew. Sustain. Energy Rev. 15 (1), 352–365.
7. Hussain, F,2013,'Design development and performance evaluation of photovoltaic/ thermal (PV/T) air base solar collector'. Renew. Sustain. Energy Rev. 25, 431– 441.
8. Othman, Mohd. Yusof Hj., Yatim, Baharudin, Sopian, Kamaruzzaman, Bakar, Mohd. Nazari Abu, 2005, 'Performance analysis of a double-pass photovoltaic/thermal (PV/ T) solar collector with CPC and fins', Renewable Energy 30, 2005–2017.
9. Othman, Mohd. Yusof, Yatim, Baharudin, Sopian, Kamaruzzaman, Bakar, Mohd. Nazari Abu, 2007,'Performance studies on a finned double-pass photovoltaic-thermal (PV/T) solar collector', Desalination, 209, 43–49
10. Sujata Nayak and 'Arvind Tiwari, 2007, 'Performance Evaluation of an Integrated Hybrid Photovoltaic Thermal (PV/T) Greenhouse System', International Journal of Agricultural Research 2 (3): 211-226.
11. Alibakhsh Kasaeian , Yasamin Khanjari , Soudabeh Golzari , Omid Mahian , Somchai Wongwises, 2017, 'Effects of Forced Convection on the Performance of a Photovoltaic Thermal System: An Experimental study', Experimental Thermal and Fluid Science, doi: <http://dx.doi.org/10.1016/j.expthermflusci.2017.02.012>.
12. Arvind Tiwari, M.S. Sodha, Avinash Chandra, J.C. Josh,2006,'Performance evaluation of photovoltaic thermal solar air collector for composite climate of India' ,Solar Energy Materials & Solar Cells 90 pp 175–189.
13. Barnwal, Arvind, Tiwari, 2009 'Thermodynamic performance analysis of a hybrid Photovoltaic-Thermal (PV/T) integrated greenhouse air heater and dryer', International Journal of Exergy January, DOI: 10.1504/IJEX.2009.023348.
14. G. K. Singh, Sanjay Agrawal, and Arvind Tiwari, 2012,'Analysis of Different Types of Hybrid Photovoltaic Thermal Air Collectors: A Comparative Study', Journal of Fundamentals of Renewable Energy and Applications Vol. 2, Article ID R120305, 4 pages doi:10.4303/jfrea/R120305.
15. Joshi AS, Tiwari A, Tiwari GN, Dincer I, Reddy BV, 2009,' Performance evaluation of a hybrid photovoltaic thermal (PV/T) (glass-to-glass) system. Int J Therm Sci ,48:154-64
16. Vineet Saini , Sumit Tiwari , G.N. Tiwari, 2017,' Environ economic analysis of various types of photovoltaic technologies integrated with greenhouse solar drying system', Journal of Cleaner Production 156 , 30-40.
17. Ooshaksaraei P, Sopian K, Zaidi SH, Zulkifli R, 2017,' Performance of four air-based photovoltaic thermal collectors configurations with bifacial solar cells', Renewable Energy 102:279–93.
18. Ilaria Guarracinoa , James Freemana , Alba Ramosa , Soteris A. Kalogiroub , Nicholas J. Ekins-Daukesc , Christos N. Markides, 2019,'Systematic testing of hybrid PV-thermal (PVT) solar collectors in steadystate and dynamic outdoor conditions', Applied Energy 240 ,1014-1030
19. Giovanni Barone , Annamari Buonomano , Cesare Forzano , Adolfo Palombo , Orestis Panagopoulod, 2019,' Experimentation, modeling and applications of a novel low-cost air-based photovoltaic thermal collector prototype', Energy Conersion and Management 195,1079-1097.
20. Swapnil Dubey , S.C. Solanki , Arvind Tiwari, 2009,'Energy and exergy analysis of PV/T air collectors connected in series', Energy and Buildings ENB-2588; No of Pages 8
21. S.C. Solanki, Swapnil Dubey , Arvind Tiwari,2009,'Indoor simulation and testing of photovoltaic thermal (PV/T) air collectors', Applied Energy.

Analysis of MAP/PH/1 Queueing model subject to Two-stage vacations policy with imperfect service, Setup time, Breakdown, Delayed Phase type repair and Reneging customer

¹G. Ayyappan, ²N. Arulmozhi

^{1,2}Department of mathematics
Puducherry Technological University
Puducherry -605014, India.

ayyappan@ptuniv.edu.in, arulmozhi.n@pec.edu

Abstract

This paper explores a continuous-time single server queueing system with infinite system capacity, a two-vacation policy with imperfect service, setup, breakdown, delayed phase-type repair, and customer reneging in this study. The Markovian Arrival Process is used when a customer arrives, and the phase-type distribution is used when offering service. That includes the two-vacation policy, which incorporates a single working vacation and multiple vacations. When the system is empty during the regular busy period, it takes a working vacation first, during which the server can continue to provide service but at a slower speed. If the system is empty after this working vacation, the server will take a vacation during which it will entirely stop serving. Otherwise, the server returns to its normal rate of service. We generate the invariant probability vector for this model using the Matrix-Analytic combination solution approach. In addition, we discuss the busy period and cost analysis. The construction of an absorbing state yields a further waiting time distribution. There are also certain performance measures obtained. Finally, some numerical findings are shown to graphically depict the 2D and 3D.

Keywords: *Markovian Arrival Process; Phase type Distribution; Two-stage vacation; Breakdown; Delayed Repair; Setup; imperfect service; Matrix-analytic method*

AMS Subject Classification (2010): 60K25, 68M20, 90B22.

Analysis of MAP/PH/1 Queueing Model with Degrading Service Rate, Phase-type Vacation, Repairs, Starting failure and Closedown

¹G. Ayyappan, ²S. Meena

^{1,2}Department of mathematics
Puducherry Technological University
Puducherry -605014, India.
ayyappan@ptuniv.edu.in, meena.s@pec.edu

Abstract

We consider a single-server queueing model with degrading service rate, phase-type vacation, repairs, starting failure and closedown in which, the arrival rate of a customer follows the Markovian Arrival Process (MAP) and the service rate of the server follows the phase-type distribution. When the server returns from vacation, if there is no one present in the system, the server will wait until the customer's arrival. If the customer arrives at the moment with no starting failure, then he provides service otherwise the server immediately goes for the repair process. Here the service is degrading service, after completing L service, the server turns to serve at a normal rate. During the period of service, the server may get a breakdown at any moment, and then the server immediately goes for a repair process. After completing the service, he switches to the closedown process, and then he goes on vacation. Using the Matrix-Analytic method, the steady-state probability of the number of customers in the system is investigated. The analysis of the busy period, the mean waiting time, and cost analysis are discussed. Some important performance measures are obtained. Finally, some numerical illustrations are provided.

Keywords: *Markovian Arrival Process; Phase type Distribution; Degrading service rate; Server Vacation; Breakdown; Repair; Starting failure; Closedown; Matrix-analytic method*

AMS Subject Classification (2010): 60K25, 68M20, 90B22.

Analysis of MAP/PH/1 Queueing Model with Differentiated Vacation, Vacation Interruption under N-Policy, Optional Service, Breakdown and Repair, Setup and Discouragement of customers

¹G. Ayyappan, ²G. Archana @ Gurulakshmi

^{1,2}Department of Mathematics
Puducherry Technological University
Puducherry, India

¹ ayyappanpec@hotmail.com; ² archanagurulakshmi@gmail.com

Abstract

In this study, we examine a classical queue with single server in which the customers arrive according to the Markovian Arrival Process(MAP), the repair and service time is according to phase type distribution. The server offers the service to the customers those who are present in the system. On the completion of its service, the server looks to the next customer for providing the service: if system size is empty, the server can take vacation. Here, we consider two types of server vacation such as type 1 vacation as single vacation and type 2 vacation as multiple vacation with distinct durations. After completing the vacation, the server has to start the setup process to provide the service. The server also provides optional service to the customers those who are in need of additional services. During both the vacation period, the arrival of customers may balk the system due to impatience. Under QBD process, we investigate the steady-state probability vector with the assistance of matrix analytic method. In addition, the stability condition, busy period analysis, cost analysis and some of the system performance measures are also examined. The impact of numerical values and graphical representations are also furnished.

Keywords: *Markovian arrival process; Phase type distribution; Two vacation policies; Optional service; Setup; Breakdown; Phase type repair; Balking*

MSC 2010 No.: 60K25, 68M30, 90B22

Analysis of $M^{[X1]}, M^{[X2]}/G_1, G_2^{(a,b)}$ /1 Queue with Priority Services, Server Breakdown, Repair, Modified Bernoulli Vacation, Immediate Feedback

¹G. Ayyappan ²S. Nithya

^{1,2}Department of Mathematics
Puducherry Technological University
Puducherry-605014

1ayyappanpec@hotmail.com; 2nithyamoultouraman@gmail.com

³B. Somasundaram

Department of Mathematics
Vel Tech Rangarajan Dr.Sagunthala
India R&D Institution of Science and Technology
Tamil Nadu-600054, India

3somu.b92@gmail.com

Abstract

In this paper, the steady state analysis of two individualistic batch arrival queues with immediate feedback, modified Bernoulli vacation and server breakdown are introduced. Two different categories of customers like priority and ordinary are to be considered. This model proposes non pre-emptive priority discipline. Ordinary and priority customers arrive as per Poisson processes. The server consistently afford single service for priority customers and the general bulk service for the ordinary customers and the service follows general distribution. The ordinary customers to be served only if the batch size should be greater than or equal to 'a', else the server should not start service until 'a' customers have accumulated. Meanwhile priority queue is empty, the server becomes idle or go for vacation. If server gets breakdown while the priority customers are being served, they may wait in the head of the queue and get fresh service after repair completion, but in case of ordinary customers they may leave the system. After completion of each priority service, customer may re-join the system as a feedback customer for receiving regular service because of inappropriate quality of service. Supplementary variable technique and probability generating function are generally used to solve the Laplace transforms of time-dependent probabilities of system states. Finally, some performance measures are evaluated and express the numerical results.

Keywords: *Batch arrivals; Bulk service; Priority queues; Breakdown; Immediate feedback; Modified Bernoulli vacation.*

AMS Subject Classification (2010): 60K25, 68M30, 90B22.

MAP/PH(1),PH(2)/2 queue with backup server, multiple vacations, optional Service, breakdowns and repairs

¹G. Ayyappan , ²S. Sankeetha

¹Department of Mathematics, Puducherry Technological University, India

²Department of Mathematics, Saradha Gangadharan College, India

e-mail: ayyappanpec@hotmail.com, sangeetha.sivarajp@gmail.com

Abstract

This paper looks at two sorts of services: classic server and main server, both of which offer both regular and optional services. Customers arrive using the Markovian Arrival Process (MAP), and service time is allocated based on phase type distribution. When the classic server fails due to a technical fault or goes on vacation, the backup server takes over at a gradual pace. This system has been modelled as a QBD Process that uses matrix analytic techniques to analyse steady state using finite-dimensional block matrices. During peak periods, the waiting time distribution of our model was investigated in greater depth. The system's performance metrics are assessed, and a few numerical and graphical representations are created.

Keywords: *Markovian Arrival Process-Phase type service-Vacation-Optional service Interruptions.*

MSC 2020 No.: 60K25, 68M20, 90B22

Enhanced Internal Quantum Efficiency of Organic Light-Emitting Diodes: A Synergistic Effect

G. Abirama sundari,¹Assistant professor Chemistry, St.Annes College of Engineering & Technology
S. Ramya² Associate professor Chemistry, St.Annes College of Engineering & Technology

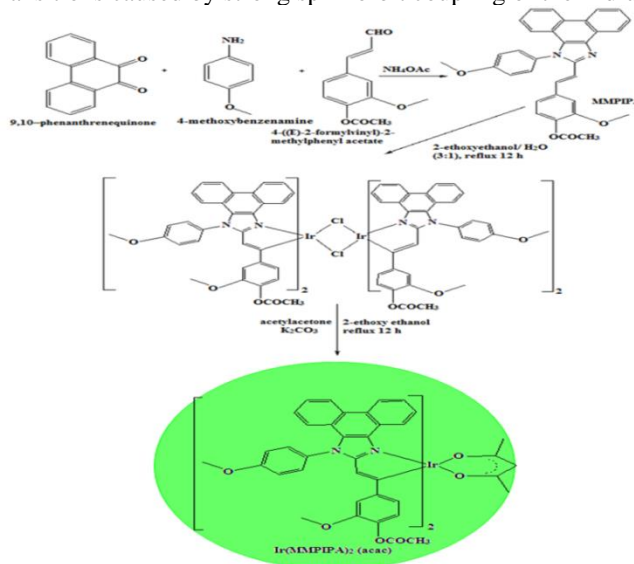
Abstract

The size effect of copper, gold and silver nanoparticles on green OLEDs with MNP-PEDOT: PSS as hole injection layer (HIL) and 4,4'-bis(9-carbazolyl)-biphenyl(CBP): Ir (MMPIPA)₂ (acac) as emissive material were analysed. The OLEDs performance was enhanced by copper, gold and silver NPs with 21, 20 and 55 nm, respectively. The external quantum efficiency (η_{ex}) of green OLEDs with Au (20 nm: III) and Ag (55 nm: IV) has been enhanced by 60% and 64%: power efficiency (η_p) enhanced by 46.9% and 38.7% and current efficiency (η_c) enhanced by 50.0% and 72.2%, when compared with control device (I) respectively. In addition higher efficiencies was harvested from OLEDs with co-doped NPs [Au (20nm) -Ag (55nm), L - 51262 cd/m²; η_{ex} - 9.8%; η_c - 35.3 cd A⁻¹ and η_p - 8.2 lm W⁻¹ and Cu (21nm) - Ag (55nm), L - 49856 cd/m²; η_{ex} - 8.3 %; η_c - 32.1 cd A⁻¹ and η_p - 7.5 lm W⁻¹]. The η_{ex} , η_p and η_c of co-doped green OLEDs with Au-Ag NPs was improved by 96.0, 67.3 and 96.1 %, respectively, compared to control device. The size-controlled NPs can synergistically enhanced OLEDs performances by improving the internal quantum efficiency.

Keywords: Phosphorescence spectrum, plasmon resonance, external quantum efficiency (η_{ex}), MLCT transitions.

1. Characterization of green emissive material [Ir(MMPIPA)₂(acac)]

For the heteroleptic iridium complex (Ir(MMPIPA)₂(acac) in (scheme 1) the absorption band at 248 nm is assigned to spin-allowed ligand-centered transition of imidazole fragment and absorptions at 304 and 345 nm attributed to MLCT transitions to singlet excited state [¹MLCT ← S₀] and triplet excited state [³MLCT ← S₀], respectively (Fig.1), both originated from ligand interaction with iridium center of Ir(MMPIPA)₂(acac).i.e., effective mixing of these transitions caused by strong spin-orbit coupling of the iridium ion.¹⁻⁸



Scheme 1: Synthesis of iridium (III)bis-2-methoxy-4-((E)-2-(1-(4-methoxyphenyl)-1H-phenanthro[9,10-d]-imidazolato-N,C2) (acetylacetonate) [Ir(MMPIPA)₂(acac):]

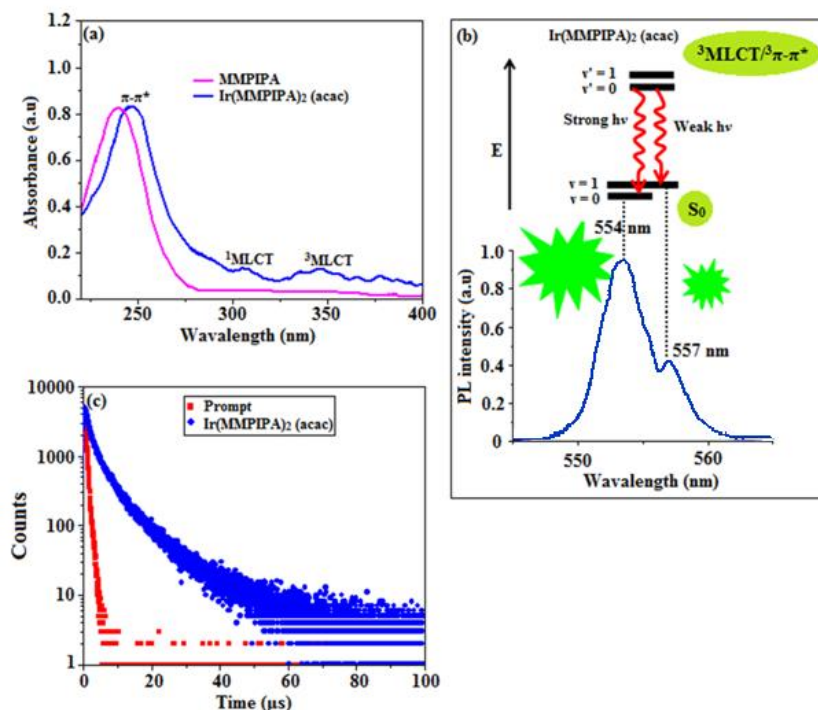


Fig.1. (a) UV spectra of MMPIPA and Ir(MMPIPA)₂(acac); (b) Franck - Condon electronic transitions of Ir(MMPIPA)₂(acac); (c) Life time spectra of Ir(MMPIPA)₂(acac).

The heteroleptic complex Ir (MMPIPA)₂(acac) shows vibronic natured green emission at 554 and 557 nm (**Fig. 1**) and the PL quantum yield (Φ) was measured as 0.49. The photoluminescence spectrum and absorption peaks reveal that Ir (MMPIPA)₂(acac) possess predominantly ³MLCT character. It is known that phosphorescence spectrum of ligand centered -π* is vibronic in nature whereas PL spectra from ³MLCT is in broad shape.⁸⁻¹⁴ The 1.7 μs decay time of Ir (MMPIPA)₂(acac) was further confirmed its MLCT nature (**Fig. 1**). The high (554 nm) and low (557 nm) intensities of the emission peaks are discussed in our previous report (**Fig. 1**).¹⁴ The electrochemical stability of the emissive heteroleptic complex was studied by CV graph which shows reversible oxidation involving single-electron at $E_{ox}^{1/2} = 0.40$ V vs. Fc/Fc⁺. From the oxidation potential, the HOMO energy is calculated as -5.20 eV and LUMO energy obtained from $E_{LUMO} = E_{HOMO} - 1239/\lambda_{onset}$ is -2.60 eV.¹⁵ The thermal characterization (decomposition temperature (T_{d5}) - 410 °C and glass transition temperature (T_g)- 154 °C) of Ir(MMPIPA)₂(acac) were analyzed by usual thermal experiments (DSC and TGA) to find the stability of the films formed (**Fig.2**).The green emissive material exhibits good thermal stability, hence it could be vacuum-evaporated easily without decomposition during fabrication process.

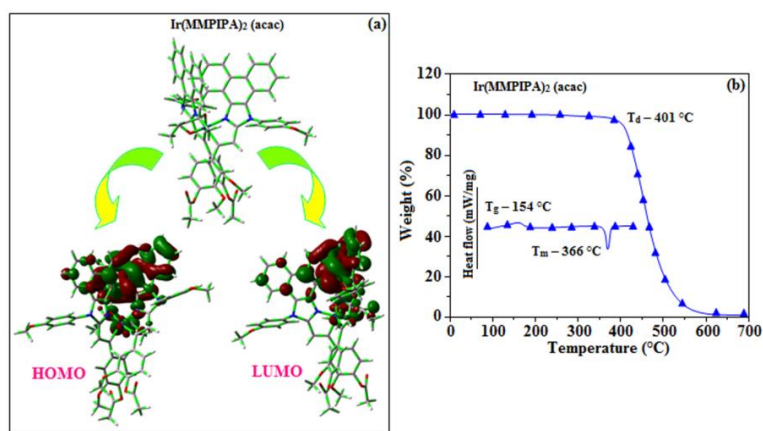


Fig.2:(a) Optimized geometry, HOMO and LUMO contour map of Ir (MMPIPA)₂(acac); (b) DSC and TGA graphs of Ir (MMPIPA)₂(acac).

1.1. Structure of iridium (III)-bis-2-methoxy-4-(*E*)-2-(1-(4-methoxyphenyl)-1*H*-phenanthro[9,10-*d*]-imidazolato-*N,C*²) (acetylacetonate) [Ir (MMPIPA)₂ (acac)]

The optimized geometry of Ir (MMPIPA)₂ (acac) was obtained using Gaussian -09 [DFT/LANL2DZ/6-31G (d,p)] (Fig.2). This complex shows an distorted octahedral geometry with *cis*-C,C and *trans*-N,N chelate disposition inspite of *trans*-C,C and *trans*-N,N chelate. The richer electron density phenyl rings normally exhibit very strong influence (*trans*effect). The obtained *trans*-C, C geometry is thermodynamically higher in energy and kinetically labile referred as “*trans*phobia”.⁶ The *Ir-C* length of complex Ir (MMPIPA)₂ (acac), i.e., *Ir-C_{av}* = 1.96 Å is shorter than *Ir-N_{av}*=2.05 Å and *Ir-O* bond length [2.13 Å] is longer than mean *Ir-O* length (2.07 Å).⁷ The two cyclometalated MMPIPA ligand with acetylacetonate (acac) ancillary moiety around iridium atom forms octahedral geometry⁵ and this was proven by the shorter bond length of *Ir-C_{av}* (1.96 Å) than *Ir-N_{av}* bond length (2.05Å).⁸

1.2. Characterisation of nanoparticles

The crystalline nature of as-synthesized copper NPs with 10 and 20 nm, silver NPs with 25 and 55 nm and gold NPs with 10 and 20 nm was confirmed by XRD (Fig.3), TEM (Fig.4) and XPS (Fig.5) analysis. The peaks observed for copper NPs at 2θ of 42.8, 50.43, 74.12 and 89.92 corresponds to (111), (200), (220), and (311) inter planar reflections of face centered cubic (FCC) crystal, respectively (JCPDS No. 04-0836). Similarly peaks at 39.28, 43.95, 65.01, 75.51 and 80.01 corresponds to (111), (200), (220), (311) and (322) interplanar reflections of face centered cubic (FCC) crystal of silver NPs, respectively (JCPDS No. 89-3722) and peaks observed for gold NPs at 38.74, 44.13, 63.95, 77.13 and 81.01 corresponds to (111), (200), (220), (311) and (222) inter planar reflections of face centered cubic (FCC) crystal, respectively (JCPDS No. 65-2870). The highly intensified peak corresponds to (111) plane of copper, silver and gold nanoparticles indicating their predominant orientation and broadening Bragg’s peak confirm the small crystallite size. The average crystallite size deduced from Debye-Scherrer equation [$D=k\lambda/\beta\cos\theta$, D - average crystal size; k - Scherer coefficient; λ - X-ray wave length; θ - Bragg’s angle; β - full width at half maximum intensity] of Cu, Ag and Au is 21, 25 and 20 nm, respectively and surface area [$S=6000/\rho\times D$] of Cu, Ag and Au is 50.30, 42.25 and 52.56 m²/g, respectively. By varying the experimental procedure, the synthesized Cu, Ag and Au with 10, 55 and 10 nm sizes (Scheme2) also determined from XRD analysis. The composition of Au, Ag, and Cu NPs was analyzed by XPS and the spectrum exhibits copper, silver and gold NPs exist in their metallic state. The peak at Ag 2p_{5/2} (368.1eV) and Ag 2p_{3/2} (374.00 eV) are attributed with metallic silver.¹⁶ Similarly, Cu 2p_{3/2} (932.4 eV) and Cu 2p_{1/2} (951.8 eV) peaks are associated with metallic Cu.¹⁷ The doublet binding energies of Au 4f_{7/2}(84.6 eV) and Au 4f_{5/2}(88.1 eV) shows gold present as Au⁰.¹⁸ The average size of copper, silver and gold 21, 25 and 20 nm calculated from DLS analysis (Fig.6) is well matches with XRD and TEM results. The repulsive forces exist with the electrical charge of the Ag, Au and Cu NPs surface accounts the negative ζ potential (-26.3, -17.0 and -19.5 mV) which increases the stability of the NPs. The gold, silver, copper, Cu-Ag and Au-Ag nanoparticles show SPR peak at 531, 430, 548, 479 and 459 nm, respectively (Fig.7).

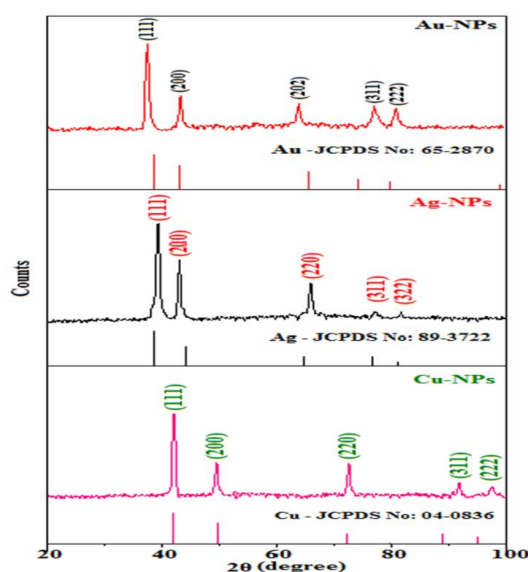


Fig.3: X-ray diffraction pattern of Au (20nm), Ag (25nm) and Cu (21nm) NPs.

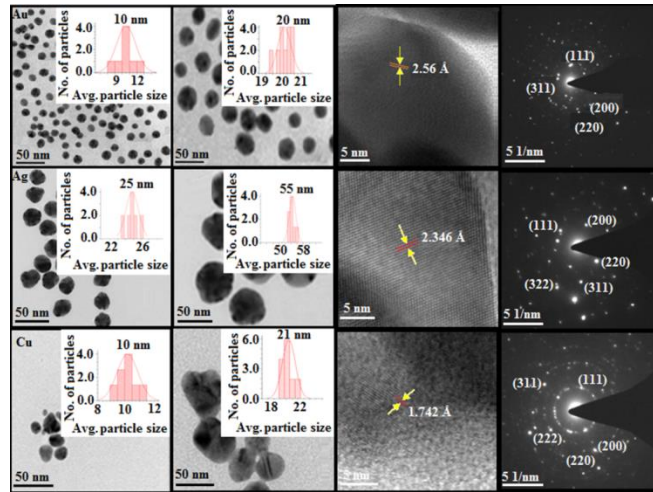


Fig.4: HR-TEM images and SAED of Au, Ag and Cu NPs

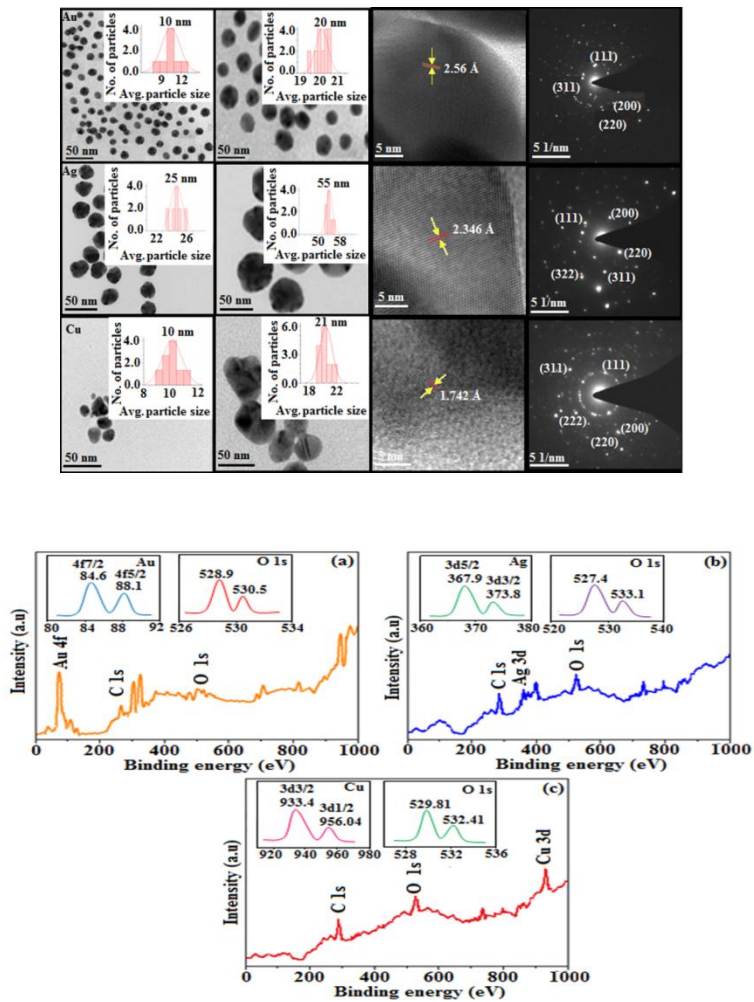
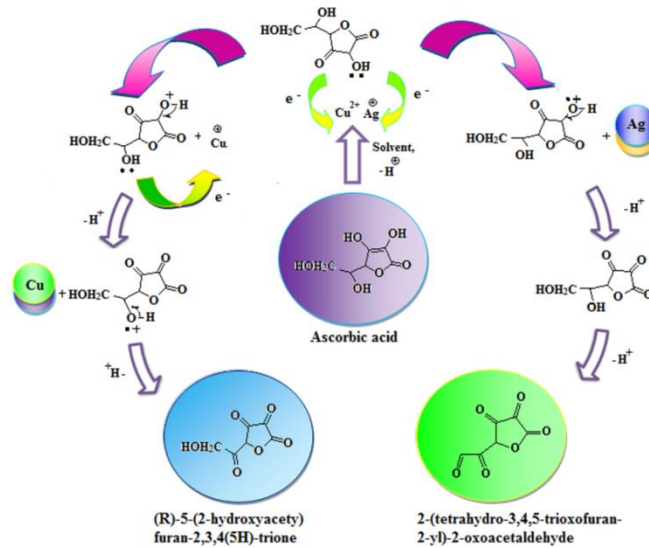


Fig.5: X-ray photoelectron spectra (XPS) of (a) Au(10nm), (b) Ag(55nm) and (c) Cu(10nm) NPs.



Scheme 2: Schematic representation of Ag^+ and Cu^{2+} reduction by ascorbic acid

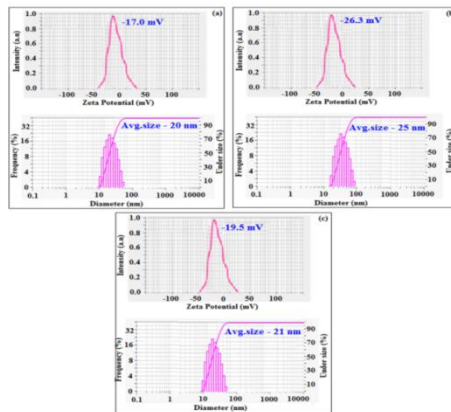


Fig.6: Dynamic light scattering (DLS) and Zeta potential of (a) Au (b) Ag and (c) Cu NPs

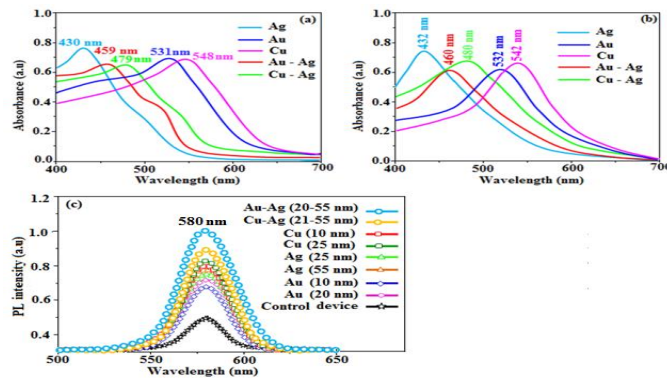


Fig.7: (a) Diffused reflectance spectra (DRS) of Au, Ag, Cu, Cu-Ag and Au-Ag NPs; (b) UV spectra of Au, Ag, Cu, Au-Ag and Cu-Ag NPs coated ITO film; (c) PL spectra of Au, Ag, Cu, Au-Ag and Cu-Ag NPs coated ITO film

1.3. Performances of OLEDs

Thin film of Au, Ag, Cu, Au-Ag and Cu-Ag nanoparticles deposited ITO glass show broad surface plasmon resonance at 532, 432, 542, 460 and 480 nm, respectively, (Fig.7). The size effect of metal nanoparticles on the PL emission of the emissive layer, Ir(MMPIPA)₂(acac) in the fabricated device have been recorded with and without metal nanoparticles. The emission intensity (580 nm) of ITO/Ag NPs or Au NPs or Cu NPs or Au-Ag NPs or Cu-Ag NPs- PEDOT:PSS(40 nm)/CBP:Ir(MMPIPA)₂(acac) (60 nm)/LiF (1nm)/Al (100nm) film is stronger than the device, ITO/without metal nanoparticles (PEDOT:PSS(40 nm)/CBP:Ir(MMPIPA)₂(acac) (60 nm)/LiF (1 nm)/Al (100nm) (Fig.9). The relative EL and PL enhancement of devices II-IX compared to control device I reveal that the enhanced light extraction from the fabricated devices could be a major reason for the enhanced efficiency of the devices [Au-10nm 20%, Au-20nm 24%, Ag-25nm 36%, Ag-55nm 40%, Cu-10nm 42%, Cu-21nm 50%, Cu- Ag 21-55nm 62%, Au-Ag 20-55nm 80% and PL: Au-10nm 24%, Au-20nm 31%, Ag-25nm 38%, Ag-55nm 44%, Cu-10nm 46%, Cu-21nm 51%, Cu- Ag 21-55nm 64%, Au-Ag 20-55nm 85%]. The fabricated green devices having the following configuration : ITO/without NPs (I) or Au [10 nm II : 20 nm III] or Ag NPs [55 nm IV : 25 nm V] or Cu NPs [10 nm VI : 21 nm VIII] or Cu-Ag NPs [21 nm/55 nm VIII] or Au-Ag [20 nm/55 nm IX]-PEDOT:PSS (40 nm)/ CBP:Ir(MMPIPA)₂(acac) (60 nm) /LiF (1 nm)/Al (100 nm) (Fig.9; Table1). (20nm/55nm). The η_c , η_p, η_{ex} efficiency of ITO/Au-Ag(20nm/55nm)-EDOT:PSS/CBP:Ir(MMPIPA)₂(acac) /LiF/Al device is increased by 67, 96 and 67%, respectively than the device without NPs[ITO/PEDOT:PSS/CBP:Ir(MMPIPA)₂(acac) /LiF/Al].The surface analysis of devices III, IV, VIII and IX along with bare were made by topographic images (Fig.10) which shows uniform distribution of metal nanoparticles on ITO anode. The J-V-L curve reveals that the efficiency was increased by co-doped Au-Ag NPs

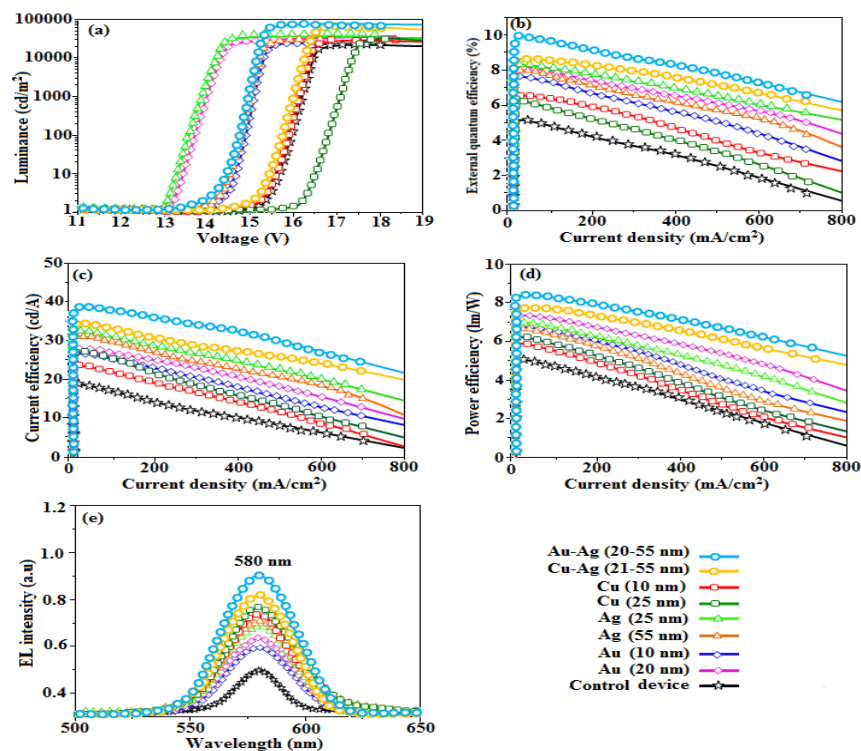


Fig.9: (a) Luminance-Voltage of devices I-IX; (b) External quantum efficiency- Current density of devices I-IX; (c) Current Efficiency-Current density of devices I-IX (d) Power efficiency -Current density I-IX; (e) Electroluminescent spectra of devices I-IX.

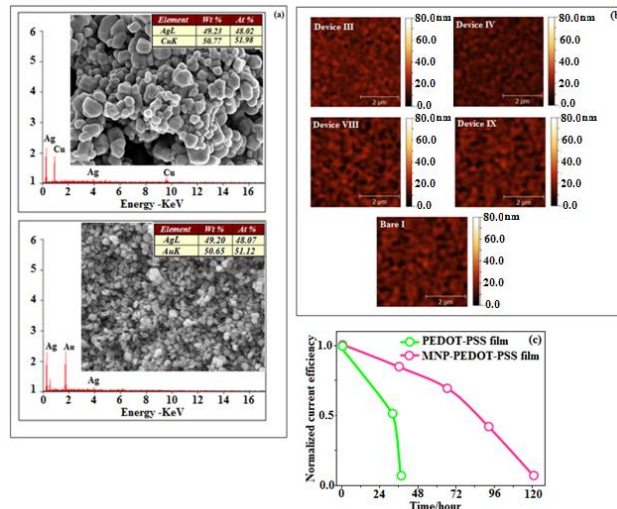


Fig.10: (a) HR-SEM image of Cu-Ag and Au-Ag NPs; (b) AFM images of device bare **I**, (**Au 20 nm**) **III**, (**Ag 55 nm**) **IV**, (**Cu-Ag 21-55 nm**) **VIII** and (**Au-Ag 20-55 nm**) **XI**; (c) Normalized current efficiency of green OLEDs as a function of time.

The root mean square (RMS) values calculated for bare, Au, Ag, Cu-Ag and Au-Ag coated ITO is, 0.40 nm (bare), 0.43 nm (Au), 0.45 nm (Ag), 0.47 nm (Cu-Ag) and 0.49 nm (Au-Ag). The mono dispersed metal nanoparticles with surface plasmonic absorption is beneficial for OLEDs otherwise the plasmonic enhancement is not possible. If there is an agglomeration between the nanoparticles, absorption moves away from visible region and make it unworthy. The SEM and EDX spectra of Au-Ag and Cu-Ag nanoparticles are shown in (Fig.10). The current (η_c), power (η_p) and external quantum efficiency (η_{ex}) of the devices doped with NPs are enhanced and the enhancement depends upon Cu, Au and Ag NPs size [η_c (cd/A): 26.6 (21 nm Cu); 27.0 (20 nm Au); 31.0 (55 nm Ag); η_p (lm/W): 6.2 (21 nm Cu); 7.2 (20 nm Au); 6.8 (55 nm Ag); η_{ex} (%) 6.3 (21 nm Cu); 8.0 (20 nm Au); 8.2 (55 nm Ag)] (Fig.9). The enhanced power efficiency [46.9 % (20 nm Au), 26.5 % (21 nm Cu) and 38.8 % (55 nm Ag)], current efficiency [50.0 % (20 nm Au), 47.7 % (21 nm Cu) and 72.2 % (55 nm Ag)] and external quantum efficiency [60 % (20 nm Au), 26 % (21 nm Cu) and 64% (55 nm Ag)] have been harvested from doped green OLEDs. The performance of green OLEDs has been enhanced by co-doped MNP *i.e.*, Au-Ag NPs (20 and 55 nm) and Cu-Ag (21 and 55 nm). This combination of NPs produces higher performance than OLEDs doped with 10 nm Au NPs, 10 nm Cu and 25 nm Ag NPs. The current (η_c), power (η_p) and external quantum efficiency (η_{ex}) of the devices co-doped with NPs are enhanced and the enhancement depends upon Cu, Au and Ag NPs size [η_c (cd/A): 32.1 (21 and 55 nm Cu-Ag); 35.3 (20 and 55 nm Au-Ag); η_p (lm/W): 7.5 (21 and 55 nm Cu-Ag); 8.2 (20 and 55 nm Au-Ag); η_{ex} (%) 8.3 (21 and 55 nm Cu-Ag); 9.8 (20 and 55 nm Au-Ag)]. The enhanced power efficiency [53.06 % (21 and 55 nm Cu-Ag) and 67.34 % (20 and 55 nm Au-Ag)] and current efficiency [78.3 % (21 and 55 nm Cu-Ag) and 96.1 % (20 and 55 nm Au-Ag)] have been obtained from the co-doped devices. The operating voltages of all the devices are almost identical (7 V at 1 cd m⁻²), indicating that the hole injection is slightly affected by the presence of MNP in the PEDOT:PSS layer. The external quantum efficiency (η_{ex}) of OLED depends upon internal quantum efficiency (η_{in} : number ratio of radiated photons to injected electron-hole pairs) and light extraction efficiency (LEE: number ratio of externally extracted photons to radiated photons). Cho *et al.*,²⁰ reveal that the enhanced dipole emission near Au and Ag NPs increases the rate of radiative recombination (k_r) and Purcell factor [$F_p = k_r(\text{MNP})/k_r(\text{control})$]. The dipole emission of Au NPs for $D < 51$ nm is larger than Ag NPs while it is smaller for $D > 51$ nm. The Ag NPs enhances multiple wavelengths over the entire spectrum, while Au NPs greatly enhances small section of the visible spectrum (550-600 nm). The wavelength enhanced by Au NPs deviate from the emission spectrum of the emitter at large distances and thus, the LSPR effect dramatically decreases. In contrary, the enhancement caused by Ag NPs does not show extreme spectral shifts because of the enhancement of multiple wavelength and broad band response. Therefore, the resonant radiation of Au NPs is stronger at short distances, while Ag NP is stronger at longer distances. The η_{in} of an OLED can be calculated from the equation, $\eta_{in} = (\gamma \times \eta_s \times k_r) / (k_r + k_{nr} + k_{sp})$, where γ is a charge-balance factor, η_s is the singlet exciton efficiency, k_r and k_{nr} are the radiative and nonradiative recombination rates of electron-hole pairs and k_{sp} is the nonradiative decay caused by surface plasmon modes. Hence, the η_{in} can be increased by LSPR induced by MNP, which increases the k_r of the emitter. The average decay time (τ) of the PL emission decreases from 8.38 ns to 7.30ns with Cu NPs, 7.81 ns with Au NPs, 9.80 ns with Ag NPs, 6.98 ns with Cu-Ag NPs and 6.35 ns with Au-Ag NPs (Fig. 11).

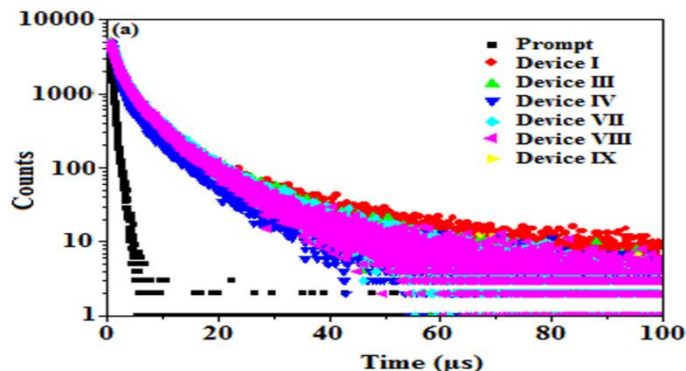
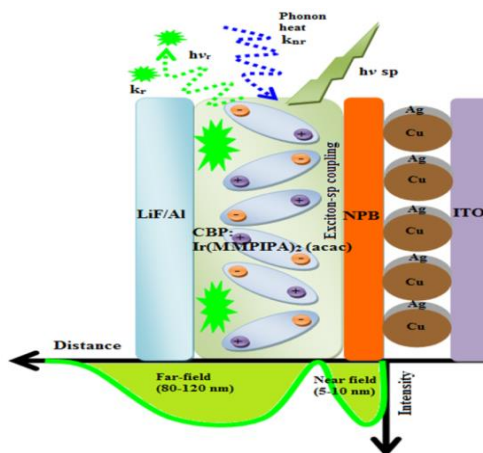


Fig.11: Life time spectra of device I, III, IV, VII, VIII and I

This reduction in τ altered k_r values of doped and co-doped OLEDs which is caused by MNP-induced LSPR and therefore the corresponding quantum yield (ϕ) of the devices increases [ϕ : 0.31 (I), 0.30 (VII), 0.38 (III), 0.51 (IV), 0.43 (VIII), 0.46 (IX)]. In addition the k_r can be calculated from $k_r = \phi/\tau$ and the values are tabulated (Table 2). By assuming that k_{nr} and k_{sp} (Scheme 3) are mostly unchanged by the addition of MNP: increased k_r of the doped and co-doped OLEDs imply that more photons are radiated and hence η_{in} of the devices are increased. The observed higher efficiencies of nano Au deposited device compared to those of Ag as well as Cu incorporated devices is in on the expected line Nano Au is known for its unique optical, electrical and surface plasmonic related properties.²¹ The co-doped Au-Ag and Cu-Ag green OLEDs shows higher efficiencies because of synergistic effect.



Scheme 3: Electron-hole recombination and exciton-surface plasmon (SP) coupling mechanism

Table 1. Lifetime (τ) (ns), quantum yield (ϕ), radiative rate (k_r) ($\times 10^7 s^{-1}$) and Purcell factor (F_p) of OLEDs.

Devices	τ	ϕ	k_r	F_p
Control (I)	8.38	0.31	3.6	-
Au (20 nm, III)	7.81	0.38	4.8	1.33
Ag (55 nm, IV)	9.80	0.51	5.2	1.44
Cu (21 nm, VII)	7.30	0.30	4.1	1.14
Cu-Ag (21/55 nm, VIII)	6.98	0.43	6.1	1.69
Au-Ag (20/55 nm, IX)	6.35	0.46	7.2	2.00

The better performances of nano Au-Ag devices than Cu-Ag is also likely to be due to the better electrical, optical and SPR related feature.²³ co-doped Au-Ag and Cu-Ag based devices were not inferior to previously reported OLEDs.²⁴⁻³⁴ The stability of OLED devices with pristine PEDOT: PSS and MNP-PEDOT:PSS HIL was carried out in ambient air. The degradation of the devices in ambient air condition was analysed in terms of varying current efficiency with time (Fig. 9). The (Fig. 9) shows that the stability of device

based on MNP-PEDOT: PSS HIL was improved than device with PEDOT: PSS HIL in ambient air. This enhanced stability of the device resulted from the alleviated acidic and hygroscopic nature of MNP-PEDOT: PSS HIL due to the usage of significantly reduced amount of PEDOT:PSS polymer. It is well known that the ITO anode is sensitive to acidic conditions and that the high acidity of PEDOT:PSS leads to corrosion of ITO anode and causes diffusion of indium into the emitting layer.^{33,34} The co-doped OLEDs exhibit highest enhancement which can be due to the synergistic effect of stronger near-field resonance of Au NPs and relatively broadband resonance of Ag NPs.

REFERENCE

- [1] J. D. Priest, G. Y. Zheng, N. Goswami, D. M. Eichhorn, C. Woods, D. P. Rillema, *Inorg. Chem.* **2000**, 39, 1955.
- [2] J. Jayabharathi, V. Thanikachalam, K. Saravanan, N. Srinivasan, *J. Fluoresc.* **2011**, 21, 507.
- [3] K. Saravanan, N. Srinivasan, V. Thanikachalam, J. Jayabharathi, *J. Fluoresc.* **2011**, 21, 65.
- [4] J. Jayabharathi, V. Thanikachalam, N. Srinivasan, K. Saravanan, *J. Fluoresc.* **2011**, 21, 596.
- [5] J. Jayabharathi, V. Thanikachalam, K. Saravanan, *J. Photochem. Photobiol. A.* **2009**, 208, 13.
- [6] S. Lamansky, P. Djurovich, D. Murphy, F. A. Razzaq, H. F. Lee, C. Adachi, P. E. Burrows, S.R. Forrest, M. E. Thompson, *J. Am. Chem. Soc.* **2001**, 123, 4304.
- [7] M. G. Colombo, A. Hauser, H. U. Gudel, *Inorg. Chem.* **1993**, 32, 3088.
- [8] S. Okada, K. Okinaka, H. Iwawaki, M. Furugori, M. Hashimoto, T. Mukaide, J. Kamatani, S. Igawa, A. T. suboyama, T. Takiguchi, K. Ueno, *Dalton Trans.* **2005**, 9, 1583.
- [9] K. C. Tang, K. L. Liu, I. C. Chen, *Chem. Phys. Lett.* **2004**, 386, 437.
- [10] D. S. McClure, *J. Chem. Phys.* **1949**, 17, 905.
- [11] H. Bessler, B. Schweitzer, *Acc. Chem. Res.* **1999**, 32, 173.
- [12] N. J. Turro, V. Ramamurthy, J. C. Scaiano, *Published by University Science Books.* **2012**, 88,1.
- [13] J. Liu, Z. Zeng, X. Cao, G. Lu, L. H. Wang, Q. L. Fan, W. Huang, H. Zhang, *Small.* **2012**, 8, 3517.
- [14] J. Jayabharathi, P. Sujatha, V. Thanikachalam, P. Jeeva, S. Panimozhi, *Ind. Eng. Chem. Res.* **2017**, 56, 6952.
- [15] Z. Wang, Y. Feng, S. Zhang, Y. Gao, Z. Gao, Y. Chen, X. Zhang, P. Lu, B. Yang, Chen, P. Ma, Y. Liuc, *Phys. Chem. Chem. Phys.* **2014**, 16, 20772.
- [16] J. Kümmerlen, A. Leitner, H. Brunner, F. R. Aussenegg, A. Wokaunt, *Mol. Phys.* **1993**, 80,1031.
- [17] J. Zhao, D. Zhang, J. Zhao, *J. Solid State Chem.* **2011**, 184, 2339.
- [18] Y. Joseph, I. Besnard, M. Rosenberger, B. Guse, H. G. Nothofer, J. M. Wessels, U. Wild, A. K. Gericke, D. Su, R. Schlog, A. Yasuda, T. Vossmeier, *J. Phys. Chem. B.* **2003**, 107,7406.
- [19] C. Cho, H. Kang, S. Baek, T. Kim, C. Lee, B. J. Kim, J. Y. Lee, *ACS Appl. Mater. Interfaces.* **2016**, 8, 27911.
- [20] K. L. Kelly, E. Coronado, L. L. Zhao, G. C. Schatz, *J. Phys. Chem. B.* **2003**, 107, 668.
- [21] S. W. Baek, G. Park, J. Noh, C. Cho, C. H. Lee, M. K. Seo, H. Song, J. Y. Lee, *ACS Nano.* **2014**, 8,3302.
- [22] A. Kumar, P. Tyagi, R. Srivastava, D. S. Mehta, M. N. Kamalasanan, *Appl. Phys. Lett.*, **2013**, 102, 203304.
- [23] P. E. Laibinis, G. M. Whitesides, D. L. Allara, Y. T. Tao, A. N. Parikh, R. G. Nuzz, *J. Am. Chem. Soc.* **1991**, 113, 7152.
- [24] S. J. Ko, H. Choi, W. Lee, T. Kim, B. R. Lee, J. W. Jung, J. R. Jeong, M. H. Song, J. C. Lee, H. Y. Woo, J. Y. Kim, *Energy Environ. Sci.* **2013**, 6, 1949.
- [25] M. Ullah, K. Tandy, A. J. Clulow, P. L. Burn, I. R. Gentle, P. Meredith, S. C. Lo, E. B. Namdass, *ACS photonics*, 2017, 4, 754
- [26] J. H. Kim, J. H. Lee, T. H. Kim, C. Seoul, *Mater. Res. Soc. Symp. Proc.* **2006**, 936, L05.
- [27] S. A. Choulis, M. K. Mathai, V. E. Choong, *Appl. Phys. Lett.* **2006**, 88, 213503.
- [28] K. Xu, Y. Li, W. Zhang, L. Zhang, W. Xie, *Curr. Appl. Phys.* **2014**, 14, 53.
- [29] Y. Xiao, J. P. Yang, P. P. Cheng, J. J. Zhu, Z. Q. Xu, Y. H. Deng, S. T. Lee, Y. Q. Li, J. X. Tang, *Appl. Phys. Lett.* **2012**, 100, 013308.
- [30] X. Wu, L. Liu, T. Yu, L. Yu, Z. Xie, Y. Mo, S. Xu, Y. Ma, *J. Mater. Chem. C.* **2013**, 1, 7020.
- [31] P. J. Jesuraj, K. Jeganathan, M. Navaneethan, Y. Hayakawa, *Synthetic Metals.* **2016**, 211, 155.
- [32] P. J. Jesuraj, K. Jeganathan, *RSC Adv.* **2015**, 5, 684.
- [34] C. Lee, D. J. Kang, H. Kang, T. Kim, J. Park, J. Lee, S. Yoo, B. J. Kim, *Adv. Energy. Mater.* **2014**, 4, 1301345.
- [34] J. K. Kim, H. S. Park, D. K. Rhee, S. J. Ham, K. J. Lee, P. J. Yoo, J. H. Park, *J. Mater. Chem.* **2012**, 22, 7718.

St. Anne's College of Engineering and Technology

Anguchettypalayam, Panruti - 607 106

Cuddalore Dt.

www.stannescet.ac.in

stannescet@gmail.com

04142 - 241661, 242661

